EVALUATION OF CELLULAR PROCESSES AND IDENTIFICATION OF CANDIDATE GENES CRITICAL TO CORNEAL EPITHELIAL DEVELOPMENT

Magdalena Nowak-Musiał

Thesis submitted to Cardiff University in accordance with the requirements for the degree of Doctor of Philosophy

Visual Neuroscience and Molecular Biology Group
School of Optometry and Vision Sciences
Cardiff University
2009

ProQuest LLC
789 East Eisenhower Parkway
P.O. Box 1346
Ann Arbor, MI 48106-1346

CARDIFF UNIVERSITY
PRIFYSGOL CAERDYDD

Declaration

This work has not previously been accepted in substance for any degree and is not being currently submitted in candidature for any degree.

Signed: ..... Date: .....

STATEMENT 1

This thesis is being submitted in partial fulfilment of the requirements for the degree of PhD.

Signed: ..... Date: .....

STATEMENT 2

This thesis is the result of my own investigations, except where otherwise stated. Other sources are acknowledged by footnotes giving explicit references. A bibliography is appended.

Signed: ..... Date: .....

STATEMENT 3

I hereby give consent for my thesis, if accepted, to be available for photocopying and for inter library loan, and for the title and summary to be made available to outside organisations.

Signed: ..... Date: .....

Dedicated to my Family

No two journeys are the same.
And when you arrive for the first time you realise that it
is not the destination, but how you got there that counts.

Acknowledgements

In the first place I would like to express profound gratitude to Dr. Julie Albon for her supervision and for giving me this opportunity. Her moral support, encouragement and continuous guidance enabled me to complete my work successfully. I am also highly thankful to my other supervisors, Prof. Mike Boulton and Dr Mike Wride for their valuable suggestions throughout this study.

I wish to express my appreciation to a number of people involved in development of my research. I gratefully acknowledge Dr. Jez Guggenheim and Paul Chen for providing experimental animals, Dr. Gillian Smith and Dr. Malyka Galay-Burgos for sharing their experience in microscopy and molecular techniques. I would also like to thank Peter Giles and members of Biostatistic and Bioinformatic Unit for performing chip processing and preliminary statistical analysis of microarray data.

I am particularly indebted to my colleagues; Tetyana Zayats for introducing real time PCR and for being an extremely supportive housemate, Miguel Jarrin for help with histology, immunohistochemistry and for emotional support, Ankush Prashar for statistical advice and patience, Llinos Williams for help with Western blotting and her optimism.

A very special thanks go to all fellow PhD students and postdocs who have been there with me at any stage of this journey, especially Kinga, Basia, Yaiza, Paulinka, Lilian, Gosia, Patrycja, Claudia, Yadan, Cris, Vedran and Aneesh for their support, smiles and friendship.

I also thank all staff in the School of Optometry and Vision Sciences whose support was essential in completing this thesis, in particular: Sue, Steve, Phil, Rob, John, Andy and Greeg for always being so helpful and friendly.

Sincere thanks go to my friends: Monika for always being there for me ready to help in every possible way, and Agnieszka, Piotr, Krzysztof and Karol for inspiration.

I am as ever, especially indebted to my parents who have always put my interests before theirs providing unconditional love and care. I would not have made it this far without their faith and encouragement.

Last but not least I would like to thank my husband. His endless support and understanding for these past four years has allowed me to chase a dream. Martin, thank you for shining your light so beautifully onto my life.

Abstract

The overall aim of this study was to determine factors and mechanisms that underlie the regulation of epithelial patterning and homeostasis during corneal development.

Histological staining was performed in chick corneas, embryonic day (ED) 4 to 21, to evaluate changes in the overall epithelial cell morphology, in particular cell shape, cell size and the number of epithelial cell layers. Epithelial differentiation patterns were identified in frozen sections of chicken corneas after immunolocalisation of pan-cytokeratins (Pan-CK) and cytokeratin 3 (CK3). Proliferating Cell Nuclear Antigen (PCNA) and caspase 3 (active) immunolocalisation studies, as well as, TUNEL-labelling (Terminal deoxynucleotidyl transferase dUTP-biotin nick-end labelling) were performed to assess temporal and spatial localisation of cell proliferation and death in the developing corneal epithelium respectively. The expression of PCNA and CK3 were later confirmed by immunoblotting. Total RNA was isolated from epithelia at selected developmental time points and collected for microarray analysis. Gene expression profiles were analysed by appropriate mathematical methods. The sensitivity of arrays in producing data trends was validated by quantitative RT-PCR.

Histological findings included changes in stratification; an increase in the number of cell layers, change in cell morphology. In this study it was demonstrated that after becoming two layered by ED4, the epithelium underwent further stratification to form intermediate cell layers at about ED14. These changes were accompanied by changes in cell shape commencing at ED10. Cell proliferation appeared high throughout corneal development, with peak proliferation between ED12 and ED14 in the limbal, peripheral and central epithelium, respectively, thereafter the level of proliferation decreased. The above coincided with changes in epithelial morphology (stratification) and changes in expression of cytokeratin (CK) epithelial markers. The appearance of pan-CK labelling was first observed at ED10 and the presence of CK3 immunolabelling appeared in epithelial cells at ED12. TUNEL-labelling and caspase 3 (active) immunolocalisation demonstrated only few TUNEL-positive cells, mostly restricted in the limbal region of the corneal epithelium, in the mid and later developmental stages. Microarray analyses identified gene families and their members (including these involved in stem cell biology) likely to be relevant in the regulation of homeostasis during corneal epithelial development, as well as, differentially expressed genes that reveal changes in biological processes due to the change in time. RT-qPCR confirmed the differential expression patterns of seven genes of interest following analysis of microarray data.

Patterns of cell proliferation and differentiation showed changes during the development of the corneal epithelium that reflect the interaction of a complex network of mitogenic, apoptotic and differentiation agents. The changes in gene expression profiles, detected by the microarray analyses, were consistent with the phenotypic changes in the developing chick corneal epithelium. The microarray data provided the first study to present a good overall picture of genes expression in the developing chick corneal epithelium.

Table of contents

List of Figures

List of Tables

Abbreviations

ABCG2	ATP-binding cassette sub-family G member 2
ALDH	Aldehyde dehydrogenase
ALV	Avian leucosis virus
AM	Arithmetic mean
ANOVA	Analysis of variance
Ap2	Activator protein 2
Apaf1	Apoptotic peptidase activating factor 1
APC	Adenomatosis polyposis coli
Api5	Apoptosis inhibitor 5
Aqp3	Aquaporin 3
ARK	Aniridia-related keratopathy
Atoh7	Atonal homolog 7
ATP	Adenosine triphosphate
Bcl2a1	Bcl2-related protein A1
Bdnf	Brain-derived neurotrophic factor
bHLH	Basic helix-loop-helix
Bid	BH3 interacting domain death agonist
βigh3	GF-β-induced gene-human clone 3
Birc2	Baculoviral IAP repeat-containing 2
Birc4	Baculoviral IAP repeat-containing 4
BL	Bowman`s layer
BMP	Bone morphogenetic protein
Bmp4	Bone morphogenetic protein 4
Bmp7	Bone morphogenetic protein 7
Bmpr1b	Bone morphogenetic protein receptor type 1b
BMSCs	Bone marrow-derived stem cells
Bnip3	BCL2/adenovirus E1B 19kDa interacting protein 3
Bok	Bcl-2-related ovarian killer protein
BrdU	Bromodeoxyuridine
Brg1	Brahama-related 1
BSA	Bovine Serum Albumin
°C	Celsius degrees
Cald1	Caldesmon 1
Casp	Caspase
CDH3	P-cadherin
Cdk	Cyclin-dependent kinase
cDNA	Complemetary deoxyribonucleic acid
Cebpb	CCAAT/enhancer binding protein beta
CHO	Chinase Hamster cell ovary line
Chx10	Visual system homeobox 2
CK	Cytokeratin
CK3	Cytokeratin 3
CK12	Cytokeratin 12
CK18	Cytokeratin18
CLS	Suppressor of Hairless/LAG-1 nuclear factor
Col1a2	Collagen type I alpha 2
Col11a1	Collagen type XI alpha 1
cRNA	Complementary ribonuleic acid
CRD	Cysteine rich-domain
Ct	Cycle treshhold
CV	Coefficient of variance
da	Day
DAB	Diaminobenzidine
dap	D-aminopeptidase
dATP	Deoxyadenosine triphosphate
DAVID	Database for Annotation, Visualization and Integrated Discovery
DCs	Dendritic Cells
dCTP	Deoxycytidine triphosphate

df	Degree of freedom
dGTP	Deoxyguanosine triphosphate
dH_2O	Distilled water
ddH_2O	Double distilled water
Dll1	Delta-like protein 1
DM	Descemet's membrane
DNA	Deoxyribonucleic acid
dNTP	Deoxynucleotide triphosphate
DPX	Xylene-based mountant
dsDNA	Double-stranded deoxyribonucleic acid
DSH	Dishevelled
dTTP	Deoxythymidine triphosphate
E2F	Eukaryotic transcription factor
ECL	Enhanced chemiluminescence
ECM	Extracellular matrix
ED	Embryonic day
Edg	Endothelial differentiation G-protein coupled receptors
EDTA	Ethylenediaminetetraacetic acid
EGF	Epidermal Growth Factor
EGFR	Epidermal Growth Factor Receptor
EN	Endothelium
EP	Epithelial layer
Epgn	Epithelial mitogen homolog
ERC	External spike-in RNA control
ES	Embryonic Stem Cells
EST	Expressed sequence tags
ET	T-box family gene for transcription factors
Eya	Eye absent
F	F statistic
FADD	Fas Associated protein with Death Domain
Faim	Fas apoptotic inhibitory molecule
Fc	Fold change
FDR	False discovery rate
Fgd3	FYVE, RhoGEF and PH domain containing 3
FGF	Fibroblast growth factor
FGF2	Fibroblast growth factor 2
Foxc1	Forkhead box C1
Foxe3	Forkhead box P3
G1	Gap 1
G2	Gap 2
G6PDH	Glucose-6-phosphate dehydrogenase
GAGs	Glycosaminoglycans
GAPDH	Glyceraldehyde 3 phosphate dehydrogenase
GCOS	GeneChip® Operating Software
Gdfs	Growth and differentiation factors
gDNA	Genomic deoxyribonucleic acid
GEFs	Guanine-nucleotide exchange factor
GF	Growth factor
GFP	Green fluorescence protein
Gjd3	Gap junction protein delta 3
Gli3	GLI family zinc finger 3
GM	Geometric mean
GO	Gene ontology
GSK	Glycogen synthase
H2afy2	H2A histone family, member Y2
H&E	Haematoxylin and eosin
HCl	Hydrogen chloride
Hes1	Hairy/Enhancer of Split 1
HGF	Hepatocyte Growth Factor
HH	Hamilton and Hamburger stages

hr	Hour
HRP	Horseradish peroxidase
IAP	Inhibitor of apoptosis protein
ICM	Inner Cell Mass
IGF-1	Insulin-like Growth Factor 1
IgG	Immunoglobulin type G
IHC	Immunohistochemistry
Ihh	Indian hedgehog homolog
Il -1	Interleukin 1
IMS	Industrial Methylated Spirit
IVT	In vitro transcription
KCl	Potassium chloride
Kcnj2	Potassium inwardly-rectifying channel, subfamily J, member 2
kDa	Kilo Dalton
KGF	Keratinocyte Growth Factor
KGFR	Keratinocyte Growth Factor Receptor
Klf4	Krüppel-like factor 4
LASIK	Laser-assisted *In Situ* Keratomileusis
Lect1	Chondromodulin-1
Lhx2	LIM homeobox protein 2
LI	Labelling index
LPA	Lysophosphatidic acid
LSCs	Limbal Stem Cells
Ly6e	Lymphocyte antigen 6 complex locus E
lys	lysine
mA	Milliamper
MAA	Agglutinin
mAb	Monoclonal antibody
Maf	V-maf musculoaponeurotic fibrosarcoma oncogene homolog (avian)
Mall	Mal T-cell differentiation protein-like
MAPKs	Mitogen-Activated Protein Kinases
Mcl1	Myeloid cell leukemia sequence 1
MEK	MAP kinase
MEKK	MAP kinase kinase
MEKK1	Kinase 1 mitogen-activated protein
Mf1	Winged-helix/forkhead transcription factor
mg	Milligram
$MgCl_2$	Magnesium chloride
Mgp	Matrix Gla protein
MHC	Major histocompatibility complex
ml	Millilitre
mm	Millimetre
mM	Millimole
mRNA	Messenger ribonucleic acid
miRNA	Micro ribonuleic acid
Mitf	Microphthalmia-associated transcription factor
Msx2	Msh homeobox 2
Myd88	Myeloid differentiation primary response gene (88)
N	Number of samples
NaCl	Sodium chloride
NBF	Neutral Buffered Formalin
NCBI	National Center for Biotechnology Information
NGF	Nerve Growth Factor
NGFR	Nerve Growth Factor Receptor
NF	Normalisation factor
Nfkbia	Nuclear factor of kappa light polypeptide gene enhancer in B-cells inhibitor
nm	Nanometer
Nog	Noggin
NTC	No template control
Ntf3	Neurotrophin 3

NUSE	Normalised unscaled standard errors
OCT	Optimal Cutting Temperature
OD	Optical density
Opa1	Optic atrophy 1
Otx2	Orthodenticle gene
Pan-CK	Pan-cytokeratins
Pax2	Paired box gene 2
Pax6	Paired box gene 6
Pax 7	Paired box gene 7
PBS	Phosphate Buffered Saline
PCA	Prinicpal component analysis
PCNA	Proliferating Cell Nuclear Antigen
PCR	Polymerase chain reaction
Pdcd2	Programmed cell death 2
PDGF	Platelet-derived Growth Factor
PDGFR α	Platelet-derived Growth Factor Receptor Alpha
PFA	Paraformaldehyde
Pgr	Progesterone receptor
Phe	Phenylalanine
PI3K	Phosphoinositide 3-kinases
Pitx2	Pituitary homeobox 2
Pitx3	Pituitary homeobox 3
PKA	Protein kinase A
PKC	Protein kinase C
PM	Perfect match
PNA	Peanut lectin
pRb	Retinoblastoma protein
Prox1	Prospero homeobox 1
Psca	Prostate stem cell antigen
Psen 1	Presenilin 1
Psen 2	Presenilin 2
QC	Quality control
QPCR	Quantitative polymerase chain reaction
R^2	Correlation coefficient
Raf1	V-raf-1 murine leukemia viral oncogene homolog 1
RIN	RNA Integrity Number
RLE	Relative log expression
RMA	Robust multiarray avarage
RNA	Ribonuleic acid
RNAi	Ribonuleic acid interference
ROCK	Rho-associated serine/threonine kinase
rRNA	Rybosomal ribonuleic acid
RT-qPCR	Reverse transcription quantitative polymerase chain reaction
RT	Reverse transcriptase
RTK	Receptor tyrosine kinase
RT-qPCR	Reverse transcription quantitative polymerase chain reaction
RX	Retinal Homeobox
S1P	Sphingosine 1-phosphate
SAPE	Streptavidin Phycoerythrin
SCs	Stem Cells (adult)
SD	Standard deviation
SDS	Sodium dodecyl sulphate
SDS-PAGE	Sodium Dodecyl Sulphate – Polyacrylamide Gel Electrophoresis
SEM	Standard error of the mean
Sfrp1	Secreted frizzled-related protein 1
Sfrp2	Secreted frizzled-related protein 2
Sh3bgr	SH3 domain-binding glutamic acid-rich protein
Shh	Sonic hedgehog
Sig.	Significance
siRNA	Small interfering ribonuleic acid

Six3	Sine oculis homeobox homolog 3
Slit2	Slit homolog 2
Slit3	Slit homolog 3
Sox3	Sex determining region Y-box 3
SP	Stromal substantia propia
SPSS	Statistical package for social sciences
SRE	Serum response element
SRF	Serum response factor
TACs	Transient Amplifying Cells
TAE	Tris base, acetic acid, EDTA buffer
TBS	Tris buffered saline
TBST	Tris-Buffered Saline Tween-20
TCF	T-cell factor
TdT	Terminal Deoxynucleotidyl Transferase
TE	Tris-EDTA Buffer
TGFRα	Transforming Growth Factor Receptor Alpha
TGFβ	Transforming Growth Factor Beta
TGFR1β	Transforming Growth Factor Receptor Beta 1
Thr	Threonine
TKT	Transketolase
T_m	Melting temperature
Tmsb4x	Thymosin beta 4 X-linked
TNF	Tumor Necrosis Factor
TNFα	Tumor Necrosis Factor Alpha
TNFR5	Tumor Necrosis Factor Receptor 5
TrkA	Receptor tyrosine kinase
TUNEL	Terminal deoxynucleotidyl transferase dUTP-biotin nick-end labelling
UB	Ubiquitin
V	Volt
Vegfa	Vascular endothelial growth factor A
Vsx1	Visual system homeobox 1 homologue
Vsx2	Visual system homeobox 2 homologue
WB	Western blotting
WM	Weight marker
Wnt	Wingless
WR	Working reagent
µg	Microgram
µl	Microlitre
µm	Micrometre
µM	Micromole

CHAPTER ONE

Introduction

1.1 The cornea

1.1.1 Introduction to the cornea

The ocular surface is a complex biological continuum, which comprises lids, conjunctival and corneal nonkeratinised epithelium bathed by the precorneal tear film (Thoft and Friend, 1983). Interactions between these components contribute to maintenance of corneal clarity and protection of the eye against microbial and mechanical insults.

The cornea is a part of the fibrous tunic that forms the tough, coat of the outer ocular surface of the eye. The position of the cornea assigns it a protective role as an effective barrier protecting the eye from outside environment and maintaining internal ocular pressure.

Transparency is another important feature of the cornea and is conferred by regularity in spatial arrangement of the collagen fibrils as well as their regular packing (Maurice, 1957; Meek *et al.*, 2003). This trait, as well as smooth surface and regular curvature, provide the refractive function of the cornea and make it essential for good vision. Being transparent, only 1% of incoming light is reflected, with the remaining being transmitted onto the crystalline lens and further refocused onto the retina.

1.1.2 Structure of adult cornea

The cornea is composed of five layers (from the outer layer): corneal epithelium, Bowman`s layer, stroma, Descemet`s membrane and the corneal endothelium (Gartner and Hiatt, 2001) (Figure 1.1). A detailed description of each layer is given in the following paragraphs.

Figure 1.1 A cross- section of human cornea, depicting the epithelial layer (EP), Bowman`s layer (BL), stromal substantia propia (SP), Descemet`s membrane (DM) and endothelium (EN). (Adapted from *http://education.vetmed.vt.edu/Curriculum/VM8054/EYE/CRNSCLRA.HTM).*

1.1.2.1 Epithelium

The epithelium is located in the anterior of the corneal structure; its thickness has been estimated to be around 50.7µm (Reinstein *et al.*, 1994). The adult human corneal epithelium is composed of four to five layers that form stratified, squamous and nonkeratinised features. A schematic view and cross section of the human corneal epithelium are shown in Figure 1.2.

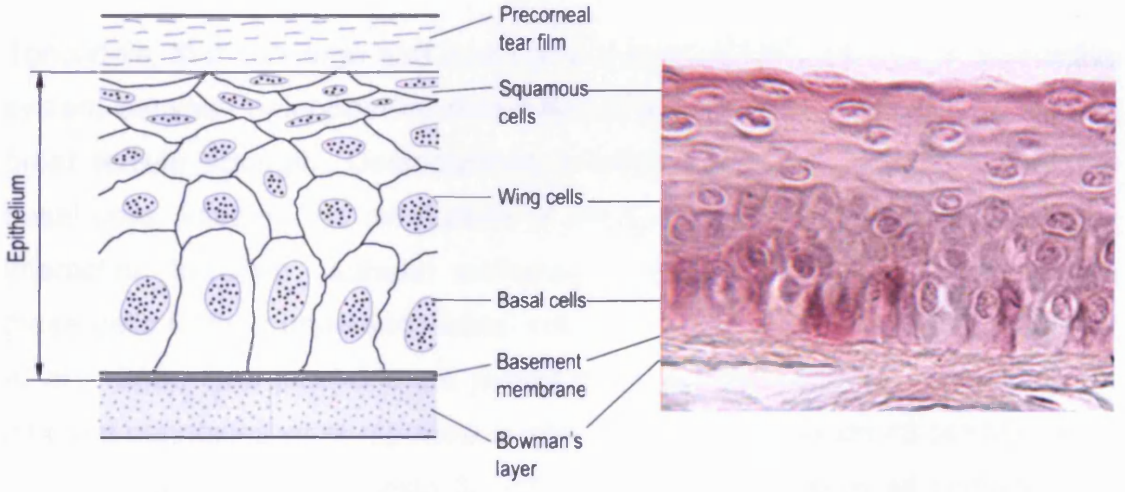

Figure 1.2 A schematic view and cross-section of human corneal epithelium showing different cell layers. (Adapted from Millodot, 2009; cross section image available online *http://cmdi.medicine.dal.ca/Human_Histology/Lab2/101_LH_CORNEA.JPG.*

The deepest layer of epithelial cells, the basal cells, rest on the underlying basement membrane (basal lamina). They are cuboidal or cylindrical in form with flat bases and rounded tops. Basal cells constitute the germinative layer of epithelium and have a higher metabolic and proliferative capacity (Davanger and Evensen, 1971).

The next two to three cell layers are constituted of polyhedral wings cells with oval nuclei. The layers near the anterior surface of the cornea consist of progressively flattened, squamous cells. The top layer is comprised of cells with the maximum surface area, flattened nuclei and projecting peculiar microvilli that secrete highly hydrophilic mucin glycocalyx (Gipson *et al.*, 1997), important in retention of the precorneal tear film.

The corneal epithelial cells tightly adhere to one another and form specialised intercellular structures, including tonofibrils (intermediate filaments), desmosomes, hemidesmosomes (between basal cells and basement membrane), tight junctions (mainly in lateral membranes of squamous cells), adherens junctions (zonula adherens, mainly in lateral membranes of basal cells) and gap junction, responsible for its barrier function against fluid loss and pathogen entrance (Fawcett, 1966; Kenyon, 1969; Gipson, 1994; Lu *et al.*, 2001). Different types of epithelial cell junctions are shown in Figure 1.3.

Tonofibrils, that converge and insert at the desmosomes, provide a connective system between neighbouring cells and extracellular matrix (ECM), as well as great tensile strength. Desmosomes provide intercellular attachment of the basal cells, keeping the membrane of contiguous cells in close proximity (by interaction between cadherin proteins), whereas, hemidesmosomes attach these cells to their underlying basal lamina (by integrins linkage) (Khodadoust *et al.*, 1968). Gap junctions are preset throughout the corneal epithelium, but different connexins were reported in different layers; connexin 43 (43 kDa) was found in basal cells, connexin 50 (50 kDa) were present in all epithelial cell types (Dong *et al.*, 1994).

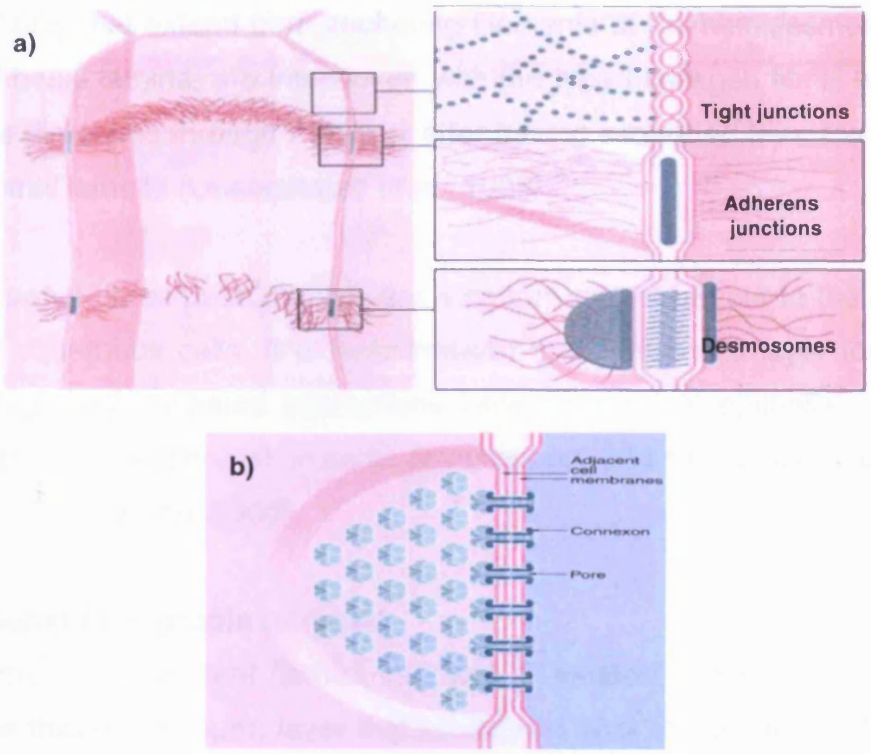

Figure 1.3 Types of intracellular **(a)** and communicating **(b)** junctions present in corneal epithelium (adapted from Young *et al.*, 2006).

Although, the corneal epithelium is considered as avascular, Hamrah *et al.* (2002) reported that the corneal epithelium contains major histocompatibility complex (MHC) class II-negative Langerhans' cells and at least three dendritic cells (DCs) phenotypes (Yamagami *et al.*, 2005). In human corneal epithelium, DCs have been detected mainly in the basal cell layer of the corneal epithelium and partly in the wing/surface layers. The number of CD45-positive cells (mature DCs with capacity to capture antigens) was shown to be significantly higher in the periphery than in the centre of the cornea (Yamagami *et al.*, 2005).

1.1.2.2 Bowman`s layer

Bowman`s layer is a characteristic, of human, primate, avian and reptile corneas, while absent in other mammals. It is an approximately 10μm thick, modified acelullar zone of the anterior stroma, also called the anterior limiting lamina, and is resistant to both mechanical and infectious trauma. The layer is

composed of randomly interplexed collagen fibrils and proteoglycans. Collagen type VII fibrils that extend from anchoring filaments of the hemidesmosomes of epithelial basal lamina, are interwoven with the type I collagen fibrils which run in various directions through the layer after having separated from the anterior-most stromal lamella (Linsenmayer *et al.*, 1998).

Sensory nerve fibres pass through this structure and reach out to the layers of epithelial squamous cells. It is hypothesised that Bowman`s layer forms as a result of cytokine-mediated interactions between corneal epithelial cells and keratocytes (in the stroma) in early development and this process continues into adulthood (Wilson, 2000).

1.1.2.3 Substantia propia (stroma)

The stroma, a transparent fibrous structure, is located under Bowman`s layer and is the thickest (500µm) layer that constitutes 90% of the corneal thickness. It is composed of 200 to 250 layers of collagenous connective tissue (mainly collagen type I and type V fibrils, with some type III and VI), arranged in lamellae (2µm thickness) (Meek and Boote, 2004). Thick flattened collagenous lamellae, embedded in a ground substance of proteoglycans, are oriented parallel to the corneal surface and continous with the sclera at the limbus. Their arrangement is more regular towards the posterior surface. Such a structure has consequences for the mechanical properties of the cornea and its resistance to intraocular pressure (Newsome *et al.*, 1981; Maurice, 1984).

Between lamellae, there is a low density population of fibroblasts (keratocytes) scattered parallel to the surface. The cell bodies of keratocytes are stellate in shape with thin cytoplasmic extensions and secrete the collagen and ECM of the stroma. Keratocytes have growth factors receptors that are activated in response to wound healing. This results in migration, transformation into myofiboblasts and formation of scar tissue. Over time the scar tissue undergoes remodelling, resulting in thinning and an increase in transparency (Cintron and Kublin, 1977).

Corneal transparency is a unique physical property that results from the regular spacing of collagen fibrils with remarkably uniform diameter and interfibrillar space (Michelacci, 2003). The latter is maintained by ECM that consists of glycosaminoglycans (GAGs) and proteoglycans forming bridges between collagen fibrils. The GAGs in the human cornea are predominantly keratan sulphate and chondroitin (dermatan) sulphates, being more concentrated in the central and peripheral stroma respectively (Michelacci, 2003).

1.1.2.4 Descemet`s membrane

Descemet`s membrane, is a basal lamina that separates the stroma from the endothelium. The function of the membrane is mostly structural, forming a tough, resistant barrier.

Its thickness ranges from 3μm at birth to 8-10μm in adults (Johnson *et al.*, 1982). This membrane comprises two layers; an anterior banded layer which appears first before birth and a homogenous/non-banded posterior which develops later. It is highly elastic, which results from collagen architecture and composition. The major protein is collagen in the anterior banded region; reported to contain the hexagonal array of type VIII collagen (Sawada *et al.*, 1990). Types V and VI collagens are dominant in the posterior zone. Other basal laminar components, such as fibronectin, have also been identified (Newsome *et al.*, 1981).

Electron microscopy studies revealed attachment sites and short fibrils extending from the stroma into Descemet`s membrane. The surface of the membrane next to the endothelium was smooth without any anchoring structures for the endothelium (Binder *et al.*, 1991). As mentioned above, uniform increase in Descemet`s membrane thickness occurs with age.

1.1.2.5 Endothelium

The corneal endothelium lines the posterior surface of the cornea and is responsible for synthesis of proteins that are necessary for secreting and maintaining Descemet`s membrane. Acting as a fluid pump, it has a critical role

in maintaining corneal hydration, and thus transparency (Gartner and Hiatt, 2001). It also serves as a barrier, protecting the cornea from oedema and allowing the passage of salts and metabolites.

The endothelium is a single layer of cells that are 4 to 6μm in height and 18-20μm in diameter. Their lateral surfaces of cells are interdigitated and neighbouring cells are bound together by apical junctional complexes (Barry *et al.*, 1995). The anterior surface of the endothelium comes in contact with Descemet`s membrane and form regular and uninterrupted polygonal or hexagonal mosaic. The posterior surface is coated with a viscous substance (Sperling and Jaobsen, 1980).

In the normal human cornea, the endothelium has low regenerative capacity. The cell loss can be overcome by the spreading and enlarging of adjacent cells that replace lost cells. However, in order to maintain its integrity and compensate for missing cells, a minimum level of 400 cells/mm^2 has to be sustained (normal average in mid-age is 2500 cells/mm^2). With age, endothelium has decreased cell density and increased cell irregularity. This is an effect of cell migration, which occurs in the aftermath of cell loss (Yee *et al.*, 1985), since the adult human endothelium is considered as non-proliferative.

1.1.3 Corneal innervation

The cornea is one of the most densely innervated tissues in the body and is richly supplied by sensory and autonomic nerve fibres, which do not compromise its transparency. The corneal innervation density differs in particular areas of the cornea, the highest density being observed in the corneal epithelium (Müller *et al.*, 2003).

Nerve bundles enter the cornea at the periphery in a radial fashion parallel to the cornea surface. Subsequently, in humans, nerves from middle and anterior stroma penetrate Bowman's layer throughout the peripheral and central cornea. At the base of epithelial layer, only beaded fibres bifurcate from the bundle, turn

upwards into the epithelium and terminate in the superficial epithelial cell layer (Müller *et al.*, 2003) (Figure 1.4).

The correct nerve distribution (Figure 1.5) and morphology is considered to be very important for proper corneal activity, especially due to the fact that in recent years neuropeptides, naturally synthesized by corneal nerve fibres, have been used to promote corneal wound healing (Müller *et al.*, 2003).

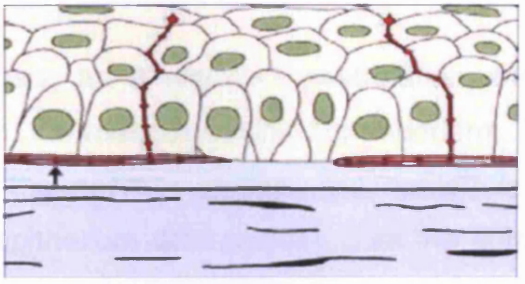

Figure 1.4 Schematic drawing of the architecture of nerve bundles in the subbasal plexus (arrow). Nerve bundles contain a mixed population of straight and beaded fibres. From this population only beaded fibres bifurcate from the bundle and turn upwards into the epithelium (adapted from Müller *et al.*, 2003).

Neurotransmitters and neuropeptides released by trigeminal neurons stimulate corneal epithelial cell growth, proliferation (i.e. substance P), differentiation, production of type VII collagen (Baker *et al*, 1993) and migration of cells (i.e. the synergistic effect of substance P and Insulin-like Growth Factor 1 (IGF-1) and/or Epidermal Growth Factor (EGF), norepinephrine and acetylcholine) (Nakamura *et al.*, 1997a,b,c). Corneal epithelial cells also release factors that promote neurite extension and survival (Emoto and Beuerman 1987), important for cornea wound healing after the laser-assisted *in situ* keratomileusis (LASIK) procedure, in which most stromal nerves are cut and ablated.

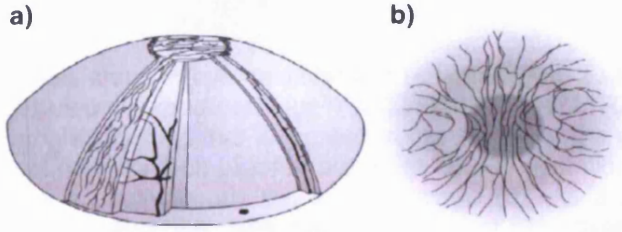

Figure 1.5 Schematic distribution of nerves in the stroma and subbasal plexus in human corneas **(a)** (adapted from Maurice,1984, Müller *et al.*, 2003) and schematic organisation of the subbasal plexus **(b)** (Müller *et al.*, 1996). The nerve bundles are orientated in the superior-inferior direction in the apex, and in the nasal-temporal direction in the surrounding area.

1.2 Corneal development

1.2.1 Early embryonic corneal development

The development of the vertebrate cornea is the last of the major inductive events in eye formation (Forrester *et al.*, 2002). Although there are differences in the structure of the cornea between species, it is believed that embryonic ocular development has been evolutionarily conserved (Oliver and Gruss, 1997). The series of events that take place during early corneal formation are described below.

In early embryogenesis, as a result of gastrulation, three germ layers are formed; the ectoderm, the mesoderm and the endoderm. The ectoderm (upper layer), gives rise to the nervous system, the epidermis and other epithelial layers. The corneal epithelium differentiates from the surface ectoderm that is rebuilt above the lens vesicle (by 4 days of gestation in chick, 6th gestational week in human). The steps of eye development are shown in Figures 1.6 and 1.7.

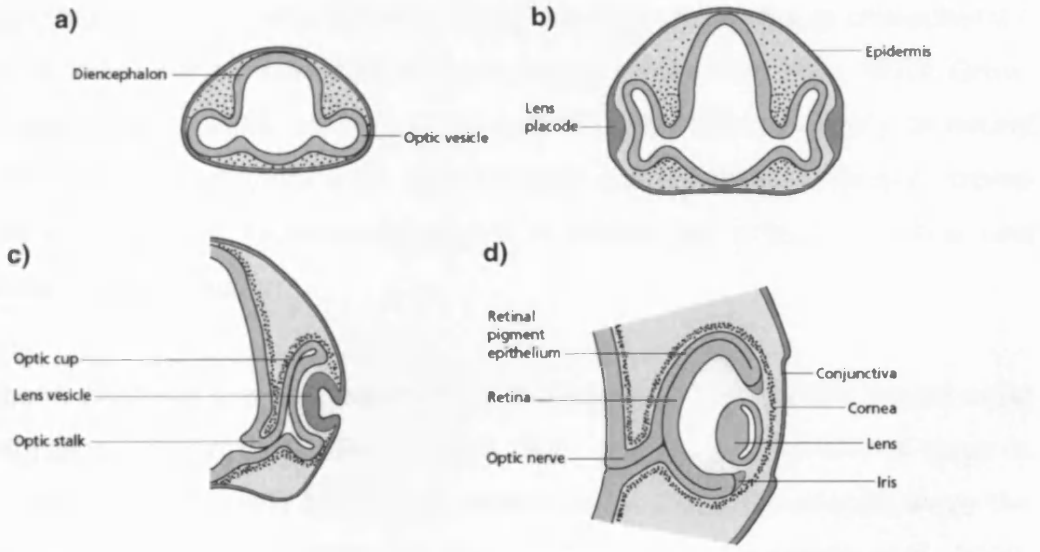

Figure 1.6 The progressive steps in eye development (adapted *from Essential Developmental Biology www.abdn.ac.uk/sms/ugradteaching/PY4302/PY4302_24112004_10.doc*). During gastrulation, from the single eye field that is located in the centre of the developing head, two lateral optic vesicles separate to reach placode stage (at 28 day gestation in human, 33 hours gestation in chick) **(a)** and subsequently the lens pit stage **(b)**. As a result of interactions between the optic vesicles and the lens placode (part of the overlying ectoderm) the neuroectoderm begins to fold inwards (**c**). Finally, the lens placode detaches from the surface ectoderm forming firstly the lens cup, then the lens vesicle (at about 33 days gestation in human, 40 hours in chick **(d)**.

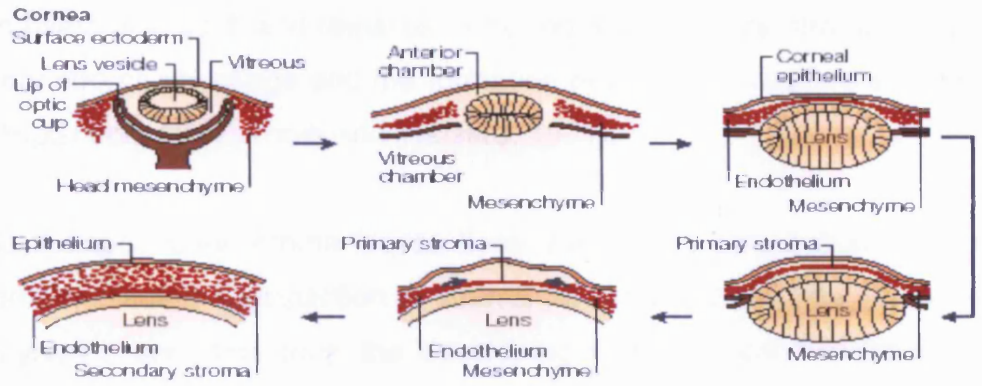

Figure 1.7 Schematic view of the developing cornea. The figure illustrates the progressive steps in cornea development. The cornea begins to develop when the surface ectoderm closes after the formation of the lens vesicle and its detachment from the surface ectoderm. Two waves of mesenchymal cells (neural crest cells) invade the cornea and form the corneal stroma after condensation (from Graw, 2003).

The lens vesicle stimulates the basal ectodermal cells to form a multilayered structure. Basal ectodermal cells increase in height and start to secrete collagen (types I, II, IV) and GAGs to form the primary stroma (a characteristic feature of lower vertebrates and avian corneas) (Meier and Hay, 1973; Graw, 2003; Jean *et al.*, 1998), which becomes a template for the activity of neural crest-derived mesenchymal cells (presumptive keratocytes). Primary stroma reaches its maximum thickness by day 6 in chicks, as a result of GAGs and hyaluronic acid deposition.

The above changes are accompanied by two waves of centripetal neural crest cell migration. In the first wave, (47-56 days gestation in human, 4 days in chick), mesenchymal cells form the endothelium, while in the second wave the corneal stroma is formed (embryonic day, ED7 in chick) (Lyngholm *et al.*, 2008; Graw, 2003). In contrast, in rodents, cats and cattle only 1 wave of mesenchymal cell migration results in the formation of the corneal endothelium and stroma (Dùblin, 1970).

The mesenchymal cells then differentiate into fibroblasts secreting more collagen type I and hyaluronidase (ED10 onwards in chicks). The latter breaks

down hyaluronic acid, and releases its bound water into the stroma, resulting in primary stroma shrinkage and the formation of secondary/mature stroma (Bard and Higginson, 1977; Toole and Trelstad, 1971).

While the secondary stroma looses thickness due to dehydration, keratocytes become quiescent. Compaction of stroma (at about ED14 in chicks) influenced by thyroxine secretion from the developing thyroid gland is associated with changes in synthesis of sulphated components of the interfibrillar matrix and the activity of the bicarbonate pump (Hay and Revel, 1969; Quantock and Young, 2008). In avian cornea, the stroma reaches approximately 50% of its earlier thickness and becomes transparent. This stage also coincides with the formation of epithelial and endothelial tight junctions, hemidesmosomes, and the appearance of the conjunctiva (Graw, 2003).

1.2.2 Development of corneal epithelium

As described in section 1.2.1, the corneal epithelium is formed about 6 weeks into gestation in human and 4 days of gestation in chick. The newly formed epithelium is subject to intense proliferation and expansion of existing cells, which results in morphological changes of the structure.

Stratification of the corneal epithelium was previously extensively studied in chicken by various authors (Trelstad *et al.*, 1974; Meier, 1977; Waggoner, 1978; Nuttall, 1976; Ozanics *et al.*, 1977; Hay, 1979). Stratification was shown to coincide with different events occurring during epithelial development such as: stroma compaction, changes in the pattern of GAGs synthesis, the appearance of non-myelinated nerve bundles, distribution of dividing cells and orientation of mitotic spindles and other cellular changes. The latter involved changes in cytoplasm, an increase in microvilli and the apperarance of glycogen and tonofilaments. The appearance of tonofilaments suggested ongoing differentiation, since the presence of tonofilaments, keratin intermediate filaments that constitute cytoplasmic protein structures in epithelial tissue (tonofibrils), in the cytoskeleton is considered a characteristic of differentiated epithelia.

It is, however, still unknown when exactly the cell commitment to a differentiated state takes place in corneal development. The corneal epithelium could be considered as developmentally differentiated when it begins to produce collagen and GAGs, which in case of avian corneal epithelium occurs about ED5 of incubation. This idea was first suggested by Coulombre and Coulombre (1971), since ED5 chick epithelium could transform into epidermis even when the developing chick lens was replaced with a mesenchymal graft, suggesting that inductive signals (from surrounding tissues and/or ECM) reached the corneal epithelium earlier than ED5. Also, as documented by Chaloin-Dufau and coauthors (1990), in the avian corneal epithelium, expression of cytokeratin 3 (CK3) (considered as a marker for differentiated state non-keratinised corneal epithelia), at ED12 preceeded expression of cytokeratin 12 (CK12) (the corneas were collected from ED11).

In human epithelia, CK3 expression was first detected in the superficial cells in the 12-13th week of gestation, with superficial cells positively labelled, providing the earliest sign of overt epithelial differentiation (Rodrigues *et al.*, 1986). At 36 weeks, the epithelium appeared morphologically mature (four to six layers), with CK3 expressed suprabasally, in contrast to the postnatal adult epithelium which exhibits uniform staining (Rodrigues *et al.*, 1986).

1.2.3 Molecular control of corneal development

Development of the eye can be divided into three phases: formation of the major structures of the eye, maturation of these structures to form the functional eye and formation of neuronal connections (Jean *et al.*, 1998). These events are strictly ordered during development via molecular signals, and mutations in the genes involved can cause numerous different disorders (Graw, 2003).

Over the past decade, several master control genes that direct distinct pathways of development and differentiation have been identified (Graw, 2003). Most of the genes code for transcription factors (i.e. retinal homeobox (*RX),* pituitary homeobox 3 (*Pitx3),* forkhead box C1 *(Foxc1),* Msh homeobox 2 *(Msx2),* musculoaponeurotic fibrosarcoma oncogene homolog (*Maf),* involved in ocular genesis of anterior segment*),* although a few code for signalling

molecules (i.e. sonic hedgehog *(Shh),* bone morphogenetic protein 4 and 7 (*Bmp4, Bmp7*) (Graw, 2003).

The paired box gene 6 (*Pax6)* is localised to human chromosome 11 in human and plays a master control role for eye formation. *Pax6* is a member of the Pax gene family, members of which encode transcription factors essential for correct spatial and temporal expression of their downstream targets (Graw, 2003). *Pax6* contains two DNA-binding domains, a paired domain and a homodomain (Oliver and Gruss, 1997). Targets of *Pax6* include structural proteins of the lens (crystallins) and cornea (CK1-12) (Van Heyningen and Willamson, 2002; Ashery-Padan and Gruss, 2001) and other transcription factors (forkhead box P3 (*Foxe3),* V-maf musculoaponeurotic fibrosarcoma oncogene homolog (avian) *(Maf),* microphthalmia-associated transcription factor (*Mitf),* prospero homeobox 1 (*Prox1),* LIM homeobox protein 2 *(Lhx2))* that regulate cornea and lens formation. *Pax6,* indispensable during the formation of chick lens placode, is expressed in the anterior neural plate, optic vesicles, lens and nasal placodes (Walther *et al.*, 1991) and may function to maintain the undifferentiated lens epithelium during later stages of lens development (Reza *et al.*, 2002). The correct *Pax6* dosage is necessary for normal clonal growth during corneal development, and correct corneal epithelial cell migration (Collinson *et al.*, 2004). The lack of, or mutations, in the *Pax6* gene leads, amongst others, to corneal changes, such as corneal stem cell deficiency and corneal opacities (Thaung *et al.*, 2002; Glaser *et al.*, 1994). As *Pax6* initiates the cascade of signals, loss of its functions leads to the eyeless phenotype in Drosophila and also causes severe ocular defects in many others animals (Ghering, 2002). Experiments on the chick embryo indicate that if the function of *Pax6* is lost, no lens structure can be detected (Reza *et al*, 2002).

One of the essential genes for anterior head formation in early development, is the orthodenticle gene (*Otx2),* identified in human, mouse and chicken. The phenotype in mutant mice is associated with microphthalmia (protruding eyes, hyperplastic retina, presence of one eye, usually without lens and cornea) (Matsuo *et al.*, 1995).

Another example is the visual system homeobox 1 homologue (*Vsx1*) gene which is localised to chromosome 20 in humans. However, although *Vsx1* is expressed by the retina, disturbances in its expression may result in corneal dystrophy (Héon *et al.*, 2002). The mammalian gene *Six3 (a* member of *sine oculis* gene family*)* is expressed in the anterior neural plate, optic stalk, optic vesicles, lens and nasal placode (Oliver *et al.*, 1995). Overexpression of *Six3* in chicken embryos prevents lens placode invagination and leads to the loss of α-crystallin expression from the lens placode (Zhu *et al.*, 2002), which presumably can affect further cornea development. *Six3* is activated by *Pax6* (Lenger and Graw, 2001) and experiments on transgenic mouse show that *Pax6* and *Six3* regulate the transcription of one another (Goudreau *et al.*, 2002).

Medina-Martinez and coauthors (2005) reported that absence of the *Foxe3*, (crucial for lens development) in homozygous mice may lead to abnormal features of the cornea, such as lack of the endothelial layer or a change in cornea epithelium thickness. Several mutations that result in loss or increase of transactivating activity in Pituitary homeobox 2 (*Pitx2)* are associated with Axenfeld-Reiger syndrome (defined by a white ring at the back of cornea) (Priston *et al*, 2001). *Mf1,* which encodes a winged-helix/forkhead transcription factor, is the murine homolog of human FKHL7/FREAC3 (Kume *et al.*, 1998; Kidson *et al.*, 1999). Mouse embryos homozygous for null mutations in *Mf1* showed severely abnormal development of the anterior segment; the cornea failed to separate from the lens, resulting in the complete absence of an anterior chamber (Kidson *et al.*, 1999).

The differentiation of the anterior part of the eye during development proceeds through a series of inductive interactions between different tissues and must be precisely coordinated by intrinsic and extracellular factors that control various signalling cascades (Fokina and Frolova, 2006; Adler and Canto-Soler, 2007). The role of morphogens secreted by the lens in corneal development has been demonstrated in several studies and is likely to indicate the cooperative action of three different signaling pathways; FGF (Fibroblast Growth Factor), BMP (Bone Morphogenetic Protein) and Wnt (wingless) (Zinn, 1970; Beebe and Coats, 2000). For instance, Wnt signals are involved in the earliest specification

of the lens placode and their interaction with BMPs and FGFs are key in this role (Litsiou *et al.*, 2005). Recently, Smith *et al.*, (2005) have shown that forced activation of Wnt/β-catenin signalling in ocular surface ectoderm abolishes lens placode development, suggestive that one of the functions of Wnts in the ocular ectoderm could be to set boundaries between lens placode and the presumptive corneal epithelium (Smith *et al.*, 2005). In chick and mouse, Wnt genes were found to be expressed in the ocular surface ectoderm, including corneal epithelium, which implies an importance of Wnts in corneal epithelial morphogenesis (Liu *et al.*, 2003; Fokina and Frolova 2006).

Since, the number of genes and factors involved in signalling pathways in particular phases of development seems to be enormous, a complete description can not be included in this chapter. Some additional examples are presented in Table 1.1.

1.3 Limbal Stem Cells

To maintain the functional properties of the corneal epithelium various mechanisms had been developed. One of them, the apical membrane covering the surface cells, constitutes the first boundary between the environment and the eye (Wolosin *et al.*, 2000). This fully polarised membrane along with high-resistant tight junctions prevents intercellular diffusion of polar solutes and is part of the volume regulatory system aimed at maintaining cells in close apposition. This control facilitates the shaping of the smooth ocular surface, thereby minimising diffraction of incoming light (Wolosin *et al.*, 2000).

However, throughout adult life, superficial corneal cells undergo a constant shedding or apoptosis (Kruse, 1994; Ren and Wilson, 1996) and thus the epithelium needs to undergo adjustments of growth and be constantly recreated through differentiation. At the beginning of postnatal life, there are two sources for epithelial layer maintenance: proliferating cells in the basal corneal epithelium (Tseng, 1989) and the population of slow-cycling limbal stem cells (LSCs) that proliferate rapidly after injury (Davanger and Evensen, 1971; Cotsarelis *et al.* 1989).

Table 1.1 Examples of various genes and factors involved in signalling pathways in different phases of eye development (adapted from Oliver and Gruss, 1997; Jean *et al.*, 1998)

Gene	*Place of expression*	*Organisms with homologue gene*	*Mutation effect*	*References*
		FORMATION OF THE OPTIC VESICLE		
Eya/eye absent (Eya1, Eya2)	anterior to the furrow	Fruitfly, human, mouse, nematode	Eyeless (*Drospohila*) branchi-oto-renal syndrome (mouse)	Xu *et al.*, 1997; Bonini and Choi, 1995; Abdelhak *et al.*, 1997
ET *(T-box family gene for transcription factors)*	Anterior neural plate, optic vesicle	Chicken, Xenopus	Not characterised functionally	Li *et al.*, 1997
		FORMATION OF THE LENS VESICLE AND OPTIC CUP		
Lhx2 *(homeobox transcription factor)*	Optic vesicle	mouse	Fail to develop the lens placode	Porter *et al.*, 1997
Gli3 *(Gli family zinc finger 3)*	Optic vesicle	Mouse	Fail to develop the lens placode, optic veisicle do not involute to form optic cup	Hui and Joyner, 1993; Franz and Besecke, 1991
Pax2 *(Paired box gene 2)*	Cells in optic vesicle that contribute to the optic stalk	Mouse, human, zebra fish	Optic nerve coloboma, aniridia (human)	Sanyanusin *et al.*, 1995; Oliver *et al.*, 1997; Krauss *et al.*, 1991
Chx10 (Vsx2, visual system homeobox 2)	optic vesicle, neuroretina	mouse, goldfish, *C.elegans*	ocular retardation (reduced cell proliferation in neural retina)	Liu *et al.*, 1994; Svendsen and McGhee, 1995; Burmeister *et al.*, 1996
Prox1/prospeo	Lens secreting cone cells (*Drosophila*), lens fibres (murine)	Chicken, frog, fruitfly, human, mouse, nematode	Axonal outgrowth (*Drosophila*)	Burglin, 1994; Tomarev *et al.*, 1996; Zinovieva *et al.*,1996
		MATURATION OF DEVELOPING CORNEA		
TGFRα *(Transforming Growth Factor Receptor Alpha)*	Lens, lens rudiment	mouse	Accumulation of mesenchymal cells	Decsi *et al.*, 1994; Luetteke *et al.*, 1994; Reneker *et al.*, 1995
PDGFRα (Platelet-derived Growth Factor Receptor Alpha)	non-neuronal derivatives of the cranial neural crest	mouse	Fail to develop the neural crest-derived structures of the eye	Morrison-Graham *et al.*, 1992

1.3.1. Definition and characteristic of adult stem cells

Despite the unquestioned totipotency of embryonic stem cells, defined by their origin and ability to indefinitely expand, self-renew, and give rise to more specialised progeny cells, there are numerous unanswered biological questions as to the regulation of their growth and differentiation (Sylvester and Longaker,

2004). In response to biological, but also political barriers, scientists have sought other possible sources of pluripotent cells.

Adult stem cells (SCs), or in newer terminology, the tissue-derived/resident stem cell population are undifferentiated (unspecialised) cells that reside in differentiated tissues and function as lineage-committed progenitors to cells able to maintain and regenerate the given tissue for a lifetime. SCs renew themselves and generate specialised progeny depending on the type of tissue from which they originate.

There are common criteria that define the phenomenon of SCs and these are described below.

- ***Capacity for unlimited self-renewal:*** it remains unknown whether stem cells have limited or unlimited division potential. Renewal of stem cells is based on their capacity to divide and give rise to a progeny, with at least one of the daughter cells remaining a stem cell.
- ***Undifferentiated state:*** Although SCs can be characterised by their undifferentiated state, they sustain high differentiation potential with a primitive phenotype – implying the ability to differentiate into all cell types of their home tissue and possibly into other cell types as well, when experimental circumstances are provided (Takacs *et al.*, 2009)
- ***Slow cell cycle:*** Most of the time, cells are in a growth arrested state and enter cell cycle on demand (i.e. tissue injury, environmental conditions) and give rise to highly proliferative and differentiating progenitor cells (Cotsarelis *et al.*, 1989).
- ***High proliferative potential:*** SCs in the mouse epidermal proliferative unit divide approximately about 1000 times, 5000-6000 times in humans (Marsham *et al.*, 2002; Potten, 2004). However, it is not yet documented how many times the LSCs in the cornea undergo division.
- ***Niche residency:*** It has been established that stem cells reside in the niche, which provides an environment critical in mainteining stem

cells properties (referred to as 'stemness') and defining stem cell destiny (Leblond, 1981; Schofield, 1983).

- ***Plasiticity:*** The potential for stem cells to undergo reprogramming under the influence of a new environment (new niche) was shown by a number of studies, providing evidence that early lineage commitments, as it is for differentiated stem cells derivates, may be reversible (Ferraris *et al.*, 2000; Pearton *et al.*, 2004). However, the underlying mechanisms of the above changes remain unidentified.

Two main strategies by which stem cells generate differentiated descendants were proposed (Hall and Watt, 1989; Morrison *et al.*, 1997). These considered: invariant asymmetry and populational asymmetry (most mammalian self-renewing tissues). The first mechanism is based on stem cell asymmetric division resulting in a population of progenitor cells with restricted proliferation potential that differentiate in response to extrinsic cues. SCs that fall into the second category give rise to daughter cells that can be either stem cells or progenitors that differentiate along different pathways, influenced by the combinations of extrinsic factors.

After division of the maternal cell, progeny could enter the differentiation pathway where a number of new genes are sequentially expressed or previously expressed genes are suppressed It is hypothesised that adult stem cells are maintained and controlled by intrinsic (i.e. proteins responsible for setting up the asymmetric cell division of precursor cells, nuclear factors controlling gene expression and chromosomal modifications) and extrinsic factors that are expressed in their microenvironment (niche) (Schofield, 1983; Watt and Hogan, 2000; Potten, 1997; Hall *et al.*, 1989; Morrison *et al.*, 1997).

A few environmental factors are known to regulate gene expression and maintain stemness of stem cells (Watt and Hogan, 2000):

1. ***Cytokines and growth factors***- Secreted by neighbouring cells, these factors support stem cells and their progeny in proliferation, differentiation and survival. In the epithelial and stromal wound healing, cytokines

modulate those processes through a number of mesenchymal-epithelial interactions. There is a wide range of factors that regulate stem cell proliferation and fate i.e. TGFβ (Transforming Growth Factor Beta), FGF, KGF (Keratinocyte Growth Factor), NGF (Nerve Growth Factor) and Wnt (Li and Tseng, 1995; Watt and Hogan, 2000). The effect of factors on a target cell depends on cell type and state of development. Wnt is responsible for asymmetric division and requires an inductive signal from its sister cell that controls spindle orientation and ectoderm specification (Jan and Jan, 1998; Xie and Spradling, 1998), while members of the TGFβ family are crucial in regulating differentiation (Peifer, 1999). TGFβ1, -β2, -β3 were shown to inhibit proliferation of limbal stem cells, thus serve to influence stem cell maintenance in the limbus (Li *et al.*, 1999, Boulton *et al.*, 2007).

2. ***Cell-matrix contact*** – Cell-matrix contacts are of major importance not only in the development of the embryo. For example, distinct collagen type IV components within the corneal and limbal basement membrane suggest that membrane composition may be responsible for the different phenotypes and proliferative capacity (Ljubimov *et al.*, 1995) of limbal stem cells. Cell adhesion to ECM is mediated by integrins that regulate differentiation of many cell types through Mitogen-Activated Protein kinases signaling (MAPKs) (Jensen *et al.*, 1999; Zhu *et al.*, 1999; Jones *et al.*, 1995) and also contribute to the activation of growth factor receptors (Moro *et al.*, 1998).
3. ***Cell-cell interactions mediated by integral membrane proteins*** – some signals that control the fate of stem cells require direct contact between cells. One of the examples, that require cell-cell contact for its activity, is the Notch transmembrane protein, important during sensory organ precursor cell division (Artavanis-Tsakonas *et al.*, 1999; Lewis, 1998) and differentiation of limbal stem cell progenitors (Ma *et al.*, 2007).

1.3.2 Limbal Stem Cells in corneal epithelial homeostasis

The phenomenon was explained by the `XYZ hypothesis' of corneal maintenance, proposed by Thoft and Friend in 1983. Stem cells from the limbal epithelium undergo division and give rise to a daughter cell. Progeny of LSCs (transient amplifying cells; TACs) migrate towards the epithelium and continue

to divide, subsequently, lose contact with the basal epithelium and become terminally differentiated in the upper layers of the central cornea before being shed from the epithelial surface (Figure 1.8).

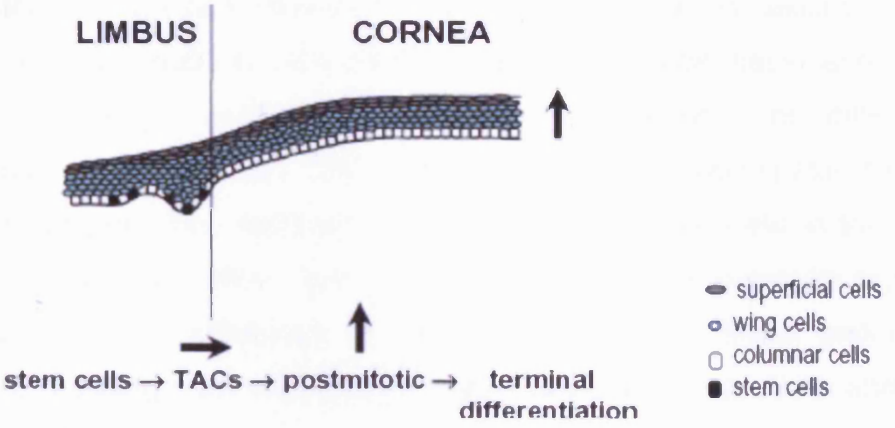

Figure 1.8 Model for the maintenance of the adult corneal epithelium. Limbal stem cells (LSCs) reside in the basal limbal epithelium at the angle between the corneal and conjunctival epithelia. They cycle slowly to produce transient amplifying cells (TACs) that migrate centripetally along the basal layer of the corneal epithelium and move apically until they reach the surface layer and are desquamated (right-hand panel) (from Boulton *et al.*, 2007).

A number of studies have tried to establish the limbal genesis during embryonic development and link these observations with the activity of limbal stem cells in adults. The beginning of limbal genesis is estimated after the formation of a distinct ectodermal zone of lens placode, which gives rise to the corneal and conjunctival epithelia (Koroma *et al.*, 1997; Williams *et al.*, 1998; Wolosin *et al.*, 2000). It is not determined precisely when in development LSCs act to replenish the population of epithelial cells. In the murine cornea, the activity of LSCs was demonstrated at the 5th postnatal week (Collinson *et al.*, 2004).

In response to tissue growth in embryonic development and later, tissue renewal of adult epithelia, constant adjustments and coordination of gene-expression and intracellular mobilisation are required. Collinson and co-authors (2004), based on their own research and previous reports, suggested that it is possible to assign two stages to the development of the corneal epithelium in mice. First is an embryonic and early postnatal phase in which epithelial cells

proliferate by randomly orientated cell division. In the second stage, directional clonal growth occurs, as well as, proliferation of LSCs (Cotsarelis *et al.*, 1989; Lehrer *et al.*, 1998).

After a stem cell division (stimulated by various factors, as described in the previous section), daughter cells either remain in the limbal basal layer, where they may undergo additional rounds of cell divison, or differentiate synchronously (Beebe *et al.,* 1996). The TACs undergo centripetal migration, as a consequence, they replenish the population of basal cells in the central section of corneal epithelium. This process, apart from the molecular signals, is caused also by the difference in compaction between limbal and corneal epithelium, resulting from sialylation of glycoconjugates in proteins and lipids) (Wolosin *et al.*, 2000).

There is a doubt as to whether the proliferative pressure in the limbus account for centripetal migration, but the increased proliferation in the periphery may play a role in this process (Lavker *et al.*, 1991; Wolosin *et al*, 2000). Following wounding, LSCs proliferation rate can be up-regulated as much as eight to nine fold within 12 hours, compared to a two-fold increase in TACs following central epithelial injury (Cotsarelis *et al.*, 1989; Lehrer *et al.*, 1998; Chung *et al.*, 1992; Boulton *et al.*, 2007).

The slow cycling limbal stem cells, responsible for long term maintenance of the tissue, can be activated by wounding or by *in vitro* culture conditions to proliferate and regenerate the tissue (Davanger and Evensen, 1971). In normal tissue, stem cells cycle infrequently with relatively long cell cycle time and their progeny, TACs, have multiple division capacity (if residing in the peripheral epithelium) or little division capacity (if residing in the centre) (Agrawal and Tsai, 2003). After stimulation by injury three different scenarios may take place: 1) more stem cells can be recruited to divide and the cell cycle time is more rapid, 2) TACs from the peripheral region are encouraged to use their full replicative potential, and 3) efficiency of TAC replication is increased by shortening the cell cycle time. When there is a need to increase a number of cells and maintain the tissue structure, as it is likely to happen during development or in wound

healing, one or all of the described mechanisms are activated. However, which of them plays a crucial role remains unknown.

Separation of a cell from its basement membrane indicates the loss of proliferative capacity, and initiates features unique in the later intra-stratal stage. It was suggested that stratification in the central cornea may follow a different path plan than stratification within the limbus (Wolosin *et al.*, 2000).

With regard to inductive methods of terminal differentiation, opinion prevails that a gradient of base to apex and base to lateral factors exist inside the limbal epithelium, which is responsible for the diverse state of maturity between cells of the limbus and those of the cornea. This confirms diverse functionality of the compartmentalisation that is observed progressing from SC to TAC to terminally differentiated cell (Revoltella *et al.*, 2007).

1.3.3 The localisation and identification of Limbal Stem Cells

The activity of LSCs located in the basal epithelium of the corneoscleral limbus (Davanger and Evensen, 1971; Schermer *et al.*, 1986; Tseng, 1989) is a prerequisite for corneal epithelial cell homeostasis as described in the above section. SC, interspersed throughout the basal cell layer most likely in small clusters (Schlötzer-Schrehardt and Kruse, 2005), represent less than 10% of the total limbal basal cell population (Lavker *et al.,* 1991).

Putative limbal stem niches (crypts) have been identified as solid cords of cells that extend from the peripheral end of the Palisades of Vogt into the underlying stroma (Dua *et al.,* 2005). The undulations of the Palisades of Vogt ensure that stem cells are hidden and protected from the environment, while nearby blood vessels provide nourishment (Boulton *et al.*, 2007).

Apart from the general criteria described in section 1.3.1, LSCs can be distinguished from other cells by morphology. They are smaller, compared to cells of the basal corneal epithelium (Romano *et al.*, 2003), and show peculiar pigmentation that confirm the notion of representation of quiescent stem cells

with high levels of melanin (protects against ultraviolet light and reactive oxygen species), that is lost with cell proliferation (Wolosin *et al.*, 2000).

A demonstration of the concept of the limbus as the germinal site for the corneal epithelium became possible following the recognition of the tissue specificity of cytokeratin (CK) pairs and their differentiation-dependent expression (Moll *et al.*, 1982). From the pattern of the CK pair K5/K14 (present in the basal cells covering the limbal rim and observed in most stratified epithelia) and CK3 expression (absent from basal epithelial cells in the limbal epithelium), it was concluded that the undifferentiated stem cells may reside within the limbal zone (Schermer *et al.*, 1986). The presence of slow-cycling cells within limbus and peak proliferative activity in the adjacent corneal periphery was later demonstrated by number of studies (Cotsarelis *et al.*, 1989; Lavker *et al.*, 1991).

For identification of LSC and their progenitors, various markers have been proposed. However, their use is still controversial. Marker-proteins are expressed depending on the type of epithelium and its state of differentiation and are not exclusive to limbal basal stem cells, therefore, the definitive marker for SC identification has yet to be found. Also, it has to be underlined, that general term 'limbal basal cells' refers not only to stem cells in a basal layer, but also to the population of TACs that reside in this zone. This fact hampers the pursuit for determination of definite LSC markers.

Candidate markers in development that are likely to identify critical stages of adult LSC maturation and/or differentiation will be determined through further study. Considering the countless studies on possible markers that could define stem cell phenotype, conviction prevails that it is not possible to identify expression of a single marker but rather that coexpression of a series of molecules by whose presence or absence identifies the characteristics of stemness (Revoltella *et al.,* 2006). Overall, the proposed markers can be divided into negative (a lack of labelling indicates undifferentiated state of cells) and positive (the presence of labelling suggests putative stem cell).

The current classification of potential stem cell markers is shown in Table 1.2.

Table 1.2 Localisation of putative stem cell markers (adapted from Schlötzer-Schrehardt and Kruse, 2005) (continued overleaf)

Marker	Limbal epithelium		Corneal epithelium		References
	basal	suprabasal	basal	suprabasal	
Cytoskeletal proteins					
Keratins K3/K12	-	+	++	++	Rodrigues *et al.*, 1987; Kasper *et al.*, 1988; Liu *et al.*, 1993; Schermer *et. al.*, 1986
Keratin 19	++	(+)/-	-	-	Chen *et al.*, 2004
Keratins K5/K14	+	(+)	-/(+)	-	Kurpakus *et al.*, 1994; Barnard *et al.*, 2001; Hsueh *et al.*, 2004; Schlötzer-Schrehardt and Kruse, 2005
Vimentin	++	(+)	-	-	Schlötzer- Schrehardt and Kruse, 2005
Cytosolic proteins					
α-enolase	++	(+)	(+)	-	Pancholi, 2001; Zieske *et al.*, 1992a,b; Zieske 1994; Chen *et al.*, 2004
Involucrin	-	(+)	+	+	Adhikary *et al.*, 2004
Aldehyde dehydrogenase (ALDH)	-	-	++	++	Kays and Piatigorsky, 1997
Transketolase (TKT)	(+)	(+)	++	+	Guo *et al.*, 1997
gamma-PKC (kinase C)	+	+	-	-	Tseng *et al.*, 1996
Nuclear proteins					
ΔNp63	(+)	(+)/-	-	-	Chen *et al.*, 2004; Koster *et al.*, 2004
p63	++	(+)	(+)	-	Pellegrini *et al.*, 2001; Chen *et al.*, 2004; Dua *et al.*, 2003
KGFR bek	(+)	-	-	-	Schlötzer- Schrehardt and Kruse, 2005
Sugar-binding proteins					
Peanut lectin (PNA)	-	++	-	-	Wolosin and Wang, 1995
TNFR1β	+	-	-	-	Iwata *et al.*, 2002; Vascotto and Griffith, 2006
Agglutinin (MAA)	-	-	(+)	++	Wolosin and Wang, 1995
TGFR1β	+	-	-	-	Joyce and Zieske, 1997
Cell surface proteins					
a) cell-cell, cell-matrix					
NGFR TrkA	+	-	+	(+)	Lambiase *et al.*, 1998; Touhami *et al.*, 2002
Connexin 43	-	+	++	+	Dong *et al.*, 1994; Matic *et al.*, 1997; Wolosin *et al.*, 2000; Chen *et al.*, 2004
P-cadherin (CDH3)	(+)/-	-/(+)	-	-	Figueira *et al.*, 2007
Integrin α6, α2, β4	-/++	+	+	+	Chen *et al.*, 2004, Schlötzer-Schrehardt and Kruse, 2005
Integrin α9	+	-	-	-	Chen *et al.*, 2004; Pajoohesh-Ganji *et al.*, 2004
b) growth factor receptors					
EGFR	++	+	++	+	Lauweryns *et al.*, 1993a; Liu *et al.*, 2001; Chen *et al.*, 2004

c) transporter molecules					
ABCG2	++	-	-	-	Chen *et al.*, 2004; Watanabe *et al.*, 2004; Wolosin *et al.*, 2004
Neuronal markers					
c-Kit	-	(+)/-	-	(+)/-	Das *et al.*, 2004; Vascotto and Griffith, 2006
Nestin	-	-	+	+	Chen *et al.*, 2004
Hematopoietic markers					
CD133 -2	+	+	+	+	Silvestri *et al.*, 1992; Yin *et al.*, 1997; Dua *et al.*, 2003
CD44	+	(+)/-	-	-	Zhu *et al.*, 1997; Vascotto and Griffith, 2006
CD34	+	+	-	-	Silvestri *et al.*, 1992; Yin *et al.*, 1997; Dua *et al.*, 2003

Key:

- undetectable
(+) weak positivity
+ moderate positivity
++ strong positivity

1.4 Implications of Limbal Stem Cell in therapeutic intervention

The eye is a highly organised complex organ. Disturbances in genetic programming during development can lead to disorders that become apparent at birth or shortly after (Graw, 2003). For instance, aniridia-related keratopathy (ARK, corneal surface degeneration, opacity) is correlated with vascularisation and epithelial fragility (Ramaesh *et al.*, 2003). ARK relates to both a deficiency within the LSC niche and nonautonomous diversion of corneal epithelial cell migration (Collinson *et al.*, 2004).

Presently, a main issue that focusses the attention of corneal scientists is ocular surface rehabilitation after grafts. Although, allogenic corneal transplantation (keratoplasty) is widely used to repair a damaged corneal stroma, in some corneal pathologies with extensive destruction of the limbus (e.g. caused by chemical/thermal burns, Steven Johnson syndrome, contact lens-induced keratopathy) the keratoplasty is unsuccessful and proper vision can not be restored (Wagoner, 1997; Pellegrini *et al.*, 2009; Boulton *et al.*, 2007). In such cases, the only way to prevent corneal conjunctivalisation is to restore the limbus.

The first suggestion, to transplant corneal epithelial stem cells to reconstruct an ocular surface, was proposed by Kenyon and Tseng (1989). This was carried out by grafting large limbal fragments from the uninjured eye onto the

diseased eye of patients with unilateral limbal-corneal destruction. Currently, the techniques of transplantation involve auto- or allografts that, apart from being undoubtedly an advantageous, can also have some drawbacks. The main limitations for auto- and allografting from living related donors, is the amount of limbal tissue and risk of tissue rejection (Kolli *et al.*, 2008). Autografting is possible only if the limbal defects are localised unilaterally. The survival of limbal allografts, from both related and cadaveric donors, requires aggressive systemic immunosuppression, which increases a risk of morbidity (Holland *et al.*, 2003; Kolli *et al.*, 2008).

Further studies provided a variety of new techniques that enabled reconstruction of the corneal epithelium by using stem cells` potential. Small limbal explants were cultured to generate limbal cells that were found to include stem cells detectable as holoclones (Pellegrini *et al.,* 1999). These can be successfully used to restore corneal integrity and improve visual acuity in patients whose corneal stroma was not destroyed, otherwise, the underlying stroma has to be resurface first (Pellegrini *et al.*, 2009).

Currently, the methods that allow *ex vivo* expansion of LSCs followed by LSCs transplantation are used in corneal epithelial reconstruction. Well established techniques are based on co-culture of limbal epithelial cells (derived from limbal explants or cell suspensions) with mitotically inactivated 3T3 mouse fibroblasts as a feeder cell, or an amniotic membrane, or a combination of those two (Koizumi *et al.*, 2000; Gruetrich *et al.*, 2003; Kinoshita *et al.*, 2004; Boulton *et al.*, 2007; Kolli *et al.*, 2008).

1.4.1 Alternative sources of cells used to resurface corneal epithelium

As described in section 1.4, there are various sources of limbal epithelial cells to be used for transplantation purposes; auto- and allografts, *ex vivo* cultures of tissues or cells obtained from live cadaver donors. Alternative sources of cells that could potentially used to resurface the corneal epithelium are derived from:

Conjunctival epithelium

The conjunctival epithelium, like most of the epithelial tissues, undergoes constant renewal with rapid cell turnover (Nagasaki and Zhao, 2005). It was suggested that the fornix and/or palpebral region (Pellegrini *et al.*, 1999; Chen *et al.* 2003) may contain conjunctival stem cell niche, due to the fact that slow-cycling cells with higher proliferative capacity have been detected in these areas (Wei *et al.,* 1995; Wirtschafter *et al.*, 1999). Although, it has been reported that limbal basal cells are the only population expressing the protein ΔNp63 in the ocular surface (Pellegrini *et al.*, 2001), results presented by Espana *et al.*, (2004) showed that the expression of ΔNp63 in conjunctiva-derived epithelium in eyes with total limbal SC deficiency was detected. The role of conjunctival epithelium in the restoration of corneal epithelial deficits requires further investigations, as it also had been shown that even small pools of slowly cycling cells within the limbus are able to regenerate the tissue on their own.

Bone-marrow derived stem cells

Bone marrow-derived stem cells (BMSCs) are an example of stem cells capacity to transdifferentiate. Nakamura *et al.*, (2005), in their experiment with bone-marrow and hematopoietic stem/progenitor cells transplantation in mice, hypothesised that bone marrow-derived cells continuously migrate into the corneal tissue and contribute to the corneal integrity. They also suggested that bone marrow-derived cells may transdifferentiate into corneal cell phenotypes or neurons. The presence of hematopoietic markers; CD34 and CD133-2 observed in the limbal epithelial zone may suggest broader interactions between BMSCs and LSCs and requires further studies.

Oral mucosa

Another source to be mentioned is the possibility of using oral mucosal epithelium as a source of cells to treat bilateral corneal limbal stem cells deficiency. The potential advantage of such an approach is no risk of immune mediated rejection, thus no need for immunosupression (Nakamura *et al.*, 2004; Inatomi *et al.*, 2006).

Long-term follow-up and experience with a large series of patients are needed to assess further the benefits and risks of the methods, which offer the potential to treat severe ocular diseases (Nishida *et al.*, 2004).

1.5 The chick as a model system to study corneal epithelial developmental biology

The chicken as a model system in biology has a long history. However, although the chicken has been a traditional model for studying embryonic development, the lack of genomic resources decreased the potential value of this system for advanced molecular research until now (Brown *et al.*, 2003). The first step to sequence chicken genome was made in 2003 when 500,000 chick ESTs (expressed sequence tags) were released. Further research resulted in compilation of a genetic map for the chicken genome, and finally, genome sequencing was accomplished in 2004 (International Chicken Genome Sequencing Consortium, 2004).

Presently, scientists are using two experimental systems: the chicken DT40 cell line and the embryos (Brown *et al.*, 2003). The DT40 cell line is derived from a chicken bursal lymphoma that has been transformed by an avian leucosis virus (ALV) (Baba *et al.*, 1985) and is used, amongst other things, to investigate gene functions, to study the mechanisms of immunoglobulin gene diversification (Sale *et al.*, 2001) and to engineer mammalian chromosomes.

Chick embryos are accessible from pre-gastrulation stages and throughout organogenesis. Furthermore, embryos can be manipulated *in ovo* for up to several days (Brown *et al.*, 2003). Although, chick embryos can be easily separated, the developmental studies of various organs cause difficulties, as

most of the later complex morphogenetic events take place in an opaque embryo which makes it difficult to disentangle. Chick cornea, however, is a unique exception to the above principle; it is accessible, geometrically simple and many events taking place during its formation are temporally and spatially separated from one another.

The availability of a chick genome database and combination of well-established embryological manipulations (e.g. "cut-and-paste" experiments, fate mapping) with recently developed techniques for gene missexpression (using electroporation, lipofection or viral transfection combined with RNA interference or morpholino oligonucleotides) provide promising perspectives for exploitation of chicken embryos in further developmental investigations. Despite various advantageous of using the chick as a model organism, there are some difficulties in carrying out classical whole-animal genetics and transgenesis. For example experiments based on the entire development of the fertilised egg require a shell-less culture environment (Brown *et al.*, 2003).

Discoveries in the field of chicken research could be related in the future to mammalian and/or human biology. Although, chickens are evolutionarily distinct, the coding genes show high similarity to human genes and only two chicken family proteins are absent from the human genome (Stern, 2005).

1.6 Hypothesis and aims

It is hypothesised that the genes involved in differentiation and cell patterning in the developing corneal epithelium will be important for the maintenance of adult corneal epithelium by limbal stem cells. These studies pave the way to understand the mechanisms that underlie the regulation of corneal epithelial homeostasis during development, as well as, in adult life.

The hypothesis put forward in this study is based on the presumption that development and maintenance of the corneal epithelial cell population is regulated by various morphogenetic mechanisms. The vast amounts of knowledge regarding molecular mechanisms that regulate progressive events in patterning of the corneal stem cell lineage are poorly understood. Previous studies in other body systems have suggested that adult and embryonic stem cells might share common pathways that are critical to stem cell survival and the maintenance of tissue they supply. Determination of the stages of development at which corneal epithelial cells proliferate, change morphology and differentiate will allow for the selection of critical time points for further investigation of gene expression profiles in the developing chick corneal epithelium. Further, microarray analyses at a global level will facilitate identification of potential specific corneal epithelial stem cell markers.

The overall objective of this study is to identify target genes that are likely to be involved in the regulation of corneal epithelial homeostasis at different stages of development, and thus, could potentially serve as markers for the generation of corneal epithelial stem cells.

Therefore, the aims of this study are:

1) To characterise spatiotemporal changes in morphology and differentiation in the developing chick corneal epithelium
2) To characterise spatiotemporal changes in cell death and proliferation during chick corneal epithelial development.
3) To examine the global gene expression during chick corneal epithelial development and identify candidate regulatory genes involved in epithelial cell

maturation and/or differentiation, thus important in corneal epithelial homeostasis.

3) To determine genes selectively expressed all along the developmental time-course of corneal epithelium and relate the findings to initial embryonic time point and posthatched epithelia
4) Identify candidate stem cell-related genes.

CHAPTER TWO

Materials and methods

2.1 Experimental animals

Fertilised white leghorn eggs, obtained from a commercial hatchery (Henry Stewart & Co, Lincolnshire, UK), were incubated broad side-up in a tray at 37.5±0.5 °C in a humidified (40% relative humidity) incubator (Octagon 100 Incubator, Brinsea, Standford, UK). Eggs were turned automatically approximately 20 times in a 24 hour period. The date and time at the start of incubation were recorded. The level of double distilled water (ddH_2O) was checked daily to ensure that the required relative humidity was maintained. Eggs were incubated until the required developmental embryonic day (ED).

2.2 Sample collection and preparation for histochemistry and immunolocalisation

2.2.1 Tissue dissection

Eggs at different time points during development, every two days (from ED4 to ED18), were removed from the incubator and stored at 4°C for 15 minutes before dissection to reduce blood pressure. Embryos were removed from the egg by cracking the shell on the broad side, or upper side of the egg using the pointed reverse end of forceps. While removing the embryo from the top of the albumen, the head was excised from the remaining embryo using dissection scissors and placed in cold phosphate buffered saline (PBS) pH 7.4 on a petri-dish (Sigma, Dorset, UK). Eyes of postnatal chick embryos (<12 hours posthatching, ED21) were collected within 30 minutes of anaesthesia (Euthatal injection, 150 mg/kg bodyweight, Merial, UK). The tissue was washed in cold PBS to remove blood and redundant tissues/membranes, and placed in fresh PBS under a dissecting microscope.

The isolated embryo (for ED4 and ED6) or anterior chamber of the right eye of each pair (for stages ED8 onwards) was fixed in 10% neutral buffered fomalin (NBF) or 4% paraformaldehyde (PFA) in PBS (see Appendix II for composition of solution). One of each pair of eyes (left eye) was processed for cryosectioning as described in section 2.3.3.4.

2.3 The principles and protocols of histology techniques

The basic techniques in histological procedures include fixation and tissue processing for further sectioning and staining. The objective of fixation is to preserve cell and tissue components in as near as identical state to *in vivo* and to ensure that this state is retained during subsequent procedures. Fixation should also provide for the preservation of tissue substances and proteins (Leong, 2000). Then stabilised tissues undergo tissue processing in order to impregnate them with a solid medium to facilitate the production of sections for microscopy. Tissue processing involves the diffusion of various substances in and out of the stabilised porous tissue.

To optimise the protocol for wax embedding of chick corneas, different approaches were tested. In order to develop the method, not only whole eyes were dissected, but also anterior chambers. Subsequently, they were fixed in 4% PFA or 10% NBF and processed for xylene- or chloroform-based technique, in different combinations.

2.3.1 Tissue fixation

2.3.1.1 PFA fixation

4% PFA (pH 7.4) was used as a non-protein coagulant fixative. After dissection, whole embryos were immersed in 4% PFA for 24 hours at 4˚C. The next day, tissue was washed twice in PBS for 30 minutes then placed in a new tube and immersed in PBS for the next 30 minutes and subsequently left overnight in new 1XPBS. Alternatively, tissue was left in PBS containing 0.1% sodium azide (Appendix II) at 4˚C for a longer period of time in preparation for the xylene-based method of tissue processing (see below).

2.3.1.2 NBF fixation

Dissected anterior chambers were immersed in 10% NBF (pH 7.2) (see Appendix II) for 48 hours at 4˚C in preparation for the chloroform-based processing technique (see below) and subsequent wax-embedding.

2.3.2 Tissue processing

The most common embedding medium for routine histology use is paraffin wax. Infiltrating and embedding media must fill all spaces within tissue to support cellular components adequately during microtomy. The first step in processing is dehydration (with alcohols increasing in concentration) followed by clearing, which is the transition step between dehydration and infiltration with the embedding medium.

2.3.2.1 Paraffin wax processing- xylene based method

PFA-fixed tissue was dehydrated through a series of graded industrial methylated spirits (IMS) as follows:

- 50% IMS for 30 minutes
- 70% IMS for 30 minutes
- 70% IMS for 30 minutes
- 90% IMS for 30 minutes
- 90% IMS for 30 minutes
- 100% IMS for 30 minutes
- 100% IMS for 30 minutes

In order to clear the tissue, it was immersed in 50% xylene in IMS for 30 minutes in glass vials and then in 100% xylene for a further 30 minutes. Excess xylene was removed and tissue was warmed by placing the glass vials on the top of a wax oven for 10 minutes. The eyes was blotted on a filter paper and placed into clean glass pots containing molten wax at 56°C for 30 minutes. Hot wax was exchanged for new hot wax and samples were left overnight in the oven (Gallenkamp, Thermo LI, UK). Next, samples were removed from the wax, dabbed on filter paper and placed in correct orientation (i.e cutting side down) in a plastic mould containing new molten wax. Blocks were left on a cold (-12°C) plate (Raymond A Lamb, UK) for 30 minutes to solidify, and then stored at 4°C.

2.3.2.2 Paraffin wax processing - chloroform based method

Tissue fixed in 10% NBF was immersed in increasing concentrations of IMS, as indicated below:

- 50% IMS for 30 minutes
- 70% IMS for 30 minutes
- 90% IMS for 30 minutes or overnight
- 100% IMS for 30 minutes
- 100% IMS for 30 minutes

For removal of dehydrating agents, tissue was first immersed in a 50% volume/volume mixture of IMS/chloroform for 30 minutes and then two immersions in 100% chloroform (each time for 30 minutes). Most of the chloroform was poured from the glass pot and the tissue was warmed on top of the wax oven for 10 minutes. The tissue was then dabbed on filter paper, placed into clean, molten wax in the oven (at 56˚C) and left for 1 hour to remove chloroform. After 1 hour, samples were transferred to clean pots containing wax and left for a further 30 minutes to ensure wax had fully impregnated the tissue. Finally, tissue was embedded in wax in moulds and left on a refrigerated base (-12˚C) for 30 minutes to harden. Solidified blocks were stored at 4˚C overnight and then subsequently at room temperature.

2.3.2.3 Optimised method of wax tissue processing for embryonic chick eyes

Two methods for fixation and further paraffin wax processing were optimised. The optimised method selected was dependent on the developmental stage as shown in a Table 2.1, in order to eliminate tissue crushing during sectioning.

Table 2.1. Optimised tissue fixation for wax embedding

Embryonic day	Embryo/Eye	Fixative	Clearing agent
4	Whole embryo	4% PFA	Xylene
6	Whole embryo	4% PFA	Xylene
8	Anterior half	10% NBF	Chloroform
10	Anterior half	10% NBF	Chloroform
12	Anterior half	10% NBF	Chloroform
13	Anterior half	10% NBF	Chloroform
14	Anterior half	10% NBF	Chloroform
16	Anterior half	10% NBF	Chloroform
18	Anterior half	10% NBF	Chloroform
21	Anterior half	10% NBF	Chloroform

2.3.2.4 Paraffin blocks sectioning

Once hardened, the blocks were removed from the mould. Wax sections (7µm thick) were cut using a microtome (Microm HM325, Germany). Wax sections were floated in a cold water bath and then in a hot (40°C) water bath (containing Mayer's albumin) (Raymond A Lamb, UK), and then transferred onto microscope slides with an adhesive coating (HistoBond, UK). Sections were dried on a hot (36°C) plate (Diswasher 2, Photax, UK) and incubated in an oven (Genlab, UK) at 56°C for 1 hour. Sections were stored at room temperature until day of use.

2.3.2.5 Tissue processing for cryoembedding

After dissection, the embryo (ED4 and ED6) or the whole eye (from ED8 to ED21 posthatch) was placed in a moist chamber (i.e. paper towel soaked in PBS inside a bijoux) at 4°C. A plastic beaker containing iso-pentane (BDH, UK) was cooled by partial immersion in liquid nitrogen. The tissue was submerged into the liquid nitrogen cooled iso-pentane. The frozen sample was then placed in an aluminium mould, containing OCT embedding media (Tissue-Tek, Agar Scientific, UK), with the cutting surface at the bottom of the mould. The sample in the aluminium mould was then immersed into the liquid nitrogen cooled iso-pentane until the embedding media had solidified. Frozen blocks were stored at -20°C, or for longer term storage at -80°C.

2.3.2.6 Cryosectioning

For sectioning of frozen tissue a Leica cryostat (Leica CM3050S) was used. Frozen blocks were attached to cryostat chucks via a small amount of OCT compound. The main cryostat chamber was set at -20°C. Sections were cut (10μm) and transferred onto Superfrost Plus electrostatically charged glass slides (Menzel-Glaser, UK), 2 sections per slide. Sections were allowed to dry at room temperature for at least 30 minutes and then stored in a freezer at -20°C for 1 week or at -80°C for longer periods of time.

2.4 Histochemistry

For the detailed examination of corneal tissue morphology Haematoxylin and Eosin (H&E) staining was employed. Cell nuclei were localised with haematoxylin and sections were counter-stained with eosin to provide overall background.

2.4.1 H&E staining of paraffin sections

Paraffin wax, being impermeable to stains, was removed by immersion in two baths of xylene each for 5 minutes and rehydrated by one-minute washes in descending grades of alcohol: 100%, 100% 90%, 70%, 50% IMS prior to 10 minutes washing in cold running tap water.

De-waxed and rehydrated sections were immersed in Harris`s Haematoxylin (BDH, UK) for 3 minutes, then rinsed in tap water for 10 minutes before counter-staining in Eosin (BDH, UK) for 3 minutes. Sections were washed for 10 minutes in tap water then dehydrated by 1-minute immersions through a series of graded alcohols (50%, 70%, 90%, 100% and 100% IMS). Clearing of sections was achieved by using two changes of xylene for 1 minute each. In a final step, sections were mounted in a xylene-based mountant, DPX (BDH, UK) and left to dry.

2.4.2 H&E staining of frozen sections

Frozen sections were warmed to room temperature, immersed in PBS, twice, for 10 minutes each and then stained with Harris`s Haematoxylin and Eosin as

described in section 2.4.1. After rinsing in tap water, sections were mounted in an aqueous mountant, Hydromount (BDH, UK).

2.5 Immunohistochemistry

2.5.1 Definition of immunohistochemistry

Immunohistochemistry is defined as a technique, which allows identification of an antigen in its tissue or cellular location by using labelled antibodies as specific reagents for localisation of tissue constituents (antigens) (Polak *et al.*, 1997). The site of antibody binding is identified either by direct labelling of the antibody, or by use of a secondary labelling method.

2.5.2 Antibodies used in immunolabelling procedures

The range of antibodies used for immunolocalisation in this study is presented in Table 2.2 below. Protocols were optimised following a number of different treatments to both wax and frozen sections. These included different antibody dilutions, with or without blocking agents (5%, 10% donkey serum) at different times of incubation. Final antibody dilutions are shown in Table 2.2. Optimised protocols are detailed below.

2.5.3 Immunolabelling protocols for frozen sections

Frozen sections of chick embryo eyes in triplicate for each stage (from ED 4 to ED21), were allowed to warm to room temperature for 15 minutes. All sections were carefully circled using a pap pen (Vector Laboratories, Inc, UK), fixed in cold (previously cooled at -20˚C for 10 minutes) 100% acetone for 10 minutes and then washed in PBS, three times for 5 minutes.

Table 2.2 Antibodies used for immunohistochemistry

Antigen	*Clone*	*Host*	*Raised against*	*Dilution*	*Company*	*Marker:*
Primary antibodies						
Cytokeratin 3	AE5 (1 mg/ml)	mouse	human	1:50	MP Biomedicals, LLC, UK	epithelial differentiation
panCK	AE1/AE3 (1 mg/ml)	mouse	human	1:100	DakoCytomation UK	epithelial differentiation
Ki67	B126.1 (0.15 mg/ml)	mouse	human	1:100	Abcam, UK	proliferation
PCNA	Pc10 (0.7 mg/ml)	mouse	human	1:500	Abcam, UK	proliferation
Caspase -3 (Active)	(n/a) (0.2 mg/ml)	rabbit	human	1:10	Millipore Upstate, UK	apoptosis
GFP	3E6 (n/a)	mouse	jellyfish	1:50 1:100	Molecular Probes, UK	negative control
Secondary antibody						
	Biotinylated anti-IgG	goat	rabbit	1:200	Vector Laboratories, UK	
	Alexa Fluor 488	donkey	mouse	1:500 1:1000	Molecular Probes, UK	

2.5.3.1 Determination of corneal epithelial cell differentiation

Immunolocalisation for cytokeratins AE1/AE3 antibody

Following fixation (see section 2.5.3), frozen sections were rinsed in three 5-minute washes in PBS. Before overnight incubation in primary antibody (diluted in PBS, as indicated in Table 2.2) in a humidified chamber at 4°C, blocking agent (5% donkey serum in PBS) was applied for 20 minutes.

The next day, sections were washed 3 times in PBS, 5 minutes each. Then sections were incubated in donkey anti-mouse Alexa Fluor 488 (Invitrogen, Molecular Probes, UK) secondary antibody (diluted 1:1000 in PBS, final concentration 0.01mg/ml) for 2 hours in the dark. In order to label cell nuclei, 3µl of Hoechst 33342 (bisbenzamide, Sigma, UK) stock solution (1mg/ml bisbenzamide in ddH_2O) per 1ml of diluted secondary antibody was included in the final antibody solution. In the final step, sections were washed with PBS,

three times for 5 minutes and mounted in Hydromount (National Diagnostics, UK). Stained slides were air dried and stored at -20˚C. As a negative control, mouse anti-GFP and mouse IgG (final concentration 0.01mg/ml) were substituted for the primary antibody.

Immunolocalisation of cytokeratin 3 (CK3)

Sections were air dried after 10 minutes acetone treatment (see 2.5.3) and rinsed three times for 5 minutes in PBS. For permeabilisation of membranes, sections were incubated with 0.1% Triton-X-100 (Sigma, UK) for 5 minutes, and once again washed in PBS for 15 minutes. Overnight incubation at 4˚C in anti-CK3 primary antibody (final concentration 0.02mg/ml) (Table 2.2) was preceded by a 20 minute incubation in 10% donkey serum. After 24 hours, sections were rinsed for 15 minutes in PBS. Secondary antibody (Alexa Fluor 488, 1:1000 in PBS) containing Hoechst 33342 (as described above) was applied for 2 hours and after that time, PBS washing was repeated (three times for 5 minutes each). Finally, sections were mounted with Hydromount (National Diagnostics, UK) and stored at -20˚C. As a negative control, mouse anti-GFP and mouse IgG (final concentration 0.02mg/ml) were substituted for the primary antibody.

2.5.4 Immunolabelling protocols for paraffin sections

Paraffin-embedded corneal embryonic corneal sections (in triplicate for each stage) from different time points (ED4 to ED21) were dewaxed in xylene (twice, 5 minutes each), rehydrated through graded alcohols (100%, 100%, 90%,70%, 50%), 5 minutes each and washed in ddH_20 for 5 minutes.

2.5.4.1 Determination of corneal epithelial cell proliferation

Immunolocalisation for PCNA

Paraffin sections, processed as described in section 2.5.4, were placed in 1600 ml of boiling dH_2O containing 15ml of antigen retrieval solution (Vector Laboratories, Inc, UK), for 2 minutes in a pressure cooker. Sections were then washed in PBS for 5 minutes and incubated with 0.2% of Tween-20 in PBS for 30 minutes. Subsequently, sections were blocked with 10% BSA (bovine serum albumin) and Tween-20 in PBS for 1 hour at room temperature and then

incubated for one hour in PCNA (Proliferating Cell Nuclear Antigen) primary antibody (diluted 1:500 in 1.5% BSA and 0.2% Tween-20 in PBS, final conc. 0.0014mg/ml). As negative controls, mouse anti-GFP (diluted as primary antibody) and mouse IgG (final concentration 0.0014mg/ml) replaced the primary antibody.

Sections were then washed three times in PBS and incubated with anti-mouse Alexa Fluor 488 diluted 1:500 in PBS containing 1.5% BSA and 0.2% Tween-20, for 2 hours at room temperature. Hoechst 33342 was added to secondary antibody solution as described above. After a lapse of 2 hours, sections were washed with PBS (3 x 5 minutes), mounted in Gelvatol (Appendix II) and stored at -4°C.

2.6 Analysis of epithelial cell death

Protocols for analyses of epithelial cell death were performed on at least triplicate sections from three different eyes at developmental time points ED4 to ED21.

2.6.1 TUNEL technique

Apoptosis was detected using terminal dUTP nick-end labeling (TUNEL) assay with ApopTag Peroxidase in situ Apoptosis Detection Kit (Chemicon International, USA). Sections were deparaffinised through xylene (three changes, 5 minutes each), rehydrated through graded alcohols (twice in 100% for 5 minutes, then 95% and 70% for 3 minutes each wash) and washed in 1XPBS. Then sections were incubated in proteinase K (20µg/ml, 60µl/5 cm^2) (Chemicon International, UK) for 15 minutes at room temperature, following incubation in 3% hydrogen peroxide (Sigma, UK) for 5 minutes and a 5-minute wash in PBS. Subsequently equilibration buffer was applied for 30 seconds, and then sections were incubated in TdT enzyme (37°C for 1 hour). Subsequently, working strength stop/wash buffer was applied for 10 minutes at room temperature.

In the next step, sections were washed in three changes of PBS for 1 minute each wash and treated with anti-digoxigenin conjugate in a humidified chamber

for 30 minutes at room temperature. Then sections were washed in PBS (four changes, for 2 minutes per wash) and peroxidase substrate (SigmaFast DAB solution, Sigma, UK) was applied for 13 minutes (Appendix II). Rat mammary gland sections (Chemicon International, UK), and DNase I (Ambion, UK) digestion of chick sections (Appendix II) acted as positive controls. Sections were incubated with DNase I (2U/µl) for 2 hours at room temperature. A negative control was performed by substitution of equilibration buffer in place of the volume of TdT enzyme reagent.

Sections were washed in 3 changes of dH_2O and counterstained in 0.5% methyl green (Vector Laboratories, UK) for 10 minutes at room temperature. Sections were rinsed with water (30 seconds) and dehydrated in n-Butanol (Fisher Scientific, UK) for 10 seconds twice, and then for 30 seconds. Finally, sections were incubated in three 2 minute changes of xylene. Subsequently, sections were mounted in DPX (BDH, UK).

2.6.2 Immunolocalisation of caspase 3 (active)

Paraffin sections, deparaffinised as described above (see section 2.6.1), were placed in 1600 ml of boiling dH_2O with 15ml of antigen retrieval solution for 2 minutes, in a pressure cooker. Sections were then washed in PBS for 5 minutes and incubated in 3% H_2O_2 for 15 minutes.

Subsequently, sections were washed in PBS three times for 5 minutes and incubated in 0.1% Triton-X-100 (Sigma, UK) for 10 minutes before three 5-minute washes in PBS. Sections were then blocked with 4% goat serum for 1 hour at room temperature and incubated for 2 hours in anti-caspase 3 (active) primary antibody, diluted 1:10 in PBS containing 4% goat serum (final concentration 0.002mg/ml). For negative and positive controls primary antibody was substituted with rabbit IgG (final concentration 0.002mg/ml) and sections were incubated with DNase I (2U/µl) for 2 hours at room temperature, respectively. Sections were then washed three times in PBS and incubated in biotinylated secondary goat anti-rabbit antibody (50µl in 10ml of PBS containing 1% goat serum, VECTASTAIN® Elite® ABC KIT, Vector Laboratories, UK) for 1 hour.

After 1 hour, sections were washed in PBS (3 x 5 minutes), and VECTASTAIN® ABC Reagent was applied. VECTASTAIN® ABC Reagent containing Reagent A (Avidin) and Reagent B (biotynylated enzyme) was prepared 30 minutes before application: 100µl of reagent A and reagent B was added to 5ml of PBS. After 1 hour, sections were washed with PBS (3 x 5 minutes) before incubation in peroxidase substrate (SigmaFast DAB solution, Sigma, UK) for 15 minutes (Appendix II). Sections were then washed in three one-minute changes and a final 5-minute wash in dH_2O before counterstaining in methyl green (Vector Laboratories, UK) for 5-minute at room temperature. In the final step, sections were washed with dH_2O for 30 seconds and dehydrated in two one-minute changes of 95% and 100% alcohol and three 2-minute changes of xylene. Sections were mounted in DPX (BDH, UK).

2.7 Image capture

All Haematoxylin and Eosin stained sections were observed via bright field microscopy using a DMRA2 microscope (Leica, UK) and images were capture using QWin v3 software (Leica, UK). Immunofluorescence was visualised by DM5500B microscopy (FW4000 software, Leica, UK) using filters for bisbenzamide (excitation 359 nm, emission 461 nm) and Alexa Fluor 488 (excitation 494 nm, emission 518 nm). Images were captured using FW4000 image analysis software (Leica, UK). For quantification of cell proliferation and TUNEL-labelled cells, sections were observed under immersion using x100 objective. At least triplicate sections of three different eyes at each developmental stage were observed in captured images for all localisation protocols. In each section three fields of view in three different corneal regions (centre, periphery and limbus) were examined.

2.8 Statistical analysis

In all experiments, at least triplicate sections of three different samples for each developmental stage were observed. In each section three fields of view in three corneal regions (limbus, periphery, centre) were investigated. Quantification of epithelial cell proliferation and apoptosis was performed by calculating the labelling index (LI), according to the equation:

LI = (number of labelled cells/total number of cells) x 100%.

Statistical analysis was carried out using parametric One-way ANOVA (SPSS v.12), followed by post-hoc Dunnett T3 test (SPSS v.12) for data with Gaussian distribution. Pearson correlation was performed in order to depict an association between two variables. A *p* value less than 0.05 ($p \leq 0.05$) was considered statistically significant.

2.9 Western Blotting

Western blotting is a method for detecting a specific antigen in a sample of tissue/cell homogenate. The method is dependent on the use of a high-quality antibody directed against a desired protein and visualisation of immobilised antigens directly or indirectly with horseradish peroxidase (HRP) labelled antibodies.

2.9.1 Sample preparation

Eyes were isolated from chick embryos at developmental stages (ED4-ED21) as described in section 2.2.1. After dissection in PBS, corneas were incubated in Dispase II (2.4U/ml) (Roche Diagnostics Ltd, UK) at 37°C. The number of corneas dissected at each stage was established experimentally in order to obtain the required protein concentration for further experiments (Table 2.3). Time of incubation in Dispase II was optimised for ease of epithelial removal and differed depending on the developmental time point as shown in Table 2.3.

Table 2.3 Number of eyes used in sample preparation and time of incubation in Dispase II for each developmental time point

Embryonic day	**6**	**8**	**10**	**12**	**13**	**14**	**16**	**18**	**21**
No. of eyes	120	120	100	100	80	80	60	40	30
Time [hours]	7/60	0.25	0.5	1	1.15	1.25	1.35	1.45	3

2.9.2 Protein extraction

The epithelia, after incubation in Dispase II, were dissected away from the stroma (Fig. 2.1) and placed into 250µl of protein extraction buffer on ice. Protein extraction buffer contained 1XRIPA buffer (0.5M Tris-HCl pH 7.4, 1.5M NaCl, 2.5% deoxycholic acid, 10% NP-40, 10mM EDTA) (Upstate, UK) with the addition of 2.5µl of protease inhibitor cocktail (Sigma-Aldrich, UK). Tissue was homogenised using a rotor (Kimble Kontes LLC, Belgium) for 30-45 seconds and placed on a rotator (Benley Spiramix, UK) for 30 minutes at 4°C. The sample was then centrifuged at 10,000g for 15 minutes at 4°C. Subsequently, supernatant was removed and aliquoted (10µl) into new ependorff tubes before storage at -20°C. Pellets were resuspended and checked for protein concentration as described below in 2.9.3.

2.9.3 Protein quantification

The protein samples collected were quantified using BCA Protein Assay Kit (Pierce, UK). The BCA™ Protein Assay is a detergent-compatible formulation based on bicinchoninic acid (BCA) for the colorimetric detection and quantification of total protein. The method combines reduction of Cu^{+2} to Cu^{+1} by protein in an alkaline medium (the biuret reaction) with the highly sensitive and selective colorimetric detection of the cuprous cation (Cu^{+1}) using a reagent containing bicinchoninic acid (Smith *et al.*, 1985). A series BSA standards were prepared from a 2µg/ml stock solution, as described in Table 2.4.

Table 2.4 The dilution series of the BSA standard for BCA protein assay

Vial	*Diluent H_2O (µl)*	*BSA (µl)*	*Final BCA concentration (µg/ml)*
A	0	300 of stock	2,000
B	125	375 of stock	1,500
C	325	325 of stock	1,000
D	175	175 of vial B	750
E	325	325 of vial C	500
F	325	325 of vial E	250
G	325	325 of vial F	125
H	400	100 of vial G	25
I	400	0	0

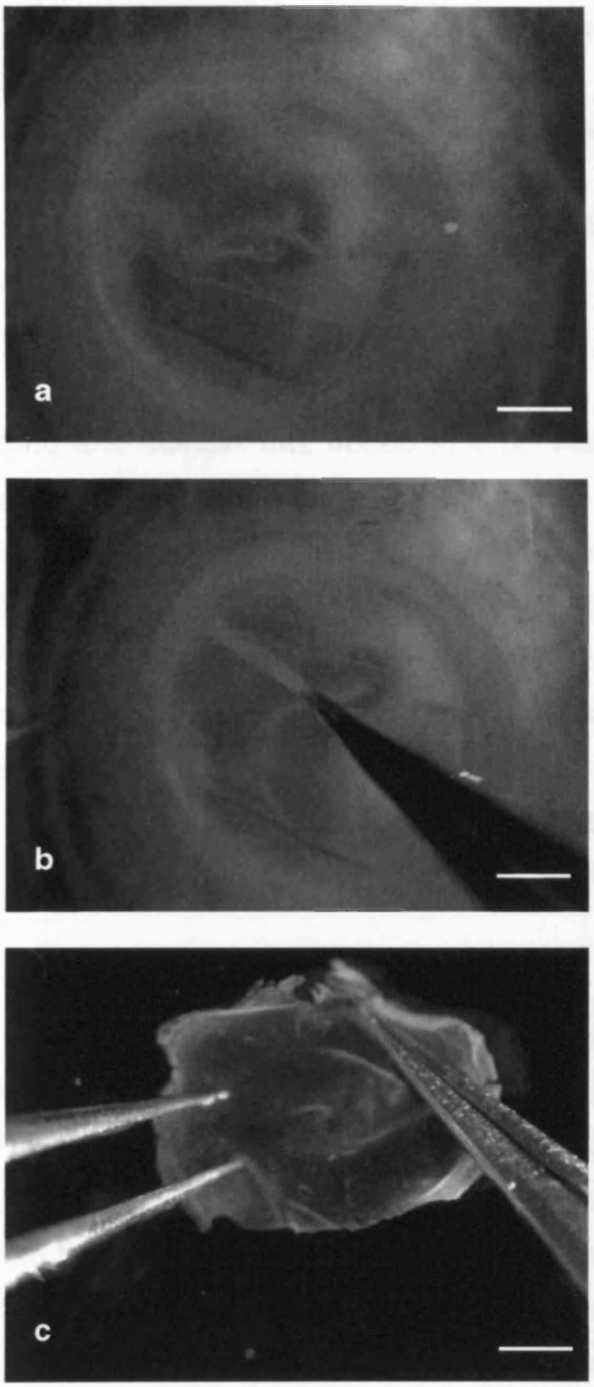

Figure 2.1 Isolation of chicken corneal epithelium from adjacent stroma. **a)** The cornea of posthatched chicken after incubation in Dispase II, **b)** the epithelium was dissected out using forceps, **c)** the removed corneal epithelial sheet. Scale bar 1mm. x 10.

The volume of BCA working reagent (WR) was calculated using the following equation:

Total volume of WR = (no. of samples + no. standards) x number of replicates (2) x volume required per sample (200µl)

The WR was prepared by adding 1 volume of BCA reagent B to 50 volumes of reagent A (50:1, Reagent A:B) in the volume required to run each sample (plus BSA standards) in duplicate.

25µl of each standard and sample was added to a 96 well microplate, then, 200µl of the WR was added to each well. The microplate was covered with aluminium foil and incubated at 37˚C for 30 minutes. Following incubation, the absorbance was measured at 570nm on a plate reader (Multiscan Ascent® Labsystems, UK). The absorbance readings were exported to Excel (Microsoft) and standard curves were created by plotting the average measurement of each dilution of BSA standard into a regression of linear fit. The concentration of total protein in each sample was calculated by reference to the standard curve.

2.9.4 Preparation of protein samples

The supernatants from ED6 to posthatch epithelia were diluted to obtain the same concentration (2.4µg/10µl and 7µg/10 µl, for PCNA and CK3 respectively) by addition of the lysis buffer (RIPA buffer, Upstate, UK). Equal volumes (10µl) of the diluted protein sample and working sample loading buffer Laemmli (Bio-Rad, UK) were added to an eppendorf (Appendix II). These samples were then boiled at 100˚C for 5 minutes on a heating block (Grant QBT2, UK) to denaturate proteins. Following boiling, the protein samples (10µl), for PCNA and CK3 respectively were loaded on the gel, prepared as described below.

2.9.5 Sodium Dodecyl Sulphate-Polyacrylamide Gel Electrophoresis (SDS-PAGE)

SDS-PAGE is a technique to separate proteins according to their electrophoretic mobility. The anionic detergent SDS dissociates and unfolds oligomeric proteins into its subunits. The SDS binds to the polypeptides to form complexes with fairly constant negative charge to mass ratios. The

electrophoretic migration rate through a gel is therefore determined only by the size of the complexes. SDS-PAGE is used to estimate a molecular mass of a protein, as well as the degree of sample purity (Shapiro *et al.*, 1967).

To run SDS-PAGE the Bio-Rad Mini-Protean® system was used. The resolving and stacking gels were made up as described in Table 2.5 (Appendix II). The percentage of the resolving gel was altered depending on the molecular weight of protein. For PCNA and CK3 - 10% and 12% gel was used respectively.

Table 2.5 Components of the resolving and stacking gels for SDS-PAGE

	Resolving gel (10 ml)		*Stacking gel (10ml)*
Final % Range (MW)	***10%*** 21-100	***12%*** 10-70	***5%***
Acrylamide 30%	3.3 ml	4.0 ml	1.67 ml
Distilled H_2O	4.0 ml	3.3 ml	5.83 ml
1.5 M Tris/HCl	2.5 ml	2.5 ml	-
0.5 M Tris/HCl	-	-	2.5 ml
10% SDS	0.1 ml	0.1 ml	0.1 ml
10% APS	0.1 ml	0.1 ml	0.5 ml
TEMED	0.02 ml	0.02 ml	0.01 ml

The resolving gel (covered with dH_2O) was allowed to set for 10 minutes, before the stacking gel mixture was layered on the top of the resolving gel. The gel was left to set for an hour, and humidity was maintained to prevent the gel from drying out. After an hour, the glass plates with the gel were removed from casting frames and placed into the electrode assembly (Bio-Rad, UK), short plates inward, to create an inner buffer chamber. The electrode assembly was then locked into the clamping frame and placed into the mini tank. The inner chamber was filled with approximately 125ml of Running Buffer (see Appendix II) and 200ml was added to the outer chamber.

Samples were loaded with equal amount of protein; 10µl of protein/loading buffer mix was added to each well (~2.4 or 7µg of protein). 5µl of molecular weight marker (Precision Plus Kaleidoscope Protein Standard, range 10-250

kDa, Bio-Rad, UK) was added to the outermost lanes. The gel was run at 120V, 300mA for 10 minutes and thereafter the power was increased to 150V for the next 50 minutes.

2.9.6 Transfer of proteins onto the nitrocellulose membrane

After completion of electrophoresis, the gel, nitrocellulose membranes (Hybond™ -ECL™, Amersham Bioscences, UK), filter paper and fibre pads were placed in Transfer Buffer (Appendix II) for 15 minutes on a rocker. The cassette with gel sandwiched between filter paper and membrane was then placed in a tank with 600ml of transfer buffer and a frozen cooling unit. Proteins were transferred from the gel to a nitrocellulose membrane at 100V, 350mA for 45 minutes. Subsequently, the nitrocellulose membrane was washed overnight with TBS/Tween20 (0.1% Tween20 in TBS washing buffer) (Appendix II) at 4˚C.

2.9.7 Blocking non-specific binding

To check the efficiency of the transfer, membranes were stained with Ponceau S staining buffer (Sigma, UK) for 3 minutes, and then washed 3 times for 5 minutes in TBS/Tween20 prior to blocking. To minimise non-specific binding approximately 20ml of 5% milk in TBS/Tween20 was applied for 1 hour at room temperature. After blocking membranes were washed six times with TBS/Tween20 for 5 minutes each time.

2.9.8 Incubation with the primary antibody

The membranes were incubated in 5ml of primary antibodies, diluted in TBS/Tween20 containing 1% milk, for 1 hour at room temperature. The optimised dilutions were used as shown in Table 2.6. Following incubation with the primary antibody, the membranes were washed in six 5-minute changes of 1x TBS/Tween20.

Table 2.6 Antibodies used for Western Boltting

Antigen	*Clone*	*Host*	*Raised against*	*Dilution*	*Company*	*Marker*
Primary antibodies						
Cytokeratin 3	AE5	mouse	human	1:2000	MP Biomedicals, LLC, UK	epithelial differentiation
PCNA	Pc10	mouse	human	1:1000	Abcam, UK	proliferation
β-actin	I-19	goat	rabbit	1:2000	Santa-Cruz, UK	loading control
Secondary antibody						
	IgG-HRP	goat	rabbit	1:10000	Santa-Cruz, UK	
	IgG-HRP	donkey	goat	1:10000	Santa-Cruz, UK	

2.9.9 Incubation with the secondary antibody

After washing, the membranes were exposed to a secondary antibody conjugated with HRP (Santa-Cruz, UK) for 1 hour at room temperature. The secondary antibodies were diluted in 1x TBS/Tween20 with 1% milk at optimised dilutions (see Table 2.6). Membranes were then washed with the TBS/Tween20 for 30 minutes with 6 changes.

2.9.10 Controls

To check specificity of the Western Blotting, one positive control sample (ED6 developing chicken brain) was used for PCNA western blotting. Negative controls included omission of the primary antibody and the use of mouse IgG instead of the primary antibody.

2.9.11 Visualisation of the specific protein antigens using ECL+^{TM}

For the detection of antibody-antigen complexes, the ECL Plus solution (ECL Plus Western Blotting Detection Reagents, Amersham Biosciences, UK) was used (Fig. 2.2). The ECL Plus Western Blotting provide a non-radioactive method for the detection of immobilised specific antigens conjugated to HRP labelled antibodies.

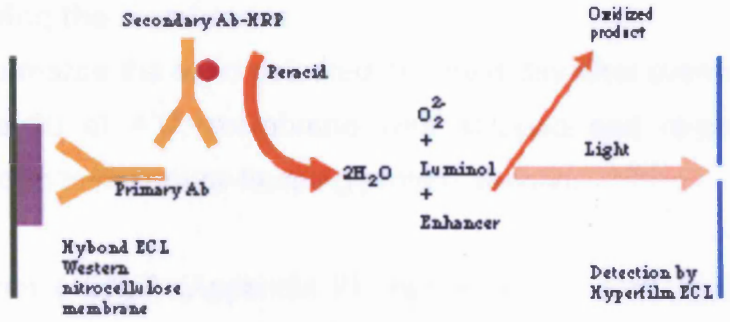

Figure 2.2 Chemiluminescent detection of protein using ECL Plus (from Amersham ECL Plus Western Blotting Detection Reaction product booklet).

The reaction is based on the peroxidase-catalyzed reaction of luminol and subsequently enhanced chemiluminescence, where HRP-labelled protein is bound to the antigen on the membrane. The resulting light is detected on Hyperfilm.

Working solution (adjusted to room temperature for 30 minutes prior to use) was prepared by mixing 50 parts of reagent A and 1 part of reagent B and then 1 ml of the solution was added to each membrane. After 5 minutes incubation, excess reagent was removed and membranes were sealed in individual plastic pockets and placed in an X-ray film cassette (Amersham, UK). A sheet of film (Hyperfilm™, Amersham Biosciences, UK) was placed on top of the plastic wallet in a dark room. A number of different exposure times were used in an attempt to obtain the best blot, ranging from 0.5 to 10 minutes. Optimised exposure times are shown in Table 2.7. Following exposure, film was incubated with developer solution (Photosol Ltd, UK) for 30 seconds and transferred to fixer solution (Photosol Ltd, UK) for the next 30 seconds. In the final step, the films were rinsed in water and air dried.

Table 2.7 Optimised protocols for detection of protein bands

	PCNA	*AE5*	*B-Actin*
Optimal exposure time to ECL+ [min]	1	15	0.5
Developing [min]	0.5	3	0.5
Fixing [mini]	1	3	1
Washing [min]	3	3	3

2.9.12 Stripping the membranes

In order to normalise the band detected, the next day after overnight incubation in TBS/Tween20 at 4˚C, membrane was stripped and re-probed with an antibody specific to the house-keeping protein, β-actin.

Stripping buffer (~20ml) (Appendix II) was added to each membrane for 10 minutes, twice. Following removal of stripping buffer, membranes were incubated in two changes of 1XPBS for 10 minutes each. Membranes were then placed into 1XTBS/Tween20 for 5 minutes before they were ready for the blocking stage. Blocking and incubating with antibodies were performed as described in sections 2.9.7-2.9.9, before detection of bands with ECL Plus (2.9.11).

2.9.13 Analysis of the Western Blotting results

The films with detected bands were scanned (Epson Expression 1680 Pro). Bands were then semi-quantified by densitometry using Labworks™ software (Media Cybernetics, UK).The optical density was measured for each band and results were imported to Microsoft® Excel. Data were collected from three experiments and normalised with β-actin level. Mean normalised band intensity along with the standard error of the mean was calculated for each protein at each time point. Comparisons between the nine time points (embryonic days) were performed using the parametric analysis of the variance test (One-way ANOVA) followed by the appropriate post-hoc test (Dunnett T3) for the data log transformed when necessary and with normal distribution (SPSS v.12). Significance was taken at $p \leq 0.05$.

2.10 Preparation of samples for microarray analysis

2.10.1 Isolation of corneal epithelium and RNA stabilisation

Chick embryos corneas were dissected from eyes isolated from different embryonic stages (ED 6, 10,12,14,16,18, posthatch) and separated into right and left eyes. After dissection in PBS (RNase, DNase – free), corneas were incubated with Dispase II (2.4U/ml) in 37˚C. Time of incubation was optimised and differed depending on the developmental time-point as detailed in Table

2.3 and the number of epithelia in each sample set is shown in Table 2.8. Following incubation, the epithelium was peeled off in two drops of RNA*later*® (Sigma-Aldrich, UK). RNA was stabilised in tissue by preservation in RNA*later*®. Tissue was stored at 4°C for up to a month or at -80°C for archiving.

Table 2.8 Number of epithelia isolated for each time point

ED	6	10	12	14	16	18	21
Set I	25	13	12	13	14	15	11
Set II	28	13	16	16	16	16	9
Set III	29	14	15	14	16	17	5

2.10.2 RNA extraction from tissue

In order to obtain high yield and pure RNA from the tissue, RNeasy® Micro Kit from Qiagen (UK) was used. The RNeasy® Micro technology combines the selective binding properties of a silica-gel-based membrane with the speed of microspin technology. The procedure allows purification of total RNA (maximum 45µg) from small amount of tissues (maximum 5mg). The maximum amount that can be used is limited by the volume of Buffer RLT required for efficient lysis and the maximum loading volume of the RNeasy MinElute Spin Column (~700µl). Guanidine-isothicyanate-containing lysis buffer and ethanol are added to the sample to create conditions that promote selective binding of RNA to the RNeasy MinElute membrane. DNase and any contaminants are washed away, and high-quality total RNA is eluted in RNase-free water (RNeasy® Micro Kit Handbook, Qiagen).

RNA was isolated from chick corneal epithelia using Qiagen Micro Kit (Qiagen, UK) according to the protocol described below. The excess RNA*later*® from the Eppendorf tube was removed and replaced with 350µl of working buffer RLT (provided with kit, see Appendix II). Tissue was homogenised immediately using a conventional rotor homogeniser (Kontes Gerresheimer, UK) and the tissue lysate was then centrifuged at 10,000g for 3 minutes at maximum speed in a microcentrifuge (Jencons-Plc, UK). Subsequently, the supernatant was

carefully transferred to a new tube by pipetting. In the next step, 350µl of 70% ethanol was added to the homogenised lysate, and mixed by pipetting.

The sample (including precipitate) was applied to an RNeasy MinElute Spin Column (Qiagen, UK), and centrifuged for 15 seconds at ≥8,000g. Next, 700µl Buffer RW1 (provided with kit) was added and the column was centrifuged for 15 seconds at ≥8,000g. Following centrifugation, the column was transferred into a new collection tube and 500µl of Buffer RPE (diluted in 4 volumes of 100% ethanol) was added. The column was then centrifuged for another 15 seconds at ≥8,000g to wash the column. Subsequently, 500 µl of 80% ethanol was added, before centrifugation for 2 minutes at ≥8,000 g. In the final step, the columns were centrifuged with open caps at full speed for 5 minutes. Then, 10µl per sample of RNase-free water was added directly onto the centre of the silica-gel membrane and columns were centrifuged for 1 minute at 10,000g. To ensure a complete RNA elution, the eluent was added again onto the column and centrifugation was repeated.

2.10.3 Optimisation of the protocol for RNA extraction

During optimisation of the protocol for RNA isolation, another approach was tested involving DNAse I (Qiagen, UK) digestion on the column to remove traces of DNA that may copurify. DNase I stock solution was prepared by dissolving lyophilised DNase I (1500 Kunitz units) in 550µl of RNase-free water. To prepare a working solution, 10µl of DNase I stock solution was added to 70µl of Buffer RDD (provided with kit). The working mix was then applied onto the RNeasy MinElute silica-gel membrane for 15 minutes at room temperature following first application of RW1 Buffer (see 2.10.2). After 15 minutes, a further 350µl of Buffer RW1 was added and the column was centrifuged for 15 seconds at 8,000g. The remaining protocol was performed as described in section 2.10.2.

2.10.4 RNA quantitative and qualitative analysis

To determine integrity and measure the concentration of total RNA, samples were obtained from chicken corneal epithelia at different developmental stages. The 3µl total RNA from each sample was checked for purity, using a PicoDrop

spectrophotometer (Genetic Research Instrumentation Ltd, UK), by measuring absorbance at 260nm and 280nm wavelength and computing the ratio.

RNA integrity and quantity of small amounts of total RNA was determined using the Agilent System (Agilent Technologies, UK). The Agilent RNA kit contains chips and reagents designed for analysis of RNA fragments. Each RNA chip contains an interconnected set of microchannels that is used for separation of nucleic acid fragments based on their size as they are driven through it electrophoretically. Workflow chart is shown in Figure 2.3. The limitation of the quantitative range of the assay is 25-500ng/µl total RNA and 5-5000ng/µl for the qualitative range.

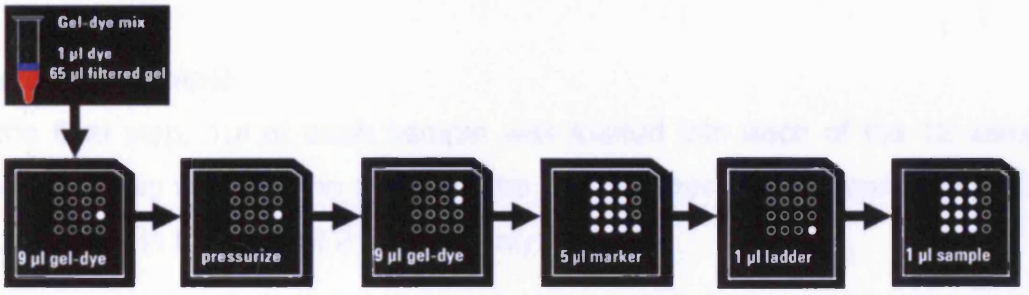

Figure 2.3 Principles of Agilent System for analysis of total RNA (from Agilent RNA 6000 Nano Kit Guide).

Gel-Dye Mix preparation

All reagents were allowed to equilibrate to room temperature for 30 minutes before use. Firstly, 200µl of gel matrix was filtered with a 0.2µm filter by centrifuging at 1,500g for 10 minutes at room temperature. Subsequently, 1µl of RNA 6000 Nano dye concentrate (Agilent Technologies, UK) was added to a 65µl of filtered RNA 6000 Nano gel (Agilent Technologies, UK) and the tube was centrifuged for 10 minutes at 13,000g.

Loading the Gel-Mix onto chip

To prepare the capillary electrophoresis chip, 9µl of the gel-dye was added to the dedicated well on the chip and dispensed using a syringe with priming station (Agilent Technologies, UK).

Loading the RNA 6000 Nano Marker and molecular weight marker

Next, 5µl of RNA 6000 Nano marker were pipetted into the molecular weight marker (WM) and sample wells, prior to the addition of 1µl of WM into the ladder well.

Sample preparation

To eliminate secondary structure formation of RNA, samples were heated at 70°C for 2 minutes before being loaded to the chip.

Loading of sample

In the final step, 1µl of each sample was loaded into each of the 12 sample wells. The chip was shaken on top of the IKA vortexer for 60 seconds at 1,000g and then run in the Agilent 2100 Bioanalyzer.

Chip processing

The chip was run in the Agilent 2100 Bioanalyzer within 5 minutes after addition of samples. Results were analysed by the integrated Agilent software.

2.11 Microarrays preparation

GeneChip® probe arrays are manufactured using technology that combines photolithography and combinational chemistry. Up to 1.3 million different oligonucleotide probes are synthesized on each array. Each oligonucleotide is located in a specific area on the array called a probe cell. Each probe cell contains hundreds of thousands to millions of copies of a given oligonucleotide. During the laboratory procedure, labelled with fluorescent markers, RNA (or DNA) fragments (referred to as the "target") are hybridised to the probe array. The amount of signal, emitted after excitation by laser at a characteristic wavelength, is directly in proportion to the amount of dye at the spot on

microarray. These values are obtained and quantified on the scanner. The following major steps include:

1. Target preparation
2. Target hybridisation
3. Fluidics station setup
4. Probe array washing and staining
5. Probe array scan
6. Data analysis

2.11.1 Preparation of Spike-in Controls and T7-Oligo (dT) Primer/Poly-A Controls Mix

Reagents for this step were supplied with the GeneChip® Eukaryotic Poly-A RNA Control Kit and in a GeneChip® One-Cycle cDNA Synthesis Kit (Affymetrix).

Preparation of Spike-in Controls

In order to monitor the amplification and labelling process, the same volume (2µl) of four controls (*lys, phe, thr, dap*) were spiked directly into RNA samples prior to amplification and labelling. The spike-in controls were diluted in Poly-A Control Dil Buffer to the final concentrations (referred to as ratio of copy number) as shown in Table 2.9.

Table 2.9 Final concentrations of Poly-A RNA controls in samples

Poly-A RNA Spike	Final concentration (ratio of copy number)
lys	1:100,000
phe	1:50,000
thr	1:25,000
dap	1:7,500

Preparation of T7-Oligo (dT) Primer/Poly A Controls Mix

2µl of diluted Poly-A controls were mixed with 2µl of 50 µM T7-Oligo(dT) Primer and were brought to the total volume of 10µl with RNase-free water (Ambion, UK).

2.11.2 First round RNA amplification

For the first round of amplification, reagents from GeneChip® One-Cycle cDNA Synthesis Kit (Affymetrix, UK) were used for cDNA synthesis.

First strand cDNA synthesis

Single strand cDNA was synthesised using an oligonucleotide that incorporated the T7 promoter at 3' end mRNA of 10 µl total RNA-control spike mixture.

Firstly, 1µg of total RNA of each sample were added to the T7-Oligo (dT) Primer/Poly A Controls Mix (1:1) with RNase-free water (final volume 12 µl). The mixture was centrifuged for approximately 5 seconds heated at 70˚C for 10 minutes to reduce secondary structure formation and the sample was left to anneal at 4˚C for at least 2 minutes.

Then, reverse transcriptase reaction mixture was prepared (buffer and reverse transcriptase premixes were provided in First-Strand Master Mix (Affymetrix) (Table 2.10), and 7µl was added to the RNA template (RNA sample/T7-Oligo(dT) Primer/Poly-A Controls Mix) and incubated at 42˚C for 2 minutes.

Table 2.10 Preparation of First - Strand Master Mix

Component	Volume [µl]
5X 1st Strand Reaction Mix	4
DTT, 0.1 M	2
dNTP, 10 mM	1
Total volume	**7**

Following incubation, 1µl of SuperScript™ II (Invitrogen, UK) (Appendix II) was added to each RNA sample for a final volume of 20µl. The RT reaction was performed at 42°C for 1 hour, and then samples were cooled for at least 2 minutes at 4°C in order to maintain RT enzyme activity.

Second strand cDNA synthesis

The second strand of cDNA was synthesised by adding 130µl of the Second-Strand Master Mix (Affymetrix) (Table 2.11) to each first-strand synthesis sample for a total volume of 150 µl. Samples were centrifuged for 5 seconds and then incubated for 2 hours at 16°C. Next, 2µl of T4 DNA polymerase were mixed with the samples and left for 5 minutes at 16°C. In the final step, 10µl of 0.5M EDTA was added.

Table 2.11 Preparation of Second - Strand Master Mix

Component	Volume [µl]
RNase-free water	91
5X 2nd Strand Reaction Mix	30
dNTP, 10 mM	3
E. coli DNA ligase	1
E. coli DNA Polymerase I	4
RNase H	1
Total volume	**130**

Cleanup of double-stranded cDNA

All components needed for this step were supplied with the GeneChip® Sample Cleanup Module (Qiagen, UK).

600µl of cDNA Binding Buffer were added to the double-stranded cDNA and 500µl was applied to the cDNA Cleanup Spin Column following centrifugation for 1 minute at 8,000g. Then columns were washed with 750µl of the cDNA Wash Buffer and centrifuged for the same time and speed. Columns were then

centrifuged with open caps for 5 minutes at maximum speed, before elution with 14µl of cDNA Elution Buffer (1 minute, at maximum speed).

2.11.3 IVT labelling reaction

For the synthesis of biotin-labelled cRNA, GeneChip® IVT (*in vitro* transcription) Labelling kit was used (Table 2.12).

Reagents were mixed with 12µl of double-stranded cDNA template and RNase-free water was added to a final volume of 40µl. The IVT labelling reaction was performed in a thermal cycler for 16 hours at 37°C.

Table 2.12 IVT Reaction Mix

Component	Volume [µl]
10X IVT Labelling Bufer	4
IVT Labelling NTP Mix	12
IVT Labelling Enzyme Mix	4
Total volume	**20**

2.11.4 Cleanup of biotin-labelled cRNA

RNA generated from the IVT labelling reaction was purified using reagents supplied with the GeneChip® Sample Cleanup Module. Each sample was mixed with 350µl of IVT cRNA Binding Buffer and then with 250µl of absolute ethanol, before being applied to the cRNA Cleanup Spin Column and centrifuged for 15 seconds at 8,000g. Subsequently, 500µl of IVT cRNA Wash Buffer was pipetted onto the spin column and centrifuged for 5 minutes at maximum speed. Before elution with 11µl of RNase-free water, 500µl of 80% ethanol was added onto the spin column and centrifuged for 15 seconds at 8,000g.

2.11.5 Fragmentation of cRNA

Fragmentation was performed using the Affymetrix Fragmentation Kit (Affymetrix, UK). 20µg of biotin-labelled cRNA (final concentration 0.5µg/µl) was mixed with 8µl of 5X fragmentation buffer, and RNase-free water was added to make a final volume of 40µl. The reaction mixture was incubated at 94°C for 35 minutes in the thermal cycler. The reaction was terminated at 4°C. 1µl of cRNA was used to check the fragmentation.

2.11.6 GeneChip® hybridisation

All components were provided by Affymterix Hybridisation Kit (Table 2.13, Appendix II).

Table 2.13 Hybridisation Cocktail for Single Probe Array

Component	Volume [µl]	Final concentration
Control Biotin Labelled oligo B2, 3 nM	5	50 pM
20X Eukaryotic Hybridisation Controls (bioB, bioC, bioD, cre)	15	1.5, 5, 25, 100 pM respectively
Herring Sperm DNA (10 mg/ml blocking agent)	3	0.1 mg/ml
Acetylated BSA (50 mg.ml blocking agent)	3	0.5 mg/ml
2X MES Hybridisation Buffer	150	1X
DMSO	30	10%
H_2O	to final volume of 300	
Final volume	**300**	

Components of Hybridisation Cocktail were mixed with 15µg of fragmented cRNA to give a total volume of 300µl. The reaction mixture was denatured at 99°C for 5 minutes prior to applying to the GeneChip®.

Chicken GeneChip® Arrays (Affymterix) were prehybridised using 200µl of 1X hybridisation buffer at 45°C for 10 minutes with rotation (60 rpm). Then, 200µl

denaturated hybridisation cocktail was applied onto the chip. The GeneChip® was hybridised for 16 hours at 45°C and 60rpm in a GeneChip® Hybridisation Oven 640.

2.11.7 Probe array wash and stain

After 16 hours of hybridisation arrays were washed and stained in an automated process using the GeneChip® Fluidics Station 400. Detailed reagent preparation protocols are shown in Appendix II. The following wash and staining steps included:

- *Post Hybridisation Wash #1:* 10 cycles of 2 mixes/cycle with wash Buffer A (non-stringent, 6x SSPE, 0.01% Tween-20) at 25°C,
- *Post Hybridisation Wash # 2:* 4 cycles of 15 mixes/cycle with wash Buffer B at 50°C (stringent, 100 mM MES, 0.1M [Na^+], 0.01% Tween-20),
- *1st Stain:* 10 minutes at 25°C in SAPE solution,
- *Post Stain Wash:* 10 cycles of 4 mixes/cycle with Wash Buffer A at 25°C,
- *2nd Stain:* 10 minutes in antibody solution at 25°C,
- *3rd Stain:* 10 minutes in SAPE solution at 25°C,
- *Final Wash:* 15 cycles of 4 mixes/cycle with Wash Buffer A at 30°C

2.11.8 Scanning of GeneChip®

GeneChips® were scanned using an Affymterix GeneChip® Scanner 3000 system. Two scans were conducted using the following settings: pixel value = 3µm, wavelength = 570nm. Absolute comparison analysis was performed using the following setting for scalling:

- All Probe Sets: Target Signal = 500,
- Normalisation: Scale factor = 1.

2.12 Standard and semiquantitative Real-Time PCR

2.12.1 cDNA synthesis

QuantiTect® Reverse Transcription System (Qiagen) was used for reverse transcription of total RNA templates. All reagents were provided with the kit. All reaction components were centrifuged before use and handled on ice.

Total RNA samples were diluted to the final concentration of 10ng/µl in RNase free water. Subsequently, 0.5µl of RNA template was mixed with components for genomic DNA elimination reaction, according to Table 2.14. Each sample was incubated for 2 minutes at 42˚C.

Table 2.14 Genomic DNA elimination reaction components (per sample)

Component	Volume/reaction [µl]	Final concentration
gDNA Wipeout Buffer, 7X	2	1x
Template RNA	0.5	0.25 ng/ µl
RNase-free water	11.5	
Final volume	**14**	

Then, the following components of master mix were combined in RNase-free tube: 1µl of Reverse Transcriptase, 4µl RT Buffer, 5X (final concentration 1X), 1µl of RT Primer Mix (includes Mg^{2+} and dNTPs). Master mix was added to the 14µl template RNA after gDNA elimination reaction and incubated for 15 minutes at 42˚. The cDNA synthesis reaction was terminated at 95˚C for 3 minutes. Reaction tubes were chilled on ice and used directly for PCR reaction or stored at -20˚C.

2.12.2 Primers

Primers used for standard and real-time PCR of housekeeping genes were taken from the publications. For selected targets, primers were designed using Primer3 (*http://frodo.wi.mit.edu/*) or Primer-Blast (*www.ncbi.nlm.nih.gov/tools/primerblast/index.cgi?LINK_LOC=BlastHome)* based on transcript sequences used to design the probes on the Affymetrix chicken array. All primers were checked for secondary structure using the DINAMelt Server (*http://www.bioinfo.rpi.edu/applications/hybrid/twostate-fold.php*) and their specificity was verified using NCBI nucleotide blast tool (*http://blast.ncbi.nlm.nih.gov/Blast.cgi*). The sequences of primers are shown in Table 2.15.

Table 2.15 Houskeeping genes and primer sequences used for semiquantitative RT-PCR of chick corneal epithelial cDNA

Gene	Site on sequence	Sequence (5`-3`)	Amplicon size (bp)	Primer Annealing temperature	Accesion number in GeneBank	Reference
GAPDH	FW (338) RV (501)	GGTGGTGCTAAGCGTGTTA CCCTCCACAATGCCAA	179	58	X01578	Li *et al.*, 2007
B-Actin	FW (973) RV (1106)	GAGAAATTGTGCGTGACATCA CCTGAACCTCTCATTGCCA	152	58	L08165	Li *et al.*, 2007
G6PDH	FW RV	CGGGAACCAAATGCACTTCGT CGCTGCCGTAGAGGTAGGGA	122	58	AI981686	De Boever *et al.*, 2008
UB	FW RV	GGGATGCAGATCTTCGTGAAA CTTGCCAGCAAAGATCAACCTT	147	58	M11100	De Boever *et al.*, .2008
Atoh7	FW (218) RV (452)	TCGTTTGAGGAAGGTGGTTC TCGCTGTGCATAAGGATCAC	235	58	AJ001178	
Psca	FW (369) RV (559)	AACAGAGCTCCCATGACCAC GTGGATTGCACACACACACA	191	58	XM_418414	
Sh3bgr	FW (273) RV (426)	AATGAGGAGCGGTATTGTGG TGTGTTCTGTGTGTGCCTCA	154	58	BX934008	
Kcnj2	FW (1210) RV (1441)	TTTAGAGGGCATGGTGGAAG AAAGGAGTTTGCGTTCGAGA	232	58	U20216	
Sfrp2	FW (268) RV (415)	AAGCAGTGTCACCCCGATAC AGCCGAAAGCAGACATCACT	148	58	AF218056	
Aqp3	FW (196) RV (401)	GGAGCTGGCATAGTCTTTGG TTGAAGGGATCCACGATAGC	206	58	AB358970	
H2afy2	FW (955) RW (1173)	GCTTAACAGCCGCAGAAGAC CTAGCTTGGCCATTTCTTGC	219	58	CR385118	

Lyophilised primers were dissolved in 1XTE buffer (pH 8.0) to a final concentration of 100µM and stored at -20°C.

2.12.3 Standard PCR

Standard PCR was carried out in order to check for primer specificity and to optimise annealing temperatures. All reactions were carried out using MegaMix~Blue kit (Cambio Ltd, UK) in 20µl reaction volume in PCR tubes (Axygen Scientific, UK). The detailed protocol and list of reagents is shown in Table 2.16.

Table 2.16 Standard PCR reaction components (per sample)

Component	Volume/reaction [µl]	Final concentration
MegaMix~Blue	17	
Forward primer (10 µM)	1	
Reverse primer (10 µM)	1	
Template cDNA	1	0.25 ng/µl
Final volume	**20**	

cDNA from different samples (embryonic day in which expression of target gene was the highest according to microarray data) were amplified in a DNA thermal cycler (MJ Research, UK) with the following programme in 30 cycles:

- Initial denaturation: 95°C for 3 minutes, 1 cycle,
- Denaturation: 95°C for 3 minutes,
- Annealing: gradient from 50°C to 70°C for 30 seconds,
- Extension: 72°C for 1 minute,
- Hold: at 72°C for 7 minutes and overnight incubation at 4°C

2.12.4 Quantitative PCR

Quantitative reverse transcription PCR (RT-qPCR) reactions were carried out in 0.1ml tubes (Corbett Research, UK) using a RotorGene 6000 (Corbett Research, UK). cDNA for all reactions was generated from the same amount of total RNA, with the same RT protocol (2.12.1). 2µl of cDNA was used in each reaction (individual tube). Samples from three separate RNA pools were run in triplicates for each primer set.

The 25µl reaction mixtures contained: 12.5µl of SYBR® Green JumpStart™ Taq Ready Mix™ (Sigma, UK) (20 mM Tris-HCl pH 8.3, 100mM KCl, 7mM $MgCl_2$, 0.05ng/µl Taq DNA Polymerase, 0.4mM of each dNTP; dATP, dCTP, dGTP, dTTP), 0.5µl of forward primer (final concentration 0.2µM), 0.5µl of reverse primer (final concentration 0.2µM), 9.5µl H_2O and 2µl of cDNA template.

Samples for standard curve were prepared as serial dilutions of cDNA sample to the final concentration 0.5ng/µl reaction, 0.25ng/µl reaction, 0.125ng/µl reaction. Amplification of a number of housekeeping genes was performed as the internal control. For negative controls similar amounts of total RNA of each sample were subjected to the cDNA synthesis protocol without reverse transcriptase. Standards, negative controls and NTC (no template control, reverse transcriptase substituted with RNase-free water) were run simultaneously with samples in all experiments.

The RT-qPCR was initiated with 3 minutes denaturation step at 95˚C. Initial denaturation was followed by 40 cycles at 95˚C for 30 seconds, annealing at 58˚C for 30 seconds, and a 1-minute extension at 72˚C. Cycling was followed by a 7 minutes hold at 72˚C. The specificity of the amplified RT-PCR products was verified by melting peak analysis (30-95˚C) after 40 cycles and confirmed on 2% agarose gel (2.14.5).

2.12.5 DNA agarose gel electrophoresis

PCR and real-time PCR products were run on 2% agarose gel prepared with RNase-free 1XTAE buffer (40mM Tris acetate pH 8.5 and 1mM EDTA). The gel was prepared by dissolving 2g of agarose (Sigma-Aldrich, UK) in 100 ml of

1XTAE buffer and heated in a microwave. 4µl ethidium bromide solution (10mg/ml) was added to the gel. Gels were cast and left to cool at room temperature. 2.5µl of 5X loading buffer (Qiagen, UK) was added to 10µl of each sample before loading on the gel. The gel was then run on a BioRad gel electrophoresis apparatus at 80V for 1 hour in 1XTAE buffer. Subsequently, the gel was visualised by placing on a UV transilluminator (UVP, UK) and and image of the gel was captured using a VisiDoc-It System (UVP, UK) equipped with a thermal printer (Sony, Japan).

2.12.6 Analysis of RT-qPCR

The threshold cycles (Ct) were calculated using RotorGene 6000 Series software (Corbett Research, UK). Ct values were transformed to quantities using the comparative cycle threshold (Ct) method (delta Ct). Normalisation was performed against the two most stable housekeeping genes; G6PDH (6-phosphate dehydrogenase) and UB (ubiquitin). Housekeeping genes stability was evaluated using the software programmes; NormFinder (*www.wzw.tum.de/gene-quantification/*), geNorm v.3.5 (*http://medgen.ugent.be/~jvdesomp/genorm/)* and BestKeeper v.1 (*http://medgen.ugent.be/~jvdesomp/genorm/).*

Statistical analysis was performed using SPSS package (v.12). Data was checked for normality (Shapiro-Wilk test) and homogeneity of variances (Lavene test). One-way ANOVA with an appropriate post-hoc test (Tukey or Dunnett T3) was performed for data with normal distribution. Otherwise, Kruskal-Wallis with post-hoc test was used to identify significant differences within the data set.

RESULTS

CHAPTER THREE

Morphology and epithelial cell differentiation in the developing corneal epithelium

MORPHOLOGY AND EPITHELIAL CELL DIFFERENTIATION IN THE DEVELOPING CHICKEN CORNEAL EPITHELIUM

3.1 Introduction

The cornea, being the primary refractive element of the eye, is transparent and forms the avascular anterior part of the eye globe. It consists of epithelial, stromal and endothelial layers, with each layer separated by a specialised basement membrane. The epithelium, a non-keratinised outermost multilayer, rests on a basement membrane adjacent to Bowman's layer (characteristic feature of primate and avian corneas). It has unique properties that prevent the entry of harmful substances into the intraocular tissue (Pajoohesh-Ganji and Stepp, 2005).

The development of avian cornea has been studied extensively by various authors (Hay, 1979; Hay and Revel, 1969; Coulombre and Coulombre, 1958; Coulombre and Coulombre, 1964; Trelstad, 1970) using light and electron microscopy for the investigation of ultrastructure and morphology. Despite detailed insight into components of the corneal epithelium at the molecular level, few quantitative analyses have been performed with respect to morphological changes during development.

In this chapter, the Hamburger-Hamilton (HH) stages description is used. Hamburger and Hamilton staged chicken embryo development in 1951 and aimed to provide a detailed description of developmental events in chronological order, starting from laying of the egg and ending with a newly hatched chick. A complete register of HH stage series in comparison to the days of incubation (embryonic days, ED) is shown in Appendix I.

3.2 Aim

The aim was to understand the pattern of changes in epithelial cell morphology and differentiation during corneal development in order to identify critical developmental time-points.

3.3 Experimental design

To evaluate changes in overall morphology of the developing chick corneal epithelium, in particular cell shape and number of cell layers, standard procedures for Haematoxylin and Eosin staining on paraffin sections of chick corneal epithelia from ED4 to ED21 (<12 hours posthatch) were performed as described in section 2.3. As described, corneas were dissected every second day, except for ED20, which is just prior to hatching.

To determine epithelial differentiation, frozen sections of chicken corneas (n=3 per stage) at different developmental stages (from ED4 to posthatching) were immunolabelled using antibodies raised against pan-CK (AE1/AE3) and CK3 (CK3, clone AE5) as described in section 2.5.3.1. AE1/AE3 antibody has previously been shown to recognise two mutually exclusive families of keratins (Tseng *et al.*, 1982) which includes subfamily A (acidic keratins: 10, 13, 14, 15, 16, 19, of molecular weights 56.5, 54, 50, 48, 40 kDa, respectively) and subfamily B (basic keratins: 1, 2, 3, 4, 5, 6, 7, 8 of molecular weights 65, 67, 64, 59, 58, 56, 54 52 kDa, respectively).

The corneal epithelium was examined by dividing it into three regions: the centre, periphery and limbus (Figs. 3.1a, b). The number of cell layers was quantified at each time-point in triplicate from three different specimens. Three fields of view for each region were analysed.

Finally, Western blotting was completed to quantitatively examine the levels of expression of CK3, as a measure of chick corneal epithelial differentiation during development, as described in section 2.9. For this purpose collection of samples started from ED6 onwards, excluding ED4, which did not provided efficient amount of protein sample.

Statistical analysis between embryonic day independent groups were performed using parametric analysis (One-way ANOVA) followed by the appropriate post-hoc test (Dunnett T3 test), since data was normally distributed (as determined by Saphiro-Wilk test) and showed unequal variances between samples (Lavene`s test) (see Appendix III). Pearson correlation was used to

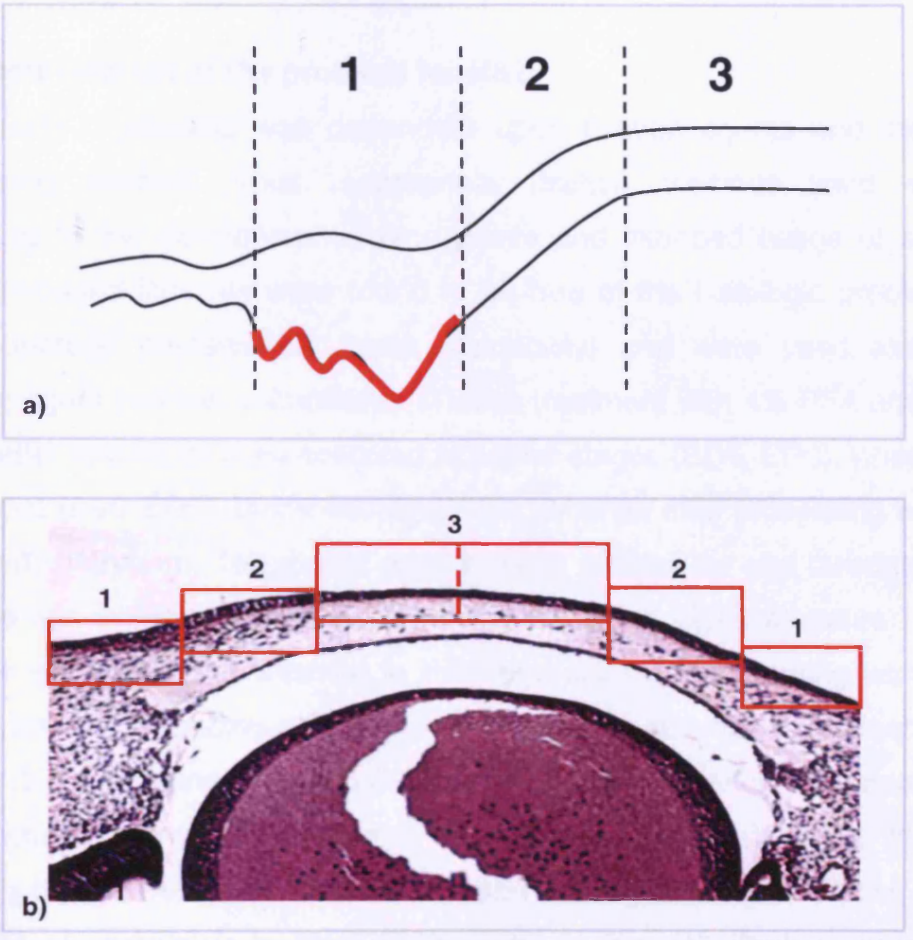

Figure 3.1 A schematic picture **(a)** and image **(b)** of the corneal epithelium showing the three regions examined: limbus (1), periphery (2), centre (3). x 5.

test tendency of values Y (i.e. number of cell layers) towards value X (developmental stage) (section 2.8 and 2.9.13).

RESULTS

3.4 Histological study of chicken corneal epithelial development

3.4.1 Optimisation of the protocol for H&E

The quality of staining was dependent upon fixation agents and the tissue processing method. Thus, appropriate fixation methods were selected according to the developmental time points and intended usage of sections. Formalin-based fixatives were found to be free of the histologic problems (ie. poor structural preservation, weak stainability) and were used along with clearing agent (xylene, chloroform). Tissue treatment with 4% PFA and xylene gave better results for eyes collected at earlier stages (ED4, ED6), whereas, for older eyes (from ED8), better sections were obtained after processing with 10% NBF and chloroform. The above combinations of fixatives and clearing agents ensured non-wrinkled, flat sections without, crushing tissue structure. Shorter fixations with additional washing in PBS and subsequent clearing with xylene worked better for specimens with newly developed structures (as described in chapter 2.3.1). Xylene, is considered to be used to clear small samples in a rapid schedule and is easily and quickly replaced by paraffin, therefore, ensuring that soft tissue is not overexposed to reagents. The number of steps and time of immersion in alcohols involved in the dehydration process was optimised to prepare the tissue for embedding.

As mentioned above, 10% NBF was used for fixation of eyes from ED8 to ED21. Using this solution ensures that the pH of the fixative remains constant before and during fixation. The 48 hours immersion with optimally buffered solution (pH 7.2) allows exchange with tissue fluid during the fixation process and thorough penetration of the tissue structure. Additionally, chloroform, being gentle on tissue with little hardening did not appear to affect structural integrity of the tissue.

For studies of tissue morphology, paraffin sections were chosen, as the tissue structure was better maintained than in frozen sections, and intense colour staining with H&E was observed (Fig. 3.2). Counterstaining with eosin (acidic dye), allowed visualisation of the basic parts of the cells, in the cytoplasm, haematoxylin stained cell nuclei, as a result of binding to lysine residues of nuclear histones in acidic conditions.

3.4.2 Morphology of the developing corneal epithelium

Changes in epithelial morphology throughout development were observed in cross-sections of H&E stained chicken corneas (Fig. 3.3). These changes included alterations in the number of cell layers and the morphology of cells in the different layers of the epithelium. One-way ANOVA demonstrated significant differences ($p \leq 0.05$) in the number of cell layers between 10 independent groups (ED4 to ED21) within each region, and also between regions within each group, except for ED4, ED10, ED12. Test results are shown in Appendix III. Values of the average number of cell layers at different developmental stages are shown in Table 3.1.

Table 3.1 Average number of cell layers at different developmental age

ED		4	6	8	10	12	14	16	18	21
Limbal epithelium	*Mean*	2.0	2.2	2.4	2.5	2.8	3.4	4.7	5.0	6.4
	±SD	±0	±0.4	±0.5	±0.5	±0.5	±0.5	±0.4	±0.5	±0.6
Peripheral epithelium	*Mean*	1.8	2.0	2.1	2.2	2.5	3.4	3.9	4.9	5.5
	±SD	±0.3	±0.1	±0.3	±0.4	±0.5	±0.5	±0.5	±0.6	±0.6
Central epithelium	*Mean*	1.8	2.0	2.1	2.3	2.8	3.8	4.6	5.3	5.7
	±SD	±0.3	±0.1	±0.1	±0.4	±0.5	±0.4	±0.4	±0.4	±0.4

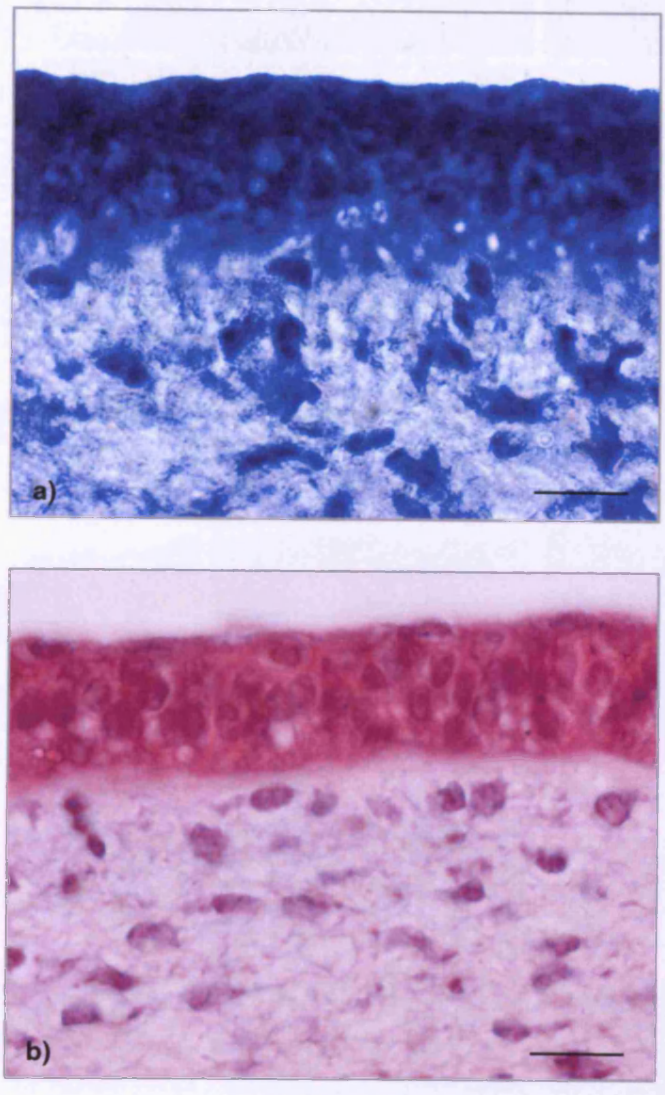

Figure 3.2 Frozen **(a)** and paraffin **(b)** cross-sections of the developing chick corneal epithelium at ED16 stained with H&E. Haematoxylin strongly stained frozen sections allowing morphological observations. Eosin stained frozen sections very weakly in comparison to paraffin. Scale bar = 100μm. x 100.

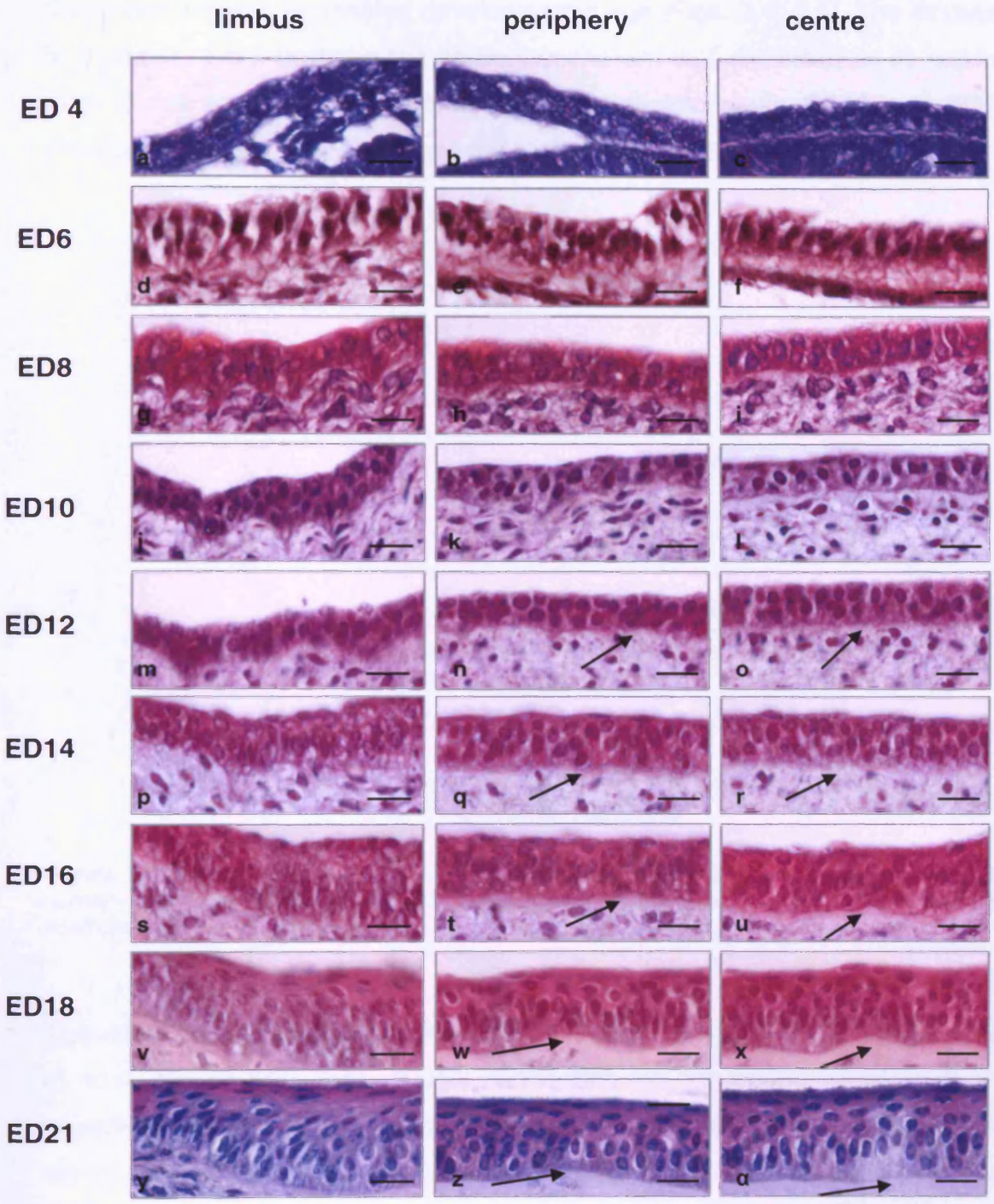

Figure 3.3 H&E staining of cross-sections of the developing chick corneal epithelium. Panels show different regions in the corneal epithelium (limbus, centre, periphery) at ED4-ED21. Between ED4 **(a-c)** and ED10 **(j-l)** the epithelium was two cells thick. Epithelial stratification began at ED10 **(g-i)** and was clearly seen at ED14 **(p-r)**. By ED18 **(v-x),** the epithelium consisted of 5 to 6 cell layers. At ED21, the posthatched epithelium was composed of 6 to 7 cell layers **(y-α)**. Arrows indicate Bowmans layer in the central and peripheral epithelium. Scale bar = 100μm. x 100.

An increase in the number of cell layers in the corneal epithelium was demonstrated with increasing developmental age (Figs. 3.4, 3.5). The increase in number of cell layers in the corneal epithelium was significant in all regions from 2 cell layers at ED4 up to 7 in later development; ED18 and ED21 (Pearson correlation r=0.891, p≤0.01, n=3) (Figs. 3.3, 3.5) (Appendix III).

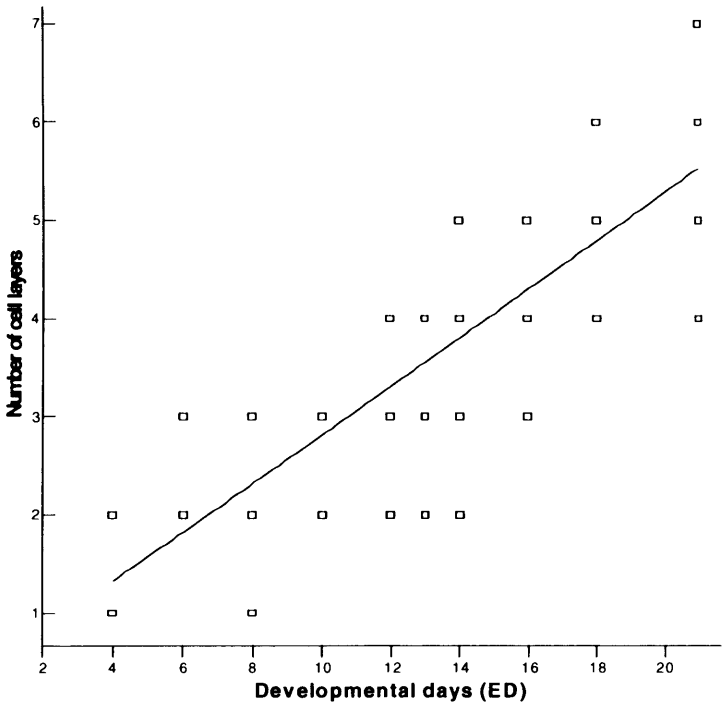

Figure 3.5 Number of cell layers in chick corneal epithelium throughout development. The number of cell layers increased significantly with increasing developmental age (correlation coefficient r=0.891 p≤0.01, n=3).

The entire corneal epithelium, was two cells thick from ED4 (HH23) (Figs. 3.3a-c) to ED8 (HH34) (Figs. 3.3g-i), consisting of one round basal and one superficial cell layer throughout the entire epithelium. By ED10 (HH36) two cell layers remained in the central epithelium (Fig. 3.3k,l), but an additional layer was observed in the limbus (Fig. 3.3j). Differences in the number of cell layers between ED4, ED6 and ED8 were not statistically significant for central and peripheral regions, whereas, in the limbal epithelium significant differences were demonstrated between ED4 and ED8 (p≤0.05).

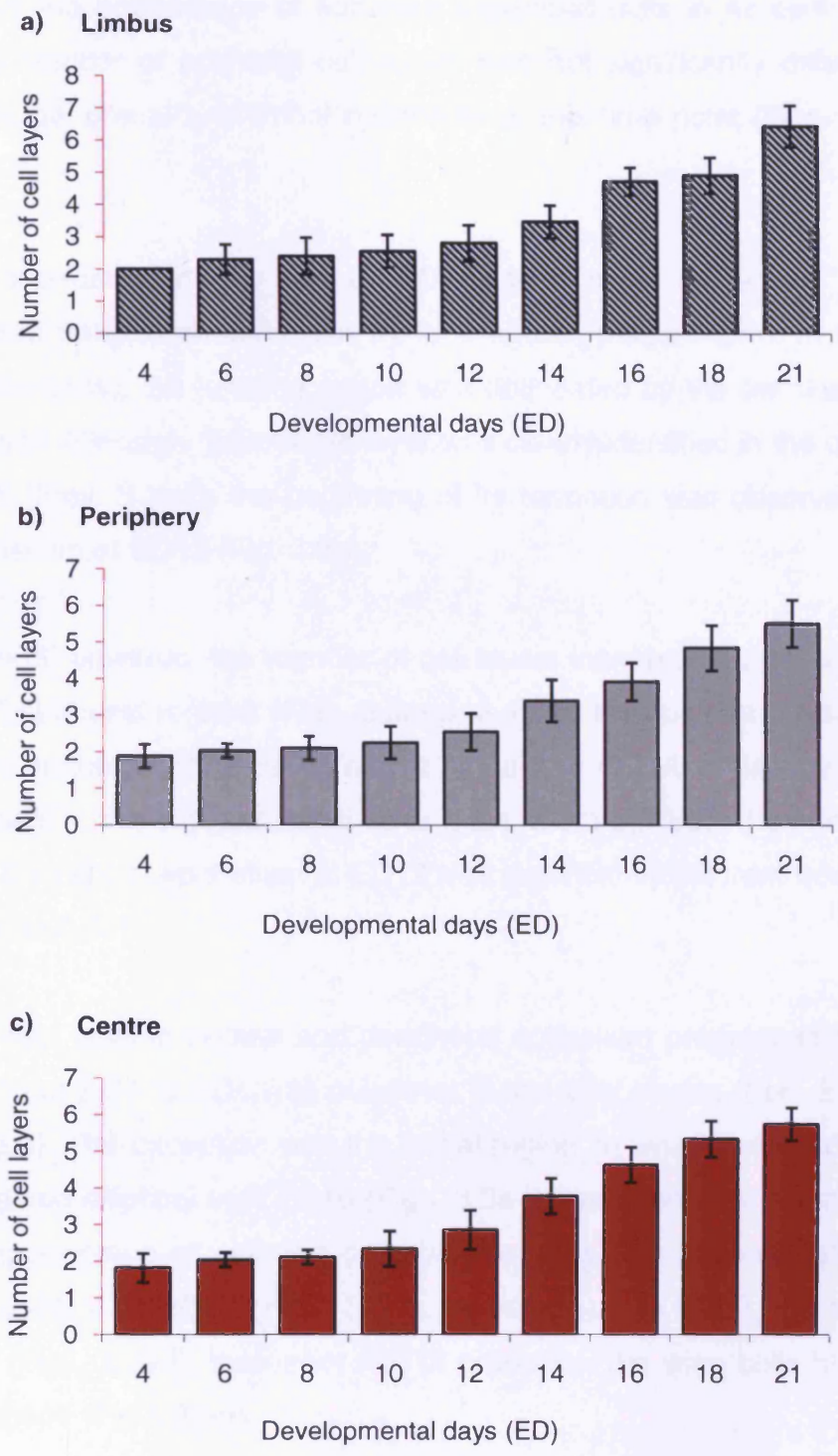

Figure 3.4 Changes in the number of epithelial cell layers throughout chick corneal development. Results obtained from three experiments were combined to give the average number of cell layers for each developmental stage. Error bars displayed represent the standard deviation from the mean. **(a)** Limbus: epithelial cell layers increased from 2 at ED4 to 6-7 by ED21, **(b)** Periphery: increased from 2 at ED4 to 5-6 layers by ED21, **(c)** Centre: from two at ED4 to 5-6 by ED21 (n=27).

From ED10 onwards, the outermost cell layer showed signs of early stratification with the appearance of flattened superficial cells in all epithelial regions but the number of epithelial cell layers was not significantly different between central, peripheral and limbal epithelium at this time point (Figs. 3.4, 3.5).

In earlier developmental stages (up to ED10) the limbal epithelium was distinguished from peripheral epithelium by its irregular, pleated form. In later stages (ED12 onwards), the junction region was delineated by the termination of Bowman's layer. Although, Bowman`s layer was clearly identified in the chick cornea at ED16 (Figs. 3.3t,u), the beginning of its formation was observed in the central epithelium at ED12 (Fig. 3.3o).

From ED12 (HH38) onwards, the number of cell layers increased from three to four layers in all epithelial regions (Figs. 3.3m-o, 3.4). All regions demonstrated the beginning of epithelial stratification at this stage with definitive flattening of the superficial cells in the outermost cell layer (Figs. 3.3m-o). Also, the number of cell layers in the central epithelium at ED12 was significantly different from all embryonic days ($p \leq 0.05$).

The shape of basal cells in central and peripheral epithelium progressed from an oval shape (from ED4 to ED13) to columnar in the later stages (from ED14 to ED21) (Fig. 3.3). The exception was the limbal region, in which the shape of basal cells remained elliptical until ED10 (Figs. 3.3a-j), and thereafter columnar in shape. The appearance of wing-like cells between basal and superficial cell layer was also evident at ED10 (Figs. 3.3j-l). However, up to ED12, the wing cells were oval (Figs. 3.3a-j), thereafter (ED14 onwards), the wing cells had a more irregular shape (Fig 3.3p-α).

At ED14 (HH40), compared to ED12, one or two additional layers of suprabasal cells were observed throughout the epithelium (Figs. 3.3m-r, 3.4). The number of cell layers in the central and limbal region at ED14 was significantly different from other embryonic days, but not from ED13 ($p \leq 0.05$). These changes

coincided with the appearance of Bowman's layer, which appeared to be fully formed by ED16 (HH42), where it clearly separated the stroma and epithelium (Figs. 3.3t-u). The latter consisted of four to five epithelial cell layers at this stage (Figs. 3.3s-u) and showed significant differences in all regions when compared to earlier and later time points ($p \leq 0.05$), with exception of the limbal epithelia at ED18.

By ED18 (HH44), the epithelium, from its superficial aspect, included one-to-two flattened superficial cell layers, three to five suprabasal wing-like cells and a single layer of columnar shaped basal cells (Figs. 3.3v-x). All cells appeared to be in close proximity to each other. The morphology of the epithelium at ED18 was similar to that observed posthatch ED21, except that posthatched epithelium had one or two additional suprabasal wing cell layers observed in all epithelial regions (Figs. 3.3y-α). Both ED18 and posthatch ED21 were statistically different in epithelial cell layer number to each other and the earlier stages within epithelial regions except for central epithelium ($p \leq 0.05$).

3.5 Epithelial cell differentiation in corneal chick development

3.5.1 Optimisation of the protocol for markers of epithelial differentiation

In order to optimise the protocol for immunofluorescent labelling with monoclonal antibodies AE1/AE3 and AE5, a number of different pretreatments were used. Immunolabelling with antibodies on both paraffin and frozen sections was carried out to determine which provided optimal labelling. An example is shown in Figure 3.6. It was observed that frozen sections provided better immunofluorescent labelling with background staining greatly reduced, when compared to that in wax sections. Although, wax is the most widely used embedding medium in routine histology, and paraffin sections produce satisfactory results for the demonstration of the majority of tissue antigens, in some cases in this study a high background was observed. Additionally, aldehyde fixation might be harmful for some antigens, and under this condition, much better results are obtained when tissue is rapidly fresh frozen in liquid nitrogen and cut with a cryostat without infiltrating with sucrose. Cryostat

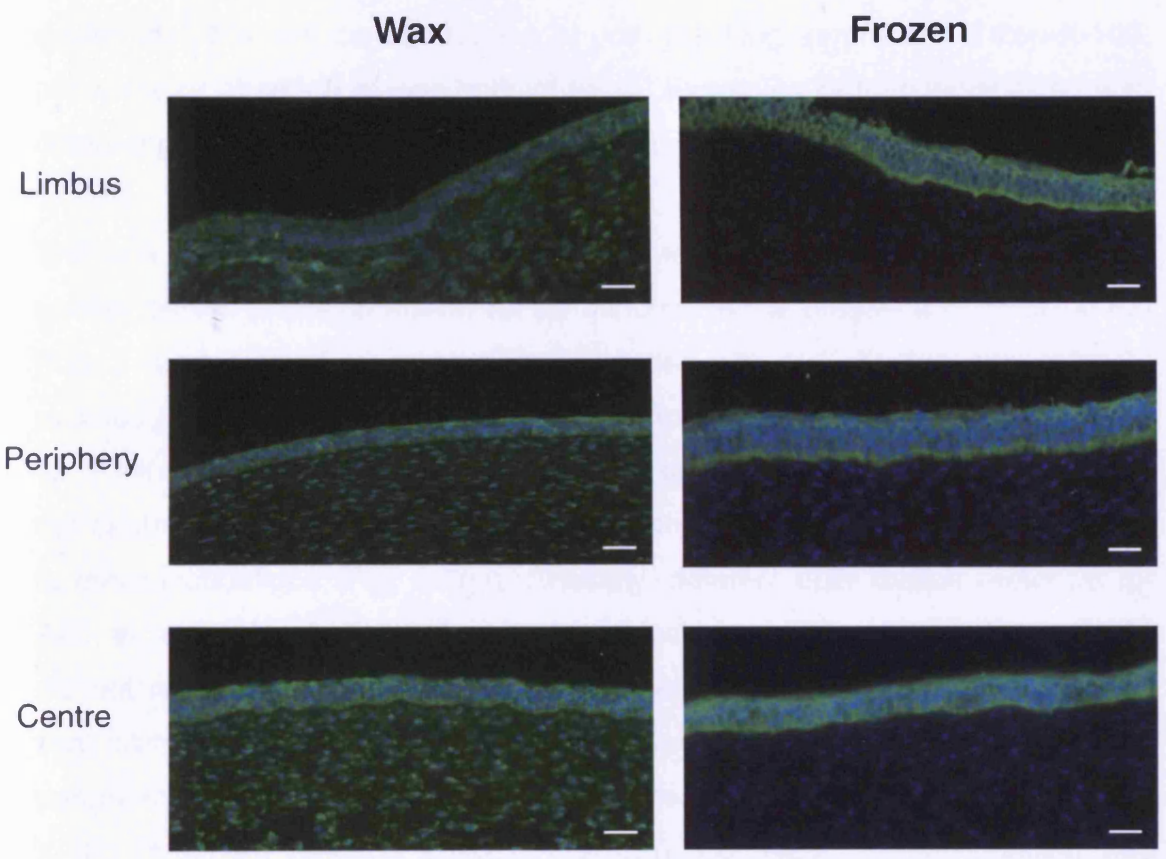

Figure 3.6 Comparison of immunolabelling for mAb AE1/AE3 (green) in paraffin (left panel) and frozen (right panel) sections of chicken cornea at ED16. mAb AE1/AE3 binding sites were labelled green (Alexa Fluor 488 conjugated secondary antibody) and cell nuclei was stained blue by Hoechst 33342. Labelling in frozen sections provided a signal of better quality with reduced background staining. Scale bars = 20μm. x 20.

sections are not processed through organic solvents or high heat, which can destroy the antigenicity.

Further modifications of the protocol included: different dilutions of primary antibodies, different concentrations of both blocking serum and Triton-X-100, presence or absence of one/both of them. Examples of immunolabelling with different parameters for AE1/AE3 and AE5 are shown in Figure 3.7.

The lack of immunofluoresence was observed in sections incubated with 5% donkey serum (blocking agent) for 20 minutes, in the presence of Triton-X-100 (Fig. 3.7a-c) as well as, in sections incubated with 10% donkey serum for 20 minutes and Triton-X-100 (Fig. 3.7d-f). Sections treated with 0.1% Triton-X-100 for 5 minutes and with 5 % blocking agent for 20 minutes revealed staining in the central and peripheral epithelium, with the reduced background compared to other incubations (Fig. 3.7g-i). Similarly, different optimisation protocols for AE5, including incubation with or without blocking agent and 0.1% Triton-X-100 did not result in appearance of AE5-positive cells (Fig. 3.7j-r). Therefore, the final pretreament protocol for AE1/AE3 immunolabelling included the following parameters: 5% blocking agent for 20 minutes, with the exclusion of the Triton-X-100 treatment (section 2.5.3.1, Fig. 3.8). For AE5, optimal labelling was obtained after pre-treatment with a 10% blocking agent for 20 minutes and 0.1% Triton-X-100 for 5 minutes (section 2.5.3.1, Fig. 3.9).

3.5.2 Immunolocalisation of a broad spectrum of cytokeratins (pan-CK, AE1/AE3 clone)

Immunolocalisation of pan-CKs was performed to evaluate cytokeratin distribution during chick corneal development, from ED4 to ED18 and ED21 (posthach <12 hours) epithelium. Frozen sections of chick cornea were labelled with mAb AE1/AE3, according to the protocol described in section 2.5.3.1.

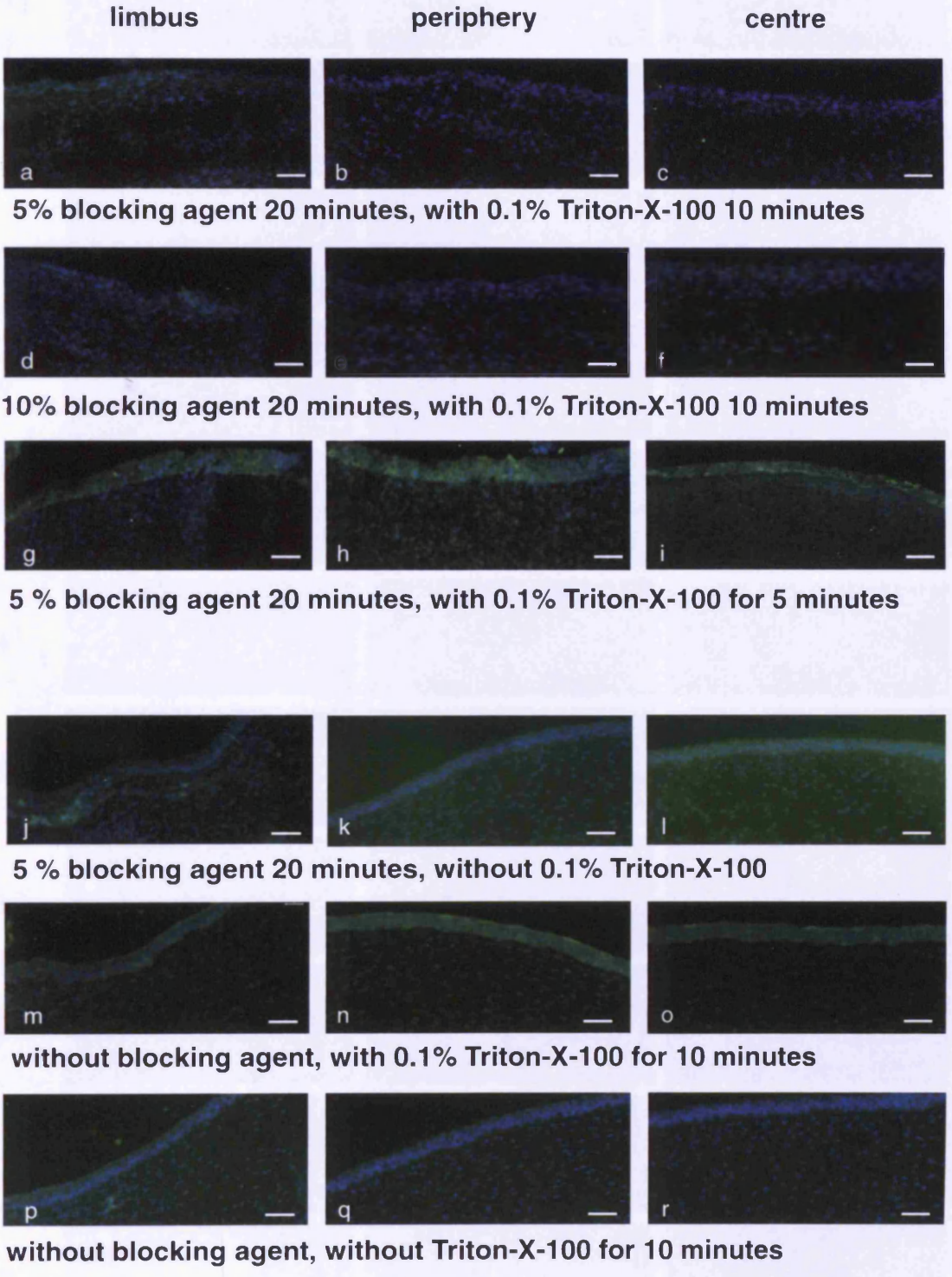

Figure 3.7 Comparison of the effects of different parameters on immunofluorescent labelling by mAb AE1/AE3 (1:100) (in ED12) and AE5(1:50) (in ED16) in different regions of chick corneal epithelium, on frozen sections. Columns represent three epithelial regions (limbus, periphery, centre). **(a-i)** sections labelled with AE1/AE3, **(j-r)** sections labelled with AE5. As blocking agent donkey serum was used in different concentrations. Scale bars = 20μm. x 20.

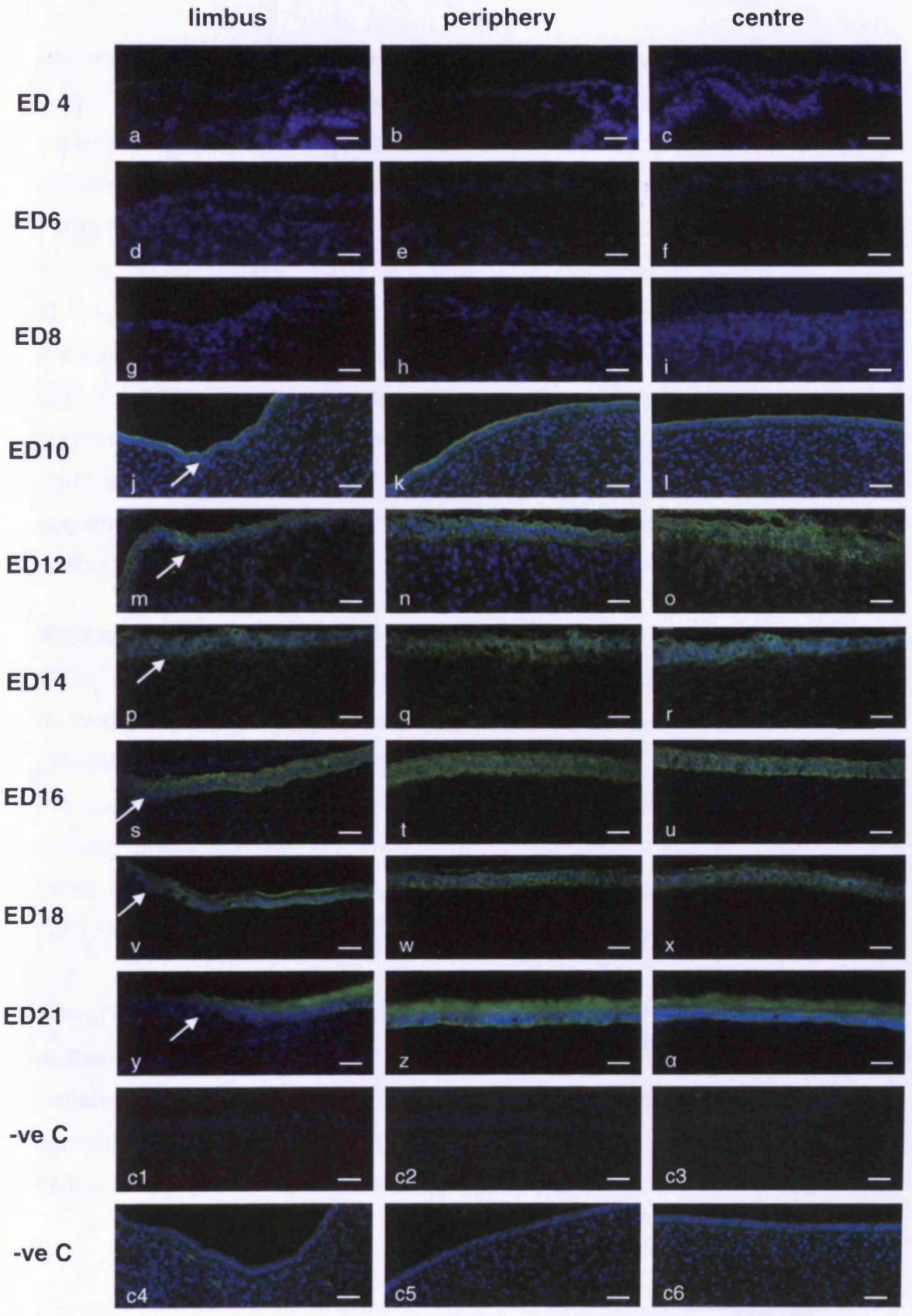

Figure 3.8 Pan-CK (AE1/AE3) immunolabelling of the developing chick corneal epithelium. Panels show different regions in the corneal epithelium (limbus, centre, periphery). Immunolabelling was absent in the epithelium from ED4 to ED8 **(a-i)**. At ED10 **(j-l)** and ED12 **(m,n)** staining was restricted to the superficial layers in the limbus and periphery. From ED16 onwards **(s-α)**, the entire corneal epithelium was labelled, with the exception of the limbal basal cells (indicated by arrows). Cell nuclei were stained blue by Hoechst 33342. Negative controls (ED12); mouse anti-GFP **(c1-c3)** and mouse IgG **(c4-c6)** show no staining in all regions **(c1-c3)**. Part of the eyelid is visible in figure **(o)**. Scale bars = 20µm. x 40 , c4-c6 x 20.

Immunofluorescent labelling was not observed between ED4 and ED8 (Figs. 3.8a-i). Pan-CK immuno-positive labelling was first observed at ED10, in the superficial cell layer throughout the corneal epithelium (Figs. 3.8j-l). By ED12, immunolabelling was present in the superficial layer in the limbal epithelium, in the peripheral epithelial basal cell layer, and throughout the whole thickness of the central epithelium (Figs. 3.8m-o). At ED16, the labelling pattern was similar to that observed at ED12 and ED14, except that, staining was also present in the subrabasal cell layers in the limbal epithelial region (Figs. 3.8s,u). By ED18 and in ED21 posthatch corneal epithelium, immunolabelling was restricted to suprabasal layers in the limbus, but observed throughout the central and peripheral corneal epithelium (Figs. 3.8p-α). Labelling was not observed in negative controls, mAb anti-GFP and mouse IgG applied in place of the primary antibody (Figs. 3.8c1-c6).

3.5.3 Immunolocalisation of cytokeratin 3 (CK3, AE5 clone)

CK3 expression in the developing chick epithelium was examined by immunostaining with mouse anti-human monoclonal antibody AE5 at different time-points (Fig. 3.9). CK3-positive cells were first observed at ED12 in the superficial cell layer of the limbal and peripheral epithelium, whereas, uniform labelling throughout the entire thickness of the central epithelium was noted (Figs. 3.9m-o). By ED14, additional labelling was observed in the basal cell layer of central and peripheral epithelium (Figs. 3.9q, r).

By ED16, immunolabelling was demonstrated in throughout the corneal epithelium with the exclusion of the limbal basal cells (Fig 3.9s-u). This labelling pattern remained constant in the ED18 (Fig. 3.9v-x) and posthatch ED21 corneal epithelia (Figs. 3.9y-α). Labelling was not observed in any corneal epithelial regions in negative control sections (Figs. 3.9c1-c6).

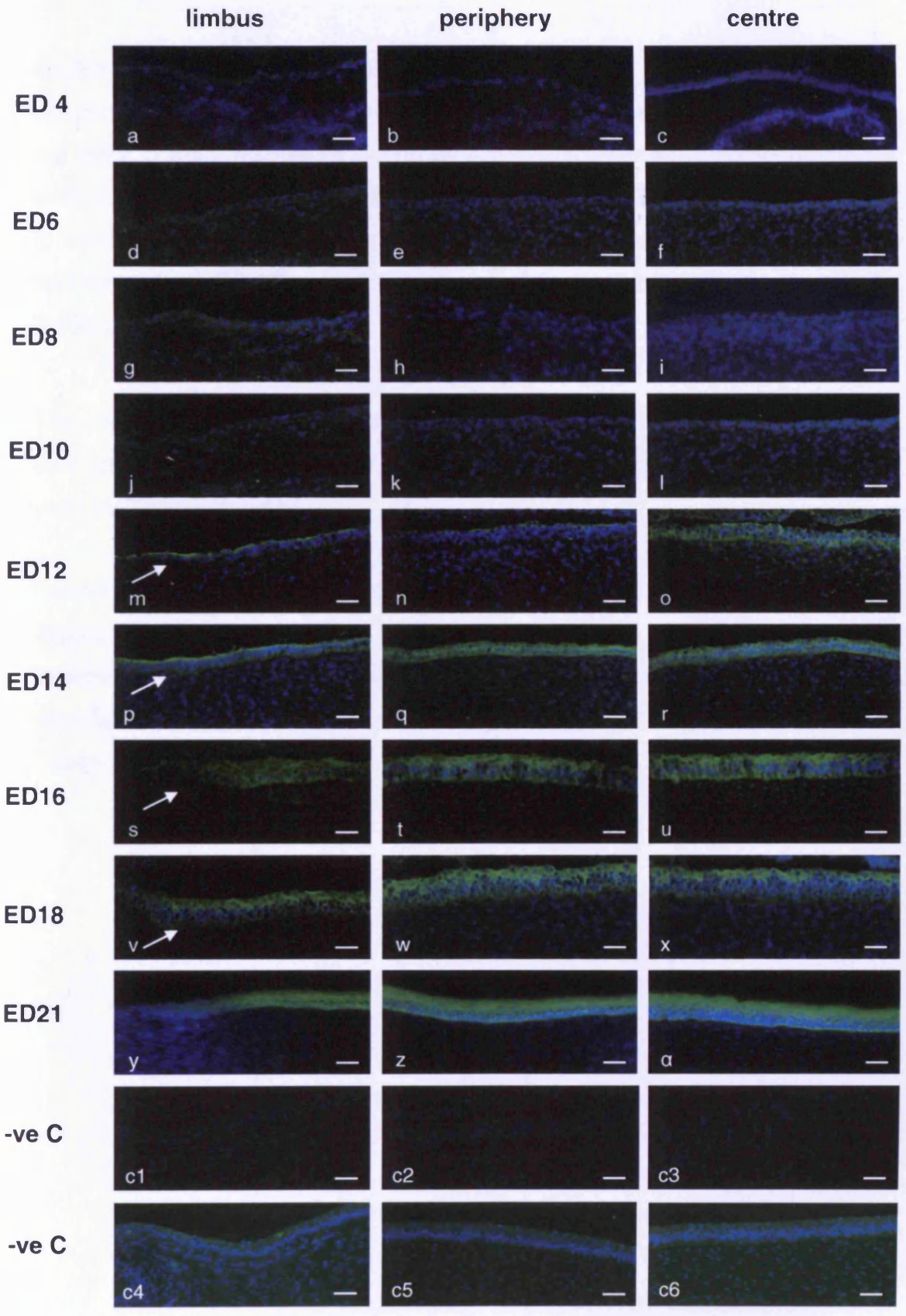

Figure 3.9 CK3 (AE5 clone) immunolabelling of chick corneal epithelium.
Panels show selected regions of corneal epithelium (limbal, peripheral, central), at ED6 to posthatch. CK3 expression in superficial cell layers of limbus and peripheral epithelium commenced at ED12 **(m, n)** and was maintained in the limbus by ED14 **(p)**. By ED14 staining was observed throughout epithelium in the peripheral **(q)** and central region **(m)**, AE5 positive cells were absent in basal cells of limbal epithelium at ED12 to ED18 (left panel, indicated by arrows). Cell nuclei were stained blue by Hoechst 33342 Negative controls (ED18); mouse anti-GFP **(c1-c3)** and mouse IgG **(c4-c6)** show no staining in all regions. Part of the eyelid is visible in figure **(o)**. Scale bars = 20μm. x 40.

3.5.3.1 Immunoblotting for CK3

Western blotting was performed to examine the expression of CK3 protein in the chick corneal epithelium during development. Eight developmental stages were evaluated: ED6, ED8, ED10, ED12, ED14, ED16, ED18 and ED21 (posthatch <12 hours). CK3 protein expression was confirmed in the corneal epithelium from ED10 onwards by immunodetection of 70 kDa bands (Figure 3.10a).

The specificity of the CK3 bands was monitored by enclosed negative controls, such as without primary antibody, or with the mouse IgG. CK3 protein was not detected in control lanes.

Densitometric analysis was carried out to identify differences in protein expression throughout epithelial development. An increase in the CK3 expression in the corneal epithelium was demonstrated with increasing developmental age (Pearson correlation r=0.891, p≤0.01, n=3) as shown in Figure 3.11.

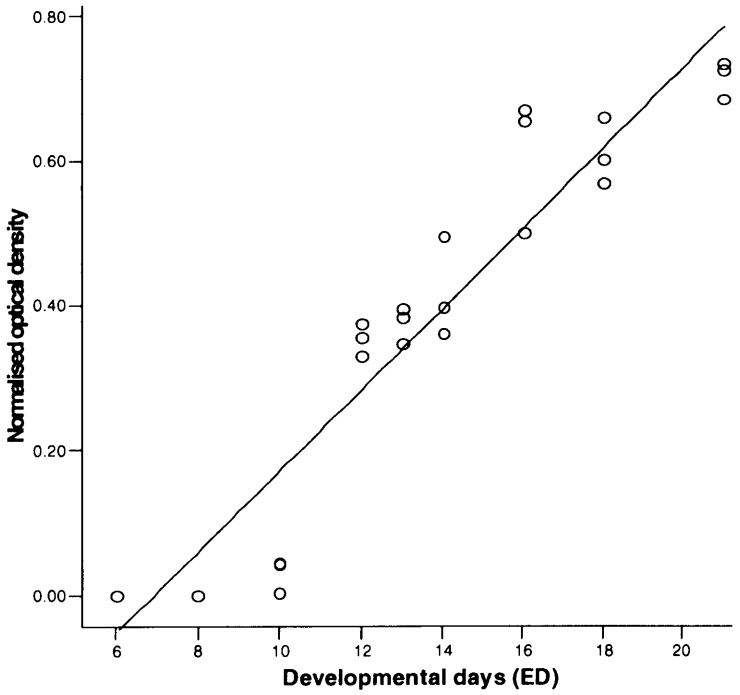

Figure 3.11 Normalised optical density of CK3 bands in developmental time points of chick corneal epithelium, ED6 to ED21. The expression level of CK3 protein increased significantly with increasing developmental age (correlation coefficient r=0.951 p≤0.01, n=3).

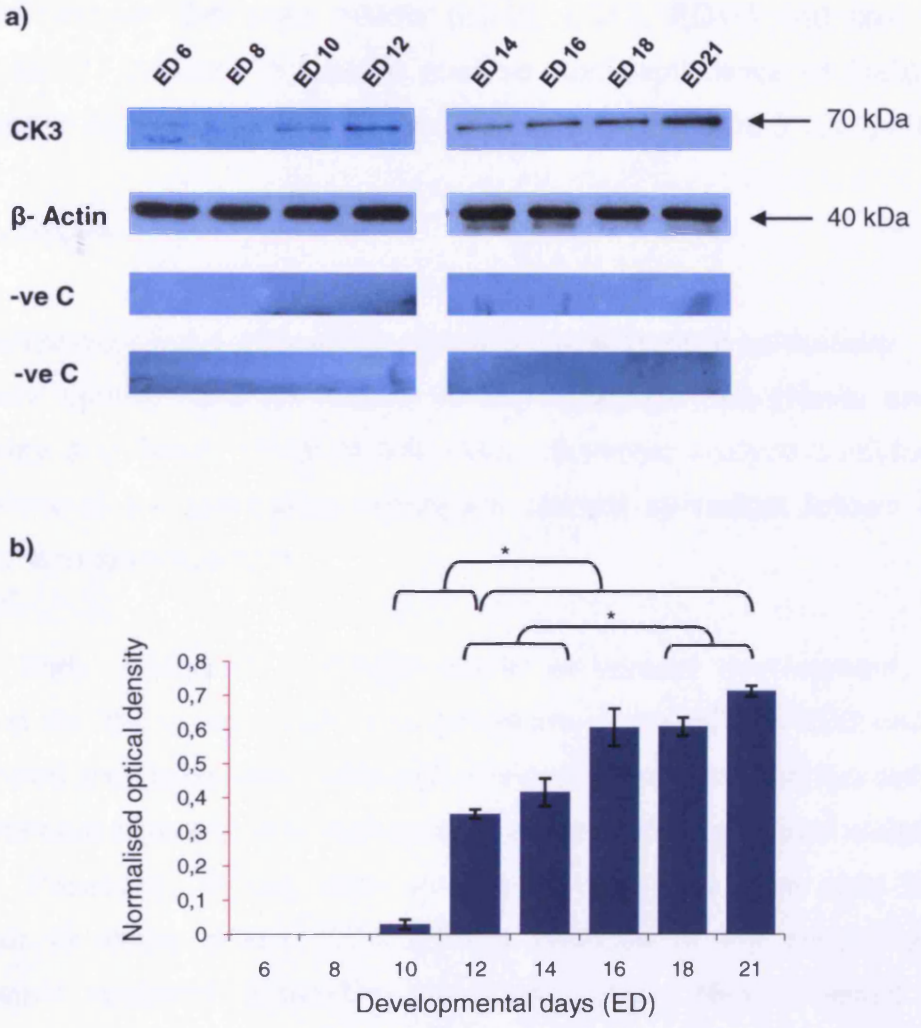

Figure 3.10 Western blot detection of CK3 protein in developing chick corneal epithelium. 10µg of protein per sample were loaded to each well electrophoresed, transferred to nitrocellulose membrane and incubated with anti-CK3 antibody. **(a)** A specific band of approximately 70 kDa was observed for CK3 from ED10, onwards. β-Actin (used as housekeeping protein) was detected as a band of 40 kDa. Negative controls (omission of the primary antibody and mouse IgG substitution for primary antibody) did not detect CK3 specific bands. **b)** Densitometric analysis of immunoblots. Results are representative of three data sets. Data were normalised to β-Actin and presented as mean ± SEM, *p≤0.05.

Low, but significant ($p \leq 0.05$) levels of CK3 expression were observed at ED10 (Fig 3.10a,b). Thereafter, levels of protein expression increased, reaching the highest level at ED21 in posthatched corneal epithelium. Statistically significant differences in protein expression were identified between ED10 and later developmental days ($p \leq 0.05$) (Fig. 3.10b). Also, significance in expression was revealed between the three middle (ED12, ED13, ED14) and final stages (ED18, ED21) ($p \leq 0.05$). Statistical analysis and significance of findings are presented in Appendix III and indicated with asterisk in Figure 3.10b ($p \leq 0.05$).

3.6 Discussion

3.6.1 Morphological profile of developing chick corneal epithelium

The chick cornea develops rapidly during embryogenesis (Revel and Hay, 1965; Hay and Revel, 1969). In this study, histologic analysis confirmed that morphology of the developing embryonic corneal epithelium follows a strict temporal and spatial pattern.

In this study, during the epithelial phase of corneal development, it was observed that the corneal epithelium transformed from ED4 to ED6; cells were reorganised and compacted. Although, the epithelium remained two cells thick; two additional layers in the cornea (the stroma and the endothelium) were formed. Previously, it has been postulated, that the basal cells become columnar in shape around ED4 (HH22) because of the accumulation of cytoplasmic secretory organelles (Hay and Revel, 1969; Trelstad 1970). However, in our studies, at these time points, basal cells shape appeared oval until ED10 in the limbal region, and basal columnar cells were not observed until ED14 in the peripheral and central regions. To precisely answer the question about shape of basal cells, measurements of cells diameters, along with confocal and/or electron microscopy studies to observe the three dimensional cell would be beneficial, as cells shape observed could also affected by sectioning angle.

The next major event evident during corneal epithelial development was the formation of Bowman`s layer and the beginning of epithelial stratification. In

avian embryos, Bowman`s layer derives from the outermost part of the primary stroma that remains as an acellular ECM after completion of invasion by the fibroblasts (by ED5.5-6) (Hay *et al.*, 1979) and in this form was observed by ED14. Presumptive Bowman`s layer formation was noted at ED12, and from ED14, onwards could be clearly distinguished between the epithelium and stroma, terminating at the border of the peripheral and limbal epithelium. Also, an increase in its thickness was observed from ED14 onwards.

Some controversies exist with respect to the presence or lack of Bowman`s layer in the corneas of lower (rodents) and higher mammals (i.e. canine, cattle). While it had been shown that Bowman`s layer is absent in rat (Jakus, 1954), bovine (Tanimura, 1977), cat and dog (Kafarnik *et al.*, 2007), other studies reported the existence of non-distinct, thin (approximately 1 to 3μm) and homogenous postepithelial layer that separates substantia propia from basal surface of epithelium in these species (Hayashi *et al.*, 2002).

Stratification (appearance of wing-like cells in the middle layers and flattening of the superficial cells) began in the limbus and was observed in all epithelial regions from ED12 (in limbus from ED10). Earlier studies, consistent with this observation, demonstrated that the period in which the avian corneal epithelium begins the process of stratification and maturation coincides with the time when the primary stroma reaches its narrowest width (between ED10 and ED14) (Hay and Revel, 1969; Chaloin-Dufau *et al.*, 1990). The processes of epithelial stratification and maturation result from complicated interactions between corneal structures and their internal components, which involve changes in the cytoplasm of epithelial cells; microvilli appear and reorganise, desmosomes multiply, and the pattern of GAGs changes (Meier, 1977; Dodson and Hay, 1971; Coulombre and Coulombre, 1964; Hay and Revel, 1969; Waggoner, 1978).

The corneal epithelium appeared to be fully formed by ED18 with no significant changes at ED21 in the posthatched cornea, in which the corneal epithelium contained five to seven cell layers. Montiani-Ferreira and coauthors (2004) showed that the cornea continues to undergo maturation in newly hatched

chick. Posthatching, an initial decrease in corneal thickness was observed until 12 days of age, which thereafter increased until 70 days, when a plateau was reached (Montiani-Ferreira *et al.*, 2004). The initial decrease in corneal thickness was possibly related to the maturation of the corneal endothelial cell function and/or rearrangements in composition in the fine structure of keratan sulphate GAGs chains in the stroma, whereas, the later increase was likely due to the general growth of the eye (Dunlevy *et al.*, 2000). The same initial pattern of corneal thickness development was observed in humans and dogs, but the unique feature of the development of the central corneal thickness in chicks was that after reaching plateau it did not significantly changed for the remainder of the study period (450 days of life) (Autzen and Bjornstorm, 1989; Portellinha and Belfort, 1991; Montiani-Ferreira *et al.*, 2003; Montiani-Ferreira *et al.*, 2004). Despite postnatal maturation processes in the cornea, it was suggested that the epithelium, being the first developed component of the cornea, did not undergo additional changes in the number of cell layers and type of cells after hatching. However, scanning electron microscopy studies demonstrated changes in the anterior epithelial surface in newborn chicks; the cell textures ranged from occasional surface microvilli to smooth surfaces (Waggoner, 1978). This was in contrast to the embryonic stages when all the surface cells had the same appearance and demonstrated abundant microvilli. Different surface textures resulted from changes in the cell membrane as a reflection of the state of differentiation or senescence and desquamation.

In this study, it has been observed that the avian limbal epithelium consisted of an additional one to two cell layers when compared to other regions (centre and periphery). Similarly, in human corneas at the limbal zone, the corneal structure changes. The epithelium thickens and forms epithelial pegs made up of approximately ten cell layers instead of the five to six layers observed in the central cornea (Takacs *et al.*, 2009). The increase in number of cell layers (thus thickness) in limbal epithelium is a result of its anatomical properties. The basement membrane of the limbus is undulating with 'pegs' of stroma extending upwards and fenestrated, forming Palisades of Vogt; the stem cell niche (Gipson, 1989; Li *et al.*, 2007; Dua *et al.*, 2005; Shanmuganathan *et al.*, 2007).

As mentioned earlier, the cornea is composed of several layers from the epithelium through to the endothelium i.e. epithelium, epithelial basement membrane, Bowman`s layer, substantia propria, Decemet`s membrane, and endothelium (Hayashi *et al.*, 2002). Previous studies have revealed morphological differences in corneas amongst species (Jakus, 1954; Pfister, 1973; Hayashi *et al.*, 2002; Collin and Collin, 2006; Zhao *et al.*, 2006; Kafarnik *et al.*, 2007). Undoubtedly, the avian corneal morphology shows high similarity to human. Similarities include the process of corneal formation in development (i.e. two waves of mesenchymal cell migration to form a primary stroma). Most importantly the avian corneas reflect similarities in corneal structure. The number of epithelial cell layers in both adult species is comparable in the central corneal epithelium; five to seven layers in chick epithelium, six to eight in human. Additionally, Bowman`s layer in the chick cornea presented as an acellular layer with homogenous reflectivity and structure is similar to those of primates (Kafarnik *et al.*, 2007).

In comparison to mammals, the avian group features some structural differences. One apparent difference is corneal thickness. The chicken cornea in its mature state is approximately 200µm thick (with approximately 30µm epithelium) (Hay *et al.*, 1979; Montiani-Ferreira *et al.*, 2004), which amounts to approximately one third of the human cornea`s thickness (approximately 600 µm, thickness of epithelium approximately 50µm) (Gipson, 1994). Another noticeable difference was the morphology of epithelial wing cells which were much larger, with cell nuclei irregularly shaped (Kafarnik *et al.*, 2007) when compared to human.

The above studies confirmed previous findings in respect to the changes in chick corneal epithelium that undergoes stratification and maturation during development. Additionally, quantification studies provided new insight into changes in number of cell layers and cell shape and allowed selection of time points which showed critical changes in the development of the corneal epithelium, important for future experiments.

3.6.2 Differentiation profile in the embryonic chick corneal epithelium

Cytokeratins form a complex family of fibrous cytoskeletal proteins that are among the major differentiation-specific proteins of epithelial cells (Fuchs, 1988). The 8nm keratin filaments, being one of the components of cytoskeletal architecture, are compromised of keratin polypeptides, which vary not only with cell type, but also with stage of differentiation and development (Fuchs, 1988; Kivela and Uusitalo, 1998; Magin *et al.*, 2007). Thus, the expression patterns of cytokeratins were investigated as a measure of cell commitment to differentiation.

Previous immunoblot analysis suggested that AE1 and AE3 antibodies react with two different groups of keratins. In combination, AE1 and AE3 recognise most known keratins, expressed by various *in vivo* epithelial tissues (Tseng *et al.*, 1982; Nelson and Sun, 1983; Woodcock-Mitchell *et al.*, 1982; Eichner *et al.,* 1984). These are: acidic keratins 10, 13, 14, 15, 16, 19 and basic keratins 1, 2, 3, 4, 5, 6, 7. Using this antibody, expression of specific keratins can be correlated with different types of epithelial differentiation (e.g. simple vs. stratified, keratinised versus nonkeratinised) (Eichner *et al.*, 1984; Moll *et al.*, 1982; Tseng *et al.*, 1982). Not all cytokeratins detected by AE1/AE3 are present in the corneal epithelium. To date the expression of the following cytokeratin pairs have been reported in corneal epithelium: K3/K12, K5/K14, K1/K10, K6/K16, K4/K19 (Kurpakus *et al.,* 1994; Chaloin-Dufau *et al.,* 1990; Schermer *et al.*, 1986, Schermer *et al.*, 1989; Yen *et al.*, 1992; Kasper *et al.*, 1992; Kasper *et al.*, 1988; Lauweryns *et al.*, 1993a).

The earliest expression of AE1/AE3 immunolabelled cells was observed at ED10 in the superficial layers of the corneal epithelium. This finding was surprising, as it has been reported that some low molecular weight cytokeratins, such as CK7, 8 and 18-20 characterise early embryogenesis and primordial simple epithelial cells (Moll *et al.*, 1982). This would presume the appearance of immuno-positive cells in earlier embryonic days. However, it has not been definitively determined whether keratin pair K8/K18 (52/53 kDa) is expressed in the corneal epithelium, since it has not been possible to document protein expression by gel electrophoresis or immunoblotting, and immunohistochemical labelling in the cornea has been inconsistent (Kivela and Uusitalo, 1998;

Kasper *et al.*, 1988; Kasper *et al.*, 1992). In contrast, high molecular weight cytokeratin types (CK1-6, 9-17) appear with epithelial differentiation and maturation and are characteristic of complex epithelia (Moll *et al.*, 1982; Cooper *et al.*, 1985, Kivela and Uusitalo, 1998). Terminal differentiation of suprabasal cells that had lost contact with basement membrane was found to be associated with synthesis of other cytokeratin pairs; epidermal-type K1/K10 and hyperproliferation K6/K16 (Klymkowsky *et al.*, 1989). Mitotically active basal cells of stratified epithelia usually express the keratin pair 5/14 (58/50 kDa) (Kivela and Uusitalo, 1998; Nelson and Sun, 1983; Moll *et al.*, 1982; Cooper *et al.*, 1985; Purkis *et al.*, 1990). Other immunohistochemical and molecular genetic studies suggested that the human cornea contains low levels of CK14 in the basal cell layer (Kasper *et al.*, 1988; Nishida *et al.*, 1996). CK19, simple epithelia type, is another protein identified in corneal epithelium and its expression was observed in the entire limbal epithelium on the conjunctival border and in the peripheral suprabasal layers (Kasper *et al.,* 1988; Kasper *et al.*, 1992; Lauweryns *et al.*, 1993a). Cornea-type epithelial differentiation is signified by the expression of the K3/K12 keratin pair of intermediate filaments essential for corneal epithelial integrity (Sun *et al.*, 1985; Liu *et al.*, 1994; Wu *et al.*, 1994). CK3 and CK12 are present in large quantities in the corneal epithelium, comprising about 30% of total protein (Rodrigues *et al.*, 1986).

In our immunolocalisation studies, the expression of CK3 was absent from the chick corneal epithelium until ED12. In subsequent stages (from ED12 onwards), CK3 labelling of epithelial cells appeared uniform throughout all cell layers, except for basal cells in the limbal region. Using AE5 monoclonal antibody, which is highly specific for the 64 kDa corneal keratin (70 kDa for the chick) (Schermer *et al.*, 1986; Chaloin-Dufau *et al.*, 1990), other investigators have demonstrated that this keratin is localised to all corneal epithelial cell layers in the rabbit, but only the suprabasal layers of the limbal epithelium. Similar CK3 labelling patterns have been observed in the macaque (Zhao *et al.*, 2006), rabbit (Schermer *et al.*, 1986; Chaloin-Dufau *et al.*, 1990) and adult human corneas (Rodrigues *et al.,* 1987). At 8 weeks of gestation, the presumptive human corneal epithelium was composed of a single layer of

cuboidal cells and neither of these cell layers was AE5 positive. At 12-13 weeks of gestation, some superficial cells of the three to four-layered epithelium appeared AE5 positive. At 36 weeks, the epithelium was morphologically mature (four to six layers) and AE5 labelling was observed suprabasally, in contrast to the adult central epithelium which demonstrated uniform staining.

The appearance of AE1/AE3 labelling at ED10 and the presence of AE5 immunolabelling in cells at ED12 suggests that these time points are critical for the onset of epithelial differentiation during corneal development. The appearance of AE1/AE3 labelling at an earlier embryonic day than was observed for AE5 suggests that CK3 is expressed later than other keratins recognised by AE1/AE3 (i.e. CK5 and CK14, expressed in mitotically active basal cells of stratified epithelia). Immunolocalisation studies also demonstrated that later developmental stages (ED16, 18) showed similar epithelial differentiation patterns to that observed in posthatch chick epithelium. The appearance of pan-CK-positive cells at ED10 in the superficial cell layer may suggest the beginning of epithelial differentiation and might be related to the detection of cells with different antigen determinants recognised by antibodies from the cocktail AE1/AE3 (as described above). Differentiation of human and rabbit cultured corneal and limbal epithelial cells was investigated and evaluated by changes in keratin profiles by Kiritoshi and coauthors (1991). After two weeks in culture, the human limbal epithelial cells did not react with AE5 but did react strongly with AE1. Later (third week in culture), only suprabasal cells exhibited a moderate reactivity with AE5, whereas AE1 binding was seen in all of the cells. After fifth to sixth weeks in culture, all of the cells reacted moderately with AE5 and AE1. The expression of CK3 in cells derived from central cornea was lost once these cells were cultured, but they expressed keratins recognised by AE1. It may be explained by the fact that cultured cells were already in an advanced stage of differentiation and had lost ability to transcribe and translate messages for CK3 synthesis. Thus, CK3 expression was associated with maturation or a later stage of differentiation.

Our observations highlighted similarities in staining pattern between pan-CK and CK3 at ED12. In the central epithelium, CK3-labelling was observed

throughout the epithelium, whereas, in the limbal and peripheral region, CK3-positive cells were present only in the superficial cell layer. Although pan-CK labelled cells were observed ED10, at ED12, the pattern of labelling was expanded to all cell layers in the central epithelium. The above suggests that epithelial differentiation may vary (suprabasal versus uniform) in different parts of the cornea and is earlier in the central corneal epithelium. It has been postulated that differentiation of suprabasal cells is associated with synthesis of cytokeratin pairs such as K3 and 12 and the hyperproliferative K6 and 16 (Kivela and Uusitalo, 1998). Our observations, especially the appearance of AE1/AE3-positive cells earlier than AE5-positive labelling support the above assumptions.

Immunoblotting confirmed the increase in protein expression level of CK3 throughout corneal epithelial development in the avian eye. Chaloin-Dufau and coauthors (1990) reported that CK3 expression was first observed in the developing chick corneal epithelium from ED12, and postulated that CK3 might be expressed at least from ED11. By contrast this study shows that CK3 protein is expressed as early as ED10. The lower levels of CK3 protein identified in the epithelia from ED10 to ED14, and subsequent increase to their highest in epithelia of samples ED16, ED18 and posthatched corneas suggests that CK3 expression plays an important role in the differentiation and maturation of the developing avian corneal epithelium. The presence of the CK3 band at ED10 was observed on a blot in a small amount, whereas, immunolocalisation studies did not show CK3-positive cells at this time-point. The most likely explanation is the increased sensitivity of immunoblotting for the detection of protein as when compared to less sensitive immunolabelling allowed for the detection of CK3 at ED10.

Future work should be aimed to testing a number of antibodies to the same antigen in the tissue under study, to exclude epitope masking caused by postranslational modifications and to exclude detection of isoforms that are antigenically distinct or shared epitopes. An identification of individual cytokeratins (CK1, 4, 6, 8, 16, 18, 19) in the developing chick corneal epithelium, both by immunolabelling and immunoblotting, requires further

investigation, as this would allow us to determine which cytokeratins were responsible for AE1/AE3 labelling in the epithelium at ED10, as well as later time points. In our studies mAb CK14 (Santa Cruz Biotechnology Inc, UK) was tested on chicken sections, but despite high homology in amino acid sequence to human CK14 (73% identities, 88% positives), positive immunolabelling was not detected. Currently, the main limitation of using chick tissue for large scale immunolocalisation studies is the poor availability of reliable antibodies.

In conclusion, the above studies indicated that the chick epithelium undergoes rapid embryonic development, accompanied by steady and continual differentiation and maturation. The most significant morphological changes in chick corneal epithelium were seen to occur between ED10, ED12 and ED14, with the increasing number of cell layers and appearance of stratified epithelial cells in all regions and changes in cell shape. Appearance of pan-CK and CK3 expression at ED10 and 12 suggested those time points might be critical for the beginning of differentiation of corneal epithelium. Pan-CK and CK3 labelling throughout the entire central corneal epithelium earlier than in the peripheral suprabasal layer, indicates that those cells might have already entered the termination pathway.

The similarities of expression patterns in avian and mammals suggest that corneas of all vertebrates share structural and molecular characteristics (Collin and Collin, 2006). It also supports the idea that avian corneas can be used as a valuable model for the study of epithelial development.

CHAPTER FOUR

Epithelial cell proliferation and death

EPITHELIAL CELL PROLIFERATION AND DEATH

4.1 Introduction

Development and maintenance of tissues is achieved by a dynamic balance between cell proliferation, differentiation and programmed cell death (Wyllie *et al.*, 1980; Ellis *et al.,* 1991; Kojima *et al.*, 1998).

The structural integrity of the corneal epithelium must be maintained in order to preserve its essential barrier function and transparency. The corneal epithelium constantly renews its cell population with cells added through mitosis in the basal cell layer and lost by shedding from the surface (Hanna and O'Brien, 1960; Ren and Wilson, 1996) and consists of cells with different proliferative capacities. Central corneal epithelial cells were shown to contain rapidly proliferating cells in the compartment adjacent to basal cell layer, which help to maintain the thickness of epithelium by replacing lost cells from the surface and suprabasal cells that excited the cell cycle (Joyce *et al.*, 1996; Lavker *et al.*, 1991; Cotsarelis *et al.*, 1989).

The contribution of LSCs for the regulation of cell proliferation and loss has been elucidated (Thoft, 1989; Tseng, 1989; Lavker *et al.*, 1991; Cotsarelis *et al.*, 1989; Chung *et al.*, 1995). Cell proliferation in the limbus contributes new cells until adequate cell density is reached. The undifferentiated progeny (TACs) interspersed amongst LSCs in the limbal basal rapidly proliferate on appropriate stimulation and migrate centripetaly to re-establish a multilayered, stratified epithelium. TACs have been also shown to have greater proliferative capacity to peripheral and central epithelium when studied in human tissue culture (Ebato *et al.*, 1987; Lindberg *et al.*, 1993, Joyce *et al.*, 1996).

Recently, *in vitro* studies of the healing response after corneal injuries, demonstrated, that after wounding, cell proliferation and migration in the centre of the cornea was just as vigorous as in cells proliferating and migrating from the limbus and periphery (Chang *et al.*, 2008). Thus, it was concluded that central human corneal epithelium cells appeared to be fully capable of corneal epithelial regeneration suggesting a role for other mechanisms in epithelial

proliferation during the first hours after acute corneal injury, before the response from LSCs takes place (Chang *et al.*, 2008).

Homeostasis in continually renewing tissues is maintained by a tightly regulated balance between cell proliferation, cell differentiation, and cell death. Naturally occurring cell death is considered distinct from pathologically induced cell death (necrosis), and the criteria (both morphological and biochemical) which distinguish between these two processes has been precisely defined (Kerr *et al.*, 1972; Ren and Wilson, 1996). Apoptosis has been identified in association with normal cell turnover in several types of mammalian epithelia (Ren and Wilson, 1996; McCall and Cohan, 1991; Gavrieli *et al.*, 1992; Haake and Polakowska, 1993) Although corneal epithelial cell death has been studied in a number of species, including human (Ren and Wilson, 1996; Yew *et al.*, 2001, Svoboda *et al.,* 2004; Ramaesh *et al.*, 2006), the scale of cell death in avian corneal epithelium during later development has not been yet investigated *in vivo*.

4.2 Aim

The aim was to examine and quantify the spatial distribution of cell proliferation and cell death during the embryonic development of the chick corneal epithelium.

4.3 Experimental design

The present study was undertaken to compare the rate of proliferation and cell death at different time points in the developing chick corneal epithelium. Transverse wax sections of chick cornea were prepared as described in section 2.3. A monoclonal anti-PCNA antibody was used to assess the proliferation pattern of the epithelium during development, as described in section 2.5.4. The PCNA protein (29 kDa) also known as cyclin or DNA polymerase δ auxiliary factor, is expressed in the nuclei during DNA synthesis (phase S or early G1 of cell cycle) (Morris and Mathews, 1989; Takasaki *et al.*, 1984). Its rate of synthesis is directly correlated with the proliferative rate of cells, therefore it is considered as a reliable marker for epithelial proliferative activity (Celis *et al.*, 1987; Gan *et al.*, 1995, Yew *et al.*, 2001).

In order to analyse the cell death profile in the corneal epithelium during chick development, the TUNEL technique and caspase 3 (active) immunolocalisation were performed (section 2.6). TUNEL, being one of the most common methods used for detection of apoptotic cells (Gavrieli *et al.*, 1992), is based on the detection of DNA fragments – a typical characteristic of apoptosis. Caspase 3, one of the key executioners of apoptosis, is responsible either partially or totally for the proteolytic cleavage of many key proteins involved in DNA replication, transcription and translation; cytoskeletal proteins, kinases, phosphatases and other caspases (Cohen, 1997; Stroh and Schulze-Osthoff, 1998; Umpierre *et al.*, 2001).

Three regions of cornea were examined: the central, peripheral and limbal. Each experiment was carried out at least three times. The quantitative analysis of proliferation and apoptotic cell death were carried out by counting PCNA-positive and TUNEL-positive cells at each time point in triplicate sections of three different specimens for each time point. Three fields of microscope view of each region were examined.

The labelling index (LI) was defined as the number of PCNA-positive cells divided by total number of cells and multiplied by 100% (Fig. 4.1) or as the number of TUNEL-positive cells divided by total number of cells and multiplied by 100%. Evaluation was performed under oil immersion using a x100 objective lens

In order to confirm expression of PCNA during development, Western blot analyses were performed on protein samples from embryonic chick epithelia (as described in section 2.9). For this purpose collection of samples started from ED6 onwards, excluding ED4, which did not provided efficient amount of protein sample.

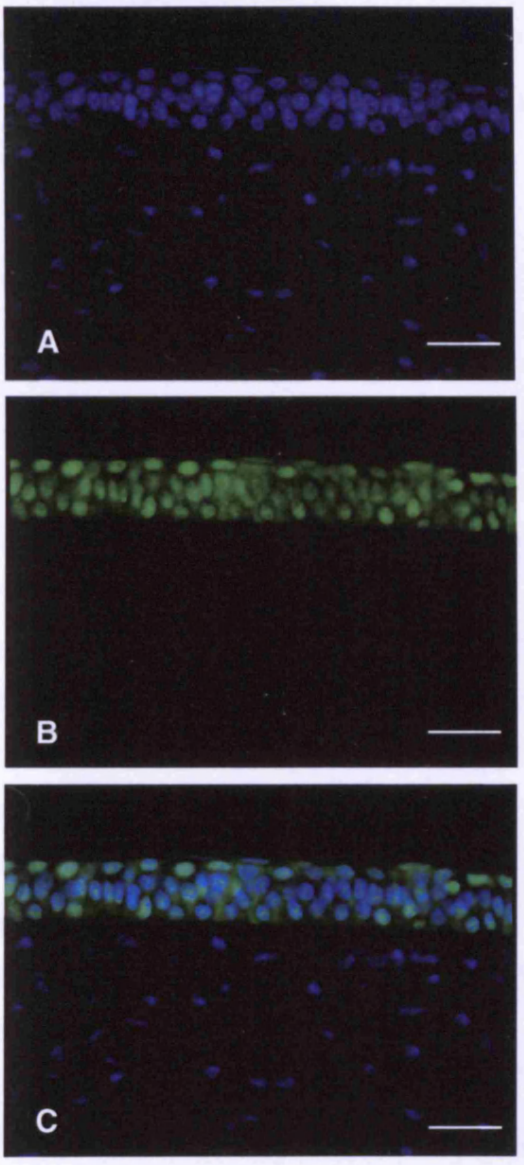

Figure 4.1 Representative images used to calculate proliferation labelling index (LI) in developing chick corneal epithelium. **(A)** central epithelium at ED16 stained with Hoechst 33342 (blue). **(B)** central epithelium immunolabelled for PCNA (green) with secondary anti-mouse antibody Alexa Fluor 488. **(C)** combined image; PCNA: green, Hoechst 33342: blue. Scale bar = 50μm. x 100.

Statistical analyses were then performed using (SPSS v12). Data was checked for distribution (Shapiro-Wilk test) and homogeneity of variances (Lavene test). Data was log transformed when necessary. One-way ANOVA and appropriate post-hoc (Dunnett T3) tests were performed (SPSS v.12) for the data showing Gaussian distribution with significance at $p \leq 0.05$. Non-parametric data was processed for interaction plots (MiniTab v.14).

RESULTS

4.4 Epithelial cell proliferation in chick corneal development

4.4.1 Optimisation of the protocols for Ki67 immunolabelling

In order to assess the proliferative activity of epithelial cells using anti-Ki67 in the developing chick cornea, numerous protocols were performed. Different combinations of individual steps (including different dilutions of primary antibody, concentrations of Triton-X-100 and blocking agent, length of incubation) both on paraffin and frozen sections were subsequently investigated. Examples are shown in Figure 4.2. A weak signal together with a high background was observed in all sections. However, no specific staining for Ki67 was achieved. Positive control sections of human corneal epithelium showed specific nuclear labelling for Ki67 (Fig. 4.2). Therefore, anti-PCNA labelling was used to characterise epithelial cell proliferation during development, as described in section 4.4.2.

4.4.2 Immunolocalisation of proliferating epithelial cells using PCNA monoclonal antibody

The results observed from PCNA immunolocalisation studies showed temporal and spatial regulation of proliferation during chick corneal epithelial development (Fig. 4.3). PCNA immunolocalisation in the chick corneal epithelium demonstrated positive labelling in all regions from ED4 to ED21 (posthatched epithelia) with regional variation dependent on developmental time point (Fig. 4.3). Negative control sections showed no staining (Figs. 4.3c1-6).

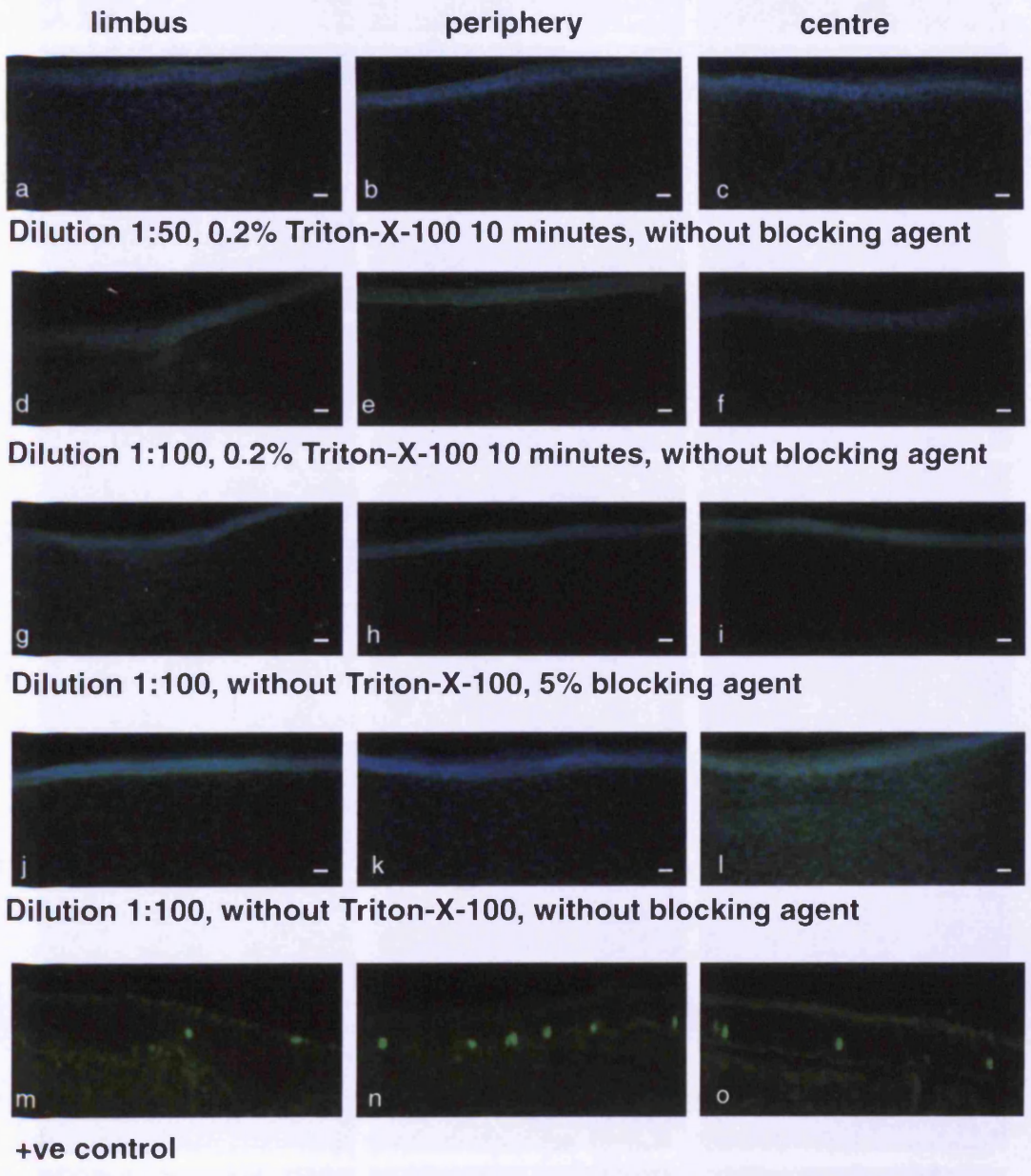

Figure 4.2 Comparison of the effects of different parameters on immunofluorescent labelling by mAb Ki67 in different regions of chick corneal epithelium at ED16, on frozen sections. Dilutions of primary antibody varied **(a-c**: 1:50, **d-l**: 1:100**)**. Donkey serum was used as a blocking agent. Non specific staining pattern for Ki67 was observed after individual treatments. In contrast, labelling for Ki67 in human cornea, used as a positive control, is shown **(m, n, o)**. Scale bars = 20μm. x 20.

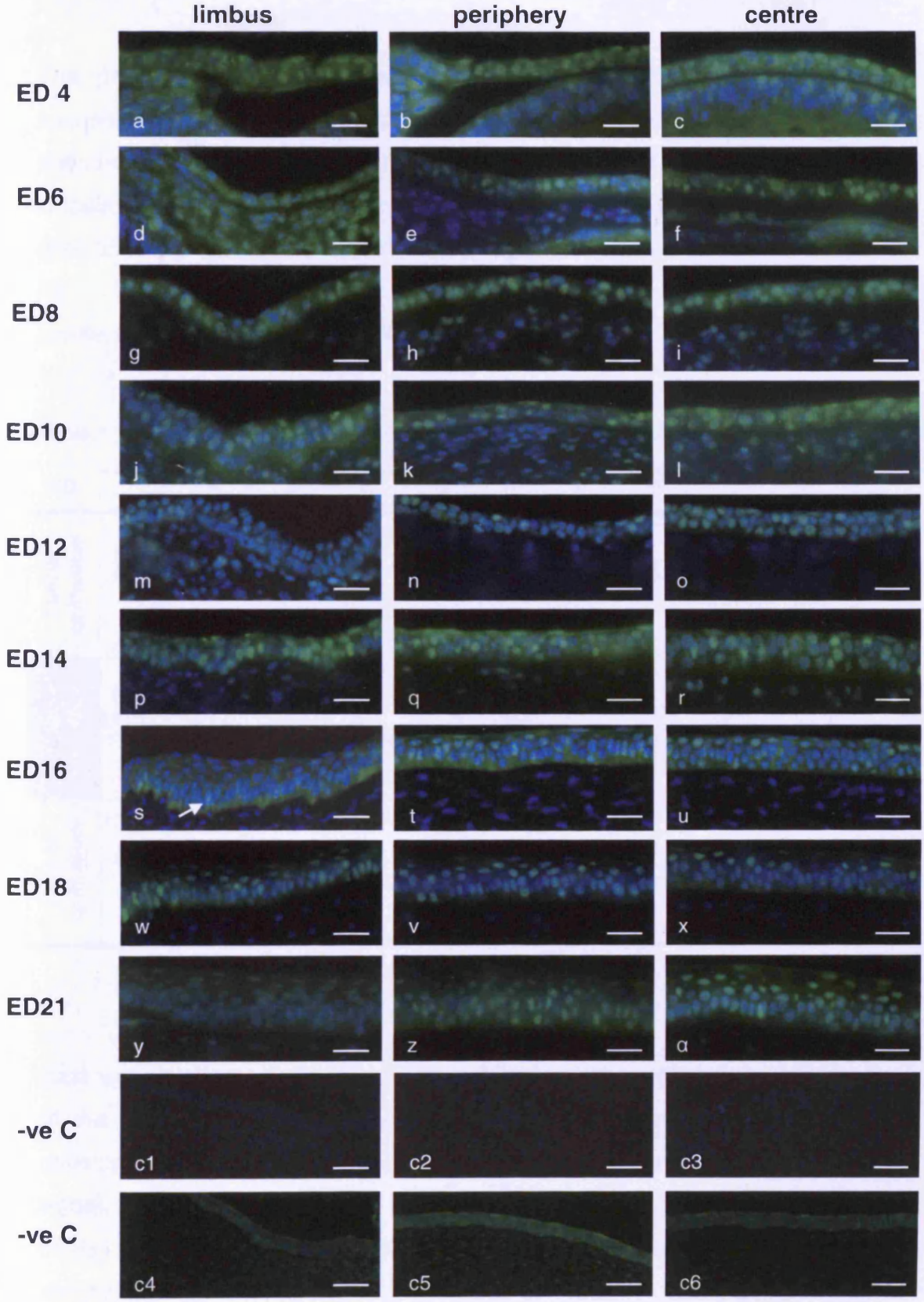

Figure 4.3 Immunolocalisation of PCNA in the developing chick corneal epithelium (ED4-ED21). PCNA-positive cells were observed in all developmental stages. From ED4 to ED12 immunolabelling was observed in cells distributed throughout the whole thickness of central, peripheral and limbal epithelium **(a-o)**. Cell proliferation appeared to peak at ED14, with PCNA-positive cells dispersed throughout the thickness of central and peripheral epithelium **(q, r)**. At ED16 PCNA labelling disappeared from suprabasal cell layers in the limbal epithelium **(m, p, s)**. PCNA-positive labelling was decreased in all regions by ED21 **(y-α)**. mAb anti-PCNA binding sites are labelled with green fluorescence and cell nuclei are stained blue by Hoechst 33342. Control sections (ED12); mouse anti-GFP **(c1-c3)** and mouse IgG **(c4-c6),** show no staining in all regions **(c1-c3)**. Scale bars = 50μm. x 100, c1-c6 x 20.

The proliferative activity of cells in the developing chick epithelium was assessed throughout epithelial thickness by means of immunohistochemical detection of PCNA-positive cells. Percentage of PCNA-positive cells (LI) was calculated for each developmental time point and significant differences ($p \leq 0.05$) were found between the three regions of corneal epithelium (Appendix III). Table 4.1 summarises results obtained from the quantification of proliferating cells in each epithelial region.

Table 4.1 Percentage of proliferation (LI) in three regions of corneal epithelium

ED		4	6	8	10	12	14	16	18	21
Limbal epithelium	*Mean*	54.8	57.1	66.1	74.1	74.4	79.4	68.9	52.8	31.3
	SD	±7.09	±7.5	±9.53	±2.9	±5.5	±4.4	±7.1	±4.09	±6.0
Peripheral epithelium	*Mean*	60.3	65.8	74.0	77.8	80.8	86.5	77.4	68.3	49.9
	SD	±10.9	±6.6	±8.5	±6.1	±6.1	±6.8	±4.5	±3.5	±5.9
Central epithelium	*Mean*	61.5	62.7	73.5	75.6	78.3	82.7	76.4	63.2	45.7
	SD	±10.5	±10.2	±9.1	±5.3	±5.5	±3.5	±7.6	±4.2	±4.9

Data were plotted as a percentage of PCNA-positive cells in the three regions of the cornea (Fig. 4.4). Percentage cell proliferation was high throughout development (LI>67.7± 12.8%). Mean percentage proliferating cells in the limbal, peripheral and central epithelium was 63.0±15.6%, 71.2±11.3% and 68.8±11.5%, respectively. Differences between these three regions were statistically significant ($p \leq 0.05$) (Appendix III).

From ED4 to ED8, labelled cells were observed in two cell layers of the epithelium in the centre, periphery and limbus, in both basal and suprabasal cell layers (Figs. 4.3a-i). The percentage of proliferating cells at ED4 was the

highest in the central epithelium (61.5±10.5%), and increased to 73.5±9.1% by ED8. At ED8, in the peripheral corneal epithelium, the number of PCNA nuclei was higher than in the limbal epithelium, but lower than the central region with 74.0±8.5%, 66.1±9.5% and 73.5±9.1% labelled cells, respectively. Statistically significant differences in percentage proliferating cells were found between central and limbal regions at ED4 and ED8, and between peripheral and limbal regions at ED6 ($p \leq 0.05$). Additionally, no statistically significant differences in the percentage of PCNA-positive cells were demonstrated between ED4 and ED6 in any of three epithelial regions.

From ED10 to ED12 PCNA-positive cells were identified in all cell layers throughout the corneal epithelium (Figs. 4.3j-o). At ED14, immunolabelled cells were observed throughout the entire central and peripheral epithelium whereas, in the limbus, more positive cells were detected towards the peripheral side of the limbal region (Figs. 4.3p-r). From ED10 to ED14, the percentage of proliferating cells increased from 74.1±2.9%, 77.8±6.1% and 75.6±5.3% to 79.4±4.4%, 86.5±6.8% and 82.7±3.5% in the limbal, peripheral and central epithelium, respectively (Fig. 4.4). The peak proliferation rate was observed from ED12 (74.4±5.5%, 80.8±6.1% and 78.3±5.5%, in limbal, peripheral and central epithelium respectively) to ED14 in all epithelial regions (Fig. 4.4). Significant differences in percentage proliferation were found between ED10 and ED14 as well as between ED12 and ED14 in all epithelial regions ($p \leq 0.05$), but not between ED10 and 12.

By ED16, fewer PCNA immunopositive cells were observed. They appeared to be restricted mainly in the basal cell layer (Fig. 4.3s) of the limbus (LI: 68.9±7.1%), although, present throughout all epithelial layers in the peripheral and central epithelium (LI: 77.4±4.5% and 76.4±7.6%) (Figs. 4.3 t,u and 4.4). Labelling of PCNA-positive cells appeared to be reduced in all cell layers at ED18 and ED21 (posthatch), particularly noticeable in the central and peripheral epithelium with mostly suprabasal localisation (Figs. 4.3w-α).

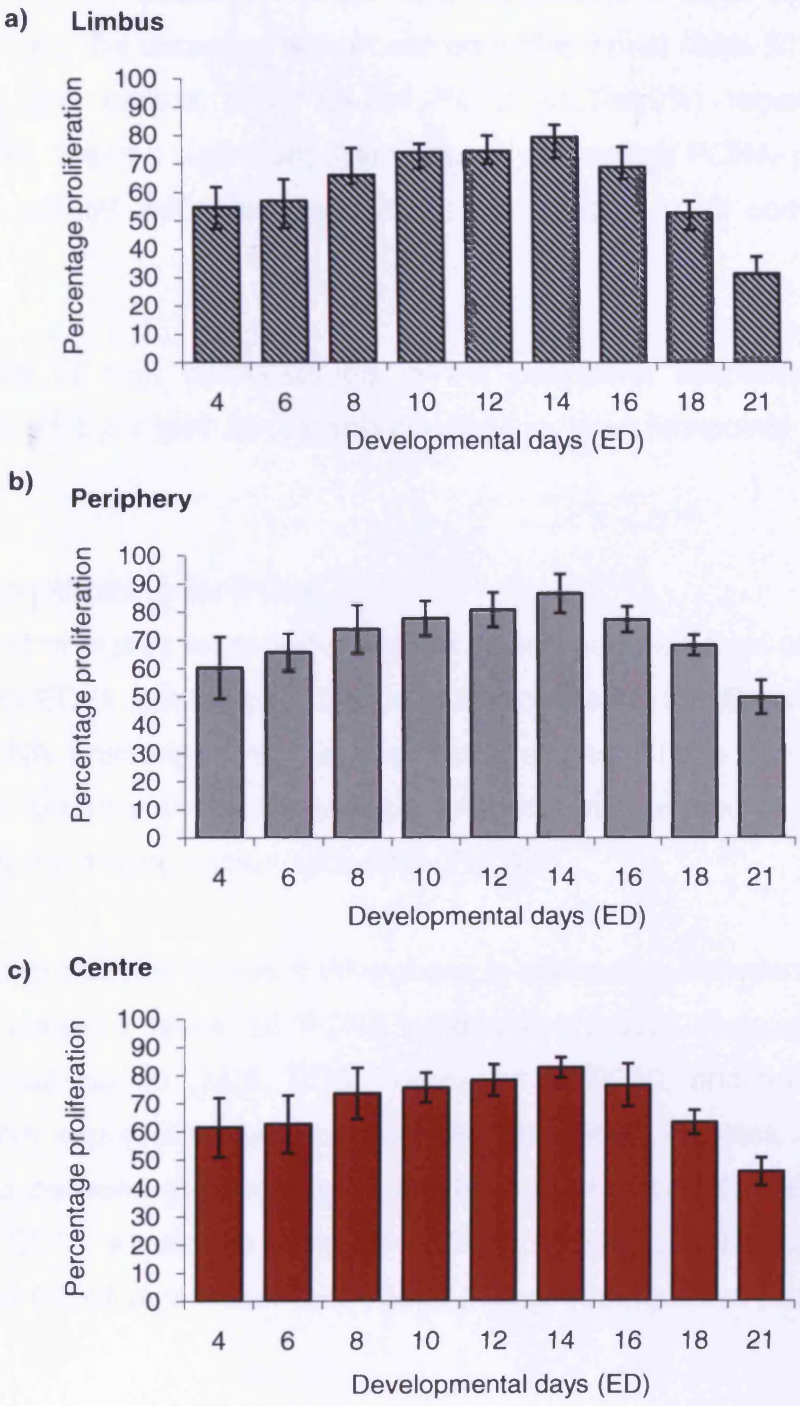

Figure 4.4 Percentage proliferation (LI) in developing chick corneal epithelium. PCNA-positive cells were quantified in three epithelial regions; limbus **(a)**, periphery **(b)**, centre **(a)**. Results obtained from three experiments were combined to give the average LI for each developmental stage. Error bars displayed represent the standard deviation from the mean. The highest LI was demonstrated in the middle time-points (ED12 to ED14), and than gradually decreased.

As quantified, in the peripheral epithelium, the percentage of PCNA-positive cells decayed from 68.3±3.5% at ED18, to 49.9±5.9% at ED21 posthatch(Fig. 4.4b). Similarly, the decrease was observed in the limbal (from 52.8±4.09% to 31.37±6%) and central (from 63.2±4.2% to 45.7±4.9%) regions. Multiple comparisons revealed significant differences in percentage PCNA–positive cells between posthatch epithelium and the earlier stages in all corneal regions ($p \leq 0.05$).

The highest LI was demonstrated in the peripheral epithelium and was significantly different ($p \leq 0.05$) to limbal epithelium in all timepoints from ED6 to ED21.

4.4.3 Immunoblotting for PCNA

Western blot analyses were performed on protein samples from chick corneas from ED6 to ED21 (posthatch). Bands of approximately 30 kDa were detected by anti-PCNA antibody in all developmental stages. These bands were not detected in controls where the primary antibody was omitted or primary was replaced by the mouse immunoglobulins (Fig. 4.5).

Densitometric analysis revealed differences in expression between time points. Relatively constant levels of PCNA protein expression observed in earlier developmental stages (ED6, ED8), increased at ED10, and thereafter from ED12, PCNA expression decayed abruptly. Statistically significant differences were found between the expression levels of PCNA at ED6/ED8 and ED10, ED10 and ED18, as well as, between ED6 and ED12 ($p \leq 0.05$). Differences in the levels of PCNA expression between any other comparisons, including ED21

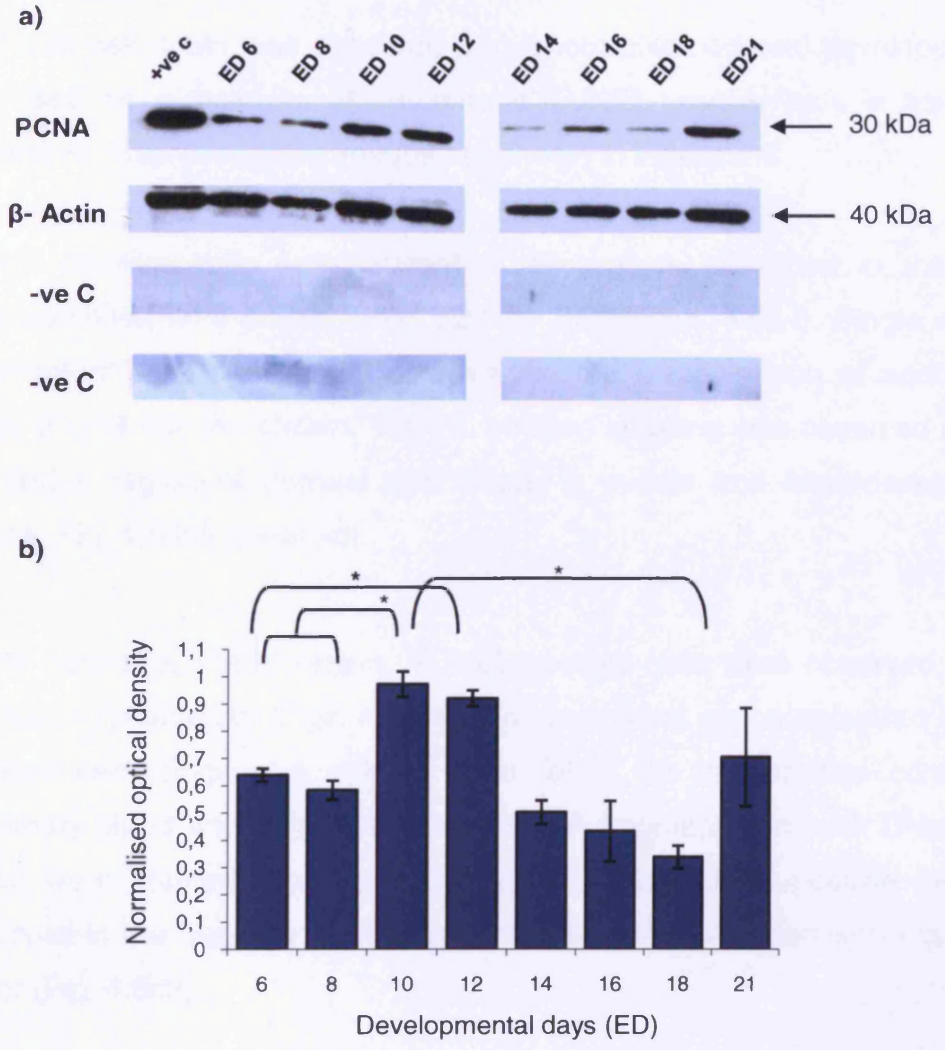

Figure 4.5 Western blot detection of PCNA in developing chick corneal epithelium. 10µg of protein per sample were loaded to the electrophoresis gel, transferred to nitrocellulose membrane and incubated with antibody raised against PCNA protein. **(a)** A specific band of approximately 30 kDa was observed for PCNA in all developmental stages. As a positive control protein sample from chick developing brain (ED6) was used. β-Actin (used as housekeeping protein) was detected as a band of 40 kDa, Negative controls (omission of the primary antibody and mouse IgG substitution for primary antibody) did not tetect PCNA specific bands. **(b)** Densitometric analysis of immunoblots. Results are representative of the three sets. Data were normalised to β-Actin and presented as mean ± SEM, *p≤0.05.

.

(posthatched) epithelia, were not statistically significant. Detailed statistical analyses of the PCNA expression are given in Appendix III.

4.5 Epithelial cell death in chick corneal development

4.5.1 TUNEL

Epithelial cell death was observed throughout chick corneal development and quantified as a measure of percentage TUNEL-positive cells in the corneal epithelium. Representative images are shown in Figure 4.6.

TUNEL-positive cells were absent in all regions examined in the earliest developmental time points; from ED4 by ED8 (Figs. 4.6a-i). Single cells with fragmented DNA were firstly observed in the limbal region of epithelium at ED10 (Fig. 4.6j). As shown, TUNEL positive labelling was observed mostly in the limbal region of corneal epithelium, in middle and later developmental stages (Fig. 4.6 left panel j-α).

In the central epithelial region, TUNEL-positive cells were observed at ED12 and ED21 (posthatch) (Figs. 4.6o,α). The peripheral region appeared devoid of labelled cells (Figs. 4.6 middle panel b-c2). In the positive controls, rat mammary gland and artificially induced DNA fragmentation (with DNase I) cell nuclei were stained brown (Figs. 4.6c2,c1). No TUNEL-positive cells were observed in the negative control, in which TdT was replaced with equilibration buffer (Fig. 4.6c3).

The highest rate of TUNEL-positivity was observed at ED18 in the limbal region, with an apoptotic index 5.7±0.7%. From ED12, TUNEL labelling was observed in the limbal epithelium in all developmental time points, with TUNEL-positivity below 5%, except for ED18.

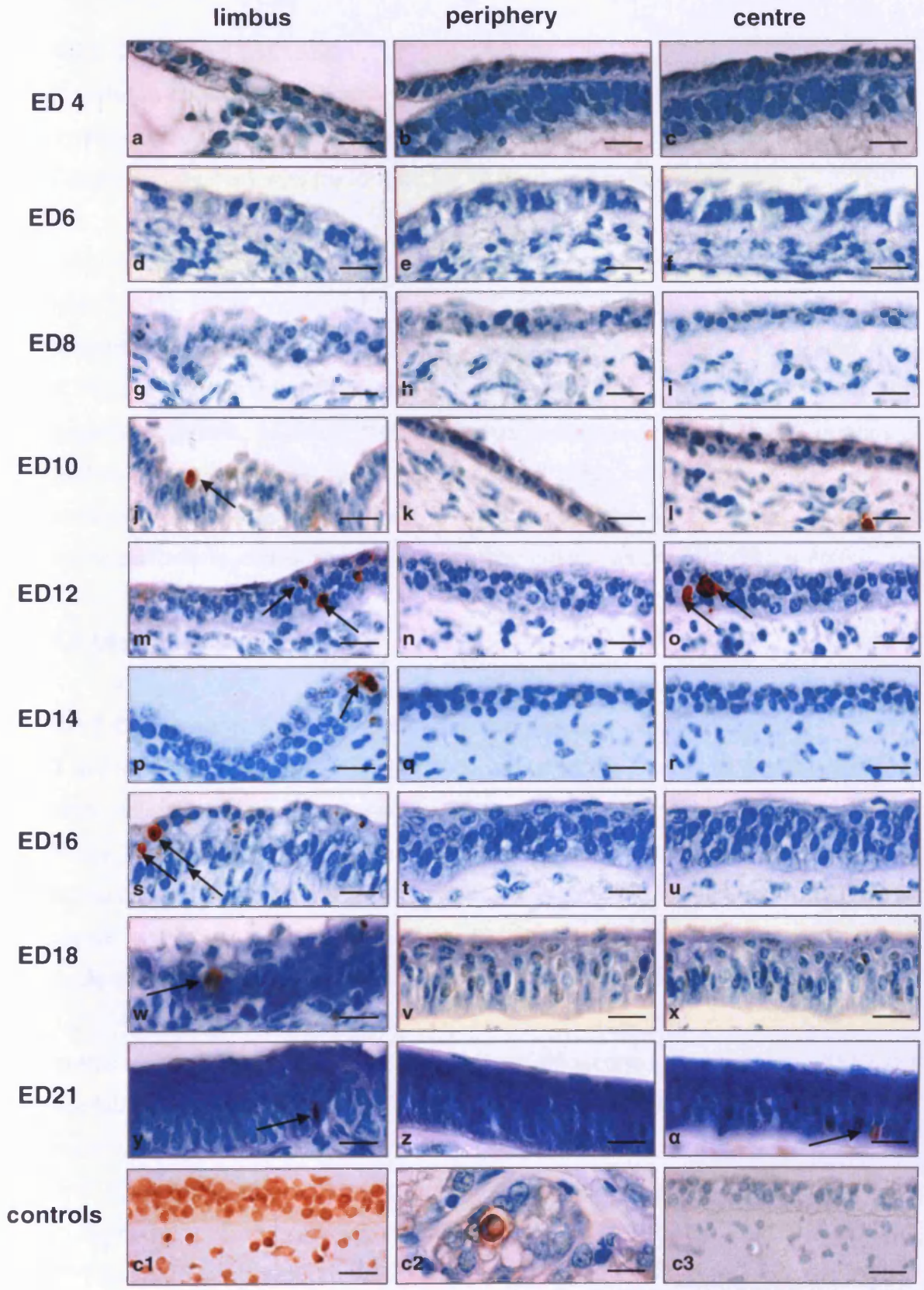

Figure 4.6 TUNEL labelling of developing chick corneal epithelium. Panels show TUNEL labelling in limbal **(a-y)**, peripheral **(b-z)** and central **(c-α)** regions of the corneal epithelium, ED4 to ED21. TUNEL-positive cells, indicated by arrows, were absent from all regions at earlier time points (ED4 - ED8) **(a-i)**. In the later stages, from ED10 onwards, TUNEL-labelling was observed in the limbal epithelium **(left panel, j-y)** and also, in the central region at ED12 **(α)**. Positive controls; DNase I digestion (**c1**) and rat mammary gland **(c2)** showed labelled cells. TUNEL-positive cells were not observed in negative control sections (substitution of equilibration buffer for TdT enzyme) **(c3)**. Scale bars = 100μm. x 100.

4.5.2 Caspase 3 activation

In order to confirm that TUNEL labelling results that suggest epithelial cell death by apoptosis during corneal development, additional immunolabelling for anti-Caspase 3 (active) was performed for all developmental time points.

Immunolocalisation of the active form of caspase 3 in chick corneal epithelium from ED4 to ED21 (posthatched) (Fig 4.7) demonstrated a lack of labelling in all regions investigated, with the exception of the limbal epithelium at ED16 (Fig. 4.7s), the central epithelium at ED18 (Fig. 4.7x) and ED21 (Fig. 4.7α). In the negative controls, in which rabbit IgG was substituted for mAb anti-Caspase 3 (active), apoptotic cells were not observed (Figs. 4.7c1,c2). In the positive controls (rat mammary gland, DNase I digestion), Caspase 3 (active) immunolabelling, characteristic of apoptotic cells, was present (Fig. 4.7c3).

4.6 Discussion

4.6.1 Cell proliferation in the developing chick corneal epithelium

The formation of corneal epithelium depends on the control of proliferation and differentiation. Although, those processes are under constant investigation, many aspects underlying those processes remain unknown. Thus, to answer some of the questions regarding molecular targets required for the regulation of signal transduction cascades, it is necessary to gain the knowledge and understanding of the changes in the pattern of proliferation in development.

In this study, despite performing various modifications to the protocol, Ki-67 did not label epithelial cells in chick cornea sections, although, Ki-67-positive cells were observed in human controls. It was revealed that Ki-67 monoclonal antibodies show little cross reactivity between species limiting their application in basic research (Endl and Gerdes, 2000; Brown and Gatter, 2002). In support of this, a BLAST search demonstrated that the Ki-67 protein is not highly conserved with only 23% homology in amino-acid sequences between human and chick.

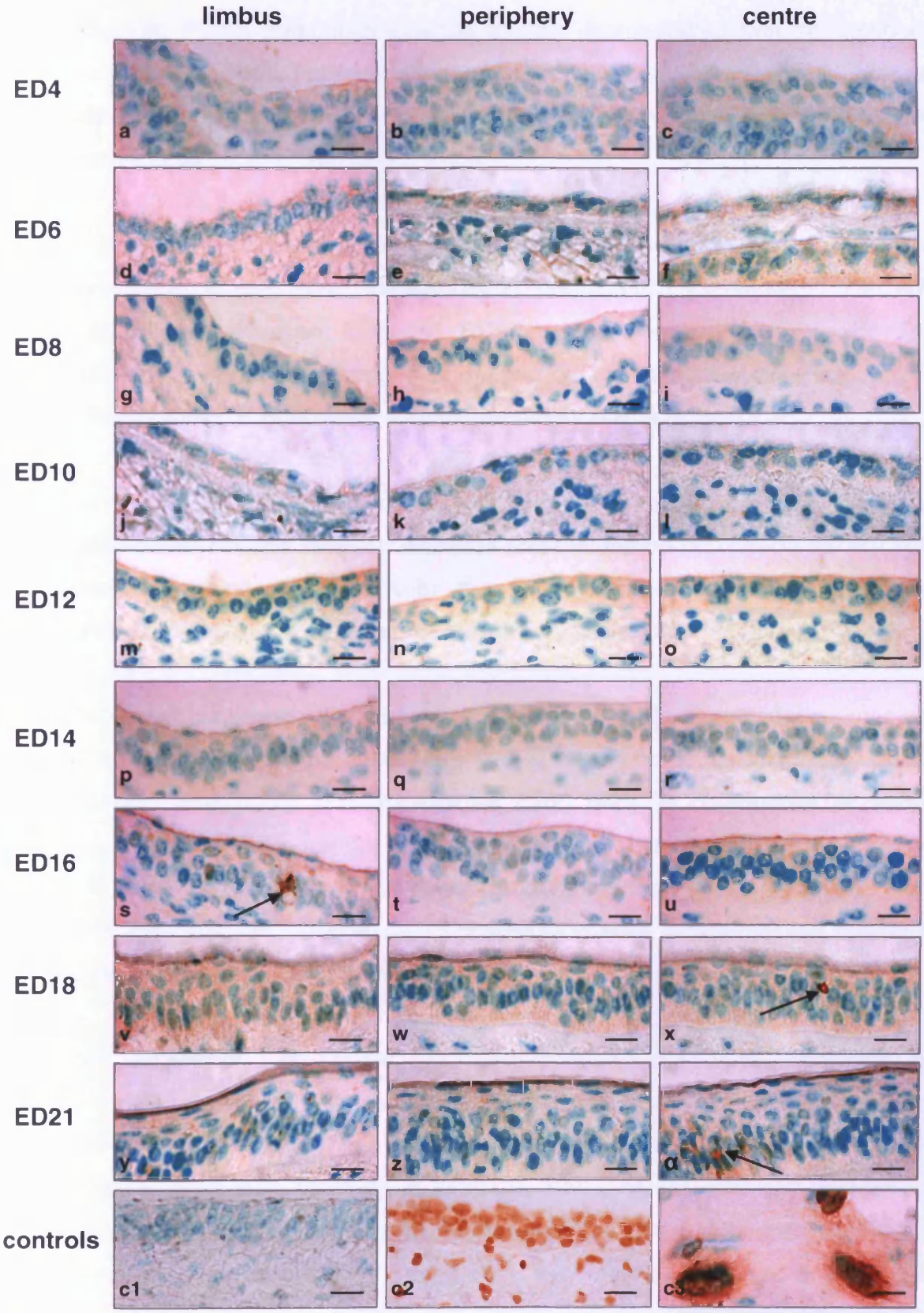

Figure 4.7 Caspase 3 immunolabelling in the developing chick corneal epithelium. Caspase 3 positive cells (indicated by arrows) were observed in the limbal epithelium at ED16 **(s)**, and central epithelial regions at ED18 **(x)** and ED21 (posthatch) **(α)**. Negative controls, rabbit IgG **(c1)** demonstrated no immunolabelling. Positive controls; Dnase I treatment **(c2)** and rat mammary gland **(c3)** showed positive labelling for caspase 3. Scale bars = 100 μm. x 100.

However, PCNA immunolocalisation studies demonstrated that this antibody successfully labelled proliferating cells in the developing chick corneal epithelium and the LI demonstrated temporal changes in the number of PCNA-positive cells.

An increase in proliferation rates in the developing chick corneal epithelium was evident from ED6 to ED12, followed by a peak, and finally a decrease of PCNA-positive cells between ED16 to ED21 in the posthatched epithelia. The proliferative rate in the peripheral epithelium was higher when compared to limbal and central epithelium at all developmental time points.

The peak proliferation rate occurs at the same time that the epithelium was observed to undergo initial stratification and maturation (ED12 and ED14). This observation also coincides with the appearance of CK3 expression and distribution of pan-CK labelling, discussed in Chapter 3.

The use of immunofluorescence allowed the study of the spatial distribution of PCNA expression in the epithelium during chick corneal development. It was observed that basal and suprabasal cells were PCNA-positive in earlier developmental time points (ED4 to ED14) in the central and peripheral epithelium. In the limbus, the fewer proliferating cells were observed. From ED16 onwards, an abundance of proliferating cells was observed mainly in suprabasal layers in all regions and basally in limbus.

The expression of PCNA in the corneal epithelium detected by immunofluorescence was confirmed by Western Blotting, PCNA protein was identified in all stages from ED6 to posthatching. The levels of protein increased from ED6, peaking at ED10 to ED12, before gradually decreasing. Although, the observed protein expression for ED21 posthatch epithelium appeared to be greater then other bands, after normalisation and analysis, the amount of protein expressed in this sample was not statistically different (Fig 4.5e, Appendix III). Opposite tendency (decrease of PCNA-positive cells when compared to embryonic time-points) was visualised by PCNA immunolabelling,

this dissagreement could be explained by different sensitivity of these two techniques.

The observed profile of proliferating cells in the epithelium during avian corneal development was different to that observed in humans. Yew and coauthors (2001) reported that before the 17th gestational week, PCNA-positive cells were not identified, although, the cornea is developed by 7-8 week of gestation (Rodrigues *et al.*, 1987). The appearance of PCNA labelling at ED4 in chick corneal epithelium and an increase in the number of proliferating cells suggested that abundant cell proliferation in earlier development is fundamental for tissue formation during development.

Additionally, in the chick epithelium the increase in proliferation was accompanied by the appearance of CK3 and pan-CK labelling, unlike in humans, where expression of CK3 was observed at 12-13 week of gestation (Rodrigues *et al.*, 1987). It has been recently reported, that mouse genetics and human diseases have provided strong support for the idea that changes in expression of certain cytokeratins (CK6, 8, 16, 18, 17, 14-3-3σ isoform) have a profound impact on cell size and cell proliferation in skin epithelium (Magin *et al.*, 2007; Pallari and Eriksson, 2006; Gu and Coulombe, 2007).

As demonstrated, in chicken corneal epithelium the peak of proliferation was followed by a steady decline from ED16 onwards in all epithelial regions. Similarly, in humans after the twentieth week of gestation, intense PCNA-labelling was observed throughout the corneal epithelium, but after twenty eight weeks, anti-PCNA labelling gradually disappeared from the central and peripheral corneal epithelium (Yew *et al.*, 2001).

In developing chick corneal epithelium, proliferating cells were observed in the limbus in both basal and suprabasal layers from earlier stages to ED16. Later, at ED18 and in posthatched epithelium, occasional basal cells showed positive nuclear labelling in all three epithelial regions with more positively labelled cells in suprabasal layers. It was similar to the results demonstrated in the postnatal human corneal epithelia after immunolabelling for Ki67. Within the corneal

epithelium, only a few basal cells were labelled, but the nuclei of cells in the above layers were more abundant. In the limbal epithelium, individual Ki-67-positive cells were located basally and more positively labelled cells were demonstrated in one or two layers above the basal layer (Joyce *et al.*, 1996). Other studies in rabbit and SENCAR mouse corneal epithelia showed that majority of the cells that incorporated ^{3}H-thymidine appeared to be suprabasally located in the central cornea (Lavker *et al.*, 1991). Those cells were shown to be basal cells that were expelled into the suprabasal layer, still connected to basement membrane via a thin stalk of cytoplasm (Lavker *et al.*, 1991). Another study, carried out by Francesconi and co-authors (2000), in developing corneal epithelium in rats after birth showed that at age 1-3 days, proliferation was maximal with Ki67-positive cells localised in the basal layers of corneal and limbal epithelium, but Ki-67 labelling was not identified in suprabasal layers. Similarly, in mouse corneas, Ki-67-positive cells were exclusively distributed through the basal cell layer in all epithelial regions (Fabiani *et al.*, 2009). In this study the percentage of PCNA-labelled cells was higher in the central than limbal epithelium both in pre- and posthatch corneas which is consistent with observations made in rat epithelia (Francesconi *et al.*, 2000).

It has been postulated, that the limbal epithelium contains a mixture of slow-cycling stem cells and more rapidly cycling transient amplifying cells, the central corneal epithelium contains rapidly proliferating basal cells and that the suprabasal cells have excited the cell cycle and become terminally differentiated (Francesconi *et al.,* 2000; Cotsarelis *et al.*, 1989; Lavker *et al.*, 1991). This study however, also showed PCNA-labelled cells in the suprabasal layers. Whether those labelled cells were basal cells expelled to above layers or undifferentiated suprabasal cells undergoing proliferation, requires further investigation.

The observation that peripheral epithelium in developing chick cornea had a higher percentage of proliferating cells than central and limbal region is in agreement with previous reports and may support the hypothesis about the role of populational pressure in the periphery that forces cells to migrate towards the central cornea (Lavker *et al.*, 1991; Fabiani *et al.*, 2009).

It is likely that in the earlier developmental stages and later, when corneal epithelium reorganises, the mechanisms of cell proliferation and differentiation are similar to that which occurs during the wound healing. Studies of epithelial wound-healing response in culture, demonstrated that as cells migrate, proliferation is suppressed in the migrating cell front, allowing these cells to maintain their cell-to-cell contacts and form a continuous advancing front in order to maintain structural integrity (Zelenka and Arpitha, 2008). Similarly, during normal homeostasis continuous centripetal movement of the peripheral corneal epithelium towards the visual axis maintains corneal epithelial mass, and balances the cellular loss resulting from anterior movement of the basal epithelial cells to the surface (Sharma and Coles, 1989; Agrawal and Tsai, 2003).

The role of different key regulatory mechanisms of the cell cycle has been studied intensively at both protein and gene levels. For instance, it has been shown that proto-oncogenes i.e c-*Fos* c-*Jun*, and *Fra-2* are expressed in normal ocular surface epithelia (Saika *et al.*, 1999; Bourcier *et al.*, 2000) and may play an important role in modulating epithelial cell functions (i.e. proliferation, migration, and differentiation) during epithelial wound healing. An immediate expression of nucleoprotein encoding proto-oncogenes could represent the molecular response that initiates the healing process (Thompson *et al.*, 1989; Bourcier *et al.*, 2000). Moreover, proto-oncogenes of the Fos/Jun family have been shown to be upregulated in many basal cell layers of the corneal epithelium after UV exposure (Wickert *et al.*, 1999; Bourcier *et al.*, 2000).

The retinoblastoma gene product (pRb) and E2F (Eukaryotic transcription factor family) appeared to regulate entrance and exit from the cell cycle by activating the transcription of genes necessary for DNA synthesis (Francesconi *et al.*, 2000, Ikeda *et al.*, 1996) and were shown to exhibit differential localisation depending primarily on the differentiative state of the corneal cells (Francesconi *et al.*, 2000). The mechanism of their activity, thus cell cycle regulation, is likely to be dependent on their translocation from the cytoplasm to the nucleus (Francesconi *et al.*, 2000).

Also, members of Notch genes family have been shown to modulate cell proliferation in the corneal epithelium (Ma *et al.*, 2007; Djalilian *et al.*, 2008). Notch signalling is initiated by the interaction between the ligand on one cell and the receptor on a neighbouring cell, which triggers the proteolytic cleavage of the Notch receptor (Djalilian *et al.*, 2008; Schroeter *et al.,* 1998). Transactivation of protein targets such as Hairy/Enhancer of Split (*Hes*) and Hairy/Enhancer of Split-related genes, which in turn affect numerous pathways involving cell-fate determination, requires translocation of Notch intracellular domain to the nucleus (Lai, 2002; Djalilian *et al.*, 2008).

Other examples of recently reported factors involved in proliferation in corneal epithelium include DeltaNp63 isoforms (Robertson *et al.*, 2008), Krüppel-like factor 4 (Klf4) (Swamynathan *et al.*, 2008), Rho-associated serine/threonine kinase (ROCK) (Chen *et al.*, 2008) and epiregulin (Morita *et al.*, 2007).

The modulators of cell proliferation and differentiation are under investigation and still many questions regarding the exact mechanisms and pathways of their actions need to be answered.

In conclusion, the above results demonstrated that proliferation in the developing chick corneal epithelium, although vigorous throughout development, was particularly increased at mid time points, ED10 to ED14. The increase in percentage proliferating cells was preceded by synthesis of PCNA protein. Decrease in number of PCNA-positive cells in later developmental time points and differences in regional localisation of PCNA-positive cells with the restriction to the suprabasal cell layers in the peripheral and central epithelium of neonates, suggested that by the time of hatching corneal epithelial proliferation acts as mechanism of control responsible for the maintenance of epithelial homeostasis.

PCNA as a marker of proliferation

In this study PCNA (PC10) antibody was used as a marker of cell proliferation due to its wide use in different species, the possibility of using it with fixed

tissue and its correlation with BrdU labelling (Hall *et al.*, 1990; Katsuda *et al.*, 1993).

Previously, techniques used for assessing cell proliferation in developing tissues included measurements of the incorporation of thymidine analogues, such as BrdU (Bromodeoxyuridine) or tritiated thymidine (Yu *et al.*, 1992). Although, both techniques were effective for evaluating cell proliferation rates, some disadvantages derived from each of those methods were indicated. The main limitation of BrdU incorporation is the fact that it can only be performed in viable cells, which requires additional animal handling and precise timing and dosage. Finally, BrdU is incorporated to cells in S phase and is a mutagen, which limits its usage (Muskhelishvili *et al.*, 2003).

The Ki-67 protein is considered to be proliferation marker in cycling cells (G1, S, G2, M phases) (Gerdes *et al.*, 1984). Ki-67 acted as a marker of actively cycling cells, as it is synthesised in the mid-G1-phase and then enters the nucleus where it is present throughout the cell cycle (Joyce *et al.*, 1996; Gerdes *et al.*, 1984). Although Ki-67 is widely used, some doubts have been reported with regards to Ki-67 protein half life, expression during the cell cycle and between cell types (Louis *et al.*, 1998; Zuber *et al.*, 1988). Other studies using anti-Ki-67 antibodies have also demonstrated an inability to obtain specific labelling in tissues other than human, including avian (Rodriguez-Burford *et al.*, 2001).

In contrast to Ki-67, PCNA, as an auxillary protein for DNA polymerase gamma is an evolutionarily conserved molecule, that may be detected in human and animal frozen or paraffin-embedded tissues (Moriuchi *et al.*, 1986; Matsumato *et al.*, 1987; Waseem and Lane, 1990), avian (94% homology in aminoacid sequence between human and chick) and plant cells (Suzuka *et al.*, 1989).

Some controversy exists, whether PCNA can be defined as a specific indicator of proliferation. It has been reported that PCNA is expressed in some replicating pathological cells, and is engaged in DNA repair (Shivji *et al.*, 1992;

Hall *et al.*, 1990). In spite of the fact that anti-PCNA immunohistochemistry may also weakly stain non-proliferating cells (Mokrý and Němecek, 1995), PCNA is the most frequently detected proliferation marker and appeared to be an excellent alternative for an evaluation of proliferating cells in the physiological tissue.

4.6.2 Epithelial cell death profile during chick corneal development

Programmed cell death (apoptosis) is a selective process of physiological cell deletion and its execution plays a major role in the control of shape and size in normal and abnormal processes (Kerr *et al.*, 1972; Wyllie *et al.*, 1980; Gavrieli *et al.*, 1992). Apoptotic death is characterised by DNA fragmentation, chromatin condensation, membrane blebbing, cell shrinkage and apoptotic bodies and a number of techniques have been developed to identify and quantify cell apoptosis (Duan *et al.*, 2003). Detection of apoptosis in tissue sections includes microscopic techniques for morphology assessment, analysis of DNA degradation (TUNEL assay, *in situ* hybridisation for DNA strand-breaks) and immunohistochemistry for apoptosis-associated proteins (Gavrieli *et al.*, 1992; Hall, 1999; Save *et al.*, 2001; Willingham, 1999; Duan *et al.*, 2003).

To examine in more detail the condensation and fragmentation state of chromatin during corneal epithelial differentiation, TUNEL and counterstaining with methyl green were performed. In situ TUNEL labelling is a method for examination of apoptosis via DNA fragmentation (Gavrieli *et al.*, 1992). The DNA strand breaks are detected by enzymatic labelling of the free 3'-OH termini with modified nucleotides. The new DNA ends are typically localised in morphologically identifiable nuclei and apoptotic bodies. The technique is highly specific; normal or proliferative nuclei (low abundant in DNA 3'-OH ends) are not stained, and it allows detection of an apoptotic cells in the early stage (where strand breaks are fewer, before the nucleus undergoes major morphological changes) (Migheli *et al.* 1995).

In our studies the mean percentage of TUNEL-positive cells was between 2.5±0.6 and 5.7±0.7 throughout epithelial development. Individually labelled cells were observed mostly in the limbal epithelium. In most cases the value

was equal to zero (i.e. no TUNEL-positive cells were observed), thus statistical analysis was impossible. It has been reported, that apoptotic cell appearance is limited to only a few minutes (Russell *et al.*, 1972; Sanderson, 1976; Kerr *et al.*, 1987) and apoptotic bodies in diverse forms are seen for only a few hours before they are phagocytosed (Wyllie *et al.*, 1980; Brusch *et al.*, 1990). A rate of tissue regression, as rapid as 25% per day, can result from apparent apoptosis in only 2-3% of the cells at any one time (Brusch *et al.*, 1990). In other words, when within a hundred cells three TUNEL-positive cells are detected at a time, it might be predicted that the actual number of cells undergoing cell death would be actually twenty five.

Previous studies, where the TUNEL technique was applied to flatmounts and frozen sections of the normal rat corneal epithelium, demonstrated very few TUNEL-positive cells in the flatmounts, with a lack of labelling in wing and basal cell layers (Ren and Wilson, 1996). The TUNEL-positive cells were found only on the epithelial surface and not in deeper layers (Ren and Wilson, 1996). Similarly a limited number of apoptotic cells on the surface of the rabbit corneal epithelium was reported by Gao and coauthors (1997). Despite the fact that the TUNEL-positive cells were detected on the surface of the cornea, it is still unknown, whether they represented a population of classically apoptotic cells or were terminally differentiated cells that can form blebs. Apoptotic bodies have not been yet found on the surface of the normal human corneal epithelium, but structures described as blebs have been reported in keratoconic corneas examined by scanning electron microscopy (Ren and Wilson, 1994; Pfister and Burstein, 1977). Also, TUNEL-positive cells were absent in the developing human cornea (Yew *et al.*, 2001). Labelled cells were first observed postnatally in the epithelium.

Although the TUNEL assay is quite sensitive and widely used, it is prone to some pitfalls; it can label non-apoptotic nuclei showing signs of active gene transcription (Kockx *et al.*, 1998). Additionally, necrosis and autolysis may generate a sufficiently high number of DNA ends that can be positively labelled under certain conditions (Grasl-Kraupp *et al.*, 1995; Duan *et al.*, 2003). The ApopTag® Kit, used for TUNEL labelling in this study, distinguishes apoptosis

from necrosis, by specifically detecting DNA cleavage and chromatin condensation associated with apoptosis, nevertheless, there may be some instances where cells exhibiting necrotic morphology may stain lightly (Gold, 1994; Perry *et al.,* 1997), and thus the evaluation of the method is crucial. TUNEL assay is also associated with a number of technical problems, mostly related to DNA strand-breaks associated with excessive levels of proteinase digestion, with fixation and processing procedures, or with the action of section cutting or other pretreatments (Baron *et al.*, 2000, Duan *et al.*, 2003). Although, care was undertaken and all steps in the procedure were monitored (i.e. time of proteinase digestion), the possibility of such negative effect of the factors mentioned above can not be excluded. In order to minimise effect of fixation and processing procedure it might be useful to perform similar studies using cryostat sections, but yet again, the effect of cutting can not be eliminated.

To confirm that TUNEL labelling represented apoptotic cell death, immunohistochemistry against caspase 3 (active) was performed. Of the 14 identified caspases in mammals, caspase 3 is known to play a key role in the apoptotic pathway as an effector caspase (Bozanic *et a*l., 2003; Reed, 2000; Kuan *et al.*, 2000; Mirkes *et al.*, 2001). In response to various apoptotic stimuli, inactive pro-caspase-3 is cleaved by other activated caspases, primarily caspase 8 (Tewari *et al.*, 1995; Boldin *et al.*, 1995) and caspase 9 (Li *et al.*, 1997), to form two subunits (17 and 12 kDa) (Mirkes *et al.*, 2001). Once activated, caspase 3 cleaves a variety of substrates involved in DNA replication, transcription, and indirectly activates a nuclease responsible for internucleosomal DNA fragmentation (Mirkes *et al.*, 2001; Nagata, 2000). To date, there are many reports available regarding examination of apoptosis with anti-caspase 3 antibodies in early eye development in various species (Bozanic *et al.*, 2003; Laemle *et al.*, 1999; Lang, 1997; Zhang *et al.*, 1997; Wride *et al.*, 1999), but none have investigated later corneal epithelial development in detail.

The pattern of caspase 3 (active) localisation did not entirely mimic the distribution of TUNEL labelling in the developing chick corneal epithelium, although some similarities were noticed. Apoptotic cell death was identified in the limbal epithelium at ED16 and in the centre at ED18 and in posthatched

epithelia. TUNEL labelling was confirmed by caspase 3 (active) immunodetection. The fewer number of cells visualised by caspase 3 immunolabelling, in comparison to TUNEL, may result from the fact that activated caspase 3 allows identification of apoptotic cells in tissue sections, even before all the morphological features of apoptosis occur.

The lack of caspase-3 immunolabelling at earlier developmental stages of chick corneal epithelium is consistent with observations in the developing human eye (Bozanic *et al.*, 2003). The morphological patterns in the corneal epithelium of 7 week-old human embryos, corresponds to changes observed at ED4 of chicken development: the surface ectoderm becomes the corneal epithelium, while mesenchyme underlying this epithelium gives rise to the substantia propia of the cornea. During this period of eye development, apoptotic cells were observed throughout the whole width of the neural retina and in the anterior lens epithelium, but were absent from the corneal epithelium (Bozanic *et al.*, 2003).

To definitively answer questions about the scale of cell apoptosis in the developing chick corneal epithelium, it would be beneficial to perform further immunohistochemistry experiments; including dual labelling (TUNEL, active caspase 3) in a number of sections, immunolocalisation of cleaved cytokeratin 18, Annexin V labelling, or *in situ* hybridisation for DNA strand-breaks. However, the use of latter method is controversial, as it has been shown, that not only apoptotic, but also necrotic cells can incorporate the label (Wijsman *et al.*, 1993).

The cytokeratin 18 (CK18) has been identified as a substrate for caspases 3, 6 and 7 (Caulin *et al.*, 1997), which during apoptosis undergoes dramatic reorganisation and is cleaved, generating the apoptotic cascade before Annexin V reactivity or positive DNA nick-end labelling (Caulin *et al.*, 1997; Leers *et al.*, 1999). Several studies have suggested that the detection of cleaved CK18 could be a promising specific assay for apoptosis identification (Leers *et al.*, 1999; Huppertz *et al.*, 1999; Duan *et al.*, 2003) and CK18 was reported to be present in the corneal epithelium. The detection of cleaved CK18 was

successfully used to investigate apoptotic response of HSV-1 infection in human corneal epithelial cells (Miles *et al.,* 2007).

In situ end-labelling technique relies on the presence of DNA strand breaks in apoptotic cells, caused by the activation of endogenous nuclease activity during the process of cell death. These strands are labelled with a non-isotopic reporter molecule in the presence of a DNA polymerase, and labelled DNA is identified immunohistochemically. It has been shown that *in situ* end-labelling stains cells with the morphological characteristics of apoptosis, but also necrotic cells that can incorporate the label (Wijsman *et al.*, 1993). Nevertheless, this method in combination with other histological techniques (H&E staining) can greatly simplify the identification of apoptotic events (Ansari *et al.,* 2005).

In conclusions, it seems likely, that after the formation of the corneal epithelium (at ED4, HH 23-24), cell mitosis is involved in morphogenesis, whereas in later development might be associated with tissue differentiation and homeostasis. Cell proliferation appeared high throughout corneal development, with peak proliferation at ED14. The level of proliferation decreased throughout the corneal epithelium in posthatch tissue. The above coincides with changes in epithelial morphology (stratification) and changes in expression of epithelial markers described in Chapter 3. The level of proliferation decreased throughout the corneal epithelium from ED16 onwards, and more apoptotic events were observed in epithelia posthatching, suggestive that proliferation and apoptosis seems to play a minor role in corneal epithelial development as a regulatory mechanism in maintaining homeostasis of the epithelial cell population in later developmental time points.

The patterns of proliferation and differentiation showed changes during the development of the corneal epithelium which reflect interaction of a complex network of mitogenic, apoptotic and differentiation agents. It has been postulated that apoptosis shares a molecular pathway with the normal cell cycle and as such is regulated by the same molecular mechanism that control cell growth and proliferation and is sensitive to the same environmental factors (Haake *et al.*, 1993; Sen, 1992). Despite the knowledge already gained in the

field, the molecular mechanisms of apoptosis, the nature of cell signalling and the intrinsic factors that promote and regulate cell death are still largely unknown. Further analysis of potential agents involved in these processes, are performed at the gene level in the next chapters of this thesis.

CHAPTER FIVE

Gene expression profiles in chick corneal epithelium during development

GENE EXPRESSION PROFILES IN CHICK CORNEAL EPITHELIUM DURING DEVELOPMENT

5.1 Introduction

Vertebrate corneal development is the result of coordination of three basic events: cell proliferation, differentiation and cell death. The regulation of these events, in order to maintain tissue homeostasis and ensure normal development, is under strict molecular control. Programmes of gene expression are believed to be instituted early in embryogenesis and sequentially altered as development proceeds (Jan and Jan, 1993; Sorrentino *et al.*, 1990). Genes expressed by a particular cell depend on its embryonic lineage, the developmental stage of the organism/tissue, cellular environment and the functions that the cell must fulfil (Andreeff *et al.,* 2000).

Since cellular states are largely determined by the coordinated expression of thousands of genes, they must be tightly regulated by complex mechanisms which involve the sequential action of cell lineage-specific or cell type-specific factors that repress or activate the gene-specific response. These mechanisms can be divided into several categories such as changes in DNA sequence, changes in DNA structure/conformation, DNA methylation, chromatin protein alterations (histone modification/exchange, non-histone protein), non-coding RNA molecules regulating transcription, transcription regulatory factors, posttranscriptional control and translational control (Roloff and Nuber, 2005).

Throughout development, and in adult organisms, the ability of a cell to proliferate is intimately connected to its state of differentiation. A variety of factors act to maintain both proliferation and the differentiation status of the cell; these include secreted molecules, transmembrane receptors, intracellular signalling molecules and transcription factors (Andreeff *et al.* 2000). In the cornea, epithelial cell proliferation and differentiation were mostly studied in the context of wound healing. The importance of growth factors (i.e. TGFβ, EGF, HGF, FGF2), their receptors and downstream signalling components (e.g. smads, ras/raf/MEK/MAP, phosphoinositide 3-kinases (PI3K), protein kinase C (PKC), src family kinase pathways) in regulation of gene transcription, was

demonstrated in a number of studies (Zhang and Akhtar, 1998; Chandrasekher *et al.*, 2001; Xu *et al.*, 2007; Zelenka *et al.*, 2008).

The role of programmed cell death as a necessary mechanism complementary to proliferation is well documented during early stages of eye development (Wilson, 1999). In corneal epithelial system apoptosis is mostly reported as an *in vitro* induced event (Lu, 2006; Chang *et al.*, 2008; Kim *et al.*, 2008). Three major pathways which result in activation of caspase 3 have been elucidated: the mitochondrial/cytochrome C pathway (mediated through Bcl-2 family members), ligation of members of the TNF-receptor family or Fas (CD95), and granzyme B (Ashkenazi and Dixit, 1998; Hengartner, 2000; Nagata and Golstein, 1997). The role of a number of natural inhibitors (IAPs) and substrates (BH3-domain molecules) of caspases, Fas/Fas ligands (*i.e.* p53, FADD) and TRAIL receptors (i.e.DcR1/DcR2, DR4/DR5) was shown to be relevant at different levels of the programmed cell death cascade (Duckett *et al.*, 1996; Wei *et al.,* 2001; Owen-Schaub *et al.*, 1995; Chinnaiyan *et al.*, 1995; Pan *et al.*, 1997a).

The molecular mechanisms behind the function and regulation of corneal epithelial homeostasis require further investigation. It is also not clear when and how during embryonic development the limbal stem cell becomes committed to become an adult stem cell and crucial to the maintenance of epithelial tissue in postnatal life. Previous studies in other body systems have shown that adult and embryonic stem cells might share common pathways that are critical to stem cell survival and maintenance of the tissue they supply. For instance, Notch signalling was shown to be an evolutionary conserved mechanism for controlling cell fate through local intercellular interactions in adult and embryonic tissues (*i.e.* corneal and mammary epithelium) and also demonstrated to influence stem-cell fate in human epidermis, mouse intestinal epithelium (Lewis, 1996; Bray, 1998; Artavanis-Tsakonas *et al.*, 1999; Lowell *et al.*, 2000; Nicolas *et al.*, 2003; Hu *et al.*, 2006; Schroder and Gossler, 2002; Ma *et al.* 2007; Djalilian *et al.*, 2008).

The roles of other signalling pathways, in epithelial stem cell biology are less clear. Lack of sonic hedgehog (Shh) signalling, for instance, resulted in a severely impaired hair-follicle morphogenesis, whereas the development of the intestine and mammary gland are relatively normal, suggestive that hedgehog signalling may promote proliferation in some epithelial cells types whereas in other epithelial cells it inhibits proliferation or has no effect (Blanpain *et al.*, 2006).

5.2 Aims

- To reveal the gene expression profile during chick corneal epithelium development and identify main biological functions
- To identify genes involved in the processes of differentiation, proliferation and apoptosis during development
- To determine genes differentially expressed in the developing embryonic corneal epithelium compared to posthatched epithelial tissue
- To identify candidate genes involved in stem cell biology/regulation.

5.3 Experimental design

The specific methods involving sample preparation and chip processing are described in detail in Chapter 2, section 2.11. The experimental design described in this chapter refers to microarray data analysis (Step 9 in Figure 6.1) following initial preprocessing of data and validation to confirm quality of data obtained for further analysis.

Sample collection

Briefly, seven developmental time points (ED6, 10, 12, 14, 16, 18 and ED21 posthatch) were selected for gene expression studies. These were selected based on earlier morphological and immunolocalisation studies discussed in Chapter 3 (sections 3.6.1, 3.6.2) and Chapter 4 (sections 4.6.1, 4.6.2).

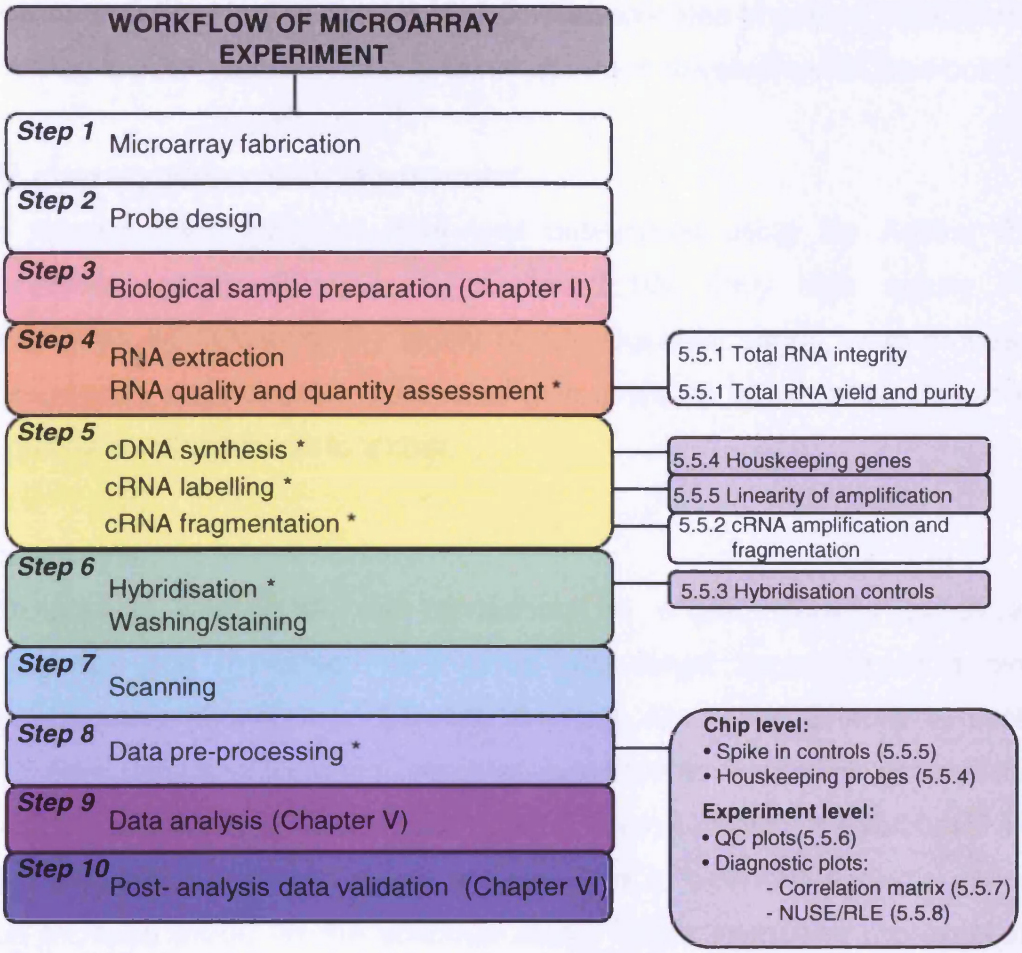

Figure 5.1 Workflow of procedures for gene expression profiling. Left panel shows successive steps, right side panels denotes controls/validation techniques involved in each of experimental step; white background: controls used to validate quality control during experimental procedures, grey background: validation carried out post-experimentally.

To minimise the influence of potential individual differences between animals and technical variation introduced by tissue preparation and dissection, total RNA, isolated from corneal epithelia of a number of animals at each developmental time point, was pooled. Three replicates of pooled RNA (derived according to RNA content) were obtained for each developmental time-point.

RNA quantity and quality assessment

The amount and quality of RNA was determined using the Agilent 2100 Bioanalyser system (Chapter 2, section 2.10). Only high quality RNA preparations, as judged by the clarity of the ribosomal bands, were processed for microarray experiments. RNA quality is a critical factor which determines the quality of hybridisation to a chip.

Microarrays

Each pool of total RNA was converted do cRNA, labelled by *in vitro* transcription and hybridised to a short oligo-target sequence on a single microarray chip (Gene Chip® Chicken Genome Array, see Chapter 2, section 2.11). Raw data after scanning were represented as an image, generated by measuring signals in defined areas (pixels) across the entire hybridised area. The main objective of this image analysis was to calculate a single intensity value for each probe on the scanned array. These intensities represent how much hybridisation has occurred for each oligonucleotide probe. After image scanning and quantification, raw intensity data was further processed to correct systematic variations and prevent artefacts before data analysis. This included background correction, summarisation, normalisation and transformation (see section 5.4.1).

5.4 Microarray Data Analysis

5.4.1 Pre-processing of data

Data pre-processing was performed using software tools that have been developed under the Bioconductor v.1.6. project (Gentleman *et al.*, 2004). Pre-processing GeneChip® expression data involved generation of 3 types of files; .DAT, .CEL and .CHP with Affymetrix GCOS software. Each .CEL file

corresponds to a single hybridisation and contains the intensities for each probe on the chip. Statistical software tools like R (Ihaka and Gentleman, 1996) in conjunction with Bioconductor allowed investigation of different quality parameters using .CEL data after background correction and normalisation (see section 5.4.2). Bioconductor uses the best known algorithms for preprocessing microarray data, such as MAS5.0, Robust Microarray Average (RMA) and GC-RMA for single channel arrays, and LOESS normalisation for two-channel arrays (Irizarry *et al.*, 2003, Yang *et al.*, 2001, Tarca *et al.*, 2006).

5.4.2 RMA normalisation

Robust Multiarray Average (RMA) was used to analyse microarray data as described by Bolstad and coauthors (2003) for vast data sets. RMA method handles background adjusted, log-transformed and normalised Perfect Match (PM) values in order to produce an expression value that is exhibiting reduced bias and non biological variability. RMA estimates are based upon robust average of log_2 *(B (PM)),* where *B (PM)* are background corrected PM intensities. RMA method was performed to increase the sensitivity and specificity of the final measure of expression and to be more powerful at lower sample sizes when compared to other methods (*i.e.* MAS5.0).

5.4.3 Identifying differentially expressed genes

Limma analysis

To identify differentially expressed genes Limma analysis was used (part of Bioconductor package). Limma is a package for differential expression analysis of microarray data and its central idea is to fit a linear model to the expression data (log-expression values) for each gene (Smyth, 2005). With one-channel data (Affymetrix GeneChip®) linear modelling is equivalent to ANOVA or multiple regression. It provides functions which summarise the results of the linear model, performs hypothesis tests and adjusts the p-values for multiple testing (p-values are multiplied by the number of comparisons) (Smyth, 2005). The p-values for each gene resulting from Limma were corrected for multiple testing using the False Discovery Rate (FDR) method (Benjamini and Hochberg, 1995) with a p-value cut off of 0.000000001. The FDR is defined as

the expected proportion of false positives (incorrectly rejected null hypotheses, type I errors) amongst all significant tests, and the p-value of an individual test is the minimum FDR at which the test may be called significant.

Fold change calculation

The fold changes (fc) calculation is another technique to identify differentially expressed genes. Although, it is commonly used in static experiments, this method is not directly applicable for time course experiments, where differential expression has to be calculated globally in the temporal space and not just between corresponding time points (Storey *et al.*, 2005; Jonnalagadda and Srinivasan, 2008). For the purpose of this study to identify genes relevant at a particular time point and select candidates for validation of microarray experiment (see Chapter 6), fc were calculated on log normalised RMA data between particular time points according to the formula: log(A/B) = log(A) - log(B).

5.4.4 Principal Component Analysis

Principal Component Analysis (PCA) was used to identify differentially expressed genes and reveal fundamental patterns within the microarray data. A statistical test (ANOVA) was used on RMA data to find the significance of differences in expression values between time points for each gene, thus identify differentially expressed genes and their p-values. PCA was applied on the data found as significant by the ANOVA at a significance of 0.05. The set of vectors (a linear transformation of the expression values of all genes) obtained from the analysis was applied back to the data in order to identify most variable elements (probe sets) that show the highest correlation (R^2>0.9) to defined vectors (components). Since only the dominant components (the first two that capture the highest variance) are used for analysis, the effect of noise in data is alleviated.

5.4.5 Gene Ontology clustering

Probe sets identified by RMA analysis were uploaded into MADRAS (*www.madras.uwcm.cf.ac.uk*, Microarray Bioinformatic Group, Cardiff University) where gene expression profiles could be visualised using heatmaps.

The tools for data mining used in this study included the Database for Annotation, Visualisation and Integration Discovery (DAVID) 2.1 v.6 (*http://david.abcc.ncifcrf.gov/)* and NetAffx (Affymetrix Analysis Centre, *http://affymetrix.com/analysis/index.affx).* All softwares incorporated the Gene Ontology (GO) approach, which compares the number of genes found in each GO category of interest with the number of genes expected to be found in the same category just by chance. If the observed number is substantially different from the one expected to be found just by chance, the category is reported as significant (Tarca *et al.*, 2006).

DAVID 2.1 software suite integrates functional genomic annotations with intuitive graphical summaries. The Classification Tool uses a novel clustering algorithm that allows the classification of highly related genes into functionally related groups based on similar biological terms between them. The Functional Annotation Tool was used to cluster related terms/annotations (gene functions) based on a gene list.

A novel heuristic partitioning procedure, applied to create clustering, allowed an object (gene) to participate in more than one cluster, when using the Classification Tool. The use of this method, in grouping related genes, better reflects the nature of biology. The same genes can be classified to several clusters, but genes that significantly fall under a specific term (function) will cause the separation of these clusters. The DAVID system calculation in Functional Classification Tool is based on the assumption that a gene group is more important if a majority of its gene members are associated with highly enriched annotation terms, as found in the traditional enrichment analysis of the total gene list (the whole genome, so called background) (Huang *et al.*, 2007). Clusters were ranked according to enrichment scores, which were calculated as a geometric mean of EASE scores (more conservative Fisher Exact p-value) of terms involved in each gene group, following minus log transformation. Since the geometric mean is a relative score instead of an absolute *p* value, the group enrichment scores are intended to order the relative importance of the gene groups instead of as absolute decision values (Huang *et al.*, 2007).

The detailed fuzzy heat map view available in DAVID software allowed examination of similarities and differences of annotation across the group gene members, as well as between different gene families, since genes and terms/annotations appear multiple times within the heatmap. An interesting area (cluster) can be then selected and viewed in detail. However, this is one of the exploratory tools available online, thus only introduced in this chapter

On the other hand, the Functional Clustering Tool clusters similar biological terms (functions). However, genes that bring each cluster together belong to different gene families. Additional advancements included in this algorithm are: the automatic determination of the optimal number of clusters, and the exclusion of members (genes) that have weak relationships. The DAVID Classification and Functional Clustering Tools were run using default parameters (medium stringency, similarity threshold at 0.35 level) for most analyses, unless stated otherwise.

The NetAffx is an online resource which was used to correlate GeneChip® array results with array design and annotations. NetAffx provides access to integrated biological annotations from a broad range of both public (GenBank, RefSeq, Ensembl, UniGene, Entrez Gene, UniProt, UCSC) and Affymetrix-specific databases through a streamlined interface. The NetAffx was used to search through lists of significant probe sets for terms of interest and to identify genes/ESTs that were recognised as 'not annotated', due to less frequent updates of other softwares' databases.

All tables presented in this chapter and Appendix V contain the Affymetrix probe set IDs, gene names, symbols, as well as, Unigene reference numbers.

RESULTS

5.5. Validation of techniques to ensure quality and reproducibility of microarray data

Generating gene expression measures by using a microarray platform like Affymetrix GeneChip® is a sophisticated and time consuming process with many potential sources of variation (Heber and Sick, 2006). Sources of variation that could compromise gene expression data and analysis results include biological variation, sample preparation (total RNA isolation, labelling) and the system used (instruments and arrays). Speculations about biological variability require earlier identification of other non-biological sources of variation. Experimental variations come from undesirable systematic error introduced during the many technical steps (Imbeaud and Auffray, 2005), involving tissue processing, labelling and hybridisation. The standardised procedure to assess the quality of individual chips within experiments involves the collection, visualisation and interpretation of a defined set of quality measurements.

5.5.1 RNA quality and quantification

Total RNA integrity

The sharp definition of the 28S and 18S ribosomal RNA species in all lines demonstrated the integrity of samples (Figure 5.2). Distinct double intensity of the 28S in relation to 18S rRNA band and non-smeared appearance of major bands indicated high quality, non-degraded RNA in all samples to be processed for microarray analysis.

Total RNA yield and purity

Yield, purity and integrity measurements for all total RNA samples are listed in the table below (Table 5.1). Samples of high quality typically had a ratio of 28S/18S close to 2 and RNA Integrity Number (RIN) close to 10. RNA purity was determined by optical density (OD) measurements at wavelengths of 260 and 280nm. Samples of high quality had a 260/280 ratio within the range 1.8-2.29.

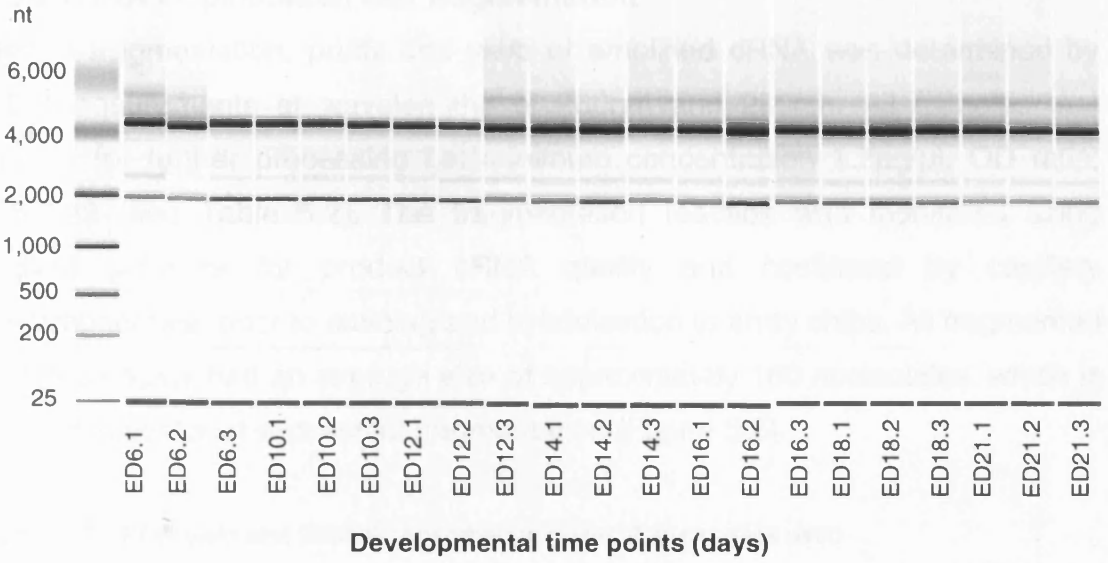

Figure 5.2 Image file output of total RNA isolated from chick corneal epithelia at different developmental time points (n=3) obtained from Lab-on-a-chip system from Agilent. When viewed as a virtual gel, the 28S, 18S are easily identifiable, and all lanes contain good quality RNA.

Table 5.1 Total RNA yield, 260/280 absorbance ratios, integrity parameters of samples used in array experiments

Sample	RNA ng/µl	260/280 ratio	rRNA ratio 28s/18s	RNA integrity number
ED6.1	173	1.97	2.7	10
ED6.2	348	2.01	1.8	9
ED6.3	267	2.03	2.7	10
ED10.1	482	2.07	2.2	9.8
ED10.2	441	2.1	2.4	10
ED10.3	410	2.05	2.5	10
ED12.1	410	2.09	2.1	9.8
ED12.2	362	2.01	2.3	10
ED12.3	564	2.04	2.4	10
ED14.1	399	2.05	2.1	9.7
ED14.2	347	2.04	2.5	10
ED14.3	471	2.03	2.5	10
ED16.1	355	2.03	2.1	9.7
ED16.2	347	2.02	2.6	10
ED16.3	383	2.03	2.3	10
ED18.1	396	2.00	2.1	9.7
ED18.2	447	2.03	2.3	9.8
ED18.3	317	2.02	2.5	10
ED21.1	344	2.07	2.0	9.6
ED21.2	290	2.05	2.3	10
ED21.3	597	2.01	2.7	10

5.5.2 cRNA amplification and fragmentation

Before fragmentation, purity and yield of amplified cRNA was determined by OD measurements at wavelengths of 260nm and 280nm. All samples met criteria for further processing i.e. minimum concentration 1.7µg/µl, OD ratio; 1.8-2.29 (see Table 5.2). The fragmentation reaction was monitored using Agilent software for product cRNA quality and confirmed by capillary electrophoresis, prior to staining and hybridisation to array chips. All fragmented cRNA samples had an average size of approximately 100 nucleotides, which is a good indicator of successful fragmentation (Figure 5.3).

Table 5.2 cRNA yield and 260/280 absorbance ratios of all samples used

Sample	RNA µg/µl	260/280 ratio
ED6.1	1.78	2.08
ED6.2	1.81	2.07
ED6.3	2.04	2.07
ED10.1	3.09	2.00
ED10.2	2.96	2.02
ED10.3	2.67	2.03
ED12.1	3.07	2.00
ED12.2	2.58	2.03
ED12.3	2.73	2.02
ED14.1	2.36	2.05
ED14.2	2.27	2.05
ED14.3	2.91	2.00
ED16.1	2.75	2.03
ED16.2	2.84	2.01
ED16.3	2.24	2.05
ED18.1	2.62	2.04
ED18.2	2.82	2.03
ED18.3	2.34	2.05
ED21.1	1.79	2.07
ED21.2	2.00	2.07
ED21.3	2.43	2.04

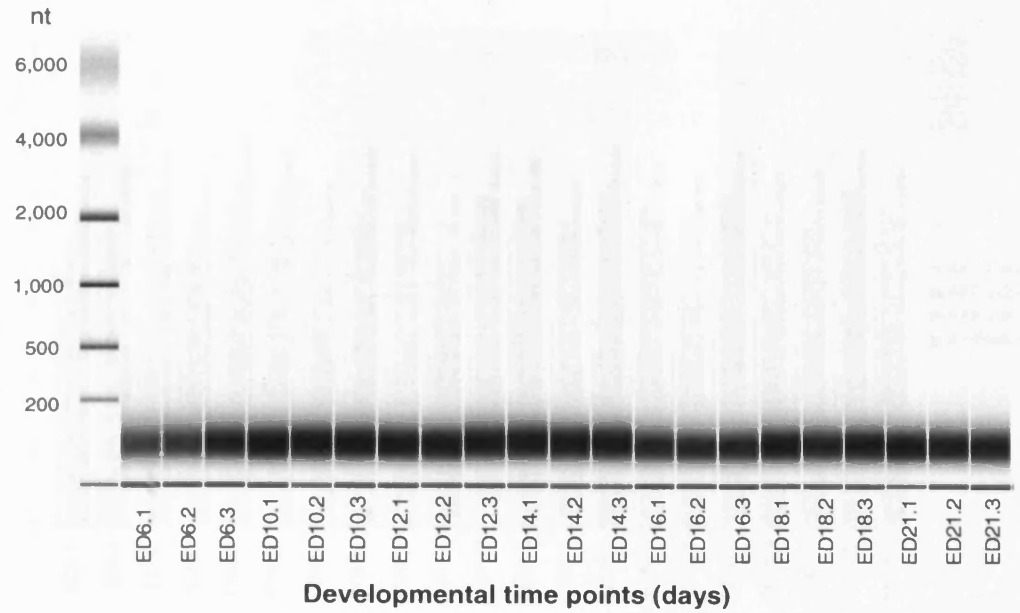

Figure 5.3 Image file output of fragmented cRNA from different samples of developmental time points (ED6-ED21, n=3) used for hybridisation to arrays.

5.5.3 Hybridisation controls

External controls (mixture of biotin-labelled cRNA transcripts of *BioB, BioC, BioD* and *Cre* prepared in staggered concentrations, section 2.11.6) gave increasing signal values (the fourth being the highest), reflecting their relative concentrations and the level of signal intensity was maintained across the arrays (Fig. 5.4). The series of quality control parameters associated with this assay and hybridisation performance are listed in Appendix IV.

5.5.4 Housekeeping genes

In addition to conventional probe sets, which are designated to be complementary to the region within 600bp of the 3' end of the transcripts, the internal controls (GAPDH, glyceraldehyde 3-phosphate dehydrogenase and β-Actin) also have 5' and middle (M) probe sets included on the array. These are intended to give an indication of the integrity of the RNA sample, and efficiency of 1st strand cDNA synthesis. As indicated in Figure 5.5, signal intensity values are consistent across the data set, suggesting minimal quality variation between samples hybridised to different chips.

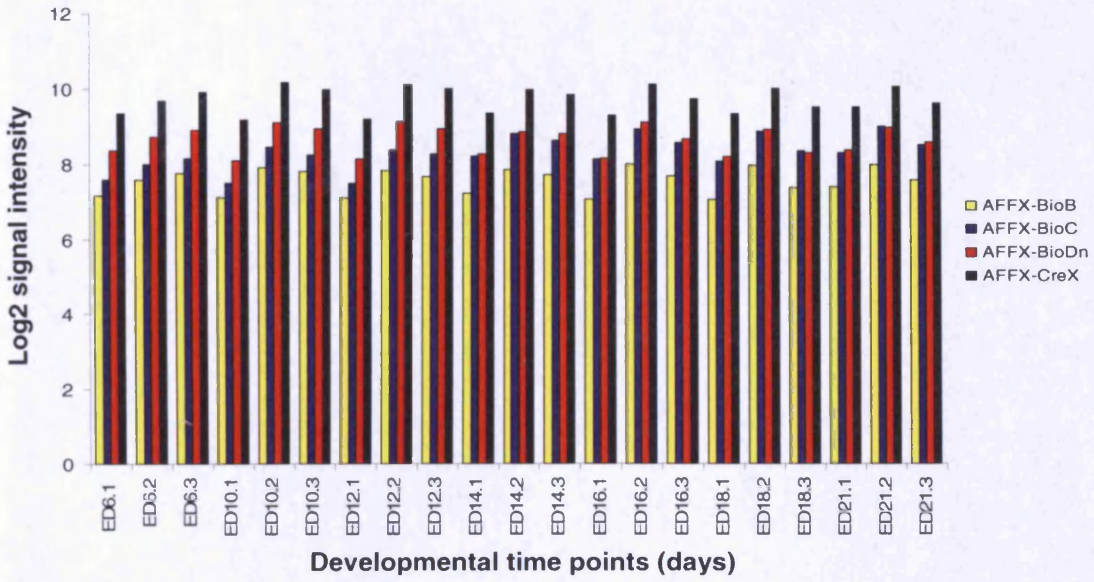

Figure 5.4 Log2 signal intensity of external spiked controls for each array. Controls (BioB, BioC BioD and cre) increase in quantity, which is reflected in the signal intensity.

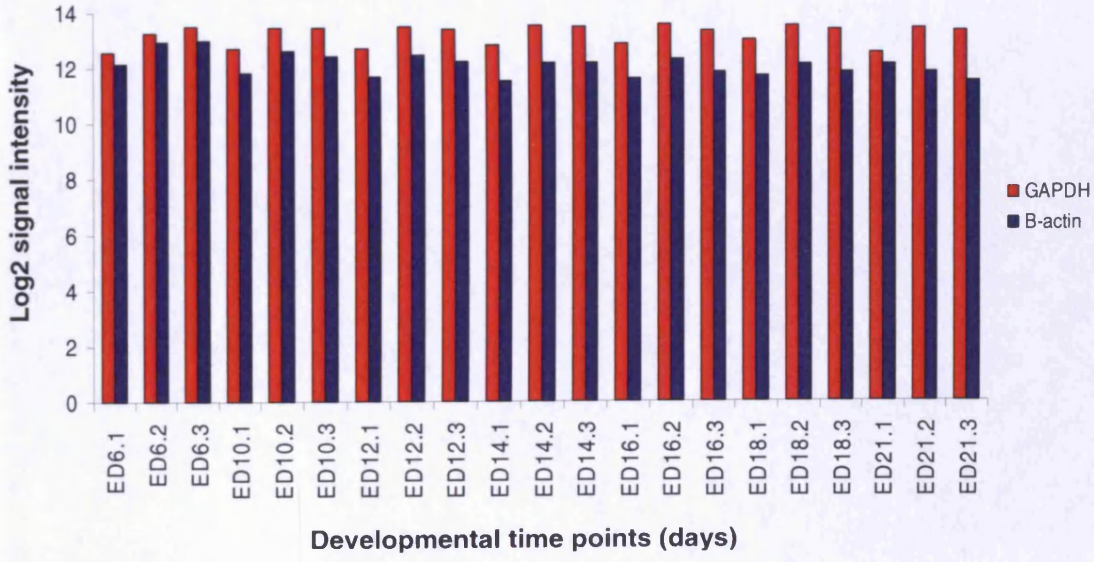

Figure 5.5 Log2 signal intensity of internal controls for each array. Controls (GAPDH and β-actin) increase in a quantity, which is reflected in the signal intensity.

The signal for the 3', M, and 5' probe sets (3' signal higher than for the M' and 5' probe sets, due to the direction of synthesis) and the ratio for the 3'/5' signal values (<3) confirmed the high quality of the samples (Appendix IV).

5.5.5 Linearity of amplification

Pre-synthesised mixture of four poly-adenylated prokaryotic RNA controls (*lys, phe, thr, dap* in increasing ratios of copy number 0.000001, 0.00002, 0.00004, 0.0001 respectively) were spiked into each RNA sample in staggered concentrations prior to RNA amplification and labelling (see section 2.11.1) to monitor the entire GeneChip® eukaryotic target labelling process.

All polyA+ controls showed increasing raw signal values in the following order: *dap>thr>phe>lys* and the consistency of signal was maintained between arrays (Fig. 5.6, Appendix IV). The values of the log transformed signal intensities of control transcripts were calculated for each array to check for correlation with their predetermined relative abundance ratios (Table 5.3). R^2 showed high correlation (R^2>0.95) between concentrations of transcripts and raw signal value, with the exception of array ED12.1 (R^2 = 0.9195) and ED16.1 (R^2 = 0.9488). However, these values are within the acceptable range and may be a result of different sample handling.

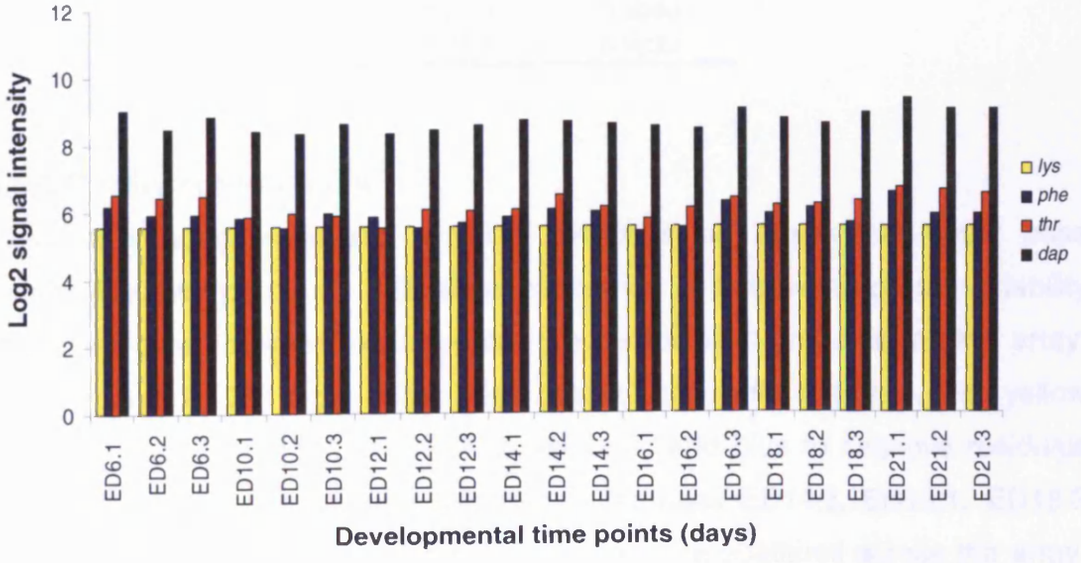

Figure 5.6 Log2 signal intensity of internal polyA+ controls for each array. The signal intensity was highest for the most abundant transcript (*dap*), and lowest for the least abundant (*lys*). Consistency of signal for each control was maintained for all chips.

Correlation between ratios of copy numbers for each control and mean signal intensities was 0.9835, indicating that 98.35% of the variance in ratios of control transcripts before and after amplification, was related. The reaction of amplification did not change these ratios, therefore, confirming the lack of experimentally induced variance.

Table 5.3 R^2 correlation values of log2 transcript relative concentration (ratio of copy number) versus log2 signal (fluorescence units) for each sample

Sample	R^2
ED6.1	0.9930
ED6.2	0.9949
ED6.3	0.9923
ED10.1	0.9594
ED10.2	0.9659
ED10.3	0.9564
ED12.1	0.9195
ED12.2	0.9706
ED12.3	0.9711
ED14.1	0.9732
ED14.2	0.9959
ED14.3	0.9769
ED16.1	0.9488
ED16.2	0.9722
ED16.3	0.9838
ED18.1	0.9784
ED18.2	0.9811
ED18.3	0.9816
ED21.1	0.9892
ED21.2	0.9949
ED21.3	0.9932

5.5.6 Quality control plots

Residual images visualised physical artefacts on arrays that could pose potential quality problems and allow evaluation of both within-group variability and effect-size between experimental groups for each probe set on the array. Quality control (QC) plots show false colour images for residuals, with yellow intensities corresponding to positive residuals, and blue to negative residuals (Fig. 5.7). A few hybridisation effects for samples ED14.3, ED18.1, ED16.3 were observed, however, as probes for genes are scattered across the array, these localised effects had negligible effect on the expression levels of the genes. Plots for other samples showed high similarity between the data.

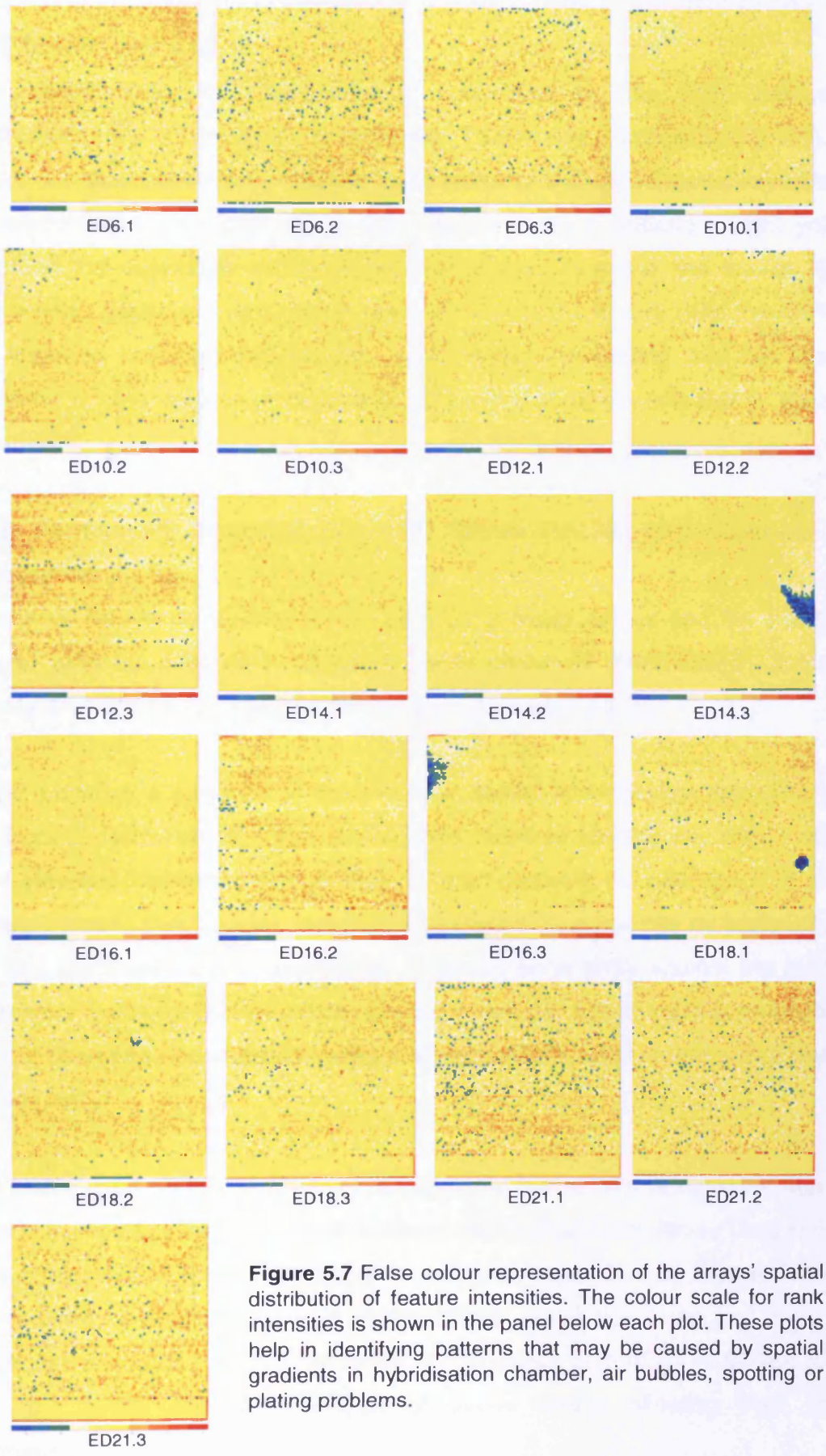

Figure 5.7 False colour representation of the arrays' spatial distribution of feature intensities. The colour scale for rank intensities is shown in the panel below each plot. These plots help in identifying patterns that may be caused by spatial gradients in hybridisation chamber, air bubbles, spotting or plating problems.

5.5.7 Correlation matrix

The reproducibility of the results is underlined by the high correlation coefficients (R^2) of the replicate samples. These had a range of 0.9 to 0.99. Figure 5.8 illustrates the correlation coefficients of the experimental repetitions. Correlation was visualised using a customised colour selection. Light yellow indicated the highest correlation coefficient values and red, the lowest. As it was shown, even the lowest correlation (R^2 value of 0.9) indicated that 90% of the variance between experiments was related, confirming that the results exhibited a high degree of reproducibility and lack of experimentally induced variance.

5.5.8 Normalised Unscaled Standard Errors (NUSE) and Relative Log Expression (RLE).

To assess the variability in gene expression between arrays and the quality of arrays, specific Affymetrix boxplots were obtained; Normalised Unscaled Standard Errors (NUSE) and Relative Log Expression (RLE).

NUSE provides a measure of relative chip quality derived from residuals from the Robust Multiarray Analysis (RMA) and helps to identify any arrays which have elevated standard errors relative to other arrays in the data set. RLE is the absolute metric that gauges variability of expression measures by summarising the $\log_2$ scale estimate of expression value on each array against the median expression value for that probe set across all arrays. Assuming that most genes are not changing in expression across arrays, ideally most of these RLE values will be near 0.

The NUSE plot shown in Figure 5.9a showed the arrays reasonably centred around the median NUSE=1, with approximately equal box sizes. They did not appear to present any quality control problems. As shown in Figure 5.9b, all arrays were centred near 0 and approximately equal box sizes and therefore presented no quality control problems. In all cases a median RLE was lower than 0.1 which confirmed a lack of outlier arrays allowing their cross comparisons.

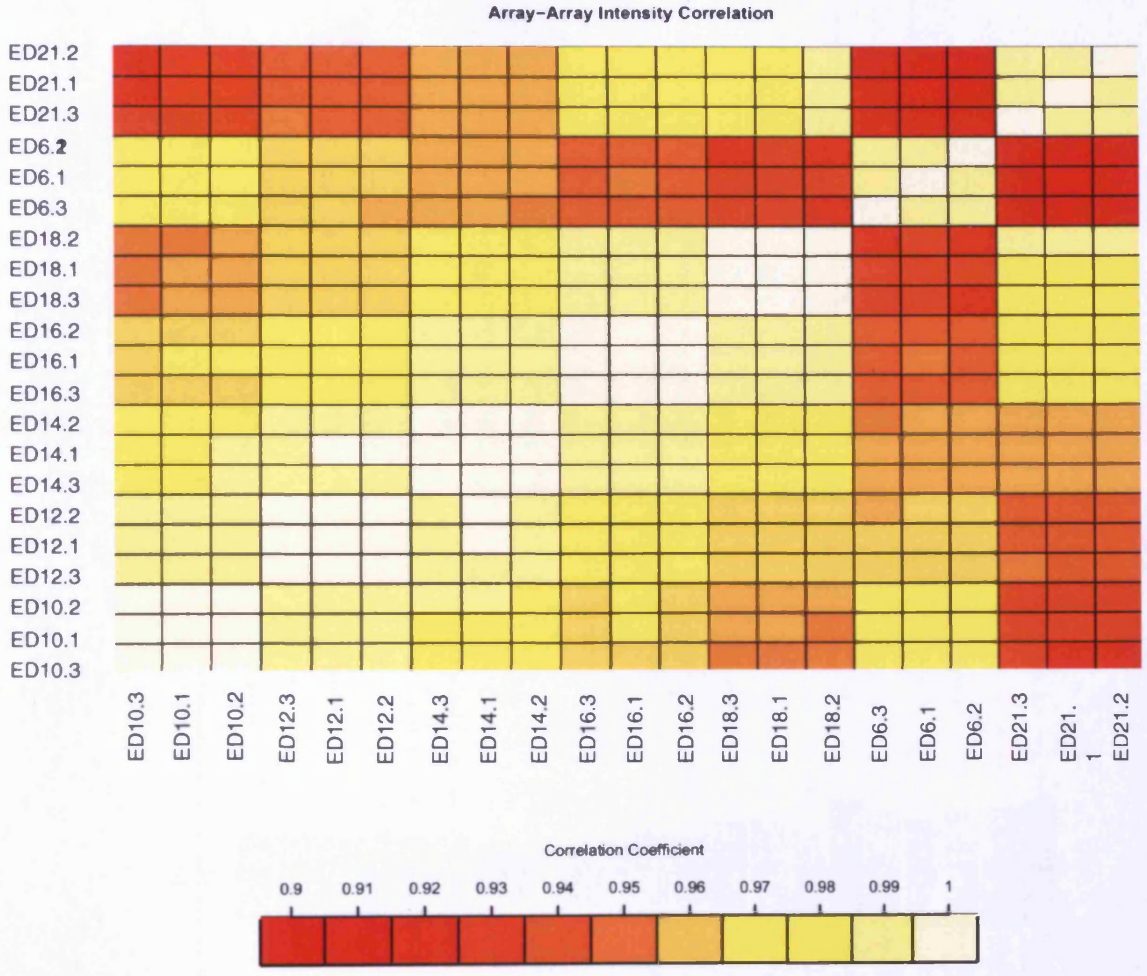

Figure 5.8 Correlation matrix for all pairwise comparisons between individual chips hybridised with different samples. The colour scale is shown in the panel, and it is proportional to the ranks. Light yellow coloured cells indicate very high correlation.

a)

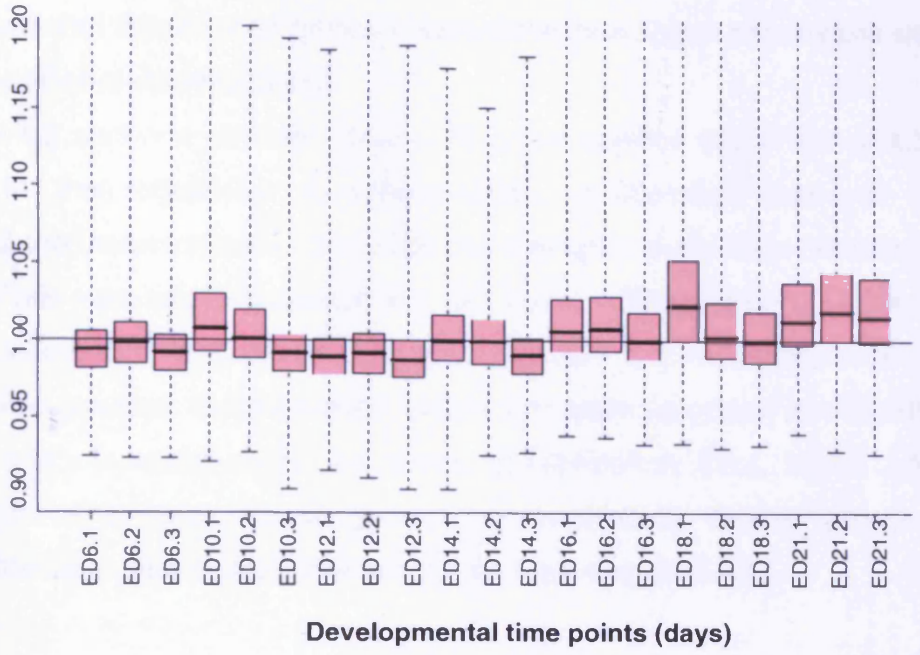

b)

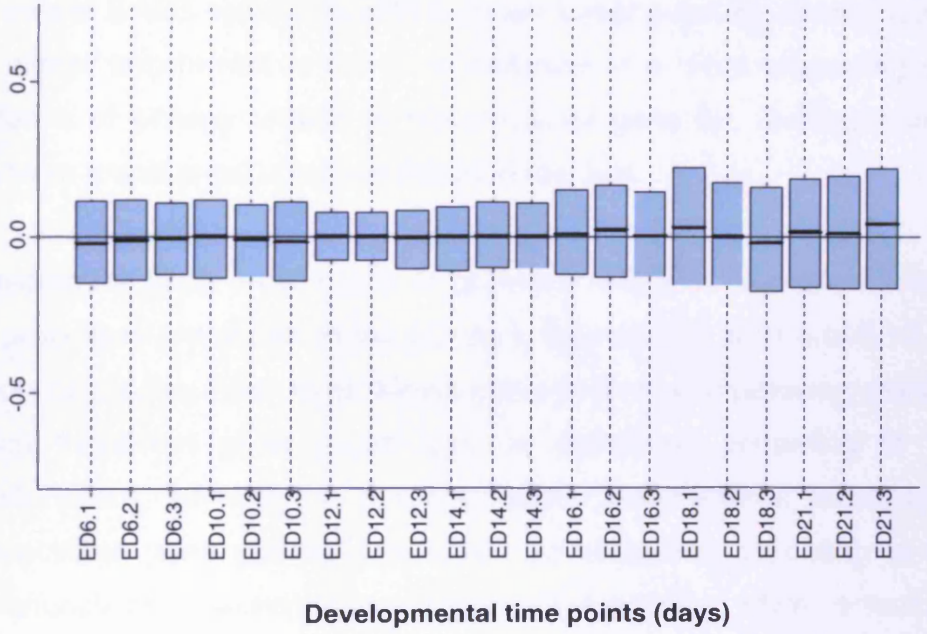

Figure 5.9 Normalised Unscaled Standard Error **(a)** and Relative Log Expression plots (**b**). Both NUSE and RLE are performed on preprocessed data after background correction and normalisation. All arrays were found to be of good quality, not significantly elevated (a) and centered at 0 (b).

5.6 Gene expression analyses

5.6.1 Functional families of genes involved in biological processes during corneal epithelial development

The following sections include outputs of gene families identified, which are involved in the regulation of differentiation, proliferation and cell death throughout the development of the chick corneal epithelium. Data obtained from RMA analysis was used to search for GO terms; differentiation, proliferation, apoptosis/cell death, and probe sets that matched any of the three areas of interest were grouped. Subsequently, probe lists were uploaded into DAVID 2.1 software and classified using the Gene Classification Tool, which allowed organisation of a large list of genes into functionally related groups and revealed the biological context of each family (see section 5.4.5).

Functional groups were organised in descending order according to the enrichment score, which ranked the biological importance of each gene groups based on overall EASE scores (modified Fisher Exact p-value), as described in 5.4.5. A higher enrichment score is an indicator of a more interesting gene family in terms of biology related to the uploaded gene list. Overrepresented GO terms were found at $p \leq 0.01$ level Fisher Exact test.

The representative fuzzy heat maps of genes involved in regulation different biological processes are shown in the following figures 5.10, 5.11 and 5.12. The organisation of a fuzzy heat map allows gene-to-term comparison (members within each functional gene group can be compared according to their annotation/function), as well as, cluster-to-cluster comparisons (members of different functional gene group/clusters can be compared according to their annotations/functions). Horizontal grey lines separate genes, while vertical grey lines separate annotation terms belonging to each functional gene group. The heatmap patterns in diagonal (blue) are the functional gene clusters identified within uploaded gene lists; the number of diagonal squares is equal to the number of functional gene groups. The heatmap patterns above and below each blue square show relationship/similarity between different functional gene families. Green patterns indicate a match between gene and term/annotation.

5.6.1.1 Functional gene families involved in regulation of differentiation

From the list of genes identified following RMA analysis, 242 probe sets (159 genes) were identified as those which match 'differentiation' gene ontology (GO:0030154). From the uploaded probe list, 10 functional gene groups and 135 non-clustered probe sets (88 genes) were identified. Functional gene families involved in differentiation of chick corneal epithelium during development included: Nerve Growth Factor Receptors, Bone Morphogenetic Proteins, Transcription regulators, Semaphorins, Growth Factors, Frizzled-Related Protein, Epidermal Growth Factors-like, Transforming Growth Factors β-like, Kinases, G-protein coupled receptors. The genes that constitute the functional group and their functional role in biological processes are summarised in Table V.1 (Appendix V). A list of unclustered genes (genes not mapped to any of the functional groups, but potentially biologically relevant) is presented in Table V.2 (Appendix V).

A global view of these 10 functional clusters derived from 71 genes involved in the regulation of differentiation during development of the chick corneal epithelium is shown in Figure 5.10.

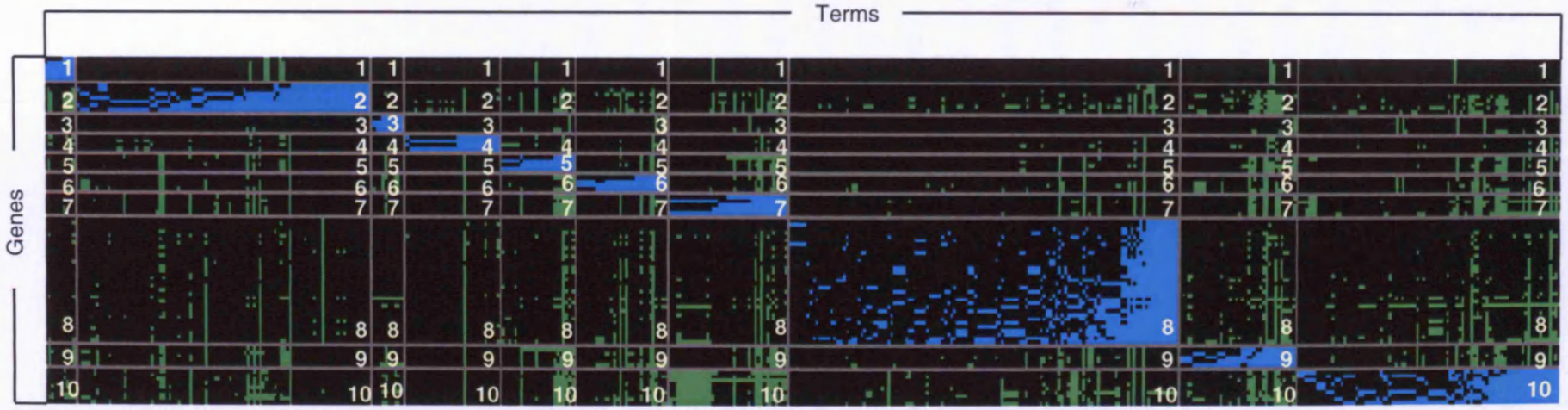

Figure 5.10 The global view of fuzzy heat map of 10 functional genes groups derived from 71 genes involved in regulation of differentiation during development of chick corneal epithelium. Horizontal grey lines separate genes belonging to each functional group, vertical grey lines separate annotation terms belonging to each functional group. The heat map patterns in diagonal (blue) are the 10 functional groups and show gene-to-term relationship within each gene family. The heat map patterns above and below (green) show cluster-to-cluster relationship between different functional gene families. Green and blue patterns visualise a match between gene and term/annotation. Numbers correspond to numbers of functional cluster in text.

5.6.1.2 Functional gene families involved in regulation of proliferation

RMA analysis and GO clustering identified 98 probe sets (64 genes) involved in cell proliferation (GO:0008283) during chick corneal epithelial development. DAVID Classification Tool clustered transcripts from uploaded probe list into 3 functional groups; Growth Factors activity (6 genes), Transcription Regulators (8 genes), Growth Factors activity (6 genes). The Classification Tool clustered genes into two gene families of Growth Factors. As described in section 5.4.5, classification in DAVID system is generates functional gene cluster, based on the terms (function) shared by the genes in the clusters; the more enriched term, the higher probability of forming separate cluster. The general terms `Regulation of progression through cell cycle` and `Regulation of cell cycle` are more enriched for several gene members that constitute the family showing the highest enrichment score (first functional group). Genes from the third gene family (Growth Factors) are grouped based on their more specialised annotations. Similarities and differences between members of all three functional gene clusters are visualised by the fuzzy heatmap shown in Figure 5.11 (see section 5.6.1). It appeared that members of first and third cluster share some common annotation, but also several genes matched more specialised terms, thus were classified to separate groups.

Table V.3 summarises identified functional gene families grouped according to the enrichment score and their functional roles (Appendix V). A list of 67 probe sets (44 genes) which were determined as unclustered is shown in Table V.4 (Appendix V).

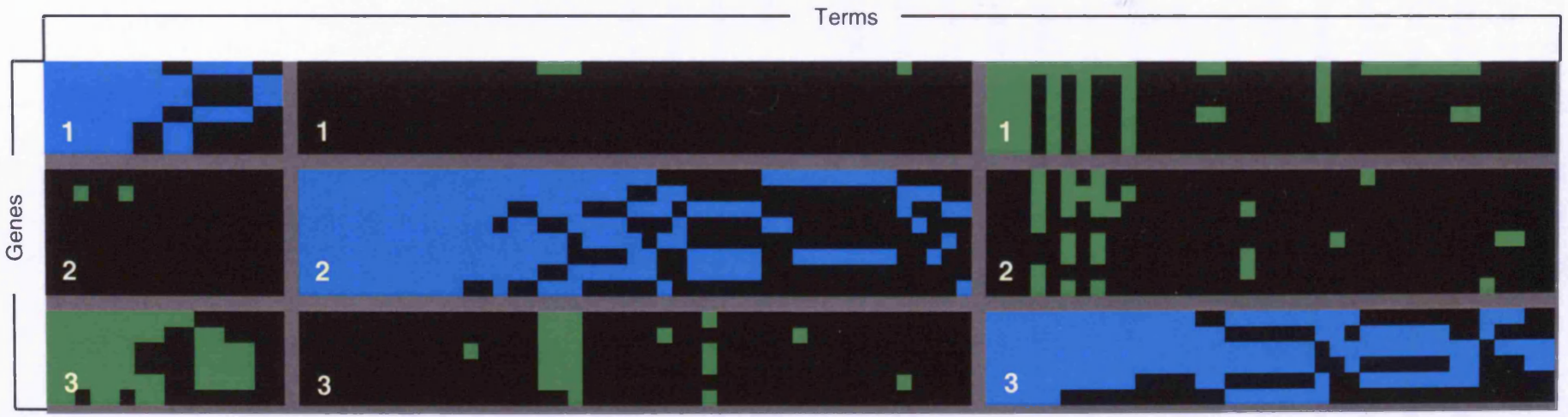

Figure 5.11 The global view of fuzzy heat map of 3 functional genes groups derived from 20 genes involved in regulation of proliferation during development of chick corneal epithelium. Horizontal grey lines separate genes belonging to each functional group, vertical grey lines separate annotation terms belonging to each functional group. The heat map patterns in diagonal (blue) are the 3 functional groups and show gene-to-term relationship within each gene family. The heat map patterns above and below (green) show cluster-to-cluster relationship between different functional gene families. Green and blue patterns visualise a match between gene and term/annotation. Numbers correspond to numbers of functional clusters in text.

5.6.1.3 Functional gene families involved in regulation of cell death

A probe list of 215 probe sets (140 genes), that match gene ontology term 'apoptosis' (GO:0006915), was used to identify functional families involved in these process during corneal epithelial development. Three relevant gene families and 45 non-clustered genes were identified using default settings. 72 genes constituted the first functional gene family. Therefore, in order to obtain more specific and cohesive clustering within this functional group, the settings were further optimised (similarity threshold at 0.5 level). This resulted in additional 7 subclusters and 16 non-clustered genes. The first class, in this ontological category, was Bcl-2-related Apoptosis Regulators family, which claimed 19 of the genes involved in programmed cell death processes. Subsequent groups, ordered according to enrichment score, included: Inhibitor Apoptosis Proteins (10 genes), Bcl-2-related Apoptosis Agonists (4 genes), Phosphotransferases (7 genes), Tumor Necrosis Factor Receptors family (4 genes), Caspase Apoptosis Regulators (10 genes), Kinases (7 genes), Transcription regulators (10 genes) and Neurotrophin family (4 genes).

The genes and names of families they belonged to are summarised in Table V.5 and unclustered transcripts are presented in Table V.6 (Appendix V). Figure 5.12 shows a fuzzy map of functional gene groups, including 7 subclusters derived from the first functional group (see section 5.6.1).

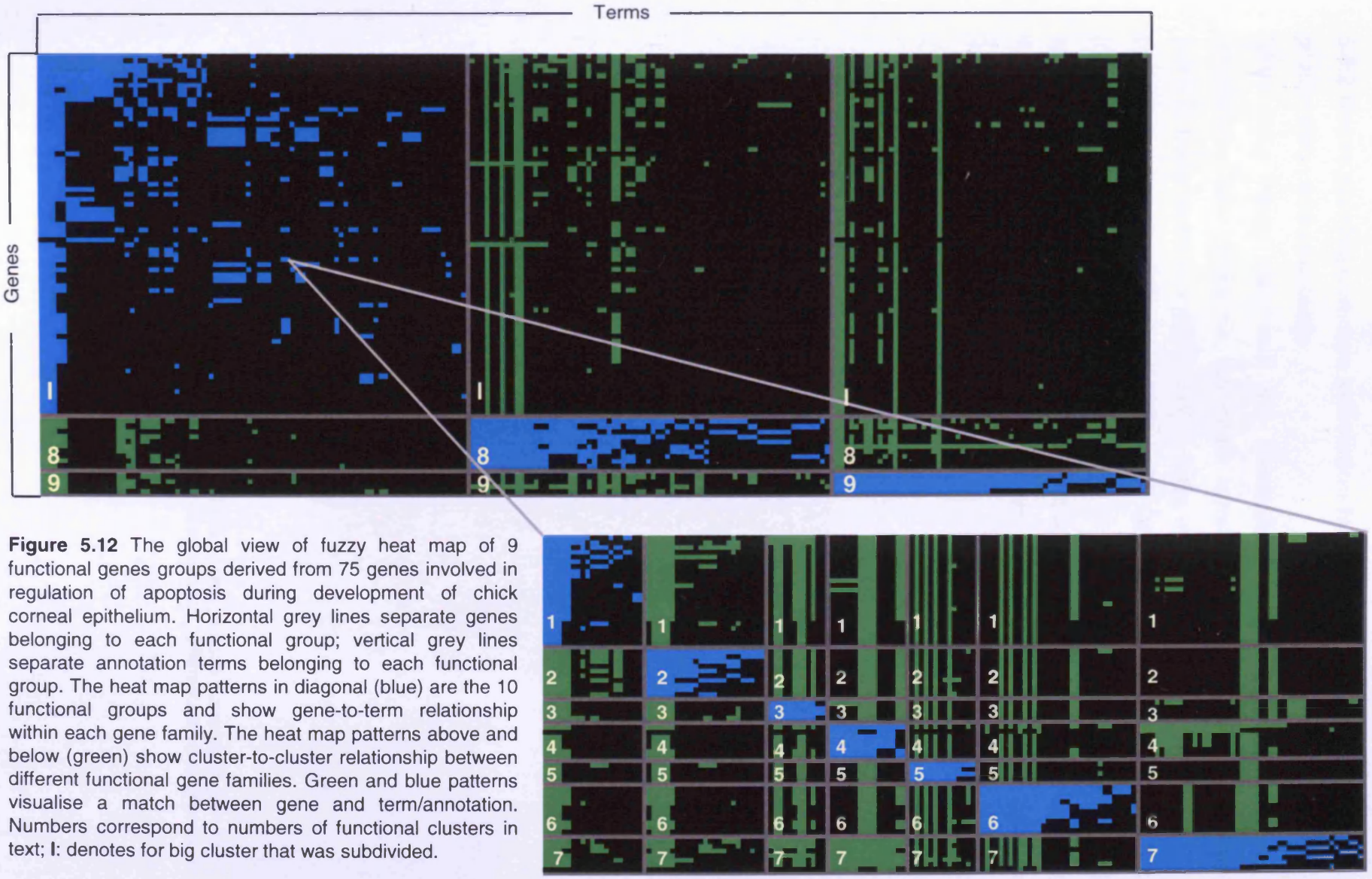

Figure 5.12 The global view of fuzzy heat map of 9 functional genes groups derived from 75 genes involved in regulation of apoptosis during development of chick corneal epithelium. Horizontal grey lines separate genes belonging to each functional group; vertical grey lines separate annotation terms belonging to each functional group. The heat map patterns in diagonal (blue) are the 10 functional groups and show gene-to-term relationship within each gene family. The heat map patterns above and below (green) show cluster-to-cluster relationship between different functional gene families. Green and blue patterns visualise a match between gene and term/annotation. Numbers correspond to numbers of functional clusters in text; **I**: denotes for big cluster that was subdivided.

5.6.2 Genes sharing common annotation for gene ontology differentiation, proliferation and apoptosis

RMA data was searched for annotation containing, 'differentiation', 'proliferation' and 'apoptosis, cell death' terms. 7 genes (12 probe sets) were found to be involved in regulation of all three biological processes. 16 genes (19 probe sets) shared common annotation for 'differentiation', and 'proliferation', 6 (8 probe sets) genes were involved both in regulation of differentiation and apoptosis, and 3 (5 probe sets) in proliferation and apoptosis (Fig. 5.13). The list of genes sharing different annotation terms, in each comparison, is presented in Table 5.4.

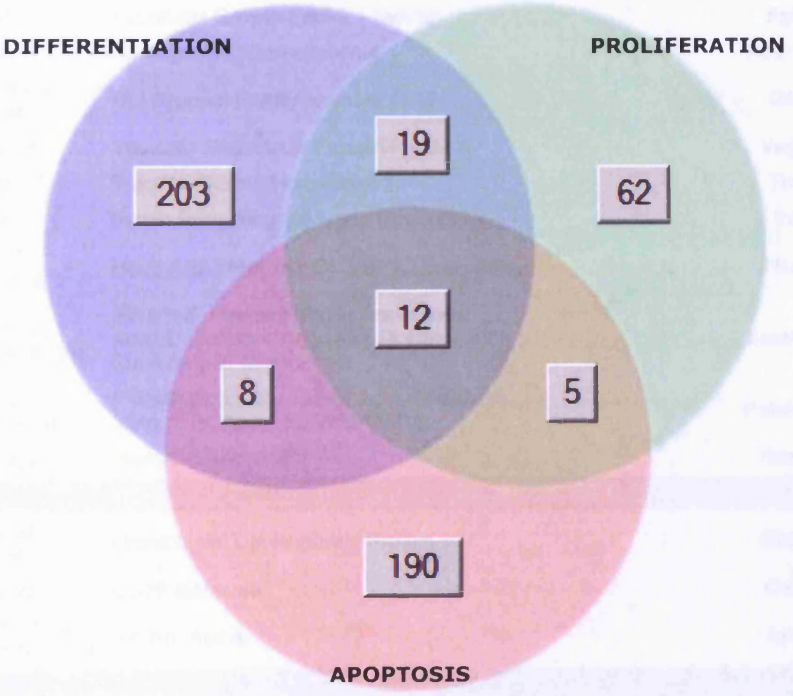

Figure 5.13 Venn diagram shows numbers of probe sets in each comparison between subgroups of genes involved in three biological processes: differentiation, proliferation and apoptosis.

Table 5.4 List of genes sharing GO annotation for more than one biological process

Affy Probe ID	Gene name	Gene Symbol	Unigene
Differentiation/Proliferation/Apoptosis			
GgaAffx.22982.1.S1_at	Transforming Growth Factor, Beta 2	**Tgfβ2**	GGA.12932
Gga.16413.3.S1_at Gga.16413.1.A1_a_at Gga.16413.1.A1_at	Fibroblast Growth Factor Receptor 3 (achondroplasia, thanatophoric dwarfism)	**Fgfr3**	GGA.16413
Gga.2396.1.S1_at	B-cell Translocation Gene 1, Anti-proliferative	**Btg1**	GGA.2396
Gga.696.1.S1_at Gga.696.1.A1_at	Brain-derived Neurotrophic Factor	**Bdnf**	GGA.696
Gga.345.1.S1_at	Sonic Hedgehog Homolog (Drosophila)	**Shh**	GGA.345
Gga.1095.1.S1_at	Signal Transducer And Activator Of Transcription 5B	**Stat5b**	GGA.1095
Gga.961.2.S1_a_at Gga.961.2.S1_at Gga.961.1.S1_at	T-box 5	**Tbx5**	GGA.961
Differentiation/Proliferation			
GgaAffx.5710.2.S1_s_at GgaAffx.5710.2.S1_at GgaAffx.5710.1.S1_at	Neural Proliferation, Differentiation And Control, 1	**Npdc1**	GGA.31961
Gga.5002.1.S1_at	Midkine (Neurite Growth-promoting Factor 2)	**Mdk**	GGA.5002
Gga.17040.2.S1_a_at	Fibroblast Growth Factor 2 (basic)	**Fgf2**	GGA.17040
Gga.648.1.S2_at	Fibroblast Growth Factor 1 (acidic)	**Fgf1**	GGA.648
Gga.570.1.S1_at	Neurogenic Differentiation 4	**Neurod4**	GGA.570
GgaAffx.7399.1.S1_at Gga.4969.1.S1_at	GLI-Kruppel Family Member GLI2	**Gli2**	GGA.4969
Gga.537.2.S1_a_at	Vascular Endothelial Growth Factor A	**Vegfa**	GGA.537
Gga.511.1.S1_at	T-cell Leukemia Homeobox 1	**Tlx1**	GGA.511
Gga.473.1.S1_at	Indian Hedgehog Homolog (Drosophila)	**Ihh**	GGA.473
Gga.3754.2.S1_at Gga.3754.1.S1_a_at	Hairy And Enhancer Of Split 1, (Drosophila)	**Hes1**	GGA.3754
Gga.4349.2.S1_s_at Gga.4349.1.S1_s_at	SWI/SNF Related, Matrix Associated, Actin Dependent Regulator Of Chromatin, Subfamily B, Member 1	**Smarcb1**	GGA.8558
Gga.3126.1.S1_at Gga.11892.1.S1_s_at	Platelet-activating Factor Acetylhydrolase, Isoform Ib, Alpha Subunit 45kDa	**Pafah1b1**	GGA.3126
Gga.3689.2.S1_a_at	Histone Deacetylase 4	**Hdac4**	GGA.3689
Proliferation/Apoptosis			
Gga.122.2.S1_a_at Gga.6790.1.A1_at	Craniofacial Development Protein 1	**Cfdp1**	GGA.122
Gga.723.1.S1_a_at	CD28 Molecule	**Cd28**	GGA.723
GgaAffx.23500.1.S1_at GgaAffx.23500.1.S1_s_at	Inhibin, Alpha	**Inha**	GGA.6881
Differntiation/Apoptosis			
Gga.4285.1.S1_at	CCAAT/enhancer Binding Protein (C/EBP), Beta	**Cebpb**	GGA.4285
Gga.3982.1.S1_at Gga.3982.1.S2_at	Inhibin, Beta A	**Inhba**	GGA.3982
Gga.11320.1.S1_s_at	Tyrosine Protein Kinase	**P56lck**	GGA.11320
GgaAffx.11482.1.S1_s_at GgaAffx.20273.1.S1_s_at	Jumonji Domain Containing 6	**Jmjd6**	GGA.21114
GgaAffx.7932.1.S1_at	Nerve Growth Factor Receptor (TNFR Superfamily, Member 16)	**Ngfr**	GGA.39799
GgaAffx.11073.1.S1_at	Neurotrophin 3	**Ntf3**	GGA.41617

5.6.3 Principal Component Analysis (PCA)

PCA is a statistical technique commonly used in microarray research, which identifies patterns in data and magnifies trends (Raychaudhuri *et al.*, 2000; Konradi, 2005). PCA applies vectors (a linear transformation of the expression values of all genes) to the data and identifies meaningful underlying variables (key variance in the data) by separating poorly correlated elements and bringing highly correlated elements together. The number of components (vectors) is equal to the number of observed variables, but only the first few are considered as ones with the highest (meaningful) variance, as they account for over 90% of the variance allowing most of the information to be visualised in two dimensions.

PCA was applied to the expression data, where gene expression measurements were the variables, and the developmental time series was the observation. PCA demonstrated, within component one (direction along which samples show the highest variation) 2 genes involved in regulation of differentiation, whereas within component two (direction uncorrelated to the first component), it revealed 6, 4 and 8 genes involved in apoptosis, proliferation and differentiation, respectively. List of genes identified by PCA is shown in Table 5.5. In two cases (genes involved in proliferation and cell death), only genes detected by the second component are demonstrated, this is due to the fact the genes correlation to the first component (first PCA vector) was lower than $R^2 < 0.9$ (Spearman`s test, see section 5.4.4).

Table 5.5 Genes identified by PCA

	Affy Probe ID	Gene name	Gene Symbol	Unigene
		Differentiation		
Component 1	Gga.540.1.S1_at	Matrix Gla Protein	**Mgp**	GGA.504
	Gga.4285.1.S1_at	Ccaat/enhancer binding protein (c/ebp), beta	**Cebpb**	GGA.706
Component 2	Gga.17397.1.S1_at GgaAffx.3703.1.S1_at	Myeloid Differentiation Primary Response Gene (88)	**Myd88**	GGA.17397
	Gga.6399.1.S1_at	Mal, T-cell Differentiation Protein-like	**Mall**	GGA.6399
	Gga.135.2.S1_a_at	Neuregulin 1	**Nrg1**	GGA.135
	Gga.665.1.S1_at	Cysteine And Glycine-rich Protein 2	**Csrp2**	GGA.665
	Gga.651.1.S1_at Gga.651.1.S2_at Gga.651.1.S2_s_at	Ephrin-A5	**Efna5**	GGA.651
	Gga.13269.1.S1_at	Sphingosine-1-phosphate Receptor 1	**S1pr1**	GGA.13269
	Gga.853.1.S1_at	Ciliary Neurotrophic Factor	**Cntf**	GGA.835
	Gga.16413.3.S1_at Gga.16413.1.A1_at Gga.16413.1.A1_a_at	Fibroblast Growth Factor Receptor 3	**Fgfr3**	GGA.16413
		Proliferation		
Component 2	Gga.4349.1.S1_s_at Gga.4349.2.S1_s_at	SWI/SNF related, matrix associated, actin dependent regulator of chromatin, subfamily b, member 1	**Smarcb1**	GGA.4349
	GgaAffx.8915.1.S1_at	xylosylprotein beta 1,4-galactosyltransferase, polypeptide 7 (galactosyltransferase I)	**B4galt7**	GGA.33756
	Gga.3219.1.S1_at	c-fos induced growth factor (vascular endothelial growth factor d)	**Figf**	GGA.3219
	Gga.1479.1.S1_at Gga.1479.2.S1_a_at	Pleiotrophin	**Ptn**	GGA.39450
		Cell death		
Component 2	Gga.122.2.S1_a_at Gga.6790.1.A1_at	craniofacial development protein 1	**Cfdp1**	GGA.122
	GgaAffx.6171.1.S1_at GgaAffx.6171.2.S1_s_at	similar to hypothetical protein flj21901	**Fastkd1**	GGA.22679
	Gga.4960.1.S1_at	defender against cell death 1	**Dad1**	GGA.4960
	Gga.1234.1.S1_s_at	bh3 interacting domain death agonist	**Bid**	GGA.1234
	GgaAffx.22169.2.S1_at	Optic Atrophy 1 (autosomal Dominant)	**Opa1**	
	GgaAffx.6512.1.S1_at	PRKC, apoptosis, WT1, regulator	**Pawr**	GGA.24903

5.6.4 Up- and downregulated genes during corneal epithelial development

Several genes involved in regulation of differentiation, proliferation and cell death were found to show a continuum (gradual increase/decrease) of up- or downregulation throughout epithelial development. Identified genes are summarised in Tables 5.6 and 5.7 including both clustered and non-clustered probe sets, as demonstrated by DAVID Classification Tool (see section 5.6.1). Changes in genes expression levels at different time points were visualised on a heatmap in Figure 5.14. As shown, the change in gene expression pattern of these genes occurred at ED14.

Table 5.6 Genes involved in regulation of biological process showing continuum of upregulation

Affymetrix ID	Gene name	Gene symbol	Unigene ID
	Differentiation		
Gga.17397.1.S1_at	myeloid differentiation primary response gene (88)	**Myd88**	GGA.17397
Gga.6399.1.S1_at	mal, T-cell differentiation protein-like	**Mall**	GGA.6399
	Proliferation		
Gga.895.1.S1_at	S100 calcium binding protein A6	**S100a6**	GGA.22951
GgaAffx.6863.1.S1_at	epithelial mitogen homolog (mouse)	**Epgn**	GGA.22922
Gga.4390.2.S1_a_at	ferritin, heavy polypeptide 1	**Fth1**	GGA.4390
	Cell death		
GgaAffx.11653.1.S1_s_at	serine/threonine kinase 17b	**Stk17b**	GGA.22951
Gga.5708.2.S1_a_at	chromosome 9 open reading frame 89	**C9orf89**	GGA.22922
Gga.4846.1.S2_at Gga.4846.1.S1_at	anti-apoptotic NR13	**LOC395193**	GGA.43428
Gga.10204.1.S1_s_at	caspase 1, apoptosis-related cysteine	**Casp1**	GGA.10204
GgaAffx.11935.1.S1_s_at	apoptosis, caspase activation inhibitor	**Aven**	GGA. 9342
GgaAffx.5618.1.S1_at	caspase 7, apoptosis-related cysteine peptidase	**Casp7**	GGA.39052
Gga.5708.2.S1_a_at	Similar To RIKEN CDNA 1110007C0	**LOC415987**	GGA.5708
Gga.104.1.S1_at	X-linked inhibitor of apoptosis	**Xiap**	GGA.104
Gga.17104.1.S1_at	BCL2-like 15	**Bcl2l15**	GGA.17104

Table 5.7 Genes involved in regulation of biological process showing continuum of downregulation

Affymetrix ID	Gene name	Gene symbol	Unigene ID
	Differentiation		
Gga.5002.1.S1_at	midkine (neurite growth-promoting factor 2)	**Mdk**	GGA.5002
GgaAffx.12403.1.S1_s_at	PDZ and LIM domain 7 (enigma)	**Pdlim7**	GGA.7667
Gga.4032.1.S1_at	neuropilin 1	**Nrp1**	GGA.4032
Gga.4349.1.S1_s_at Gga.4349.2.S1_s_at	SWI/SNF related, matrix associated, actin dependent regulator of chromatin, subfamily b, member 1	**Smarcb1**	GGA.4349
GgaAffx.20498.1.S1_s_at	monocyte to macrophage differentiation-associated	**Mmd**	GGA.5197
GgaAffx.11995.1.S1_s_at GgaAffx.11995.1.S1_at	basic leucine zipper and W2 domains 2	**Bzw2**	GGA.7693
Gga.4345.1.S1_at	secreted frizzled-related protein 2	**Sfrp2**	GGA.4345
Gga.909.1.S1_at	slit homolog 2 (Drosophila)	**Slit2**	GGA.39631
	Proliferation		
Gga.5002.1.S1_at	midkine (neurite growth-promoting factor 2)	**Mdk**	GGA.5002
Gga.18937.1.S1_s_at GgaAffx.13116.1.S1_at	RAP1B, member of RAS oncogene family	**Rap1b**	GGA.18937
Gga.4349.1.S1_s_at Gga.4349.2.S1_s_at	SWI/SNF related, matrix associated, actin dependent regulator of chromatin, subfamily b, member 1	**Smarcb1**	GGA.4349
Gga.3219.1.S1_at	c-fos induced growth factor (vascular endothelial growth factor D)	**Figf**	GGA.3219
GgaAffx.8915.1.S1_at	xylosylprotein beta 1,4-galactosyltransferase, polypeptide 7 (galactosyltransferase I)	**B4galt7**	GGA.33756
	Cell death		
Gga.1234.1.S1_s_at	BH3 interacting domain	**Bid**	GGA.1234
GgaAffx.13220.1.S1_s_at	apoptosis-inducing factor, mitochondrion-associated, 1	**Aifm1**	GGA.4923
Gga.4960.1.S1_at	defender against cell death 1	**Dad1**	GGA.4960
GgaAffx.6512.1.S1_at	PRKC, apoptosis, WT1, regulator	**Pawr**	GGA.24903

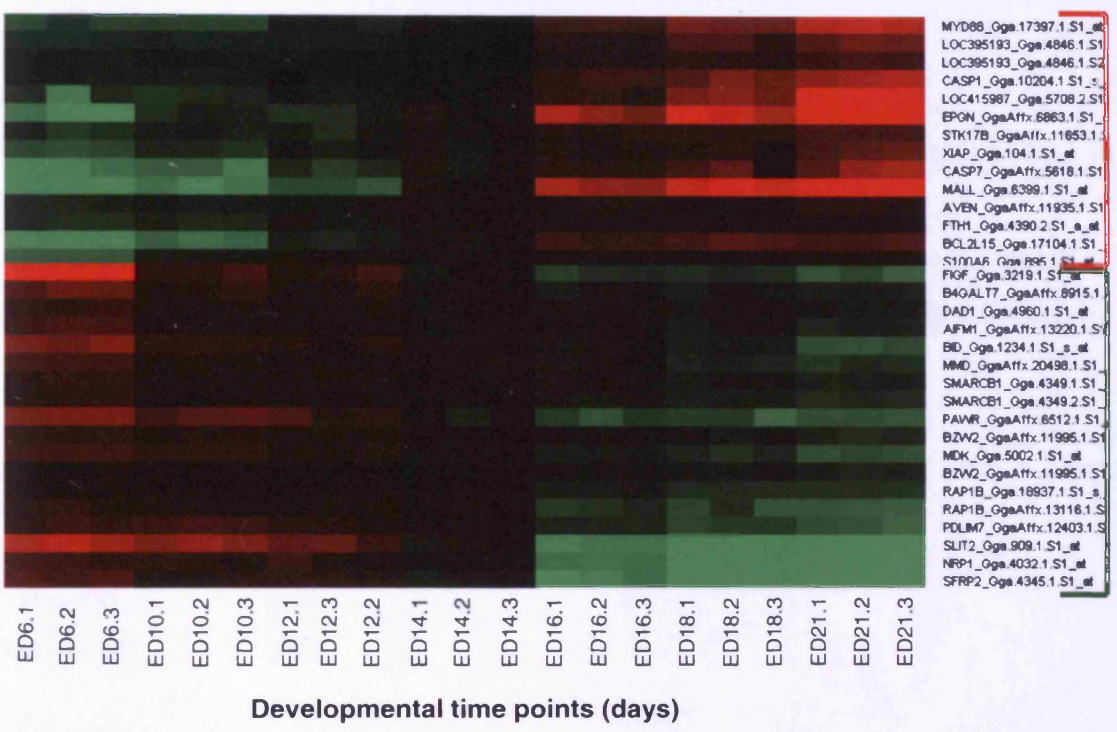

Figure 5.14 Heatmap of genes showing continuum of up- or downregulation during corneal epithelial development. Genes were selected from probe lists involved in three major biological processes (differentiation, proliferation and apoptosis). Colour rank refers to changes in expression, with red being characteristic of gene upregulation and green for downregulation.

5.6.5 Genes differentially expressed in development

To identify differentially expressed genes in corneal epithelia throughout the development, the Limma analysis was applied to RMA normalised microarray data, as described in section 5.4.3. In time course experiments the choice of analysis depends on the comparison of interest. However in this kind of investigation, reference design is commonly used since it provides the advantage of easy analysis and interpretation (Chu *et al.,* 1998; Spellman *et al.*, 1998; Sekiya *et al.*, 2002; Yang *et al.*, 2002).

5.6.5.1 Functional clustering of genes differentially expressed in comparison to ED6 baseline

Limma analysis with ED6 (intital time point) used as a reference identified differentially expressed genes at each time point. The number of probe sets for each comparison is given below:

ED6 vs ED10	300
ED6 vs ED12	757
ED6 vs ED14	1217
ED6 vs ED16	1863
ED6 vs ED18	2486
ED6 vs ED21	3714

The list of identified probe sets was uploaded into the Functional Annotation Clustering Tool in DAVID, which clusters genes based on their function according to gene ontology terms. Analysis was performed with default parameters which provided high specificity for detection of enriched terms. Clusters were ranked according to their enrichment score (the geometric mean in log scale of member`s p-values in a corresponding annotation cluster). From the demonstrated annotation clusters overrepresented GO terms found significant at $p \leq 0.01$ level Fisher Exact test are presented in Table 5.8.

Due to the restriction in data loading (less than 3000 probe sets in an uploaded list) there was a need to reduce the number of differentially expressed probe sets demonstrated for the ED21, the posthatching time point. Venns analysis demonstrated 2275 probe sets common for ED18 and ED21, 211 differentially

expressed probe sets between ED6 and ED18, and 1439 between ED6 and ED21. The latter was then uploaded into the Functional Annotation Clustering Tool and analysed separately.

Table 5.8 Over-represented functional classes of genes amongst differentially expressed transcripts between ED6 baseline and developmental time points (continued overleaf)

ED6 versus ED10

GO Category	GO Term	p-value	Number of genes
Annotation cluster 1 (enrichment score 2.26)			
Molecular function	Cell-comunication	3.7E-6	9
	Structural molecule activity	5.1E-3	11
Cellular component	Intermediate filament cytoskeleton	1.3E-2	12
Annotation cluster 2 (enrichment score 1.27)			
Biological process	Gas transport	1.0E-2	3
Molecular function	Oxygen transporter activity	8.2E-3	3
Cellular component	Hemoglobin complex	3.9E-3	3
Annotation cluster 3 (enrichment score 1.25)			
Biological process	Multicellular organismal development	7.7E-3	13
	Regulation of cell differentiation	1.0E-21	4

ED6 versus ED12

GO Category	GO Term	p-value	Number of genes
Annotation cluster 1 (enrichment score 2.48)			
Molecular function	Cell communication	7.7E-6	12
Cellular component	Intermediate filament	5.3E-4	6
	Keratin type I	2.2E-3	4
Annotation cluster 2 (enrichment score 1.59)			
Molecular function	EGF-like calcium binding	8.2E-3	6
Annotation cluster 3 (enrichment score 1.25)			
Biological process	Multicellular organismal development	4.4E-3	30
	Neurogenesis	3.4E-3	7
	Anatomical structure development	9.2E-3	18
	Nervous system development	5.3E-3	10
Annotation cluster 3 (enrichment score 1.2)			
Cellular component	Extracellular matrix	4.8E-3	12
	Extracellular region part	7.1E-3	14
Annotation cluster 4 (enrichment score 1.2)			
Cellular component	Cytoskeleton constituent	2.0E-3	22
Annotation cluster 5 (enrichment score 1.15)			
Biological process	Cell proliferation	3.2E-3	9
	Negative regulation of transcription from RNA polymerase II promoter	1.0E-2	4
Annotation cluster 6 (enrichment score 1.11)			
Biological process	Gas transport	6.3E-3	4
Annotation cluster 7 (enrichment score 0.91)			
Molecular function	Transcription regulator activity	4.4E-3	31
	Sequence-specific DNA binding	9.2E-3	19
Cellular component	Intracellular part	3.5E-3	102

ED6 versus ED14

GO Category	GO Term	p-value	Number of genes
Annotation cluster 1 (enrichment score 2.57)			
Biological process	Multicellular organismal development	1.2E-4	44
	Developmental process	1.3E-4	54
	Anatomical structure development	5.2E-4	31
	Nervous system development	1.7E-3	48
	Anatomical structure morphogenesis	3.8E-3	20
Molecular function	Developmental protein	6.3E-3	24
Annotation cluster 2 (enrichment score 1.91)			
Cellular component	Cytoskeleton	4.7E-5	36
	Cytoskeletal part	1.5E-3	24
Annotation cluster 3 (enrichment score 1.74)			
Molecular function	EGF	6.1E-3	10
	EGF-like calcium binding	3.5E-4	9
Annotation cluster 4 (enrichment score 1.7)			
Cellular component	Intermediate filament	5.8E-5	8
	Keratin type I	8.3E-4	5
Annotation cluster 5 (enrichment score 1.53)			
Cellular component	Intracellular part	1.5E-4	167
Annotation cluster 6 (enrichment score 1.25)			
Biological process	Proteinaceous extracellular matrix	6.6E-3	15
Annotation cluster 7 (enrichment score 1.08)			
Biological process	Alcohol metabolic process	5.9E-3	12
Molecular function	Oxidoreductase activity, acting on CH-OH group of donors	7.9E-3	8
Annotation cluster 8 (enrichment score 0.99)			
Molecular function	Lipid metabolism	6.7E-3	5
Annotation cluster9 (enrichment score 0.97)			
Molecular function	Iron ion binding	2.4E-3	17
Annotation cluster10 (enrichment score 0.53)			
Biological process	Glycine metabolic process	4.4E-3	4

ED6 versus ED16

GO Category	GO Term	p-value	Number of genes
Annotation cluster 1 (enrichment score 3.37)			
Biological process	Multicellular organismal development	8.6E-5	60
	Developmental process	3.8E-5	76
	Anatomical structure development	2.3E-3	39
Annotation cluster 2 (enrichment score 2.69)			
Molecular function	EGF	3.4E-4	15
	EGF-like type 3	6.6E-4	14
	EGF-like calcium binding	1.1E-3	10
Annotation cluster 3 (enrichment score 2.38)			
Cellular component	Cytoplasm	7.0E-7	139
	Intracellular organelle	5.7E-3	184
Annotation cluster 4 (enrichment score 2.12)			
Biological process	Neurogenesis	6.8E-3	8
Molecular function	Semaphorin/CD100 antigen	3.7E-3	5
Annotation cluster 5 (enrichment score 1.98)			
Molecular function	Oxidoreductase activity, acting on CH-OH group of donors, NAD or NADP as aceptor	2.9E-3	10

Annotation cluster 6 (enrichment score 1.67)			
Cellular component	Extracellular matrix	7.6E-3	20
	Proteinaceous extracellular matrix	6.6E-3	19
Annotation cluster 7 (enrichment score 1.5)			
Biological process	Cell adhesion	9.4E-3	31
Annotation cluster 8 (enrichment score 1.48)			
Biological process	Phenol metabolic process	8.3E-3	4
Annotation cluster 9 (enrichment score 1.35)			
Molecular function	Zinc-finger LIM domain	7.6E-3	8
Annotation cluster 10 (enrichment score 1.29)			
Cellular component	Intermediate filament	7.1E-4	8
	Keratin type I	3.7E.3	5
Annotation cluster 11 (enrichment score 1.28)			
Biological process	Anterior/posterior pattern formation	4.7E-3	6
Annotation cluster 12 (enrichment score 1.07)			
Biological process	Cell proliferation	4.7E-3	15

ED6 versus ED18

GO Category	GO Term	p-value	Number of genes
Annotation cluster 1 (enrichment score 3.69)			
Cellular component	Intracellular part	2.4E-8	324
	Intracellular membrane-bound organelle	9.6E-4	207
Annotation cluster 2 (enrichment score 2.88)			
Biological process	Cell differentiation	2.2E-5	56
	Multicellular organismal development	1.8E-3	69
	Developmental process	8.3E-5	94
Annotation cluster 3 (enrichment score 2.46)			
Cellular component	Cytoskeleton	4.3E-4	54
	Microtubule cytoskeleton	9.4E-3	20
Annotation cluster 4 (enrichment score 2.27)			
Biological process	Cell cycle process	2.3E-4	27
	Mitosis	1.8E-3	12
	Regulation of progression through cell cycle	2.0E-3	18
Annotation cluster 5 (enrichment score 1.9)			
Molecular function	EGF	6.9E-3	15
	EGF-like type 3	1.7E-3	16
	EGF-like calcium binding	3.1E-3	11
Annotation cluster 6 (enrichment score 1.88)			
Biological process	Differentiation	4.2E-3	16
Annotation cluster 7 (enrichment score 1.87)			
Cellular component	Proteinaceous extracellular matrix	1.8E-3	25
	Extracellular matrix	2.9E-3	26
Annotation cluster 8 (enrichment score 1.72)			
Biological process	Neurogenesis	8.7E-3	9
Molecular function	Semaphorin/CD100 antigen	2.0E-3	5
Annotation cluster 9 (enrichment score 1.71)			
Cellular component	Intermediate filament	9.5E-4	9
Annotation cluster 10 (enrichment score 1.57)			
Biological process	Zinc-finger LIM domain	8.7E-4	11
Annotation cluster 12 (enrichment score 1.42)			
Biological process	Intracellular transport	5.2E-3	32

Annotation cluster 13 (enrichment score 1. 17)			
Biological process	Cytoskeleton organisation and biogenesis	3.1E-3	22
Cellular component	Microtubule	1.5E-3	14
	Microtubule cytoskeleton	9.4E-3	20

ED6 versus ED21

GO Category	GO Term	p-value	Number of genes
Annotation cluster 1 (enrichment score 2.7)			
Cellular component	Intracellular part	1.7E-4	194
	Intracellular membrane-bound organelle	7.1E-4	128
	Nucleus	3.0E-3	100
Annotation cluster 2 (enrichment score 2.16)			
Biological process	Protein modification	2.8E-3	64
Molecular function	Nucleotide binding	1.7E-4	105
Annotation cluster 3 (enrichment score 1.86)			
Cellular component	Intracellular non-membrane-bound organelle	4.8E-3	52
Annotation cluster 4 (enrichment score 1.75)			
Biological process	Biopolymer metabolic process	3.4E-4	145
	Primary metabolic process	4.4E-3	214
Annotation cluster 5 (enrichment score 1.55)			
Cellular component	Nuclear envelope	2.8E-3	9
Annotation cluster 6 (enrichment score 1.49)			
Biological process	Antigen processing and presentation of peptide or polysaccharide antigen via MHC class II	2.7E-4	11
Molecular function	MHC class II protein complex	4.5E-4	11
Annotation cluster 7 (enrichment score 1.39)			
Biological process	Establishment of cellular localisation	1.6E-3	26
Annotation cluster 8 (enrichment score 1.27)			
Biological process	Cell cycle process	7.8E-3	16
Annotation cluster 9 (enrichment score 1.01)			
Cellular component	Endoplasmic reticulum lumen	8.3E-3	5

5.6.5.2 Genes differentially expressed in comparison to ED6 baseline involved in regulation of differentiation, proliferation and cell death

Probe lists of differentially expressed transcripts in comparison to ED6 obtained from Limma analysis (see section 5.4.3) were searched for genes involved in regulation of differentiation, proliferation and cell death (according to gene ontology), described in section 5.6.1 and showing at least 1.6 fold expression between time points. This approach allowed identification of genes differentially expressed at each time point from genes involved in regulation of these three biological processes, thus likely to be relevant for spatiotemporal changes in the corneal epithelium at particular developmental time points. Identified genes from each comparison are presented in Table V.7 (Appendix V).

5.6.5.3 Genes differentially expressed in development in comparison to ED21 baseline

42 genes were found to be common for all comparisons between ED21 and each of the embryonic time points. The list of identified probe sets was uploaded into the Functional Annotation Clustering Tool in DAVID, and clustered into functional annotation groups, as described in section 5.4.5.

Analysis of the biological function of genes whose expression differed between embryonic and posthatch (ED21) time points revealed over-representation of those related to cell membrane constitution (10 genes), cytoplasmic and cytoskeleton composition (19 genes), ion transport (5 genes) and ribonucleoide binding (4 genes). Candidate genes with potential involvement cellular metabolic processes, including protein modification were found among genes clustered to over-represented groups linked to transferase and kinase activity (16 genes). Furthermore molecular function of 4 other gene was linked to ion binding. Identified annotation clusters are shown in Table 5.9.

Table 5.9 Functional clusters of genes differentially expressed between embryonic and posthatch time points

GO Category	GO Term	p-value	Gene symbol
Annotation cluster 1 (enrichment score 0.47)			
Cellular component	Membrane	4.0E-1	*Lgals3, Scarb1, Gjd3, Ephb6, Moxd1, Fcgbp, Cyp3a37, Kcna5, Rhoc, St6gal1*
	Integral to membrane	5.6E-1	
Annotation cluster 2 (enrichment score 0.44)			
Cellular component	Cell part	3.2E-1	*Mx1, Scarb1, Col11a1, Gjd3, RCJMB04_24f23, Ephb6, Tmsb4x, Kcna5, Rhoc, Hic2, Col1a2, Cald1,* Lgals3, *Moxd1, Fcgbp, LOC408038, Cyp3a37, LOC396479, St6gal1*
	Intracellular part	5.5E-1	
	Cytoplasmic part	2.3E-1	
	Cytoskeleton part	1.8E-1	
	Non-membrane bound organelle	5.9E-1	
Annotation cluster 3 (enrichment score 0.32)			
Biological process	Ion transport	3.0E-1	*Col11a1, RCJMB04_24f23, Tmsb4x, Kcna5, Col1a2*
	Establishment of localisation	5.7E-1	
Annotation cluster 4 (enrichment score 0.29)			
Molecular function	Ribonucleotide binding	4.6E-1	*Mx1, Rps6ka2, Ephb6, Rhoc*
Annotation cluster 5 (enrichment score 0.21)			
Molecular function	Transferase activity	1.8E-1	Mx1, *Scarb1, Gjd3, Col11a1, Ephb6, RCJMB04_24f23, RCJMB04_8a2, Tmsb4x, Rhoc, Gk5, Rps6ka2, Moxd1, Fcgbp, Ugt1a, Cyp3a37, St6gal1*
	Kinase activity	3.3E-1	
	Catalytic activity	3.8E-1	
Biological process	Cellular process	9.3E-1	
	Metabolic process	9.7E-1	
	Protein modification process	6.2E-1	
Annotation cluster 6 (enrichment score 0.11)			
Molecular function	Ion binding	7.9E-1	*Moxd1, Kcna5, Cyp3a37, Hic2*

Amongst the 42 differentially genes, 30 and 12 were demonstrated to be up- or downregulated, respectively. Genes are listed in Table 5.10 and visualised using heatmaps (Fig. 5.15).

Table 5.10 Genes differentially expressed between embryonic and posthatch time points, showing up- or downregulation (continued overleaf)

Affymetrix ID	Gene name	Gene symbol	Unigene ID
	Upregulated		
Gga.6289.1.S1_at	Calcium binding protein 39-like	**Cab39l**	GGA.44652
Gga.8190.1.S1_at Gga.17775.1.S1_s_at GgaAffx.23468.7.S1_s_at	calpain 9	**Capn9**	GGA.8190
GgaAffx.4382.2.S1_s_at	cartilage acidic protein 1	**Crtac1**	GGA.34442
Gga.1163.1.S1_at GgaAffx.21825.1.S1_s_at	cytochrome P450 A 37	**Cyp3a37**	GGA.1163
GgaAffx.3047.2.S1_s_at	Family with sequence similarity 101, member B	**Fam101b**	GGA.43287
GgaAffx.4504.1.S1_at	Fc fragment of IgG binding protein	**Fcgbp**	GGA.18502
GgaAffx.1780.1.S1_s_at	Glycerol kinase 5 (putative)	**Gk5**	GGA.22519
Gga.9082.1.S1_at	potassium voltage-gated channel, shaker-related subfamily, member 5	**Kcna5**	GGA.9082
Gga.155.1.S1_s_at	lectin, galactoside-binding, soluble, 3	**Lgals3**	GGA.667
Gga.844.1.S1_at	Keratin	**LOC396479**	GGA.844
Gga.5589.1.S1_at	beta-keratin	**LOC408038**	GGA.5589
Gga.12861.1.S1_at	similar to Hypothetical protein CBG04537	**LOC415708**	GGA.12861
Gga.10351.2.S1_x_at	similar to RIKEN cDNA 1600014C10	**LOC415755**	GGA.10351
Gga.17984.1.S1_at	Similar to multidrug resistance protein 1a	**LOC420606**	GGA.17984
GgaAffx.2182.4.S1_at	similar to ALDH7	**LOC428812**	GGA.35434
Gga.10746.1.S1_at	Hypothetical protein LOC769486	**LOC769486**	GGA.10746
Gga.1660.2.S1_s_at	Hypothetical protein LOC770534	**LOC770534**	GGA.30168
Gga.7197.1.S1_at	similar to Cytochrome P450 4A2 precursor (CYPIVA2) (Lauric acid omega-hydroxylase) (P450-LA-omega 2) (P450 K-5) (P-450 K-2)	**LOC771974**	GGA.47408
Gga.8243.1.S1_at	Hypothetical Gene Supported By CR390716	**LOC425623**	Gga.37213
Gga.131.1.S1_at	myxovirus (influenza virus) resistance 1, interferon-inducible protein p78 (mouse)	**Mx1**	GGA.131
GgaAffx.24960.1.S1_at	PQ loop repeat containing 3	**Pqlc3**	GGA.41231
GgaAffx.2035.2.S1_s_at	RAB11 family interacting protein 4 (class II)	**Rab11fip4**	GGA.27810
GgaAffx.12005.1.S1_s_at	Epidermal Retinal Dehydrogenase 2	**RCJMB04_8a2 (RDHE2)**	GGA.4788
Gga.17535.1.S1_at	Ras homolog gene family, member C	**Rhoc**	GGA.17535
GgaAffx.7275.1.S1_at	ribosomal protein S6 kinase, 90kDa, polypeptide 2	**Rps6ka2**	GGA.30233
Gga.9027.1.S1_at	scavenger receptor class B, member 1	**Scarb1**	GGA.9027
Gga.1148.1.S1_at Gga.1148.1.S2_at	ST6 beta-galactosamide alpha-2,6-sialyltranferase 1	**St6gal1**	GGA.1148
Gga.10343.1.S1_a_at	tubulin polymerization promoting protein	**Tppp**	GGA.10343
GgaAffx.26133.1.S1_s_at	UDP glucuronosyltransferase 1 family, polypeptide A1 similar to UDP-glucuronosyltransferase	**Ugt1a1**	GGA.30083
GgaAffx.8298.1.S1_at	uridine phosphorylase 1	**Upp1**	GGA.20540

Affymetrix ID	Gene name	Gene symbol	Unigene ID
	Downregulated		
Gga.4988.1.S1_at Gga.4988.2.S1_a_at	Caldesmon 1	**Cald1**	GGA.4988
GgaAffx.22999.1.S1_s_at	collagen, type I, alpha 2	**Col1a2**	GGA.42179
Gga.16392.1.S1_at GgaAffx.26432.1.S1_s_at	Collagen, type XI, alpha 1	**Col11a1**	GGA.16392
Gga.13980.1.S1_at	chemokine (C-X-C motif) receptor 7	**Cxcr7**	GGA.13980
Gga.633.1.S1_at	EPH receptor B6	**Ephb6**	GGA.633
Gga.16710.2.S1_a_at	Family with sequence similarity 132, member A	**Fam132a**	GGA.16710
Gga.7018.1.S1_s_at	FYVE, RhoGEF and PH domain containing 3	**Fgd3**	GGA.7018
Gga.862.1.S1_at	Gap junction protein, alpha 7, 45kDa (connexin45)	**Gjd3**	GGA.862
Gga.5574.1.S1_at	hypermethylated in cancer 2	**Hic2**	GGA.25061
Gga.969.1.S1_at	monooxygenase, DBH-like 1	**Moxd1**	GGA.969
GgaAffx.20726.1.S1_s_at	Endoplasmic reticulum protein 29	**RCJMB04_24f23 (C12orf8,ERP29)**	GGA.4806
Gga.4472.2.S1_x_at	Thymosin Beta 4, X-linked	**Tmsb4x**	GGA.42171

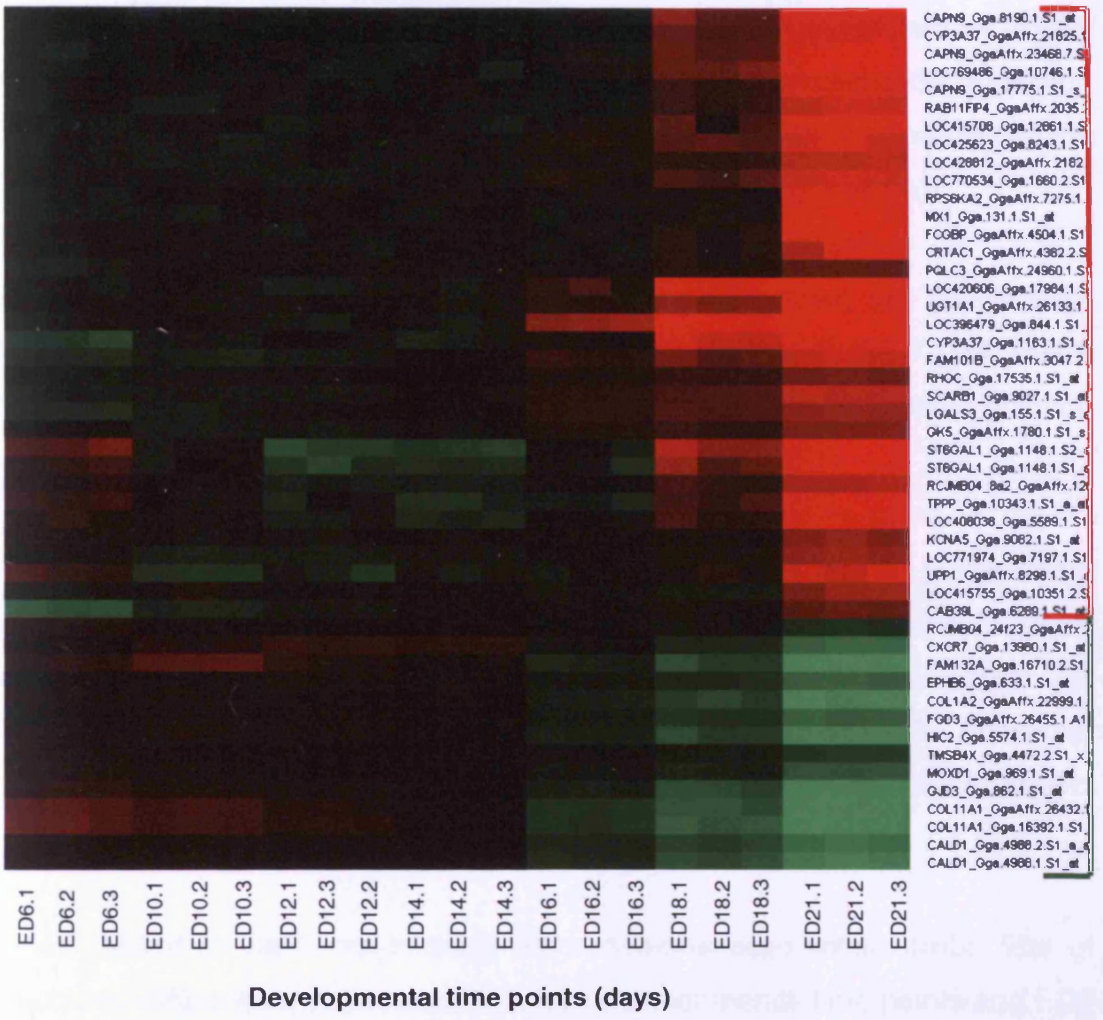

Figure 5.15 Heatmap showing expression levels of 43 differentially expressed genes between embryonic and posthatch chick corneal epithelium. Colour rank refers to changes in expression, with red being characteristic of gene upregulation and green for downregulation.

5.6.6 Genes involved in stem cell biology

Genes from uploaded probe lists were searched for the 'stem cell' annotation term using NetAffx application. Eleven genes were found to be involved in the regulation of differentiation and stem cell biology. Included genes were *Dll1*, *Tgfβ2*, *Gata2*, *Notch1*, *Cebpb* (CCAAT/enhancer binding protein (C/EBP), beta), *Fgf2* (fibroblast growth factor 2 basic), *Myod 1* (myogenic differentiation 1), *Bmp4* (bone morphogenetic protein 4), *Sox3* (SRY sex determining region Y-box 3), *Vegfa* (vascular endothelial growth factor A), *Nog* (noggin).

From the genes involved in the regulation of proliferation, six genes were identified to have an ontology related to stem cell biology; *Tgfβ2, Tgfβ3, Nfkbia (*nuclear factor of kappa light polypeptide gene enhancer in B-cells inhibitor, Alpha), *Vsx2* (visual system homeobox 2), *Vegfa* and *Fgf2*.

Amongst the genes involved in of cell death regulation, 10 genes were established to share this ontology term. These included: *Bcl2a1* (Bcl2-related protein A1), *Psen2* (presenilin 2, Alzheimer disease 4), *Mcl1* (myeloid cell leukemia sequence 1), *Loc396098* (B6.1), *Psen1* (presenilin 1, Alzheimer disease 3), *Loc395193* (anti-apoptotic NR13), *Pax7* (paired box 7), *Cebpb* and *Tgfβ2*.

Genes related to stem cell biology were demonstrated within probe lists of transcripts differentially expressed between developmental time points and ED6 and ED21 baselines, except for the probe lists ED18 versus ED21 comparison, in which stem cell-related genes were not identified. Genes obtained from all comparisons are listed in Table V.8 and all stem cell-related genes and their ontology description are summarised in Table V.9 (Appendix V).

5.7 Discussion

5.7.1 Experimental and post-experimental quality assessment

Sample collection and handling can adversely affect results; therefore, quality metrics are required to detect and assess the potential errors induced by these factors. The major aspect of experimental validation is the assessment of the hybridisation step, which is determined by several conditions such as temperature, humidity, time, buffering conditions and washing protocol (Ehrenreich, 2006). Although, automated hybridisation stations are often used to run programmed protocols to ensure reproducibility of the experiments, non-specific hybridisation is one of the common causes of poor quality microarray data (Draghici *et al.*, 2006).

Hybridisation quality controls were examined by internal and external spike-in RNA controls (ERCs), which are synthetic or naturally occurring RNA species. ERCs enable quality control for different steps of the assay including sample labelling and hybridisation. All internal and externals controls, along with standard quality metrics, such as GAPDH and Actin 3`/5` ratio, background and scaling factor, met criteria to allow further processing of microarray data.

Many of the quality assessment techniques for microarray experiments are available as post-experiment measurements of signal intensity data (Sauer *et al.*, 2005) and provide an insight into overall data quality. In practice, this type of quality assessment is highly dependent on the experimental context. Therefore, the general consistency between samples in an experiment is often more important than absolute parameter values themselves (Heber and Sick, 2006).

Various types of graphical displays were used in this study to determine the overall quality of an experiment based on signal intensities. At the chip level these were: log transformation of intensities from RMA model fit, correlation matrix plot, NUSE and RLE. All of these confirmed the good quality of the hybridised arrays and the high reproducibility of the data.

Brettschneider *et al.*, (2008) laid out concepts for microarray quality assessment data by introducing numerical measures (NUSE, RLE). The approach was derived based on the RMA model for microarray gene expression value estimation by Irizarry *et al.*, (2003).

NUSE and RLE have been previously shown to be able to detect systematic variation within certain participant sets that were not detectable using the standard Affymetrix quality metrics only. In the developmental time series experiments, application of these methods only, is likely not to be sufficient, as biological variation may often be misinterpreted as technologically-caused noise. Especially, since NUSE and RLE quality assessment is based on the assumption that the majority of genes are not differentially expressed. Developmental microarray data differs in this aspect from most other kinds of microarray data: the fraction of non-differentially expressed genes is much higher and is inhomogeneous over time. This explains the need for using additional visualisation tools and a combination of different assessment methods. Each array was checked for a number of quality controls, and was required to pass the majority of these. Failure to pass would lead to exclusion from further analyses as this would be a potential source of error.

The techniques used for sample preparation and GeneChip® processing were validated. A high quality of starting material was demonstrated and maintained throughout the experiment. Post-experimental quality controls eliminated the risk of including flawed arrays in further statistical processing of the data which could affect the outcome of differential gene expression analysis.

5.7.2 Gene expression analyses

In this study, the gene expression profile of chick corneal epithelium was evaluated throughout development, using microarray technology. Identification of these profiles is an essential prerequisite for future functional studies aimed at gaining insights into the role of these genes in corneal development, maturation and physiology. For the purpose of this thesis, particular emphasis was given on the mechanisms that are relevant to corneal epithelial homeostasis i.e. differentiation, proliferation and apoptosis and differentially

expressed genes that are likely to be relevant for morphological changes in different developmental time points.

For the studies of gene expression using the microarray approach, a number of platforms are available; both commercial (i.e. Illumina, Operon Technologies, NimbleGen Systems, Inc) and those designed for individual use (i.e. Clonetech Laboratories, BioRobotics, Ltd, Agilent Technologies etc.). The primary advantage of selecting a commercial platform is the elimination of the manufacturing expertise required and quality uncertainties, thus permitting the user to obtain robust, reproducible results and focus solely on the biology of interest. One of the reasons for choosing the Affymetrix system was the possibility to perform infinite data comparisons amongst other Affymetrix chips, since labelling and hybridisation protocols have been standardised. A high degree of Affymetrix data concordance even when run by different groups has been documented emphasising intra-platform reproducibility (Dobbin *et al.*, 2005). Another advantage of this platform is the number of programs that are built based on Affymterix chip design (Hipp and Atala, 2007). An incorporation of various global data bases into softwares for data mining and linking it with Affymetrix platform is essential in deriving biological meaning from microarray data. However, despite the availability of various applications, their main limitation is a restriction in regard to the type of input file. The majority of free online softwares preferentially allows analysis of data obtained from human, rat or mice, with only a few application available for chick data analysis (i.e. DAVID, Onto-Express).

The DAVID software, used in this study, collects and integrate diverse gene identifiers (including Affymetrix IDs from Chicken Arrays) as well as, available annotation categories from more than 40 well-known public databases, which are then centralised by internal DAVID identifiers (Huang *et al.*, 2009). The core strategy is to systematically map a large number of interesting genes in a list to the associated biological annotations (i.e. gene ontology terms) and then statistically highlight the most over-represented (enriched) biological annotations. This increases the likelihood of identifying biological processes most pertinent to the biological phenomena under study (Huang *et al.*, 2009)

Clustering of genes into groups involved in the regulation of differentiation, proliferation and apoptosis according to gene ontology, allowed the identification of functional gene families that might be relevant for understanding the developmental changes observed in the morphology of corneal epithelium. This procedure provided the possibility of exploring and viewing functionally related genes and to concentrate on the larger biological networks. The output of gene lists presented in this chapter was a result of an exploratory, computational procedure rather than a purely statistical solution.

Analysis of probe lists associated with 'differentiation' identified a number of genes that play a role in blood vessel morphogenesis and immune system development, neurogenesis, epidermal cell differentiation and somitogenesis. Most of these genes belonged to different families of growth factors and their receptors, which are known as inducers of signal transmissions to the cytoplasm through activation of the kinase (i.e. *Vegfa, Fgfs)*, or involved in TGFβ signaling pathway (i.e. growth and differentiation factors, *Gdfs*). A number of genes involved in bone morphogenetic proteins (BMP), Wnt, G-protein coupled receptor and Notch signalling pathways were also revealed by this study. Several genes were linked to negative regulation of transcription DNA-dependent and from RNA polymerase II promoter and Kinase activity.

The roles of BMPs, multi-functional growth factors that belong to the TGFβ superfamily, in embryonic development and cellular functions in postnatal and adult animals have been extensively studied in recent years. BMP signalling appeared to influence the activation of multiple different types of epithelial stem cells (Blanpain *et al.*, 2006); it was documented in early development to direct epidermal fate (Wilson *et al.*, 2001). Inhibition of BMP signalling by overexpression of *Nog* resulted in induction of hair placode formation as well as *de novo* formation of the intestinal crypt (Botchkarev *et al.*, 2001; Haramis *et al.*, 2004; He *et al.*, 2004). *Bmp4* and *Bmpr1b* were previously detected to be expressed *ex vivo* and in cultured human corneal epithelia. The *Lect1* (Chondromodulin 1) gene, relevant for chondrocyte growth and inhibition of angiogenesis, was demonstrated in the epithelial layer of rat cornea (You *et al.*, 1999; Fukushima *et al.*, 2003).

Wnt/β-catenin signalling pathways have been shown to control the specification, maintenance, and activation of stem cells. The deregulation of this pathway often resulted in the development of familial and/or sporadic epithelial cancers (Reya and Clevers, 2005). In this study, several genes that belong to frizzled- related protein family were identified, i.e. *Sfrp2, Sfrp1, Frzb.* The first two contain a cysteine-rich domain homologous to the putative Wnt-binding site of Frizzled proteins and act as extracellular signalling ligands (Rattner *et al.*, 1997). *Sfrp1* gene (an antagonist of the Wnt signalling patway) was earlier identified as the evolutionarily conserved target of the Hedgehog-Gli signalling pathway (Katoh and Katoh, 2006). *Gli* genes were identified in this study among transcripts involved in the regulation of proliferation (described below).

G protein-coupled receptors, also known as seven-transmembrane domain receptors, comprise a large protein family of transmembrane receptors that activate inside signal transduction pathways and, ultimately, cellular response (Bjarnadottir *et al.*, 2006). In this study, several members of this gene family were demonstrated to be involved in the regulation of differentiation. The majority of these were classified as the endothelial differentiation G-protein coupled receptors (Edg). Edg1, Edg2 and Edg6 elicit responses after binding sphingosine 1-phosphate (S1P) extracellular mediator, whereas Edg3 binds lysophosphatidic acid (LPA) ligand (Svetlov *et al.*, 2002). This evokes a number of responses, depending on the cell type including activation of MAP kinase pathways, alterations in the cytoskeleton, antiapoptotic effects and mitogenesis (Zhang *et al.*, 1999; Liu *et al.*, 2000; Wang *et al.*, 2002).

Gene classification clustered four genes (*Slit2, Slit3, Dll1, Notch1*) to a functional family involved in the Notch signalling pathway. Physiological function of Notch signalling within different self-renewing tissues is very diverse, ranging from gate-keeper functions for progenitor and/or stem cells in the brain and the gut to lineage specification of lymphoid progenitor cells in the hematopoietic system (Wison and Radke, 2006). In the epidermis, a structure which is morphologically similar to the corneal epithelium, Notch signalling functions as a commitment switch signal for the epithelial cells to leave the

basal layer and begin terminal differentiation (Blanpain *et al.*, 2006; Lefort *et al.*, 2007). In the mouse and human corneal epithelium *Notch 1* was primarly expressed in the basal and early suprabasal cells, which further supports the involvement of Notch in the commitment of a cell to proliferate or differentiate (Vauclair *et al.*, 2007; Djalilian *et al.,* 2008). Slit proteins have emerged as essential developmental molecules, potentially controlling multiple phases of neural development in both invertebrates and vertebrates. However, the expression of the *Slit* genes in a broad array of tissues outside the central neural system suggests that the Slit family may play a wider role during embryonic development and adult life (Piper and Little, 2002). The expression of the Slit family encompasses a diverse array of morphological events, including development of tooth primordia, and limb formation (Loes *et al.*, 2001; Vargesson *et al.*, 2001). In chick corneal epithelium, expression of *Slit2* was previously demonstrated at ED5 (HH27) (Holmes and Niswander, 2001).

One group of genes identified within genes involved in differentiation includes members of the Semaphorin/CD100 antigen family. Semaphorins are a large and diverse family of widely expressed secreted and membrane-associated proteins, which are conserved both structurally and functionally across divergent animal (Yazdani and Terman, 2006). The expression patterns of the individual semaphorins are best characterised in the nervous system, particularly during development, where most, or perhaps all, semaphorins are widely expressed by neuronal and nonneuronal cells (Fiore and Puschel, 2003). The signal transduction cascades used by semaphorins are poorly understood. It is known that semaphorins exert the majority of their effects by serving as a ligand and binding to members of the plexin family of transmembrane receptors (Negishi *et al.*, 2000). The activitvation of Sema4d/PlexB1 complex enhances the activity of Rho GEFs (guanine-nucleotide exchange factors) and leads to cytoskeletal rearrangement and axon guidance (Fiore and Puschel, 2003). *Sema3a* was postulated to be involved in cell death, proliferation, cell adhesion and aggregation, cell migration and patterning and cytoskeletal organisation in different tissues, including epithelia (Giger *et al.*, 1996; Gagliardini and Fankhauser, 1999; Osborne *et al.*, 2005; Catalano *et al.*, 2004; Kashiwagi *et al.*,

2005). *Sema3c* and *Sema3d* play role in cell survival and neural connectivity (Halloran *et al.*, 1999; Moreno-Flores *et al.*, 2003)

Genes from the gene ontology 'proliferation' category were grouped into functional clusters, which contained genes showing growth factors activity and genes involved in regulation of DNA-dependent transcription. These groups included members of the following gene families: fibroblast, platelet derived, vascular endothelial and heparin-binding growth factors. Additionally, gene clustering based on similarity in function was performed on the probe list from this category (including non-clustered probe sets). This allowed further exploration of gene functionality involved in cell proliferation. As mentioned earlier, functional clustering is based on grouping similar biological terms (functions of genes) together, but members that bring the cluster together belong to different families (described further below). The procedure revealed several genes linked to MAPKKK signalling cascades *(Fgfr3, Epgn, Stat5b, Cer1, Fgf8),* signal transduction (i.e. *Epgn, Ihh, Tgfβ2, Gli2, Fzd10*), zinc ion binding and epithelial morphogenesis (*i.e.* s100a6, *Gli2, Pgr*) or intracellular signalling cascade and GTP-binding (*i.e. Epgn, Ihh, Cd3e*).

This example shows that, even though, a gene may be excluded from created functional groups (e.g. *Epgn, Gli2*), it may actually play an interesting (multiple) role in cell/tissue biology, potentially being a gene of interest for further analysis. This is discussed further below.

In a category of genes involved in the regulation of cell death, the first detected functional group was enriched by genes related biologically to zinc-ion binding and Bcl-2 activity. This group contained most pro-apoptotic genes *(i.e. Bok, Faim, Fadd, Pdcd2*), whereas, the second (Inhibitor Apoptosis Proteins) and third (Bcl-2 related Apoptosis Agonists) ranked functional gene families were constituted by genes recognised as anti-apoptotic (*i.e. Bid, Bnip3, Birc2, Birc4, Api5).* All products of Bcl-2 family members' gene expression contain at least one of four conserved motifs, termed Bcl-2 Homology (BH) domains (Reed, 1998). Bcl-2 subfamily proteins, which contain a BH1 and BH2 (*i.e Bid*), promote cell survival by displacing the adapters, thus inhibiting, adapters

needed for the activation of caspases (Kirkin *et al.*, 2004; Adams and Cory, 1998). The caspase gene family, demonstrated by gene ontology clustering, contained a diverse set of genes, including initiator caspases (*Casp8, Casp9, Casp10*), effector caspases (*Casp3, Casp6, Casp9*) and Casp2 which play a pivotal role in DNA damaged induced-cell death (Lassus *et al.*, 2002). Several genes were demonstrated to be members of Kinase and Phosphotransferases functional families which act as modulators of the apoptotic pathway by either inhibiting (i.e. *Raf1*) or promoting (i.e. *Apaf1,*) apoptotic factors (von Giese *et al.*, 2001; Chu *et al.*, 2001), whereas others were classified as Neurotrophins. From the latter group of genes, *Ntf3* and *Bdnf*, which act via tyrosine kinase receptors, were shown to promote the survival and/or differentiation of cells from different populations of the peripheral and central nervous system (Maisonpierre *et al.*, 1990; Kalcheim *et al.*, 1992; Liu and Jaenisch, 2000). The above suggests, that the balance between agonist and antagonistic members of the Bcl-2 family, caspase gene family and kinases and phosphotransferase modulators is likely to play a role in determining cell fate during corneal epithelial development.

This study demonstrated a number of genes within each biological category that were excluded from a functional classification. Some of these genes (*i.e. bcl2l15, Fzd10, Notch homolog 2*) were assigned to the unclustered group, even though their name would suggest an affiliation to a functional gene family. The possible reasons for this are that: 1) the gene does not have a relationship with any of other genes above the similarity threshold, 2) the gene has a relationship with a few other genes, but there are not enough members to form a functional group based on a minimum of final cluster members and 3) the gene might be a false negative, as the current algorithm used for gene clustering might have up to a 2% false negative rate. Although such genes were not mapped to any of the functional groups (as it was in the case of genes involved in the regulation of proliferation) they might still be biologically relevant (*i.e. Epgn, Gli2*).

PCA provided a way to identify predominant gene expression patterns across the data. Although, PCA is commonly used to summarise microarray data, it is

a statistical tool, thus may not always reflect the biological importance of genes detected. PCA identified within the first discrete distribution; two genes involved in differentiation; *Mgp* and *Cebpb.* The first gene was classified to unclustered genes, but showed a high change in expression between the earliest and mid-developmental time points and between embryonic and posthatch stages. *Cebpb* also showed a similar expression pattern to *Mgp* throughout development and was identified as a gene involved in all three major biological processes (proliferation, differentiation and apoptosis). PCA also showed a population of genes (except for *Fgfr3, Myd88* and *Mall*) that were not classified to any of the functional gene families, and additionally their expression throughout the development appeared to be stable. This was also observed for the apoptosis-related *Opa1* gene. Thus, in future studies, it would be interesting to investigate the role of the above genes in the corneal epithelium as well as their interaction network.

The functional annotation clustering approach was used for differentially expressed genes between posthatching (ED21) and embryonic time points. This procedure uses a similar concept as functional classification by measuring the relationship amongst the annotation terms on the basis of the degree of their coassociation with genes within the probe list to cluster heterogenous, yet highly similar annotation into functional annotation groups (Huang *et al.*, 2009). This type of grouping provides a more insightful view of the relationships between annotation categories allowing the biological interpretation to be more focusses at the 'biological module' level.

Functional annotation clustering was performed for genes differentially expressed genes between each embryonic time point when compared to ED6 (initial time point) baseline. From reported overrepresented biological terms (significant at $p \leq 0.01$ level) annotation clusters with the highest rank for each comparison were shown in this chapter. Analysis revealed the importance of particular biological processes at different time points throughout development. For instance, it was demonstrated that the activity of genes in the two earliest embryonic days (ED10, ED12) in reference to ED6 basline, was oriented towards the formation of cell communication and constitution of intermediate

filaments in cytoskeleton. Annotation clustering at ED12 revealed additionally a role of differentially expressed genes in constitution of ECM and importance of genes involved in multicellular development as well as cell proliferation. In the middle developmental time-points (ED14, ED16) gene activity is likely to be primarily directed at further multicellular and anatomical structure development, reorganisation of cytoskeleton and acceleration of metabolic processes. Also, analyses identified a number of genes that contain EGF-like domain motif, thus they are likely to act in similar way to EGF (e.g. participation in various signalling patwhays). A number of genes differentially expressed at ED16 and ED18 were shown to be involved in neurogenesis and further formation of cytoskeletal/intracellular componets. Analysis of intitial time point versus ED21 posthatch, revealed additional clusters of differentially expressed genes that play a role in primary metabolic processes and post-translational protein modification, immunoresponse and the establishment of cellular localisation. Interestingly, it was observed that some clusters are shared by different time points, but their order (and thus biological importance) is changed. Above results from increasing number of differentially expressed genes that constitute each cluster, and share similar annotation terms; the more enriched term, the higher significance (p-value) and final enrichment score. Individual genes that constitute each cluster should be investigated further in order to answer more detailed questions regarding their role and relationship to other members of the cluster they belong to.

Within differentially expressed genes between ED6 and other developmental time points were those involved in different biological processes, as described in section 5.6.1. Some of them might be of particular interest, as they were identified also in PCA analysis and are stem cell-related. For instance *Cebpb* was shown in this study to be upregulated in the mid-developmental time-points, differentially expressed between ED6 and EDs 10, 12, 14, 16. It was also identified as a stem cell related gene. *Cebpb* is a nuclear factor that binds to SRE (serum response element), a promoter element essential for transcriptional activation of immediate early genes, such as c-fos and early growth response-1, by mitogenic signals. The interaction of the *Cebpb* with *Ras GTPases* and role of Cepb proteins in regulating the balance between cell

growth and differentiation were suggested (Umek *et al.*, 1991; Hanlon and Sealy, 1999).

Also, genes which belong to Semaphorin/CD100 antigen, *Myd88* (Myeloid Differentiation Primary Response Gene (88)), *Mall* (Mal, T-cell Differentiation Protein-like) appeared to be relevant in regulation of differentiation during corneal epithelial development. *Myd88* and *Mall* were identified in PCA, and also shown to be upregulated continuously throughout the development and diferrentially expressed in later developmental time points (from ED16 onwards) (Fig. 5.14). While previous study demonstrated role of *Myd88* in positive regulation of NF-kappaB transcription factor activity, little is known about *Mall* (Jefferies *et al.*, 2001). It might participte in signal transcduction through Toll-like receptor (TLRs) (similarily to Myd88) as regulator of NF-kappaB transcription factor and MAP kinase signalling, which give rise to increased expression of a multitude of pro-inflammatory proteins (O'Neill *et al.*, 2003).

In this study, genes differentially expressed in embryonic development when compared to posntal corneal were demonstrated. 43 genes, either up- or downregulated were clustered into 6 functinal groups. While downregulation of several genes (*i.e Cald1, Gjd3, Col1a2, Col11a1, Tmsb4x, Fgd3*) might be related to processes occurring during epithelial development such as collagen reorganisation, constitution of ECM and formation of actin filaments and gap junction or cell migration, role of transcripts identified as upregulated in posthatched epithelium is not clear and requires further investigation.

Finally, this study demonstrated genes that were involved in stem cell biology within uploaded probe lists of genes from the main biological categories (differentiation, proliferation and cell deah), and differentially expressed between embryonic time points when compared to ED6 and posthatch epithelia as a baseline. Mechanisms that some of these genes control, are likely to be important also in limbal stem cell and/or transient amplifying cell fate determination and maintenance (e.g. *Cebpb, Atoh7, Ly6e, Psca*). This however requires further investigation and confirmation.

In summary, the analysis of gene expression using high density oligonucleotide arrays delivered a complete gene expression profile of the developing chick corneal epithelium and allowed identification of control mechanisms and factors involved in major processes that potentially may regulate important biological functions in corneal epithelial homeostasis. Additionally, several genes were selected for further experiments to validate the microarray data. However, this study was performed using the whole corneal epithelium, thus, one must be are aware of the fact there is potentially difference in expression of individual gene between different epithelial regions and/or cell layers as well as between different cell types. This will be investigated in the future experiments.

CHAPTER SIX

Confirmation and characterisation of microarray targets

CONFIRMATION AND CHARACTERISATION OF MICROARRAY TARGETS

6.1 Introduction

To investigate local tissue-specific expression even in tissues with low abundances, very sensitive methods are required which allow reliable RNA quantification (Pfaffl, 2003). Different techniques have been developed for analysis and quantification of gene expression. These include: Northern Blotting, RNAse protection assay and *in situ* hybridisation. However, reverse transcription combined with real-time (quantitative) Polymerase Chain Reaction (RT-qPCR) has been proven to be the most specific and sensitive for quantitative analysis of gene expression (Murphy *et al.*, 1990; Horikoshi *et al.*, 1992; Livak and Schmittgen, 2001).

In conventional PCR, the amplified product (amplicon) is detected by end-point analysis and running the PCR product on an agarose gel after the reaction has finished. In contrast, qPCR allows the accumulation of amplified product to be detected and measured as the reaction progresses (real time). Quantitative data is collected at a point in which every sample is in the exponential phase of amplification, as its most reproducible, before the reaction enters the plateau phase (when one or more of the reaction components becomes limiting) (Fig 6.1).

Additionally, qPCR data can be evaluated without gel electrophoresis once the reaction is optimised, resulting in reduced experiment time and increased throughput. Another advantage is that reactions are run and data are evaluated in a closed-tube system, thereby reducing the risk of contamination and eliminating the need for postamplification manipulation.

Different types of qPCR use different approaches to detect the new products synthesised at each new PCR cycle. The chemistry used depends mainly on the application and cost consideration. The two basic chemistries, along with highly specific primers and optimised reagents, decide technique sensitivity.

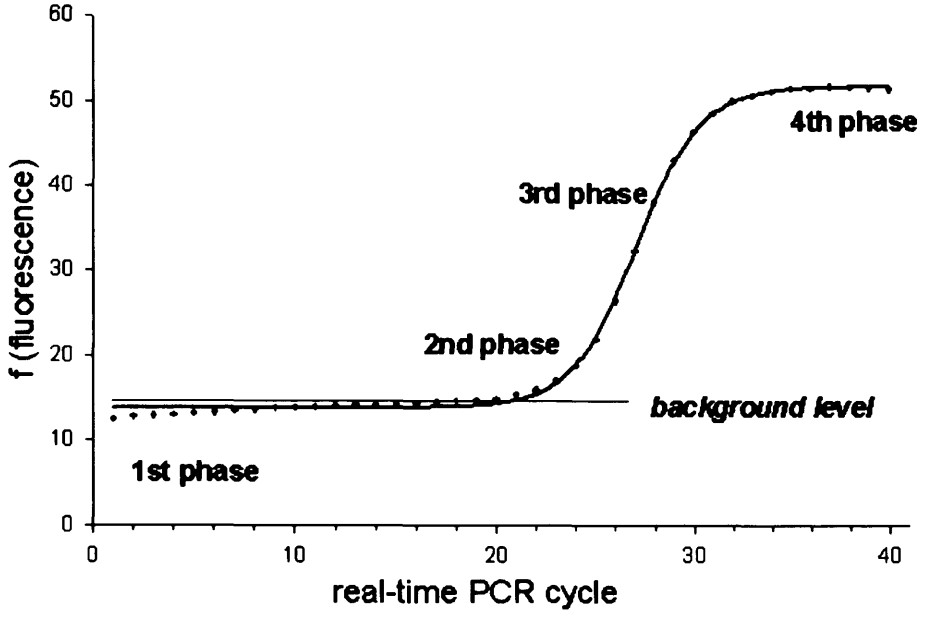

Figure 6.1 The four characteristic phases of real-time PCR evaluated by fluorescence acquisition. 1st phase: hidden under background fluorescence, where an exponential amplification is expected, 2nd phase: exponential amplification that can be detected above the background, 3rd phase linear amplification and a steep increase in fluorescence, 4rd phase (plateau) (Tichopad *et al.* 2003; Pfaffl, 2003).

The first one, used in high-throughput experiments is based on fluorescent primer- or probe-based assays (singleplex or multiplex reaction). For low-throughput, singleplex experiments intercalating dyes are preferable. DNA-binding dyes fluoresce only when bound to double-stranded products generated by PCR.

In this study SYBR Green I, the most commonly used DNA-binding dye for qPCR and was used. Since SYBR Green I exhibits little fluorescence when it is free in solution, at early stages of the qPCR reaction the emitted fluorescence is too low to be registered by the machine, but it increases up to 1000-fold when binding to double-stranded DNA (dsDNA) during the exponential phase of the reaction. The overall fluorescent signal from the reaction is proportional to the amount of dsDNA present, and will increase as the target is amplified.

Although, microarray technology is a powerful technique used to analyse the expression of thousands of genes in a short time and high quality arrays are

available from several manufacturers, problems encountered include high variability and sensitivity not sufficient for low abundant expressed genes (i.e. growth factors and their receptors) (Pfaffl, 2003). Also, discrepancy in fold-change calculation and lack of specificity for different isoforms or differentially expressed genes has been suggested. Therefore, additional confirmation check of array results is required (Schena *et al.*, 1995; Harrington *et al.*, 2000; Bustin, 2002).

The microarray based screening of tissue specific gene expression and confirmation of putative candidate target genes by kinetic qPCR represents a powerful and optimal combination (Rajeevan *et al.,* 2001, Pfaffl, 2003). The advantages of both quantification systems can be added – the high throughput capacity of the microarray platform, as well as sensitivity and specificity of real-time RT-PCR (Schena *et al.*, 1995, Pfaffl, 2003).

6.2 Aims

- To identify suitable housekeeping genes as an internal control for normalisation of RT-qPCR results
- To validate the reproducibility of the microarray results
- To analyse and quantify the expression of genes of interest during the development of chick corneal epithelium.

6.3 Experimental design

The details of primer design and protocols for conventional and RT-qPCR are described in section 2.12.

Briefly, three sets of chick corneal epithelia RNA obtained from separate sample isolations (previously subjected to microarray experiments) were used for relative quantification of genes of interests. The three pools of RNA at each developmental time point (ED6, 10, 12, 14, 16, 18, ED21 posthatch), were transcribed to cDNA and processed for real-time RT-PCRs. Specificity of primers and products was confirmed by electrophoresis and melting peak analysis (Chapter 2, sections 2.12.4, 2.12.5).

All reactions were replicated thrice with cDNA samples collected from different sets of pooled chick corneal epithelia. Amplification of housekeeping genes; G6PDH and UB, was performed as an internal control. For negative controls, similar amounts of total RNA of each sample were subjected to the same cDNA synthesis protocol without the reverse transcriptase. Both negative controls (exclusion of reverse transcriptase) and NTC were run simultaneously in all experiments to ensure a specificity of the assay and detection of carryover contamination (Chapter 2, section 2.12.4).

Average threshold cycle (Ct) values obtained form triplicates after qPCR reactions, were transformed to linear scale expression quantities using the comparative delta-Ct method. The sample with the highest expression (lowest Ct) for each gene was used as a calibrator and set to 1 and subsequently raw expression values of remaining samples were calculated according to the formula as follows:

$$Q = (1+ Ex)^{(\text{calibrator Ct} - \text{sample Ct})},$$

where *Ex* was the efficiency of qPCR reaction (0.95-1.10 range), *Q* was quantity.

Several houskeeping genes; GAPDH, β-Actin, G6PDH and UB, were checked for stability throughout development allowing selection of the most stable pair after pairwise comparison. All softwares programmes used for the calculations are free accessible and it is recommended to evaluate candidate genes using at least two of them.

The NormFinder applies an algorithm for identifying the optimal normalisation gene among set of candidates. It ranks the set of candidate normalisation genes according to their expression stability in a given sample set and given experimental design. NormFinder calculates a gene-stability value with a mathematical model based on separate analysis of the sample subgroups and estimation of both intra- and intergroup variation in expression levels (Andersen *et al.*, 2004)

geNorm is a software developed by Vandesompele and coauthors (2002). Its approach relies on the principle, that the expression ratio of two perfect reference genes would be identical in all samples in all experimental conditions or cell types (Ishii *et al.*, 2006). geNorm calculates the individual stability of a gene within pool of genes, and calculates stability (*M* value) according to the similarity of their expression profile by pairwise comparison, using the geometric means as a normalising factor.

The third software used, BestKeeper, developed by Pfaffl and coauthors (2004), calculates the gene expression variation for all individual housekeeping genes based on Ct. The best suited candidates are determined and combined into an index. Gene stability was deducted from the calculated SD (standard deviation) and coefficient of variance. To estimate gene relations, pairwise correlation analyses were performed by calculating the Pearson correlation coefficient.

After evaluation of the most stable housekeeping genes, the normalisation factor (NF) was calculated as a geometric mean of the expression of the pair of the most stable housekeeping genes. NF is reported to be more accurate as an internal control than one housekeeping gene (Vandesompele *et al.*, 2002). By dividing the relative quantities (raw expression) for each gene of interest and time point (sample) by the appropriate NF, the relative expression levels of all target genes and time points were calculated. The standard errors for normalisation factors and normalised expression of each sample were calculated and data was shown as a mean of results from three independent experiments. In order to make data comparable between runs, a dilution series of the same standard was used.

Statistical analysis on normalised RT-qPCR data (after log transformation when necessary) was performed One-way ANOVA with appropriate post-hoc test (Tukey or Dunnett T3) and/or Kruskal-Wallis with post-hoc test (Appendix VI). Fold changes were calculated on log normalised microarray and RT-qPCR data, based on the formula: log(A/B) = log(A) - log(B).

.

6.4 Optimisation for the RT-qPCR

The optimum annealing temperature (T_a) was established, using standard PCR, by trying a range of T_a above and below the calculated melting temperature (T_m) of the primers. Samples from developmental time points where the relative expression of each gene was the highest, according to microarray data, were chosen to check for optimal T_a of each pair of primers. The temperatures varied between 50 and 72°C (Figure 6.2). Optimum T_a was determined by the temperature that offered a single, sharply defined band when visualised: set at 58°C for all primer sets. In most cases, the T_a was 5°C below the lowest T_m of one of the primers from a pair, as suggested by Innis and Gelfand (1990). Although, for some primer pairs, the difference between T_m and T_a was higher (i.e. G6PDH, UB) or slightly lower (i.e. GAPDH) than 5°C, in all cases a distinct band was observed at 58°C.

The efficiency, reproducibility and dynamic range of SYBR Green I assay was determined by constructing a standard curve using serial dilutions of a known template. The range of template concentrations used for standard curve encompassed the concentration of the test samples; results from test samples were within the linear dynamic range of the assay. In all assays the efficiency estimated by the software was between 90% and 105%, the coefficient of determination (R^2) of was >0.97 and Pearson`s correlation coefficient (r)>0.98 as estimated by the software, indicating good reproducibility across assays.

During optimisation of qPCR conditions, primers were checked for their specificity and melting peak analysis was used to confirm that the observed fluorescence was derived from the target product, rather than from non-specific amplification. Results were confirmed by running qPCR products on an agarose gel.

As shown in Figure 6.3, each primer set generated one amplified band using chick corneal epithelia cDNA. An additional peak observed in early T_m resulted from primer-dimer formation but not contamination. This was confirmed by agarose gel analysis which did not showed the presence of additional peaks.

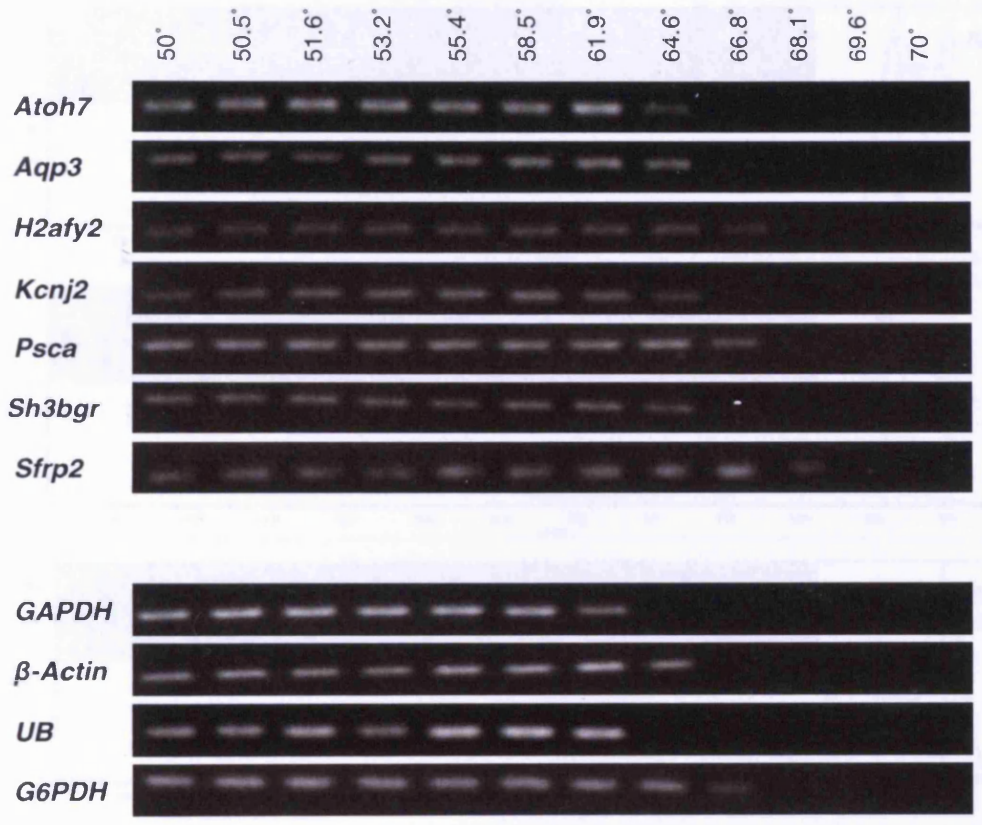

Figure 6.2 Annealing temperature optimisation. An annealing temperature gradient of 50°C to 70°C was performed using standard PCR and 30 cycles. The 58°C was selected as the optimal annealing temperature for all assays.

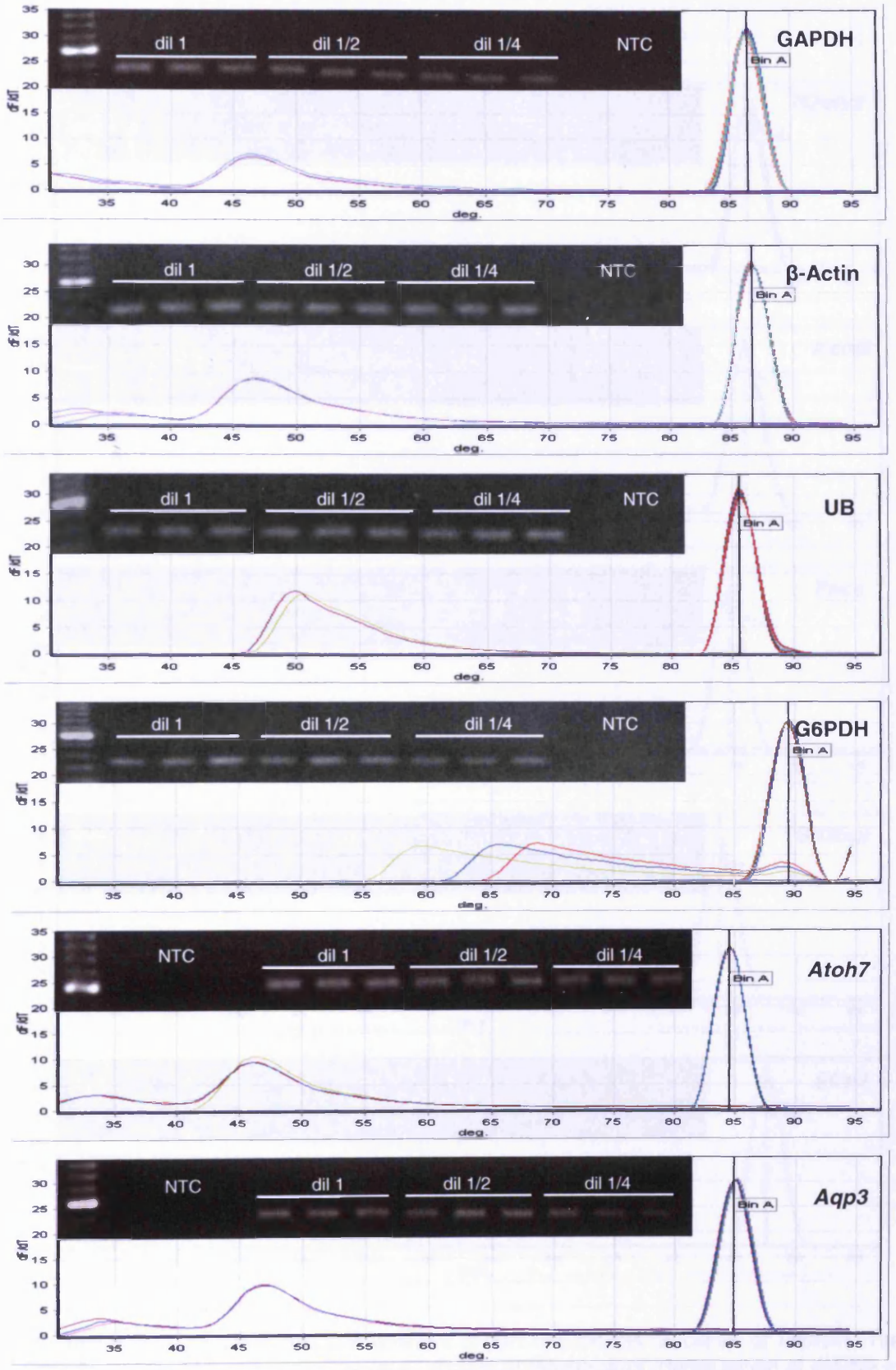

Figure 6.3a Melt-curve and gel analysis of qPCR products for reference genes (GAPDH, β-Actin, UB, G6PDH) and two genes of interest (*Atoh7*, *Aqp3*). The change in fluorescence is plotted as a function of temperature (denaturation of dsDNA in degrees). For standard curve analysis serial dilutions of known sample were used. The higher melt peaks represent the specific product, and correspond to the lanes with bands on a gel. Additional peaks at low T_m indicate the formation of primer-dimers. Lane 1: 50-500bp molecular ruler (intense band indicates 250bp), lanes 2-9 for reference genes and 5-13 for *Atoh7* and *Aqp3* represent bands from triplicate dilutions for standard curve. NTC: no template control.

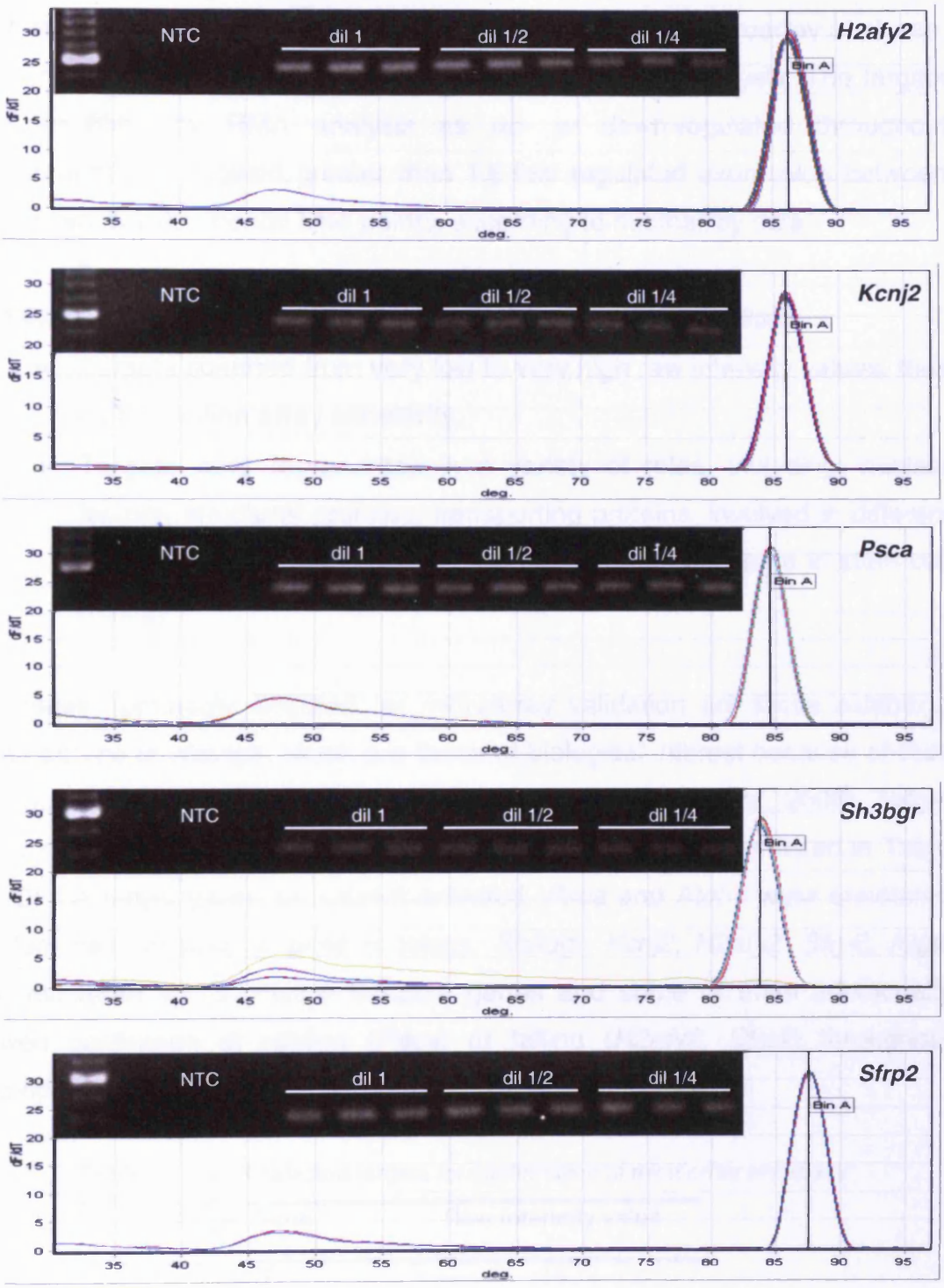

Figure 6.3b Melt-curve and gel analysis of qPCR products of genes of interest. The change in fluorescence is plotted as a function of temperature (denaturation of dsDNA in degrees). For standard curve analysis serial dilutions of known sample were used. The higher melt peaks represent the specific product, and correspond to the lanes with bands on gel. Additional peaks at low T_m indicate the formation of primer-dimers. Lane 1, 50-500bp molecular ruler (intense band indicates 250bp), 5-13 for represent bands from triplicate dilutions for standard curve. NTC: no template control.

6.5 Selection of microarray targets for RT-qPCR analysis

In order to confirm the levels of gene expression found by microarray analyses, selected gene targets were chosen for further RT-qPCR analysis. The targets were identified by RMA analysis as up- or down-regulated throughout development and showed greater then 1.6-fold regulated expression between at least two developmental time points, according to microarray data.

In addition, the following criteria of selection of genes were applied:

- Targets spanned from very low to very high raw intensity values, thus could confirm array sensitivity,
- Targets were represented in a variety of roles, including; nuclear factors, structural proteins, transporting proteins, involved in different biological processes and had the potential to participate in stem cell biology.

The genes commonly selected for microarray validation are those exhibiting large degrees of change, which are those of biological interest because of their response to some challenge or change in condition (Morey *et al.*, 2006). Target genes of interest, selected for validation of microarray data, are listed in Table 6.1. Of the target genes of interest selected, *Psca* and *Atoh7* were annotated for stem cells related by gene ontology. *Sh3bgr, Kcnj2, H2afy2, Sfrp2, Aqp3* were clustered in 1000 most variable genes and some of them additionally showed continuum of raising (*Psca*) or falling (*H2afy2, Sfrp2*) throughout development.

Table 6.1 List of selected targets for confirmation of microarray sensitivity

Target Gene	Raw Intensity value
Atoh7	15
Sh3bgr	150
Kcnj2	155
H2afy2	287
Sfrp2	712
Aqp3	1337
Psca	>6000

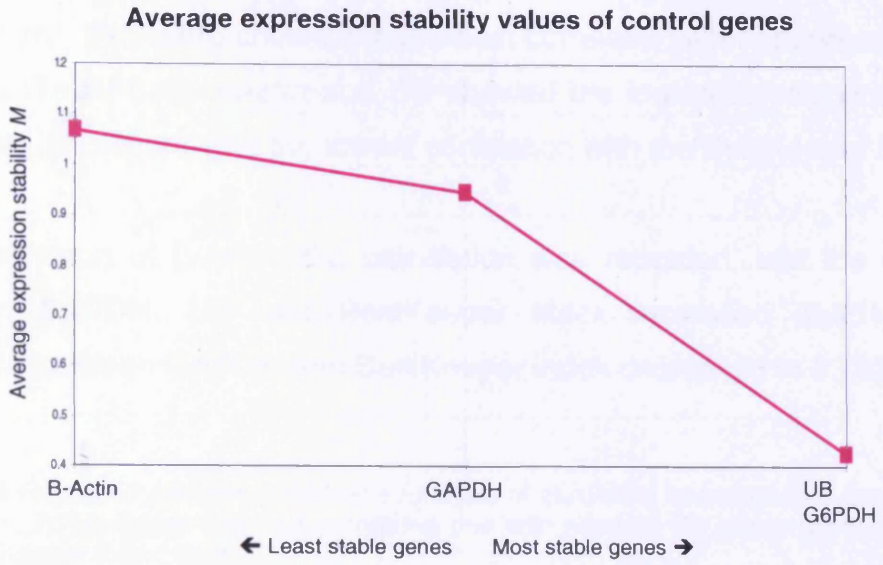

Figure 6.4 Avarage expression stability values of control genes. The UB and G6PDH were identified as the most accurate reference genes in the chick corneal epithelial model using geNorm.

BestKeeper analysis confirmed that UB and G6PDH were the best housekeeping gene combination. Descriptive statistics of the derived Ct were computed for each housekeeping gene is presented in Table 6.3

Table 6.3 Descriptive statistic of four candidate housekeeping genes based on their Ct values. Abbreviations: N: number of samples; GM: geometric mean; AM: arithmetic mean; Min and Max: the extreme values of Ct; SD: standard deviation; CV (%): coefficient of variance expressed as a percentage on the Ct level.

	GAPDH	β -Actin	UB	G6PDH	BestKeeper
n	7	7	7	7	7
GM [Ct]	11.24	14.76	27.49	16.15	16.47
AM [Ct]	11.25	14.77	27.51	16.20	16.49
min [Ct]	11.01	13.93	25.84	14.61	15.64
max [Ct]	12.08	15.45	28.81	18.11	17.60
SD [± Ct]	0.24	0.42	1.03	1.14	0.51
CV [% Ct]	2.12	2.87	3.75	7.02	3.10

Subsequently, the individual housekeeping genes levels were calculated and genes were ordered from the most (showing lowest variation) to the least stably expressed (showing the highest variation). In agreement with analyses, GAPDH showed the highest stability (*CV*=2.12, *SD*=0.24). Although, UB and G6PDH

showed a high Ct variation (as shown in Table 6.3) and could be considered as inconsistent, they were shown to have best correlation after pairwise correlation analysis (Table 6.4). β-Actin and UB showed the lowest correlation among all pairs and β-Actin showed the lowest correlation with the BestKeeper index.

After exclusion of β-Actin, the calculation was repeated, and the correlation between G6PDH, UB and BestKeeper index increased ($0.951<r<0.990$), whereas, between GAPDH and BestKeeper index decreased to 0.783.

Table 6.4 Repeated pairwise correlation analysis of candidate housekeeping genes (Pearson correlation, *r*). (A) genes pairwise correlated one with another; (B) genes pairwise correlation with BestKeeper index (n=4).

(A)

	GAPDH	β -Actin	UB	G6PDH
vs. β -Actin	0.290	-	-	-
p-value	0.527	-	-	-
vs. UB	0.582	0.073	-	-
p-value	0.170	0.879	-	-
vs. G6PDH	0.708	0.146	0.955	-
p-value	0.075	0.755	0.001	-

B)

BestKeeper vs.	GAPDH	β -Actin	UB	G6PDH
Corr. coeff. (*r*)	0.808	0.343	0.883	0.970
p-value	0.028	0.450	0.008	0.001

6.6.2 Validation of microarray data of differentially expressed genes

6.6.2.1 Genes upregulated during chick corneal epithelial development

Aquaporin 3 (Gill Blood Group)

Quantitative analysis showed that the Aquaporin 3 (Gill Blood Group) transcript (*Aqp3*) was upregulated throughout development in relation to the earliest developmental time point ED6 studied. Figure 6.5 shows the log normalised relative expression of *Agp3* between time points determined by RT-qPCR and microarray. As shown by RT-qPCR, the *Aqp3* transcript was expressed at a detectable level from ED12 onwards (Appendix VI, Table VI.1). Statistically significant differences in expression of Aqp3 were demonstrated between ED6 and two latest developmental time points, and also between ED10 and ED18, and between ED12 and ED18 ($p \leq 0.05$, see Appendix VI, Table VI.5).

The fold change differences between ED6 (used as a calibrator) and the rest of the developmental time points, as estimated by RT-qPCR and microarray analysis are detailed in Table 6.5.

Table 6.5 Fold changes in abundance of *Aqp3* transcript between developmental time points

Symbol	Functional group	Fold change EDs	6	10	12	14	16	18	21
Aqp3	Transporter activity, water and glycerol channel activity	Microarray	1	1.8	4.9	6.6	7.6	7.9	7.8
		RT-qPCR	1	2.3	2.8	2.9	3.1	3.3	3.2

Prostate Stem Cell Antigen

Microarray and RT-qPCR demonstrated the lowest expression levels of Prostate Stem Cell Antigen (*Psca*) at ED6 with a gradual upregulation thereafter to the highest levels in posthatched corneal epithelia. This is illustrated in Figure 6.6, where the log normalised relative expression of *Psca* transcript throughout the development is indicated. By quantitative RT-PCR, *Psca* transcript appeared to be expressed at low detectable level up to ED10 (Appendix VI, Table VI.1). Statistically significant differences in expression were identified between ED6 and ED18, posthatched (ED21) epithelia, as well

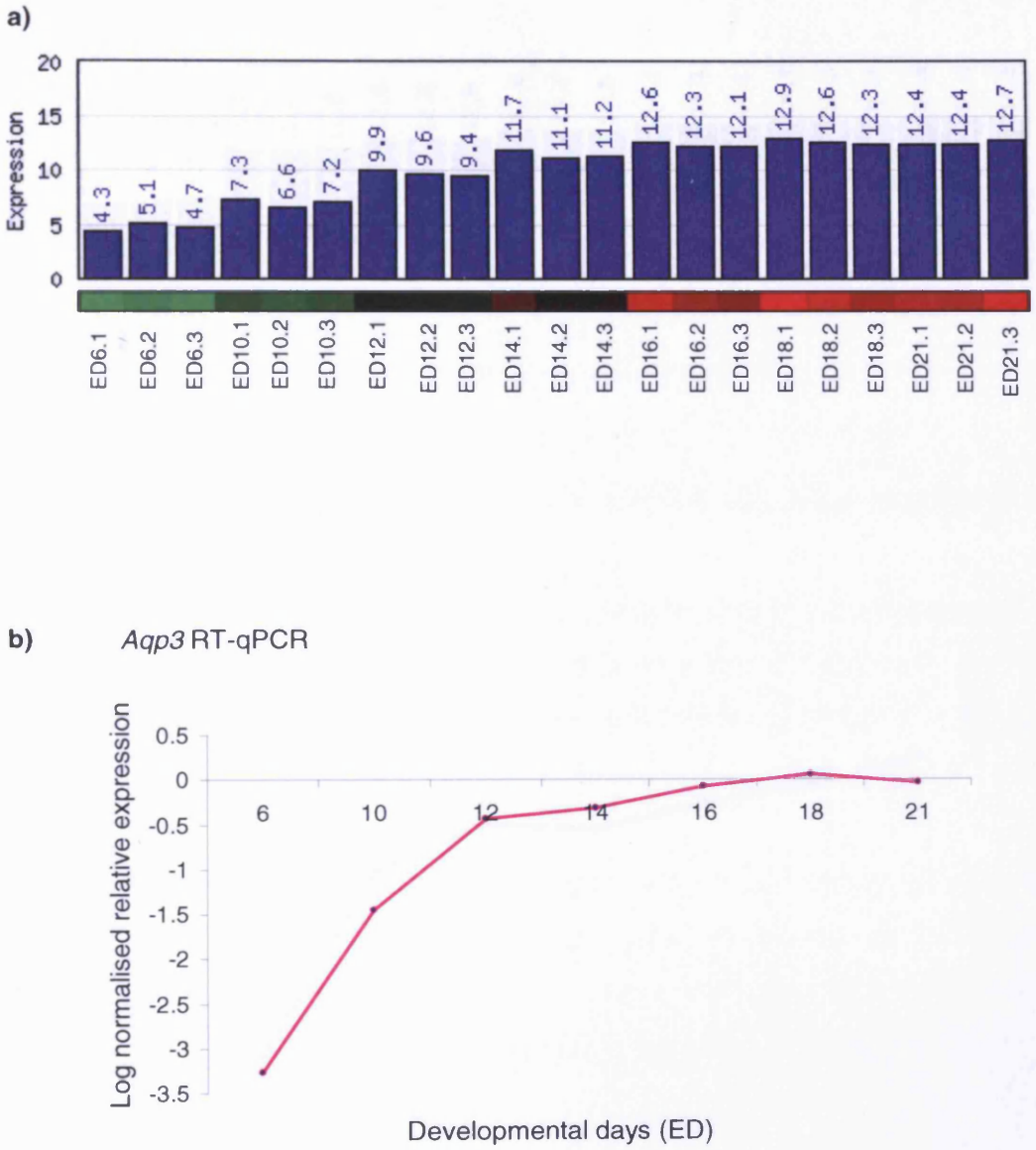

Figure 6.5 Microarray **(a)** and real-time RT-PCR **(b)** of *Aqp3* expression profile. RT-qPCR confirmed upregulation of the transcript throughout development. Blue bars represent levels of expression obtained from normalised RMA data, colour rank of heatmap underneath graph refers to relative changes in expression, with red being characteristic of gene upregulation and green for downregulation.

as, between ED10 and ED21 (K>8.46, p=0.05) (Appendix VI, Table VI.25). Fold changes calculated from microarray and quantitative RT-PCR using ED6 as a reference time are shown in Table 6.6.

Table 6.6 Fold changes in abundance of *Psca* transcript between developmental time points

Symbol	Functional group	Fold change EDs	6	10	12	14	16	18	21
Psca	Kinase and TGFβ receptor activity	Microarray	1	4.7	5.9	6.9	7.2	7.4	7.7
		RT-qPCR	1	1.7.	2.2	2.2	2.4	2.6	2.9

6.6.2.2 Genes downregulated during chick corneal epithelial development

Atonal Homolog 7 (Drosophila)

Atonal Homolog 7 (Drosophila) (*Atoh7*) also called Math5 is a homologue of the Drosophila gene. Microarray analysis as well as real-time RT-PCR showed that the *Atoh7* transcript was significantly downregulated in development (ED10 to ED21), compared to the highest expression levels at ED6 (Figs. 6.7a,b).

Significant differences in *Atoh7* gene expression were also demonstrated between ED10 and other embryonic days, with exception of ED12, and between ED14 and ED6, ED10 ($p \leq 0.05$, Appendix VI). The fold change differences in expression of the *Atoh7* transcript between developmental stages are shown in Table 6.7.

Table 6.7 Fold changes in abundance of *Atoh7* transcript between developmental time points

Symbol	Functional group	Fold change EDs	6	10	12	14	16	18	21
Atoh7	Transcription regulator activity	Microarray	1	-3.7	-3.6	-3.8	-3.6	-3.6	-3.5
		RT-qPCR	1	-1.7.	-2.0	-2.3	-2.6	-2.5	-2.7

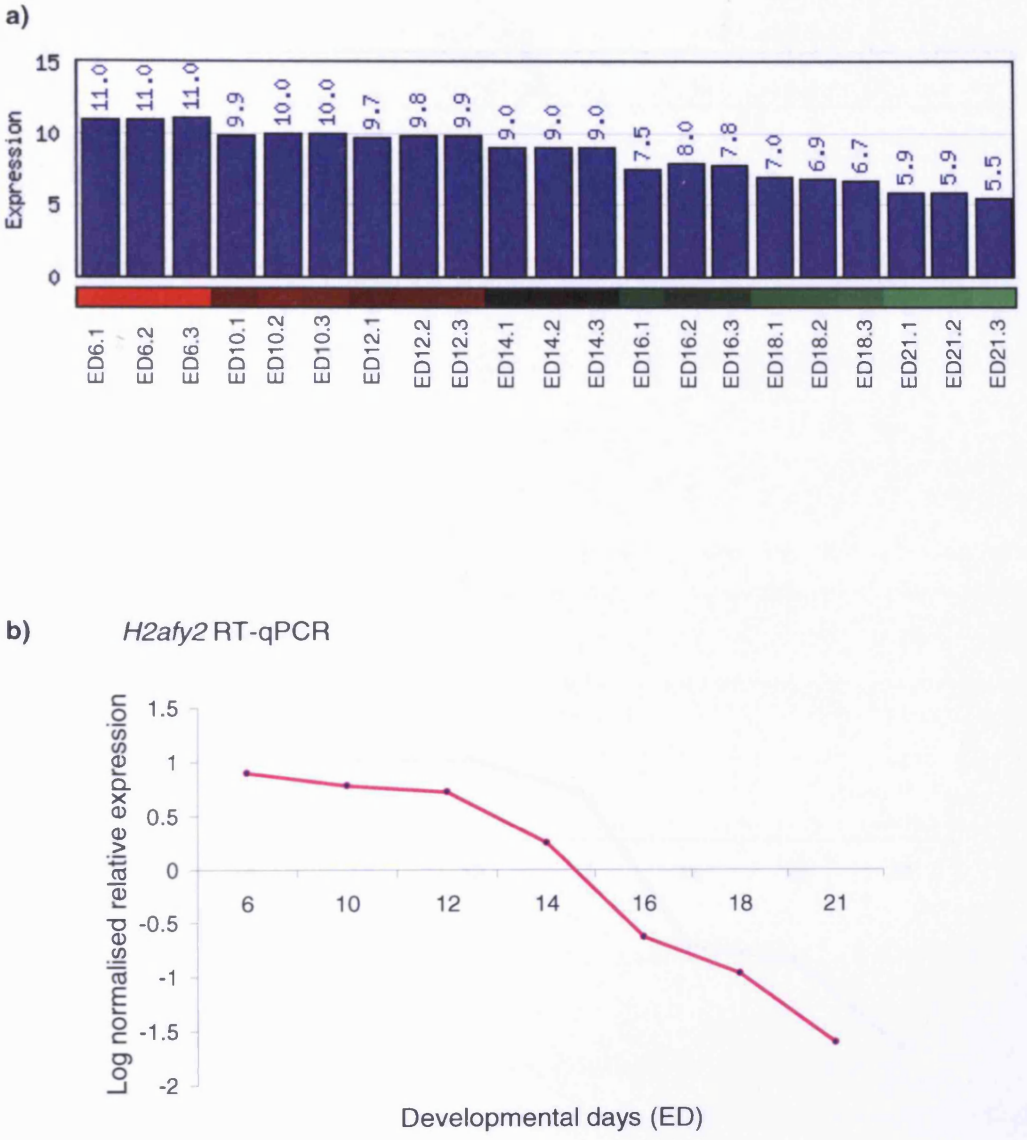

Figure 6.8 Microarray **(a)** and real-time RT-PCR **(b)** of *H2afy2* expression profile. RT-qPCR confirmed downregulation of the transcript throughout development. Blue bars represent levels of expression obtained from normalised RMA data, colour rank of heatmap underneath graph refers to relative changes in expression, with red being characteristic of gene upregulation and green for downregulation.

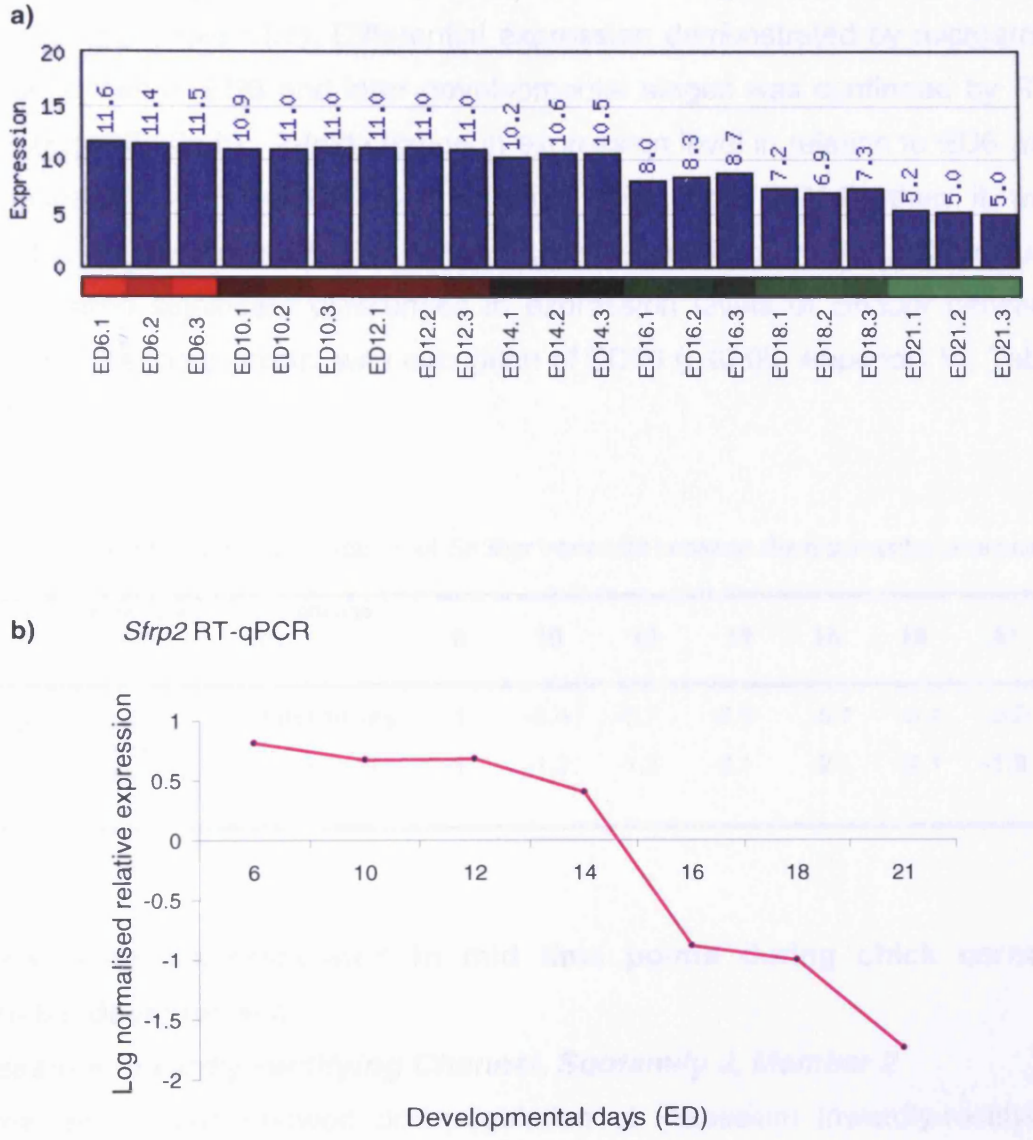

Figure 6.9 Microarray **(a)** and real-time RT-PCR **(b)** of *Sfrp2* expression profile. RT-qPCR confirmed down-regulation of the transcript throughout development. Blue bars represent levels of expression obtained from normalised RMA data, colour rank of heatmap underneath graph refers to relative changes in expression, with red being characteristic of gene upregulation and green for downregulation.

SH3 Domain Binding Glutamic Acid-rich Protein

Quantitative analysis showed that SH3 Domain Binding Glutamic Acid-rich Protein (*Sh3bgr*) gene is downregulated throughout chick corneal development (Appendix VI, Table VI.1). Differential expression demonstrated by microarray analysis between ED6 and later developmental stages was confirmed by RT-qPCR (Figs. 6.10a,b). 2-fold change in expression level in relation to ED6 was demonstrated by RT-qPCR in later time point (from ED14), then it was estimated by microarray (Table 6.10). Statistical analysis of RT-qPCR results demonstrated significant differences in expression levels of *Sh3bgr* between ED6 and other time points, with exception of ED10 ($p \leq 0.05$, Appendix VI, Table VI.17).

Table 6.10 Fold changes in abundance of *Sh3bgr* transcript between developmental time points

Symbol	Functional group	Fold change EDs	6	10	12	14	16	18	21
Sh3bgr	Protein complex assembly	Microarray	1	-5.4	-5.7	-5.9	-5.7	-5.4	-5.2
		RT-qPCR	1	-1.2	-1.3	-2.1	-2.1	-2.1	-1.8

6.6.2.3 Gene downregulated in mid time points during chick corneal epithelial development

Potassium Inwardly-rectifying Channel, Subfamily J, Member 2

Microarray analysis showed downregulation of Potassium Inwardly-rectifying Channel, Subfamily J, Member 2 transcript (*Kcnj2*) from ED6 to ED14, with later upregulation until posthatched (ED21) time point (Fig. 6.11a). The pattern of *Kcnj2* expression throughout development was confirmed by quantitative RT-PCR analysis, however, lowest expression level was demonstrated at ED16 (Fig. 6.11b). Statistically significant differences were demonstrated between ED6 and the rest of developmental time points, with the exception of ED18 and other statistically significant variations in gene expression are shown in Table VI.13. Fold changes estimates from microarray and RT-qPCR data are listed in Table 6.11.

a)

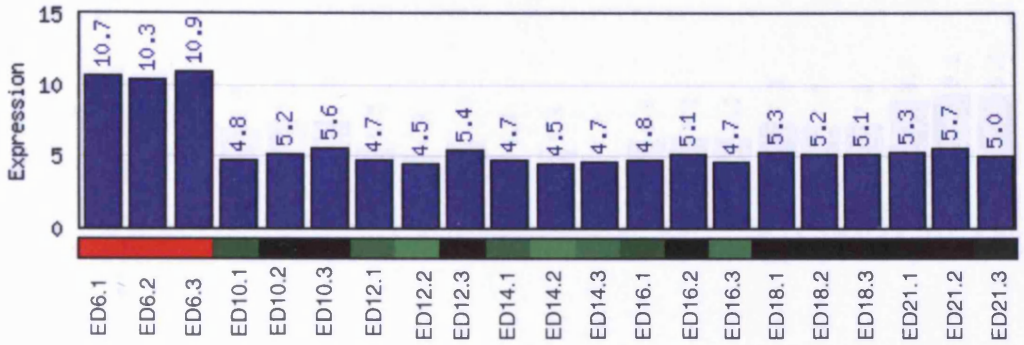

b) *Sh3bgr* RT-qPCR

Figure 6.10 Microarray **(a)** and real-time RT-PCR **(b)** of *Sh3bgr* expression profile. RT-qPCR confirmed down-regulation of the transcript throughout development. Blue bars represent levels of expression obtained from normalised RMA data, colour rank of heatmap underneath graph refers to relative changes in expression, with red being characteristic of gene upregulation and green for downregulation.

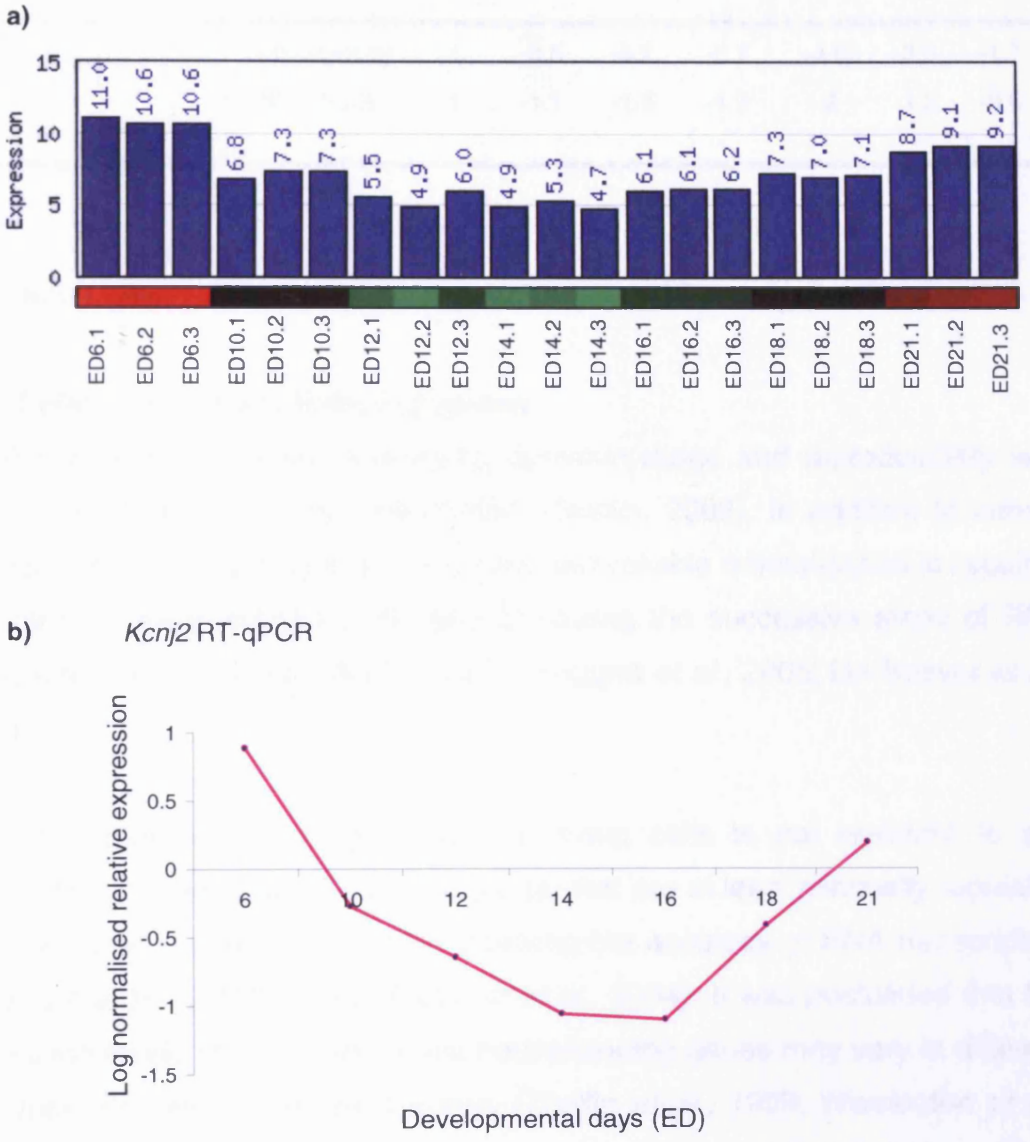

Figure 6.11 Microarray **(a)** and real-time RT-PCR **(b)** of *Kcnj2* expression profile. RT-qPCR confirmed downregulation of the transcript throughout development. Blue bars represent levels of expression obtained from normalised RMA data, colour rank of heatmap underneath graph refers to relative changes in expression, with red being characteristic of gene upregulation and green for downregulation.

Table 6.11 Fold changes in abundance of *Kcnj2* transcript between developmental time points

Symbol	Functional group	Fold change EDs	6	10	12	14	16	18	21
Kcnj2	Potassium ion transport	Microarray	1	-3.5	-5.2	-5.7	-4.5	-3.5	-1.7
		RT-qPCR	1	-1.1	-1.5	-1.9	-2	-1.2	-0.6

6.7 Discussion

6.7.1 Selection of housekeeping genes

qPCR combines accuracy, sensitivity, dynamic range and reproducibility with speed and potential for high throughput (Bustin, 2002). In addition to careful reaction setup and optimisation, accurate and reliable normalisation is required to control for experimental error induced during the successive steps of RNA extraction and processing (Bustin, 2002; Huggett *et al.*, 2005; De Boever *et al.*, 2008).

Since the transcription of any gene in living cells is not resistant to cell fluctuations, it is important to identify genes that are at least minimally regulated and may serve as reference genes allowing the accuracy of RNA transcription analysis that RT-qPCR offers (Radonic *et al.*, 2004). It was postulated that the expression levels of commonly used housekeeping genes may vary in different cell types, tissues and disease states (Thellin *et al.*, 1999; Warrington *et al.*, 2000, Bustin, 2000, Ishii *et al.*, 2006). It also has been reported that some of the housekeeping genes with assumed stable expression can exhibit either up- or downregulation under some experimental conditions (Foss *et al.*, 1998; Schmittgen and Zakrajsek, 2000). Because, the result of qPCR experiment is expressed as a target/reference ratio, thus, it is important that the expression level of housekeeping genes remains constant under different experimental conditions (Ishii *et al.*, 2006).

The possibility of large variability (biological or experimentally induced) may lead to large errors, and needs to be taken into account particularly in the developmental experiments. Normalisation by multiple control genes instead of a single gene is recommended to measure expression levels accurately (De Boever *et al.*, 2008). The validity of the approach is related to the number of samples and candidates analysed, i.e. the more samples and candidates, the better estimates (Andersen *et al.,* 2004). The sample set should contain at least 6 samples per group and the number of candidates should be at least 3 for technical reasons. Validation of housekeeping genes is highly specific for a particular experimental model and is crucial in assessing a new model (Dheda *et al.*, 2004; De Boever *et al.*, 2008).

Two out of four candidate reference genes; GAPDH and β-Actin had been previously used in various gene expression studies. In chickens, the β-Actin gene (encoding for cytoskeletal protein) was commonly used as an internal control for normalisation in several experimental designs. In our studies it was observed that β-Actin was the least stable throughout development. Pairwise comparisons also excluded GAPDH as a housekeeping gene in time course experiment, although, it was demonstrated to be most stable analysis when used as a single reference gene. These findings are consistent with a number of studies which reported that GAPDH and β-Actin genes, and alternatives (18S and 28S rRNA genes), are unsuitable references, because their transcription is significantly regulated in various experimental settings and variable in different tissues, as well as between individuals and between samples from the same individual (Selvey *et al.*, 2001; Goidin *et al.*, 2001; Glare *et al.*, 2002; Radonic *et al.*, 2004).

In this study G6PDH and UB were shown to be the most stable genes in pairwise comparison, which was confirmed by three independent software packages. These genes also appear to be stable in chickens after virus infection (Xing and Schat, 2000; Hong *et al.*, 2006; Li *et al.*, 2007; De Boever *et al.*, 2008). Li and coauthors (2007) tested the stability of 28 cellular genes in chicken embryo cell cultures. In their experimental setup, the expression of

G6PDH and UB also proved to be stable. In addition, proteins of the selected genes belong to different functional classes, thus reducing the chance of their coregulation.

6.7.2 Validation of differentially expressed genes by RT-qPCR

The differences in gene expression found by microarray analyses were validated by using quantitative RT-PCR. The selected genes of interest, used to carry out this validation were *Aqp3, Psca, Atoh7, H2afy2. Sfrp2, Sh3bgr* and *Kcnj2.*

In this study, all genes showed a differential expression of at least 1.6 fold in at least one time point, which is a major criterion for the selection of genes in order to validate time course microarray experiment (Wurmbach *et al.*, 2003; Ryan *et al.*, 2005, Morey *et al.*, 2006). Although, variation concerning the degree of regulation was observed, the data obtained with microarray analysis were substantially confirmed for all genes of interest by RT-qPCR.

Several studies attempted to determine factors which contribute to the variation in results obtained by microarray versus qPCR (Rajeevan *et al.*, 2001; Etienne *et al.*, 2004; Wurmbach *et al.* 2003; Beckman *et al.*, 2004; Morey *et al.*, 2006). Lower correlations were reported for genes exhibiting small degrees of change (less than 2-fold), as compared to those showing greater than 2-fold change. Differences in calculated fold changes between microarray and RT-qPCR data may result from various sources of pitfalls in long methodologies; these include different efficiencies of reverse transcriptase used in both qPCR and RNA amplification procedures for microarray labelling (Freeman *et al.*, 1999).

Previous reports showed that, the effects of dye biases, non-specific and/or cross hybridisations of labelled targets to array probes, may have an impact on microarray procedures (Freeman *et al.*, 1999; Yang *et al.*, 2002). In addition, potential sources of error in qPCR include, among others, amplification biases, mispriming or the formation of primer dimers, and the changing efficiency of qPCR at later cycles, finally, analysis of images (Chuaqui *et al.*, 2002; Bustin, 2002; Freeman *et al.*, 1999).

Although the selection and application of normalisation criteria was performed with care, it must be mentioned that normalisation procedures differ between microarray and qPCR analysis; the former requires global normalisation, while the latter generally utilizes the expression of one or more reference genes against which all other gene expression is calibrated (Morey *et al.*, 2006).

6.7.3 Selected genes and their potential roles in corneal development

Upregulated genes

Upregulation of two out of seven genes of interest was demonstrated; included *Aqp3* and *Psca*. *Aqp3* gene coding for member of the homologous water channels protein family. A product of *Aqp3* gene is expressed in many cell types in the eye, where its primary function is to facilitate transmembrane flow of solute-free water in response to osmotic gradients (Verkman, 2003; Verkman *et al.*, 2008). The expression of water and glycerol-transporting aquaglyceroporin Aqp3 was demonstrated in stratified corneal epithelia of mouse, rat, and human (Patil *et al.*, 1997; Hamann *et al.*, 1998; Levin and Verkman, 2004). Recently, Aqp3-dependent cell migration was shown to be involved in epithelial cell proliferation indicating a potential role in corneal epithelial wound healing (Levin and Verkman, 2006). The proposed mechanism of Aqp3-facilitated cell proliferation in epidermis involved increase of cellular glycerol metabolism and biosynthesis, therefore increased ATP content and altered MAP kinase signalling (Verkman *et al.*, 2008; Hara-Chikuma and Verkman, 2008). Its role in similar mechanisms within corneal epithelium requires further investigation.

It is likely, that the increase in levels of *Aqp3* gene expression in development of the chick corneal epithelium is associated with structural and functional changes in cornea. As shown by microarrays and RT-qPCR, the level of *Aqp3* expression gradually increased from ED6 to ED14, and then plateaued. Changes in Aqp3 expression pattern in mid time points coincide with dehydration of secondary stroma and beginning of epithelial stratification, which were postulated to begin around ED12 (Hay, 1979). The role of Aquaporins in maintenance of corneal stromal transparency was studied and their involvement in stromal dehydration processes has been suggested

(Thiagarajah and Verkman, 2002; Verkman *et al.*, 2008). Recent studies by Swamynathan and coauthors (2008) demonstrated that the Aqp3 promoter is regulated by Klf4 (Krüppel-like factor 4) which plays a crucial role in the development and maintenance of the mouse cornea. *Aqp3*, as a potential member of genetic network regulating embryonic morphogenesis and maturation, may be a regulating factor in maintenance in chick corneal epithelial homeostasis. However, further study needs be undertaken to confirm this.

Psca also appeared to be upregulated in corneal epithelia development. *Psca* was expressed at the lowest level at ED6, with 1.7 fold change expression relative ED10, as shown by RT-qPCR. The increase in expression level of *Psca* transcripts coincides with the beginning of epithelial stratification during chick corneal development. *Psca* is so-named for its strong homology to the thymocyte marker stem cell antigen 2 (*LOC420301*) and is a member of the Thy-1/Ly-6 family of glycosylphosphatidylinositol (GPI)-anchored cell surface antigens (Reiter *et al.*, 1998). Both *LOC420301* and *Ly6y* (paralog for Psca) were identified in this studies by RMA (see Chapter 6). *In situ* hybridisation analysis localised *Psca* expression in normal prostate, with predominant restriction to a subset of basal cell epithelium, the putative stem cell compartment of the prostate (Reiter *et al.*, 1998). A murine homologue of *Psca* shows a similar pattern of expression (Dubey *et al.*, 2001). Psca was suggested to be a unique marker of an intermediate subpopulation of prostate epithelial cells in transition from a basal to terminally differentiated secretory phenotype (Tran *et al.*, 2002). To date, one study has reported *Psca* expression in *Gallus Gallus*, in the shell gland of both juvenile and laying hens (Dunn *et al.*, 2009). However, to the best of our knowledge, this thesis is the first to report *Psca* expression in the corneal epithelium.

Downregulated genes

Four out of seven genes used in RT-qPCR analysis were downregulated during chick corneal epithelial development. *Atoh7* gene expression in the chicken corneal epithelium was shown to be highest at ED6. When other time points were compared to ED6, *Atoh7* exhibited greater than 2 and 3 fold change in relative expression by RT-qPCR and microarray, respectively.

Atoh7, also known as *Math5/Ath5* (mouse), or *Ath5/Cath5* (chicken) is a transcription factor involved in the differentiation of retinal ganglion cells. *Atoh7* was shown to be crucial for cell cycle progression and differentiation of embryonic retinal progenitor cells from several species (*i.e.* mouse, frog, zebrafish and chicken) (Le *et al.*, 2006; Kanekar *et al.*, 1997; Kay *et al.*, 2001; Liu e*t al.*, 2001). *In situ* hybridisation studies in developing chicken retina (from ED2 to ED18) demonstrated that the intense expression of *Atoh7* continues until ED9.5, and thereafter appears to be downregulated (Liu *et al.*, 2001). The dynamic pattern of *Atoh7* expression was correlated with the genesis of ganglion cells, which were previously shown to exit cell cycle between ED2 and ED9 during chick retinogenesis (Liu *et al.*, 2001; Prada *et al.*, 1991). Although, it is postulated that activation of *Atoh7* is a key initiating event in the mammalian eye, the regulation of this process has not been well characterised (Riesenberg *et al.*, 2009).

H2afy2 in the developing chick corneal epithelium was also confirmed by RT-qPCR. From ED6 to hatching a decrease in H2afy2 relative expression by more than 2.5-fold was indicated. The expression pattern was similarly demonstrated by microarray data, however, the fold change difference was higher (discussed above). *macroH2a* is a conserved family of replication-dependant core histone proteins with expression restricted to the S phase of cell cycle (Costanzi and Pehrson, 2001; Chadwick and Willard, 2001). *H2afy2,* a subtype of *macroH2a,* is non-allelic gene located on human chromosome 10 or chicken chromosome 6. In mouse the H2afy2 protein is concentrated in the inactive X chromosome suggestive that *H2afy2* is involved in establishing and/or maintaining transcriptionally silent chromatin domains (Costanzi and Pehrson, 1998, 2001). Accessibility of DNA sequences for transcription regulatory factors depends on chromatin state, which is regulated, among others, by histone variants and covalent modifications of histones (i.e. phosphorylation, acetylation, methylation) throughout the cell cycle (Van Leeuven and Gottschling, 2003; Cheung *et al.*, 2000; Roloff and Nuber, 2005). Several studies have linked histone modification phenomenon with undifferentiated stem or progenitor cells and their differentiated progeny (Fajas *et al.*, 2002; Lee *et al.*, 2004b, Milhem *et al.,* 2004). Combination of certain histone variants and their dynamic

interactions with chromatin-associated proteins may play important role in gene expression patterns associated with maintenance of embryonic stem (ES) cell line pluripotency and during cell differentiation (Shukla *et al.,* 2008, Roloff and Nuber, 2005). For instance, *H2a.z* (a subtype of H2a2 gene), which in human shows 56% identity in amino acid sequence to H2afy2 protein, is highly expressed in embryonic stem cells, with much lower expression in differentiated cells (Hatch and Bonner, 1996).

Sfrp2, also known as Secreted apoptosis-related protein 1, as shown by both microarray and RT-qPCR was downregulated from ED14. This gene encodes a member of the SFRP family that contains a cysteine-rich domain homologous to the putative Wnt-binding site of Frizzled proteins and acts as an antagonist of Wnt signalling (Rattner *et al.*, 1997, Ladher *et al.*, 2000). The Wnt genes have a number of different roles during development varying from controlling patterning to proliferation, cell adhesion and differentiation (Wodarz and Nusse, 1998). Studies in chicken embryo suggested that *Sfrp2* may play an active role in embryogenesis, especially in development of the neural system, eyes, muscles and limbs (Terry *et al.*, 2000, Lin *et al.*, 2007). Previous studies have identified *Sfrp2* expression at stages 4 (18-19 hours) to 32 (ED7.5) in chick mesodermal and ectodermal derivatives (Terry *et al.*, 2000). As shown by Lin and coauthors (2007), the developing chick eye contains an intracellular distribution of *Sfrp2* in the pigmented layer of the retina and photoreceptors until ED10. However, *Sfrp2* expression in developing chick corneal epithelium has not been reported previously.

Sh3bgr downregulation occured over the time course of chick cornel epithelial development as confirmed by microarray data analysis and RT-qPCR. However, expression fold changes differed with a greater than 5 fold change beginning in early developmental stages following microarray data analysis and a 2 fold difference by RT-qPCR. In the latter, downregulation of Sh3bgr appeared later, from ED14 onwards. The *Sh3bgr* gene is differentially expressed in heart and skeletal muscle and was cloned in an effort to identify genes mapping to human chromosome 21 (chicken chromosome 1), which could be involved in pathogenesis of congenital heart disease associated with

Down syndrome (Scartezzini *et al.*, 1997; Mazzocco *et al.*, 2002). *Sh3bgr* encodes for a protein with proline-rich middle region containing a Sh3 binding motif and a proline-rich peptide sequences, which were shown to be relevant for protein interactions involved in signal transduction pathways (Scartezzini *et al.*, 1997; Egeo *et al.*, 1998). So far, the expression and role of *Sh3bgr* has not been reported in the eye and biological functions of this gene need to be elucidated further.

Kcnj2, also known as *Kir2.1* and *Hhbirk1,* was shown to be downregulated in the developing chick corneal epithelium from ED6 to ED16, and then upregulated from ED16 to posthatch. *Kcnj2* is a member of Kir2 gene family and encodes for integral membrane protein (inward-rectifier type potassium channel protein) (Doupnik *et al.*, 1995). Inwardly rectifying potassium channels play a key role in stabilising the resting membrane potential in both excitable and non-excitable cells (Giovannardi *et al.,* 2002). *Kcnj2*, originally cloned by Kubo and co-authors (1993) from a mouse macrophage cell line, was shown to be highly expressed in mouse forebrain, heart ventricle, and skeletal muscle in mouse and chicken (Morishige *et al.*, 1933; Ishihara and Hiraoka, 1994; Navaratnam *et al.*, 1995). Ras and MAP kinase pathways, which play a pivotal role in cell proliferation, survival, and differentiation, were demonstrated to modulate inward rectifying potassium current by reducing the cell surface channel availability (Giovannardi *et al.*, 2002; Fakler *et al.*, 1994). Modulation of electrophysiological response may represent one of the events that control the electrical activity of the cell, a mechanism likely to be important for the cell fate determination (cell assignment for either proliferation or differentiation) (Giovannardi *et al.*, 2002; Johns *et al.*, 1999; Bianchi *et al.*, 1998). Recently, *Kcnj2* was demonstrated to be involved in differentiation of myoblasts (Hinard *et al.*, 2008). The earliest event in this process requires hyperpolarisation, which occurs via an increased activity of *Kcnj2* K^+ channels due to dephosphotylation of tyrosine (Liu *et al.*, 1998; Fischer-Lougheed *et al.*, 2001; Hinard *et al.*, 2008). In proliferating myoblast *Kcnj2* channels were found to be localised at the cell surface in silent state (Hinard *et al.*, 2008).

Ion channels play central roles in maintaining electrophysiological stabilisation and fluid balance in order to dehydrate the cornea and to prevent corneal swelling (Lu, 2006). Recent reports demonstrated that of K^+ channels activity is linked to proliferation and activation of stress-related signalling pathways in corneal epithelium (Lu, 2006; Wang *et al.*, 2003; Roderick *et al.*, 2003). Changes in K^+ channel activity in corneal epithelial cells and other cell types can be modulated by a variety of growth factors (i.e. EGF, NGF), and cytokines (*i.e.* TNFα), and when affected in short term, may play the major role in regulation of proliferation and apoptosis (Lu, 2006; Minami *et al.*, 2002). For instance, as suggested by Lu (2006), TNFα-induced stimulation of K^+ channel is required for NfκB nuclear translocation and DNA binding activity, which in turn promotes cell survival.

6.8 Conclusions

The objective of RT-qPCR studies described in this chapter was to confirm the array sensitivity. There was a general conformity between the microarray and RT-qPCR results, indicating that the microarray results demonstrated the extent of changes in gene expression. The analysis of gene expression using high density oligonucleotide arrays and performing RMA analysis delivered genes of interest that reflected true differences in gene expression levels throughout development of chick corneal epithelium.

Further studies to evaluate gene distribution and protein expression are required to determine the role of these selected genes in corneal epithelial development and homeostasis. These will include immunohistochemical localisation of proteins and the spatial localisation and distribution of mRNA transcripts using *in situ* hybridisation.

CHAPTER SEVEN

General discussion and future work

7.1 General Discussion

The overall aim of this study was to determine factors and mechanisms that underlie the regulation of epithelial patterning and homeostasis during corneal development. This was achieved firstly by examination of spatiotemporal changes in morphology, cell differentiation, proliferation and apoptosis of the developing chick corneal epithelium using histological staining, immunohistochemistry and cytochemical techniques, and secondly by an investigation of the gene expression profiles by microarray. For the purpose of this study, chicken corneas were used, which provided an excellent model due to the ease of eye collection, short time of embryonic development and similarity to human corneal epithelium.

Embryonic corneas from early stages of development ED4 (HH28-29) to ED18 (HH44) and lastly corneas of chicks <12 hours after hatching (labelled as ED21 throughout the thesis) were isolated and processed for the studies mentioned above. Procedures for Haematoxylin and Eosin staining were optimised in order to evaluate changes in the overall morphology, in particular cell shape, cell size and the number of epithelial cell layers. Epithelial differentiation patterns were identified in frozen sections of chicken corneas after immunolocalisation of pan-CK (acidic: 10, 13, 14, 15, 16, 19 and basic: 1, 2, 3, 4, 5, 6, 7) and CK3 (Chapter 3). PCNA and caspase 3 (active) immunolocalisation studies, as well as, TUNEL-labelling were performed to assess temporal and spatial localisation of cell proliferation and death in the developing corneal epithelium (Chapter 4). The expression of PCNA and CK3 were later confirmed by immunoblotting.

Subsequently, techniques to isolate corneal epithelia at different developmental time points, in a manner that would not compromise the quality of RNA were optimised and developed. RNA samples of high purity and integrity, were amplified, labelled and hybridised to high density oligonucleotide arrays. All experimental steps were monitored, using a number of validation processes, to ensure accurate microarray data for gene expression analysis. The performance of microarrays and appropriate mathematical methods, such as Robust Multiarray Avarage and Limma provided a vast amount of data. To reduce the complexity of these results, and reveal biological implications of

gene profiles in the developing corneal epithelium, data were further analysed using probabilistic clustering according to gene ontology and principal component analysis (Chapter 5). The sensitivity of arrays in producing data trends was validated in a small number of selected genes by quantitative RT-PCR (Chapter 6).

A summary of the results of this thesis, determined following morphological, immunohistochemical and cytochemical examination of the developing chick corneal epithelium, as well as, from microarray studies is provided below. The following discussion offers general observations as to the importance of differentially expressed genes and gene families identified in this study and underlines their potential role in the regulation of corneal epithelial homeostasis during development and following hatching.

7.2 Evaluation of changes in morphology, differentiation, proliferation and cell death during chick corneal epithelial development

Results demonstrating changes in epithelial cell morphology, differentiation, proliferation and cell death during chick corneal development, described in Chapters 3 and 4, are summarised below and presented in Table 7.1.

Corneal epithelial morphogenesis is a dynamic process involving the formation of new layers and horizontal expansion in the developing eye. Highlights of corneal epithelial development include stratification; an increase in the number of cell layers, change in cell morphology, and terminal differentiation of newly formed cells. The chick fetal corneal epithelium is derived from a single layer of ectoderm overlying the lens vesicle. In this study it was demonstrated that after becoming two layered by ED4, the epithelium underwent further stratification to form intermediate cell layers at about ED14. As demonstrated, these changes are accompanied by changes in cell shape commencing at ED10. This was in agreement with earlier studies of Hay and Revel (1969), which revealed that the early developed epithelium was two cells thick with basal cuboidal cells and became three-layered between ED10 and ED14.

Table 7.1 Summary of the findings of histological, immunohistochemical and cytochemical studies

	ED4			ED6			ED8			ED10			ED12			ED14			ED16			ED18			ED21		
	L	P	C	L	P	C	L	P	C	L	P	C	L	P	C	L	P	C	L	P	C	L	P	C	L	P	C
Histological observation																											
Stratification:																											
No. of cell layers	2	2	2	2	2	2	2	2	2	3	2	2	3	3	3	4	3	3	5	4	5	6	5	5	7	6	6
basal-ovoid	+	+	+	+	+	+	+	+	+		+	+		+	+												
basal-columnar										+			+			+	+	+	+	+	+	+	+	+	+	+	+
wing-like										±	±	±	+	+	+	+	+	+	+	+	+	+	+	+	+	+	+
no. of layers													1	1	1	2	1	1	3	2	3	4	3	3	5	4	4
superficial-not flat	+	+	+	+	+	+	+	+	+																		
superficial-flattened										+	+	+	+	+	+	+	+	+	+	+	+	+	+	+	+	+	+
Immunolocalisation studies																											
Epithelial differentiation:																											
Pan-CK basal														+	+		+	+		+	+	+	+	+	+	+	+
suprabasal															+	+	+	+	+	+	+	+	+	+	+	+	+
superficial										+	+	+	+	+	+	+	+	+	+	+	+	+	+	+	+	+	+
CK3 basal															+		+	+		+	+		+	+		+	+
suprabasal															+		+	+	+	+	+	+	+	+	+	+	+
superficial													+	+	+	+	+	+	+	+	+	+	+	+	+	+	+
Proliferation:																											
PCNA basal	+	+	+	+	+	+	+	+	+	+	+	+	+	+	+	+	+	+	+	+	+	±	±	±	±	±	±
suprabasal	+	+	+	+	+	+	+	+	+	+	+	+	+	+	+	+	+	+	+	+	+	+	+	+	±	+	+
superficial	+	+	+	+	+	+	+	+	+	+	+	+	+	+	+	+	+	+	±	+	+	±	±	±	±	±	±
Cell death:																											
Caspase 3 basal																											
suprabasal																			+								+
superficial																											
Cytochemical analysis of cell death																											
TUNEL basal													+		+	+			+			+			+		+
suprabasal													+		+	+			+			+			+		+
superficial										+																	

Legend: L: limbus, P: periphery, C: centre; +: present, ±: sparsely present, **+**: greater activity, +: peak activity, blank: absent

Survival, proliferation and differentiation of an epithelium, depends on a complex system of interactions between its cells, the external environment and the underlying mesenychme (Revoltella *et al.*, 2006). The newly formed epithelium is a subject to intense proliferation and expansion of existing cells. PCNA immunolocalisation studies suggested that after the formation of the corneal epithelium (at ED4), cell mitosis is involved in morphogenesis, whereas in later development its decrease might be associated with ongoing tissue differentiation. Cell proliferation appeared high throughout corneal development, with peak proliferation between ED12 (limbal epithelium: 74.4±5.5%, periphery: 80.8±6.1% and centre: 78.3±5.5%) and ED14 (79.4±4.4, 86.5±6.8%, 82.7±3.5% in the limbal, peripheral and central epithelium, respectively), thereafter the level of proliferation decreased. The above coincided with changes in epithelial morphology (stratification) and changes in expression of epithelial markers (described below). It is likely that by ED14 cells divide rapidly to increase the population of epithelial cells. Some of those cells differentiate and are designated for stratification before the epithelium is fully formed. Once the epithelium is fully formed and stratified, less cells divide, and the newly developed epithelium undergoes maturation. While the level of proliferation decreased throughout the corneal epithelium from ED16 onwards, more apoptotic events were observed in neonate epithelia, suggesting that proliferation and apoptosis play a regulatory role in maintaining homeostasis during development.

Earlier studies conducted by Nuttall (1976) established the distribution of dividing cells during epithelial stratification in the avian cornea using electron microscopy. Study revealed that at about day 9 of incubation 70% of mitotic spindles in the basal layer were oriented parallel to the basement membrane, whereas, in mid-developmental time points (ED12-ED16) the mitotic spindles change orientation to vertical (with 80% of basal cells showing this characteristic). Once the epithelium is fully stratified, the high level of perpendicularly orientated mitotic spindles falls off and mitosis was rarely observed in the flattened superficial layers of the corneal epithelium (Nuttall, 1976; Hay, 1979). It was therefore postulated that the changing orientation of

the spindles may initiate stratification, but stratification was not considered to result from an increase in local cell division.

It is still unknown when exactly the cell commitment to a given line in differentiation takes place in corneal development. The hypothesis of early differentiation of corneal epithelial cells was first put forward by Coulombre and Coulombre (1971). The experiments, based on the replacement of a developing chick lens with mesenchymal graft *in vivo* and *in vitro* led to the conclusion that the avian epithelium at day 5 of incubation was capable of transformation into epidermis, suggesting that inductive signals (from surrounding tissues and/or ECM) reach the corneal epithelium earlier than the 5th day of development.

The appearance of desmosmes and tonofilaments following stratification may suggested ongoing differentiation of corneal epithelia (Hay and Revel, 1969). A presence of tonofilaments, keratin intermediate filaments that constitute cytoplasmic protein structures (tonofibrils), in the cytoskeleton is considered a hallmark of differentiated epithelia. A pattern of expression of cytokeratins of epithelial cells provides a simple and reliable method for determination of epithelial differentiation state (Wolosin *et al.*, 2000). The present study used the advantage of the co-expression of different cytokeratins and CK3 as differentiation markers signifying the commitment of corneal-type epithelial cells. The appearance of pan-CK labelling was first observed at ED10 and the presence of CK3 immunolabelling appeared in epithelial cells at ED12. However, low levels of CK3 protein expression were noted at ED10 by immunoblotting. The results indicated that during chick corneal development, the ED10 and ED12 appeared to be critical for the onset of epithelial differentiation during corneal development.

Identified differences in staining pattern between pan-CK and CK3 at ED12; pan-CK-positive cells in basal layer of peripheral epithelium, and lack of such labelling for CK3; suggested that differentiation may vary (suprabasal versus uniform) in different parts of the cornea and is most advanced in the central corneal epithelium. In later developmental time points, immunolabelling showed similar characteristics for both pan-CK and CK3, with positive cells present

throughout the thickness of central and peripheral epithelium, and restriction to suprabasal layer in the limbal region.

Similar labelling patterns have been observed in the zebrafish (Zhao *et al.*, 2006) and rabbit corneas (Schermer *et al.*, 1986; Chaloin-Dufau *et al.*, 1990). In the developing human corneal epithelium, CK3 was firstly detected at the 12-13th week of gestation, with superficial cells positively labeled (Rodrigues *et al,* 1987). By the time the epithelium was morphologically matured (four to six layers at 36 weeks). CK3 was expressed suprabasally, in contrast to adult epithelium which exhibited uniform staining.

The terminal differentiation process of keratocytes in human epidermis was suggested to utilise members of the apoptotic pathway and the fragmented DNA, as seen during classical apoptosis, and the activation of caspase 3 have both been demonstrated in differentiating keratinocytes (Polakowska *et al.*, 1994; Weil *et al.*, 1999). This supported an idea of apoptosis being a specialised form of terminal differentiation in epidermal keratinocytes, which in the final stage leads to tissue keratinisation (Yamanishi *et al.*, 2005). Since, corneal epithelium is stratified, non-keratinising tissue, the role of apoptosis in process of differentiation is not clear, however, apoptosis signalling might also have a more direct role in differentiation independent of apoptosis itself.

In this study, TUNEL-labelling demonstrated the presence of positive cells mostly in the limbal region of the corneal epithelium, in the mid and later developmental stages. However, immunolocalisation of the active form of caspase 3 revealed a lack of labelling in all regions investigated, with the exception of the limbal epithelium at ED16 and the central epithelium at ED18. Thus, it appeared that apoptosis in the developing chick corneal epithelium plays a minor role, which is in agreement with studies of cell death in developing human corneal epithelium (Yew *et al.*, 2001), in which TUNEL-labelled cells were first observed postnatally.

It has been postulated that apoptosis shares a molecular pathway with the normal cell cycle and as such is regulated by the same molecular mechanism

that control cell growth and proliferation and is sensitive to the same environmental factors in tissues of ectodermal origin (Haake and Polakowska, 1993; Sen, 1992). A number of protooncogenes/anti-oncogenes (e.g. *p53, c-Myc*), growth factors (e.g. TGFβ, retinoic acid) and hormones, which initiate or suppress the self destruction program under experimental conditions, are known to affect cell proliferation (Haake and Polakowska, 1993; Lane, 1992; Evans *et al.*, 1995). In the presence of survival factors (cytokines), a normal cell could proliferate and in the absence the cell would either differentiate or turn on the death pathway (Haake and Polakowska, 1993). Extracellular inducers, such as Ca^{2+} ionophores, EGF, TNFα are also known to trigger either cell death or division, dependent on activation of appropriate second signals that execute further cell response (McConkey *et al.*, 1990; Lu *et al.*, 2001).

The patterns of cell proliferation and differentiation showed changes during the development of the corneal epithelium. These changes reflect the interaction of a complex network of mitogenic, apoptotic and differentiation agents, many of which remain to be identified.

7.3 Regulatory mechanisms of epithelial cell patterning during corneal development and their implications

The aim of the microarray time course experiment was to identify gene families and their members likely to be relevant in the regulation of homeostasis during corneal epithelial development. Additionally, the study demonstrated differentially expressed genes that reveal changes in biological processes due to the change in time, which is essential to understand differences in the dynamics during development.

Functional studies in developing organs and cell lines of different species, have shown that Wnt/β-catenin, Nfκβ, Notch, Shh and TGF-b/BMP pathway signalling are crucial in the control of several cellular processes, including proliferation, cell transformation/fate and cell adhesion (Fig. 7.1). Mutual regulations between different signalling pathways and their ligands are important both during early development and in adult tissues (Guo and Wang, 2009). The above mechanisms were also extensively studied in order to understand their roles in the niche control of different types of stem cells, which are crucial in the genesis and maintenance of adult tissue (Li and Xie, 2005).

The microarrays provided a vast amount of data and revealed genes that participated in different regulatory pathways and are likely to be crucial in the regulation of biological processes throughout development and/or in life following hatching. Some of the genes are of particular interest and might be proposed as critical for maintenance of epithelial homeostasis. These putative genes involved in epithelial cell patterning during corneal development are described below and presented in diagram (Fig. 7.2).

7.3.1 *H2Afy2* in chromatin remodelling and switching between active and inactive gene programs

Expression of H2afy2 gene was downregulated throughout development of the corneal epithelium, with the lowest level of expression observed posthatching.

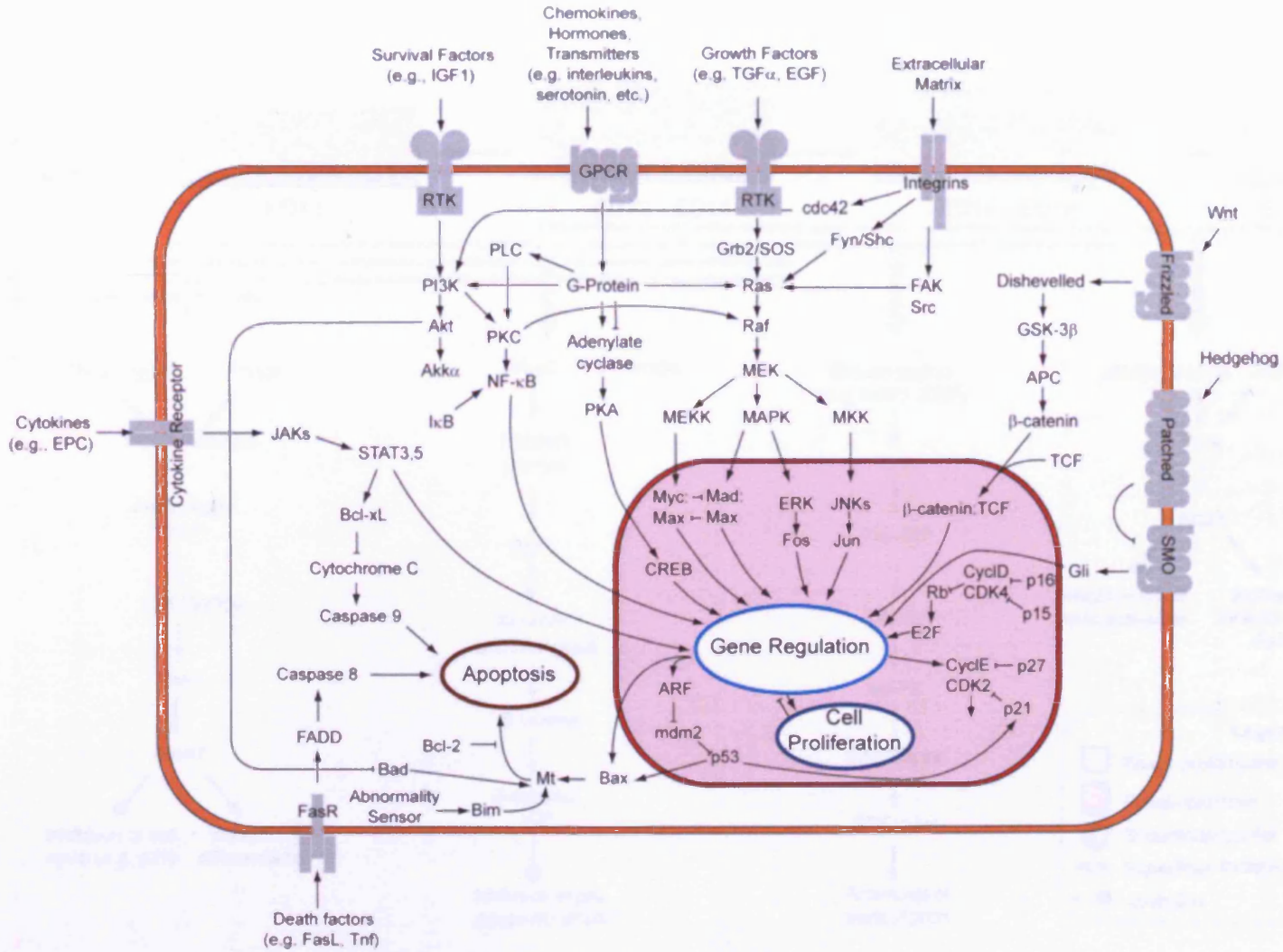

Figure 7.1 Overview of general interaction between different signal transduction pathways crucial in control of several cellular processes, including proliferation, cell transformation/fate and cell death (adapted from Lodish, 2003).

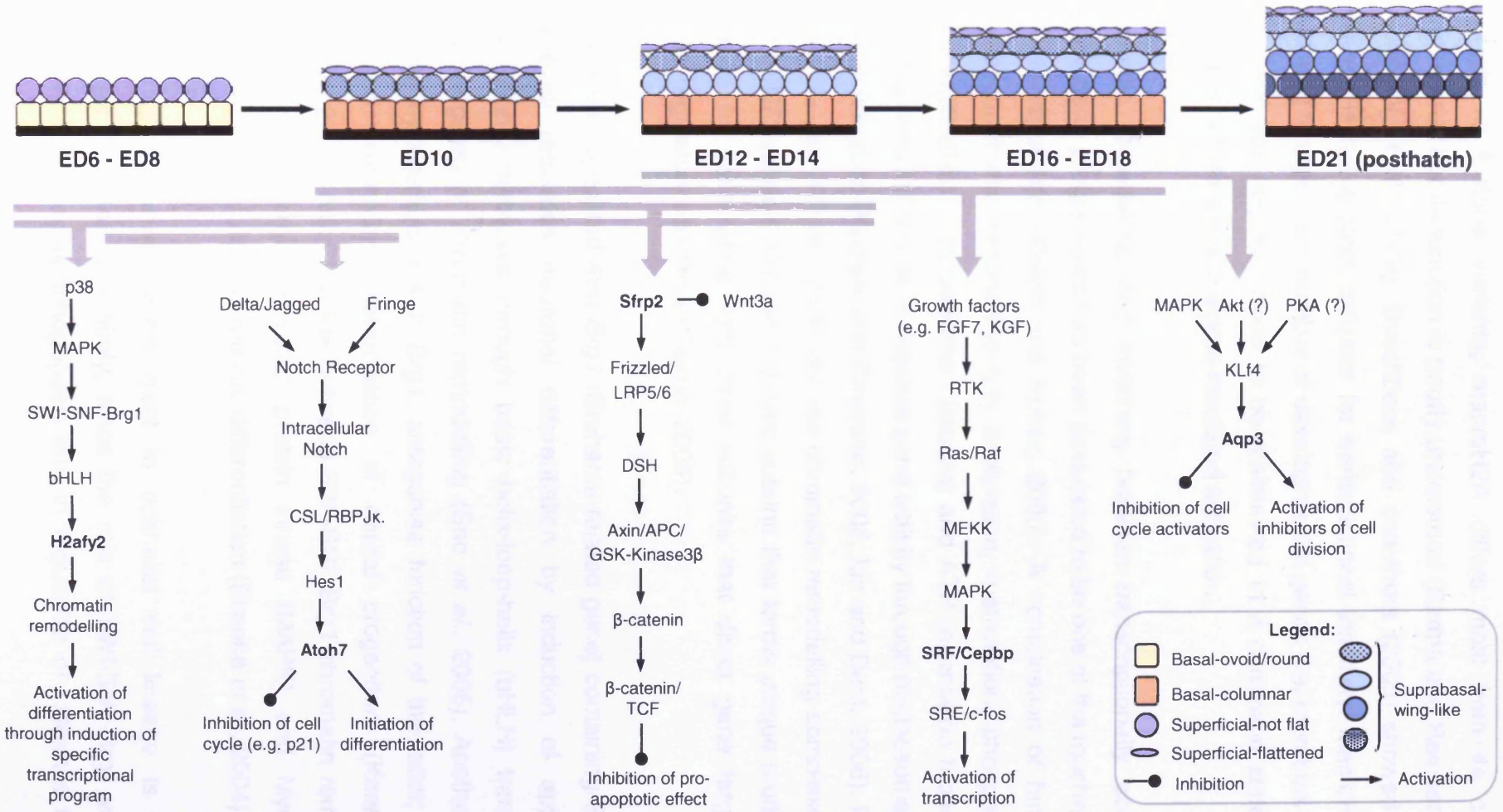

Figure 7.2 Putative molecular mechanisms for corneal epithelial differentiation, stratification, survival during development. Several genes of interest (*H2afy2, Atoh7, Sfrp2, Cebpb, Aqp3*) identified in microarray study, confirmed by RT-qPCR and involved in regulation of corneal epithelial homeostasis during development are presented in context of signalling pathways they are likely to participate in. Grey lines indicate time points in which the expression of gene was the highest.

Amongst all histone variants, macroH2A differs most from its canonical counterparts, but its function is poorly understood (Sarma and Reinberg, 2005; Buschbeck *et al.*, 2009). Buschbeck and coauthors (2009) showed that its presence is not a strict indicator for transcriptional inactivity. MacroH2A was postulated to regulate a number of developmental genes (i.e. members of HOX, DLX, LHX families) that need to be maintained in a chromatin state that is repressed but sensitive to signal-mediated activation.

Chromatin remodelling and switching between transcriptionally active and inactive gene programmes has been postulated to be one of the mechanisms of cell fate regulation (Roloff and Nuber, 2005). A combination of functionally diverse chromatin remodelling (i.e. acetylation, methylation, phosphorylation and ubiquitination of nucleosmal histones) and ATP (adenosine triphosphate) modifying complexes acts to regulate gene activity through nucleosome mobility and specialisation (Kaeser and Emerson, 2006; Lin and Dent, 2006). Identified distinct classes of functionally diverse chromatin-remodelling complexes share a SWI-SNF2-related ATPase catalytic subunit that forms unique multi-subunit enzymes by associating with other subunits that direct gene targeting or specific regulatory functions (Cairns, 2005).

It has been suggested that *Brg1* (Brahama-related gene) containing SWI-SNF complexes regulates neuronal differentiation by induction of appropriate transcriptional pathways through basic helix-loop-helix (bHLH) transcription factors targeted at chromatin remodelling (Seo *et al.*, 2005). Another factor, *Geminin*, by interaction with *Brg1*, antagonise function of the latter, thereby preventing premature differentiation of neural progenitors (Kaeser and Emerson, 2006). Also, the link between SWI-SNF-Brg1 chromatin remodelling complex, p38 mitogen-activated protein kinase (MAPK) and MyoD was revealed in study of skeletal muscle differentiation (Simone *et al.*, 2004).

Whether similar mechanisms exist in epithelial cell lineage is not yet determined, however it is likely, since the role of SWI-SNF-Brg1 was also demonstrated during lymphogenesis and in regulation of response to niche

BMP signals that control the self-renewal of different stem cell types (Chi *et al.*, 2002; Xi and Xie, 2005).

7.3.2 Role of *Atoh7* in cell cycle progression and differentiation

Atonal homolog 7 (Drosophila) (*Atoh7*) gene expression in the chicken corneal epithelium was shown to be highest at ED6, thereafter expression was downregulated and remained on constant level.

As described in section 7.7.2, Atoh7 was previously recognised as a transcription factor involved in the differentiation of retinal ganglion cells. *Atoh7* was postulated to be one of the first genes of bHLH transcription regulators, targeted by *Pax6* during retinogenesis (Brown *et al.*, 1998; Marquardt *et al.*, 2001; Vetter and Brown, 2001; Riesenberg *et al.*, 2009). Studies of Lee and coauthors (2005) in mouse showed that *Hes1* is an upstream regulator for *Atoh7* during retinal ganglion cell genesis independent of *Pax6*.

Hes1 is known to code for a bHLH transcription factor functioning downstream of the Notch receptor (Jarriault *et al.*, 1998) and after transactivation affects numerous pathways involving cell-fate determination (Lai, 2002). Recently Djalilian and coauthors (2008) demonstrated higher expression of *Notch1* and *Jagged1* in the human limbal epithelium while the expression of *Hes1* was higher in the central cornea, and their expression was found predominantly in the basal and immediate suprabasal cells. Notch activity in the mouse corneal epithelial wound healing model was inversely proportional to the degree of proliferation, confirming its role in control of proliferation and promotion of differentiation (Djalilian *et al.*, 2008).

Atoh7-expressing cells were described as "transitional" (Dyer *et al.*, 2005), since they are nonmitotic, migratory cells that are undifferentiated but committed to particular fates (Le *et al.*, 2006). *Ath5* cells appeared evolutionarily conserved since *Drosophila atonal* is found in G_1-arrested retinal cells and chick and zebrafish *Atoh7* are excluded from S phase (Ma *et al.*, 2004; Masai *et al.*, 2005). *In situ* hybridisation studies in developing chicken retina (from ED2 to ED18) demonstrated that the intense expression of *Atoh7*

continues until ED9.5, and thereafter appears to be downregulated (Liu *et al.*, 2001). The dynamic pattern of *Atoh7* expression was correlated with the genesis of ganglion cells, which were previously shown to exit the cell cycle between ED2 and ED9 during chick retinogenesis (Liu *et al.*, 2001; Prada *et al.*, 1991).

The above suggests that *Atoh7* may play a similar role in morphogenesis and cell progression in the developing chick corneal epithelium. In the early phase of epithelial morphogenesis, its action may be directed at suppression of cell proliferation and initiation of differentiation.

7.3.3 *Sfrp2* involvement in epithelial cell survival during development

In this study, expression of *Sfrp2* in chick corneal epithelium was shown to be downregulated throughout development; a constant level of expression was observed from ED6 to ED14, with a decrease from ED16.

Secreted-frizzled-related proteins are thought to bind and regulate Wnt activity through a cysteine rich-domain (CRD), preventing Wnt from interacting with Frizzleds (Lin *et al.*, 1997; Rattner *et al.*, 1997). SFRPs are also able to downregulate Wnt signaling by the formation of an inhibitory complex with the Frizzled receptors (Chim *et al.*, 2007). The mechanisms mediating Sfrp2`s cellular survival effect have not been precisely elucidated. Recently it has been postulated that *Sfrp2*, through interaction with Frizzled receptor, could potentially influence cell fate and survival by antagonising *Wnts* with pro-apoptotic properties. Evidence supporting this hypothesis was derived from a Wnt signalling study in rat embryonic heart-derived myoblasts (Zhang *et al.*, 2009).

Although, it is likely that *Sfrp2* plays a similar role in the corneal epithelial system, its role in cell survival during chick corneal epithelium development requires further investigation. *Sfrp2* was previously demonstrated to block pro-apoptotic signalling of *Wnt* in neural crest cells of chick embryos (Ellies *et al.*, 2000), whereas another study demonstrated that *Wnt3a* expression in the ocular ectoderm starts later at ED4 and coincides with the onset of the

secondary corneal stroma development (Fokina and Forlova, 2006). Ellies and coauthors (2000) also indicated an important role for Wnt signalling, coordinated by Bmp4 signalling, in the induction of programmed cell death in developing chicken hindbrain. Interestingly, Sfrp2 was not detected by *in situ* hybridisation analysis in the developing murine corneal epithelium (E12.5-18.5, postnatal E7 and adult), although an expression of several Wnts, including Wnt-3, was demonstrated (Liu *et al.,* 2003).

7.3.4 Role of *Cebpb* in epithelial cell proliferation and commitment to terminal differentiation

Microarray analysis identified *Cebpb* (Ccaat/enhancer binding protein c/ebp, beta) in the development of corneal epithelium. The highest expression of *Cebpb* was observed from ED10 to ED16, and was thereafter downregulated.

The evidence for the proposed role of *Cebpb,* a member of the basic leucine zipper family of transcription factors, in growth arrest and terminal cell differentiation has come from studies of adipogenesis and adipose-specific genes that are expressed only upon terminal differentiation (Kaestner *et al.*, 1990, Umek *et al.*, 1991).

The involvement of *Cebpb* in Ras/Raf/MAPK-dependent signalling pathway was demonstrated by Hanlon and Sealy (1999). Initiation of Ras signalling leads to activation of downstream serum response factor (SRF), which binds to SRE in a promoter region of *c-fos* gene. *C-fos* proto-oncogene is a member of the set of 'immediate early' genes whose transcription is rapidly activated in the absence of protein synthesis by mitogenic signals (Cohen and Curran, 1989). *Cebpb* gives rise to three translation products that bind to the SRE region; p38, p35 and p20 (murine and rat). The N-terminal half of the first two proteins contains strong transactivation domains, whereas p20 lacks this domain and acts as an inhibitor of transcription (Hanlon and Sealy, 1999).

More recently, Yuan and coauthors (2004) suggested a role for *Cebpb* in the regulation of *βigh3* gene transcription (GF-β-induced gene-human, clone 3), which was considered as an essential constituent of the ECM responsible for

cell adhesion and cell-matrix interactions. The temporal expression of *βigh3* mRNA during corneal healing and development indicated that it plays a role in the synthesis and regulation of new tissue (Rawe *et al.*, 1997). *βigh3* gene, which codes for keratoepithelin protein, was shown to be upregulated by TGFβ1 in corneal epithelial cells in a cell density-dependent way (Wang *et al.*, 2002).

Cebpb has been implicated in differentiation and tumor development of several epithelial cells including mammary epithelial cells and keratinocytes (Johnson, 2005). In epidermis, C*ebpb* induced expression of early keratinocyte differentiation markers keratin-1 and 10 through the transcription factor, activator protein 2 (Ap2) (Maytin *et al.*, 1999).

Above suggested, that *Cebpb* may act as an auxiliary factor that, at the appropriate time, assists in the regulation of cell cycle and execution of the predetermined differentiation programs in developing corneal epithelium.

7.3.5 Role of *Aqp3* in regulation of epithelial barrier formation

The corneal epithelium, outermost component of the cornea, is a primary barrier that protects the eye from mechanical trauma and microbial insults. The protective function of the chick corneal epithelium is established during embryonic development, in the final step of epithelial stratification, as a result of a complex and precisely coordinated program of morphogenesis.

As described in section 6.6.2.1, *Aqp3* was upregulated at the transcriptional level during the development of chick corneal epithelium, showing the lowest expression between ED6 and ED12, and an increase from ED14. The proposed mechanism of *Aqp3*-facilitated cell proliferation in the epidermis involved increased of cellular glycerol metabolism and biosynthesis, therefore increase ATP content and altered MAP kinase signalling (Verkman *et al.*, 2008; Hara-Chikuma and Verkman, 2008). In contrast to the epidermal epithelium, in which differentiated cells began to express proteins that generate the external cornified layer, the differentiation of external layers of corneal epithelia was

accompanied by the expression of proteins delegated for metabolites, and ion transport (Revoltella *et al.,* 2006).

Recent studies by Swamynathan and coauthors (2008) demonstrated that the Aqp3 promoter is regulated by *Klf4* which plays a crucial role in the development and maintenance of the mouse cornea. In the epidermal system *Klf4* is one of the best-studied transcription factors in respect to regulation of epidermal barrier formation (Koster and Roop, 2007). It was also shown that the CK12 promoter was bound and upregulated by Klf4 and that the downregulation of keratin CK12 may be responsible for *Klf4*-conditional null corneal epithelial fragility in mice (Swamynathan *et al.,* 2007).

Above suggests that *Aqp3* may be a downstream target for *Klf4,* and act similarly to *Klf4;* by upregulating inhibitors of cell division, and downregulating activators of the cell cycle, reported in earlier studies (Whitney *et al.*, 2006; Swamynathan *et al.,* 2008). It remains to be established whether Aqp3 plays a direct role in coordinating the regulation of the groups of genes whose expression is affected by the *Klf4* in the cornea.

In conclusion, the changes in gene expression profiles, detected by the microarray analyses in this investigation, are consistent with the phenotypic changes in the developing chick corneal epithelium. The microarray data provided a good overall picture of gene expression in the developing chick corneal epithelium, although further exploration to ascertain exact roles and functions of differentially expressed genes and their proteins in corneal epithelial cell homeostasis is required.

7.4 Future work

The present study is a first step in order to shed light on how corneal epithelial development is regulated and how the structure is maintained during embryonic development and posthatched life.

The results presented in this study show expression profiles of several genes of interests at developmental time points, however, it can not be determined from this study in which subcompartment of the developing corneal epithelium the identified genes are expressed. Thus future work on selective genes and regulatory mechanisms will involve cellular localisation of gene transcripts of interest by mRNA *in situ* hybridisation

Further studies could be completed to demonstrate protein expression of genes and post translational modifications of the proteins of interest by Western blotting and additional immunohistochemistry experiments. Above experiments should be complemented by analyses of adult chick tissue, as well as tissues of other species, in steady state homeostasis, during wound healing and/or in tissues with pathological characteristics.

Several methods might be applied in order to examine the gene of interest functions. RNAi (i.e. siRNA) or Cre/LoxP system under the control of promoters of genes might be utilised to knock-down target genes *in vivo*. An alternative method could be *in ovo* electroporation of iRNA (miRNA such as morpholinos) to silence endogenous gene products.

APPENDICES

APPENDIX I

Table I.1 Hamburger Hamilton Stages

(adapted from http://embryology.med.unsw.edu.au/OtherEmb/chick1.htm, UNSW Embryology, accessed 19.07.2006) (continued overleaf)

Hamburger Hamilton Stages	Age	Identification of Stages
		Before laying
Early cleavage	3.5-4.5 hr	Shell membrane of egg formed in isthmus of oviduct
During cleavage		Germ wall formed from marginal periblast
Late cleavage	4.5-24.0 hr	Shell of egg formed in uterus
		After laying
1		Preprimitive streak (embryonic shield)
2	6-7 hr	Initial primitive streak, 0.3-0.5 mm long
3	12-13 hr	Intermediate primitive streak
4	18-19 hr	Definitive primitive streak, ±1.88 mm long
5	19-22 hr	Head process (notochord)
6	23-25 hr	Head fold
7	23-26 hr	1 somite; neural folds
7 to 8	ca. 23-26 hr	1-3 somites; coelom
8	26-29 hr	4 somites; blood islands
9	29-33 hr	7 somites; primary optic vesicles
9+ to 10+	ca. 33 hr	8-9 somites; anterior amniotic fold
10	33-38 hr	10 somites; 3 primary brain vesicles
11	40-45 hr	13 somites; 5 neuromeres of hindbrain
12	45-49 hr	16 somites; telencephalon
13	48-52 hr	19 somites; atrioventricular canal
13+ to 14-	ca. 50-52 hr	20-21 somites; tail bud
14	50-53 hr	22 somites; trunk flexure; visceral arches I and II, clefts 1 and 2
14+ to 15-	ca. 50-54 hr	23 somites; premandibular head cavities
15	50-55 hr	24-27 somites; visceral arch III, cleft 3
16	51-56 hr	26-28 somites; wing bud; posterior amniotic fold
17	52-64 hr	29-32 somites; leg bud; epiphysis
18	3 da	30-36 somites extending beyond level of leg bud; allantois
19	3.0-3.5 da	37- 40 somites extending into tail; maxillary process
20	3.0-3.5 da	40-43 somites; rotation completed; eye pigment
21	3.5 da	43-44 somites; visceral arch IV, cleft 4
22	3.5-4.0 da	Somites extend to tip of tail

23	4 da	Dorsal contour from hindbrain to tail is a curved line
24	4.5 da	Dorsal contour from hindbrain to tail is a curved line
25	4.5-5.0 da	Elbow and knee joints
26	5 da	1st 3 toes
27	5.0-5.5 da	Beak
28	5.5-6.0 da	3 digits, 4 toes
29	6.0-6.5 da	Rudiment of 5th toe
30	6.5-7.0 da	Feather germs; scleral papillae; egg tooth
31	7.0-7.5 da	Web between 1st and 2nd digits
32	7.5 da	Anterior tip of mandible has reached beak
33	7.5-8.0 da	Web on radial margin of wing and 1st digit
34	8 da	Nictitating membrane
35	8.5-9.0 da	Phalanges in toes
36	10 da	Length of 3rd toe from tip to middle of metatarsal joint = 5.4±0.3mm; length of beak from anterior angle of nostril to tip of
37	11 da	Length of 3rd toe = 7.4±0.3mm; length of beak = 3.0 mm
38	12 da	Length of 3rd toe = 8.4±0.3 mm; length of beak = 3.1 mm
39	13 da	Length of 3rd toe = 9.8±0.3 mm; length of beak = 3.5 mm
40	14 da	Length of beak = 4.0 mm; length of 3rd toe = 12.7±0.5 mm
41	15 da	Length of beak from anterior angle of nostril to tip of upper bill = 4.5 mm; length of 3rd toe = 14.9±0.8 mm
42	16 da	Length of beak = 4.8 mm; length of 3rd toe = 16.7±0.8 mm
43	17 da	Length of beak = 5.0 mm; length of 3rd toe = 18.6±0.8 mm
44	18 da	Length of beak = 5.7 mm; length of 3rd toe = 20.4±0.8 mm
45	19-20 da	Yolk sac half enclosed in body cavity; chorio-allantoic membrane contains less blood and is "sticky" in living embryo
46	20-21 da	Newly-hatched chick

APPENDIX II

List of reagents and composition of kits used in the study.

HISTOLOGY/HISTOCHEMISTRY

10X PBS [1L]

NaCl	80g
KCl	2g
Na_2PO_4	14.4g
KH_2PO_4	2.4g
HCl to pH 7.4	
dH_2O	1000 ml

Gelvatol Mounting Medium

Double distilled water	40ml
Na_2HPO_4	0.08g
KH_2PO_4	0.03g
NaCl	0.327g
Sodium azide	0.024g
1,4 – Diazabicyclo – [2.2.2] octane	0.6g
Gelvatol	10g
Glycerol	20ml

10% Neutral Buffered Formalin [1L]

NaH_2PO_4	4g
Na_2HPO_4	6.4ml
dH_2O	900ml
36% Formaldehyde	100ml

4% Paraformaldehyde [100ml]

1X PBS	90ml
PFA	4g
1M NaOH	1ml

0.1% Sodium Azide [100ml]

Sodium azide	0.1g
1X PBS	100ml

Peroxidase substrate [5ml]

DAB/Cobalt [0.5 mg/ml]	1 tablet
Urea Hydrogen Peroxide/ Tris Buiffer	1 tablet
dH_2O	5ml

DNAseI [per slide]

1x Reaction Buffer	100µl
DNaseI stock	100µl

WESTERN BLOTTING

1.5 M Tris/HCl pH 8.8 [150ml]

Tris base	27.23g
dH_2O	150ml
HCL to pH 8.8	

0.5 M Tris/HCl pH 6.8 [100ml]

Tris base	6g
dH_2O	100ml
HCL to pH 6.8	

10% APS

Ammonium persulphat e	1g
dH_2O	10ml

10% SDS

SDS	10g
dH_2O	100ml

10x TBS [1L]

10 mM Tris base	12.1g
150 mM NaCl	87g
dH_2O	1000ml

1x TBS/Tween20

10x TBS	100ml
dH_2O	900ml
Tween20	1ml
pH 7.4	

Working sample buffer [100µl]

Laemlli Buffer	95µl
β-mercapthoethanol	5µl

Running Buffer [1L]

10x Tris/glycine/SDS	100ml
dH_2O	900ml

Transfer Buffer [1L]

Tris/glycine	100ml
Methanol	200ml
dH_2O	700ml

Stripping Buffer[1L]

Glycine	15g
SDS	1g
Tween20	10ml
HCl to pH 2.2	
dH_2O	1000ml

RNA ISOLATION

Working RLT

β-Mercaptoethanol	10µl
Buffer RLT	1ml

MICROARRAYS

12X MES Stock Buffer, 1.22M Mes, 0.89M [Na^+] [1L]

MES hydrate	64.61ml
MES Sodium Salt	193.3g
Molecular Biology Grade water	800ml
dH_2O to 1L	
Adjust pH to 6.5-6.7	

2X Hybridisation Buffer [50ml]

12X MES Stock Buffer	8.3ml
5M NaCl	17.7ml
0.5M EDTA	4.0ml
10% Tween20	0.1ml
dH_2O	19.9ml

Final 1X concentration is 100mM MES, 1M [Na^+], 20mM EDTA, 0.01% Tween20.

Wash Buffer A [1L]

20X SSPE	300ml
10% Tween-20	1.0ml
dH_2O	699ml
Filter through a 0.2µm filter.	

Wash Buffer B [1L]

12 X MES Stock Buffer	83.3ml
5M NaCl	5.2ml
10% Tween-20	1.0ml
dH_2O	910.5ml

SAPE

2X Stain Buffer	300µl
50mg/mL BSA	24µl
1mg/mL Streptavidin Phycoerythrin	6µl
RNase-free H_20	270µl

Antibody solution mix

2X MES Stain Buffer	300µl
50mg/mL BSA	24µl
10mg/mL Normal Goat IgG	6µl
0.5mg/mL Anti-streptavidin Antibody, biotinylated	3.6µl
Nuclease-free H_20	266.4µl

Streptavidin Stock [1mg/ml]

Stretpavidin Stock	5mg
1X PBS	5ml

Goat IgG Stock [10mg/mL]

Goat IgG	50mg
150mM NaCl	5ml

COMPOSITIONS OF SOLUTIONS PROVIDED WITH KITS

VECTASTAIN® Elite® ABC KIT, Vector Laboratories

Reagent A: avidin
Reagent B: biotinylated enzyme

BCA™ Protein Assay, Pierce

Reagent A: sodium carbonate, sodium bicarbonate, bicinchonic acid and sodium tartrate in 0.1M sodium hydroxide
Reagent B: 4% cupric sulphate
Albumin Standard Ampules 2 mg/ml: bovine serum albumin at 2.0mg/ml in 0.9% saine and 0.05% sodium azide.

ECL Plus, Amersham

Solution A: ECL Plus substrate solution containing tris buffer
Solution B: Stock Acridam solution in Dioxane and Ethanol

RNeasy® Micro Kit, Qiagen

RLT Buffer: containing guanidinium thicyanate
RW1 Buffer: guanidinium thicyanate, ethanol

ApopTag® Peroxidase in situ Apoptosis Detection Kit, Chemicon

Equlibration Buffer: contains potassium cacodylate (dimethylarsinic acid)
Reaction Buffer: contains potassium cacodylate (dimethylarsinic acid)

SuperScript™ II, Invitrogen

Primer: Pd(N) oligos
DEPC water
Random primers
First-Strand Buffer
RNase Inhibitor

GeneChip® Sample Cleaup Module

cDNA Binding Buffer: containing guanidine hydrochloride and isopropanol
IVT cRNA Binding Buffer: guanidine thiocyanate

Affymetrix Fragmentation Kit

5X Fragmentation Buffer: 200mM Tris-Acetate (pH 8.1), 500mM potassium acetate, 150mM magnesium acetate.

APPENDIX III

STATISTICAL ANALYSIS OUTPUTS

Chapter 3, section 3.4.2 Morphology of the developing corneal epithelium

One-way ANOVA with Dunnett T3 post-hoc test were performed in SPSS v.12 to compare data obtained after quantification of number of cell layers in developing chick corneal epithelium.

Table III.1 Shapiro-Wilk results for test of normality. The mean difference is significant at the 0.05 level.

	Shapiro-Wilk		
	Statistic	df	Sig.
number	.869	729	.135

Table III.2 One-way ANOVA results obtained from analysis of the number of epithelial cell layers. **(a)** comparisons between groups (ED4-ED21), **(b)** comparisons between EDs within regions (centre, periphery, limbus), **(c)** comparisons between regions within EDs. The mean difference is significant at the 0.05 level.

a)

ANOVA

	Sum of Squares	df	Mean Square	F	Sig.
Between Groups	1388.149	8	154.239	568.202	.000
Within Groups	217.160	700	.271		
Total	1605.310	709			

b)

ANOVA

region		Sum of Squares	df	Mean Square	F	Sig.
centre	Between Groups	498.519	8	55.391	273.449	.000
	Within Groups	52.667	260	.203		
	Total	551.185	269			
periphery	Between Groups	396.478	8	44.053	194.499	.000
	Within Groups	58.889	260	.226		
	Total	455.367	269			
limbus	Between Groups	514.800	8	57.200	229.979	.000
	Within Groups	64.667	260	.249		
	Total	579.467	269			

c) **ANOVA**

group		Sum of Squares	df	Mean Square	F	Sig.
day 4	Between Groups	.469	2	.235	2.714	.073
	Within Groups	6.741	78	.086		
	Total	7.210	80			
day 6	Between Groups	1.210	2	.605	6.245	.003
	Within Groups	7.556	78	.097		
	Total	8.765	80			
day 8	Between Groups	1.580	2	.790	4.449	.015
	Within Groups	13.852	78	.178		
	Total	15.432	80			
day 10	Between Groups	1.284	2	.642	2.805	.067
	Within Groups	17.852	78	.229		
	Total	19.136	80			
day 12	Between Groups	1.407	2	.704	2.478	.090
	Within Groups	22.148	78	.284		
	Total	23.556	80			
day 14	Between Groups	2.543	2	1.272	4.649	.012
	Within Groups	21.333	78	.274		
	Total	23.877	80			
day 16	Between Groups	10.543	2	5.272	23.324	.000
	Within Groups	17.630	78	.226		
	Total	28.173	80			
day 18	Between Groups	2.543	2	1.272	3.837	.026
	Within Groups	25.852	78	.331		
	Total	28.395	80			
day 21	Between Groups	13.728	2	6.864	20.078	.000
	Within Groups	26.667	78	.342		
	Total	40.395	80			

Table III.3 Levene's test of homogeneity of variances

number

Levene Statistic	df1	df2	Sig.
13.577	8	700	.000

Table III.4 Post-hoc Dunnett T3 test results obtained from analysis of the number of epithelial cell layers. **(a)** comparisons between EDs within regions (centre, periphery, limbus), **(b)** comparisons between regions within EDs. The mean difference is significant at the 0.05 level.

a)

Multiple Comparisons

Dependent Variable: number
Dunnett T3

region	(I) group	(J) group	Mean Difference (I-J)	Std. Error	Sig.	95% Confidence Interval	
						Lower Bound	Upper Bound
centre	day 4	day 6	-.222	.085	.378	-.52	.07
		day 8	-.296	.098	.151	-.63	.04
		day 10	-.519(*)	.120	.003	-.93	-.11
		day 12	-1.037(*)	.128	.000	-1.48	-.60
		day 14	-2.000(*)	.120	.000	-2.41	-1.59
		day 16	-2.852(*)	.120	.000	-3.26	-2.44
		day 18	-3.519(*)	.131	.000	-3.97	-3.07
		day 21	-3.926(*)	.115	.000	-4.32	-3.53
	day 6	day 4	.222	.085	.378	-.07	.52
		day 8	-.074	.072	1.000	-.32	.18
		day 10	-.296	.100	.189	-.65	.05
		day 12	-.815(*)	.109	.000	-1.20	-.43
		day 14	-1.778(*)	.100	.000	-2.13	-1.42
		day 16	-2.630(*)	.100	.000	-2.98	-2.28
		day 18	-3.296(*)	.113	.000	-3.70	-2.90
		day 21	-3.704(*)	.094	.000	-4.03	-3.37
	day 8	day 4	.296	.098	.151	-.04	.63
		day 6	.074	.072	1.000	-.18	.32
		day 10	-.222	.111	.850	-.61	.16
		day 12	-.741(*)	.120	.000	-1.16	-.33
		day 14	-1.704(*)	.112	.000	-2.09	-1.32
		day 16	-2.556(*)	.111	.000	-2.94	-2.17
		day 18	-3.222(*)	.123	.000	-3.65	-2.79
		day 21	-3.630(*)	.106	.000	-3.99	-3.27
	day 10	day 4	.519(*)	.120	.003	.11	.93
		day 6	.296	.100	.189	-.05	.65
		day 8	.222	.111	.850	-.16	.61
		day 12	-.519(*)	.138	.019	-.99	-.04
		day 14	-1.481(*)	.131	.000	-1.93	-1.03
		day 16	-2.333(*)	.131	.000	-2.78	-1.88
		day 18	-3.000(*)	.141	.000	-3.48	-2.52
		day 21	-3.407(*)	.126	.000	-3.84	-2.97
	day 12	day 4	1.037(*)	.128	.000	.60	1.48
		day 6	.815(*)	.109	.000	.43	1.20
		day 8	.741(*)	.120	.000	.33	1.16
		day 10	.519(*)	.138	.019	.04	.99
		day 14	-.963(*)	.139	.000	-1.44	-.49
		day 16	-1.815(*)	.138	.000	-2.29	-1.34
		day 18	-2.481(*)	.148	.000	-2.99	-1.97
		day 21	-2.889(*)	.134	.000	-3.35	-2.43
	day 14	day 4	2.000(*)	.120	.000	1.59	2.41
		day 6	1.778(*)	.100	.000	1.42	2.13

		day 8	1.704(*)	.112	.000	1.32	2.09
		day 10	1.481(*)	.131	.000	1.03	1.93
		day 12	.963(*)	.139	.000	.49	1.44
		day 16	-.852(*)	.131	.000	-1.30	-.40
		day 18	-1.519(*)	.142	.000	-2.00	-1.03
		day 21	-1.926(*)	.127	.000	-2.36	-1.49
	day 16	day 4	2.852(*)	.120	.000	2.44	3.26
		day 6	2.630(*)	.100	.000	2.28	2.98
		day 8	2.556(*)	.111	.000	2.17	2.94
		day 10	2.333(*)	.131	.000	1.88	2.78
		day 12	1.815(*)	.138	.000	1.34	2.29
		day 14	.852(*)	.131	.000	.40	1.30
		day 18	-.667(*)	.141	.001	-1.15	-.18
		day 21	-1.074(*)	.126	.000	-1.51	-.64
	day 18	day 4	3.519(*)	.131	.000	3.07	3.97
		day 6	3.296(*)	.113	.000	2.90	3.70
		day 8	3.222(*)	.123	.000	2.79	3.65
		day 10	3.000(*)	.141	.000	2.52	3.48
		day 12	2.481(*)	.148	.000	1.97	2.99
		day 14	1.519(*)	.142	.000	1.03	2.00
		day 16	.667(*)	.141	.001	.18	1.15
		day 21	-.407	.137	.171	-.88	.06
	day 21	day 4	3.926(*)	.115	.000	3.53	4.32
		day 6	3.704(*)	.094	.000	3.37	4.03
		day 8	3.630(*)	.106	.000	3.27	3.99
		day 10	3.407(*)	.126	.000	2.97	3.84
		day 12	2.889(*)	.134	.000	2.43	3.35
		day 14	1.926(*)	.127	.000	1.49	2.36
		day 16	1.074(*)	.126	.000	.64	1.51
		day 18	.407	.137	.171	-.06	.88
periphery	day 4	day 6	-.148	.072	.810	-.40	.10
		day 8	-.222	.087	.420	-.52	.08
		day 10	-.370(*)	.106	.043	-.73	-.01
		day 12	-.667(*)	.115	.000	-1.07	-.27
		day 14	-1.519(*)	.126	.000	-1.96	-1.08
		day 16	-2.074(*)	.117	.000	-2.48	-1.67
		day 18	-3.037(*)	.134	.000	-3.50	-2.57
		day 21	-3.630(*)	.138	.000	-4.11	-3.15
	day 6	day 4	.148	.072	.810	-.10	.40
		day 8	-.074	.072	1.000	-.32	.18
		day 10	-.222	.094	.567	-.55	.11
		day 12	-.519(*)	.104	.001	-.89	-.15
		day 14	-1.370(*)	.116	.000	-1.78	-.96
		day 16	-1.926(*)	.106	.000	-2.30	-1.55
		day 18	-2.889(*)	.124	.000	-3.33	-2.45
		day 21	-3.481(*)	.129	.000	-3.94	-3.02
	day 8	day 4	.222	.087	.420	-.08	.52
		day 6	.074	.072	1.000	-.18	.32
		day 10	-.148	.106	.998	-.51	.22
		day 12	-.444(*)	.115	.016	-.84	-.05
		day 14	-1.296(*)	.126	.000	-1.74	-.86
		day 16	-1.852(*)	.117	.000	-2.26	-1.45
		day 18	-2.815(*)	.134	.000	-3.28	-2.35

		day 21	-3.407(*)	.138	.000	-3.89	-2.92
	day 10	day 4	.370(*)	.106	.043	.01	.73
		day 6	.222	.094	.567	-.11	.55
		day 8	.148	.106	.998	-.22	.51
		day 12	-.296	.130	.643	-.74	.15
		day 14	-1.148(*)	.140	.000	-1.63	-.67
		day 16	-1.704(*)	.132	.000	-2.16	-1.25
		day 18	-2.667(*)	.146	.000	-3.17	-2.16
		day 21	-3.259(*)	.151	.000	-3.78	-2.74
	day 12	day 4	.667(*)	.115	.000	.27	1.07
		day 6	.519(*)	.104	.001	.15	.89
		day 8	.444(*)	.115	.016	.05	.84
		day 10	.296	.130	.643	-.15	.74
		day 14	-.852(*)	.147	.000	-1.36	-.35
		day 16	-1.407(*)	.139	.000	-1.89	-.93
		day 18	-2.370(*)	.153	.000	-2.90	-1.84
		day 21	-2.963(*)	.157	.000	-3.50	-2.42
	day 14	day 4	1.519(*)	.126	.000	1.08	1.96
		day 6	1.370(*)	.116	.000	.96	1.78
		day 8	1.296(*)	.126	.000	.86	1.74
		day 10	1.148(*)	.140	.000	.67	1.63
		day 12	.852(*)	.147	.000	.35	1.36
		day 16	-.556(*)	.149	.020	-1.07	-.05
		day 18	-1.519(*)	.162	.000	-2.07	-.96
		day 21	-2.111(*)	.166	.000	-2.68	-1.54
	day 16	day 4	2.074(*)	.117	.000	1.67	2.48
		day 6	1.926(*)	.106	.000	1.55	2.30
		day 8	1.852(*)	.117	.000	1.45	2.26
		day 10	1.704(*)	.132	.000	1.25	2.16
		day 12	1.407(*)	.139	.000	.93	1.89
		day 14	.556(*)	.149	.020	.05	1.07
		day 18	-.963(*)	.155	.000	-1.49	-.43
		day 21	-1.556(*)	.159	.000	-2.10	-1.01
	day 18	day 4	3.037(*)	.134	.000	2.57	3.50
		day 6	2.889(*)	.124	.000	2.45	3.33
		day 8	2.815(*)	.134	.000	2.35	3.28
		day 10	2.667(*)	.146	.000	2.16	3.17
		day 12	2.370(*)	.153	.000	1.84	2.90
		day 14	1.519(*)	.162	.000	.96	2.07
		day 16	.963(*)	.155	.000	.43	1.49
		day 21	-.593(*)	.171	.046	-1.18	-.01
	day 21	day 4	3.630(*)	.138	.000	3.15	4.11
		day 6	3.481(*)	.129	.000	3.02	3.94
		day 8	3.407(*)	.138	.000	2.92	3.89
		day 10	3.259(*)	.151	.000	2.74	3.78
		day 12	2.963(*)	.157	.000	2.42	3.50
		day 14	2.111(*)	.166	.000	1.54	2.68
		day 16	1.556(*)	.159	.000	1.01	2.10
		day 18	.593(*)	.171	.046	.01	1.18
limbus	day 4	day 6	-.296	.090	.101	-.62	.03
		day 8	-.407(*)	.110	.040	-.81	-.01
		day 10	-.556(*)	.097	.000	-.91	-.20
		day 12	-.815(*)	.107	.000	-1.20	-.43

		day 6	2.704(*)	.139	.000	2.23	3.18
		day 8	2.593(*)	.153	.000	2.07	3.12
		day 10	2.444(*)	.145	.000	1.95	2.94
		day 12	2.185(*)	.151	.000	1.67	2.70
		day 14	1.519(*)	.145	.000	1.02	2.02
		day 16	.222	.134	.980	-.24	.68
		day 21	-1.481(*)	.163	.000	-2.04	-.92
	day 21	day 4	4.481(*)	.124	.000	4.03	4.93
		day 6	4.185(*)	.153	.000	3.66	4.71
		day 8	4.074(*)	.166	.000	3.51	4.64
		day 10	3.926(*)	.157	.000	3.38	4.47
		day 12	3.667(*)	.164	.000	3.10	4.23
		day 14	3.000(*)	.158	.000	2.46	3.54
		day 16	1.704(*)	.148	.000	1.19	2.22
		day 18	1.481(*)	.163	.000	.92	2.04

* The mean difference is significant at the .05 level.

b) **Multiple Comparisons**

Dependent Variable: number
Dunnett T3

group	(I) region	(J) region	Mean Difference (I-J)	Std. Error	Sig.	95% Confidence Interval	
						Lower Bound	Upper Bound
day 4	centre	periphery	-.074	.098	.833	-.32	.17
		limbus	-.185	.076	.064	-.38	.01
	periphery	centre	.074	.098	.833	-.17	.32
		limbus	-.111	.062	.224	-.27	.05
	limbus	centre	.185	.076	.064	-.01	.38
		periphery	.111	.062	.224	-.05	.27
day 6	centre	periphery	.000	.052	1.000	-.13	.13
		limbus	-.259(*)	.097	.033	-.50	-.02
	periphery	centre	.000	.052	1.000	-.13	.13
		limbus	-.259(*)	.097	.033	-.50	-.02
	limbus	centre	.259(*)	.097	.033	.02	.50
		periphery	.259(*)	.097	.033	.02	.50
day 8	centre	periphery	.000	.087	1.000	-.21	.21
		limbus	-.296	.126	.069	-.61	.02
	periphery	centre	.000	.087	1.000	-.21	.21
		limbus	-.296	.126	.069	-.61	.02
	limbus	centre	.296	.126	.069	-.02	.61
		periphery	.296	.126	.069	-.02	.61
day 10	centre	periphery	.074	.126	.913	-.24	.39
		limbus	-.222	.134	.278	-.55	.11
	periphery	centre	-.074	.126	.913	-.39	.24
		limbus	-.296	.130	.078	-.62	.02
	limbus	centre	.222	.134	.278	-.11	.55
		periphery	.296	.130	.078	-.02	.62
day 12	centre	periphery	.296	.142	.118	-.05	.65
		limbus	.037	.149	.992	-.33	.40
	periphery	centre	-.296	.142	.118	-.65	.05
		limbus	-.259	.145	.218	-.62	.10

	limbus	centre	-.037	.149	.992	-.40	.33
		periphery	.259	.145	.218	-.10	.62
day 14	centre	periphery	.407(*)	.144	.020	.05	.76
		limbus	.333(*)	.135	.050	.00	.67
	periphery	centre	-.407(*)	.144	.020	-.76	-.05
		limbus	-.074	.147	.943	-.44	.29
	limbus	centre	-.333(*)	.135	.050	-.67	.00
		periphery	.074	.147	.943	-.29	.44
day 16	centre	periphery	.704(*)	.136	.000	.37	1.04
		limbus	-.111	.123	.748	-.41	.19
	periphery	centre	-.704(*)	.136	.000	-1.04	-.37
		limbus	-.815(*)	.129	.000	-1.13	-.50
	limbus	centre	.111	.123	.748	-.19	.41
		periphery	.815(*)	.129	.000	.50	1.13
day 18	centre	periphery	.407(*)	.159	.040	.01	.80
		limbus	.333	.151	.091	-.04	.71
	periphery	centre	-.407(*)	.159	.040	-.80	-.01
		limbus	-.074	.159	.954	-.47	.32
	limbus	centre	-.333	.151	.091	-.71	.04
		periphery	.074	.159	.954	-.32	.47
day 21	centre	periphery	.222	.151	.375	-.15	.59
		limbus	-.741(*)	.151	.000	-1.11	-.37
	periphery	centre	-.222	.151	.375	-.59	.15
		limbus	-.963(*)	.175	.000	-1.39	-.53
	limbus	centre	.741(*)	.151	.000	.37	1.11
		periphery	.963(*)	.175	.000	.53	1.39

* The mean difference is significant at the .05 level.

Table III.5 Pearson correlation of number of cell layers in chick corneal epithelium and developmental time point. Correlation is significant at the 0.01 level (2-tailed).

Descriptive Statistics

	Mean	Std. Deviation	N
number	3.35	1.409	729
ED	12.20	5.079	729

Correlations

		number	ED
number	Pearson Correlation	1	.891(**)
	Sig. (2-tailed)		.000
	N	729	729
ED	Pearson Correlation	.891(**)	1
	Sig. (2-tailed)	.000	
	N	729	729

Chapter 3, section 3.5.3.1 Immunoblotting for cytokeratin 3

One-way ANOVA with Dunnett T3 post-hoc test were performed in SPSS v.12 to compare the normalised band intensities across time points in an attempt to identify significant changes in expression.

Table III.6 Shapiro Wilk results for test of normality. The mean difference is significant at the 0.05 level.

	Shapiro-Wilk		
	Statistic	df	Sig.
normdata	.907	21	.067

Table III.7 One-way ANOVA results obtained from analysis of the chicken cytokeratin 3 Western blot. The mean difference is significant at the 0.05 level.

ANOVA

normdata

	Sum of Squares	df	Mean Square	F	Sig.
Between Groups	.938	6	.156	59.985	.000
Within Groups	.036	14	.003		
Total	.975	20			

Table III.8 Levene's test of homogeneity of variances

normdata

Levene Statistic	df1	df2	Sig.
3.614	5	12	.022

Table III.9 Post-hoc test results obtained from analysis of the chicken cytokeratin 3 Western blot. The mean difference is significant at the 0.05 level.

Multiple Comparisons

Dependent Variable: normdata
Dunnett T3

(I) ed	(J) ed	Mean Difference (I-J)	Std. Error	Sig.	95% Confidence Interval	
					Lower Bound	Upper Bound
10.00	12.00	-.32335(*)	.01881	.001	-.4261	-.2207
	14.00	-.38727(*)	.04248	.036	-.7219	-.0526
	16.00	-.57801(*)	.05620	.034	-1.0619	-.0942
	18.00	-.58017(*)	.02980	.002	-.7776	-.3828
	21.00	-.68458(*)	.02036	.000	-.7961	-.5731
12.00	10.00	.32335(*)	.01881	.001	.2207	.4261
	14.00	-.06391	.04224	.848	-.4033	.2755
	16.00	-.25466	.05602	.189	-.7433	.2340
	18.00	-.25682(*)	.02945	.025	-.4571	-.0565
	21.00	-.36123(*)	.01985	.001	-.4709	-.2516
14.00	10.00	.38727(*)	.04248	.036	.0526	.7219
	12.00	.06391	.04224	.848	-.2755	.4033
	16.00	-.19075	.06774	.359	-.5790	.1975
	18.00	-.19290	.04815	.158	-.4803	.0945
	21.00	-.29732	.04295	.063	-.6238	.0292

16.00	10.00	.57801(*)	.05620	.034	.0942	1.0619
	12.00	.25466	.05602	.189	-.2340	.7433
	14.00	.19075	.06774	.359	-.1975	.5790
	18.00	-.00216	.06060	1.000	-.4149	.4106
	21.00	-.10657	.05656	.711	-.5817	.3685
18.00	10.00	.58017(*)	.02980	.002	.3828	.7776
	12.00	.25682(*)	.02945	.025	.0565	.4571
	14.00	.19290	.04815	.158	-.0945	.4803
	16.00	.00216	.06060	1.000	-.4106	.4149
	21.00	-.10441	.03047	.251	-.2976	.0888
21.00	10.00	.68458(*)	.02036	.000	.5731	.7961
	12.00	.36123(*)	.01985	.001	.2516	.4709
	14.00	.29732	.04295	.063	-.0292	.6238
	16.00	.10657	.05656	.711	-.3685	.5817
	18.00	.10441	.03047	.251	-.0888	.2976

* The mean difference is significant at the .05 level.

Chapter 4, section 4.4.2 Immunolocalisation of proliferating epithelial cells using PCNA monoclonal antibody

One-way ANOVA with Dunnett T3 post-hoc test was performed in SPSS v.12 to percentage of PCNA-positive cells across the time points and corneal epithelial regions in an attempt to identify significant changes.

Table III.10 Shapiro-Wilk results for test of normality (n=27). The mean difference is significant at the 0.05 level.

	Shapiro-Wilk		
	Statistic	df	Sig.
number	.973	729	.214

Table III.11 One-way ANOVA results obtained from quantification of proliferating cells. **(a)** comparisons between groups (ED4 – ED21), **(b)** comparisons between EDs within regions (centre, periphery, limbus), **(c)** comparisons between regions within EDs. The mean difference is significant at the 0.05 level.

a)

ANOVA

	Sum of Squares	df	Mean Square	F	Sig.
Between Groups	11814.416	2	5907.208	31.151	.000
Within Groups	153033.535	807	189.633		
Total	164847.951	809			

b)

ANOVA

region		Sum of Squares	df	Mean Square	F	Sig.
centre	Between Groups	32816.714	8	3646.302	72.829	.000
	Within Groups	13017.352	260	50.067		
	Total	45834.066	269			
periphery	Between Groups	32601.349	8	3622.372	79.449	.000
	Within Groups	11854.376	260	45.594		
	Total	44455.724	269			
limbus	Between Groups	52960.055	8	5884.451	156.378	.000
	Within Groups	9783.689	260	37.630		
	Total	62743.744	269			

c)

ANOVA

group		Sum of Squares	df	Mean Square	F	Sig.
day 4	Between Groups	695.952	2	347.976	3.706	.029
	Within Groups	7322.949	78	93.884		
	Total	8018.901	80			
day 6	Between Groups	1053.748	2	526.874	7.652	.001
	Within Groups	5370.313	78	68.850		
	Total	6424.061	80			
day 8	Between Groups	1077.874	2	538.937	6.528	.002
	Within Groups	6439.459	78	82.557		
	Total	7517.333	80			
day 10	Between Groups	190.849	2	95.424	3.825	.026
	Within Groups	1946.156	78	24.951		
	Total	2137.005	80			
day 12	Between Groups	555.793	2	277.896	8.433	.000
	Within Groups	2570.456	78	32.955		
	Total	3126.249	80			
day 14	Between Groups	692.314	2	346.157	13.107	.000
	Within Groups	2059.916	78	26.409		
	Total	2752.230	80			
day 16	Between Groups	1165.474	2	582.737	13.354	.000
	Within Groups	3403.831	78	43.639		
	Total	4569.305	80			
day 18	Between Groups	3350.595	2	1675.297	105.192	.000

	Within Groups	1242.240	78	15.926		
	Total	4592.834	80			
day 21	Between Groups	5125.065	2	2562.533	80.164	.000
	Within Groups	2493.346	78	31.966		
	Total	7618.411	80			

Table III.12 Levene`s test of homogeneity of variance

number

Levene Statistic	df1	df2	Sig.
4.406	2	807	.012

Table III.13 Post-hoc test results obtained from quantification of proliferating cells. **(a)** comparisons between EDs within regions (centre, periphery, limbus), **(b)** comparisons between regions within EDs. The mean difference is significant at the 0.05 level.

a)

Multiple Comparisons

Dependent Variable: number
Dunnett T3

region	(I) group	(J) group	Mean Difference (I-J)	Std. Error	Sig.	95% Confidence Interval	
						Lower Bound	Upper Bound
centre	day 4	day 6	-1.14519	2.83118	1.000	-10.854	8.5643
		day 8	-12.03333(*)	2.68745	.002	-21.259	-2.8074
		day 10	-14.05815(*)	2.27617	.000	-22.007	-6.1085
		day 12	-16.77444(*)	2.29623	.000	-24.780	-8.7680
		day 14	-21.20185(*)	2.14535	.000	-28.802	-13.6011
		day 16	-14.92667(*)	2.51135	.000	-23.581	-6.2715
		day 18	-1.67889	2.19101	1.000	-9.3968	6.0391
		day 21	15.76889(*)	2.24093	.000	7.9170	23.6208
	day 6	day 4	1.14519	2.83118	1.000	-8.5643	10.8547
		day 8	-10.88815(*)	2.64221	.006	-19.955	-1.8211
		day 10	-12.91296(*)	2.22256	.000	-20.666	-5.1598
		day 12	-15.62926(*)	2.24310	.000	-23.441	-7.8174
		day 14	-20.05667(*)	2.08839	.000	-27.448	-12.6645
		day 16	-13.78148(*)	2.46287	.000	-22.262	-5.3006
		day 18	-.53370	2.13527	1.000	-8.0472	6.9797
		day 21	16.91407(*)	2.18646	.000	9.2620	24.5661
	day 8	day 4	12.03333(*)	2.68745	.002	2.8074	21.2593
		day 6	10.88815(*)	2.64221	.006	1.8211	19.9552
		day 10	-2.02481	2.03632	1.000	-9.0965	5.0468
		day 12	-4.74111	2.05872	.624	-11.879	2.3969
		day 14	-9.16852(*)	1.88897	.001	-15.829	-2.5074
		day 16	-2.89333	2.29621	1.000	-10.780	4.9935
		day 18	10.35444(*)	1.94067	.000	3.5551	17.1538
		day 21	27.80222(*)	1.99686	.000	20.8453	34.7592

	day 10	day 4	14.05815(*)	2.27617	.000	6.1085	22.0078
		day 6	12.91296(*)	2.22256	.000	5.1598	20.6662
		day 8	2.02481	2.03632	1.000	-5.0468	9.0965
		day 12	-2.71630	1.48218	.934	-7.7996	2.3670
		day 14	-7.14370(*)	1.23561	.000	-11.412	-2.8747
		day 16	-.86852	1.79752	1.000	-7.0718	5.3348
		day 18	12.37926(*)	1.31328	.000	7.8642	16.8943
		day 21	29.82704(*)	1.39498	.000	25.0416	34.6125
	day 12	day 4	16.77444(*)	2.29623	.000	8.7680	24.7809
		day 6	15.62926(*)	2.24310	.000	7.8174	23.4411
		day 8	4.74111	2.05872	.624	-2.3969	11.8792
		day 10	2.71630	1.48218	.934	-2.3670	7.7996
		day 14	-4.42741(*)	1.27218	.047	-8.8292	-.0257
		day 16	1.84778	1.82286	1.000	-4.4350	8.1305
		day 18	15.09556(*)	1.34775	.000	10.4574	19.7337
		day 21	32.54333(*)	1.42747	.000	27.6442	37.4425
	day 14	day 4	21.20185(*)	2.14535	.000	13.6011	28.8026
		day 6	20.05667(*)	2.08839	.000	12.6645	27.4488
		day 8	9.16852(*)	1.88897	.001	2.5074	15.8296
		day 10	7.14370(*)	1.23561	.000	2.8747	11.4127
		day 12	4.42741(*)	1.27218	.047	.0257	8.8292
		day 16	6.27519(*)	1.62870	.019	.5691	11.9813
		day 18	19.52296(*)	1.07065	.000	15.8457	23.2003
		day 21	36.97074(*)	1.16942	.000	32.9408	41.0007
	day 16	day 4	14.92667(*)	2.51135	.000	6.2715	23.5818
		day 6	13.78148(*)	2.46287	.000	5.3006	22.2624
		day 8	2.89333	2.29621	1.000	-4.9935	10.7801
		day 10	.86852	1.79752	1.000	-5.3348	7.0718
		day 12	-1.84778	1.82286	1.000	-8.1305	4.4350
		day 14	-6.27519(*)	1.62870	.019	-11.981	-.5691
		day 18	13.24778(*)	1.68839	.000	7.3732	19.1223
		day 21	30.69556(*)	1.75269	.000	24.6301	36.7610
	day 18	day 4	1.67889	2.19101	1.000	-6.0391	9.3968
		day 6	.53370	2.13527	1.000	-6.9797	8.0472
		day 8	-10.35444(*)	1.94067	.000	-17.153	-3.5551
		day 10	-12.37926(*)	1.31328	.000	-16.894	-7.8642
		day 12	-15.09556(*)	1.34775	.000	-19.733	-10.4574
		day 14	-19.52296(*)	1.07065	.000	-23.200	-15.8457
		day 16	-13.24778(*)	1.68839	.000	-19.122	-7.3732
		day 21	17.44778(*)	1.25121	.000	13.152	21.7430
	day 21	day 4	-15.76889(*)	2.24093	.000	-23.620	-7.9170
		day 6	-16.91407(*)	2.18646	.000	-24.566	-9.2620
		day 8	-27.80222(*)	1.99686	.000	-34.759	-20.8453
		day 10	-29.82704(*)	1.39498	.000	-34.612	-25.0416
		day 12	-32.54333(*)	1.42747	.000	-37.442	-27.6442
		day 14	-36.97074(*)	1.16942	.000	-41.000	-32.9408
		day 16	-30.69556(*)	1.75269	.000	-36.761	-24.6301
		day 18	-17.44778(*)	1.25121	.000	-21.743	-13.1525
periphery	day 4	day 6	-5.52333	2.46224	.673	-14.062	3.0154
		day 8	-13.75407(*)	2.67395	.000	-22.951	-4.5564
		day 10	-17.52852(*)	2.41564	.000	-25.930	-9.1270
		day 12	-20.53852(*)	2.41315	.000	-28.932	-12.1442

	day 14	-26.26333(*)	2.48439	.000	-34.868	-17.6582
	day 16	-17.13741(*)	2.28108	.000	-25.164	-9.1106
	day 18	-8.03444(*)	2.21687	.041	-15.896	-.1726
	day 21	10.36630(*)	2.39985	.004	2.0105	18.7221
day 6	day 4	5.52333	2.46224	.673	-3.0154	14.0621
	day 8	-8.23074(*)	2.08263	.011	-15.396	-1.0653
	day 10	-12.00519(*)	1.73858	.000	-17.969	-6.0413
	day 12	-15.01519(*)	1.73512	.000	-20.967	-9.0629
	day 14	-20.74000(*)	1.83291	.000	-27.026	-14.4540
	day 16	-11.61407(*)	1.54618	.000	-16.952	-6.2760
	day 18	-2.51111	1.44978	.961	-7.5604	2.5382
	day 21	15.88963(*)	1.71657	.000	9.9997	21.7795
day 8	day 4	13.75407(*)	2.67395	.000	4.5564	22.9517
	day 6	8.23074(*)	2.08263	.011	1.0653	15.3961
	day 10	-3.77444	2.02733	.921	-10.763	3.2150
	day 12	-6.78444	2.02437	.065	-13.764	.1957
	day 14	-12.50926(*)	2.10878	.000	-19.759	-5.2594
	day 16	-3.38333	1.86496	.936	-9.8837	3.1170
	day 18	5.71963	1.78585	.111	-.5624	12.0017
	day 21	24.12037(*)	2.00849	.000	17.1899	31.0508
day 10	day 4	17.52852(*)	2.41564	.000	9.1270	25.9300
	day 6	12.00519(*)	1.73858	.000	6.0413	17.9691
	day 8	3.77444	2.02733	.921	-3.2150	10.7639
	day 12	-3.01000	1.66834	.944	-8.7313	2.7113
	day 14	-8.73481(*)	1.76982	.000	-14.807	-2.6619
	day 16	.39111	1.47084	1.000	-4.6753	5.4575
	day 18	9.49407(*)	1.36915	.000	4.7396	14.2485
	day 21	27.89481(*)	1.64903	.000	22.2395	33.5501
day 12	day 4	20.53852(*)	2.41315	.000	12.1442	28.9328
	day 6	15.01519(*)	1.73512	.000	9.0629	20.9674
	day 8	6.78444	2.02437	.065	-.1957	13.7646
	day 10	3.01000	1.66834	.944	-2.7113	8.7313
	day 14	-5.72481	1.76643	.085	-11.786	.3368
	day 16	3.40111	1.46675	.610	-1.6506	8.4529
	day 18	12.50407(*)	1.36476	.000	7.7657	17.2425
	day 21	30.90481(*)	1.64539	.000	25.2621	36.5476
day 14	day 4	26.26333(*)	2.48439	.000	17.6582	34.8684
	day 6	20.74000(*)	1.83291	.000	14.4540	27.0260
	day 8	12.50926(*)	2.10878	.000	5.2594	19.7592
	day 10	8.73481(*)	1.76982	.000	2.6619	14.8077
	day 12	5.72481	1.76643	.085	-.3368	11.7864
	day 16	9.12593(*)	1.58122	.000	3.6609	14.5909
	day 18	18.22889(*)	1.48710	.000	13.0428	23.4149
	day 21	36.62963(*)	1.74821	.000	30.6288	42.6305
day 16	day 4	17.13741(*)	2.28108	.000	9.1106	25.1642
	day 6	11.61407(*)	1.54618	.000	6.2760	16.9521
	day 8	3.38333	1.86496	.936	-3.1170	9.8837
	day 10	-.39111	1.47084	1.000	-5.4575	4.6753
	day 12	-3.40111	1.46675	.610	-8.4529	1.6506
	day 14	-9.12593(*)	1.58122	.000	-14.590	-3.6609
	day 18	9.10296(*)	1.11471	.000	5.2695	12.9364
	day 21	27.50370(*)	1.44476	.000	22.5309	32.4766
day 18	day 4	8.03444(*)	2.21687	.041	.1726	15.8963

		day 6	2.51111	1.44978	.961	-2.5382	7.5604
		day 8	-5.71963	1.78585	.111	-12.001	.5624
		day 10	-9.49407(*)	1.36915	.000	-14.248	-4.7396
		day 12	-12.50407(*)	1.36476	.000	-17.242	-7.7657
		day 14	-18.22889(*)	1.48710	.000	-23.414	-13.0428
		day 16	-9.10296(*)	1.11471	.000	-12.936	-5.2695
		day 21	18.40074(*)	1.34109	.000	13.7487	23.0528
	day 21	day 4	-10.36630(*)	2.39985	.004	-18.722	-2.0105
		day 6	-15.88963(*)	1.71657	.000	-21.779	-9.9997
		day 8	-24.12037(*)	2.00849	.000	-31.050	-17.1899
		day 10	-27.89481(*)	1.64903	.000	-33.550	-22.2395
		day 12	-30.90481(*)	1.64539	.000	-36.547	-25.2621
		day 14	-36.62963(*)	1.74821	.000	-42.630	-30.6288
		day 16	-27.50370(*)	1.44476	.000	-32.476	-22.5309
		day 18	-18.40074(*)	1.34109	.000	-23.052	-13.7487
limbus	day 4	day 6	-2.30370	2.00084	1.000	-9.1669	4.5595
		day 8	-11.29000(*)	2.28739	.000	-19.167	-3.4122
		day 10	-19.29185(*)	1.47906	.000	-24.496	-14.0873
		day 12	-19.66926(*)	1.73125	.000	-25.62	-13.7137
		day 14	-24.60815(*)	1.60971	.000	-30.184	-19.0321
		day 16	-14.15259(*)	1.94168	.000	-20.811	-7.4939
		day 18	1.92556	1.57674	1.000	-3.5524	7.4036
		day 21	23.42926(*)	1.78950	.000	17.2838	29.5747
	day 6	day 4	2.30370	2.00084	1.000	-4.5595	9.1669
		day 8	-8.98630(*)	2.34615	.016	-17.052	-.9197
		day 10	-16.98815(*)	1.56840	.000	-22.520	-11.4558
		day 12	-17.36556(*)	1.80817	.000	-23.597	-11.1342
		day 14	-22.30444(*)	1.69217	.000	-28.181	-16.4277
		day 16	-11.84889(*)	2.01056	.000	-18.744	-4.9528
		day 18	4.22926	1.66083	.431	-1.5564	10.0149
		day 21	25.73296(*)	1.86402	.000	19.3230	32.1430
	day 8	day 4	11.29000(*)	2.28739	.000	3.4122	19.1678
		day 6	8.98630(*)	2.34615	.016	.9197	17.0529
		day 10	-8.00185(*)	1.92059	.010	-14.824	-1.1797
		day 12	-8.37926(*)	2.12091	.013	-15.746	-1.0122
		day 14	-13.31815(*)	2.02292	.000	-20.406	-6.2296
		day 16	-2.86259	2.29590	1.000	-10.767	5.0423
		day 18	13.21556(*)	1.99678	.000	6.1977	20.2334
		day 21	34.71926(*)	2.16872	.000	27.2097	42.2288
	day 10	day 4	19.29185(*)	1.47906	.000	14.0873	24.4964
		day 6	16.98815(*)	1.56840	.000	11.4558	22.5205
		day 8	8.00185(*)	1.92059	.010	1.1797	14.8240
		day 12	-.37741	1.20570	1.000	-4.5792	3.8244
		day 14	-5.31630(*)	1.02356	.000	-8.8536	-1.7790
		day 16	5.13926	1.49218	.061	-.1135	10.3920
		day 18	21.21741(*)	.97088	.000	17.8706	24.5643
		day 21	42.72111(*)	1.28794	.000	38.2178	47.2244
	day 12	day 4	19.66926(*)	1.73125	.000	13.7137	25.6248
		day 6	17.36556(*)	1.80817	.000	11.1342	23.5970
		day 8	8.37926(*)	2.12091	.013	1.0122	15.7463
		day 10	.37741	1.20570	1.000	-3.8244	4.5792
		day 14	-4.93889(*)	1.36282	.029	-9.6241	-.2537
		day 16	5.51667	1.74247	.106	-.4790	11.5123

		day 18	21.59481(*)	1.32371	.000	17.0353	26.1544
		day 21	43.09852(*)	1.57111	.000	37.7087	48.4883
	day 14	day 4	24.60815(*)	1.60971	.000	19.0321	30.1841
		day 6	22.30444(*)	1.69217	.000	16.4277	28.1812
		day 8	13.31815(*)	2.02292	.000	6.2296	20.4067
		day 10	5.31630(*)	1.02356	.000	1.7790	8.8536
		day 12	4.93889(*)	1.36282	.029	.2537	9.6241
		day 16	10.45556(*)	1.62178	.000	4.8356	16.0755
		day 18	26.53370(*)	1.16024	.000	22.5536	30.5138
		day 21	48.03741(*)	1.43609	.000	43.0901	52.9848
	day 16	day 4	14.15259(*)	1.94168	.000	7.4939	20.8113
		day 6	11.84889(*)	2.01056	.000	4.9528	18.7449
		day 8	2.86259	2.29590	1.000	-5.0423	10.7675
		day 10	-5.13926	1.49218	.061	-10.392	.1135
		day 12	-5.51667	1.74247	.106	-11.512	.4790
		day 14	-10.45556(*)	1.62178	.000	-16.075	-4.8356
		day 18	16.07815(*)	1.58906	.000	10.5551	21.6012
		day 21	37.58185(*)	1.80036	.000	31.3980	43.7657
	day 18	day 4	-1.92556	1.57674	1.000	-7.4036	3.5524
		day 6	-4.22926	1.66083	.431	-10.014	1.5564
		day 8	-13.21556(*)	1.99678	.000	-20.233	-6.1977
		day 10	-21.21741(*)	.97088	.000	-24.564	-17.8706
		day 12	-21.59481(*)	1.32371	.000	-26.154	-17.0353
		day 14	-26.53370(*)	1.16024	.000	-30.513	-22.5536
		day 16	-16.07815(*)	1.58906	.000	-21.601	-10.5551
		day 21	21.50370(*)	1.39903	.000	16.6725	26.3349
	day 21	day 4	-23.42926(*)	1.78950	.000	-29.574	-17.2838
		day 6	-25.73296(*)	1.86402	.000	-32.143	-19.3230
		day 8	-34.71926(*)	2.16872	.000	-42.228	-27.2097
		day 10	-42.72111(*)	1.28794	.000	-47.224	-38.2178
		day 12	-43.09852(*)	1.57111	.000	-48.488	-37.7087
		day 14	-48.03741(*)	1.43609	.000	-52.984	-43.0901
		day 16	-37.58185(*)	1.80036	.000	-43.765	-31.3980
		day 18	-21.50370(*)	1.39903	.000	-26.334	-16.6725

b) **Multiple Comparisons**

Dependent Variable: number
Dunnett T3

group	(I) region	(J) region	Mean Difference (I-J)	Std. Error	Sig.	95% Confidence Interval	
						Lower Bound	Upper Bound
day 4	centre	periphery	1.24593	2.92677	.964	-5.9659	8.4577
		limbus	6.74667(*)	2.44825	.025	.6869	12.8065
	periphery	centre	-1.24593	2.92677	.964	-8.4577	5.9659
		limbus	5.50074	2.51061	.097	-.7182	11.7197
	limbus	centre	-6.74667(*)	2.44825	.025	-12.8065	-.6869
		periphery	-5.50074	2.51061	.097	-11.7197	.7182
day 6	centre	periphery	-3.13222	2.34781	.461	-8.9482	2.6838
		limbus	5.58815	2.45460	.079	-.4761	11.6524
	periphery	centre	3.13222	2.34781	.461	-2.6838	8.9482
		limbus	8.72037(*)	1.93979	.000	3.9379	13.5028

	limbus	centre	-5.58815	2.45460	.079	-11.6524	.4761
		periphery	-8.72037(*)	1.93979	.000	-13.5028	-3.9379
day 8	centre	periphery	-.47481	2.40965	.996	-6.4130	5.4633
		limbus	7.49000(*)	2.54178	.014	1.2268	13.7532
	periphery	centre	.47481	2.40965	.996	-5.4633	6.4130
		limbus	7.96481(*)	2.46556	.006	1.8875	14.0421
	limbus	centre	-7.49000(*)	2.54178	.014	-13.7532	-1.2268
		periphery	-7.96481(*)	2.46556	.006	-14.0421	-1.8875
day 10	centre	periphery	-2.22444	1.56533	.406	-6.0838	1.6349
		limbus	1.51296	1.17244	.490	-1.4020	4.4279
	periphery	centre	2.22444	1.56533	.406	-1.6349	6.0838
		limbus	3.73741(*)	1.31139	.021	.4657	7.0091
	limbus	centre	-1.51296	1.17244	.490	-4.4279	1.4020
		periphery	-3.73741(*)	1.31139	.021	-7.0091	-.4657
day 12	centre	periphery	-2.51815	1.59059	.314	-6.4385	1.4022
		limbus	3.85185(*)	1.50862	.040	.1346	7.5691
	periphery	centre	2.51815	1.59059	.314	-1.4022	6.4385
		limbus	6.37000(*)	1.58661	.001	2.4594	10.2806
	limbus	centre	-3.85185(*)	1.50862	.040	-7.5691	-.1346
		periphery	-6.37000(*)	1.58661	.001	-10.2806	-2.4594
day 14	centre	periphery	-3.81556(*)	1.48618	.042	-7.5156	-.1155
		limbus	3.34037(*)	1.09534	.011	.6377	6.0430
	periphery	centre	3.81556(*)	1.48618	.042	.1155	7.5156
		limbus	7.15593(*)	1.56850	.000	3.2705	11.0414
	limbus	centre	-3.34037(*)	1.09534	.011	-6.0430	-.6377
		periphery	-7.15593(*)	1.56850	.000	-11.0414	-3.2705
day 16	centre	periphery	-.96481	1.71587	.922	-5.2237	3.2941
		limbus	7.52074(*)	2.02066	.001	2.5412	12.5003
	periphery	centre	.96481	1.71587	.922	-3.2941	5.2237
		limbus	8.48556(*)	1.63409	.000	4.4359	12.5353
	limbus	centre	-7.52074(*)	2.02066	.001	-12.5003	-2.5412
		periphery	-8.48556(*)	1.63409	.000	-12.5353	-4.4359
day 18	centre	periphery	-5.10963(*)	1.07193	.000	-7.7533	-2.4660
		limbus	10.35111(*)	1.13696	.000	7.5495	13.1527
	periphery	centre	5.10963(*)	1.07193	.000	2.4660	7.7533
		limbus	15.46074(*)	1.04758	.000	12.8781	18.0434
	limbus	centre	-10.35111(*)	1.13696	.000	-13.1527	-7.5495
		periphery	-15.46074(*)	1.04758	.000	-18.0434	-12.8781
day 21	centre	periphery	-4.15667(*)	1.48830	.022	-7.8282	-.4852
		limbus	14.40704(*)	1.49336	.000	10.7228	18.0913
	periphery	centre	4.15667(*)	1.48830	.022	.4852	7.8282
		limbus	18.56370(*)	1.63045	.000	14.5463	22.5811
	limbus	centre	-14.40704(*)	1.49336	.000	-18.0913	-10.7228
		periphery	-18.56370(*)	1.63045	.000	-22.5811	-14.5463

* The mean difference is significant at the .05 level.

Chapter 4, section 4.4.3 Immunoblotting for PCNA

One-way ANOVA and Dunnett post-hoc test of log transformed data were performed in SPSS v.12 to compare the normalised band intensities across time points in an attempt to identify significant changes in expression.

Table III.14 Shapiro Wilk results for test of normality of log transformed data (n=3). The mean difference is significant at the 0.05 level.

	Shapiro-Wilk		
	Statistic	df	Sig.
transformed	.951	27	.230

Table III.15 One-way ANOVA results obtained from analysis of the PCNA Western blot. The mean difference is significant at the 0.05 level.

ANOVA

transformed

	Sum of Squares	df	Mean Square	F	Sig.
Between Groups	.548	7	.068	4.605	.003
Within Groups	.268	16	.015		
Total	.815	23			

Table III.16 Levene`s test of homogeneity of variances

transformed

Levene Statistic	df1	df2	Sig.
4.868	7	16	.003

Table III.17 Post-hoc test results obtained from analysis of the chicken PCNA Western blot. The mean difference is significant at the 0.05 level.

Multiple Comparisons

Dependent Variable: transformed
Dunnett T3

(I) ed	(J) ed	Mean Difference (I-J)	Std. Error	Sig.	95% Confidence Interval	
					Lower Bound	Upper Bound
6	8	.04063	.03028	.956	-.1617	.2429
	10	-.18179(*)	.02629	.035	-.3443	-.0193
	12	-.15857(*)	.02097	.021	-.2832	-.0340
	14	.10712	.04149	.540	-.2234	.4376
	16	.20349	.13062	.881	-1.1484	1.5553
	18	.28184	.05507	.167	-.2104	.7741
	21	-.00571	.13677	1.000	-1.4255	1.4141
8	6	-.04063	.03028	.956	-.2429	.1617
	10	-.22243(*)	.03339	.036	-.4239	-.0210
	12	-.19920	.02938	.056	-.4065	.0081
	14	.06648	.04631	.938	-.2299	.3629
	16	.16286	.13223	.961	-1.1325	1.4582
	18	.24120	.05879	.216	-.1911	.6735
	21	-.04634	.13831	1.000	-1.4114	1.3187
10	6	.18179(*)	.02629	.035	.0193	.3443

	8	.22243(*)	.03339	.036	.0210	.4239
	12	.02323	.02525	.998	-.1398	.1862
	14	.28891	.04381	.059	-.0171	.5949
	16	.38528	.13138	.474	-.9390	1.7096
	18	.46363(*)	.05684	.048	.0064	.9209
	21	.17608	.13749	.951	-1.2171	1.5693
12	6	.15857(*)	.02097	.021	.0340	.2832
	8	.19920	.02938	.056	-.0081	.4065
	10	-.02323	.02525	.998	-.1862	.1398
	14	.26568	.04084	.090	-.0759	.6073
	16	.36206	.13042	.515	-.9977	1.7218
	18	.44040	.05458	.067	-.0644	.9452
	21	.15285	.13658	.977	-1.2745	1.5802
14	6	-.10712	.04149	.540	-.4376	.2234
	8	-.06648	.04631	.938	-.3629	.2299
	10	-.28891	.04381	.059	-.5949	.0171
	12	-.26568	.04084	.090	-.6073	.0759
	16	.09637	.13524	1.000	-1.1143	1.3071
	18	.17472	.06527	.478	-.2318	.5812
	21	-.11283	.14119	.999	-1.3941	1.1684
16	6	-.20349	.13062	.881	-1.5553	1.1484
	8	-.16286	.13223	.961	-1.4582	1.1325
	10	-.38528	.13138	.474	-1.7096	.9390
	12	-.36206	.13042	.515	-1.7218	.9977
	14	-.09637	.13524	1.000	-1.3071	1.1143
	18	.07835	.14000	1.000	-1.0391	1.1958
	21	-.20920	.18782	.991	-1.3166	.8982
18	6	-.28184	.05507	.167	-.7741	.2104
	8	-.24120	.05879	.216	-.6735	.1911
	10	-.46363	.05684	.048	-.9209	-.0064
	12	-.44040	.05458	.067	-.9452	.0644
	14	-.17472	.06527	.478	-.5812	.2318
	16	-.07835	.14000	1.000	-1.1958	1.0391
	21	-.28755	.14576	.748	-1.4735	.8984
21	6	.00571	.13677	1.000	-1.4141	1.4255
	8	.04634	.13831	1.000	-1.3187	1.4114
	10	-.17608	.13749	.951	-1.5693	1.2171
	12	-.15285	.13658	.977	-1.5802	1.2745
	14	.11283	.14119	.999	-1.1684	1.3941
	16	.20920	.18782	.991	-.8982	1.3166
	18	.28755	.14576	.748	-.8984	1.4735

* The mean difference is significant at the .05 level.

APPENDIX IV

Table IV.1 Output of microarray controls

Samples:	6.1	6.2	6.3	10.1	10.2	10.3	12.1	12.2	12.3
AFFX-BioB-5_at	123.7[P]	194.2[P]	217.1[P]	142.2[P]	238.3[P]	238.1[P]	133.3[P]	235.7[P]	205.1[P]
AFFX-BioB-3_at	159.6[P]	190[P]	219.3[P]	135.5[P]	244.9[P]	211.9[P]	142.5[P]	218.9[P]	201.7[P]
AFFX-BioC-5_at	383.8[P]	512.5[P]	566.9[P]	359.3[P]	704[P]	609.8[P]	358.1[P]	663.1[P]	623.1[P]
AFFX-BioC-3_at	498.1[P]	648.4[P]	733.6[P]	407.3[P]	861.5[P]	775[P]	428.5[P]	900.3[P]	782.9[P]
AFFX-BioDn-5_at	922.7[P]	1140.7[P]	1353.6[P]	810.5[P]	1597.9[P]	1437.6[P]	831.2[P]	1580.7[P]	1442.3[P]
AFFX-BioDn-3_at	1494.5[P]	2002.1[P]	2304.2[P]	1315.1[P]	2553.5[P]	2190.1[P]	1357.1[P]	2598.4[P]	2398[P]
AFFX-CreX-5_at	4383.2[P]	6170.2[P]	7107.9[P]	4087.1[P]	8084.2[P]	7134.3[P]	4163.2[P]	7791.1[P]	7062[P]
AFFX-CreX-3_at	4896.9[P]	6351.3[P]	7784.2[P]	4812[P]	9021[P]	8169.9[P]	4847.4[P]	9163.1[P]	8111.2[P]
AFFX-Gga-gapdh-5_a_at	6121.6	9944.9	11533.6	6582.4	10897.9	10710	6265.6	11264	10670.2
AFFX-Gga-gapdh-M_a_at	5842.9	8961.5	10740.5	6288.8	10659.7	10388	6710.1	11106	10433.1
AFFX-Gga-gapdh-3_a_at	6282.1	10467.7	12262.3	7230.3	11659.1	12026	7070.1	12125.5	10765.9
AFFX-Gga-actin-5_a_at	3590.2	5717.2	6469	2664.8	4287.1	3850.9	2535.1	3852.2	3348
AFFX-Gga-actin-M_at	3985.4	7284.4	7498	3113.9	5467.8	4913.4	3025.9	4943.3	4295.4
AFFX-Gga-actin-3_at	5854.1	10716.4	10407.9	4990.5	8940.3	7882.6	4417.6	7987.8	6907.3
Gapdh 3'/5'	1.02622	1.05257	1.063181	1.09843	1.06985	1.1229	1.1284	1.07648	1.00897
Actin 3'/5'	1.630578	1.874414	1.6088885	1.872748	2.085396	2.04695	1.74257	2.073568	2.063112
AFFX-LysX-M_at	46.8	46.8	46.8	46.8	46.8	46.8	46.8	46.8	46.8
AFFX-PheX-M_at	72.8	61.2	60.2	56	45.9	61.9	57.8	46.2	51.4
AFFX-ThrX-M_at	93.6	86.1	89	58.3	62.8	58.9	46	66.9	65.9
AFFX-DapX-M_at	520.5	353.6	456.1	336.3	319.3	389	324.3	346.2	386.3

Samples:	14.1	14.2	14.3	16.1	16.2	16.3	18.1	18.2	18.3	21.1	21.2	21.3
AFFX-BioB-5_at	154.3[P]	241.9[P]	217.3[P]	130.6[P]	261.3[P]	202.2[P]	117.7[P]	221[P]	166.5[P]	157[P]	223.3[P]	170.9[P]
AFFX-BioB-3_at	148[P]	221.3[P]	208.3[P]	139.3[P]	256.7[P]	211.8[P]	155.1[P]	288.4[P]	172.3[P]	183.9[P]	296.7[P]	220.5[P]
AFFX-BioC-5_at	413.6[P]	649.8[P]	545.9[P]	393.8[P]	665.6[P]	494.5[P]	364.7[P]	640.2[P]	458.9[P]	427.7[P]	674.1[P]	458[P]
AFFX-BioC-3_at	472.3[P]	719.1[P]	701.9[P]	439.9[P]	868[P]	610.7[P]	439.6[P]	712.2[P]	467.6[P]	492.9[P]	724[P]	563.6[P]
AFFX-BioDn-5_at	911.5[P]	1378.1[P]	1318.8[P]	878.5[P]	1597.9[P]	1228.8[P]	961.9[P]	1493.2[P]	1048.5[P]	1081.8[P]	1505.9[P]	1151.3[P]
AFFX-BioDn-3_at	1486.3[P]	2049.2[P]	2064.1[P]	1384.9[P]	2836.1[P]	2091.3[P]	1663.6[P]	2471.5[P]	1809.9[P]	1848.4[P]	2595.7[P]	1907.2[P]
AFFX-CreX-5_at	4738.5[P]	7753.6[P]	7029.1[P]	4677.2[P]	8191.6[P]	6567.3[P]	5064.6[P]	7376.6[P]	6085.2[P]	5974.3[P]	7655.6[P]	6804.1[P]
AFFX-CreX-3_at	5368.4[P]	8124.4[P]	8205.7[P]	5469.5[P]	9342.7[P]	7801.2[P]	5969[P]	8693.3[P]	7057.9[P]	7119.9[P]	8841[P]	7445.8[P]
AFFX-Gga-gapdh-5_a_at	7101.5	11713	11309.1	7370.5	12023.9	10446	7958.9	11834.2	10520.4	6121.6	11158.2	10650.5
AFFX-Gga-gapdh-M_a_at	7112.7	11207.4	11088.1	7434.2	11797.8	10099	8194.6	10894.4	10166	5842.9	10390.7	9353.6
AFFX-Gga-gapdh-3_a_at	7520.1	13028.9	12074.8	7862.4	12589.8	10485	8755.6	12638.5	11687.6	6282.1	12366.8	11266
AFFX-Gga-actin-5_a_at	2256.4	3356.9	3219	2324.4	3594	2375.6	2476.9	3344.4	2375.3	3590.2	2335.7	1921.1
AFFX-Gga-actin-M_at	2638.5	4128.4	4087.4	2893.4	4495.5	3211.9	3063.8	4229.7	3612.2	3985.4	3324.8	2724
AFFX-Gga-actin-3_at	4137.3	6481.5	6871.9	4352	7322.1	5656.3	4644.4	6006.5	5302.5	5854.1	5495.5	4252.7
Gapdh 3'/5'	1.05895	1.11235	1.067707	1.06674	1.04706	1.0037	1.1001	1.06796	1.11095	1.026219	1.108315	1.057791
Actin 3'/5'	1.833584	1.930799	2.1347934	1.872311	2.037312	2.380998	1.87509	1.795987	2.23235	1.6305777	2.3528278	2.2136797
AFFX-LysX-M_at	46.8	46.8	46.8	46.8	46.8	46.8	46.8	46.8	46.8	46.8	46.8	46.8
AFFX-PheX-M_at	58.5	67.8	64.8	42.5	46.1	79.2	60.7	69	50.5	94.7	61.5	61.4
AFFX-ThrX-M_at	67.8	92	70.3	55.6	68.9	85.4	72	74.6	80.9	107.2	99.8	94.5
AFFX-DapX-M_at	426.1	416.7	391.1	377.8	359.5	534.2	438.1	390.6	495.5	669.7	534.4	526.7

APPENDIX V

Table V.1 Functional groups of genes involved in the regulation of differentiation. Genes may appear in more than one group if they have more than one term associated with them (continued overleaf)

Functional group 1 Nerve Growth Factor Receptor (NGF-R)

Enrichment score 21.79

	GO term	p-value
Biological process	Nervous system development	9.7E-15
	Neurogenesis	3.0E-20
	Axonogenesis	4.3E-20
	Neurite development	1.2E-19
	Neuron differentiation	1.7E-18
Molecular function	Receptor binding	2.2E-6
Cell component	Cytoplasmic membrane	4.8E-2

Affymetrix ID	Gene name	Gene symbol	Unigene ID
GgaAffx.7932.1.S1_at	nerve growth factor receptor (tnfr superfamily, member 16)	**Ngfr**	GGA.39799
Gga.696.1.A1_at, Gga.696.1.S1_at	brain-derived neurotrophic factor	**Bdnf**	GGA.696
GgaAffx.11073.1.S1_at	neurotrophin 3	**Ntf3**	Gga.41617
Gga.4032.1.S1_at	neuropilin 1	**Nrp1**	GGA.4032
Gga.5163.1.S1_at	nerve growth factor, beta polypeptide	**Ngfb**	GGA.5163
Gga.651.1.S1_at	ephrin-a5	**Efna5**	GGA.651
Gga.766.1.S1_at	sema domain, immunoglobulin domain (ig), transmembrane domain (tm) and short cytoplasmic domain, (semaphorin) 4d	**Sema4d**	GGA.766
Gga.2142.1.S1_at	ephrin-b1	**Efnb1**	GGA.2142
Gga.487.1.S1_at	sema domain, immunoglobulin domain (ig), short basic domain, secreted, (semaphorin) 3a	**Sema3a**	GGA.487

Functional group 2 Bone Morphogenetic Proteins (BMP)

Enrichment score 19.83

	GO term	p-value
Biological process	Skeletal development	1.0E-9
	Cartilage development	1.9E-5
	Negative regulation of signal transduction	4.3E-7
	Cell surface receptor linked signal transduction	1.2E-4
	BMP signalling pathway	1.5E-5
Molecular function	Receptor activity	4.3E-2

Affymetrix ID	Gene name	Gene symbol	Unigene ID
Gga.449.1.S1_at	noggin	**Nog**	GGA.449
Gga.4723.1.S1_at	leukocyte cell derived chemotaxin 1	**Lect1**	GGA.4723
Gga.4213.1.S1_at Gga.4213.1.S2_at	twisted gastrulation homolog 1 (drosophila)	**Twsg1**	GGA.4213
Gga.10863.1.S1_s_at Gga.686.1.S1_at	bone morphogenetic protein 4	**Bmp4**	GGA.686
Gga.607.1.S1_at	bone morphogenetic protein receptor, type ib	**Bmpr1b**	GGA.607
Gga.4955.1.S1_at	frizzled-related protein	**Frzb**	GGA.4955

Functional group 3 Transcription Regulators

Enrichment score 17.41

	GO term	p-value
Biological process	Regulation of transcription DNA-dependant	7.2E-22
	RNA biosynthetic process	1.0E-21
	Regulation of cellular metabolic process	6.6E-20
	Regulation of nucleobase, nucleoside, nucleotide and nucleic acid metabolic process	2.4E-20
Molecular function	DNA binding	7.3E-22
Cell component	Nucleus	1.2E-14
	Intracellular membrane-bound organelle	1.3E-11

Affymetrix ID	Gene name	Gene symbol	Unigene ID
Gga.961.2.S1_a_at	t-box 5	**Tbx5**	GGA.961
Gga.3754.2.S1_at	hairy and enhancer of split 1, (drosophila)	**Hes1**	GGA.3754

Gga.281.1.S1_at	v-maf musculoaponeurotic fibrosarcoma oncogene homolog f (avian)	**Maff**	GGA.281
Gga.750.1.S1_at	myogenic differentiation 1	**Myod1**	GGA.750
Gga.8.1.S1_at	myogenin (myogenic factor 4)	**Myog**	GGA.8
Gga.379.1.S1_at	myogenic factor 5	**Myf5**	GGA.379
Gga.608.1.S1_at	myogenic factor 6 (herculin)	**Myf6**	GGA.608
Gga.4285.1.S1_at	ccaat/enhancer binding protein (c/ebp), beta	**Cepbp**	GGA.4285
Gga.4418.1.S1_at	interferon regulatory factor 8	**Irf8**	GGA.4418
Gga.570.1.S1_at	neurogenic differentiation 4	**Neurod4**	GGA.570
Gga.6758.1.S1_s_at Gga.752.1.S1_at	t-cell acute lymphocytic leukemia 1	**Tal1**	GGA.752
Gga.3795.1.S1_at	sry (sex determining region y)-box 3	**Sox3**	GGA.3795
GgaAffx.11738.1.S1_s_at	early growth response 1	**Egr1**	GGA.4922
Gga.511.1.S1_at	t-cell leukemia homeobox 1	**Tlx1**	GGA.511
GgaAffx.20591.2.S1_s_at	sry (sex determining region y)-box 10	**Sox10**	GGA.4428
Gga.11154.1.S1_s_at Gga.8567.1.S1_at GgaAffx.20135.1.S1_s_at GgaAffx.20135.1.S1_at	Signal transducer and activator of transcription 3 (acute-phase response factor)	**Stat3**	GGA.32114
Gga.1840.1.S1_at	neurogenic differentiation 1	**Neurod1**	GGA.1840
GgaAffx.11567.1.S1_at GgaAffx.11567.1.S1_s_at	endothelial differentiation-related factor 1	**Edf1**	GGA.4585
Gga.745.1.S1_at	gata binding protein 2	**Gata2**	GGA.745
Gga.614.1.S1_at	gli protein	**Gli1**	GGA.614
Gga.13567.1.S1_at Gga.13567.1.S1_s_at	t-cell leukemia homeobox 3	**Tlx3**	GGA.21135
GgaAffx.6770.1.S1_at	similar to dmrt-like family b with proline-rich c-terminal, 1	**Dmrtb1**	GGA.30315
Gga.260.1.S1_a_at Gga.260.5.S1_a_at Gga.260.6.A1_at Gga.260.6.S1_at Gga.260.7.S1_x_at GgaAffx.6391.2.S1_s_at Gga.260.7.A1_a_at Gga.260.6.S1_a_at Gga.260.2.S1_a_at	ankyrin repeat domain 15	**Ankrd15**	GGA.260

Functional group 4 Semaphorin/CD100 antigen

Enrichment score 16.01

	GO term	p-value
Biological process	Nervous system development	1.1E-7
	Regulation of neurogenesis	5.4E-21
	Develomental protein	1.1E-5
Molecular function	Receptor activity	3.1E-2

Affymetrix ID	Gene name	Gene symbol	Unigene ID
Gga.766.1.S1_at	sema domain, immunoglobulin domain (ig), transmembrane domain (tm) and short cytoplasmic domain, (semaphorin) 4d	**Sema4d**	GGA.766
Gga.1846.1.S1_at Gga.1846.1.S2_at	sema domain, immunoglobulin domain (ig), short basic domain, secreted, (semaphorin) 3c	**Sema3c**	GGA.1846
Gga.487.1.S1_at	sema domain, immunoglobulin domain (ig), short basic domain, secreted, (semaphorin) 3a	**Sema3a**	GGA.487
Gga.3972.1.S1_at Gga.3972.1.S2_at	sema domain, immunoglobulin domain (ig), short basic domain, secreted, (semaphorin) 3d	**Sema3d**	GGA.3972
Gga.136.1.S1_at	sema domain, immunoglobulin domain (ig), short basic domain, secreted, (semaphorin) 3e	**Sema3e**	GGA.136

Functional group 5 Growth Factors

Enrichment score 15.46

	GO term	p-value
Biological process	Angiogenesis	4.0E-5
	Blood vessel morphogenesis	8.5E-5
	Regulation of cellular metabolic process	6.6E-20
	Regulation of progression through cell cycle	4.9E-4
Molecular function	Heparin binding	5.5E-9
	Glycosaminoglycan binding	3.5E-8
	Polisaccharide binding	4.9E-8

Affymetrix ID	Gene name	Gene symbol	Unigene ID
Gga.5002.1.S1_at	midkine (neurite growth-promoting factor 2)	**Mdk**	GGA.5002
Gga.648.1.S2_at	fibroblast growth factor 1 (acidic)	**Fgf1**	GGA.648
Gga.537.2.S1_a_at	vascular endothelial growth factor	**Vegfa**	GGA.537
Gga.17040.2.S1_a_at	fibroblast growth factor 2 (basic)	**Fgf2**	GGA.17040

Functional group 6 Frizzled-Related Protein (sFRP)

Enrichment score 13.5

	GO term	p-value
Biological process	Wnt receptor signalling pathway	2.4E-4
	Somitogenesis	2.5E-3
	Segmentation	3.6E-3
	Anterior/posterior pattern formation	7.6E-3
	Embryonic development ending in birth or egg hatching	1.2E-2
	Cell surface receptor linked signal transduction	3.0E-2

Affymetrix ID	Gene name	Gene symbol	Unigene ID
Gga.4345.1.S1_at	secreted frizzled-related protein 2	**Sfrp2**	GGA.4345
Gga.4830.1.S1_at Gga.4830.1.S2_at	secreted frizzled-related protein 1	**Sfrp1**	GGA.4830
Gga.136.1.S1_at	sema domain, immunoglobulin domain (ig), short basic domain, secreted, (semaphorin) 3e	**Sema3e**	GGA.136
Gga.4955.1.S1_at	frizzled-related protein	**Frzb**	GGA.4955

Functional group 7 Epidermal Growth Factors-like (EGFs-like)

Enrichment score 7.52

	GO term	p-value
Biological process	Cell differentiation	1.3E-4
	Noch signalling pathway	6.1E-3
Molecular function	Calcium ion binding	1.6E-4

Affymetrix ID	Gene name	Gene symbol	Unigene ID
Gga.2000.1.S1_at GgaAffx.20384.1.S1_at	slit homolog 3 (drosophila)	**Slit3**	GGA.2000
Gga.909.1.S1_at	slit homolog 2 (drosophila)	**Slit2**	GGA.909
Gga.2283.1.S1_at	delta-like 1 (drosophila)	**Dll1**	GGA.2283
Gga.182.1.S1_at Gga.9548.1.S1_at GgaAffx.1586.1.S1_at Gga.3837.1.S1_at Gga.16356.1.S1_at	Notch homolog 1, translocation-associated (drosophila)	**Notch 1**	GGA.9548

Functional group 8 Transforming Growth Factors Beta-like (TGFβ-like)

Enrichment score 6.86

	GO term	p-value
Molecular function	Growth factor activity	1.3E-6
	Receptor biinding	3.8E-5

Affymetrix ID	Gene name	Gene symbol	Unigene ID
Gga.3403.1.S1_at Gga.3403.1.S2_at	growth differentiation factor 5 (cartilage-derived morphogenetic protein-1)	**Gdf5**	GGA.3403
Gga.811.1.S1_at	growth differentiation factor 2	**Gdf2**	GGA.811
Gga.13143.1.S1_at GgaAffx.20103.1.S1_s_at	growth differentiation factor 9	**Gdf9**	GGA.13143
Gga.4324.2.S1_a_at	growth differentiation factor 3	**Gdf3**	GGA.4324

Functional group 9 Kinase type family

Enrichment score 4.93

	GO term	p-value
Biological process	Enzyme linked receptor protein signalling pathway	2.7E-9
	Protein amino acid phosphorylation	5.7E-8
	Ribonucleotide binding	6.8E-6
	Eye development	1.8E-2
	Blood vessel development	3.2E-2
Molecular function	Protein kinase activity	1.6E-8
	Phosphotransferase activity, alcohol group as acceptor	4.0E-8
	ATP binding	2.1E-6
Cellular component	Intristic to membrane	1.6E-8

Affymetrix ID	Gene name	Gene symbol	Unigene ID
Gga.2833.1.S1_at	salt-inducible kinase 1	**Sik1**	GGA.2833
Gga.509.1.S1_at	neurotrophic tyrosine kinase, receptor, type 3	**Ntrk3**	GGA.509
Gga.150.1.S1_at Gga.150.2.S1_a_at Gga.150.2.S2_at	fms-related tyrosine kinase 1 (vascular endothelial growth factor/vascular permeability factor receptor)	**Flt1**	GGA.150
Gga.681.1.S1_at Gga.681.2.S1_a_at	neurotrophic tyrosine kinase, receptor, type 2	**Ntrk2**	GGA.681
Gga.607.1.S1_at	bone morphogenetic protein receptor, type ib	**Bmpr1b**	GGA.607

Gga.5483.1.S1_s_at GgaAffx.2058.2.S1_at GgaAffx.2058.1.S1_s_at GgaAffx.2058.1.S1_at	conserved helix-loop-helix ubiquitous kinase	**RCJMB04_19H23**	GGA.5483
Gga.16413.1.A1_a_at Gga.16413.3.S1_at Gga.16413.1.A1_at	fibroblast growth factor receptor 3 (achondroplasia, thanatophoric dwarfism)	**Fgfr3**	GGA.16413

Functional group 10 G-protein Coupled Receptor Family (GPCRs)

Enrichment score 1.6

	GO term	p-value
Biological process	G-protein coupled receptor protein signalling pathway	1.4E-4
	Cell surface receptor inked signal transduction	5.3E-4
Molecular function	Transmembrane receptor activity	2.2E-6
	G-protein coupled receptor activity	3.5E-5
	Rhodopsin-like receptor activity	2.1E-5
Cellular component	Intristic to membrane	1.5E-3

Affymetrix ID	**Gene name**	**Gene symbol**	**Unigene ID**
GgaAffx.8514.1.S1_at	similar to sphingosine 1-phosphate receptor edg-6 (s1p receptor edg-6) (endothelial differentiation g-protein coupled receptor 6)	**Edg6**	GGA.41534
GgaAffx.6752.1.S1_at	similar to endothelial differentiation, sphingolipid g-protein-coupled receptor, 3; s1p receptor edg3; g protein-coupled receptor, endothelial differentiation gene-3; sphingosine 1-phosphate receptor 3; chromosome 9 open reading frame 47 ...	**Edg3**	GGA.26638
Gga.9756.1.S1_at	endothelial differentiation, lysophosphatidic acid g-protein-coupled receptor, 2	**Edg2**	GGA.9756
Gga.13269.1.S1_at	endothelial differentiation, sphingolipid g-protein-coupled receptor, 1	**Edg1**	GGA.13269
GgaAffx.5710.1.S1_at GgaAffx.5710.2.S1_s_at GgaAffx.5710.2.S1_at	similar to olfactory receptor olr461; similar to olfactory receptor mor260-5	**LOC417291**	GGA.31961
Gga.17397.1.S1_at GgaAffx.3703.1.S1_at	myeloid differentiation primary response gene (88)	**RCJMB04_14H3**	GGA.17397

Table V.2 Unclustered genes involved in regulation of differentiation. Gene name, symbol and Unigene database reference ID are listed.

Affymetrix ID	Gene name	Gene symbol	Unigene ID
GgaAffx.8847.1.S1_at	similar to histone-lysine n-methyltransferase, h3 lysine-9 specific 2 (histone h3-k9 methyltransferase 2) (h3-k9-hmtase 2) (suppressor of variegation 3-9 homolog 2) (su(var)3-9 homolog 2)	RCJMB04_5F7	GGA.13450
GgaAffx.7399.1.S1_at	gli-kruppel family member gli2	Gli2	GGA.4969
GgaAffx.20135.1.S1_at Gga.11154.1.S1_s_at GgaAffx.20135.1.S1_s_at	signal transducer and activator of transcription 3 (acute-phase response factor)	RCJMB04_38L20	GGA.32114
Gga.13567.1.S1_s_at	ribosomal protein l17	Tlx3	GGA.4385
Gga.3982.1.S2_at	inhibin, beta a (activin a, activin ab alpha polypeptide)	Inhba	GGA.3982
GgaAffx.11073.1.S1_at	neurotrophin 3 swi/snf related, matrix associated, actin dependent regulator of chromatin, subfamily b, member 1	Ntf3	GGA.41617
Gga.4349.1.S1_s_at Gga.4349.2.S1_s_at	swi/snf related, matrix associated, actin dependent regulator of chromatin, subfamily b, member 1	RCJMB04_13F19	GGA.8558
Gga.3689.2.S1_a_at	histone deacetylase 4	Hdac4	GGA.3689
Gga.3707.1.S1_a_at Gga.3707.2.A1_at	ccaat/enhancer binding protein (c/ebp), gamma	Cepbg	GGA.3707
Gga.1057.1.S1_at	nuclear factor of kappa light polypeptide gene enhancer in b-cells 2 (p49/p100)	Nfkb2	GGA.1057
GgaAffx.21048.1.S1_s_at GgaAffx.24927.1.S1_s_at	development and differentiation enhancing factor 1	Ddef1	GGA.20746
GgaAffx.12873.1.S1_at	spermatid perinuclear rna binding protein	RCJMB04_25E3	GGA.22384
Gga.1960.2.S1_a_at	myoglobin	Mb	GGA.1960
Gga.135.2.S1_a_at Gga.135.2.S1_at Gga.135.3.S1_a_at	neuregulin 1	Nrg1	GGA.135
Gga.6399.1.S1_at	mal, t-cell differentiation protein-like	Mall	GGA.6399
Gga.3615.1.S1_at Gga.3615.1.S2_at	follistatin	Fst	GGA.3615
Gga.7667.1.S1_at GgaAffx.12403.1.S1_s_at	pdz and lim domain 7	Pdlim7	GGA.7667
Gga.473.1.S1_at	indian hedgehog homolog (drosophila)	Ihh	GGA.473
Gga.4783.1.S2_at GgaAffx.20356.1.S1_s_at	radical fringe	Rfng	GGA.4783
Gga.3168.1.S1_a_at Gga.3168.2.S2_at	quaking homolog, kh domain rna binding (mouse)	Qki	GGA.3168
Gga.2396.1.S1_at	b-cell translocation gene 1, anti-proliferative	Btg1	GGA.2396
Gga.3311.1.S1_at Gga.12322.1.S1_at GgaAffx.3505.1.S1_at GgaAffx.3520.1.S1_at GgaAffx.3517.1.S1_at GgaAffx.3551.1.S1_at	neurofibromin 1 (neurofibromatosis, von recklinghausen disease, watson disease)	Nf1	GGA.3311
Gga.1962.2.S1_a_at GgaAffx.8715.1.S1_s_at GgaAffx.8716.1.S1_s_at GgaAffx.24252.1.S1_s_at GgaAffx.24252.1.S1_at	similar to erythroid differentiation-related factor 1	LOC430674	GGA.31156
Gga.16196.1.S1_at	keratin 14 (epidermolysis bullosa simplex, dowling-meara, koebner)	Krt14	GGA.16196
Gga.11892.1.S1_s_at Gga.3126.1.S1_at	platelet-activating factor acetylhydrolase, isoform ib, alpha subunit	Pafah1b1	GGA.3126
Gga.2396.1.S1_at	b-cell translocation gene 1, anti-proliferative	Btg1	GGA.2396
Gga.16469.1.S1_at GgaAffx.9985.1.S1_s_at GgaAffx.20531.1.S1_s_at	similar to regulator of differentiation (in s. pombe) 1	Rod1	GGA.20566
Gga.13567.1.S1_s_at	ribosomal protein l17	Tlx3	GGA.21135
Gga.9093.1.S1_a_at Gga.9093.3.S1_a_at	drebrin 1	Dbn1	GGA.9093
Gga.239.1.S1_at	tolloid-like 1	Tll1	GGA.239
Gga.651.1.S2_at Gga.651.1.S2_s_at	ephrin-A5	Efna5	GGA.651

Gga.3147.1.S1_at	myosin vi	**Myo6**	GGA.3147
Gga.2458.1.S1_at GgaAffx.21710.1.S1_s_at	interferon-related developmental regulator 1	**Ifrd1**	GGA.2458
Gga.3039.1.S1_at GgaAffx.22277.1.S1_s_at	cyclin d1	**Ccnd1**	GGA.3039
Gga.377.1.S1_at	neural src interacting protein, long form	**Ldb1**	GGA.377
Gga.8015.1.S1_at	development and differentiation enhancing factor	**Ddef2**	GGA.35857
Gga.12231.1.S1_at Gga.12231.2.S1_s_at Gga.12231.2.S1_at	similar to differentiation-associated na-dependent inorganic phosphate cotr; differentiation-associated na-dependent inorganic phosphate cotransporter	**LOC422972**	GGA.12231
GgaAffx.3720.1.S1_at	similar to prepro bone inducing protein	**Gdf10**	GGA.12231
Gga.15179.1.S1_at	development and differentiation enhancing factor 2	**Ddef2**	GGA.35857
Gga.540.1.S1_at	matrix gla protein	**Mgp**	GGA.540
Gga.10980.2.S1_at Gga.10980.1.S1_at Gga.10980.2.S1_s_at GgaAffx.22148.2.S1_s_at	similar to bm426j14.1 (pregnancy-associated plasma protein a)	**Pappa**	GGA.10980
Gga.3136.1.S1_at	syndecan 3 (n-syndecan)	**Sdc3**	GGA.3136
Gga.701.1.S1_s_at	similar to rsfr	**LOC396194**	GGA.703
Gga.701.1.S1_s_at Gga.703.1.S1_at	ribonuclease a/angiogenin	**Rsfr**	GGA.701
Gga.9529.1.S1_s_at GgaAffx.24741.1.S1_at	ganglioside-induced differentiation-associated protein 1	**Gdap1**	GGA.9529
Gga.9831.1.S1_at	Ganglioside-induced differentiation-associated protein 1-like 1	**Gdap1l1**	GGA.30627
Gga.853.1.S1_at	ciliary neurotrophic factor	**Cntf**	GGA.853
GgaAffx.22982.1.S1_at	transforming growth factor, beta 2	**Tgfb2**	GGA.12932
Gga.10652.1.S1_at Gga.14211.1.S1_at	similar to neurogenic locus notch homolog protein 2 precursor (notch 2) (hn2)	**LOC424378**	GGA.10652
Gga.4462.1.S1_at GgaAffx.23937.1.S1_s_at	myosin, heavy polypeptide 9, non-muscle	**Myh9**	GGA.4462
Gga.18916.1.S1_at GgaAffx.20944.1.S1_at	notch homolog 2 (drosophila)	**Notch2**	GGA.18916
GgaAffx.8715.2.S1_at	similar to erythroid differentiation-related factor 1	**LOC430674**	GGA.31156
Gga.16564.1.S1_a_at Gga.16564.2.S1_s_at Gga.16564.3.S1_s_at	ribosomal protein sa	**Rpsa**	GGA.16564
Gga.2494.1.S1_at Gga.2494.1.S2_at	xanthine dehydrogenase	**Xdh**	GGA.2494
Gga.11320.1.S1_s_at	tyrosine protein kinase	**p56lck**	GGA.11320
GgaAffx.21489.1.S1_s_at GgaAffx.8793.1.S1_s_at	transducin (beta)-like 1x-linked receptor 1	**RCJMB04_8J10**	GGA.20641
Gga.6665.1.A1_at GgaAffx.5387.1.S1_at	mal, T-cell differentiation protein	**Mal**	GGA.29846
Gga.17936.1.S1_at	sema domain, immunoglobulin domain (Ig), short basic domain, secreted, (semaphorin) 3D	**Sema3d**	GGA.3972
GgaAffx.20498.1.S1_s_at	monocyte to macrophage differentiation-associated	**RCJMB04_11O17**	GGA.5197
GgaAffx.24252.1.S1_s_at	similar to erythroid differentiation-related factor 1	**LOC430674**	GGA.31156
GgaAffx.26163.1.S1_at	ganglioside-induced differentiation-associated protein 1-like 1	**Gdap1l1**	GGA.30627
GgaAffx.2775.1.S1_s_at	pappalysin 2	**Pappa2**	429071
GgaAffx.5498.1.S1_at	endothelial differentiation, lysophosphatidic acid G-protein-coupled receptor, 7	**Edg7**	GGA.47476
Gga.3569.1.S1_a_at	dihydropyrimidinase-like 2	**Dpysl2**	GGA.3569
GgaAffx.11482.1.S1_s_at GgaAffx.20273.1.S1_s_at	phosphatidylserine receptor	**RCJMB04_1M8**	GGA.21114
GgaAffx.3230.1.S1_at	cell cycle exit and neuronal differentiation 1	**Cend1**	GGA.30146
Gga.5769.1.S1_at	yip1 domain family, member 3	**Yipf3**	GGA.5769
GgaAffx.20430.1.S1_at	Ephrin-A5	**Efna5**	GGA.651
Gga.184.1.S1_a_at	chondroitin sulfate proteoglycan 5 (neuroglycan c)	**Cspg5**	GGA.184

Gga.665.1.S1_at	cysteine and glycine-rich protein 2	**Csrp2**	GGA.665
Gga.19170.1.S1_s_at GgaAffx.21764.1.S1_at GgaAffx.21764.1.S1_s_at	zinc finger protein 403	**Ggnbp2**	GGA.19170
Gga.1095.1.S1_at	signal transducer and activator of transcription 5b	**Stat5b**	GGA.1095
Gga.7938.2.S1_a_at	similar to progestin and adipoq receptor family member x	**Mmd2**	GGA.7938
GgaAffx.8850.1.S1_s_at	dna cross-link repair 1c (pso2 homolog, s. cerevisiae)	**Dclre1c**	GGA.22874
GgaAffx.24331.1.S1_s_at	ndrg family protein member 3	**Ndrg3**	GGA.39122
Gga.9906.1.S1_at	meteorin, glial cell differentiation regulator-like	**Metrln**	GGA.9906
Gga.12707.1.S1_s_at Gga.14179.1.S1_at	development and differentiation enhancing factor 1	**Ddef1**	GGA.35879
Gga.345.1.S1_at	sonic hedgehog homolog (drosophila)	**Shh**	GGA.345
Gga.5133.1.S1_at	deleted in azoospermia-like	**Dazl**	GGA.5133
Gga.12508.1.S1_at	similar to ganglioside-induced differentiation-associated-protein 2	**Gdap2**	GGA.12508
GgaAffx.9584.1.S1_at	adipose differentiation-related protein	**RCJMB04_4D23**	GGA.22793
GgaAffx.7753.1.S1_at	neurogenic differentiation factor 6 (neurod6) (my051 protein)	**Neurod6**	GGA.26741
Gga.13269.1.S1_at	Sphingosine-1-phosphate Receptor 1	**S1pr1**	GGA.13269
GgaAffx.11995.1.S1_at GgaAffx.11995.1.S1_s_at	basic leucine zipper and w2 domains 2	**Bzw2**	GGA.7693
GgaAffx.5026.1.S1_at	leukemia inhibitory factor (cholinergic differentiation factor)	**Lif**	GGA.427718
Gga.3768.1.S1_s_at Gga.5610.1.A1_at GgaAffx.12327.1.S1_at GgaAffx.20199.1.S1_s_at Gga.3768.2.S1_at	rcd1 required for cell differentiation1 homolog (s. pombe)	**Rqcd1**	GGA.3768
Gga.8737.1.S1_at	mal, t-cell differentiation protein 2	**Mal2**	GGA.8737

Table V.3 Functional groups of genes involved in regulation of proliferation. Genes may appear in more than one group if they have more than one term associated with them (continued overleaf)

Functional group 1 Growth Factors

Enrichment score 13.64

	GO term	p-value
Biological process	Regulation of progression through cell cycle	3.1E-10
	Regulation of cell cycle	3.3E-10
Molecular function	Receptor binding	4.3E-8
	Growth factor activity	1.4E-10

Affymetrix ID	Gene name	Gene symbol	Unigene ID
Gga.1907.1.S1_at	platelet derived growth factor c	**Pdgfc**	GGA.1907
GgaAffx.4716.1.S1_at	fibroblast growth factor 4 (heparin secretory transforming protein 1, kaposi sarcoma oncogene)	**Fgf4**	GGA.32086
Gga.71.1.S1_at	platelet-derived growth factor beta polypeptide (simian sarcoma viral (v-sis) oncogene homolog)	**Pdgfb**	GGA.71
Gga.2701.1.S1_at Gga.2701.1.S2_at	fibroblast growth factor 3 (murine mammary tumor virus integration site (v-int-2) oncogene homolog)	**Fgf3**	GGA.2701
Gga.3219.1.S1_at	c-fos induced growth factor (vascular endothelial growth factor d)	**Figf**	GGA.3219
Gga.3899.1.S1_a_at Gga.3899.3.S1_a_at	platelet-derived growth factor alpha polypeptide	**Pdgfa**	GGA.3899

Functional group 2 Transcription Regulators

Enrichment score 9.94

	GO term	p-value
Biological process	Regulation of transcription, DNA-dependant	2.0E-7
	RNA biosynthetic process	2.2E-7
	Regulation of nucleobase, nucleoside, nucleotide and nucleic acid metabolic process	6.1E-7
	System development	2.3E-6
	Biopolymer metabolic process	2.4E-4
Molecular function	DNA binding	1.2E-5
Cell component	Intracellular membrane-bound organelle	3.5E-4
	Nucleus	3.8E-5

Affymetrix ID	Gene name	Gene symbol	Unigene ID
Gga.17307.1.S1_at Gga.6791.1.A1_s_at Gga.709.2.S1_a_at	nuclear factor i/b	**Nfib**	GGA.709
Gga.289.1.S1_at	ceh-10 homeodomain containing homolog (c. elegans)	**Vsx2**	GGA.289
Gga.961.1.S1_at Gga.961.2.S1_at Gga.961.2.S1_a_at	t-box 5	**Tbx5**	GGA.961
Gga.4349.1.S1_s_at Gga.4349.2.S1_s_at	swi/snf related, matrix associated, actin dependent regulator of chromatin, subfamily b, member 1	**RCJMB04_13F19**	GGA.8558
Gga.3689.2.S1_a_at	histone deacetylase 4	**Hdac4**	GGA.3689
Gga.4131.1.S1_at	homeobox protein hoxd13	**Hoxg13**	GGA.4131
Gga.570.1.S1_at	neurogenic differentiation 4	**Neurod4**	GGA.570
Gga.511.1.S1_at	t-cell leukemia homeobox 1	**Tlx1**	GGA.511

Functional group 3 Growth Factors

Enrichment score 9.42

	GO term	p-value
Biological process	Regulation of cell cycle	1.3E-7
	Organ morphogenesis	1.5E-7
	Angiogenesis	4.5E-7
	Specification of organ identity	1.7E-6
	Cell-cell signalling during cell fate commitment	1.7E-6
	Sensory organ development	3.1E-2
Molecular function	Glycosaminoglycan binding	3.4E-7
	Heparin binding	5.5E-8
	Growth factor activity	1.4E-10
	Receptor binding	4.3E-8

Affymetrix ID	Gene name	Gene symbol	Unigene ID
Gga.661.1.S1_at	fibroblast growth factor 8	**Fgf8**	GGA.661
Gga.2701.1.S1_at Gga.2701.1.S2_at	fibroblast growth factor 3 (murine mammary tumor virus integration site (v-int-2) oncogene homolog)	**Fgf3**	GGA.2701
Gga.5002.1.S1_at	midkine (neurite growth-promoting factor 2)	**Mdk**	GGA.5002
Gga.648.1.S2_at	fibroblast growth factor 1 (acidic)	**Fgf1**	GGA.648
Gga.537.2.S1_a_at	vascular endothelial growth factor	**Vegfa**	GGA.537
Gga.17040.2.S1_a_at	fibroblast growth factor 2 (basic)	**Fgf2**	GGA.39646

Table V.4 Unclustered genes involved in regulation of proliferation. Gene name, symbol and Unigene database reference ID are listed.

Affymetrix ID	Gene name	Gene symbol	Unigene ID
GgaAffx.6863.1.S1_at	epigen	**Epgn**	GGA.22922
Gga.3027.1.S1_at	cd40 ligand (tnf superfamily, member 5, hyper-igm syndrome)	**Cd40lg**	GGA.3027
Gga.122.2.S1_a_at Gga.6790.1.A1_at	craniofacial development protein 1	**Cfdp1**	GGA.122
Gga.4969.1.S1_at GgaAffx.7399.1.S1_at	gli-kruppel family member gli2	**Gli2**	GGA.4969
Gga.196.1.S1_at	nibrin	**Nbn**	GGA.196
Gga.1065.1.S1_at	guanine nucleotide binding protein (g protein), alpha inhibiting activity polypeptide 2	**Gnai2**	GGA.1065
Gga.473.1.S1_at	indian hedgehog homolog (drosophila	**Ihh**	GGA.473
GgaAffx.26679.1.S1_at	similar to proliferation-associated protein 1	**Pa2g4**	
GgaAffx.11558.1.S1_s_at	nude nuclear distribution gene e homolog 1 (a. nidulans)	**Nde1**	GGA.22352
Gga.8771.1.S1_at	fibroblast growth factor receptor-like 1	**Fgfrl1**	GGA.8771
Gga.3754.1.S1_a_at Gga.3754.2.S1_at	hairy and enhancer of split 1, (drosophila)	**Hes1**	GGA.3754
Gga.2396.1.S1_at	b-cell translocation gene 1, anti-proliferative	**Btg1**	GGA.2396
GgaAffx.1.1.S1_s_at	nuclear factor of kappa light polypeptide gene enhancer in b-cells inhibitor, alpha	**Nfkbia**	GGA.2937
Gga.15747.1.S1_at GgaAffx.20937.1.S1_at Gga.15747.2.S1_s_at	similar to androgen-induced prostate proliferative shutoff associated protein; androgen-induced shutoff 3	**RCJMB04_6G19**	GGA.15747
GgaAffx.23500.1.S1_s_at GgaAffx.23500.1.S1_at	inhibin, alpha	**Inha**	GGA.6881
Gga.723.1.S1_a_at	cd28 antigen (tp44)	**Cd28**	GGA.723
Gga.11892.1.S1_s_at Gga.3126.1.S1_at	platelet-activating factor acetylhydrolase, isoform ib, alpha subunit 45kda	**Pafah1b1**	GGA.3126
Gga.12097.1.S1_s_at GgaAffx.24932.3.S1_s_at	polymerase (dna directed), alpha	**Pola1**	GGA.12097
Gga.1250.1.S1_at Gga.1250.1.S2_at	protein phosphatase 1, catalytic subunit, beta isoform	**Ppp1cb**	GGA.1250
GgaAffx.8915.1.S1_at	xylosylprotein beta 1,4-galactosyltransferase, polypeptide 7	**B4galt7**	GGA.33756
Gga.1095.1.S1_at	signal transducer and activator of transcription 5b	**Stat5b**	GGA.1095
GgaAffx.23427.1.S1_s_at GgaAffx.23427.1.S1_at Gga.15420.1.S1_at	signal-induced proliferation-associated 1 like 2	**Sipa1l2**	GGA.20062
Gga.4970.1.S1_at	cd3e antigen, epsilon polypeptide (tit3 complex)	**Cd3e**	GGA.4970
Gga.12636.1.A1_at Gga.4847.1.S1_x_at Gga.4847.3.S1_a_at	nucleophosmin	**Npm1**	GGA.4847
Gga.4390.2.S1_a_at Gga.4390.4.S1_s_at Gga.4390.4.S1_a_at	ferritin, heavy polypeptide 1	**Fth1**	GGA.4390
Gga.15420.1.S1_at GgaAffx.23427.2.S1_at GgaAffx.23427.2.S1_s_at Gga.20062.1.S1_s_at	signal-induced proliferation-associated 1 like 2	**Sipa1l2**	GGA.20062
Gga.6791.1.A1_at	nuclear factor I/B	**Nfib**	GGA.709
Gga.109.1.S1_at	frizzled homolog 10 (drosophila)	**Fzd10**	GGA.109
Gga.696.1.A1_at Gga.696.1.S1_at	brain-derived neurotrophic factor	**Bdnf**	GGA.696
Gga.1479.1.S1_at Gga.1479.2.S1_a_at	pleiotrophin (heparin binding growth factor 8, neurite growth-promoting factor 1)	**Ptn**	GGA.39450
Gga.345.1.S1_at	sonic hedgehog homolog (drosophila)	**Shh**	GGA.345
Gga.1861.1.S1_at	mago-nashi homolog, proliferation-associated (drosophila)	**Magoh**	GGA.1861
Gga.895.1.S1_at	s100 calcium binding protein a6 (calcyclin)	**S100a6**	GGA.22951
GgaAffx.22982.1.S1_at	transforming growth factor, beta 2	**Tgfb2**	GGA.12932
Gga.7066.1.S1_at	signal-induced proliferation-associated 1 like 1	**Sipa1l1**	GGA.29067

Gga.6276.3.S1_at GgaAffx.22359.1.S1_at GgaAffx.22359.1.S1_s_at Gga.6276.3.S1_s_at	pescadillo homolog 1, containing BRCT domain (zebrafish)	**Gal3st1**	GGA.6276
Gga.705.1.S1_at	progesterone receptor	**Pgr**	GGA.705
GgaAffx.13116.1.S1_at	rap1b, member of ras oncogene family	**Rap1b**	GGA.18937
Gga.355.1.S1_at	cerberus 1, cysteine knot superfamily, homolog (xenopus laevis)	**Cer1**	GGA.355
Gga.3849.1.S1_at	v-ha-ras harvey rat sarcoma viral oncogene homolog	**Hras**	GGA.3849
Gga.1686.1.S1_s_at GgaAffx.21450.2.S1_s_at	transforming growth factor, beta 3	**Tgfb3**	GGA.1686
GgaAffx.21801.1.S1_at	thrombopoietin	**Thpo**	GGA.21063
Gga.1479.1.S1_at Gga.1479.2.S1_a_at	Pleiotrophin	**Ptn**	GGA.39450
Gga.16413.1.A1_a_at Gga.16413.1.A1_at Gga.16413.3.S1_at	fibroblast growth factor receptor 3 (achondroplasia, thanatophoric dwarfism)	**Fgfr3**	GGA.16413

Table V.5 Genes that belong to the gene ontology clusters related to regulation of apoptosis. Genes may appear in more than one group if they have more than one term associated with them (continued overleaf)

Functional group 1 Bcl-2 Related Apotosis Regulators

Enrichment score 100.73

	GO term	p-value
Biological process	Programmed cell death	2.6E-38
	Regulation of apoptosis	5.4E-28
Molecular function	Zinc ion binding	2.2E-2
	Transition metal ion binding	4.5E-2

Affymetrix ID	Gene name	Gene symbol	Unigene ID
Gga.4846.1.S1_at Gga.4846.1.S2_at	anti-apoptotic nr13	**LOC395193**	GGA.4846
Gga.3811.1.S1_at Gga.3811.1.S2_at	bcl2-related ovarian killer	**Bok**	GGA.3811
GgaAffx.11795.1.S1_s_at	apaf1 interacting protein	**RCJMB04_5F12**	GGA.22458
Gga.1234.1.S1_s_at	bh3 interacting domain death agonist	**Bid**	GGA.1234
Gga.5164.1.S1_at	bcl2-related protein a1	**Bcl2a1**	GGA.5164
Gga.16560.1.S1_at Gga.16560.2.S1_a_at Gga.16560.2.S1_s_at	myeloid cell leukemia sequence 1 (bcl2-related)	**Mcl1**	GGA.16560
GgaAffx.3610.1.S1_at GgaAffx.3610.4.S1_s_at GgaAffx.3610.4.S1_at GgaAffx.3610.2.S1_s_at	similar to baculoviral iap repeat-containing protein 4 (inhibitor of apoptosis protein 3) (x-linked inhibitor of apoptosis protein) (x-linked iap) (iap-like protein) (hilp)	**LOC419239**	GGA.23967
Gga.10125.1.S1_a_at GgaAffx.23776.1.S1_at	similar to fas apoptotic inhibitory molecule 1 (rfaim)	**Faim**	GGA.39768
Gga.12655.1.S1_at Gga.12655.2.S1_at	tnf receptor-associated factor 3	**Traf3**	GGA.12655
GgaAffx.7095.1.S1_at GgaAffx.7095.2.S1_at GgaAffx.7095.1.S1_s_at	programmed cell death 2	**Pdcd2**	GGA.21558
Gga.16457.1.S1_s_at GgaAffx.23449.1.S1_at	interferon induced with helicase c domain 1	**Ifih1**	GGA.16457
GgaAffx.23578.1.S1_at	similar to apoptotic protease activating factor 1 (apaf-1)	**Apaf1**	GGA.34905
Gga.1729.1.S1_at	bcl2-like 13 (apoptosis facilitator)	**Bcl2l13**	GGA.1729
Gga.11428.1.S1_at Gga.2796.1.S1_ at	b-cell cll/lymphoma 10	**Bcl10**	GGA.11428
GgaAffx.7894.1.S1_at GgaAffx.7894.2.S1_at	similar to caspase recruitment domain protein 10; card-containing maguk 3 protein; bcl10 binding protein and activator of nfkb	**Card10**	GGA.25961

Gga.7057.1.S1_at GgaAffx.13169.1.S1_s_at GgaAffx.26202.1.S1_at	caspase recruitment domain family, member 11	**Card11**	GGA.7057
Gga.10782.1.S1_at	similar to mort1	**Fadd**	GGA.10782
Gga.12955.1.S1_at GgaAffx.25775.1.S1_at	bcl2-antagonist/killer	**RCJMB04_3P2**	GGA.12955
Gga.5708.2.S1_a_at	similar to riken cdna 1110007c09	**LOC415987**	GGA.5708
GgaAffx.12782.1.S1_s_at	programmed cell death 10	**Pdcd10**	GGA.6335
Gga.4304.1.S1_at	dna fragmentation factor, 40kda, beta polypeptide (caspase-activated dnase)	**Dffb**	GGA.4304
GgaAffx.1822.1.S1_at	similar to dna fragmentation factor alpha subunit (dna fragmentation factor 45 kda subunit) (dff-45) (inhibitor of cad) (icad)	**Dffa**	GGA.41944
Gga.16931.1.S1_at	bcl2-associated athanogene 4	**Bag4**	GGA.16931

Functional group 2 Inhibitor Apoptosis Proteins (IAP)

Enrichment score 43.77

	GO term	p-value
Biological process	Negative regulation of apoptosis	4.9E-14
	Anti-apoptosis	3.3E-11
Molecular function	Zinc ion binding	4.2E-4
	Transition metal ion binding	1.1E-3
Cellular component	Cytoplasm	1.4E-2

Affymetrix ID	**Gene name**	**Gene symbol**	**Unigene ID**
Gga.4384.1.S1_at Gga.4384.1.S2_at Gga.4384.1.S2_s_at	baculoviral iap repeat-containing 2	**Birc2**	GGA.4384
Gga.104.1.S1_at	baculoviral iap repeat-containing 4	**Birc4**	GGA.104
Gga.122.2.S1_a_at Gga.6790.1.A1_at	craniofacial development protein 1	**Cfdp1**	GGA.122
GgaAffx.11795.1.S1_s_at	apaf1 interacting protein	**RCJMB04_5F12**	GGA.22458
Gga.5127.1.S1_s_at GgaAffx.12475.1.S1_at	tnf receptor-associated factor 5	**Traf5**	GGA.5127
GgaAffx.13009.1.S1_at GgaAffx.13009.1.S1_s_at	tumor necrosis factor, alpha-induced protein 8	**RCJMB04_29H8**	GGA.11736
Gga.5885.1.S1_s_at GgaAffx.11374.1.S1_at	apoptosis inhibitor 5	**Api5**	GGA.5885

GgaAffx.3610.1.S1_at GgaAffx.3610.4.S1_at GgaAffx.3610.4.S1_s_at GgaAffx.3610.2.S1_s_at	similar to baculoviral iap repeat-containing protein 4 (inhibitor of apoptosis protein 3) (x-linked inhibitor of apoptosis protein) (x-linked iap) (iap-like protein) (hilp)	**LOC419239**	GGA.23967
Gga.10125.1.S1_a_at GgaAffx.23776.1.S1_at	similar to fas apoptotic inhibitory molecule 1 (rfaim)	**Faim**	GGA.39768
Gga.12655.1.S1_at Gga.12655.2.S1_at	tnf receptor-associated factor 3	**Traf3**	GGA.12655

Functional group 3 Bcl-2 Related Apoptosis Agonists

Enrichment score 36.9

	GO term	p-value
Biological process	Positive regulation of apoptosis	1.4E-7
Cellular component	Mitochondrial envelope	3.8E-2

Affymetrix ID	Gene name	Gene symbol	Unigene ID
Gga.2008.1.S1_at Gga.2008.2.S1_a_at	bcl2/adenovirus e1b 19kda interacting protein 3	**Bnip3**	GGA.2008
Gga.1234.1.S1_s_at	bh3 interacting domain death agonist	**Bid**	GGA.1234
GgaAffx.11837.1.S1_s_at	bcl2/adenovirus e1b 19kda interacting protein 3-like	**Bnip3l**	GGA.22016
Gga.9467.1.S1_at	integral membrane protein 2b	**Itm2b**	GGA.9467

Functional group 4 Phosphotransferase activity

Enrichment score 36.22

	GO term	p-value
Biological process	Regulation of apoptosis	3.2E-3
Molecular function	ATP binding	2.1E-6
	Ribonucleotide binding	6.8E-6
	Protein kinase activity	2.5E-4
	Transferase activity, alcohol group as acceptor	1.6E-4
	Transferase activity, transferring phosphorus-containing groups	4.4E-4

Affymetrix ID	Gene name	Gene symbol	Unigene ID
GgaAffx.23578.1.S1_at	apoptotic protease activating factor 1 (apaf-1)	**Apaf1**	GGA.34905
Gga.16457.1.S1_s_at GgaAffx.23449.1.S1_at	interferon induced with helicase c domain 1	**Ifih1**	GGA.16457
GgaAffx.10124.2.S1_at GgaAffx.12451.1.S1_s_at GgaAffx.10124.2.S1_s_at	receptor-interacting serine-threonine kinase 2	**RCJMB04_15N4**	GGA.22379
GgaAffx.4315.1.S1_at	similar to apoptosis-associated tyrosine kinase	**LOC422076**	GGA.30387
Gga.7702.1.S1_at	similar to cell cycle progression 2 protein	**Tbrg4**	GGA.31062
Gga.11617.1.S1_at	similar to hypothetical protein mgc5297	**Fastkd3**	GGA.11617
GgaAffx.6171.1.S1_at GgaAffx.6171.2.S1_s_at	similar to hypothetical protein flj21901	**Fastkd1**	GGA.22679

Functional group 5 Tumor Necrosis Factor Receptor (TNF-R)

Enrichment score 35.59

	GO term	p-value
Biological process	Cell death	1.1E-5
	Signal transduction	8.4E-3
Molecular function	Transmembrane receptor activity	4.0E-4

Affymetrix ID	Gene name	Gene symbol	Unigene ID
Gga.100.1.S1_a_at	fas (tnf receptor superfamily, member 6)	**Fas**	GGA.100
Gga.5148.1.S1_at Gga.5148.1.S1_s_at GgaAffx.12029.1.S1_at Gga.5148.1.S2_s_at	tumor necrosis factor receptor superfamily, member 1b	**Tnfrsf1b**	GGA.5148
Gga.197.1.S1_at	cd40 antigen (tnf receptor superfamily member 5)	**Cd40**	GGA.197
Gga.8546.1.S1_a_at Gga.8546.2.S1_at	death domain-containing tumor necrosis factor receptor superfamily member 23	**LOC378902**	GGA.8546

Functional group 6 Caspase Apoptosis Regulators

Enrichment score 28.45

	GO term	p-value
Biological process	Programmed cell death	6.9E-16
	Proteolysis	8.7E-12
	Cellular protein metabolic process	2.1E-6
Molecular function	Caspase activity	1.3E-27
	Cysteine-type endopeptidase activity	5.1E-21

Affymetrix ID	Gene name	Gene symbol	Unigene ID
Gga.2960.1.S1_at	caspase 6, apoptosis-related cysteine peptidase	**Casp6**	GGA.2960
Gga.4346.1.S1_at Gga.4346.1.S2_at	caspase 3, apoptosis-related cysteine peptidase	**Casp3**	GGA.4346
GgaAffx.5264.1.S1_at	initiator caspase	**Casp18**	GGA.32077
GgaAffx.7181.1.S1_at	similar to cell death adaptor molecule	**RCJMB04_16C14**	GGA.22811
Gga.504.1.S1_at Gga.14486.1.S1_at	caspase 2, apoptosis-related cysteine peptidase (neural precursor cell expressed, developmentally down-regulated 2)	**Casp2**	GGA.504
Gga.2451.1.S1_at	caspase 8, apoptosis-related cysteine peptidase	**Casp8**	GGA.2451
Gga.4116.1.S1_at	caspase 9, apoptosis-related cysteine protease	**Casp9**	GGA.4116
GgaAffx.5246.1.S1_at	similar to casp10 protein	**Casp10**	GGA.39974
GgaAffx.5618.1.S1_at	caspase-7, apoptosis-related cysteine peptidase	**Casp7**	GGA.39052
Gga.10204.1.S1_s_at Gga.1747.2.S1_a_at	caspase 1, apoptosis-related cysteine peptidase (interleukin 1, beta, convertase)	**Casp1**	GGA.1747

Functional group 7 Kinase Family

Enrichment score 20.63

	GO term	p-value
Biological process	Phosphate metabolic process	4.0E-7
	Post-translational protein modification	1.3E-6
	Protein amino acid phosphorylation	5.7E-8
Molecular function	Protein serine/threonine kinase activity	1.0E-5
	Transferase activity, transferring phosphorus groups	1.9E-7
	Ribonucleotide binding	6.8E-6

Affymetrix ID	Gene name	Gene symbol	Unigene ID
Gga.14403.1.S1_at GgaAffx.12794.1.S1_at Gga.14403.1.S1_s_at	dual-specificity tyrosine-(Y)-phosphorylation regulated kinase 2	**Dyrk2**	GGA.14403
Gga.15820.1.S1_s_at GgaAffx.12533.1.S1_at	serine/threonine kinase 4	**RCJMB04_17l1**	GGA.15820
Gga.9012.1.S1_at GgaAffx.11653.1.S1_s_at	serine/threonine kinase 17b (apoptosis-inducing)	**RCJMB04_3F1**	GGA.9012
GgaAffx.4315.1.S1_at	similar to apoptosis-associated tyrosine kinase	**LOC422076**	GGA.30387
Gga.685.1.S1_at Gga.685.2.S1_at Gga.685.3.A1_at Gga.685.1.S2_at	v-raf-1 murine leukemia viral oncogene homolog 1	**Raf1**	GGA.685
Gga.3580.1.S1_at Gga.3580.2.S1_a_at GgaAffx.2310.1.S1_at	insulin receptor precursor	**Insr**	GGA.3580
GgaAffx.10124.2.S1_at GgaAffx.12451.1.S1_s_at GgaAffx.10124.2.S1_s_at	receptor-interacting serine-threonine kinase 2	**RCJMB04_15N4**	GGA.22379

Functional group 8 Transcription Regulators

Enrichment score 29.58

	GO term	p-value
Biological process	Positive regulation of transcription DNA-dependant	2.4E-9
	Regulation of nucleobase, nucleoside, nucleotide and nucleic acid metabolic process	1.0E-8
	RNA biosynthetic process	2.8E-9
	Biopolymer metabolic process	2.2E-5
Cellular component	Intracellular membrane bound organelle	7.2E-4
	Nucleus	8.7E-4
	Cytoplasm	8.1E-3

Affymetrix ID	Gene name	Gene symbol	Unigene ID
Gga.961.1.S1_at Gga.961.2.S1_a_at Gga.961.2.S1_at	t-box 5	**Tbx5**	GGA.961
Gga.3982.1.S1_at Gga.3982.1.S2_at	inhibin, beta a (activin a, activin ab alpha polypeptide)	**Inhba**	GGA.3982
Gga.706.1.S1_at	tumor protein p53	**Tp53**	GGA.706
Gga.4285.1.S1_at	ccaat/enhancer binding protein (c/ebp), beta	**Cebpb**	GGA.706

Gga.4396.1.S1_at	v-rel reticuloendotheliosis viral oncogene homolog (avian)	**Rel**	GGA.4396
GgaAffx.11073.1.S1_at	neurotrophin 3	**Ntf3**	GGA.41617
Gga.3213.1.S1_at	e2f transcription factor 1	**E2f1**	GGA.3213
Gga.7539.1.S1_at	transcription factor foxl2	**Foxl2**	GGA.7539
Gga.48.1.S1_at	d4, zinc and double phd fingers family 2	**Dpf2**	GGA.48
Gga.555.1.S1_at	paired box gene 7	**Pax7**	GGA.555

Functional group 9 Neurotrophin Family

Enrichment score 17.1

	GO term	p-value
Biological process	Axon guidance	2.8E-8
	Axonogenesis	6.7E-8
	Neurite morphogenesis	7.6E-8
	Neuron development	1.3E-7
	Cell part morphogenesis	3.6E-7
	Cell migration	5.1E-7
	Regulation of neuron apoptosis	3.6E-6
Molecular function	Growth factor activity	3.6E-4
	Receptor binding	3.3E-3
Cellular component	Cytoplasmic membrane-bound vesicle	2.9E-2

Affymetrix ID	**Gene name**	**Gene symbol**	**Unigene ID**
GgaAffx.11073.1.S1_at	neurotrophin 3	**Ntf3**	GGA.41617
GgaAffx.22982.1.S1_at	transforming growth factor, beta 2	**Tgfb2**	GGA.12932
Gga.696.1.A1_at Gga.696.1.S1_at	brain-derived neurotrophic factor	**Bdnf**	GGA.696
GgaAffx.7932.1.S1_at	nerve growth factor receptor (tnfr superfamily, member 16)	**Ngfr**	GGA.39799

Table V.6 Unclustered genes involved in regulation of apoptosis. Gene name, symbol and Unigene database reference ID are listed.

Affymetrix ID	Gene name	Gene symbol	Unigene ID
Affx-Gga-gapdh-3_a_at Affx-Gga-gapdh-3_x_at Affx-Gga-gapdh-5_a_at Affx-Gga-gapdh-M_a_at Gga.1374.4.S1_a_at Gaga374.4.S1_x_at	glyceraldehyde-3-phosphate dehydrogenase	**Gapdh**	GGA.1374
Gga.1095.1.S1_at	signal transducer and activator of transcription 5b	**Stat5b**	GGA.1095
Gga.12309.1.S1_at	apoptosis-inducing factor (aif)-like mitochondrion-associated inducer of death	**Aifm2**	GGA.12309
Gga.1551.2.S1_a_at	baculoviral iap repeat-containing 5 (survivin)	**Birc5**	GGA.1551
Gga.1661.1.S1_at Gga.1661.2.S1_s_at Gga.1661.3.S1_s_ at GgaAffx.20215.1.S1_at	engulfment and cell motility 1	**RCJMB04_7b13**	GGA.20205
Gga.17022.1.S1_at	ww domain containing oxidoreductase	**RCJMB04_28b1**	GGA.7638
Gga.17166.1.S1_at	tnf-related apoptosis inducing ligand-like	**Trail-like**	GGA.17166
Gga.17305.1.S1_s_at Gga.2939.1.S1_at	shingomyelin synthase 1	**Sgms1**	GGA.2939
Gga.18742.1.S1_at Gga.18742.1.S1_x_at GgaAffx.22341.1.S1_at GgaAffx.4807.1.S1_s_at	apoptosis inducing factor mitochondrion-associated 3	**Aifm3**	GGA.18742
Gga.189.1.S1_at Gga.189.1.S2_at	protein kinase, dna-activated, catalytic polypeptide	**Prkdc**	GGA.189
Gga.1902.1.S1_at	hypothetical protein		GGA.42092
Gga.2719.1.S2_at Gga.2719.2.S1_a_at	presenlin 2 (alzheimer disease 4)	**Psen2**	GGA.2719
Gga.345.1.S1_at	sonic hedgehog homolog (drosophila)	**Shh**	GGA.345
Gga.3864.1.S1_at Gga.3864.1.S2_at	presenlin 1 (alzheimer disease 3)	**Psen1**	GGA.3864
Gga.4219.1.S1_at	heat shock 70kda protein 5 (glucose-regulated protein, 78kda)	**Hspa5**	GGA.4219
Gga.4394.1.S1_at	b-cell cll/lymphoma 2	**Bcl2**	GGA.4394
Gga.4510.1.S1_a_at	albumin	**Alb**	GGA.4510
Gga.5455.2.S1_s_at Gga Affx.12635.1.S1_s_at	cytokine induced apoptosis ihibitor 1	**Ciapin1**	GGA.5455
Gga.5675.3.S1_A_at	death associated protein 3	**Dap3**	GGA.5675
Gga.673.1.S1_at	insulin	**Ins**	GGA.673
Gga.723.1.S1_A_at	cd28 antigen (tp44)	**Cd28**	GGA.723
Gga.7468.1.S1_at	perp, tp53 apoptosis effector	**Perp**	GGA.7468
Gga.9342.1.S1_at GgaAffx.11935.1.S1_s_at	Apoptosis, caspase activation inhibitor	**Aven**	GGA.9342
Gga.9385.1.S1_A_at	cd27-binding (siva) protein	**Siva1**	GGA.9385
Gga.955.1.A1_at Gga.955.1.S1_at	apoptosis asscociated protein	**Loc395325**	GGA.955
GgaAffx.11281.1.S1_at	similar to death receptor 3	**Loc425564**	GGA.3003
GgaAffx.11604.1.S1_s_at	ras homolog gene family, member T2	**RCJMB04_2o8**	GGA.34587
GgaAffx.11996.1.S1_s_at Ggaaffx.26111.2.S1_s_at	cell division cycle and apoptosis regulator 1	**Ccar1**	GGA.17450
GgaAffx.12955.1.S1_s_at	programmed cell death-2-like	**RCJMB04_27n18**	GGA.5383
GgaAffx.13220.1.S1_s_at Gga.11032.1.A1_at	apoptosis-inducing factor mitochondrion-associated	**Aifm1**	GGA.4923
GgaAffx.25742.1.S1_at	bifunctional apoptosis regulator	**Bfar**	GGA.39205
GgaAffx.3404.1.S1_s_at GGAAFFX.12861.1.S1_s_at	similar to apoptosis antagonizing transcription factor	**Aatf**	GGA.7407
GgaAffx.5200.1.S1_v GgaAffx.5200.2.S1_at GgaAffx.5200.2.S1_s_at	casp8 and fadd-like apoptosis regulator	**Cflar**	GGA.21431

GgaAffx.5947.1.S1_s_at GgaAffx.12756.1.S1_at	bcl2-associated athanogene 3	**Bag3**	GGA.21928
GgaAffx.6512.1.S1_at	similar to prostate apoptosis response protein 4	**Pawr**	GGA.24903
GgaAffx.7315.1.S1_at	bcl2-like14 (apoptosis faciliator)	**Bcl2l14**	GGA.41240
GgaAffx.9801.1.S1_at	thap domain containing, apoptosis associated protein 1	**Thap1**	GGA.27477
Gga.11011.1.S1_at	cell death-inducing dffa-like effector	**Cidea**	GGA.36618
Gga.13392.1.S1_at	similar to riken cdna 1110007c09	**Loc415987**	GGA.5708
Gga.15359.1.S1_ at Gga.15359.1.S1_s_ at	apoptotic peptidase activating factor 1	**Apaf1**	GGA.34905
GGA.17104.1.S1_ at	bcl2-like 15	**Bcl2l15**	GGA.17104
Gga.2345.1.S1_ at Gga.2345.2.S1_a_ at GgaAffx.21274.1.S1_s_ at	Tp53 regulated inhibitor of apoptosis 1	**Triap1**	GGA.2345
Gga.2856.1.S1_a_ at	apoptosis-inducing, taf9-like domain 1	**Apitd1**	GGA.2856
Gga.4367.1.S1_ at	myeloid cell leukaemia sequence 1 (bcl2-related)	**Mcl1**	GGA.34519
Gga.2875.1.S1_at Gga.2875.2.S1_a_at	activin a receptor, type	**Acvr1**	GGA.2875
GgaAffx.1941.1.S1_at	fas ligand (tnf superfamily, member 6)	**Fasl g**	GGA.29896
GgaAffx.11614.1.S1_s_at	ras homolog gene family, member t1	**Rhot1**	GGA.1088
Gga.1247.1.S1_at GgaAffx.12136.1.S1_s_at	b6.1	**Loc396098**	GGA.1247
Gga.1721.1.S1_at	bcl2-associated athanogene 5	**RCJMB04_2E5**	GGA.1721
Gga.4944.1.S2_at Gga.4944.2.S1_a_at Gga.4944.2.A1_at	bcl2-like 1	**Bcl2l1**	GGA.4944
GgaAffx.11482.1.S1_s_at GgaAffx.20273.1.S1_s_at	phosphatidylserine receptor	**RCJMB04_1M8**	GGA.21114
Gga.555.1.S1_at	paired box gene 7	**Pax7**	GGA.555
Gga.2396.1.S1_at	b-cell translocation gene 1, anti-proliferative	**Btg1**	GGA.2396
GgaAffx.23500.1.S1_at GgaAffx.23500.1.S1_s_at	Inhibin, alpha	**Inha**	GGA.6881
GgaAffx.22169.2.S1_at GgaAffx.22169.1.S1_s_at Gga.3605.1.S1_s_at Gga.17273.1.S1_at	similar to optic atrophy 1 isoform 7	**RCJMB04_1M16**	
Gga.48.1.S1_at	d4, zinc and double phd fingers family 2	**Dpf2**	GGA.48
Gga.16137.1.S1_at	bcl2-associated athanogene	**Bag1**	GGA.16137
Gga.11320.1.S1_s_at	tyrosine protein kinase	**P56LCK**	GGA.11320
Gga.4960.1.S1_at	defender against cell death 1	**Dad1**	GGA.4960
Gga.16413.1.A1_a_at Gga.16413.3.S1_at Gga.16413.1.A1_at	fibroblast growth factor receptor 3 (achondroplasia) thanatophoric (dwarfism)	**Fgfr3**	GGA.16413

Table V.7 Differentially expressed genes identified for each developmental time point when compared to ED6 baseline and involved in regulation of biological processes (continued overleaf)

ED6 versus ED10

Affymetrix ID	Gene name	Gene symbol	Unigene ID	Fold change
Differentiation				
Gga.4723.1.S1_at	leukocyte cell derived chemotaxin 1	**Lect1**	GGA.4723	-3.1
Gga.2833.1.S1_at	salt-inducible kinase 1	**Sik1**	GGA.2833	2
Proliferation				
Gga.3219.1.S1_at	c-fos induced growth factor (vascular endothelial growth factor d)	**Figf**	GGA.3219	-2.3
GgaAffx.11558.1.S1_s_at	nudE nuclear distribution gene E homolog 1 (A. nidulans)	**Nde1**	GGA.22352	-1.5
GgaAffx.1.1.S1_s_at	Nuclear Factor Of Kappa Light Polypeptide Gene Enhancer In B-cells Inhibitor, Alpha	**Nfkbia**	GGA.41891	2.4
Gga.895.1.S1_at	S100 calcium binding protein A6	**S100a6**	GGA.22951	1.4

ED6 versus ED12

Affymetrix ID	Gene name	Gene symbol	Unigene ID	Fold change
Differentiation				
Gga.4285.1.S1_at	ccaat/enhancer binding protein (c/ebp), beta	**Cebpb**	GGA.706	2.2
GgaAffx.11738.1.S1_s_at	early growth response 1	**Egr1**	GGA.4922	3.2
Gga.3754.2.S1_at Gga.3754.1.S1_a_at	hairy and enhancer of split 1, (drosophila)	**Hes1**	GGA.3754	1.6
Gga.2833.1.S1_at	salt-inducible kinase 1	**Sik1**	GGA.2833	3.3
Proliferation				
Gga.3219.1.S1_at	c-fos induced growth factor (vascular endothelial growth factor d)	**Figf**	GGA.3219	-2.4
Gga.3754.2.S1_at Gga.3754.1.S1_a_at	hairy and enhancer of split 1, (drosophila)	**Hes1**	GGA.3754	1.6
GgaAffx.11558.1.S1_s_at	nudE nuclear distribution gene E homolog 1 (A. nidulans)	**Nde1**	GGA.22352	-1.6
Gga.709.2.S1_a_at	nuclear factor i/b	**Nfib**	GGA.709	2
GgaAffx.1.1.S1_s_at	Nuclear Factor Of Kappa Light Polypeptide Gene Enhancer In B-cells Inhibitor, Alpha	**Nfkbia**	GGA.41891	3.3
GgaAffx.21450.2.S1_s_at	transforming growth factor, beta 3	**Tgfb3**	GGA.1686	1.6
Gga.895.1.S1_at	S100 calcium binding protein A6	**S100a6**	GGA.22951	1.8
Cell death				
Gga.17104.1.S1_at	BCL2-like 15	**Bcl2l15**	GGA.17104	1.7
Gga.4285.1.S1_at	ccaat/enhancer binding protein (c/ebp), beta	**Cebpb**	GGA.706	2.2

ED6 versus ED14

Affymetrix ID	Gene name	Gene symbol	Unigene ID	Fold change
Differentiation				
Gga.4285.1.S1_at	ccaat/enhancer binding protein (c/ebp), beta	**Cebpb**	GGA.706	1.9
Gga.16413.3.S1_at Gga.16413.1.A1_a_at	fibroblast growth factor receptor 3 (achondroplasia, thanatophoric dwarfism)	**Fgfr3**	GGA.16413	1.7
Gga.4723.1.S1_at	leukocyte cell derived chemotaxin 1	**Lect1**	GGA.4723	-2.9
Gga.6399.1.S1_at	mal, T-cell differentiation protein-like	**Mall**	GGA.6399	2.5
Gga.509.1.S1_at	neurotrophic tyrosine kinase, receptor, type 3	**Ntrk3**	GGA.509	1.6
Gga.487.1.S1_at	Sema Domain, Immunoglobulin Domain (Ig), Short Basic Domain, Secreted, (semaphorin) 3A	**Sema3a**	GGA.487	-3.1
Gga.3972.1.S1_at	sema domain, immunoglobulin domain (ig), short basic domain, secreted, (semaphorin) 3d	**Sema3d**	GGA.3972	-2.5
Gga.2833.1.S1_at	salt-inducible kinase 1	**Sik1**	GGA.2833	3.3
Gga.909.1.S1_at	Slit Homolog 2 (Drosophila)	**Slit2**	GGA.909	-1.7
Gga.4213.1.S1_at	twisted gastrulation homolog 1 (drosophila)	**Twsg1**	GGA.4213	
Proliferation				
Gga.16413.3.S1_at Gga.16413.1.A1_a_at	Fibroblast Growth Factor Receptor 3	**Fgfr3**	GGA.16413	1.7
Gga.3219.1.S1_at	c-fos induced growth factor (vascular endothelial growth factor d)	**Figf**	GGA.3219	-2.9
Gga.709.2.S1_a_at	nuclear factor i/b	**Nfib**	GGA.709	1.9
GgaAffx.1.1.S1_s_at	Nuclear Factor Of Kappa Light Polypeptide Gene Enhancer In B-cells Inhibitor, Alpha	**Nfkbia**	GGA.41891	3.7
Gga.1479.1.S1_at Gga.1479.2.S1_a_at	Pleiotrophin	**Ptn**	GGA.39450	-3.6
Gga.895.1.S1_at	S100 calcium binding protein A6	**S100a6**	GGA.22951	1.9
Cell death				
Gga.17104.1.S1_at	BCL2-like 15	**Bcl2l15**	GGA.17104	2.1
Gga.4285.1.S1_at	ccaat/enhancer binding protein (c/ebp), beta	**Cebpb**	GGA.706	1.9
Gga.16413.3.S1_at Gga.16413.1.A1_a_at	Fibroblast Growth Factor Receptor 3	**Fgfr3**	GGA.16413	1.7
Gga.17166.1.S1_at	TNF-related apoptosis inducing ligand-like	**Trail-like**	GGA.17166	1.7

ED6 versus ED16

Affymetrix ID	Gene name	Gene symbol	Unigene ID	Fold change
Differentiation				
Gga.4285.1.S1_at	ccaat/enhancer binding protein (c/ebp), beta	**Cebpb**	GGA.706	1.7
Gga.16413.3.S1_at Gga.16413.1.A1_a_at	fibroblast growth factor receptor 3 (achondroplasia, thanatophoric dwarfism)	**Fgfr3**	GGA.16413	1.9
Gga.4723.1.S1_at	leukocyte cell derived chemotaxin 1	**Lect1**	GGA.4723	-4.3
Gga.6399.1.S1_at	mal, T-cell differentiation protein-like	**Mall**	GGA.6399	4.2
Gga.17397.1.S1_at	myeloid differentiation primary response gene (88)	**Myd88**	GGA.17397	1.6
Gga.135.2.S1_a_at	neuregulin 1	**Nrg1**	GGA.135	1.6
Gga.4032.1.S1_at	neuropilin 1	**Nrp1**	GGA.4032	-1.9
Gga.509.1.S1_at	neurotrophic tyrosine kinase, receptor, type 3	**Ntrk3**	GGA.509	2.2
Gga.487.1.S1_at	Sema Domain, Immunoglobulin Domain (Ig), Short Basic Domain, Secreted, (semaphorin) 3A	**Sema3a**	GGA.487	-3.1
Gga.1846.1.S1_at Gga.1846.1.S2_at	sema domain, immunoglobulin domain (ig), short basic domain, secreted, (semaphorin) 3c	**Sema3c**	GGA.1846	2.1
Gga.3972.1.S1_at	sema domain, immunoglobulin domain (ig), short basic domain, secreted, (semaphorin) 3d	**Sema3d**	GGA.3972	-2.7
Gga.136.1.S1_at	sema domain, immunoglobulin domain (ig), short basic domain, secreted, (semaphorin) 3e	**Sema3e**	GGA.136	2.1
Gga.4345.1.S1_at	Secreted Frizzled-related Protein 2	**Sfrp2**	GGA.4345	-3.2
Gga.2833.1.S1_at	salt-inducible kinase 1	**Sik1**	GGA.2833	3.4
Gga.909.1.S1_at	Slit Homolog 2 (Drosophila)	**Slit2**	GGA.909	-3.3
Proliferation				
GgaAffx.6863.1.S1_at	epithelial mitogen homolog (mouse)	**Epgn**	GGA.22922	2.8
Gga.16413.3.S1_at Gga.16413.1.A1_a_at	Fibroblast Growth Factor Receptor 3	**Fgfr3**	GGA.16413	1.9
Gga.3219.1.S1_at	c-fos induced growth factor (vascular endothelial growth factor d)	**Figf**	GGA.3219	-3.5
GgaAffx.11558.1.S1_s_at	nudE nuclear distribution gene E homolog 1 (A. nidulans)	**Nde1**	GGA.22352	2.8
GgaAffx.1.1.S1_s_at	Nuclear Factor Of Kappa Light Polypeptide Gene Enhancer In B-cells Inhibitor, Alpha	**Nfkbia**	GGA.41891	3.8
Gga.1479.1.S1_at Gga.1479.2.S1_a_at	Pleiotrophin	**Ptn**	GGA.39450	-4
GgaAffx.21450.2.S1_s_at	transforming growth factor, beta 3	**Tgfb3**	GGA.1686	1.7
Gga.895.1.S1_at	S100 calcium binding protein A6	**S100a6**	GGA.22951	2.2

Cell death				
Gga.17104.1.S1_at	BCL2-like 15	**Bcl2l15**	GGA.17104	3
Gga.4384.1.S1_at	baculoviral iap repeat-containing 2	**Birc2**	GGA.4384	2.8
Gga.4285.1.S1_at	ccaat/enhancer binding protein (c/ebp), beta	**Cebpb**	GGA.706	1.7
Gga.16413.3.S1_at Gga.16413.1.A1_a_at	Fibroblast Growth Factor Receptor 3	**Fgfr3**	GGA.16413	1.9
Gga.16560.1.S1_at Gga.16560.2.S1_a_at Gga.16560.2.S1_s_at	myeloid cell leukemia sequence 1 (bcl2-related)	**Mcl1**	GGA.16560	1.8
Gga.7468.1.S1_at	PERP, TP53 Apoptosis Effector	**Perp**	GGA.7468	1.9
Gga.17166.1.S1_at	TNF-related apoptosis inducing ligand-like	**Trail-like**	GGA.17166	1.9

ED6 versus ED18

Affymetrix ID	Gene name	Gene symbol	Unigene ID	Fold change
Differentiation				
Gga.16413.3.S1_at Gga.16413.1.A1_a_at	fibroblast growth factor receptor 3 (achondroplasia, thanatophoric dwarfism)	**Fgfr3**	GGA.16413	2
Gga.4723.1.S1_at	leukocyte cell derived chemotaxin 1	**Lect1**	GGA.4723	-4.4
Gga.6399.1.S1_at	mal, T-cell differentiation protein-like	**Mall**	GGA.6399	4.9
Gga.5002.1.S1_at	midkine (neurite growth-promoting factor 2)	**Mdk**	GGA.5002	-1.9
Gga.17397.1.S1_at	myeloid differentiation primary response gene (88)	**Myd88**	GGA.17397	2.1
Gga.135.2.S1_a_at	Neuregulin 1	**Nrg1**	GGA.135	1.6
Gga.4032.1.S1_at	neuropilin 1	**Nrp1**	GGA.4032	-2.4
Gga.509.1.S1_at	neurotrophic tyrosine kinase, receptor, type 3	**Ntrk3**	GGA.509	2.4
GgaAffx.12403.1.S1_s_at	pdz and lim domain 7 (enigma)	**Pdlim7**	GGA.7667	2.8
Gga.487.1.S1_at	Sema Domain, Immunoglobulin Domain (Ig), Short Basic Domain, Secreted, (semaphorin) 3A	**Sema3a**	GGA.487	-3.1
Gga.1846.1.S1_at Gga.1846.1.S2_at	sema domain, immunoglobulin domain (ig), short basic domain, secreted, (semaphorin) 3c	**Sema3c**	GGA.1846	-2.1
Gga.3972.1.S1_at	sema domain, immunoglobulin domain (ig), short basic domain, secreted, (semaphorin) 3d	**Sema3d**	GGA.3972	-2.9
Gga.136.1.S1_at	sema domain, immunoglobulin domain (ig), short basic domain, secreted, (semaphorin) 3e	**Sema3e**	GGA.136	2.1
Gga.2833.1.S1_at	salt-inducible kinase 1	**Sik1**	GGA.2833	3.2
Gga.4345.1.S1_at	Secreted Frizzled-related Protein 2	**Sfrp2**	GGA.4345	-4.4
Gga.2494.1.S1_at	Xanthine Dehydrogenase	**Xdh**	GGA.2494	1.7

Proliferation				
GgaAffx.6863.1.S1_at	epithelial mitogen homolog (mouse)	**Epgn**	GGA.22922	3.3
Gga.16413.3.S1_at Gga.16413.1.A1_a_at	Fibroblast Growth Factor Receptor 3	**Fgfr3**	GGA.16413	2
Gga.3219.1.S1_at	c-fos induced growth factor (vascular endothelial growth factor d)	**Figf**	GGA.3219	-3.4
Gga.4390.2.S1_a_at	ferritin, heavy polypeptide 1	**Fth1**	GGA.4390	1.6
Gga.5002.1.S1_at	midkine (neurite growth-promoting factor 2)	**Mdk**	GGA.5002	-1.9
GgaAffx.1.1.S1_s_at	Nuclear Factor Of Kappa Light Polypeptide Gene Enhancer In B-cells Inhibitor, Alpha	**Nfkbia**	GGA.41891	3.7
Gga.1479.1.S1_at Gga.1479.2.S1_a_at	Pleiotrophin	**Ptn**	GGA.39450	-4.1
Gga.895.1.S1_at	S100 calcium binding protein A6	**S100a6**	GGA.22951	2.2
GgaAffx.21450.2.S1_s_at	transforming growth factor, beta 3	**Tgfb3**	GGA.1686	1.6
Cell death				
Gga.17104.1.S1_at	BCL2-like 15	**Bcl2l15**	GGA.17104	3
Gga.1234.1.S1_s_at	bh3 interacting domain death agonist	**Bid**	GGA.1234	-1.6
Gga.4384.1.S1_at	baculoviral iap repeat-containing 2	**Birc2**	GGA.4384	2.9
Gga.16413.3.S1_at Gga.16413.1.A1_a_at	Fibroblast Growth Factor Receptor 3	**Fgfr3**	GGA.16413	2
Gga.16560.1.S1_at Gga.16560.2.S1_a_at Gga.16560.2.S1_s_at	myeloid cell leukemia sequence 1 (bcl2-related)	**Mcl1**	GGA.16560	1.7
GgaAffx.6512.1.S1_at	PRKC, apoptosis, WT1, regulator	**Pawr**	GGA.24903	-1.6
Gga.7468.1.S1_at	PERP, TP53 Apoptosis Effector	**Perp**	GGA.7468	2.2
Gga.17166.1.S1_at	TNF-related apoptosis inducing ligand-like	**Trail-like**	GGA.17166	1.7

ED6 versus ED21

Affymetrix ID	Gene name	Gene symbol	Unigene ID	Fold change
Differentiation				
Gga.16413.3.S1_at Gga.16413.1.A1_a_at	fibroblast growth factor receptor 3 (achondroplasia, thanatophoric dwarfism)	**Fgfr3**	GGA.16413	1.8
Gga.4723.1.S1_at	leukocyte cell derived chemotaxin 1	**Lect1**	GGA.4723	-4.7
Gga.6399.1.S1_at	mal, T-cell differentiation protein-like	**Mall**	GGA.6399	5.3
Gga.5002.1.S1_at	midkine (neurite growth-promoting factor 2)	**Mdk**	GGA.5002	-2.7
Gga.17397.1.S1_at	myeloid differentiation primary response gene (88)	**Myd88**	GGA.17397	3
Gga.4032.1.S1_at	neuropilin 1	**Nrp1**	GGA.4032	3.1
Gga.681.1.S1_at Gga.681.2.S1_a_at	neurotrophic tyrosine kinase, receptor, type 2	**Ntrk2**	GGA.681	1.9
Gga.509.1.S1_at	neurotrophic tyrosine kinase, receptor, type 3	**Ntrk3**	GGA.509	1.6
GgaAffx.12403.1.S1_s_at	pdz and lim domain 7 (enigma)	**Pdlim7**	GGA.7667	-2
Gga.487.1.S1_at	Sema Domain, Immunoglobulin Domain (Ig), Short Basic Domain,	**Sema3a**	GGA.487	-2.1

	Secreted, (□emaphoring) 3A			
Gga.1846.1.S1_at Gga.1846.1.S2_at	sema domain, immunoglobulin domain (ig), short basic domain, secreted, (semaphorin) 3c	**Sema3c**	GGA.1846	-2.3
Gga.3972.1.S1_at	sema domain, immunoglobulin domain (ig), short basic domain, secreted, (semaphorin) 3d	**Sema3d**	GGA.3972	-2.8
Gga.136.1.S1_at	sema domain, immunoglobulin domain (ig), short basic domain, secreted, (semaphorin) 3e	**Sema3e**	GGA.136	2
Gga.2833.1.S1_at	salt-inducible kinase 1	**Sik1**	GGA.2833	3.4
Gga.4830.1.S1_at Gga.4830.1.S2_at	Secreted Frizzled-related Protein 1	**Sfrp1**	GGA.4830	-1.9
Gga.4345.1.S1_at	Secreted Frizzled-related Protein 2	**Sfrp2**	GGA.4345	-6.5
Gga.909.1.S1_at	Slit Homolog 2 (Drosophila)	**Slit2**	GGA.909	-4.1
Gga.2494.1.S1_at	Xanthine Dehydrogenase	**Xdh**	GGA.2494	2.5
Proliferation				
GgaAffx.6863.1.S1_at	epithelial mitogen homolog (mouse)	**Epgn**	GGA.22922	3.8
Gga.16413.3.S1_at Gga.16413.1.A1_a_at	Fibroblast Growth Factor Receptor 3	**Fgfr3**	GGA.16413	1.8
Gga.3219.1.S1_at	c-fos induced growth factor (vascular endothelial growth factor d)	**Figf**	GGA.3219	-3.9
Gga.5002.1.S1_at	midkine (neurite growth-promoting factor 2)	**Mdk**	GGA.5002	-2.7
GgaAffx.1.1.S1_s_at	Nuclear Factor Of Kappa Light Polypeptide Gene Enhancer In B-cells Inhibitor, Alpha	**Nfkbia**	GGA.41891	2.8
Gga.71.1.S1_at	platelet-derived growth factor beta polypeptide (simian sarcoma viral (v-sis) oncogene homolog)	**Pdgfb**	GGA.71	-1.6
Gga.1479.1.S1_at Gga.1479.2.S1_a_at	Pleiotrophin	**Ptn**	GGA.39450	-3.9
Gga.895.1.S1_at	S100 calcium binding protein A6	**S100a6**	GGA.22951	2.3
Cell death				
Gga.17104.1.S1_at	BCL2-like 15	**Bcl2l15**	GGA.17104	2.8
Gga.1234.1.S1_s_at	bh3 interacting domain death agonist	**Bid**	GGA.1234	-2.3
Gga.4384.1.S1_at	baculoviral iap repeat-containing 2	**Birc2**	GGA.4384	2
Gga.1551.2.S1_a_at	baculoviral iap repeat-containing 5 (survivin)	**Birc5**	GGA.1551	-1.9
Gga.10204.1.S1_s_at	caspase 1, apoptosis-related cysteine	**Casp1**	GGA.10204	1.8
GgaAffx.5618.1.S1_at	caspase 7, apoptosis-related cysteine peptidase	**Casp7**	GGA.39052	2.3
Gga.16413.3.S1_at Gga.16413.1.A1_a_at	Fibroblast Growth Factor Receptor 3	**Fgfr3**	GGA.16413	1.8
GgaAffx.23449.1.S1_at	Interferon Induced With Helicase C Domain	**Ifih1**	GGA.16457	2.4
Gga.4846.1.S2_at Gga.4846.1.S1_at	anti-apoptotic NR13	**LOC395193**	GGA.43428	1.6
Gga.16560.1.S1_at Gga.16560.2.S1_a_at Gga.16560.2.S1_s_at	myeloid cell leukemia sequence 1 (bcl2-related)	**Mcl1**	GGA.16560	1.7
GgaAffx.6512.1.S1_at	PRKC, apoptosis, WT1, regulator	**Pawr**	GGA.24903	-1.6
Gga.7468.1.S1_at	PERP, TP53 Apoptosis Effector	**Perp**	GGA.7468	2.1

Gga.104.1.S1_at	X-linked inhibitor of apoptosis	**Xiap**	GGA.104	1.8

ED10 versus ED6

Affymetrix ID	Gene name	Gene symbol	Unigene ID	Fold change
Gga.1171.1.S1_at	lymphocyte antigen 6 complex, locus E	**Ly6e**	GGA.1171	1.8
Gga.6070.1.S1_at	prostate stem cell antigen	**Psca**	GGA.6070	4.7
GgaAffx.1.1.S1_s_at	nuclear factor of kappa light polypeptide gene enhancer in B-cells inhibitor, alpha	**Nfkbia**	GGA.41891	2.4
Gga.1899.1.S1_a_at	nestin	**Nes**	GGA.1899	-3.1
Gga.157.1.S1_at	runt-related transcription factor 2	**Runx2**	GGA.157	2.1
Gga.199.1.S1_at	atonal homolog 7 (Drosophila)	**Atoh7**	GGA.199	-3.7

Table V.8 Stem cell-related genes identified within differentially expressed genes in comparison to ED6 and posthatch basline (continued overleaf)

ED10 versus ED21

Affymetrix ID	Gene name	Gene symbol	Unigene ID	Fold change
Gga.1171.1.S1_at	lymphocyte antigen 6 complex, locus E	**Ly6e**	GGA.1171	1.9
Gga.34.1.S1_at	calcium channel, voltage-dependent, gamma subunit 4	**Cacng4**	GGA.34	-2.1
Gga.6070.1.S1_at	prostate stem cell antigen	**Psca**	GGA.6070	3
Gga.16560.2.S1_s_at	myeloid cell □eukaemia sequence 1 (BCL2-related)	**Mcl1**	GGA.34519	1.6
Gga.4846.1.S1_at Gga.4846.1.S2_at	anti-apoptotic NR13	**LOC395193**	GGA.43428	1.5
Gga.3776.1.S1_at	hippocalcin-like 1	**Hpcal1**	GGA.3776	3.6
Gga.13301.1.S1_at	glycerophosphodiester phosphodiesterase domain containing 5	**Gdpd5**	GGA.13301	-2.1
Gga.4982.1.S1_at	Aldolase A	**LOC395492**	GGA.4982	1.4
Gga.7004.1.S1_at	similar to stem cell antigen 2	**LOC420301**	GGA.7004	2.2
Gga.170.1.S1_at Gga.170.1.S2_at	wingless-type MMTV integration site family, member 2B	**Wnt2b**	GGA.170	-3.7
Gga.4058.1.S2_s_at Gga.4058.1.S1_at	Myristoylated alanine-rich C kinase substrate (MARCKS)	**LOC396473**	GGA.4058	-2.7
Gga.9293.1.S1_at Gga.3994.3.S1_x_at	fibronectin 1	**Fn1**	GGA.3994	-3.3
Gga.4046.1.S1_at	Meis homeobox 2	**Meis2**	GGA.4046	-2.4
Gga.4457.1.S1_s_at GgaAffx.11648.1.S1_at	B-cell CLL/lymphoma 6 (zinc finger protein 51)	**Bcl6**	GGA.42204	3.2
Gga.764.1.S1_at	activin A receptor, type IIB	**Acvr2b**	GGA.764	-1.6
Gga.3950.1.S1_at	bone morphogenetic protein 2	**Bmp2**	GGA.3950	-2.3
Gga.2283.1.S2_at	delta-like 1 (Drosophila)	**Dll1**	GGA.2283	-2.6
Gga.4285.1.S1_at	CCAAT/enhancer Binding Protein (C/EBP), Beta	**Cebpb**	GGA.4285	-2.3

Gga.15614.1.S1_a_at	PTK2 protein tyrosine kinase 2	**Ptk2**	GGA.42870	-1.5
Gga.4971.1.S1_at	potassium voltage-gated channel, shaker-related subfamily, beta member 1	**Kcnab1**	GGA.4971	-2

ED12 versus ED6

Affymetrix ID	Gene name	Gene symbol	Unigene ID	Fold change
Gga.9293.1.S1_at Gga.3994.3.S1_x_at	fibronectin 1	**Fn1**	GGA.3994	-2.2
Gga.6070.1.S1_at	prostate stem cell antigen	**Psca**	GGA.6070	5.9
Gga.1171.1.S1_at	lymphocyte antigen 6 complex, locus E	**Ly6e**	GGA.1171	2.7
GgaAffx.1.1.S1_s_at	nuclear factor of kappa light polypeptide gene enhancer in B-cells inhibitor, alpha	**Nfkbia**	GGA.41891	2.5
Gga.1899.1.S1_a_at	nestin	**Nes**	GGA.1899	-4
Gga.199.1.S1_at	atonal homolog 7 (Drosophila)	**Atoh7**	GGA.199	-3.6
Gga.209.2.S1_at Gga.209.1.S1_a_at	wingless-type MMTV integration site family, member 3	**Wnt3**	GGA.209	1.2
GgaAffx.21450.2.S1_s_at	transforming growth factor, beta 3	**Tgfb3**	GGA.42150	1.6
Gga.4457.1.S1_s_at GgaAffx.11648.1.S1_at	B-cell CLL/lymphoma 6 (zinc finger protein 51)	**Bcl6**	GGA.42204	1.7
Gga.758.1.S1_at	LIM homeobox transcription factor 1, beta	**Lmx1b**	GGA.758	-2.4
Gga.488.1.S1_at	achaete-scute complex homolog 1 (Drosophila)	**Ascl1**	GGA.488	-3.9
Gga.4285.1.S1_at	CCAAT/enhancer Binding Protein (C/EBP), Beta	**Cebpb**	GGA.4285	2.2

ED12 versus ED21

Affymetrix ID	Gene name	Gene symbol	Unigene ID	Fold change
Gga.606.1.S1_at	-kit Hardy-Zuckerman 4 feline sarcoma viral oncogene homolog	**Kit**	GGA.606	2.9
Gga.34.1.S1_at	calcium channel, voltage-dependent, gamma subunit 4	**Cacng4**	GGA.34	-1.7
Gga.6070.1.S1_at	prostate stem cell antigen	**Psca**	GGA.6070	1.8
Gga.3776.1.S1_at	hippocalcin-like 1	**Hpcal1**	GGA.3776	2.9
Gga.13301.1.S1_at	glycerophosphodiester phosphodiesterase domain containing 5	**Gdpd5**	GGA.13301	-2.3
Gga.4982.1.S1_at	Aldolase A	**LOC395492**	GGA.4982	1.3
Gga.170.1.S1_at Gga.170.1.S2_at	wingless-type MMTV integration site family, member 2B	**Wnt2b**	GGA.170	-3.2
Gga.4058.1.S2_s_at Gga.4058.1.S1_at	Myristoylated alanine-rich C kinase substrate (MARCKS)	**LOC396473**	GGA.4058	-2.3
Gga.4846.1.S1_at	anti-apoptotic NR13	**LOC395193**	GGA.43428	1.4
Gga.4846.1.S2_at Gga.4046.1.S1_at	Meis homeobox 2	**Meis2**	GGA.4046	-1.9

Gga.4457.1.S1_s_at GgaAffx.11648.1.S1_at	B-cell CLL/lymphoma 6 (zinc finger protein 51)	**Bcl6**	GGA.42204	2.2
Gga.764.1.S1_at	activin A receptor, type IIB	**Acvr2b**	GGA.764	-1.6
Gga.2283.1.S2_at	delta-like 1 (Drosophila)	**Dll1**	GGA.2283	-2.4
Gga.4285.1.S1_at	CCAAT/enhancer Binding Protein (C/EBP), Beta	**Cebpb**	GGA.4285	-2.9
Gga.7004.1.S1_at	similar to stem cell antigen 2	**LOC420301**	GGA.7004	2.4

ED14 versus ED6

Affymetrix ID	Gene name	Gene symbol	Unigene ID	Fold change
Gga.488.1.S1_at	achaete-scute complex homolog 1 (Drosophila)	**Ascl1**	GGA.488	-4
Gga.170.1.S1_at Gga.170.1.S2_at	wingless-type MMTV integration site family, member 2B	**Wnt2b**	GGA.170	-3.2
Gga.209.2.S1_at Gga.209.1.S1_a_at	wingless-type MMTV integration site family, member 3	**Wnt3**	GGA.209	1.3
Gga.9293.1.S1_at Gga.3994.3.S1_x_at	fibronectin 1	**Fn1**	GGA.3994	-3.5
Gga.4457.1.S1_s_at GgaAffx.11648.1.S1_at	B-cell CLL/lymphoma 6 (zinc finger protein 51)	**Bcl6**	GGA.42204	2.8
Gga.4285.1.S1_at	CCAAT/enhancer Binding Protein (C/EBP), Beta	**Cebpb**	GGA.4285	1.9
GgaAffx.21450.2.S1_s_at	transforming growth factor, beta 3	**Tgfb3**	GGA.42150	1.6
Gga.199.1.S1_at	atonal homolog 7 (Drosophila)	**Atoh7**	GGA.199	-3.8
Gga.758.1.S1_at	LIM homeobox transcription factor 1, beta	**Lmx1b**	GGA.758	-2.8
Gga.1171.1.S1_at	lymphocyte antigen 6 complex, locus E	**Ly6e**	GGA.1171	3
GgaAffx.1.1.S1_s_at	nuclear factor of kappa light polypeptide gene enhancer in B-cells inhibitor, alpha	**Nfkbia**	GGA.41891	3.7
Gga.6070.1.S1_at	prostate stem cell antigen	**Psca**	GGA.6070	6.9
Gga.1899.1.S1_a_at	nestin	**Nes**	GGA.1899	-3.9
Gga.4046.1.S1_at	Meis homeobox 2	**Meis2**	GGA.4046	-2.1

ED14 versus ED21

Affymetrix ID	Gene name	Gene symbol	Unigene ID	Fold change
Gga.606.1.S1_at	-kit Hardy-Zuckerman 4 feline sarcoma viral oncogene homolog	**Kit**	GGA.606	3.4
Gga.3776.1.S1_at	hippocalcin-like 1	**Hpcal1**	GGA.3776	2.1
Gga.13301.1.S1_at	glycerophosphodiester phosphodiesterase domain containing 5	**Gdpd5**	GGA.13301	-2
Gga.170.1.S1_at Gga.170.1.S2_at	wingless-type MMTV integration site family, member 2B	**Wnt2b**	GGA.170	-1.7
Gga.4058.1.S2_s_at Gga.4058.1.S1_at	Myristoylated alanine-rich C kinase substrate (MARCKS)	**LOC396473**	GGA.4058	-2.1
Gga.4285.1.S1_at	CCAAT/enhancer Binding Protein	**Cebpb**	GGA.4285	-2.6

	(C/EBP), Beta			
Gga.7004.1.S1_at	similar to stem cell antigen 2	**LOC420301**	GGA.7004	1.8

ED16 versus ED6

Affymetrix ID	Gene name	Gene symbol	Unigene ID	Fold change
Gga.488.1.S1_at	achaete-scute complex homolog 1 (Drosophila)	**Ascl1**	GGA.488	-4.1
Gga.170.1.S1_at Gga.170.1.S2_at	wingless-type MMTV integration site family, member 2B	**Wnt2b**	GGA.170	-5.1
Gga.7004.1.S1_at	similar to stem cell antigen 2	**LOC420301**	GGA.7004	2.7
Gga.4058.1.S2_s_at Gga.4058.1.S1_at GgaAffx.20325.1.S1_at	Myristoylated alanine-rich C kinase substrate (MARCKS)	**LOC396473**	GGA.4058	-2.2
Gga.9293.1.S1_at Gga.3994.3.S1_x_at	fibronectin 1	**Fn1**	GGA.3994	-4.5
Gga.4457.1.S1_s_at GgaAffx.11648.1.S1_at	B-cell CLL/lymphoma 6 (zinc finger protein 51)	**Bcl6**	GGA.42204	3.6
Gga.4285.1.S1_at	CCAAT/enhancer Binding Protein (C/EBP), Beta	**Cebpb**	GGA.4285	1.7
GgaAffx.21450.2.S1_s_at	transforming growth factor, beta 3	**Tgfb3**	GGA.42150	1.7
Gga.199.1.S1_at	atonal homolog 7 (Drosophila)	**Atoh7**	GGA.199	-3.6
Gga.758.1.S1_at	LIM homeobox transcription factor 1, beta	**Lmx1b**	GGA.758	-2.8
Gga.1171.1.S1_at	lymphocyte antigen 6 complex, locus E	**Ly6e**	GGA.1171	3.2
GgaAffx.1.1.S1_s_at	nuclear factor of kappa light polypeptide gene enhancer in B-cells inhibitor, alpha	**Nfkbia**	GGA.41891	3.8
Gga.6070.1.S1_at	prostate stem cell antigen	**Psca**	GGA.6070	7.2
Gga.4046.1.S1_at	Meis homeobox 2	**Meis2**	GGA.4046	-2.3
Gga.3776.1.S1_at	hippocalcin-like 1	**Hpcal1**	GGA.3776	-2.1
Gga.16560.2.S1_s_at Gga.16560.2.S1_a_at	myeloid cell □eukaemia sequence 1 (BCL2-related)	**Mcl1**	GGA.34519	1.6
Gga.34.1.S1_at	calcium channel, voltage-dependent, gamma subunit	**Cacng4**	GGA.34	-1.8
Gga.2283.1.S2_at	delta-like 1 (Drosophila)	**Dll1**	GGA.2283	-2.1
Gga.1899.1.S1_a_at	nestin	**Nes**	GGA.1899	-4.1

ED16 versus ED21

Affymetrix ID	Gene name	Gene symbol	Unigene ID	Fold change
Gga.4058.1.S2_s_at Gga.4058.1.S1_at	Myristoylated alanine-rich C kinase substrate (MARCKS)	**LOC396473**	GGA.4058	-1.2
Gga.4285.1.S1_at	CCAAT/enhancer Binding Protein (C/EBP), Beta	**Cebpb**	GGA.4285	-2.4
Gga.606.1.S1_at	-kit Hardy-Zuckerman 4 feline sarcoma viral oncogene homolog	**Kit**	GGA.606	3.3

ED18 versus ED6

Affymetrix ID	Gene name	Gene symbol	Unigene ID	Fold change
Gga.488.1.S1_at	achaete-scute complex homolog 1 (Drosophila)	**Ascl1**	GGA.488	-3.9
Gga.170.1.S1_at Gga.170.1.S2_at	wingless-type MMTV integration site family, member 2B	**Wnt2b**	GGA.170	-5.3
Gga.7004.1.S1_at	similar to stem cell antigen 2	**LOC420301**	GGA.7004	3.4
Gga.4058.1.S2_s_at Gga.4058.1.S1_at GgaAffx.20325.1.S1_at	Myristoylated alanine-rich C kinase substrate (MARCKS)	**LOC396473**	GGA.4058	-2.8
Gga.9293.1.S1_at Gga.3994.3.S1_x_at	fibronectin 1	**Fn1**	GGA.3994	-4.1
Gga.4457.1.S1_s_at GgaAffx.11648.1.S1_at	B-cell CLL/lymphoma 6 (zinc finger protein 51)	**Bcl6**	GGA.42204	3.8
GgaAffx.21450.2.S1_s_at	transforming growth factor, beta 3	**Tgfb3**	GGA.42150	1.6
Gga.199.1.S1_at	atonal homolog 7 (Drosophila)	**Atoh7**	GGA.199	-3.6
Gga.758.1.S1_at	LIM homeobox transcription factor 1, beta	**Lmx1b**	GGA.758	-2.8
Gga.1171.1.S1_at	lymphocyte antigen 6 complex, locus E	**Ly6e**	GGA.1171	3.5
GgaAffx.1.1.S1_s_at	nuclear factor of kappa light polypeptide gene enhancer in B-cells inhibitor, alpha	**Nfkbia**	GGA.41891	3.7
Gga.6070.1.S1_at	prostate stem cell antigen	**Psca**	GGA.6070	7.4
Gga.4046.1.S1_at	Meis homeobox 2	**Meis2**	GGA.4046	-2.5
Gga.3776.1.S1_at	hippocalcin-like 1	**Hpcal1**	GGA.3776	-2.8
Gga.16560.2.S1_s_at Gga.16560.2.S1_a_at	myeloid cell □eukaemia sequence 1 (BCL2-related)	**Mcl1**	GGA.34519	1.7
Gga.34.1.S1_at	calcium channel, voltage-dependent, gamma subunit	**Cacng4**	GGA.34	-2.1
Gga.2283.1.S2_at	delta-like 1 (Drosophila)	**Dll1**	GGA.2283	-2.2
Gga.2305.1.S1_at	chemokine (C-X-C motif) receptor 4	**Cxcr4**	GGA.2305	-2.8
Gga.4367.1.S1_at Gga.4846.1.S1_at Gga.4846.1.S2_at Gga.1899.1.S1_a_at	anti-apoptotic NR13 nestin	**LOC395193** **Nes**	GGA.43428 GGA.1899	1.5 -5

ED6 versus ED21

Affymetrix ID	Gene name	Gene symbol	Unigene ID	Fold change
Gga.606.1.S1_at	-kit Hardy-Zuckerman 4 feline sarcoma viral oncogene homolog	**Kit**	GGA.606	2.9
Gga.1171.1.S1_at	lymphocyte antigen 6 complex, locus E	**Ly6e**	GGA 1171	3.7
Gga.34.1.S1_at	calcium channel, voltage-dependent, gamma subunit	**Cacng4**	GGA.34	-1.9
GgaAffx.1.1.S1_s_at	nuclear factor of kappa light polypeptide gene enhancer in B-cells inhibitor, alpha	**Nfkbia**	GGA.41891	2.8
Gga.6070.1.S1_at	prostate stem cell antigen	**Psca**	GGA.6070	7.7
Gga.16560.2.S1_s_at	myeloid cell leukemia sequence 1 (BCL2-	**Mcl1**	GGA.34519	1.7

Gga.16560.2.S1_a_at	related)			
Gga.4367.1.S1_at Gga.4846.1.S1_at Gga.4846.1.S2_at	anti-apoptotic NR13	**LOC395193**	GGA.43428	1.6
Gga.488.1.S1_at	achaete-scute complex homolog 1 (Drosophila)	**Ascl1**	GGA.488	-4
Gga.3776.1.S1_at	hippocalcin-like 1	**Hpcal1**	GGA.3776	3.1
Gga.13301.1.S1_at	glycerophosphodiester phosphodiesterase domain containing 5	**Gdpd5**	GGA.13301	-1.9
Gga.7004.1.S1_at	similar to stem cell antigen 2	**LOC420301**	GGA.7004	2.7
Gga.170.1.S1_at Gga.170.1.S2_at	wingless-type MMTV integration site family, member 2B	**Wnt2b**	GGA.170	-4.9
Gga.4058.1.S2_s_at Gga.4058.1.S1_at	Myristoylated alanine-rich C kinase substrate (MARCKS)	**LOC396473**	GGA.4058	-3.4
Gga.9293.1.S1_at Gga.3994.3.S1_x_at	fibronectin 1	**Fn1**	GGA.3994	-4.2
Gga.2305.1.S1_at	chemokine (C-X-C motif) receptor 4	**Cxcr4**	GGA.2305	-2.5
Gga.758.1.S1_at	LIM homeobox transcription factor 1, beta	**Lmx1b**	GGA.758	-3
Gga.1899.1.S1_a_at	nestin	**Nes**	GGA.1899	-3.8
Gga.4046.1.S1_at	Meis homeobox 2	**Meis2**	GGA.4046	-3.2
Gga.4457.1.S1_s_at GgaAffx.11648.1.S1_at	B-cell CLL/lymphoma 6 (zinc finger protein 51)	**Bcl6**	GGA.42204	3.9
Gga.764.1.S1_at	activin A receptor, type IIB	**Acvr2b**	GGA.764	-1.8
Gga.3950.1.S1_at	bone morphogenetic protein 2	**Bmp2**	GGA.3950	-1.8
Gga.2283.1.S2_at	delta-like 1 (Drosophila)	**Dll1**	GGA.2283	-2.5
Gga.199.1.S1_at	atonal homolog 7 (Drosophila)	**Atoh7**	GGA.199	-3.5

Table V.9 Genes identified as 'stem cell-related' by gene ontology (continued overleaf)

Affymetrix ID	Gene name	Gene symbol	Unigene ID	GO biological process	GO molecular function	GO cellular component
GgaAffx.22982.1.S1_at	transforming growth factor, beta 2	**Tgfβ2**	GGA.10343	cell morphogenesis skeletal system development blood vessel development eye development response to hypoxia hair follicle development protein amino acid phosphorylation induction of apoptosis SMAD protein nuclear translocation regulation of epithelial cell proliferation epithelial cell migration positive regulation of phosphoinositide 3-kinase cascade extracellular matrix organization collagen fibril organization regulation of cell growth hair follicle morphogenesis positive regulation of stress-activated MAPK cascade wound healing regulation of apoptosis somatic stem cell division neuron fate commitment	beta-amyloid binding receptor signaling protein serine/threonine kinase activity receptor binding type II transforming growth factor beta receptor binding transforming growth factor beta receptor binding protein binding growth factor activity protein homodimerization activity	extracellular region axon cell soma
GgaAffx.1.1.S1_s_at	nuclear factor of kappa light polypeptide gene enhancer in B-cells inhibitor, alpha	**Nfkbia**	GGA.41891	regulation of fibroblast proliferation		cytoplasm
Gga.5164.1.S1_at	BCL2-related protein A1	**Bcl2a1**	GGA.5164	regulation of apoptosis	protein binding	
Gga.2719.2.S1_a_at Gga.2719.1.S2_at	presenilin 2 (Alzheimer disease 4)	**Psen2**	GGA.2719	Notch signaling pathway intracellular signaling cascade	peptidase activity hydrolase activity	Golgi membrane endoplasmic reticulum endoplasmic reticulum membrane Golgi apparatus membrane integral to membrane

Gga.16560.1.S1_at Gga.16560.2.S1_s_at Gga.16560.2.S1_a_at Gga.4367.1.S1_at	myeloid cell leukemia sequence 1 (BCL2-related)	**Mcl1**	GGA.34519	regulation of apoptosis	protein binding protein heterodimerization activity	
Gga.1247.1.S1_at	B6.1	**LOC396098**	GGA.1247	DNA fragmentation involved in apoptosis apoptosis induction of apoptosis activation of caspase activity homophilic cell adhesion apoptotic mitochondrial changes	death receptor activity protein dimerization activity	integral to plasma membrane
Gga.4846.1.S1_at Gga.4846.1.S2_at	anti-apoptotic NR13	**LOC395193**	GGA.43428	apoptosis regulation of apoptosis		plasma membrane membrane integral to membrane
Gga.3864.1.S2_at Gga.3864.1.S1_at	presenilin 1 (Alzheimer disease 3)	**Psen1**	GGA.3864	activation of MAPKK blood vessel development cell fate specification somitogenesis neuron migration protein amino acid phosphorylation hemopoietic progenitor cell differentiation Notch signaling pathway negative regulation of protein kinase activity regulation of epidermal growth factor receptor	sugar binding	integral to membrane
Gga.606.1.S1_at	-kit Hardy-Zuckerman 4 feline sarcoma viral *oncogene homolog*	**Kit**	GGA.606	protein amino acid phosphorylation transmembrane receptor protein tyrosine kinase signaling pathway	nucleotide binding protein kinase activity protein tyrosine kinase activity transmembrane receptor protein tyrosine kinase activity receptor activity ATP binding kinase activity transferase activity	membrane integral to membrane
Gga.1171.1.S1_at	lymphocyte antigen 6 complex, locus E	**Ly6e**	GGA 1171			plasma membrane membrane anchored to membrane

Gga.488.1.S1_at	achaete-scute complex homolog 1 (Drosophila)	**Ascl1**	GGA.488	regulation of transcription	DNA binding transcription regulator activity	nucleus
Gga.199.1.S1_at	atonal homolog 7 (Drosophila)	**Atoh7**	GGA.199	transcription regulation of transcription, DNA-dependent multicellular organismal development nervous system development circadian rhythm entrainment of circadian clock cell differentiation regulation of transcription	DNA binding transcription regulator activity	nucleus
Gga.34.1.S1_at	calcium channel, voltage-dependent, gamma subunit	**Cacng4**	GGA.34	calcium ion transport transmission of nerve impulse	structural molecule activity voltage-gated calcium channel activity	tight junction membrane integral to membrane
Gga.4971.1.S1_at	potassium voltage-gated channel, shaker-related subfamily, beta member 1	**Kcnab1**	GGA.4971	transport ion transport potassium ion transport oxidation reduction	ion channel activity voltage-gated ion channel activity voltage-gated potassium channel activity oxidoreductase activity	cytoplasm integral to membrane
Gga.13301.1.S1_at	glycerophosphodiester phosphodiesterase domain containing 5	**Gdpd5**	GGA.13301	glycerol metabolic process lipid metabolic process	phosphoric diester hydrolase activity glycerophosphodiester phosphodiesterase activity	
Gga.6070.1.S1_at	prostate stem cell antigen	**Psca**	GGA.6070			
Gga.3776.1.S1_at	hippocalcin-like 1	**Hpcal1**	GGA.3776		calcium ion binding	
Gga.7004.1.S1_at	similar to stem cell antigen 2	**LOC420301**	GGA.7004			
Gga.4285.1.S1_at	CCAAT/enhancer Binding Protein (C/EBP), Beta	**Cebpb**	GGA.4285	embryonic placenta development transcription regulation of transcription, DNA-dependent anti-apoptosis induction of apoptosis neuron differentiation regulation of interleukin-6 biosynthetic process fat cell differentiation	DNA binding transcription factor activity RNA polymerase II transcription factor activity, enhancer binding protein binding transcription activator activity protein homodimerization activity	nucleus cytoplasm

				positive regulation of transcription positive regulation of transcription from RNA polymerase II promoter	sequence-specific DNA binding protein heterodimerization activity protein dimerization activity	
Gga.4058.1.S2_s_at Gga.4058.1.S1_at	Myristoylated alanine-rich C kinase substrate (MARCKS)	**LOC396473**	GGA.4058		actin binding calmodulin binding	cytoplasm cytoskeleton membrane
Gga.1899.1.S1_a_at	nestin	**Nes**	GGA.1899		structural molecule activity	intermediate filament
Gga.4982.1.S1_at	Aldolase A	**LOC395492**	GGA.4982	glycolysis metabolic process	catalytic activity fructose-bisphosphate aldolase activity lyase activity	
Gga.4046.1.S1_at	Meis homeobox 2	**Meis2**	GGA.4046	regulation of transcription, DNA-dependent regulation of transcription	transcription factor activity sequence-specific DNA binding	nucleus
Gga.2283.1.S2_at	delta-like 1 (Drosophila)	**Dll1**	GGA.2283	somitogenesis somite specification cell communication Notch signaling pathway multicellular organismal development determination of left/right symmetry compartment specification negative regulation of cell differentiation negative regulation of auditory receptor cell differentiation inner ear development	Notch binding calcium ion binding protein binding	plasma membrane membrane integral to membrane cytoplasmic vesicle

Gga.3950.1.S1_at	bone morphogenetic protein 2	**Bmp2**	GGA.3950	osteoblast differentiation epithelial to mesenchymal transition inflammatory response multicellular organismal development negative regulation of cell proliferation embryonic development organ morphogenesis cell differentiation BMP signaling pathway negative regulation of gene-specific transcription growth cell fate commitment positive regulation of cell differentiation positive regulation of osteoblast differentiation negative regulation of cell cycle positive regulation of transcription	cytokine activity protein binding growth factor activity specific transcriptional repressor activity	extracellular region extracellular space
Gga.170.1.S1_at Gga.170.1.S2_at	wingless-type MMTV integration site family, member 2B	**Wnt2b**	GGA.170	Wnt receptor signaling pathway, calcium modulating pathway multicellular organismal development Wnt receptor signaling pathway	signal transducer activity	extracellular region proteinaceous extracellular matrix
Gga.4457.1.S1_s_at GgaAffx.11648.1.S1_at	B-cell CLL/lymphoma 6 (zinc finger protein 51)	**Bcl6**	GGA.42204	protein import into nucleus, translocation negative regulation of transcription from RNA polymerase II promoter cell morphogenesis negative regulation of cell-matrix adhesion germinal center formation negative regulation of T-helper 2 type immune response regulation of transcription, DNA-dependent response to DNA damage stimulus Rho protein signal transduction protein localization actin cytoskeleton organization negative regulation of cell growth regulation of Rho GTPase activity negative regulation of mast cell	nucleic acid binding DNA binding chromatin binding protein binding zinc ion binding transcription repressor activity chromatin DNA binding sequence-specific DNA binding metal ion binding	intracellular nucleus replication fork

				cytokine production negative regulation of Rho protein signal transduction regulation of cell proliferation regulation of apoptosis regulation of differentiation		
Gga.15614.1.S1_a_at	PTK2 protein tyrosine kinase 2	**PTK2**	GGA.42870	protein amino acid phosphorylation signal complex assembly	nucleotide binding SH2 domain binding protein tyrosine kinase activity non-membrane spanning protein tyrosine kinase activity signal transducer activity protein binding ATP binding kinase activity transferase activity	cytoplasm cytoskeleton plasma membrane focal adhesion membrane cell junction
Gga.764.1.S1_at	activin A receptor, type IIB	**Acvr2b**	GGA.764	protein amino acid phosphorylation signal transduction transmembrane receptor protein serine/threonine kinase signaling pathway anterior/posterior pattern formation positive regulation of bone mineralization activin receptor signaling pathway positive regulation of activin receptor signaling pathway regulation of transcription positive regulation of osteoblast differentiation	nucleotide binding magnesium ion binding protein kinase activity protein serine/threonine kinase activity transmembrane receptor protein serine/threonine kinase activity receptor signaling protein serine/threonine kinase activity receptor activity transforming growth factor beta receptor activity ATP binding kinase activity transferase activity activin receptor activity growth factor binding manganese ion binding metal ion binding	cytoplasm cell surface membrane integral to membrane
Gga.9293.1.S1_at Gga.3994.3.S1_x_at	fibronectin 1	**Fn1**	GGA.3994	acute-phase response cell-substrate junction assembly cell adhesion cell-matrix adhesion regulation of cell shape wound healing	protein binding heparin binding peptidase activator activity	extracellular region proteinaceous extracellular matrix basement membrane apical plasma membrane

Gga.2305.1.S1_at	chemokine (C-X-C motif) receptor 4	**Cxcr4**	GGA.2305	patterning of blood vessels ameboidal cell migration neuron migration signal transduction G-protein coupled receptor protein signaling pathway germ cell development brain development motor axon guidance germ cell migration regulation of cell migration T cell proliferation	signal transducer activity receptor activity G-protein coupled receptor activity C-C chemokine receptor activity C-X-C chemokine receptor activity	extracellular matrix integral to membrane growth cone
Gga.758.1.S1_at	LIM homeobox transcription factor 1, beta	**Lmx1b**	GGA.758	neuron migration transcription regulation of transcription,	DNA binding transcription factor activity	nucleus
Gga.209.1.S1_a_at	wingless-type MMTV integration site family, member 3	**Wnt3**	GGA.209	in utero embryonic development somitogenesis heart looping Wnt receptor signaling pathway, calcium modulating pathway multicellular organismal development determination of left/right symmetry axonogenesis anterior/posterior pattern formation Wnt receptor signaling pathway hippocampus development Wnt receptor signaling pathway in forebrain neuroblast division hemopoiesis mammary gland development inner ear morphogenesis regulation of cell differentiation somatic stem cell division paraxial mesodermal cell fate commitment	signal transducer activity protein binding	extracellular region proteinaceous extracellular matrix extracellular space
Gga.157.1.S1_at	runt-related transcription factor 2	**Runx2**	GGA.157	regulation of transcription, DNA-dependent regulation of transcription	DNA binding transcription factor activity ATP binding	nucleus

Appendix VI

Chapter 6, section 6.6 RT- qPCR data analysis

Table VI.1 Normalised relative expression values and standard errors of seven genes of interests (results from three sets of RT-qPCR reactions)

	Normalised relative expression ± SE						
	ED6	**ED10**	**ED12**	**ED14**	**ED16**	**ED18**	**ED21**
Aqp3	0.0005 ±8.326E-05	0.0343 ±0.0104	0.3583 ±0.0260	0.4744 ±0.0802	0.8268 ±0.1167	1.1312 ±0.1796	0.9258 ±0.1394
Psca	0.0020 ±0.0003	0.1268 ±0.0199	0.3631 ±0.0315	0.3255 ±0.0352	0.5787 ±0.0608	0.8526 ±0.1287	1.6276 ±0.2086
Atoh7	10.4127 ±1.9995	0.2033 ±0.0391	0.0848 ±0.0139	0.0477 ±0.0092	0.0218 ±0.0021	0.0291 ±0.0060	0.0170 ±0.0047
H2afy2	7.7609 ±1.4518	5.9730 ±0.9571	5.2191 ±0.4654	1.7158 ±0.2151	0.2337 ±0.0417	0.1055 ±0.0145	0.0240 ±0.0041
Sfrp2	6.4664 ±0.9691	4.7068 ±0.6921	4.8101 ±0.4922	2.5186 ±0.2701	0.1293 ±0.0128	0.0985 ±0.0124	0.0178 ±0.0024
Sh3bgr	10.4127 ±1.9392	0.5750 ±0.1306	0.4703 ±0.0853	0.0778 ±0.0127	0.0775 ±0.0075	0.0683 ±0.0088	0.1453 ±0.0270
Kcnj2	7.5944 ±1.4503	0.5260 ±0.0960	0.2249 ±0.0403	0.0852 ±0.0176	0.0773 ±0.0127	0.3811 ±0.0683	1.5428 ±0.1638

Table VI.2 Shapiro-Wilk results for test of normality of *Aqp3* gene expression. The mean difference is significant at the 0.05 level.

Aqp3

	Shapiro-Wilk		
	Statistic	df	Sig.
var	.911	21	.058

Table VI.3 One-way ANOVA results obtained from analysis of the *Aqp3* gene expression. The mean difference is significant at the 0.05 level.

ANOVA

	Sum of Squares	df	Mean Square	F	Sig.
Between Groups	3.494	6	.582	25.371	.000
Within Groups	.321	14	.023		
Total	3.815	20			

Table VI.4 Levene`s test of homogeneity of variances

Test of Homogeneity of Variances

Levene Statistic	df1	df2	Sig.
5.897	6	14	.003

Table VI.5 Post-hoc Dunnett T3 test results obtained from analysis of *Aqp3* gene expression

Multiple Comparisons

Dependent Variable: var
Dunnett T3

(I) group	(J) group	Mean Difference (I-J)	Std. Error	Sig.	95% Confidence Interval	
					Lower Bound	Upper Bound
ed6	ed10	-.0338372	.0108157	.386	-.140170	.072496
	ed12	-.3577988	.0440785	.073	-.791776	.076179
	ed14	-.4739555	.1065633	.219	-1.523212	.575301
	ed16	-.8263488	.0911983	.059	-1.724311	.071614
	ed18	-1.1307246(*)	.0658293	.017	-1.778885	-.482565
	ed21	-.9252911	.1657942	.014	-2.557769	.707187
ed10	ed6	.0338372	.0108157	.386	-.072496	.140170
	ed12	-.3239616	.0453844	.075	-.716753	.068830
	ed14	-.4401183	.1071101	.246	-1.469345	.589108
	ed16	-.7925115	.0918366	.061	-1.667366	.082342
	ed18	-1.0968873(*)	.0667108	.015	-1.714385	-.479390
	ed21	-.8914538	.1661461	.155	-2.510788	.727880
ed12	ed6	.3577988	.0440785	.073	-.076179	.791776
	ed10	.3239616	.0453844	.075	-.068830	.716753
	ed14	-.1161567	.1153192	.980	-.958587	.726274
	ed16	-.4685499	.1012911	.135	-1.159993	.222893
	ed18	-.7729257(*)	.0792229	.010	-1.242619	-.303232
	ed21	-.5674923	.1715531	.330	-2.023647	.888662
ed14	ed6	.4739555	.1065633	.219	-.575301	1.523212
	ed10	.4401183	.1071101	.246	-.589108	1.469345
	ed12	.1161567	.1153192	.980	-.726274	.958587
	ed16	-.3523932	.1402595	.446	-1.127365	.422579
	ed18	-.6567690	.1252561	.079	-1.423698	.110160
	ed21	-.4513356	.1970870	.540	-1.638627	.735956
ed16	ed6	.8263488	.0911983	.059	-.071614	1.724311
	ed10	.7925115	.0918366	.061	-.082342	1.667366
	ed12	.4685499	.1012911	.135	-.222893	1.159993
	ed14	.3523932	.1402595	.446	-.422579	1.127365
	ed18	-.3043758	.1124743	.392	-.953622	.344870
	ed21	-.0989423	.1892212	1.000	-1.317503	1.119618
ed18	ed6	1.1307246(*)	.0658293	.017	.482565	1.778885
	ed10	1.0968873(*)	.0667108	.015	.479390	1.714385
	ed12	.7729257(*)	.0792229	.010	.303232	1.242619
	ed14	.6567690	.1252561	.079	-.110160	1.423698
	ed16	.3043758	.1124743	.392	-.344870	.953622

ed21	ed21	.2054335	.1783846	.955	-1.119825	1.530692
	ed6	.9252911	.1657942	.014	-.707187	2.557769
	ed10	.8914538	.1661461	.155	-.727880	2.510788
	ed12	.5674923	.1715531	.330	-.888662	2.023647
	ed14	.4513356	.1970870	.540	-.735956	1.638627
	ed16	.0989423	.1892212	1.000	-1.119618	1.317503
	ed18	-.2054335	.1783846	.955	-1.530692	1.119825

* The mean difference is significant at the .05 level.

Table VI.6 Shapiro-Wilk results for test of normality of *Atoh7* gene expression. The mean difference is significant at the 0.05 level.

Atoh7

	Shapiro-Wilk		
	Statistic	df	Sig.
transformed1	.893	21	.062

Table VI.7 One-way ANOVA results obtained from analysis of the *Atoh7* gene expression. The mean difference is significant at the 0.05 level.

ANOVA

transformed

	Sum of Squares	df	Mean Square	F	Sig.
Between Groups	86.707	6	14.451	45.660	.000
Within Groups	4.431	14	.316		
Total	91.138	20			

Table VI.8 Levene`s test of homogeneity of variances

transformed

Levene Statistic	df1	df2	Sig.
2.701	6	14	.059

Table VI.9 Post-hoc Tukey test results obtained from analysis of *Atoh7* gene expression

Multiple Comparisons

Dependent Variable: transformed
Tukey HSD

(I) group	(J) group	Mean Difference (I-J)	Std. Error	Sig.	95% Confidence Interval	
					Lower Bound	Upper Bound
ed6	ed10	3.82756(*)	.45935	.000	2.2591	5.3960
	ed12	4.48483(*)	.45935	.000	2.9164	6.0533
	ed14	5.63672(*)	.45935	.000	4.0682	7.2052
	ed16	6.02995(*)	.45935	.000	4.4615	7.5984

	ed18	5.86608(*)	.45935	.000	4.2976	7.4346
	ed21	6.15424(*)	.45935	.000	4.5858	7.7227
ed10	ed6	-3.82756(*)	.45935	.000	-5.3960	-2.2591
	ed12	.65727	.45935	.778	-.9112	2.2257
	ed14	1.80916(*)	.45935	.019	.2407	3.3776
	ed16	2.20239(*)	.45935	.004	.6339	3.7709
	ed18	2.03852(*)	.45935	.008	.4700	3.6070
	ed21	2.32668(*)	.45935	.003	.7582	3.8952
ed12	ed6	-4.48483(*)	.45935	.000	-6.0533	-2.9164
	ed10	-.65727	.45935	.778	-2.2257	.9112
	ed14	1.15189	.45935	.228	-.4166	2.7204
	ed16	1.54512	.45935	.055	-.0234	3.1136
	ed18	1.38125	.45935	.102	-.1872	2.9497
	ed21	1.66941(*)	.45935	.034	.1009	3.2379
ed14	ed6	-5.63672(*)	.45935	.000	-7.2052	-4.0682
	ed10	-1.80916(*)	.45935	.019	-3.3776	-.2407
	ed12	-1.15189	.45935	.228	-2.7204	.4166
	ed16	.39323	.45935	.974	-1.1752	1.9617
	ed18	.22936	.45935	.998	-1.3391	1.7978
	ed21	.51752	.45935	.909	-1.0510	2.0860
ed16	ed6	-6.02995(*)	.45935	.000	-7.5984	-4.4615
	ed10	-2.20239(*)	.45935	.004	-3.7709	-.6339
	ed12	-1.54512	.45935	.055	-3.1136	.0234
	ed14	-.39323	.45935	.974	-1.9617	1.1752
	ed18	-.16387	.45935	1.000	-1.7323	1.4046
	ed21	.12429	.45935	1.000	-1.4442	1.6928
ed18	ed6	-5.86608(*)	.45935	.000	-7.4346	-4.2976
	ed10	-2.03852(*)	.45935	.008	-3.6070	-.4700
	ed12	-1.38125	.45935	.102	-2.9497	.1872
	ed14	-.22936	.45935	.998	-1.7978	1.3391
	ed16	.16387	.45935	1.000	-1.4046	1.7323
	ed21	.28816	.45935	.995	-1.2803	1.8566
ed21	ed6	-6.15424(*)	.45935	.000	-7.7227	-4.5858
	ed10	-2.32668(*)	.45935	.003	-3.8952	-.7582
	ed12	-1.66941(*)	.45935	.034	-3.2379	-.1009
	ed14	-.51752	.45935	.909	-2.0860	1.0510
	ed16	-.12429	.45935	1.000	-1.6928	1.4442
	ed18	-.28816	.45935	.995	-1.8566	1.2803

* The mean difference is significant at the .05 level.

Table VI.10 Shapiro-Wilk results for test of normality of *Kcnj2* gene expression. The mean difference is significant at the 0.05 level.

Kcnj2

	Shapiro-Wilk		
	Statistic	df	Sig.
transformed	.918	21	.079

Table VI.11 One-way ANOVA results obtained from analysis of the *Kcnj2* gene expression. The mean difference is significant at the 0.05 level.

ANOVA

transformed

	Sum of Squares	df	Mean Square	F	Sig.
Between Groups	48.902	6	8.150	62.478	.000
Within Groups	1.826	14	.130		
Total	50.728	20			

Table VI.12 Levene`s test of homogeneity of variances

transformed

Levene Statistic	df1	df2	Sig.
4.446	6	14	.010

Table VI.13 Post-hoc Dunnett test results obtained from analysis of *Kcnj2* gene expression

Multiple Comparisons

Dependent Variable: transformed
Dunnett T3

(I) group	(J) group	Mean Difference (I-J)	Std. Error	Sig.	95% Confidence Interval	
					Lower Bound	Upper Bound
ed6	ed10	2.67231(*)	.05448	.001	2.2064	3.1382
	ed12	3.59298(*)	.28411	.030	.8110	6.3749
	ed14	4.52846(*)	.19443	.009	2.6365	6.4204
	ed16	4.62286(*)	.19185	.008	2.7566	6.4891
	ed18	3.14047	.37160	.067	-.5066	6.7876
	ed21	1.60257(*)	.09449	.015	.7168	2.4883
ed10	ed6	-2.67231(*)	.05448	.001	-3.1382	-2.2064
	ed12	.92067	.28864	.363	-1.7083	3.5496
	ed14	1.85614(*)	.20100	.041	.1602	3.5521
	ed16	1.95055(*)	.19850	.035	.2816	3.6195
	ed18	.46816	.37508	.924	-3.0559	3.9922
	ed21	-1.06974(*)	.10736	.013	-1.7534	-.3861
ed12	ed6	-3.59298(*)	.28411	.030	-6.3749	-.8110
	ed10	-.92067	.28864	.363	-3.5496	1.7083
	ed14	.93548	.34373	.391	-1.0868	2.9578
	ed16	1.02988	.34227	.317	-.9940	3.0537
	ed18	-.45251	.46737	.990	-3.1034	2.1984
	ed21	-1.99041	.29879	.075	-4.3700	.3892
ed14	ed6	-4.52846(*)	.19443	.009	-6.4204	-2.6365
	ed10	-1.85614(*)	.20100	.041	-3.5521	-.1602
	ed12	-.93548	.34373	.391	-2.9578	1.0868
	ed16	.09440	.27246	1.000	-1.3905	1.5793
	ed18	-1.38798	.41895	.279	-4.1496	1.3737
	ed21	-2.92589(*)	.21531	.008	-4.3973	-1.4544
ed16	ed6	-4.62286(*)	.19185	.008	-6.4891	-2.7566

	ed10	-1.95055(*)	.19850	.035	-3.6195	-.2816
	ed12	-1.02988	.34227	.317	-3.0537	.9940
	ed14	-.09440	.27246	1.000	-1.5793	1.3905
	ed18	-1.48239	.41776	.242	-4.2529	1.2881
	ed21	-3.02029(*)	.21299	.006	-4.4671	-1.5735
ed18	ed6	-3.14047	.37160	.067	-6.7876	.5066
	ed10	-.46816	.37508	.924	-3.9922	3.0559
	ed12	.45251	.46737	.990	-2.1984	3.1034
	ed14	1.38798	.41895	.279	-1.3737	4.1496
	ed16	1.48239	.41776	.242	-1.2881	4.2529
	ed21	-1.53790	.38294	.236	-4.8322	1.7564
ed21	ed6	-1.60257(*)	.09449	.015	-2.4883	-.7168
	ed10	1.06974(*)	.10736	.013	.3861	1.7534
	ed12	1.99041	.29879	.075	-.3892	4.3700
	ed14	2.92589(*)	.21531	.008	1.4544	4.3973
	ed16	3.02029(*)	.21299	.006	1.5735	4.4671
	ed18	1.53790	.38294	.236	-1.7564	4.8322

* The mean difference is significant at the .05 level.

Table VI.14 Shapiro-Wilk results for test of normality of *Sh3bgr* gene expression. The mean difference is significant at the 0.05 level.

Sh3bgr

	Shapiro-Wilk		
	Statistic	df	Sig.
transformed	.909	21	.054

Table VI.15 One-way ANOVA results obtained from analysis of the *Sh3bgr* gene expression. The mean difference is significant at the 0.05 level.

ANOVA

transformed

	Sum of Squares	df	Mean Square	F	Sig.
Between Groups	12.921	6	2.154	7.598	.001
Within Groups	3.968	14	.283		
Total	16.889	20			

Table VI.16 Levene`s test of homogeneity of variances

transformed

Levene Statistic	df1	df2	Sig.
1.289	6	14	.324

Table VI.17 Post-hoc Tukey test results obtained from analysis of *Sh3bgr* gene expression

Multiple Comparisons

Dependent Variable: transformed
Tukey HSD

(I) group	(J) group	Mean Difference (I-J)	Std. Error	Sig.	95% Confidence Interval	
					Lower Bound	Upper Bound
ed6	ed10	1.44922	.43468	.058	-.0350	2.9335
	ed12	1.59888(*)	.43468	.031	.1146	3.0831
	ed14	2.13426(*)	.43468	.003	.6500	3.6185
	ed16	2.32142(*)	.43468	.002	.8372	3.8057
	ed18	2.40980(*)	.43468	.001	.9255	3.8941
	ed21	2.22288(*)	.43468	.002	.7386	3.7071
ed10	ed6	-1.44922	.43468	.058	-2.9335	.0350
	ed12	.14965	.43468	1.000	-1.3346	1.6339
	ed14	.68503	.43468	.698	-.7992	2.1693
	ed16	.87220	.43468	.452	-.6121	2.3565
	ed18	.96058	.43468	.349	-.5237	2.4448
	ed21	.77365	.43468	.580	-.7106	2.2579
ed12	ed6	-1.59888(*)	.43468	.031	-3.0831	-.1146
	ed10	-.14965	.43468	1.000	-1.6339	1.3346
	ed14	.53538	.43468	.870	-.9489	2.0196
	ed16	.72255	.43468	.649	-.7617	2.2068
	ed18	.81092	.43468	.530	-.6733	2.2952
	ed21	.62400	.43468	.775	-.8603	2.1083
ed14	ed6	-2.13426(*)	.43468	.003	-3.6185	-.6500
	ed10	-.68503	.43468	.698	-2.1693	.7992
	ed12	-.53538	.43468	.870	-2.0196	.9489
	ed16	.18717	.43468	.999	-1.2971	1.6714
	ed18	.27554	.43468	.994	-1.2087	1.7598
	ed21	.08862	.43468	1.000	-1.3956	1.5729
ed16	ed6	-2.32142(*)	.43468	.002	-3.8057	-.8372
	ed10	-.87220	.43468	.452	-2.3565	.6121
	ed12	-.72255	.43468	.649	-2.2068	.7617
	ed14	-.18717	.43468	.999	-1.6714	1.2971
	ed18	.08838	.43468	1.000	-1.3959	1.5726
	ed21	-.09854	.43468	1.000	-1.5828	1.3857
ed18	ed6	-2.40980(*)	.43468	.001	-3.8941	-.9255
	ed10	-.96058	.43468	.349	-2.4448	.5237
	ed12	-.81092	.43468	.530	-2.2952	.6733
	ed14	-.27554	.43468	.994	-1.7598	1.2087
	ed16	-.08838	.43468	1.000	-1.5726	1.3959
	ed21	-.18692	.43468	.999	-1.6712	1.2973
ed21	ed6	-2.22288(*)	.43468	.002	-3.7071	-.7386
	ed10	-.77365	.43468	.580	-2.2579	.7106
	ed12	-.62400	.43468	.775	-2.1083	.8603
	ed14	-.08862	.43468	1.000	-1.5729	1.3956
	ed16	.09854	.43468	1.000	-1.3857	1.5828
	ed18	.18692	.43468	.999	-1.2973	1.6712

* The mean difference is significant at the .05 level.

Table VI.18 Shapiro-Wilk results for test of normality of *Psca* gene expression. The mean difference is significant at the 0.05 level.

Psca

	Shapiro-Wilk		
	Statistic	df	Sig.
var	.865	21	.008

Table VI.19 Kruskal-Wallis results obtained from analysis of the *Psca* gene expression. The mean difference is significant at the 0.05 level.

Ranks

	group	N	Mean Rank
var	ed6	3	2.00
	ed10	3	5.00
	ed12	3	10.00
	ed14	3	10.00
	ed16	3	13.67
	ed18	3	16.33
	ed21	3	20.00
	Total	21	

Test Statistics(a,b)

	var
Chi-Square	18.355
df	6
Asymp. Sig.	.005

a Kruskal Wallis Test
b Grouping Variable: group

Table VI.20 Shapiro-Wilk results for test of normality of *Sfrp2* gene expression. The mean difference is significant at the 0.05 level.

Sfrp2

	Shapiro-Wilk		
	Statistic	df	Sig.
transformed	.470	21	.000

a Lilliefors Significance Correction

Table VI.21 Kruskal-Wallis results obtained from analysis of the *Sfrp2* gene expression. The mean difference is significant at the 0.05 level.

Ranks

	group	N	Mean Rank
var	ed6	3	18.67
	ed10	3	16.00
	ed12	3	16.33
	ed14	3	11.00
	ed16	3	7.00
	ed18	3	6.00
	ed21	3	2.00
	Total	21	

Test Statistics(a,b)

	var
Chi-Square	18.251
df	6
Asymp. Sig.	.006

a Kruskal Wallis Test
b Grouping Variable: group

Table VI.22 Shapiro-Wilk results for test of normality of *Sfrp2* gene expression. The mean difference is significant at the 0.05 level.

H2afy2

	Shapiro-Wilk		
	Statistic	df	Sig.
var	.814	21	.001

a Lilliefors Significance Correction

Table VI.23 Kruskal-Wallis results obtained from analysis of the *Sfrp2* gene expression. The mean difference is significant at the 0.05 level.

Ranks

	group	N	Mean Rank
var	ed6	3	18.33
	ed10	3	16.67
	ed12	3	16.00
	ed14	3	11.00
	ed16	3	7.00
	ed18	3	6.00
	ed21	3	2.00
	Total	21	

Test Statistics(a,b)

	var
Chi-Square	18.147
df	6
Asymp. Sig.	.006

a Kruskal Wallis Test
b Grouping Variable: group

Post-hoc pairs comparison after Kruskal-Wallis (groups equal in size (N=3))

N- the number of cases in each sample group
Each mean rank them multiplied by the N for that group (N=3) gives rank total for each group

Paired comparison of interest between two groups calculated as follows:

d = rank total of one group – rank total of the other,
K = (d-0.8)/(N*sqrt(N))

If *K* is equal to of grater than the table value, then the difference is significant at the level indicated by *p* (table adapted from R. Lanhgley *Practical Statistic Simply Explained* Pan Books 1979, p. 220).

Table VI.24 List of K values for different levels of significance

Total number of groups in the analysis	When comparing any groups with each other in pairs		When comparing several groups with a control	
	p = 0.05	p = 0.01	p = 0.05	p = 0.01
3	2.89	3.60	2.72	3.45
4	4.22	5.12	3.86	4.80
5	5.60	6.69	5.00	6.16
6	7.01	8.30	6.17	7.53
7	**8.46**	9.92	7.37	8.94
8	9.46	11.58	8.55	10.33
9	11.43	13.25	9.77	11.77
10	12.97	14.95	11.01	13.19

Calculated K values for each pair comparison are shown in Tables below.

Table VI.25 List of K values calculated for *Psca*. Asterisks indicate statistical significance

Psca	**6**	**10**	**12**	**14**	**16**	**18**	**21**
6	-	1.57	4.4	4.4	7.7	**9.2***	**10.2***
10		-	2.73	2.73	4.85	6.39	**8.51***
12			-	0.15	1.96	3.5	5.62
14				-	1.96	3.5	5.6
16					-	1.3	3.5
18						-	1.9
21							-

Table VI.26 List of K values calculated for *Sfrp2*. Asterisks indicate statistical significance

Sfrp2	**6**	**10**	**12**	**14**	**16**	**18**	**21**
6	-	1.38	1.19	4.2	6.59	7.18	**9.48***
10		-	0.03	2.7	5.04	5.62	7.93
12			-	2.92	5.23	5.8	8.12
14				-	2.15	2.73	5.04
16					-	0.4	2.7
18						-	2.15
21							-

Table VI.27 List of K values calculated for *H2afy2*. Asterisks indicate statistical significance

H2afy2	**6**	**10**	**12**	**14**	**16**	**18**	**PN**
6	-	0.8	1.19	4.08	6.3	6.9	**9.2***
10		-	0.25	3.14	5.45	6.03	**8.54***
12			-	2.73	5.04	5.6	7.9
14				-	2.1	2.7	5.01
16					-	0.4	2.7
18						-	2.1
21							-

REFERENCES

Abdelhak S, Kalatzis V, Heilig R, Compain S, Samson D, Vincent C, Weil D, Cruaud C, Sahly I, Leibovici M, Bitmer-Glindzicz M, Francis M, Lacombe D, Vigneron J, Charachon R, Boven K, Bedbeder P, Van Regemorter N, Weissenbach J, Petit C. 1997. A human homologue of the Drosophila eyes absent gene underlies branchio-oto-renal (BOR) syndrome and identifies a novel gene family. Nat Genet. 15: 157-164.

Adams JM, Cory S. 1998. The Bcl-2 protein family: arbiters of cell survival. Science. 281: 1322-1326.

Adhikary G, Crish J, Lass J, Eckert RL. 2004. Regulation of involucrin expression in normal human corneal epithelial cells: a role for activator protein one. Invest Ophthalmol Vis Sci. 45: 1080–1087.

Adler R, Canto-Soler MV. 2007. Molecular mechanisms of optic vesicle development: complexities, ambiguities and controversies. Dev Biol. 305: 1-13.

Agrawal VB, Tsai RJ. 2003. Corneal epithelial wound healing. J Opthalmol. 51: 5-15.

Andersen CL, Jensen JL, Ørntoft TF. 2004. Normalization of real-time quantitative reverse transcription-PCR data: a model-based variance estimation approach to identify genes suited for normalization, applied to bladder and colon cancer data sets. Cancer Res. 64: 5245-5250.

Andreeff M, Goodrich DW, Pardee AB. 2000. Cell Proliferation, Differentiation and Apoptosis. Chapter 2. Cancer Medicine 5th edition. B.C. Decker, Inc, Hamilton, Ontario, Canada. pp.17-32.

Ansari B, Coates AJ, Greenstein BD, Hall PA. 2005. *In situ* end-labelling detects DNA strand breaks in apoptosis and other physiological and pathological states. J Pathol. 170: 1-8.

Artavanis-Tsakonas S, Rand MD, Lake RJ. 1999. Notch signaling: cell fate control and signal integration in development. Science. 284: 770–776.

Ashery-Padan R, Gruss P. 2001. Pax6 lights-up the way for eye development. Curr Opin Cell Biol. 13: 706-714.

Ashkenazi A, Dixit VM. 1998. Death receptors: Signaling and modulation. Science. 281: 1305-1308.

Autzen T, Bjornstrom L. 1989. Central corneal thickness in full-term newborns. Acta Ophthalmologica. 67: 719–720.

Baba TW, Giroir BP, Humphries EH. 1985. Cell lines derived from avian lymphomas exhibit two distinct phenotypes. Virology. 144: 139-151.

Baker KS, Anderson SC, Romanowski EG, Thoft RA, SundarRaj N. 1993. Trigeminal ganglion neurons affect corneal epithelial phenotype. Influence on type VII collagen expression in vitro. Invest Opthalmol Vis Sci. 34: 137-144.

Bard JB, Higginson K. 1977. Fibroblast-collagen interactions in the formation of the secondary stroma of the chick cornea. J Cell Biol. 74: 816-827.

Barnard Z, Apel AJG, Harkin DG. 2001. Phenotypic analyss of limba epithelial cell cultures derived from donor corneoscleral rims. Clin Exp Ophthalmol. 29: 138-142.

Barry PA, Petroll WM, Andrews PM, Cavanagh HD, Jester JV. 1995. The spatial organization of corneal endothelial cytoskeletal proteins and their relationship to the apical junctional complex. Invest Opthalmol Vis Sci. 36: 1115-1124.

Beckman KB, Lee KY, Golden T, Melov S. 2004. Gene expression profiling in mitochondrial disease: assessment of microarray accuracy by highthroughput Q-PCR. Mitochondrion. 4: 453-470.

Beebe DC, Masters BR. 1996. Cell lineage and the differentiation of corneal epithelial cells. Invest Ophthalmol Vis Sci. 37: 1815–1825.

Beebe DC, Coats JM. 2000. The lens organizes the anterior segment: specification of neural crest cell differentiation in the avian eye. Dev Biol. 220: 424–431.

Benjamini Y, Hochberg Y. 1995. Controlling the false discovery rate: a practical and powerful approach to multiple testing. J R Stat Soc. 57: 289-300.

Bianchi L, Wible B, Arcangeli A, Taglialatela M, Morra F, Castaldo P, Crociani O, Rosati B, Faravelli L, Olivotto M, Wanke E. 1998. Herg encodes a K+ current highly conserved in tumors of different histogenesis: a selective advantage for cancer cells? Cancer Res. 58: 815–822.

Binder PS, Rock ME, Schmidt KC, Anderson JA. 1991. High-voltage electron microscopy of normal human cornea. Invest Opthalmol Vis Sci. 32: 2234-2243.

Bjarnadottir TK, Gloriam DE, Hellstrand SH, Kristiansson H, Fredriksson R, Schioth HB. 2006. Comprehensive repertoire and phylogenetic analysis of the G protein-coupled receptors in human and mouse. Genomics. 88: 263–273.

Blanpain C, Lowry WE, Pasolli HA, Fuchs E. 2006. Canonical notch signaling functions as a commitment switch in the epidermal lineage. Genes Dev. 20: 3022-3035.

Boldin MP, Varfolomeev EE, Pancer Z, Mett IL, Camonis JH, Wallach D. 1995. A novel protein that interacts with the death domain of Fas/APO1 contains a sequence motif related to the death domain. J Biol Chem. 270: 7795-7798.

Bolstad BM, Irizarry RA, Astrand M, Speed TP. 2003. A comparison of normalization methods for high density oligonucleotide array data based on variance and bias. Bioinformatics. 2: 185-193.

Bonini NM, Choi KW. 1995. Early decisions in Drosophila eye morphogenesis. Curr Opin Genet Dev. 5: 507-515.

Botchkarev VA, Botchkareva NV, Nakamura M, Huber O, Funa K, Lauster R, Paus R, Gilchrest, BA. 2001. Noggin is required for induction of the hair follicle growth phase in postnatal skin. Fed Am Soc Exp Biol J. 15: 2205–2214.

Boulton M, Albon J, Grant ME. 2007. Stems Cells in the Eye. In: Principles of Tissue Engineering. Chapter 67. 3rd Edition. pp.1011-1023.

Bourcier T, Forgez P, Borderie V, Scheer S, Roste`ne W, Laroche1 L. 2000. Regulation of human corneal epithelial cell proliferation and apoptosis by dexamethasone. Invest Ophthalmol Vis Sci. 41: 4133-4141.

Bozanic D, Tafra R, Saraga-Babić M. 2003. Role of apoptosis and mitosis during human eye development. Eur J Cell Biol. 82: 421-429.

Bray S. 1998. Notch signalling in Drosophila: three ways to use a pathway. Semin Cell Dev Biol. 9: 591-597.

Brettschneider J, Collin F, Bolstad BM, Speed TP. 2008. Quality Assessment for Short Oligonucleotide Microarray Data. Technometrics. 50: 241-264.

Brown DC, Gatter KC. 2002. Ki67 protein: the immaculate deception? Histopathology. 40: 2-11.

Brown NL, Kanekar S, Vetter ML, Tucker PK, Gemza DL, Glaser T. 1998. *Math5* encodes a murine basic helix-loop-helix transcription factor expressed during early stages of retinal neurogenesis. Development. 125: 4821-4833.

Brown WRA, Hubbard SJ, Tickle S, Wilson SA. 2003. The chicken as a model for large-scale analysis of vertebrate gene function. Nature. 4: 87-98.

Brusch W, Kleine L, Tenniswood M. 1990. The biochemistry of cell death by apoptosis. Biochem. Cell. Biol. 88: 1071-1074.

Burglin TR. 1994. A *Caenorhabditis elegans prospero* homologue defines a novel domain. Trends Biochem Sci. 19: 70-71.

Burmeister M, Novak J, Liang MY, Basu S, Ploder L, Hawes NL, Vidgen D, Hoover F, Goldman D, Kalnins VI, Roderick TH, Taylor Ba, Hankin MH, McInnes RR. 1996. Ocular retardation mouse caused by Chx10 homeobox null allele: impaired retinal progenitor proliferation and bipolar cell differentiation. Nat Genet. 12: 376-384.

Buschbeck M, Uribesalgo I, Wibowo I, Rué P, Martin D, Gutierrez A, Morey L, Guigó R, López-Schier H, Di Croce L. 2009. The histone variant macroH2A is an epigenetic regulator of key developmental genes. Nature. 16: 1074-1079.

Bustin SA. 2000. Absolute quantification of mRNA using real-time reverse transcription polymerase chain reaction assays. J Mol Endocrinol. 25: 169-193.

Bustin SA. 2002. Invited review: quantification of mRNA using real-time reverse transcription PCR (RT-PCR): trends and problems. J Mol Endocrinol. 29: 23–39.

Cairns BR. 2005. Chromatin remodeling complexes: strength in diversity, precision through specialization. Curr Opin Genet Dev. 15: 185–190.

Catalano A, Caprari P, Rodilossi S, Betta P, Castellucci M, Casazza A, Tamagnone L, Procopio A. 2004. Cross-talk between vascular endothelial growth factor and semaphorin-3A pathway in the regulation of normal and malignant mesothelial cell proliferation. FASEB J. 18: 358-360.

Caulin C, Salvesen GS, Oshima RG. 1997. Caspase cleavage of keratin 18 and reorganization of intermediate filaments during epithelial cell apoptosis. J. Cell Biol. 138: 1379–1394.

Celis JE, Madsen P, Celis A, Nielsen HV, Gesser B. 1987. Cyclin (PCNA, auxiliary protein of DNA polymerase delta) is a central component of the pathway(s) leading to DNA replication and cell division. FEBS Lett. 220: 1-7.

Chadwick BP, Willard HF. 2001. Histone H2A variants and the inactive X chromosome: identification of a second macroH2A variant. Hum. Mol. Genet. 10: 1101-1113.

Chaloin-Dufau C, Sun T-T, Dhouailly D. 1990. Appearance of the keratin pair K3/K12 during embryonic and adult corneal epithelial differentiation in the chick and in the rabbit. Cell Differ Dev. 32: 97-108.

Chandrasekher G, Kakazu AH, Bazan HE. 2001. HGF- and KGF-induced activation of PI-3K/p70 s6 kinase pathway in corneal epithelial cells: its relevance in wound healing, Exp Eye Res. 73: 191–202.

Chang CY, Green CR, McGhee CN, Sherwin T. 2008. Acute wound healing in the human central corneal epithelium appears to be independent of limbal stem cell influence. Invest Ophthalmol Vis Sci. 49: 5279-5286.

Chang EJ, Im YS, Kay EP, Kim JY, Lee JE, Lee HK. 2008. The role of nerve growth factor in hyperosmolar stress induced apoptosis. J Cell Physiol. 216: 69-77.

Chen J, Guerriero E, Lathrop K, SundarRaj N. 2008. Rho/ROCK signaling in regulation of corneal epithelial cell cycle progression. Invest Ophthalmol Vis Sci. 49: 175-183.

Chen W, Ishikawa M, Yamaki K, Sakuragi S. 2003. Wistar rat palpebral conjunctiva contains more slow-cycling stem cells that have larger proliferative capacity: implication for conjunctival epithelial homeostasis. Jpn J Ophthalmol. 47: 119–128.

Chen Z, de Paiva CS, Luo L, Kretzer FL, Pflugfelder SC, Li DQ. 2004. Characterization of putative stem cell phenotype in human limbal epithelia. Stem Cells. 22: 355-366.

Cheung P, Allis CD, Sassone-Corsi P. 2000. Signaling to chromatin through histone modifications. Cell. 103: 263-271.

Chi TH, Wan M, Zhao K, Taniuchi I, Chen L, Littman DR, Crabtree GR. 2002. Reciprocal regulation of CD4/CD8 expression by SWI/SNF-like BAF complexes. Nature. 418:195-199.

Chim CS, Pang R, Fung TK, Choi CL, Liang R. 2007. Epigenetic dysregulation of Wnt signaling pathway in multiple myeloma. Leukemia. 21: 2527–2536.

Chinnaiyan AM, O'Rourke K, Tewari M, Dixit VM. 1995. FADD, a novel death domaincontaining protein, interacts with the death domain of Fas and initiates apoptosis. Cell. 81: 505–512.

Chu S, DeRisi J, Eisen M, Mulholland J, Botstein D, Brown PO, Herskowitz I. 1998. The transcriptional program of sporulation in budding yeast. Science. 282: 699–705.

Chu ZL. Pio F, Xie Z, Welsh K, Krajewska M, Krajewski S, Godzik A, Reed J C. 2001. A novel enhancer of the Apaf1 apoptosome involved in cytochrome c-dependent caspase activation and apoptosis". J Biol Chem. 276: 9239-9245.

Chuaqui RF, Bonner RF, Best CJM, Gillespie JW, Flaig MJ, Hewitt SM, Phillips JL, Krizman DB, Tangrea MA, Ahram M, Linehan WM, Knezevic V, Emmert-Buck MR. 2002. Post-analysis follow-up and validation of microarray experiments. Nat Genet. 32:509–514.

Chung EH, Bukusolglu G, Zieske JD. 1992. Localization of corneal epithelial stem cells in the developing rat. Inves. Ophthalmol Vis Sci. 33: 121–128.

Chung EH, DeGregorio PG, Wasson M, Zieske JD. 1995. Epithelial regeneration after limbus-to-limbus debridement. Expression of alpha-enolase in stem and transient amplifying cells. Invest Ophthalmol Vis Sci. 36: 1336-1343.

Cintron C, Kublin CL. 1977. Regeneration of corneal tissue. Dev Biol. 61: 346-357.

Cohen DR, Curran T. 1989. Fra-1: a serum-inducible, cellular immediate-early gene that encodes a fos-related antigen. Mol Cell Biol. 8: 2063–2069.

Cohen GM. 1997. Caspases: the executioners of apoptosis. Biochem J. 326: 1-16.

Collin SP, Collin HB. 2006. The corneal epithelial surface in the eyes of vertebrates: environmental and evolutionary influences on structure and function. J Morphol. 267: 273-291.

Collinson JM, Chanas SA, Hill RE, West JD. 2004. Corneal development, Limbal Stem Cell Function, and Corneal Epithelial Cell Migration in the $Pax6^{+/-}$ Mouse. Invest Invest Ophthalmol Vis Sci. 45: 1101-1108.

Cooper D, Schermer A, Sun TT. 1985. Classifiation of human epithelia and their neoplasms using monoclonal antibodies to keratins: strategies, applications and limitations. Lab Invest. 52: 243-256.

Costanzi C, Pehrson JR. 1998. Histone macroH2A1 is concentrated in the inactive X chromosome of female mammals. Nature. 393: 599-601.

Costanzi C, Pehrson JR. 2001. MACROH2A2, a new member of the MARCOH2A core histone family. J Biol Chem. 276: 21776-21784.

Cotsarelis G, Cheng S-Z, Dong G, Sun T-T, Lavker RM. 1989. Existence of slow-cycling limbal epithelial basal cells that can be preferentially stimulated to proliferate: implication on epithelial stem cells. Cell. 57: 201-209.

Coulombre AJ, Coulombre JL. 1958. Corneal development 1. Corneal transparency. J Cell Physiol. 51: 1-11.

Coulombre AJ, Coulombre JL. 1964. Corneal development 3. The role of the thyroid in dehydration and the development of transparcency. Exp Eye Res. 75: 105-14.

Coulombre JL, Coulombre AJ. 1971. Metaplastic induction of scales and feathers in the corneal anterior epithelium of the chick embryo. Dev Biol. 25:464-78.

Das AV, James J, Zhao X, Rahnenfuhrer J, Ahmad I. 2004. Identification of c-Kit receptor as a regulator of adult neural stem cells in the mammalian eye: interactions with Notch signaling. Dev Biol. 273: 87–105.

Davanger M, Evensen A. 1971. Role of the pericorneal papillary structure in renewal of corneal epithelium. Nature. 229: 560-561.

De Boever S, Vangestel C, De Backer P, Croubles S, Sys SU. 2008. Identification and validation of housekeeping genes as internal control for gene expression in intravenous LPS inflammation model in chickens. Vet Immunol Immunopathol. 122: 312-317.

Decsi A, Peiffer RL, Qiu T, Lee DC, Friday JT, Bautch VL. 1994. Lens expression of TGF alpha in transgenic mice produces two distinct eye pathologies in the absence of tumors. Oncogene. 9: 1965-75.

Dheda K, Huggett JF, Bustin SA, Johnson MA, Rook G, Zumla A 2004. Validation of housekeeping genes for normalizing RNA expression in real-time PCR. Biotechniques. 37: 112-119.

Djalilian AR, Namavari A, Ito A, Balali S, Afshar A, Lavker RM, Yue BY. 2008. Down-regulation of Notch signaling during corneal epithelial proliferation. Mol Vis. 14: 1041-1049.

Dobbin KK, Beer DG, Meyerson M, Yeatman TJ, Gerald WL, Jacobson JW, Conley B, Buetow KH, Heiskanen M, Simon RM. 2005. Interlaboratory comparability study of cancer gene expression analysis using oligonucleotide microarrays. Clin Cancer Res. 11: 565-572.

Dodson JW, Hay ED. 1971. Secretion of collagenous stroma by isolated epithelium grown in vitro. Exp Cell Res. 65: 215-220.

Dong Y, Roos M, Gruijters T, Donaldson P, Bullivant S, Beyer E, Kistler J. 1994. Differential expression of two gap junction proteins in corneal epithelium. Eur J Cell Biol. 64: 95-100.

Doupnik CA, Davidson N, Lester HA. 1995. The inward rectifier potassium channel family. Curr Opin Neurobiol. 5: 268–277.

Draghici S, Kharti P, Eklund AC, Szallasi Z. 2006. Reliability and reproducibility issues in DNA microarray measurements. Trends Genet. 22: 101-109.

Dua HS, Joseph A, Shanmuganathan VA, Jones RE. 2003. Stem cell differentiation and the effects of deficiency. Eye. 17: 87-885.

Dua HS, Shanmuganathan VA, Powell-Richards A, Tiqhe PJ, Joseph A. 2005. Limbal epithelial crypts:a novel anatomical structure and a putative limbal stem cell niche. Br J Ophthalmol. 89: 529–532.

Duan WR, Garner DS, Williams SD, Funckes-Shippy CL, Spath IS, Blomme EA. 2003. Comparison of immunohistochemistry for activated caspase-3 and cleaved cytokeratin 18 with the TUNEL method for quantification of apoptosis in histological sections of PC-3 subcutaneous xenografts. J Pathol. 199: 221-228.

Dubey P, Wu H, Reiter RE, Witte ON. 2001. Alternative pathways to prostate carcinoma activate prostate stem cell antigen expression. Cancer Res. 61: 3256-3261.

Düblin I. 1970. Comparative embryologic studies of the early development of the cornea and the pupillary membrane in reptiles, birds and mammals. Acta Anat. 76: 381-408.

Duckett CS, Nava VE, Gedrich RW, Clem RJ, Vandongen JL, Gilfillan MC, Shiels H, Hardwick JM, Thompson CB. 1996. A conserved family of cellular genes related to the baculovirus iap gene and encoding apoptosis inhibitors. EMBO J. 15: 167-178..

Dunlevy JR, Beales MP, Berryhill BL, Cornuet PK, Hassell JR. 2000. Expression of the keratan sulfate proteoglycans lumican, keratocan and osteoglycin/mimecan during chick corneal development. Exp Eye Res. 70: 349-362.

Dunn IC, Wilson PW, Lu Z, Bain MM, Crossan CL, Talbot RT, Waddington D. 2009. New hypotheses on the function of the avian shell gland derived from microarray analysis comparing tissue from juvenile and sexually mature hens. Gen Comp Endocrinol. 163: 225-232.

Ebato B, Friend J, Thoft RA. 1987. Comparison of central and peripheral human corneal epithelium in tissue culture. Invest Ophthalmol Vis Sci. 28: 1450-1456.

Egeo A, Mazzocco M, Arrigo P, Vidal-Taboada JM, Oliva R, Pirola B, Giglio S, Rasore-Quartino A, Scartezzini P. 1998. Identification and characterization of a new human gene encoding a small protein with high homology to the poline-rich region of the SH3BGR gene. Biochem Biophys Res Commun. 247: 302-306.

Ehrenreich A. 2006. DNA microarray technology for the microbiologist: an overview. Appl Microbiol Biotechnol. 73: 255-273.

Eichner R, Bonitz P, Sun TT. 1984. Classification of epidermal keratins according to their immunoreactivity, isoelectric point, and mode of expression. J Cell Biol. 98: 1388-1396.

Ellies DL, Church V, Francis-West P, Lumsden A. 2000. The WNT antagonist cSFRP2 modulates programmed cell death in the developing hindbrain. Development. 127: 5285–5295.

Ellis RE, Yuan J, Horvits HR. 1991. Mechanisms and functions of cell death. Ann Rev Cell Biol. 7: 663-698.

Emoto I, Beuerman RW. 1987. Stimulation of neurite growth by epithelial implants into corneal stroma. Neurosci Lett. 23: 140-144.

Endl E, Gerdes J. 2000. The Ki-67 Protein: Fascinating Forms and an Unknown Function. Exp Cell Res. 257: 231–237.

Espana EM, Di Pascule MA, He H, Kawakita T, Raju VK, Liu CY, Tseng SC. 2004. Characterization of corneal pannus removed from patients with total limbal stem cell deficiency. Invest Ophthalmol Vis Sci. 45: 2961-2966.

Etienne W, Meyer MH, Peppers J, Meyer RA Jr. 2004. Comparison of mRNA gene expression by RT-PCR and DNA microarray. BioTechniques. 36: 618-621.

Evans GI, Brown L, Whyte M, Harrington E. 1995. Apoptosis and the cell cycle. Curr Opin Cell Biol. 7: 825-834.

Fabiani C, Barabino S, Rashid S, Dana MR. 2009. Corneal epithelial proliferation and thickness in a mouse model of dry eye. Exp Eye Res. 89: 166-171.

Fajas L, Egler V, Reiter R, Hansen J, Kristiansen K, Debril MB, Miard S, Auwerx J. 2002. The retinoblastoma- histone deacetylase 3 complex inhibits PPARgamma and adipocyte differentiation. Dev Cell. 3: 903–991.

Fakler B, Brändle U, Glowatzki E, Zenner HP, Ruppersberg JP. 1994. Kir2.1 inward rectifier K+ channels are regulated independently by protein kinases and ATP hydrolysis. Neuron.13: 1413–1420.

Fawcett DW. 1966. The occurrence of fibrous lamina on the inner aspect of the nuclear envelope in certain cells of vertebrates. Am J Anat. 119: 129-145.

Ferraris C, Chevalier G, Favier B, Jahoda CA, Dhouailly D. 2000. Adult corneal epithelium basal cells possess the capacity to activate epidermal, pilosebaceous and sweat genetic programmes in response to embryonic dermal stimuli. Development. 127: 5487–5495.

Figueira EC, Di Girolamo N, Coroneo MT, Wakefield D. 2007. The phenotype of Limbal Epithelial Stem Cells. Invest Opthalmol Vis Sci. 48: 144-156.

Fiore R, Puschel AW. 2003. The function of semaphorins during nervous system development. Front Biosci. 8: 484-499.

Fischer-Lougheed J, Liu JH, Espinos E, Mordasini D, Bader CR, Belin D, Bernheim L. 2001. Human myoblast fusion requires expression of functional inward rectifier Kir2.1 channels. J. Cell Biol. 153: 677-686.

Fokina VM, Frolova EI. 2006. Expression patterns of Wnt genes during development of an anterior part of the chicken eye. Dev Dyn. 235: 496–505.

Forrester JV, Dick AM, McMenamin PG, Lee WR. 2002. The eye; basic sciences in practice. 2nd ed. Edinburgh. W.B. Saunders. p. 447.

Foss DL, Baarsch MJ, Murtaugh MP. 1998. Regulation of hypoxanthine bv phosphoribosyltransferase, glyceraldehyde-3-phosphate dehydrogenase and beta-actin mRNA expression in porcine immune cells and tissues. Anim. Biotechnol. 9: 67–78.

Francesconi CM, Hutcheon AE, Chung EH, Dalbone AC, Joyce NC, Zieske JD. 2000. Expression patterns of retinoblastoma and E2F family proteins during corneal development. Invest Ophthalmol Vis Sci. 41:1054-62.

Franz T, Besecke A. 1991. The development of the eye in homozygotes of the mouse mutant Extra-toes. Anat Embryol. 184: 355-61.

Freeman WM, Walker SJ, Vrana KE. 1999. Quantitative RT-PCR: pitfalls and potential. BioTechniques. 26: 112–125.

Fuchs E. 1988. Keratins as biochemical markers of epithelial differentiation. Trends Genet. 4: 277-81.

Fukushima A, Funaki H, Yaoeda K, Tanaka T, Shirakashi M, Yoshida Y, Yaoita E, Abe H Yamamoto T. 2003. Localization and expression of chondromodulin-I in the rat cornea. Arch Histol Cytol Vol. 66: 445-452.

Gagliardini V, Fankhauser C. 1999. Semaphorin III can induce death in sensory neurons. Mol Cell Neurosci. 14: 301-316.

Gan L, van Setten G, Seregard S, Fagerholm P. 1995. Proliferating cell nuclear antigen colocalization with corneal epithelial stem cells and involvement in physiological cell turnover. Acta Ophthalmol Scand. 73: 491-495.

Gao J, Gelber-Schwalb TA, Addeo JV, Stern ME. 1997. Apoptosis in the rabbit cornea after photorefractive keratectomy. Cornea.16: 200-208.

Gartner LP, Hiatt JL. 2001. Color Textbook of Histology. WB Saunders Company. Chapter 22. pp.512-525.

Gavrieli Y, Sherman Y, Ben-Sasson SA. 1992. Identification of programmed cell death *in situ* via specific labeling of nuclear DNA. J Cell Biol. 119: 493-319.

Gentleman RC, Carey VJ, Bates DM, Bolstad B, Dettling M, Dudoit S. 2004. Bioconductor: open software development for computational Biology and bioinformatics. Genome Biol. 5: R80.

Gerdes J, Lemke H, Baisch H, Wacker HH, Schwab U, Stein H. 1984. Cell cycle analysis of a cell proliferation-associated human nuclear antigen defined by the monoclonal antibody Ki-67. J Immunol. 133: 1710-1715.

Ghering WJ. 2002. The genetic control of the eye development and its implicants for the evolution of the various eye-types. Int J Dev Biol. 46: 65-73.

Giger RJ, Wolfer DP, De Wit GMJ, Verhaagen J. 1996. Anatomy of rat semaphorin III/collapsin-1 mRNA expression and relationship to developing nerve tracts during neuroembryogenesis. J Comp Neurol. 375: 378-392.

Giovannardi S, Forlani G, Balestrini M, Bossi E, Tonini R, Sturani E, Peres A, Zippel R. 2002. Modulation of the inward rectifier potassium channel IRK1 by the ras signaling pathway. J Biol Chem. 277: 12158–12163.

Gipson IK. 1989. The epithelial basement membrane zone of the limbus. Eye. 3: 132–140.

Gipson IK. 1994. Anatomy of the conjunctiva, cornea, and limbus. In: Smolin G, Thoft RA, eds. The cornea. Boston: Little, Brown. pp.3-24.

Gipson IK, Ho SB, Spurr-Michaud SJ, Tisdale AS, Zhan Q, Torlakovic E, Pudney J, Anderson DJ, Toribara NW, Hill JA 3rd. 1997. Mucin genes expressed by human female reproductive tract epithelia. Biol Reprod. 56: 999-1011.

Glare EM, Divjak M, Bailey MJ, Walters EH. 2002. Beta-actin and GAPDH housekeeping gene expression in asthmatic airways is variable and not suitable for normalising mRNA levels. Thorax. 57: 765–770.

Glaser T, Jepeal L, Edwards JG, Young SR, Favor J, Maas RL. 1994. Pax-6 gene dosage effect in a family with congenital cataracts, aniridia, anopthalamia and central nervous system defects. Nature Genet. 7: 463-471.

Goidin D, Mamessier A, Staquet MJ, Schmitt D, Berthier-Vergnes O. 2001. Ribosomal 18S RNA prevails over glyceraldehyde-3-phosphate dehydrogenase and beta-actin genes as internal standard for quantitative comparison of mRNA levels in invasive and noninvasive human melanoma cell subpopulations. Anal Biochem. 95: 17-21.

Gold R. 1994. Differentiation between cellular apoptosis and necrosis by combined use of *in situ* tailing and nick translation techniques. Lab Invest. 71: 219-225.

Goudreau G, Petrou P, Reneker LW, Graw J, Loster J, Gruss P. 2002. Mutually regulated expression of *Pax6* and *Six3* and its implications for the *Pax6* haploinsufficient lens phnotype. Proc Natl Acad Sci USA 99: 8719-8724.

Grasl-Kraupp B, Ruttkay-Nedecky B, Koudelka H, Bukowska K,Bursch W, Schulte-Hermann R. 1995. In situ detection of fragmented DNA (TUNEL assay) fails to discriminate among apoptosis, necrosis, and autolytic cell death: a cautionary note. Hepatology. 21: 1465–1468.

Graw J. 2003. The genetic and molecular basis of congenital eye defects. Nat Rev Genet. 4: 876-888.

Gruetrich M, Espana EM, Tseng SCG. 2003. *Ex vivo* expansion of limbal stem cells: amniotic membrane serving as a stem cell niche. Surv Ophthalmol. 48: 631–646.

Gu LH, Coulombe PA. 2007. Keratin function in skin epithelia: a broadening palette with surprising shades. Curr Opin Cell Biol. 19: 13-23.

Guo J, Sax CM, Piatigorsky J. Xu FX. 1997. Heterogeneous expression of transketolase in ocular tissues. Curr Eye Res. 16: 467–474.

Guo X, Wang XF. 2009. Signaling cross-talk between TGF-β/BMP and other pathways. Cell Res. 19: 71-88.

Haake AR, Polakowska RR. 1993. Cell death by apoptosis in epidermal biology. J Invest Dermatol. 101: 107-112.

Hall PA, Watt FM. 1989. Stem cells: the generation and maintenance of cellular diversity. Development. 106: 619-633.

Hall PA, Levison DA, Woods AL, Yu CC-W, Kellock DB, Watkins JA, Barnes DM, Gillett CE, Camplejohn R, Dover R, Waseem NH, Lane DP. 1990. Proliferating cell nuclear antigen (PCNA) immunolocalization in paraffin sections: An index of cell proliferation with evidence of deregulated expression in some neoplasms. J Pathol. 162: 285-294.

Hall PA. 1999. Assessing apoptosis: a critical survey. Endocr Relat Cancer. 6: 3-8.

Halloran MC, Severance SM, Yee CS, Gemza DL, Raper JA, Kuwada JY. 1999. Analysis of a zebrafish semaphorin reveals potential functions in vivo. Dev Dyn. 214: 13-25.

Hamann S, Zeuthen T, La Cour M. 1998. Aquaporins in complex tissues: distribution of aquaporins 1–5 in human and rat eye. Am J Physiol. 274: C1332–C1345.

Hamburger V, Hamilton HL. 1951. Series of Embryonic Chicken Growth. J Morphology. 898: 49-92.

Hamrah P, Zhang Q, Liu Y, Dana MR. 2002. Novel characterization of MHC class II-negative population of resident corneal Langerhans cell-type dendritic cells. Invest Ophthalmol Vis Sci. 43: 639–646.

Hanlon M, Sealy L. 1999. Ras regulates the association of serum response factor and CAATT/enhaner-binding protein beta. J Biol Chem. 274:14224-14228

Hanna C, O'Brien JE. 1960. Cell production and migration in the epithelial layer of the cornea. Arch Ophthalmol. 64: 536-539.

Hara-Chikuma M, Verkman AS. 2008. Prevention of skin tumorigenesis and impairment of epidermal cell proliferation by targeted Aquaporin-3 gene disruption. Mol Cell Biol. 28: 326-332.

Haramis AP, Begthel H, van den Born M, van Es J, Jonkheer S, Offerhaus GJ, Clevers H. 2004. De novo crypt formation and juvenile polyposis on BMP inhibition in mouse intestine. Science. 303: 1684–1686.

Harrington CA, Rosenow C, Retief J. 2000. Monitoring gene expression using DNA microarrays. Curr Opin Microbiol. 3: 285–291.

Hatch CL, Bonner WM. 1996. An upstream region of the H2AZ gene promoter modulates promoter activity in different cell types. Biochem Biophys Act. 1305: 59-62.

Hay ED, Linsenmayer TF, Trelstad RL, von der Mark K. 1979. Origin and distribution of collagens in the developing avian cornea. Curr Top Eye Res. 1: 1-35.

Hay ED, Revel JP. 1969. Fine structure of the developing avian cornea. Departament of Anatomy, Harvard Medical School, Boston, Mass. Copyright by S.Kager, Basel, Switzerland. Chapter 4. Fine structure of the corneal epithelium. pp.66-74.

Hay ED. 1979. Development of the vertebrate cornea. Inter Rev Cytol. 63: 263-322.

Hayashi S, Osawa T, Tohyama K. 2002. Comparative observations on corneas, with special reference to Bowman`s layer and Decemet`s membrane in mammmals and amphibians. J Morphol. 254: 247-258.

He XC, Zhang J, Tong WG, Tawfik O, Ross J, Scoville DH, Tian Q, Zeng X, He X, Wiedemann LM. 2004. BMP signalling inhibits intestinal stem cell self-renewal through suppression of Wnt-beta-catenin signaling. Nat Genet. 36: 1117-1121.

Heber S, Sick B. 2006. Quality assessment of Affymetrix GeneChip data. OMICS. 10: 358-68.

Hedgecock EM, Sulston JE, Thomson JN. 1983. Muattions affecting programmed cell deaths in nematode *C. elegans*. Science. 220: 1277-1279.

Hengartner MO. 2000. The biochemistry of apoptosis. Nature. 407: 770-776.

Héon E, Greenberg A, Kopp KK, Rootman D, Vincent AL, Billingsley G, Priston M, Dorval KM, Chow RL, McInnes RR, Heathcote G, Westall C, Sutphin JE, Semina E, Bremner R, Stone EM. 2002. VSX1: a gene for posterior polymorphous dystrophy and keratoconus. Hum Mol Genet. 11: 1029-1036.

Hinard V, Belin D, Konig S, Bader CR, Bernheim L. 2008. Initiation of human myoblast differentiation via dephosphorylation of Kir2.1 K+ channels at tyrosine 242. Development. 135: 859-867.

Hipp J, Atala A. 2007. Principles of Regenerative Medicine. GeneChips in regenerative medicine. 3rd Edition. Academic Press. p.532.

Holland EJ, Djalilian AR, Schwartz GS. 2003. Management of aniridic keratopathy with keratolimbal allograft: a limbal stem cell transplantation technique. Opthalmology. 110: 125-130.

Holmes G, Niswander L. 2001. Expression of *slit-2* and *slit-3* during chick development. Dev Dyn. 222: 301-307.

Hong YH, Lillehoj HS, Lee SH, Dalloul R, Lillehoj EP. 2006. Analysis of chicken cytokine and chemokine gene expression following Eimeria acervulina and Eimeria tenella infections. Vet Immunol Immunopathol. 114: 209–223.

Horikoshi T, Danenberg KD, Stadlbauer TH, Volkenandt M, Shea LC, Aigner K, Gustavsson B, Leichman L, Frösing R, Ray M. 1992. Quantitation of thymidylate synthase, dihydrofolate reductase, and DT-diaphorase gene expression in human tumors using the polymerase chain reaction. Cancer Res. 52: 108-116.

Hsueh Y-J, Wang D-Y, Chng C-C, Chen J-K. 2004. Age-related expression of p63 and other keratinocyte stem cell makers in rat cornea. J Biomed Sci. 11: 641-651.

Hui CC, Joyner Al. 1993. A mouse model of greig cephalopolysyndactyly syndrome: the extra-toesJ mutation contains an intragenic deletion of the Gli3 gene. Nat Genet. 3: 241-246.

Hu C, Dievart A, Lupien M, Calvo E, Tremblay G, Jolicoeur P. 2006. Overexpression of activated murine Notch1 and Notch3 in transgenic mice blocks mammary gland development and induces mammary tumors. Am J Pathol. 168: 973–990.

Huang da W, Sherman BT, Tan Q, Collins JR, Alvord WG, Roayaei J, Stephens R, Baseler MW, Lane HC, Lempicki RA. 2007. The DAVID Gene Functional Classification Tool: a novel biological module-centric algorithm to functionally analyze large gene lists. Genome Biol. 8: R183.

Huang da W, Sherman BT, Lempicki RA. 2009. Systematic and integrative analysis of large gene lists using DAVID bioinformatics resources. Nat Prot. 4: 44-57.

Huggett J, Dheda K, Bustin S, Zumla A. 2005. Real-time RT-PCR normalization; strategies and considerations. Genes Immun. 6: 279-284.

Huppertz B, Frank HG, Kaufmann P. 1999. The apoptosis cascade – morphological and immunohistochemical methods for its visualization. Anat Embryol (Berlin). 200: 1-18.

Ihaka R, Gentleman R. 1996. A language for data analysis and graphics. J Comp and Graph Stat. 5: 299-314.

Ikeda MA, Jakoi L, Nevins JR. 1996. A unique role for the Rb protein in controling E2F Accumulation during cell grwoth and differentiation. Proc Natl Acad Sci USA. 93: 3215-3220.

Inatomi T, Nakamura T, Koizumi N, Sotozono C, Yokoi N, Kinoshita S. 2006. Midterm results on ocular surface reconstruction using cultivated autologous oral mucosal epithelial transplantation. Am J Ophthalmol. 141: 267-275.

Innis MA, Gelfand DH. 199. Optimization of PCRs. in: PCR Protocols (Innis, Gelfand, Sninsky and White, eds. Academic Press, New York. pp.3-12.

Irizarry RA, Hobbs B, Collin F, Beazer-Barclay YD, Antonellis KJ, Scherf U, Speed TP. 2003. Exploration, normalization, and summaries of high density oligonucleotide array probe level data. Biostatistic. 4: 249-284.

Ishihara K, Hiraoka M. 1994. Gating mechanism of the cloned inward rectifier potassium channel from mouse heart. J Membr Biol. 142: 55-64.

Ishii T, Wallace AM, Zhang X, Gosselink J, Abboud RT, English JC, Pare PD, Sandford PD. 2006. Stability of housekeeping genes in alveolar macrophages from COPD patients. Eur Respir J. 27: 300-306.

Iwata M, Soya K, Sawa M, Sakimoto T, Hwang DG. 2002. CD40 expression in normal human cornea and regulation of CD40 in cultured human corneal epithelial and stromal cells. Invest Ophthalmol Vis Sci. 43: 348–357.

Jakus MA. 1954. Studies on the cornea. I. The fine structure of the rat cornea. Amer J Opthal 38: 40-53.

Jan YN, Jan LY. 1993. HLH proteins, fly neurogenesis, and vertebrate myogenesis. Cell. 75: 827-830.

Jan YN, Jan LY. 1998. Asymmetric cell division. Nature. 392: 775-778.

Jarriault S, Le Bail O, Hirsinger E, Pourquié O, Logeat F, Strong CF, Brou C, Seidah NG, Isra I A. 1998. Delta-1activation of notch-1 signaling results in HES-1 transactivation. Mol Cell Biol. 18: 7423-7431.

Jean D, Ewan K, Gruss P. 1998. Molecular regulators involved in vertebrate eye development. Mech Dev. 76: 3-18.

Jefferies C, Bowie A, Brady G, Cooke EL, Li X, O'Neill LA. 2001. Transactivation by the p65 subunit of NF-kappaB in response to interleukin-1 (IL-1) involves MyD88, IL-1 receptor-associated kinase 1, TRAF-6, and Rac1. Mol. Cell. Biol. 21: 4544-4552.

Jensen UB, Lowell S, Watt FM. 1999. The spatial relationship between stem cells and their progeny in the basal layer of human epidermis: a new view based on whole-mount labelling and lineage analysis. Development.126: 2409-2418.

Johns DC, Marx R, Mains RE, O'Rourke B, Marbán E. 1999. Inducible Genetic Suppression of Neuronal Excitability. J Neurosci. 19: 1691–1697.

Johnson DH, Bourne WM, Campbell RJ. 1982. The ultrastructure of Descemet's membrane. I. Changes with age in normal cornea. Arch Ophthalmol. 100: 1942-1950.

Johnson PF. 2005. Molecular stop signs: regulation of cell-cycle arrest by C/EBP transcription factors. J Cell Sci 118: 2545-2555.

Jones PH, Harper S, Watt FM. 1995. Stem cell patterning and fate in human epidermis. Cell. 80: 83-93.

Jonnalagadda S, Srinivasan R. 2008. Principal components analysis based methodology to identify differentially expressed genes in time-course microarray data. BMC Bioinf. 9: 267-283.

Joyce NC, Meklir B, Joyce SJ, Zieske JD. 1996. Cell cycle protein expression and proliferative status in human corneal cells. Invest Opthalmol Vis Sci. 37: 645-655.

Joyce NC, Zieske JD. 1997. Transforming growth factor-beta receptor expression in human cornea. Invest Ophthalmol Vis Sci. 38:1922–1928.

Kaeser MD, Emerson BM. 2006. Remodeling plans for cellular specialization: unique styles for every room. Curr Opin Gen Develop. 16: 508–512.

Kaestner KH, Christy RJ, Lane MD. 1990. The mouse insulin-responsive glucose transporter genes: characterization and transactivation by the CCAAT/enhancer binding protein. In: (2nd rev. ed.). Proc Natl Acad Sci USA. 87: 251–255.

Kafarnik C, Fritsche J, Reese S. 2007. In vivo confocal microscopy in the normal corneas of cats, dogs, birds. Vet Ophthal. 10: 222-230.

Kalcheim C, Carmeli C, Rosenthal A. 1992. Neurotrophin 3 is a mitogen for cultured neural crest cells. Proc Natl Acad Sci USA. 89: 1661-1665.

Kanekar S, Perron M, Dorsky R, Harris WA, Jan LY, Jan YN, Vetter ML. 1997. *Xath5* participates in a network of bHLH genes in the developing *Xenopus* retina. Neuron. 19: 981–994.

Kashiwagi H, Shiraga M, Kato H, Kamae T, Yamamoto N, Tadokoro S, Kurata Y, Tomiyama Y, Kanakura Y. 2005. Negative regulation of platelet function by a secreted cell repulsive protein, semaphoring 3A. Blood. 106: 913-921.

Kasper M, Moll R, Stosiek P, Karsten U. 1988. Patterns of cytokeratin and vimentin expression in the human eyes. Acta Histochem. 89: 369-377.

Kasper M, Stosiek P, Lane B. 1992. Cytokeratin and vimentin heterogenity in human cornea. Acta Histochem. 89: 369-377.

Katoh Y, Katoh M. 2006. WNT antagonist, SFRP1, is Hedgehog signaling target. Int J Mol Med. 17: 171-175.

Katsuda S, Coltrera MD, Ross R, Gown AM. 1993. Human atherosclerosis. IV. Immunocytochemical analysis of cell activation and proliferation in lesions of young adults. Am J Pathol. 142: 1787-1793.

Kay IN, Finger-Baier KC, Roeser T, Staub W, Baier H. 2001. Retinal ganglion cell genesis requires lakritz, a Zebrafish atonal Homolog. Neuron. 30: 725–736.

Kays WT, Piatigorsky J. 1997. Aldehyde dehydrogenase class 3 expression: identification of a cornea-preferred gene promoter in transgenic mice. Proc Natl Acad Sci USA. 94: 13594–13599.

Kenyon KR. 1969. The synthesis of basement membrane by the corneal epithelium in bullous keratopathy. Invest Opthalmol Vis Sci. 8: 156-168.

Kenyon KR, Tseng SC. 1989. Limbal autograft transplantation for ocular surface disorders. Ophthalmology. 96: 709–722.

Kerr JF, Searle J, Harmon BV, Bishop CJ. 1987. Apoptosis. In Perspectives on Mammalian Cell Death. Edited by Potten CS, editor. Oxford University Press, Oxford. pp.93-128.

Kerr JF, Wyllie AH, Currie AR. 1972. Apoptosis: a basic biological phenomenon with wide-ranging implications in tissue kinetics. Br J Cancer. 26: 239–257.

Khodadoust AA, Silvestein AM, Kenyon DR, Dowling JR. 1968. Adhesion of regenerating corneal epithelium. The role of basement membrane. Am J Opthalmol. 65: 339-348.

Kidson SH, Kume T, Deng K, Winfrey V, Hogan BLM. 1999. The Forkhead/Winged-Helix gene, Mf1, is necessary for the normal development of the cornea and formation of the anterior chamber in the mouse eye. Dev Biol. 211: 306-322.

Kim JM, McOptom FS, Willcox MDP. 2008. induction of apoptosis in human corneal epithelial cells *in* vitro. Aus New Zel J Opthalmol. 27: 214-217.

Kinoshita S, Koizumi N, Nakamura T. 2004. Tranplantable cultivated mucosal epithelial sheet for ocular surface reconstruction. Exp. Eye Res. 78: 483–491.

Kiritoshi A, SundarRaj N, Thoft RA. 1991. Differentiation in cultured limbal epithelium as defined by keratin expression. Invest Ophthalmol Vis Sci. 32: 3073–3087.

Kirkin V, Joos S, Zörnig M. 2004. The role of Bcl-2 family members in tumorigenesis. Biochem Biophys Act. Mol Cell Res. 1644: 229-249.

Kivela T, Uusitalo M. 1998. Structure, development and function of cytoskeleta elements in non-neuronal cells of the human eye. Prog in Ret and Eye Res. 17: 385-428.

Klymkowsky MW, Bachant HB, Domingo A. 1989. Functions of intermediate filaments. Cell Motil Cytoskel. 14: 309-331.

Kockx MM, Muhring J, Knaapen MW, de Meyer GR. 1998. RNA synthesis and splicing interferes with DNA in situ end labelling techniques used to detect apoptosis. Am J Pathol . 152: 885–888.

Koizumi N, Inatomi T, Quantock AJ, Fullwood NJ, Dota A, Kinoshita S. 2000. Amniotic membrane as a substrated for cultivating limbal corneal epithelial cells for autologous transplantation in rabbits. Cornea. 19: 65-71.

Kojima H, Tanaka Y, Tanaka T, Miyazaki H, Shiwa M, Kamide Y, Moriyam H. 1998. Cell Proliferation and Apoptosis in Human Middle Ear Cholesteatoma. Arch Otolaryngol Head Neck Surg. 124: 261-264.

Kolli S, Lako M, Figueiredo F, Muhar H, Ahmad S. 2008. Loss of corneal epithelial stem cell properties in outgrowths from human limbal explants cultured on intact amniotic membranes. Regen Med. 3: 329-342.

Konradi C. 2005. Gene expression microarray studies in polygenic psychiatric disorders: applications and data analysis. B Res Rev. 50: 142-155.

Koroma BM, Yang JM, Sundin OH. 1997. The Pax-6 homeobox gene is expressed throughout the corneal and conjunctival epithelia. Invest Ophthalmol Vis Sci. 38: 108–120.

Koster MI, Kim S, Mills AA, DeMayo FJ, Roop DR. 2004. p63 is the molecular switch for initiation of an epithelial stratification program. Genes Dev. 18:126–131.

Koster MI, Roop DR. 2007. Mechanisms regulating epithelial stratification. Annual Cell Dev Biol. 23: 93-113.

Krauss S, Johansen T, Korzh V, Fjose A. 1991. Expression of the zebrafish paired box gene pax[zf-b] during early neurogenesis. Development. 103: 1197-1206.

Kruse FE. 1994. Stem cells and corneal epithelium regeneration. Eye. 8: 170-183.

Kuan CY, Roth KA, Flavell RA, Rakic P. 2000. Mechanisms of programmed cell death in the developing brain. Trends Neurosci. 23: 291-297.

Kubo Y, Baldwin TJ, Jan YN, Jan LY. 1993. Primary structure and functional expression of a mouse inward rectifier potassium channel. Nature. 362:127-133.

Kume T, Deng KY, Winfrey V, Gould DB, Walter MA, Hogan BL. 1998. The forkhead/winged helix gene Mf1 is disrupted in the pleiotropic mouse mutation congenital hydrocephalus. Cell. 93: 985–996.

Kurpakus MA, Maniaci MT, Esco M. 1994. Expression of keratins K12, K4 and K14 during development of ocular surface epithelium. Curr Eye Res. 13:805-814.

Ladher RK, Church VL, Allen S, Robson L, Abdelfattah A, Brown NA, Hattersley G, Rosen V, Luyten FP, Dale L, Francis-West PH. 2000. Cloning and expression of the Wnt antagonists Sfrp-2 and Frzb during chick development. Dev Biol. 218:183-198.

Laemle LK, Puszkarczuk M, Feinberg RN. 1999. Apoptosis in early ocular morphogenesis in the mouse. Brain Res Dev Brain Res. 112: 129-133.

Lai EC. 2002. Keeping a good pathway down: transcriptional repression of Notch pathway target genes by CSL proteins. EMBO Rep. 3: 840–845.

Lambiase A, Bonini S, Micera A, Rama P, Aloe L. 1998. Expression of nerve growth factor receptors on the ocular surface in healthy subjects and during manifestation of inflammatory diseases. Invest Ophthalmol Vis Sci. 39: 1272-1275.

Lane DO. 1992. P53, guardian of the genome. Nature. 358: 15-16.

Lang RA. 1997. Apoptosis in mammalian eye development: lens morphogenesis, vascular regression and immune privilege. Cell Death Differ. 4: 12-20.

Lassus P, Opitz-Araya X, Lazebnik Y. 2002. Requirement for Caspase-2 in stress-induced apoptosis before mitochondrial permeabilization. Science. 297: 1352-1354.

Lauweryns B, Van den Oord JJ, Missotten L. 1993a. The transitional zone between limbus and peripheral cornea. Invest Opthalmol Vis Sci. 34: 1991-1999.

Lavker RM, Dong G, Cheng SZ, Kudoh K, Cotsarelis G, Sun TT. 1991. Relative proliferative rates of limbal and corneal epithelia. Implications of corneal epithelial migration, circadian rhythm, and suprabasally located DNA-synthesizing keratinocytes. Invest Ophthalmol Vis Sci. 39: 301-307.

Le TT, Wroblewski E, Patel S, Riesenberg AN, Brown NL. 2006. *Math5* is required for both early retinal neuron differentiation and cell cycle progression. Develop Biol. 295: 764-778.

Leblond CP. 1981. The life history of cells in renewing systems. Am J Anat. 160: 114-158.

Lee HY, Wroblewski E, Philips GT, Stair CN, Conley K, Reedy M, Mastick GS, Brown NL. 2005. Multiple requirements for Hes1 during early eye formation. Dev Biol. 284: 464-478.

Lee JH, Hart SR, Skalnik DG. 2004b. Histone deacetylase activity is required for embryonic stem cell differentiation. Genesis. 38: 32–38.

Leers MP, Kolgen W, Bjorklund V. 1999. Immunocytochemical detection and mapping of a cytokeratin 18 neo-epitope exposed during early apoptosis. J Pathol. 187: 567–572.

Lefort K, Mandinova A, Ostano P, Kolev V, Calpini V, Kolfschoten I, Devgan V, Lieb J, Raffoul W, Hohl D, Neel V, Garlick J, Chiorino G, Dotto GP. 2007. Notch1 is a p53 target gene involved in human keratinocyte tumor suppression through negative regulation of ROCK1/2 and MRCKalpha kinases. Genes Dev. 21: 562-577.

Lehrer MS, Sun TT, Lavker RM. 1998. Strategies of epithelial repair: modulation of stem cell and transit amplifying cell proliferation. J Cell Sci. 111: 2867–2875.

Lenger J, Graw J. 2001. Regulation of the human SIX3 promoter. Biochem Biophys Res Comun. 287: 372-376.

Leong ASY, Milios J, Duncis CG. 2000. Antigen preservation in microwave-irradiated tissues: A comparison with formaldehyde fixation. J Pathol. 156: 275-282.

Levin MH, Verkman AS. 2004. Aquaporin-dependent water permeation at the mouse ocular surface: in vivo microfluorimetric measurements in cornea and conjunctiva. Invest Ophthalmol Vis Sci. 45: 4423-4432.

Levin MH, Verkman AS. 2006. Aquaporin-3-dependent cell migration and proliferation during corneal re-epithelialization. Invest Ophthalmol Vis Sci. 47: 4365-4372.

Lewis J. 1996. Neurogenic genes and vertebrate neurogenesis. Curr Opin Neurobiol. 6: 3-10.

Lewis J. 1998. Notch signaling and the control of cell fate choices in vertebrates. Cell Dev Biol. 9: 583-589.

Li DQ, Lee SB, Tseng SC. 1999. Differential expression and regulation of TGF-B1, TGF-B2, TGF-B3, TGF-BRI, TGF-BRII, TGF-BRIII in cultured human corneal, limbal and conjunctival fi broblasts. Curr Eye Res. 19: 154–161.

Li DQ, Tseng SC. 1995. Three pattern of cytokine expression potentially involved in epithelial fibroblast interactions of human ocular surface. J Cell Physiol. 163: 61-79.

Li H, Tierney C, Wen L, Wu JY, Rao Y. 1997. A single morphogenetic field gives rise to two retina primordia under the influence of the prechordal plate. Development. 124: 603-615.

Li L, Xie T. 2005. Stem cell niche: structure and function. Annu Rev Cell Dev Biol. 21: 605-631.

Li P, Nijhawan D, Budihardjo I, Srinivasula SM, Ahmad M, Alnemri ES, Wang X. 1997. Cytochrome c and dATP-dependent formation of Apaf-1/caspase-9 complex initiates an apoptotic protease cascade. Cell. 91: 479-489.

Li W, Hayashida Y, Chen YT, Tseng SC. 2007. Niche regulation of corneal epithelial stem cells at the limbus. Cell Res. 17: 26-36.

Li YP, Handberg KJ, Kabell S, Kusk M, Zhang MF, JØrgensen. 2007. Relative quantification and detection of different types of infectious bursal disease virus in bursa of Fabricius and cloacal swabs using real time RT-PCR SYBR green technology. Res Vet Sci. 82: 126-133.

Lin CT, Lin YT, Kuo TF. 2007. Investigation of mRNA expression for secreted frizzled-related protein 2 (sFRP2) in chick embryos. J Reprod Dev. 53: 801-810.

Lin K, Wang S, Julius MA, Kitajewski J, Moos M jr, Luyten FP. 1997. The cysteine-rich frizzled domain of Frzb-1 is required and sufficient for modulation of WNT signalling. Proc Natl Acad Sci USA. 94: 11196-11200.

Lin W, Dent SY. 2006. Functions of histone-modifying enzymes in development. Curr Opin Genet Dev. 16:137-142.

Lindberg K, Brown ME, Chaves H, Kenyon KR, Reinwald JG. 1993. In vitro propagation of human ocular epithelial cells for transplantation. Invest Ophthalmol Vis Sci. 34: 2672-2679.

Linsenmayer TF, Fitch JM, Gordon MK, Cai CX, Igoe F, Marchant JK, Birk DE. 1998. Development and roles of collagenous matrices in the embryonic avian cornea. Prog Retin Eye Res. 17: 231-265.

Litsiou A, Hanson S, Streit A. 2005. A balance of FGF, BMP and WNT signalling positions the fuure placode territory in the head. Development. 132: 4051-4062.

Liu CY, Zhu G, Westerhausen-Larson A, Converse R, Kao CW, Sun TT, Kao WW. 1993. Cornea-specific expression of K12 keratin during mouse development. Curr Eye Res. 12: 963-974.

Liu H, Mohamed O, Dufort D, Wallace VA. 2003. Characterization of Wnt signalling components and activation of the Wnt canonical patway in the murine retina. Dev Dyn. 227: 323-334.

Liu IS, Chen JD, Ploder L, Vidgen D, van der Kooy D, Kalnins VI, McInnes RR. 1994. Developmental expression of a novel murine homeobox gene (Chx10): evidence for roles in determination of the neuroretina and inner nuclear layer. Neuron. 13: 377-393.

Liu JH, Bijlenga P, Fischer-Lougheed J, Occhiodoro T, Kaelin A, Bader CR, Bernheim L. 1998. Role of an inward rectifier K+ current and of hyperpolarization in human myoblast fusion. J. Physiol. 510: 467-476.

Liu W, Mo Z, Xiang M. 2001. The Ath5 proneural genes function upstream of Brn3 POU domain transcription factor genes to promote retinal ganglion cell development. Proc Natl Acad Sci USA. 98: 1649–1654.

Liu X, Jaenisch R. 2000. Severe peripheral sensory neuron loss and modest motor neuron reduction in mice with combined defi ciency of brain-derived neurotrophic factor, neurotrophin 3 and neurotrophin 4/5. Dev Dyn. 218: 94-101.

Liu Y, Wada R, Yamashita T, Mi Y, Deng CX, Hobson JP, Rosenfeldt HM, Nava VE, Chae SS, Lee MJ, Liu CH, Hla T, Spiegel S, Proia RL. 2000. Edg-1, the G protein–coupled receptor for sphingosine-1-phosphate, is essential for vascular maturation. J Clin Invest. 106: 951-961.

Liu Z, Carvajal M, Carraway CAC, Carraway K, Pflugfelder SC. 2001. Expression of the receptor tyrosine kinases, epidermal growth factor receptor, ErbB2, and ErbB3, in human ocular surface epithelia. Cornea. 20: 81–85.

Livak KJ, Schmittgen TD. 2001. Analysis of relative gene expression data using real-time quantitative PCR and the 2(-Delta Delta C(T)) Method. Methods. 25: 402-408.

Ljubimov AV, Burgeson RE, Butkowski RJ, Michael AF, Sun T-T, Kenney MC. 1995. Human corneal basement membrane heterogeneity; topographical differences in the expression of type IV collagen and laminin isoforms. Lab Invest. 72: 461-472.

Lodish HF. 2003. Molecular cell biology. 5th Edition. WH. Freeman and Co. NY. p.973.

Loes S, Luukko K, Kvinnsland IH, Kettunen P. 2001. Slit1 is specifically expressed in the primary and secondary enamel knots during molar tooth cusp formation. Mech Dev. 107:155-157.

Louis H, Van Laethem JL, Wu W, Quertinmont E, Degraef C, Van den Berg K, Demols A, Goldman M, Le Moine O, Geerts A, Devière J. 1998. Interleukin-10 controls neutrophilic infiltration, hepatocyte proliferation, and liver fibrosis induced by carbon tetrachloride in mice. Hepatology. 28: 1607-1615.

Lowell S, Jones P, Le Roux I, DunneJ, Watt FM. 2000. Stimulation of human epidermal differentiation by Delta–Notch signalling at the boundaries of stem-cell clusters. Curr Biol. 10: 491-500.

Lu L, Reinach PS, Kao WW. 2001. Corneal epithelial wound healing. Exp Biol Med. 226: 6536-64.

Lu L. 2006. Stress-induced corneal epithelial apoptosis mediated by K^+ channel activation. Prog Retin Eye Res. 25: 515–538.

Luetteke NC, Phillips HK, Qiu TH, Copeland NG, Earp HS, Jenkins NA, Lee DC. 1994. The mouse waved-2 phenotype results from a point mutation in the EGF receptor tyrosine kinase. Genes Dev. 8: 399-413.

Lyngholm M, Hoyer PE, Vorum H, Nilsen K, Ehlers N, Mollgard K. 2008. Immunohistochemical markers for corneal stem cells in the early developing human eye. Exp Eye Res. 87: 115-121.

Ma A, Boulton M, Zhao B, Connon C, Cai J, Albon J. 2007. A role for Notch signaling in human corneal epithelial cell differentiation and proliferation. Invest Ophthalmol Vis Sci. 48: 3576-3585.

Ma W, Yan RT, Xie W, Wang SZ. 2004. *A* role of ath5 in inducing neuroD and the photoreceptor pathway. J. Neurosci. 24*:* 7150–7158.

Magin TM, Vijayaraj P, Leube RE. 2007. Structural and regulatory functions of keratins. Exp Cell Res. 313: 2021-2032.

Maisonpierre PC, Belluscio L, Squinto S, Ip NY, Furth ME, Lindsay RM, Yancopoulos GD. 1990. Neurotrophin-3: a neurotrophic factor related to NGF and BDNF. Science. 247: 1446-1451.

Marquardt T, Ashery-Padan R, Andrejewski N, Scardigli R, Guillemot F, Gruss P. 2001. Pax6 is required for the multipotent state of retinal progenitor cells. Cell. 105: 43–55.

Marsham E, Booth C, Potten CS. 2002. The intestinal epithelial stem cell. Bioessays. 24: 91–98.

Masai M. Yamaguchi, N. Tonou-Fujimori, A. Komori and H. Okamoto. 2005. The hedgehog-PKA pathway regulates two distinct steps of the differentiation of retinal ganglion cells: the cell-cycle exit of retinoblasts and their neuronal maturation, Development. 132: 1539–1553.

Matic M, Petrov IN, Chen S, Wang C, Dimitrijevich SD, Wolosin JM. 1997. Stem cells of the corneal epithelium lack connexins and metabolite transfer capacity. Differentiation. 61: 251-260.

Matsuo I, Kuratani S, Kimura C, Takeda N, Aizawa S. 1995. Mouse Otx2 functions in the formation and patterning of rostral head. Genes Dev. 9: 2646-2658.

Matsumato K, Moriuchi T, Koji T, Nakane PK. 1987. Molecular cloning of cDNA coding for rat proliferating cell nuclear antigen (PCNA)/cyclin. EMBO J. 6: 637-642.

Maurice DM. 1957. The structure and transparency of the cornea. J physiol. 136: 263-286.

Maurice DM. 1984. The cornea and sclera. In: Davson H: The eye. Vol 1b. Vegetative physiology and biochemistry. 3rd Edition. Academic Press, Orlando, FL. pp.1-158.

Maytin EV, Lin JC, Krishnamurthy R, Batchvarova N, Ron D, Mitchell PJ, Habener JF. 1999. Keratin 10 gene expression during differentiation of mouse epidermis requires transcription factors C/EBP and AP-2. Dev Biol. 216: 164-181.

Mazzocco M, Maffei M, Egeo A, Vergano A, Arrigo P, Di Lisic R, Ghiotto F, Scartezzini P. 2002. The identification of a novel human homologue of the SH3 binding glutamic acid-rich (SH3BGR) gene establishes a new family of highly conserved small proteins related to Thioredoxin Superfamily. Gene. 291: 233–239.

McCall CA, Cohan JJ. 1991. Programmed cell death in terminally differentiating keratinocytes. Role of endogenous endonuclease. J Invest Dermatol. 97: 111-114.

McConkey DJ, Orrenius S, Jondal M. 1990. Cellular signalling in programmed cell death (apoptosis). Immunol Today. 11: 120-121.

Medina-Martinez O, Brownell I, Amaya-Manzanares F, Hu Q, Behriger RR, Jamrich M. 2005. Severe Defects in Proliferation and Differentiation of Lens Cells in *Foxe3* Null Mice. Mol Cell Biol. 25: 8854-8863.

Meek KM, Leonard DW, Connon CJ, Dennis S, Khan S. 2003. Transparency, swelling and scarring in the corneal stroma. Eye. 17: 927–936.

Meek KM, Boote C. 2004. The organization of collagen in the corneal stroma. Exp Eye Res. 78: 503-512.

Meier S, Hay ED. 1973. Synthesis of sulfated glycosaminoglycans by embryonic corneal epithelium. Dev Biol. 35: 318-331.

Meier S. 1977. Initiation of corneal differentiation prior to cornea-lens association. Cell Tissue Res. 184: 255-267.

Michelacci YM. 2003. Collagens and proteoglycans of the corneal extracellular matrix. Braz J Med Biol Res. 36: 1037-1046.

Migheli A, Attanasio A, Schiffer D. 1995. Ultrastructural detection of DNA strand breaks in apoptotic neural cells by in situ end-labelling techniques. J Pathol. 176: 27-35.

Miles DH, Thakur A, Cole N, Willcox MD. 2007. The induction and suppression of the apoptotic response of HSV-1 in human corneal epithelial cells. Invest Ophthalmol Vis Sci. 48: 789-796.

Milhem M, Mahmud N, Lavelle D, Araki H, DeSimone J, Saunthararajah Y, Hoffman R. 2004. Modification of hematopoietic stem cell fate by 5aza 2'deoxycytidine and trichostatin A. Blood. 103: 4102–4110.

Millodot M. 2009. Dictionary of Optometry and Visual Science, 7th Edition. Butterworth-Heinemann. p.56.

Minami M, Kita M, Yan XQ, Yamamoto T, Iida T, Sekikawa K, Iwakura Y, Imanishi J. 2002. Role of IFNgamma and tumor necrosis factor-alpha in herpes simplex virus type 1 infection. J Interferon Cytokine Res. 22: 671–676.

Mirkes PE, Little SA, Umpierre CC. 2001. Co-localization of active caspase-3 and DNA fragmentation (TUNEL) in normal and hyperthermia-induced abnormal mouse development. Teratology. 63: 134-143.

Mokrý J, Němecek S. 1995. Immunohistochemical detection of proliferative cells. Sb Ved Pr Lek Fak Karlovy Univerzity Hradci Kralove. 38: 107-113.

Moll R, Franke WW, Schiller DL, Geiger B, Krepler R. 1982. The catalog of human cytokeratins: patterns of expression in normal epithelia, tumors and cultured cells. Cell. 31: 11-24.

Montiani-Ferreira F, Cardoso F, Petersen-Jones S. 2004. Postnatal development of corneal thickness in chicks of *Gallus gallus domesticus*. Vet Ophthal. 7: 37-39.

Montiani-Ferreira F, Petersen-Jones S, Cassotis N. 2003. Early postnatal development of central corneal thickness in dogs. *Veterinary Ophthalmology*. 6: 19–22.

Moreno-Flores MT, Martin-Aparicio E, Martin-Bermejo MJ, Agudo M, McMahon S, Avila J, Diaz-Nido J, Wandosell F. 2003. Semaphorin 3C preserves survival and induces neuritogenesis of cerebellar granule neurons in culture. J Neurochem. 87: 879-890.

Morey JS, Ryan JC, Van Dolah FM. 2006. Microarray validation: factors influencing correlation between oligonucleotide microarrays and real-time PCR. Biol Proced Online. 8: 175-193.

Morishige K-I, Takahashi N, Findlay I, Koyama H, Zanelli JS, Peterson C, Jenkins NA, Copeland NG, Mori N, Kurachi Y. 1993. Molecular cloning, functional expression and localization of an inward rectifier potassium channel in the mouse brain. FEBS Left. 336: 375-380.

Morita S, Shirakata Y, Shiraishi A, Kadota Y, Hashimoto K, Higashiyama S, Ohashi Y 2007. Human corneal epithelial cell proliferation by epiregulin and its cross-induction by other EGF family members. Mol Vis. 13: 2119-2128.

Moriuchi T, Matsumato K, Koji T, Nakane PK. 1986. Molecular cloning and nucleotide sequence analysis of rat PCNA/cyclin cDNA. Nucl Acids Symp Ser. 17: 117-120.

Moro L, Venturino M, Bozzo C, Silengo L, Altruda F, Beguinot L, Tarone G, Defilippi P. 1998. Integrins induce activation of EGF receptor: role in MAP kinase induction and adhesion-dependent cell survival. EMBO J. 17: 6622-6632.

Morris GF, Mathews MB. 1989. Regulation of proliferation cell nuclear antigen during the cell cycle. J Biol Chem. 264: 13856 -13864.

Morrison SJ, Shah NM, Anderson DJ. 1997. Regulatory Mechanisms in Stem Cell Biology. Cell. 88: 287-298.

Morrison-Graham K, Schatteman GC, Bork T, Bowen-Pope DF, Weston JA. 1992. A PDGF receptor mutation in the mouse (Patch) perturbs the development of a non-neuronal subset of neural crest-derived cells. Development. 115: 133-42.

Müller LJ, Pels L, Vrensen GF. 1996. Ultrastructural organization of human corneal nerves. Invest Opthalmol Vis Sci. 37: 476-488.

Müller LJ, Marfurt CF, Kruse F, Tervo TM. 2003. Corneal nerves: structure, contents and function. Exp Eye Res. 76: 521-542.

Murphy LD, Herzog CE, Rudick JB, Fojo AT, Bates SE. 1990. Use of the polymerase chain reaction in the quantitation of mdr-1 gene expression. Biochemistry. 29: 10351-10366.

Muskhelishvili L, Latendresse JR, Kodell RL, Henderson EB. 2003. Evaluation of cell proliferation in rat tissues with BrdU, PCNA, Ki-67(MIB-5) immunohistochemistry and in situ hybridization for histone mRNA. J Histochem Cytochem. 51: 1681-1688.

Nagata S, Golstein P. 1997. The Fas death receptor. Science. 267: 1449-1456.

Nagata S. 2000. Apoptotic DNA fragmentation. Exp Cell Res. 256: 12-18.

Nagasaki T, Zhao J. 2005. Uniform distribution of epithelial stem cells in the bulbar conjunctiva. Invest Ophthalmol Visual Sci. 46: 126–132.

Nakamura M, Nishida T, Ofuji K, Reid TW, Mannis MJ, Murphy CJ. 1997a. Synergistic effect of substance P with epidermal growth factor on epithelial migration in rabbit cornea. Exp Eye Res. 65: 321-329.

Nakamura M, Ofuji K, Chikama T, Nishida T. 1997b. Combined effect of substance P and insulin-like growth factor-1 on corneal epithelial wound closure of rabbit in vivo. Curr Eye Res. 16: 275-278.

Nakamura M, Ofuji K, Chikama T, Nishida T. 1997c. The NK1 receptor and its participation in the synergistic enhancment of corneal epithelial migration by substancje P and insulin-like growth factor-1. Br J Pharmacol. 120: 547-552.

Nakamura T, Inatomi T, Sotozono C, Amemiya T, Kanamura N, Kinoshita S. 2004. Transplantation of cultivated autologous oral mucosal epithelial cells in patients with severe ocular surface disorders. Br J Ophthamol. 88: 1280–1284.

Nakamura T, Ishikawa F, Sonoda KH, Hisatomi T, Qiao H, Yamada J, Fukata M, Ishibashi T, Harada M, Kinoshita S. 2005. Characterization and distribution of bone marrow-derived cells in mouse cornea. Invest Ophthalmol Vis Sci. 46: 497-503.

Navaratnam DS, Escobar L, Covarrubias M, Oberholtzer JC. 1995. Permeation properties and differential expression across the auditory receptor epithelium of an inward rectifier K+ channel cloned from the chick inner ear. J Biol Chem. 270: 19238-19245.

Negishi M, Oinuma I, Katoh H. 2000. Plexins: axon guidance and signal transduction. Cell Mol Life Sci. 62:1363-1371.

Nelson WG, Sun TT. 1983. The 50- and 58-kdalton keratin classes as molecular markers for stratified squamous epithelia: cell culture studies. J Cell Biol. 97: 244-251.

Newsome DA, Foidart JM, Hassell JR. 1981. Detection of specific collagen types in normal and keratoconus corneas. Invest Opthalmol Vis Sci. 20: 738-750.

Nicolas M, Wolfer A, Raj K, Kummer JA, Mill P, van Noort M, Hui CC, Clevers H, Dotto GP, Radtke F.2003. Notch1 functions as a tumor suppressor in mouse skin. Nat Genet. 33: 416-421.

Nishida K, Adachi W, Shimizu-Matsumoto A, Kinoshita A, Mizuno K, Matsubara K, Okubo K. 1996. A gene expression profile of human corneal epithelium and the isolation of human keratin 12 cDNA. Invest Opthalmol Vis Sci. 37: 1800-1809.

Nishida K, Yamato M, Hayashida Y, Watanabe K, Yamamoto K, Adachi E, Nagai S, Kikuchi A, Maeda N, Watanabe H, Okano T, Tano Y. 2004. Corneal reconstruction with tissue-engineered cell sheets composed of autologous oral mucosal epithelium. N Engl J Med. 351: 1187–1196.

Nuttall RP. 1976. Epithelial stratification in the developing chick cornea. J Exp Zool. 198: 185-192.

Oliver G, Mailhos A, Wehr R, Copeland NG, Jenkins NA, Gruss P. 1995. Six3, a murine homologue of the sine oculis gene, demarcates the most anterior border of the developing neural plate and is expressed during eye development. Development 121: 4045-4055.

Oliver G, Gruss P. 1997. Current views on eye development. Trends in Neurosciences. 20: 415-421.

O'Neill LA, Dunne A, Edjeback M, Gray P, Jefferies C, Wietek C. 2003. Mal and Myd88 adapter proteins involved in signalling transduction by Toll-like receptors. J Endotoxin Res. 9: 55-59.

Osborne NJ, Begbie J, Chilton JK, Schmidt H, Eickholt BJ. 2005. Semaphorin/neuropilin signaling influences the positioning of migratory neural crest cells within the hindbrain region of the chick. Dev Dyn. 232: 939-949.

Owen-Schaub LB, Zhang W, Cusack JC, Angelo LS, Santee SM, Fujiwara T, Roth JA, Deisseroth AB, Zhang WW, Kruzel E. 1995. Wild-type human p53 and a temperature-sensitive mutant induce Fas/APO-1 expression. Mol Cell Biol. 15: 3032–3040.

Ozanics V, Rayborn M, Sagun D. 1977. Observations on the morphology of the developing primate corneal epithelium, its innervation and anterior stroma. J Morphol. 153: 263–297.

Pajoohesh-Ganji A, Ghosh SP, Stepp MA. 2004. Regional distribution of alpha9beta1 integrin within the limbus of the mouse ocular surface. Dev Dyn. 230: 518-28.

Pajohesh-Ganji A, Stepp MA. 2005. In search of markers for the stem cells of the corneal epithelium. Biol Cell. 97: 265-276.

Pallari HM, Eriksson JE. 2006. Intermediate filaments as signaling platforms. Sci STKE. 366: 53-56.

Pan G, Ni J, Wei YF, Yu G, Gentz R, Dixit VM. 1997a. An antagonist decoy receptor and a death domain-containing receptor for TRAIL. Science. 277: 815–818.

Pancholi V. 2001. Multifunctional α-enolase: its role in diseases. Cell Mol Life Sci. 58: 902-920.

Patil RV, Saito I, Yang X, Wax MB. 1997. Expression of aquaporins in the rat ocular tissue. Exp Eye Res. 64: 203–209.

Pearton DJ, Ferraris C, Dhouailly D. 2004. Transdifferentiation of corneal epithelium: evidence for a linkage between the segregation of epidermal stem cells and the induction of hair follicles during embryogenesis. Int J Dev Biol. 48: 197-201.

Peifer M. 1999. Signal transduction: Neither straight nor narrow. Nature. 400: 213-215.

Pellegrini G, Dellambra E, Golisano O, Martinelli E, Fantozzi I, Bondanza S, Ponzin D, McKeon F, De Luca M. 2001. p63 identifies keratinocyte stem cells. Proc Natl Acad Sci USA. 98:3156–3161.

Pellegrini G, Golisano O, Paterna P, Lambiase A, Bonini S, Rama P. 1999. Location and clonal analysis of stem cells and their differentiated progeny in the human ocular surface. J Cell Biol. 145: 769–782.

Pellegrini G, Rama P, Mavilio F, De Luca M. 2009. Epithelial stem cells in corneal regeneration and epidermal gene therapy. J Pathol. 217: 217-228.

Perry SW, Epstein LG, Gelbard HA. 1997. Simultaneous *in situ* detection of apoptosis and necrosis in monolayer cultures by TUNEL and trypan blue staining. BioTechnigues. 22: 1102-1106.

Pfaffl MW. 2003. Live transcriptomics: Quantitative mRNA analytics in molecular endocrinology and physiology. Habilitation. Faculty Center of Life and Food Sciences, Technische Universität München – Weihenstephan, Germany. pp.1-41.

Pfaffl MW, Tichopad A, Prgomet C, Neuvians TP. 2004. Determination of stable housekeeping genes, differentially regulated target genes and sample integrity: BestKeeper – Excel-based tool using pair-wise correlations. Biotech Lett. 26: 509-515.

Pfister RR, Burstein NL. 1977. The normal and abnormal human corneal epithelial surface: A scanning electron microscope study. Invest Opthalmol Vis Sci. 16: 610-622.

Pfister RR. 1973. The normal surface of the corneal epithelium: a scanning electron microscopic study. Invest Ophthalmol. 12: 654-668.

Piper M, Little M. 2002. Movement through slits: Cellular migration via the Slit family. BioEssays. 25: 32-38.

Polak JM, Van Noorden S. 1997. Introduction to Immunochostochemistry. Second edition. Springer. Chapter 1.1. p.14-25.

Polakowska RR, Piacentini M, Bartlett R, Goldsmith LA, Haake AR. 1994. Apoptosis in human skin development: morphogenesis, periderm and stem cells. Dev Dyn. 199: 176-188.

Portellinha W, Belfort R Jr. 1991. Central and peripheral corneal thickness in newborns. Acta Ophthalmologica. 69: 247–250.

Porter FD, Drago J, Xu Y, Cheema SS, Wassif C, Huang SP, Lee E, Grinberg A, Massalas JS, Bodine D, Alt F, Westphal H. 1997. Lhx2, a LIM homeobox gene, is required for eye, forebrain, and definitive erythrocyte development. Development. 124: 2935-2944.

Potten CS. 1997. Growth factor and the regulation of haemopoietic stem cells. In: Stem Cells. Academic Press, London. pp. 433–445.

Potten CS. 2004. Keratinocyte stem cells, label-retaining cells and possible genome protection mechanisms. J Invest Dermat Symp Proc. 9: 183-195.

Prada C, Puga J, Perez-Mendez L, Lopez R, Ramirez G. 1991. Spatial and temporal patterns of neurogenesis in the chick retina. Eur. J. Neurosci. 3: 559–569.

Priston M, Kozlowski K, Gill D, Letwin K, Buys Y, Levin AV, Walter MA, Héon E. 2001. Functional analyses of two newly identified PITX2 mutants revealed a novel molecular mechanism for Axenfeld-Reiger syndrome. Hum Mol Genet. 10: 1631-1638.

Purkis PE, Steel JB, Mackenzie IC, Nathrath WB, Leigh IM, Lane EB. 1990. Antibody markers of basal cells in complex epithelia. J Cell Sci. 97: 39-50.

Quantock AJ, Young RD. 2008. Development of the corneal stroma, and the collagen-proteoglycan associations that help define its structure and function. Dev Dyn. 237: 2607-2621.

Radonic A, Thulke S, Mackay IM, Landt O, Siegert W, Nitsche A. 2004. Guideline to reference gene selection for quantitative real-time PCR. Biochem Biophys Res Comm. 313: 856–862.

Rajeevan MS, Ranamukhaarachchi DG, Vernon SD, Unger ER. 2001. Use of real-time quantitative PCR to validate the results of cDNA array and differential display PCR technologies. Methods. 25: 443-451.

Rajeevan MS, Vernon SD, Taysavang N, Unger ER. 2001. Validation of array-based gene expression profiles by real-time (kinetic) RT-PCR. J Mol Diagn. 3: 36-31.

Ramaesh T, Collinson JM, Ramaesh K, Kaufman MH, West JD, Dhillon B. 2003. Corneal abnormalities in Pax $6^{+/-}$ (small eye) mice mimic human Aniridia-related keratophaty. Invest Ophthalmol Vis Sci. 44:1871-1878.

Ramaesh T, Ramaesh K, Leask R, Springbett A, Riley SC, Dhillon B, West JD. 2006 Increased apoptosis and abnormal wound-healing responses in the heterozygous Pax6+/- mouse cornea. Invest Ophthalmol Vis Sci. 47: 1911-1817.

Rattner A, Hsieh JC, Smallwood PM, Gilbert DJ, Copeland NG, Jenkins NA, Nathans J. 1997. A family of secreted proteins contains homology to the cysteine-rich ligand-binding domain of frizzled receptors. Proc Natl Acad Sci USA. 94: 2859-2863.

Rawe IM, Zhan Q, Burrows R, Bennett K, Cintron C. 1997. Beta-ig molecular cloning and in situ hybridization in corneal tissues. Invest Opthalmol Vis Sci. 38: 839-900.

Raychaudhuri S, Stuart JM, Altman R. 2000. Prinicpal components analysis to summarize microarray experiments: application to sporulation time series. Pac Symp. Biocomput. 2000: 455-466.

Reed JC. 1998. Dysregulation of apoptosis in cancer. Oncogene. 17: 3225-3236.

Reed JC. 2000. Mechanisms of apoptosis. Am J Pathol. 157: 1415-1430.

Reinstein DZ, Silvermann RH, George AJT. Larkin DFP. 1994. Epithelial and corneal thickness measurements by high-frequency ultrasound digital signal processing. Opthalmology 101: 140-146.

Reiter RE, Gu Z, Watabe T, Thomas G, Szigeti K, Davis E, Wahl M, Nisitani S, Yamashiro J, Le Beau MM, Loda M, Witte ON. 1998. Prostate stem cell antigen: a cell surface marker overexpressed in prostate cancer. Proc Natl Acad Sci USA. 95: 1735-1740.

Ren H, Wilson G. 1994. The effect of ultraviolet-B irradiation on the cell shedding rate of the corneal epithelium. Acta Ophthalmol (Copenh). 72: 447-452.

Ren H, Wilson G. 1996. Apoptosis in corneal epithelium. Invest Ophthalmol Vis Sci. 37: 1017-1025.

Reneker LW, Silversides DW, Patel K, Overbeek PA. 1995. TGF alpha can act as a chemoattractant to perioptic mesenchymal cells in developing mouse eyes. Development. 121: 1669-80.

Revel JP, Hay ED. 1965. Fine structure of the developing chick cornea. Anat. Rec. 151: 492-502.

Revoltella RP, Papini S, Rosellini A, Michelini M. 2006. Epithelial stem cells of the surface eye. Cell Prolif. 40: 455-461.

Reya T, Clevers H. 2005. Wnt signaling in stem cells and cancer. Nature. 434: 843–850.

Reza HM, Ogino H, Yasuda K. 2002. L-Maf, a downstream target of Pax6, is essential for chick lens development. Mech Dev. 116: 61-73.

Riesenberg AN, Le TT, Willardsen MI, Blackburn DC, Vetter ML, Brown NL. 2009. Pax6 regulation of math5 during mouse retinal neurogenesis. Genesis. 47: 175-187.

Robertson DM, Ho SI, Cavanagh HD. 2008. Characterization of DeltaNp63 isoforms in normal cornea and telomerase-immortalized human corneal epithelial cells. Exp Eye Res. 86: 576-585.

Roderick C, Reinach PS, Wang L, Lu L. 2003. Modulation of rabbit corneal epithelial cell proliferation by growth factor-regulated K(+) channel activity. J Membr Biol. 196: 41–50.

Rodrigues M, Ben-Zvi A, Krachmer J, Schremer A, Sun T-T. 1987. Suprabasal expression of 4-kilodalton keratin (no. 3) in developing human corneal epithelium. Differentiation. 34: 60-67.

Rodrigues MM, Krachmer JH, Sun TT. 1986. Clinical, electron microscopic, and monoclonal antibody studies of intraocular epithelial downgrowth. Trans Am Opthalmol Soc. 84: 146-196.

Rodriguez-Burford C, Barnes MN, Berry W, Partridge EE, Grizzle WE. 2001. Immunohistochemical expression of molecular markers in an avian model: a potential model for preclinical evaluation of agents for ovarian cancer chemoprevention. Gynecol Oncol. 81: 373-379.

Roloff TC, Nuber UA. 2005. Chromatin, epigenetics and stem cells. Eur J Cell Biol. 84: 123-135.

Romano AC, Espana EM, Yoo SH, Budak MT, Wolosin JM, Tseng SCG. 2003. Different cell sizes in human limbal and central corneal basal epithelia measured by confocal microscopy and flow cytometry. Invest Ophthalmol Vis Sci. 44: 5125-5129.

Russell SW, Rosenau W, Lee JC. 1972. Cytolysis induced by human lymphotoxin. Am J Pathol. 69: 103-118.

Ryan JC, Morey JS, Ramsdell JS, Van Dolah FM. 2005. Acute phase gene expression in mice exposed to the marine neurotoxin domoic acid; excititoxicity stimulates ischemia. *Neuroscience.* 136: 1121–1132.

Saika S, Kawashima Y, Miyamoto T. 1999. Immunolocalization of transcription factor AP1 in human ocular surface epithelia. Curr Eye Res. 18: 477–489.

Sale JE, Calandrini DM, Takata M, Takeda S, Neuberger MS. 2001. Ablation of XRCC2/3 transforms immunoglobulin V gene conversion into somatic hypermutation. Nature. 412: 921-926.

Sanderson CJ. 1976. The mechanism of T cell mediated cytotoxicity. II. Morphological studies of cell death by time-lapse microcinematography. Proc R Soc Lond B Biol Sci. 192: 241–255.

Sanyanusin P, Schimmenti LA, McNoe LA, Ward TA, Pierpont ME, Sullivan MJ, Dobyns WB, Eccles MR. 1995. Mutation of the PAX2 gene in a family with optic nerve colobomas, renal anomalies and vesicoureteral reflux. Nat Genet. 9: 358-364.

Sarma K, Reinberg, D. 2005. Histone variants meet their match. Nat Rev Mol Cell Biol. 6: 139–149.

Sauer U, Preininger C, Hany-Schmatzberger R. 2005. Quick and simple: quality control of microarray data. Bioinformatics. 21:1572-1578.

Sawada H, Konomi H, Hirosawa K. 1990. Characterization of the collagen in the hexagonal lattice of Descemet's membrane: its relation to type VIII collagen. J Cell Biol. 110: 219-227.

Save V, Coates PJ, Hall PA. 2001. Analysis of apoptosis in tissue sections. Methods Mol Biol. 174: 347–359.

Scartezzini P, Egeo A, Colella S, Fumagalli P, Arrigo P, Nizetic, D,Taramelli R, Rasore-Quartino A. 1997. Cloning a new human gene from chromosome 21q22.3 encoding a glutamic acid-rich protein expressed in heart and skeletal muscle. Hum Genet. 99: 387-392.

Schena M, Shalon D, Davis RW, Brown PO. 1995. Quantitative monitoring of gene expression patterns with a complementary DNA microarray. Science. 270: 368-371.

Schermer A, Galvin S, Sun T. 1986. Differentiation-related expression of major 64K corneal keratin in vivo and in culture. J Cell Biol. 103: 49-62.

Schermer A, Jester JV, Hardy C, Milano D, Sun TT. 1989. Transient synthesis of K6 and K16 keratins in regenerating rabbit corneal epithelium: keratin markers for an alternative pathway of keratinocyte differentiation. Differentiation. 42: 103-110.

Schlötzer-Schrehardt U, Kruse FE. 2005. Identification and characterization of limbal stem cells. Exper Eye Res. 81: 247-264.

Schmittgen TD, Zakrajsek BA. 2000. Effect of experimental treatment of housekeeping gene expression: validation by real-time quantitative RT-PCR. J Biochem Biophys Meth. 46: 69-81.

Schofield R. 1983. The stem cell system. Biomed Pharmacother. 37: 375-380.

Schroder N, Gossler A. (2002). Expression of Notch pathway components in fetal and adult mouse small intestine. Gene Expr Patterns. 2: 247–250.

Schroeter EH, Kisslinger JA, Kopan R. 1998. Notch-1 signalling requires ligand-induced proteolytic release of intracellular domain. Nature. 393: 382–386.

Sekiya I, Vuoristo JT, Larson BL, Prockop DJ. 2002. In vitro cartilage formation by human adult stem cells from bone marrow stroma defines the sequence of cellular and molecular events during chondrogenesis. Proc Nat Acad Sci. 99: 4397-4402.

Selvey S, Thompson EW, Matthaei K, Lea RA, Irving MG, Griffiths ML. 2001. Beta-actin- an unsuitable internal control for RT-PCR. Mol. Cell Probes. 15: 307-311.

Sen S. 1992. Programmed cell death: concept, mechanism and control. Biol Rev Camb Philos Soc. 67:287-319.

Seo S, Richardson GA, Kroll KL. 2005. The SWI/SNF chromatin remodeling protein Brg1 is required for vertebrate neurogenesis and mediates transactivation of Ngn and NeuroD. Development.132:105-115.

Shanmuganathan VA, Foster T, Kulkarni BB, Hopkinson A, Gray T, Powe DG, Lowe J, Dua HS. 2007. Morphological Characteristics of the Limbal Epithelial Crypt. Br J Ophthalmol. 91: 514-519.

Shapiro AL, Viñuela E, Maizel JV Jr. 1967. Molecular weight estimation of polypeptide chains by electrophoresis in SDS-polyacrylamide gels. Biochem Biophys Res Commun. 28: 815–820.

Sharma A, Coles WH. 1989. Kinetics of corneal epithelial maintenance and graft loss. Invest Opthalmol Vis Sci. 30: 1962-1971.

Shivji MKK, Kenny MK, Wood RD. 1992. Proliferating cell nuclear antigen is required for DNA excision repair. Cell. 69: 367-374.

Shukla V, Vaissiere T, Herceg Z. 2008. Histone acetylation and chromatin signature in stem cell identity and cancer. Mut Res. 637: 1-15.

Silvestri F, Banavali S, Baccarani M, Preisler HD. 1992. The CD34 hemopoietic progenitor cell associated antigen: biology and clinical applications. Haematologica. 77: 265–273.

Simone C, Forcales SV, Hill DA, Imbalzano AN, Latella L, Puri PL. 2004. p38 pathway targets SWI-SNF chromatinremodeling remodelling complex to muscle-specific loci. Nat Genet. 36: 738-743.

Smith AN, Miller LA, Song N, Taketo MM, Lang RA. 2005. The duality of beta-catenin function: A requirement in lens morphogenesis and signaling suppression of lens fate in periocular ectoderm. Dev Biol. 285: 477-489.

Smyth GK. 2005. Limma: linear models for microarray data. Bioinformatics and Computational Biology Solutions using R and Bioconductor. Springer, New York. pp.397-420.

Sorrentino V, Pepperkok R, Davis RL, Ansorge W, Philipson L. 1990. Cell proliferation inhibited by MyoD1 independently of myogenic differentiation. Nature. 345: 813-815.

Spellman PT, Sherlock G, Zhang MQ, Iyer VR, Anders K, Eisen MB, Brown PO, Botstein D,Futcher B. 1998. Comprehensive identification of cell cycle-regulated genes of the yeast Saccharomyces cerevisiae by microarray hybridization. Mol Biol Cell. 9: 3273-3297.

Sperling S, Jaobsen SR. 1980. The surface coat on human corneal endothelium. Acta Opthalmol (Copenh). 58: 96-102.

Stern CD. 2005. The chick: A great model system becomes even greater. Dev Cell. 8: 9-17.

Storey JD, Xiao W, Leek JT, Tompkins RG, Davis RW. 2005. Significance analysis of time course microarray experiments. Proceed Nation Acad Sci. 102: 12837-12842.

Stroh C, Schulze-Osthoff K. 1998. Death by a thousand cuts: an ever increasing list of caspase substrates. Cell Death Differ. 5: 997-1000.

Sun TT, Tseng SC, Huang AJ, Cooper D, Schermer A, Lynch MH, Weiss R, Eichner R. 1985. Monoclonal antibody studies of mammalian epithelial keratins: a review. Ann NY Acad Sci. 455: 307-29.

Suzuka I, Daidoji H, Matsuoka M, Kadowaki K, Takasaki Y, Nakane PK, Moriuchi T. 1989. Gene for proliferating-cell nuclear antigen (DNA polymerase *6* auxiliary protein) is present in both mammalian and higher plant genomes. Proc Natn Acad Sci USA. 86: 3189-3193.

Svendsen PC, McGhee JD. 1995. The C. elegans neuronally expressed homeobox gene ceh-10 is closely related to genes expressed in the vertebrate eye. Development. 121: 1253-1262.

Svetlov SI, Sautin YY, Crawford JM. 2002. EDG receptors and hepatic pathophysiology of LPA and S1P: EDG-ology of liver injury. Biochem Biophys Act Mol Cell Biol Lip. 1582: 251-256.

Svoboda KK, Moessner P, Field T, Acevedo J. 2004. ROCK inhibitor (Y27632) increases apoptosis and disrupts the actin cortical mat in embryonic avian corneal epithelium. Dev Dyn. 229: 579-90.

Swamynathan SK, Katz JP, Kaestner KH, Ashery-Padan R, Crawford MA, Piatigorsky J. 2007. Conditional deletion of the mouse Klf4 gene results in corneal epithelial fragility, stromal edema, and loss of conjunctival goblet cells. Mol Cell Biol. 27: 182–194.

Swamynathan SK, Davis J, Piatigorsky J. 2008. Identification of candidate Klf4 target genes reveals the molecular basis of the diverse regulatory roles of Klf4 in the mouse cornea. Invest Ophthalmol Vis Sci. 49: 3360-3370.

Sylvester KG, Longaker MT. 2004. Stem cells. Review and update. Arch Surg. 139: 93-99.

Thaung C, Thaung C, West K, Clark BJ, McKie L, Morgan JE, Arnold K, Nolan PM, Peters J, Hunter AJ, Brown SDM, Jackson JJ, Cross SH. 2002. Novel ENU-induced eye mutations in the mouse: model for human disease. Hum Mol Genet. 11: 755-767.

Takacs L, Tóth E, Berta A, Vereb G. 2009. Stem cells of the adult cornea: from cytometric markers to therapeutic applications. Cytometry. 75: 54-66.

Takasaki Y, Fishwild D, Tan EM. 1984. Characterization of prolifarting cell nuclear antigen recognized by autoantibodies in luipus sera. J Exp Med. 159: 981-992.

Tanimura I. 1977. Comparative morphology of the bulbus oculi of the domestic animals revealed by scanning electron microscopy. J Vet Sci. 39: 643-649.

Tarca AL, Romero R, Draghici S. 2006. Analysis of microarray experiments of gene expression profiling. Am J Obst Gyn. 195: 373-388.

Terry K, Magan H, Baranski M, Burrus LW. 2000. Sfrp-1 and sfrp-2 are expressed in overlapping and distinct domains during chick development. Mech Dev. 97: 177-182.

Tewari M, Quan LT, O'Rourke K, Desnoyers S, Zeng Z, Beidler DR, Poirier GG, Salvesen GS, Dixit VM. 1995. Yama/CPP32 beta, a mammalian homolog of CED-3, is a CrmA-inhibitable protease that cleaves the death substrate poly(ADP-ribose) polymerase. Cell. 81: 801-809.

Thellin O, Zorzi W, Lakaye B. 1999. Houskeeping genes as internal standards: use and limits. J Biotechnol. 75: 291-295.

Thiagarajah JR, Verkman AS. 2002. Aquaporin deletion in mice reduces corneal water permeability and delays restoration of transparency after swelling. J Biol Chem. 277: 19139-19144.

Thoft RA, Friend J. 1983. The X, Y, Z hypothesis of corneal epithelial maintenance. Invest Ophthalmol Vis Sci. 24: 1442-1443.

Thoft RA. 1989. The role of the limbus in ocular surface maintenance and repair. Acta Ophthalmol Suppl. 192: 91-94.

Thompson H, Thompson J, Lockyer J, Beuerman RW. 1989. Protooncogene expression during corneal wound healing. In: Beuerman RW, Crosson GE, Kaufman HE. Advances in Applied Biotechnology Series. Vol.1. Healing Processes in the Cornea. The Woodlands, Texas: Portfolio Publishing. pp.59–68.

Tichopad A, Dilger M, Schwarz G, Pfaffl MW. 2003. Standardized determination of real-time PCR effciency from a single reaction set-up. Nucl Aci Res. 31: e122.

Tomarev SI, Sundin O, Banerjee-Basu S, Duncan MK, Yang JM, Piatigorsky J. 1996. Chicken homeobox gene Prox 1 related to Drosophila prospero is expressed in the developing lens and retina. Dev Dyn. 206: 354-367.

Toole BP, Trelstad RL. 1971. Hyaluronate production and removal during corneal development in the chick. Dev Biol. 26: 28-35.

Touhami A, Grueterich M, Tseng SC. 2002. The role of NGF signaling in human limbal epithelium expanded by amniotic membrane culture. Invest Ophthalmol Vis Sci. 43:987-994.

Tran CP, Lin C, Yamashiro J, Reiter RE. 2002. Prostate stem cell antigen is a marker of late intermediate prostate epithelial cells. Mol Cancer Res. 1: 113-121.

Trelstad RL, Hayashi K, Toole BP. 1974. Epithelial collagens and glycosaminoglycans in the embryonic cornea. Macromolecular order and morphogenesis in the basement membrane. J Cell Biol. 62: 815-830.

Trelstad RL. 1970. The Golgi apparatus in chick corneal epithelium: changes in intracellular position during development. J Cell Biol. 45: 34- 42.

Tseng SCG, Li DQ. 1996. Comparison of protein kinase C subtype expression between normal and aniridic human ocular surfaces: implications for limbal stem cell dysfunction in aniridia. Cornea. 15: 168–178.

Tseng SC. 1989. Concept and application of limbal stem cells. Eye. 3: 141-157.

Tseng SC, Jarvinen MJ, Nelson WG, Huang JW, Woodcock-Mitchell J, Sun TTI. 1982. Correlation of specific keratins with different types of epithelial differentiation: Monoclonal antibody studies. Cell. 30: 361-366.

Umek RM, Friedman AD, McKnight SL. 1991. CAAT-enhancer binding protein: a component of differentiation switch. Science. 251: 288-292.

Umpierre CC, Little SA, Mirkes PE. 2001. Co-localization of active Caspase-3 and DNA fragmentation (TUNEL) in normal and hyperthermia-induced abnormal mouse development. Teratology. 63: 134-143.

Van Heyningen V, Willamson KA. 2002. *PAX6* in sensory development. Hum Mol Genet. 11: 1161-1167.

Van Leeuven F, Gottschling DE. 2003. The histone minority report: the variant shall not be silenced. Cell. 112: 591-593.

Vandesompele J, De Peter K, Pattyn F, Poppe B, Van Roy N, De Paepe, Speleman F. 2002. Accurate normalization of real-time quantitative RT-PCR data by geometric averaging of multiple internal control genes. Genome Biol. 7: 1-11.

Vargesson N, Luria V, Messina I, Erskine L, Laufer E. 2001. Expression patterns of Slit and Robo family members during vertebrate limb development. Mech Dev. 106: 175–180.

Vascotto SG, Griffith M. 2006. Localization of candidate stem and progenitor cell markers within the human cornea, limbus, and bulbar conjunctiva in vivo and in cell culture. Anat Rec Discov Mol Cell Evol Biol. 288: 921-31.

Vauclair S, Majo F, Durham AD, Ghyselinck NB, Barrandon Y, Radtke F. 2007. Corneal epithelial cell fate is maintained during repair by Notch1 signaling via the regulation of vitamin A metabolism. Dev Cell. 13: 242-253.

Verkman AS. 2003. Role of aquaporin water channels in eye function. Exp Eye Res. 76: 137-143.

Verkman AS, Ruzi-Ederra J, Levin MH. 2008. Functions of aquaporins in the eye. Prog Ret Eye Res. 27: 420-433.

Vetter ML, Brown NL. 2001. The role of basic helix-loop-helix genes in vertebrate retinogenesis. Semin Cell Dev Biol.12: 491-498.

Von Giese A, Lorenz P, Wellbrock C, Hemmings B, Berberich-Siebelt F, Rapp U, Troppmair T. 2001. Apoptosis suppression by Raf-1 and MEK1 requires MEK- and Phosphatidylinositol 3-Kinase-dependent signals. Mol Cell Biol. 21: 2324-2336.

Walther C, Guenet JL, Simon D, Deutsch U, Jostes B, Goulding MD, Plachov D, Balling R, Gruss P. 1991. Pax: a murine multigene family of paired box-containing genes. Genomics 11: 424-434.

Waggoner PR. 1978. Scanning electron microscopy of the developing chick anterior corneal epithelium. J Embryol Exp Morphol. 44: 217-225.

Wagoner MD. 1997. Chemical injuries of the eye: current concepts in pathophysiology and therapy. Surv Ophthalmol. 41: 275–313.

Wang DA, Haming D, Jaggar JH, Brindley DN, Tigyi GJ, Watsky MA. 2002. Injury-elicited differential transcriptional regulation of phospholipid growth factor receptors in the cornea. Am J Physiol Cell Physiol. 52: C1646-C1654.

Wang L, Li T, Lu L. 2003. UV-induced corneal epithelial cell death by activation of potassium channels. Invest Ophthalmol Vis Sci. 44: 5095-5101.

Wang M, Munier F, Araki-Saski Km Schorderet D. 2002. TGFβ1 gene transcript is transfroming growth factor-beta1-responsive and cell density-dependent in human corneal epithelial cell line. Opthalamic Genet. 23: 237-245.

Warrington JA, Nair A, Mahadevappa M., Tsyganskaya M. 2000. Comparison of human adult and fetal expression and identification of 535 houskeeping/maintenance genes. Physiol Genomics. 2: 143-147.

Waseem NH, Lane DP. 1990. Monoclonal antibody analysis of the proliferating cell nuclear antigen (PCNA). J Cell Scien. 96: 121-129.

Watanabe K, Nishida M, Yamato T, Umemoto T, Sumide T, Yamamoto K, Maeda N, Watanabe H, Okano T, Tano Y. 2004. Human limbal epithelium contains side population cells expressing the ATP-binding cassette transporter ABCG2. FEBS Lett. 565: 6–10.

Watt FM, Hogan BLM. 2000. Out of Eden; Stem Cells and Their Niches. Science. 287: 1427-1430.

Wei ZG, Cotsarelis G, Sun TT, Lavker RM. 1995. Label-retaining cells are preferentially located in fornical epithelium: implications on conjunctival epithelial homeostasis. Invest Ophthalmol Vis Sci. 36: 236–246.

Wei MC, Zong WX, Cheng EH, Lindsten T, Panoutsakopoulou V, Ross AJ, Roth KA, MacGregor GR, Thompson CB, Korsmeyer SJ. 2001. Proapoptotic BAX and BAK: A requisite gateway to mitochondrial dysfunction and death. Science. 292: 727-730.

Weil M, Raff MC, Braga VM. 1999. Caspase activation in the terminal differentiation of human epidermal keratinocytes. Curr Biol. 9: 361–364.

Whitney EM, Ghaleb AM, Chen X, Yang VW. 2006. Transcriptional profiling of the cell cycle checkpoint gene kru¨ppel-like factor 4 reveals a global inhibitory function in macromolecular biosynthesis. Gene Expr. 13: 85–96.

Wickert H, Zaar K, Grauer A, John M, Zimmermann M, Gillardon F. 1999. Differential induction of proto-oncogene expression and cell death in ocular tissues following ultraviolet irradiation of the rat eye. Br J Ophthalmol. 83: 225-230.

Wijsman JH, Jonker RR, Keijzer R, Van de Velde CJ, Cornelisse CJ, Van Dierendonck JH. 1993. A new method to detect apoptosis in paraffin sections: in situ end- labeling of fragmented DNA. J Histochem Cytochem. 41: 7-12.

Williams SC, Altmann CR, Chow RL, Hemmani-Brivalou A, Lang R. 1998. A highly conserved lens transcriptional control element from the Pax-6 gene. Mech Dev. 73: 225–229.

Willingham MC. 1999. Cytochemical methods for the detection of apoptosis. J Histochem Cytochem. 47: 1101–1110.

Wison A, Radke F. 2006. Multiple functions of Notch signaling in self-renewing organs and cancer. FEBS Letters. 580: 2860-2868.

Wilson ES. 1999. Stimulus-specific and cell type-specific cascades: emerging principles relating to control of apoptosis in the eye. Exp Eye Res. 69: 255-266.

Wilson ES. 2000. Bowman's Layer Structure and Function: Critical or Dispensable to Corneal Function? A Hypothesis. Cornea. 19: 417-420.

Wilson SI, Rydstroem A, Trimborn T, Willert K, Nusse R, Jessell TM, Edlund T. 2001. The status of Wnt signalling regulates neural and epidermal fates in the chick embryo. Nature. 411: 325-330.

Wirtschafter JD, Ketcham JM, Weinstock RJ, Tabesh T, McLoon LK. 1999. Mucocutaneous junction as the major source of replacement palpebral conjunctival epithelial cells. Invest Ophthalmol Vis Sci. 40: 3138-3146.

Wodarz A, Nusse R. 1998. Mechanisms of Wnt signalling in development. Annu Rev Cell Dev Biol. 14: 59-88.

Wolosin JM, Wang Y. 1995. α-2,3 Sialylation differentiates the limbal and corneal epithelial cell phenotypes. Invest Ophthalmol Vis Sci. 36: 2277–2286.

Wolosin JM, Xiong X, Schütte M, Stegman Z, Tieng A. 2000. Stem cells and differentiation stages in the limbo-corneal epithelium. Prog Retin Eye Res. 19: 223-55.

Woodcock-Mitchell J, Eichner R, Nelson WG, Sun TT. 1982. Immunolocalization of keratin polypeptides in human epidermis using monoclonal antibodies. J Cell Biol. 95: 580-588.

Wride MA, Parker E, Sanders EJ. 1999. Members of the bcl-2 and caspase families regulate nuclear degeneration during chick lens fibre differentiation. Dev Biol. 213: 142-156.

Wu RL, Zhu G, Galvin S, Xu C, Haseba T, Chaloin-Dufau C, Dhouailly D, Wei ZG, Lavker RM, Kao WY. 1994. Lineage-specific and differentiation-dependent expression of K12 keratin in rabbit corneal/limbal epithelial cells: cDNA cloning and northern blot analysis. Differentiation. 55: 137-144.

Wurmbach E, Yuen SJ, Vrana T, Sealfon SC. 2003. Focused microarray analysis. Methods. 31: 306-316.

Wyllie AH, Kerr JF, Currie AR. 1980. Cell death: the significance of apoptosis. Int Rev Cytol. 68: 251-306.

Xi R, Xie T. 2005. Stem cell self-renewal controlled by chromatin remodeling factors. Science. 310: 1487-1489.

Xie T, Spradling AC. 1998. *Decapentaplegic* Is Essential for the Maintenance and Division of Germline Stem Cells in the *Drosophila* Ovary. Cell. 94: 251-260.

Xing Z., Schat KA. 2000. Expression of cytokines genes in Marek's disease virus-infected chickens and chicken embryo fibroblast cultures. Immunology. 100: 70–76.

Xu PX, Woo I, Her H, Beier DR, Maas RL. 1997. Mouse Eya homologues of the Drosophila eyes absent gene require Pax6 for expression in lens and nasal placode. Development 124: 219-231.

Xu XP, Yin J, Yu FS. 2007, Lysophosphatidic acid promoting corneal epithelial wound healing by transactivation of epidermal growth factor receptor. Invest Ophthalmol Vis Sci. 48: 636–643.

Yamagami S, Usui T, Amano S, Ebihara N. 2005. Bone marrow-derived cells in mouse and human cornea. Cornea. 24: S71-S74.

Yamanishi K, Shen CS, Mizutani H. 2005. Apoptosis in epidermis. Chapter 19. Epidermal cells: methods and protocols. Methods in molecular biology. K.Turksen, Humana Press Inc, Totowa, NJ. 289: p.171.

Yang S, Dudoit S, Luu P, Speed TP. 2001. Normalization for cDNA microarray data. Proc of Spie Bios. 4266: 31-53.

Yang YH, Dudoit S, Luu P, Lin DM, Peng V, Ngai J, Speed TP. 2002. Normalization for cDNA microarray data: a robust composite method addressing single and multiple slide systematic variation. Nucl Acids Res. 30: e15.

Yang YH, Speed T. 2002. Design issues for cDNA microarray experiments. Nat Rev. 3: 579-588.

Yazdani U, Terman JR. 2006. The semaphorins. Gen Biol. 7: 211-225.

Yee RW, Matsuda M, Schultz RO, Edelhauser HF. 1985. Changes in the normal corneal endothelial cellular pattern as a function of age. Curr Eye Res. 4: 671-678.

Yen MT, Pflugfelder SC, Crouse CA, Atherton SS. 1992. Cytoskeletal antigen expression in ocular mucosa-associated lymphoid tissue. Invest Opthalmol Vis Sci. 33: 3235-3241.

Yew DT, Sha O., Li WWY, Lam TT, Lorke DE. 2001. Proliferation and apoptosis in the epithelium of the developing human cornea and conjunctiva. Life Sciences. 68: 2987-3003.

Yin AH, Miraglia S, Zanjani ED, Almeida-Porada G, Ogawa M, Leary AG, Olweus J, Kearney J, Buck DW. 1997. AC133, a novel marker for human hematopoietic stem and progenitor cells. Blood. 90: 5002–5012.

You L, Kruse FE, Pohl J, Völcker HE. 1999. Bone morphogenetic proteins and growth and differentiation factors in the human cornea. Invest Ophthalmol Vis Sci. 40: 296-311.

Young B, Wheater P, Lowe JS, Stevens A, Deakin PJ, Heath JW. 2006. Wheater's functional histology: a text and colour atlas. 5th Edition. Philadelphia, Churchill Livingstone. pp.88-89.

Yu CC-W, Woods AI., Levison DA. 1992. The assessment of cellular proliferation by immunohistochemistry: a review of currently available methods and their applications. Histochem J. 24: 121-131.

Yuan C, Yang MC, Zins EJ, Boehlke CS, Huang AJW. 2004. Identification of the promoter region of the human βIGH3 gene. Mol Vis. 10: 351-360.

Zelenka PS, Arpitha P. 2008. Coordinating cell proliferation and migration in the lens and cornea. Semin Cell Dev Biol. 19: 113-124.

Zhang G, Contos JJ, Weiner JA, Fukushima N, Chun J. 1999. Comparative analysis of three murine G-protein coupled receptors activated by sphingosine-1-phosphate. Gene. 227: 89-99.

Zhang Q, Ahuja HS, Zakeri ZF, Wolgemuth DJ. 1997. Cyclin-dependent kinase 5 is associated with apoptotic cell death during development and tissue remodeling. Dev Biol. 183: 222-233.

Zhang Y, Akhtar RA. 1998. Epidermal growth factor stimulates phospholipase D independent of phospholipase C, protein kinase C or phosphatidylinositol-3 kinase activation in immortalized rabbit corneal epithelial cells. Curr Eye Res. 17: 294–300.

Zhang Z, Deb A, Zhang Z, Pachori A, He W, Guo J, Pratt R, Dzau VJ. 2009. Secreted frizzled related protein 2 protects cells from apoptosis by blocking the effect of canonical Wnt3a. J Mol Cell Card. 46: 370–377.

Zhao CX, Yee RW, Norcom E, Burgess H, Avanesov AS, Barrish JP, Malicki J. 2006. The zebrafish cornea: structure and development. Invest Opthalmol Vis Sci. 47: 4341-4348.

Zhu AJ, Haase I, Watt FM. 1999. Signaling via beta1 integrins and mitogen-activated protein kinase determines human epidermal stem cell fate in vitro. Proc Natl Acad Sci USA. 96: 6728-6733.

Zhu SN, Nolle B, Duncker G. 1997. Expression of adhesion molecule CD44 on human corneas. Br J Ophthalmol. 81: 80–84.

Zhu CC, Dyer MA, Uchikawa M, Kondoh H, Lagutin OV, Oliver G. 2002. Six3-mediated auto repression and eye development requires its interaction with members of the Groucho-related family of co-repressors. Development. 129: 2835-2849.

Zieske JD, Bukusoglu G, Yankauckas MA, Wasson ME, Keutmann HT. 1992a. Alpha-enolase is restricted to basal cells of stratified squamous epithelium. Dev Biol 115: 18-26.

Zieske JD, Bukusoglu G, Yankauckas MA. 1992b. Characterization of potential marker of corneal epithelial stem cells. Invest Ophthalmol Vis Sci. 33: 143-152

Zieske JD. 1994. Perpetuation of stem cells in the eye. Eye. 8: 163-169.

Zinn KM. 1970. Changes in corneal ultrastructure resulting from early lens removal in the developing chick embryo. Invest Ophthalmol Vis Sci. 9: 165–182.

Zinovieva RD. Duncan MK, Johnson TR, Torres R, Polymeropoulos MH, Tomarec SI. 1996. Structure and Chromosomal Localization of the Human Homeobox Gene Prox 1. Genomics 35: 517-522.

Zuber P, Hamou MF, de Tribolet N. 1988. Identification of proliferatin cells in human gliomas using monoclonal antibody Ki-67. Neurosurgery. 22: 364-368.